Journal of Biological Regulators & Homeostatic Agents

Volume 29, No. 2, April - June, 2015

CONTENTS

EDITORIAL

DYSMICROBISM, INFLAMMATORY BOWEL DISEASE AND THYROIDITIS: ANALYSIS OF THE LITERATURE

G. TOMASELLO[1,2*], P. TRALONGO[3*], F. AMOROSO[4], P. DAMIANI[5], E. SINAGRA[2,6], M. NOTO[1], V.M. ARCULEO[1], R. JURJUS ZEIN[7], W. SAAD[8], A. JURJUS[8*] A. GERBINO[9] and A. LEONE[9*]

[1]School of Medicine and Surgery, University of Palermo, Italy; [2]IEMEST, Euro-Mediterranean Institute of Science and Technology, Palermo, Italy; [3]Department of Health Promotion, Tumor Immunology Laboratory, School of Medicine and Surgery, Palermo University, Italy; [4]Student School of Medicine and Surgery, University of Palermo, Italy; [5]Geriatric School of Medicine, University of Palermo, Italy; [6]Fondazione Istituto S. Raffaele- G. Giglio, Gastroenterology and Endoscopy Unit, Cefalù, Italy; [7]Department of Anatomy and Regenerative Biology, Faculty of Medicine and Health Sciences, George Washington University, Washington DC, USA; [8]Department of Anatomy, Cell Biology and Physiological Sciences, Faculty of Medicine, American University of Beirut, Beirut, Lebanon; [9]Department of Experimental Biomedicine and Clinical Neuroscience, Section of Histology and Embryology, School of Medicine and Surgery, Palermo, Italy

Received December 9, 2014 – Accepted February 27, 2015

*These authors share the first authorship

The human body is colonized by a large number of microbes that are collectively referred to as the microbiota. They interact with the hosting organism and some do contribute to the physiological maintenance of the general good health thru regulation of some metabolic processes while some others are essential for the synthesis of vitamins and short-chain fatty acids. The abnormal variation, in the quality and/or quantity of individual bacterial species residing in the gastro-intestinal tract, is called "dysmicrobism". The immune system of the host will respond to these changes at the intestinal mucosa level which could lead to Inflammatory Bowel Diseases (IBD). This inflammatory immune response could subsequently extend to other organs and systems outside the digestive tract such as the thyroid, culminating in thyroiditis. The goal of the present study is to review and analyze data reported in the literature about thyroiditis associated with inflammatory bowel diseases such as Ulcerative Colitis (UC) and Crohn's Disease (CD). It was reported that similarities of some molecular bacterial components with molecular components of the host are considered among the factors causing IBD through an autoimmune reaction which could involve other non-immune cell types. The axis dysmicrobism-IBD-autoimmune reaction will be investigated as a possible etiopathogenic mechanism to Autoimmune Thyroiditis. If such is the case, then the employment of specific probiotic strains may represent a useful approach to moderate the immune system.

Key words: extra-intestinal manifestations of IBD, thyroiditis, IBD, ulcerative colitis, Crohn's disease, microbiota, gut microflora, dysbiosis

Mailing address: Dr Giovanni Tomasello,
Medico Chirurgo, Professore Aggregato di Chirurgia Generale,
Universita' degli Studi di Palermo,
Scuola di Medicina e Chirurgia,
Azienda Ospedaliera Universitaria "P. Giaccone",
via del Vespro 127, 90127 Palermo, Italy
Tel.: +39 0916553518
e-mail: giovanni.tomasello@unipa.it

0393-974X (2015)

DISCLOSURE: ALL AUTHORS REPORT NO CONFLICTS OF INTEREST RELEVANT TO THIS ARTICLE.

The microbiota contributes to the human health. Depending on their beneficial or harmful activity, there will be either a normal physiological or a pathological state (1). The maintenance of a balance between the different microrganisms inhabiting the gastro-intestinal tract is called "homeostasis of microbiota" (2, 3). When this equilibrium is disrupted towards the more harmful organisms the resulting condition takes the name of dysmicrobism. The course of any disease will vary depending on the species involved. For example, pseudo membranous colitis is characterized by the prevalence of C. Difficile and in typhoid fever Salmonella Typhi prevails (4).

In such situations, the lymphatic system in the intestinal mucosa, called Gut Associated Lymphatic Tissue (GALT), protects the gut from pathogenic microbes. The GALT is represented by the ring of Waldeyer at the pharyngeal level and Payer's patches in the small intestine. Since the gastrointestinal tract is in direct communication with the external environment the substantial GALT immune system protects the body from external pathogens but also from the harmful microbiota. Normally, a physical barrier, consisting of enterocytes, separates the immune cells from the microbiota, but in case of injury to this barrier, resulting from physical damage by chemicals or by exotoxins produced by bacteria, the microbiota will be in direct contact with GALT. Which is then activated causing the release of cytokines that lead to inflammation. It does this by creating a specific immune (adaptive) response and also by a non-specific response (innate). Even in the absence of a direct damage to the mucosa, the immune system may also act in an indirect way, thru the action of Antigen Presenting Cells (APC) that by diapedesis can detect the presence of foreign antigens in the lumen and present them to lymphoid tissues (5).

The immune system represented by GALT has also a positive role by inducing tolerance to beneficial microbes. Initially, all microorganisms trigger an inflammatory process by GALT but when a non-pathogenic organism is met, the immune system learns to recognize it as non-self as well as non-pathogenic, and it will stop triggering the same level of response. Laboratory studies have shown that administration of microorganisms normally present in the intestinal flora to germ-free mice caused an immune response that led to colitis, however, this was resolved in a short time and activation of specific genes of the small and large intestine was noted (5). This process represents the basis of tolerance which is essential for the maintenance of a healthy status.

When there is an infection by pathologic organisms, the immune inflammatory process starts by recognizing some components of pathogens presented to the lymphocytes as antigen. This leads to selection and multiplication of those lymphocyte clones that will be responsible to manage the inflammatory process in a specific manner. However, sometimes an unexpected cross-reaction of the antibodies with autologous components happens. This is due to the structural analogy of bacterial components to self components (6). Consequently, the antibodies produced against the antigens will recognize self elements as foreign and will attack various cells of the body. This process is in fact at the basis of the progression of autoimmune diseases. In the intestinal tract, inflammatory pathologies that are related to dysmicrobism and in association with other various factors, like genetic factors and food cause alterations of the immune system characterized in IBD including Crohn's disease(CD) and Ulcerative Colitis (UC) (7). In fact, UC and CD have been observed with an altered microbial framework somehow specific for each disease. Also certain genetic mutations, for example Nod2/CARD15 (pattern recognition receptor) are involved in the loss of the immune tolerance mechanisms (8, 9). Children with altered microbial flora have

a higher incidence of developing IBD during adulthood. When an inflammatory situation resulting from a non-specific GALT response extends to extra-intestinal organs, it will cause a systemic inflammatory response leading to systemic manifestations of IBD; the reaction will affect multiple parts of the whole body (10-16), as shown in Table I.

Thyroiditis: Is microbiota a triggering factor?

Inflammatory diseases of the thyroid are often of idiopathic etiology. Recent articles demonstrate that alterations of the intestinal microbiota can be associated with some forms of thyroiditis characterized by an autoimmune reaction, the exact etiopathogenesis of which is still unclear. Auto-antibodies formed in the intestine may hit directly the thyroid gland and cause immune thyroiditis. But also, when the intestinal mucosa is inflamed and no longer able to act as a barrier, microorganisms can pass into the circulation and make contact with the submucosa and with the vascular lining. Since some of these bacterial components have similarities in structure with the host cells, the circulating antibodies in the blood will react with the bacterial antigen causing inflammation including thyroiditis (10). It is reasonable, therefore, that the etiopathogenesis of Hashimoto's Thyroiditis may involve dysmicrobism (Fig. 1). In fact, ulcerative colitis has been associated with thyroid dysfunction such as Grave's disease, Hashimoto's thyroiditis and thyrotoxicosis as presented in Table II.

On the other hand, it is well known that colonic microbiota contributes to the bioavailability of thiamine that is synthesized in the form of thiamine pyrophosphate (TPP). The absorption of thiamine is regulated by a carrier-mediated uptake system for TPP in human cells lining the colon, probably controlled by the SLC44A4 gene (17). The microbiota is able to influence the genetic expression of colonocytes and trigger an inflammatory process. The role of thiamine deficiency in cases of altered microbiota is documented in a study conducted on fatigue as a disorder related to IBD. It has been observed that treatment with high-dose thiamine leads to significant benefits (18). Also, although the main treatment for patients affected by Hashimoto's thyroiditis is levothyroxine, fatigue symptoms of a significant number of subjects did not subside despite good control of the thyroid function as documented by thyroid tests being in the normal range. In these cases, fatigue regressed only after the administration of thiamine supplement. It has been hypothesized that thiamine deficiency

Table I. *Reported systemic manifestations of IBD.*

Association between IBD and Extra-intestinal manifestations	
Authors	Extra-intestinal Manifestations
[11] Geraci A, Tomasello G, Termine S, Damiani P, Alongi G, Sanfilippo A, D'Arienzo M.	Arthritis
[12] Shivashankar R, Loftus EV Jr, Tremaine WJ, Harmsen WS, Zinsmeister AR, Matteson EL.	Spondyloarthropathy
[13] Calvo P, Pablo L.	Ocular manifestations
[14] Weizman AV, Huang B, Targan S, Dubinsky M, Fleshner P, Kaur M, Ippoliti A, Panikkath D, Vasiliauskas E, Shih D, McGovern DP, Melmed GY.	Cutaneous manifestations
[15] Alkhateeb H, Said S, Cooper CJ, Elhanafi S, Teleb M, Saifuddin F, Mukherjee D, Abbas A, Davis HE 2nd.	Myocarditis
[16] Lankarani KB, Sivandzadeh GR, Hassanpour S.	Oral manifestations

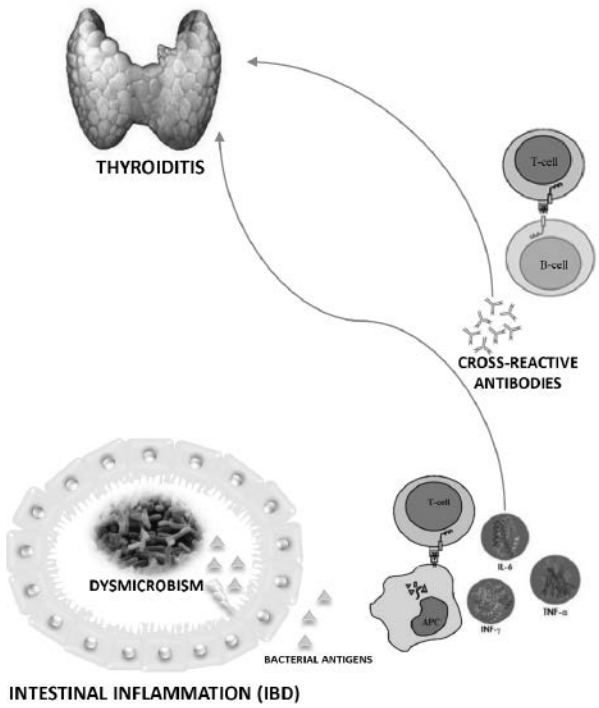

Fig. 1. *Intestinal manifastations of IBD; The possible mechanism responsible for the induction of thyroiditis consequent to IBD inflammatory process.*

may be a cofactor involved in the chronic fatigue accompanying inflammatory and autoimmune conditions (19). The mechanism is probably due to a dysfunction of the intracellular transport or to enzymatic abnormalities, most likely related to the autoimmune process of the disease. Conversely, patients with associated UC and hyperthyroidism were less responsiveness to UC treatment before the control of thyroid function (20).

Heat shock proteins (HSP) are stress proteins that have a role in protection of cells against stress. They and also have been implicated in antigen presentation with the role of transferring antigenic peptides to the class I and class II molecules of the major histocompatibility complexes (21). Using immuno-histochemical detection, Hsp60 and Hsp10 in colonic mucosa were found to be high in IBD patients localization in epithelial cells of mucosal glands and not always in the connective tissue cells of the lamina propria (22). It was also noted that patients with IBD have increased blood levels of specific antibodies to the Hsp60 that are cross-reactive with regions of the bacterial counterpart Hsp65 (23). In the blood of patients with Hashimoto's thyroiditis, Hsp60 levels were increased as compared to controls and they were immunolocalized in the thyroid tissue, both in thyrocytes and oncocytes (Hurthle cells). It was found also that there was a structural similarity between regions in Hsp60 molecule with the thyroglobulin (TG) and thyroid peroxidase (TPO) molecules. Anti-TG and anti-TPO antibodies cross-react with Hsp60 (21).

Probiotics: a potential weapon against IBD and Hashimoto's thyroiditis

The complex consortium of microbes that we harbor within our gastrointestinal tract are not just passive bystanders, rather these organisms seem to actively shape our immune system responses both inside and outside the intestine.

Butyrate and other compounds derived from bacterial fermentation of undigested fibers in the intestine reduce significantly the nuclear factor-kappa B (NF-kB) which is a protein transcription factor involved in the control of immune and inflammatory responses and is active in a number of disease states, including chronic inflammation (24). This process diminishes the production of pro-inflammatory molecules, interleukin 6 (IL6) and tumor-necrosis factor (TNFα), simulated by endotoxins, thus decreasing the inflammatory response (25).

Also, the great importance of gastro-intestinal colonization by bacteria has been demonstrated in germ-free mice models. The latter reported maturation defects in regulatory T cells (T-reg) differentiation in the intestinal lamina propria, leading to a dysregulation of

Table II. *Clinical cases of subjects affected by IBDs and thyroiditis reported in the literature.*

Authors	Biochemical and immunological parameters	Comorbidities								
(33) Yakut et al., 2011		Free T3 (picomol/L)	Free T4 (picomol/L)	TSH (micro IU/ml)	Anti TPO (IU/ml)		IBD (n = 146)	UC (n = 113)	CD (n = 33)	Control (n = 66)
	IBD	4.4 ± 1.27	14.4 ± 4.01	2.1 ± 3.6	14.1 ± 29.1	Thyroid Disease	14 (9.5%)	11 (9.7%)	3 (9.0%)	1 (1.5%)
	UC	4.5 ± 1.42	14.3 ± 4.015	1.8 ± 2.13	14.2 ± 30.25	Hyperthyroidism	5 (3.4%)	5 (4.4%)	0 (0%)	0 (0%)
	CD	4.3 ± 0.89	14.46 ± 3.81	2.7 ± 5.59	14.07 ± 28.35	Hypothyroidism	1 (0.06 %)*	0 (0%)	0 (0%)	0 (0%)
	Control	4.8 ± 0.85	15.04 ± 2.9	4 ± 15.3	22.4 ± 82.6	Subclinical Hypothyroidism	0 (0%)	0 (0%)	0 (0%)	0 (0%)
						Subclinical Hyperthyroidism	5 (3.4%)	2 (1.7%)	3 (9.0%)	0 (0%)
		Thyroidits	4 (2.7%)	4 (3.5%)	0 (0%)	1 (1.5%)				
(34) Najafi et al., 2012		Free T4 (picomol/L)	TSH (micro IU/ml)	Anti-Thyroglobulin	Anti TPO (IU/ml)	23-month-old infant affected by UC, Autoimmune Hypothyroidism, Type 1 Diabetes and Autoimmune Hepatitis				
		3.5	6	700	250					
(20) Modebe 1986	CASE 1)	1) 41-year-old African woman with Thyrotoxicosis followed by UC after two years.								
	T3 resin uptake test	Free T3 ng/dl	Free T4 mg/dl	Iodide perchlorate discharge test	Anti Thyroglobulin					
	39%	318	13	43.50%	negative					
	CASE 2)	2) 38-year-old Caucasian woman affected initially by UC which evolved into Thyrotoxicosis.								
			Free T3 ng/dl	T3 resin uptake test	Free T4 mg/dl					
			328	44%	15					

the normal mechanisms of immunological homeostasis. The above mentioned maturation defect is reverted after colonization of murine intestine by *Bacteroides fragilis* (26).

There is also evidence that selected lactic acid bacterial (LAB) strains induce a certain maturation of the dendritic cells (DC) conferring protection against induced colitis, and that these probiotic-treated DC do stimulate regulatory functions by targeting specific pattern-recognition receptors and pathways producing an anti-inflammatory activity (27). This evidence is substantiated by the fact that mice treated with probiotics show an increase in interleukin 10 production which is responsible for prevention of autoimmune disorders (28). Supplementation of the diet with LAB to mice did enhance several indices of natural and acquired immunity in

healthy mice. It increased the phagocytic activity of peripheral blood leucocytes and peritoneal macrophages. The serum antibody response was also significantly enhanced. In addition, spleen cells produced significantly higher amounts of interferon-gamma (IFNγ) (29).

However, it has also been reported that some probiotic strains are responsible for a worsening of colitis characterized by a marked and aberrant increase in IFNγ production and by a reduced T-reg activity (30). Though probiotics usually inhibit DC activation by inflammatory bacteria, some immunostimulatory probiotics not only fail to protect against colitis but they actually can amplify the disease progression (31). Probiotic with LAB did not stimulate induced experimental autoimmune thyroiditis but also did not have an inhibitory effect on the inflammatory disease development (32).

CONCLUSIONS

Based on the data in this review, it is clear that alterations of the normal flora of the intestines may result in an inflammatory process. At the origin of this pathology there is an improper reaction of the immune system that activates other secondary pathways. Dysbiosis can also alter the cell junctions leading to an increase in mucosal permeability thus allowing the passage of microorganisms or their antigenic components into the circulation, which could result in extra-intestinal manifestations of IBD; including the thyroid and causing thyroiditis. This mechanism could explain the correlation between dysbiosis and thyroiditis. Some cases of autoimmune thyroiditis may therefore be a systemic expression of IBD triggered by a stimulation of GALT due to a dysmicrobic condition.

Getting to know all the species that make up the intestinal flora should enable recognition of the possible pathogens and their specific role in the etiopathogenesis of IBD as well as of the extra-intestinal manifestations including thyroiditis. Therapy could then be directed towards correcting homeostasis of the intestinal flora. Specific probiotic mixes may then contribute to the resolution of dysmicrobism and hopefully of the thyroid inflammatory pathology.

In conclusion, caution must be exercised when choosing a probiotic strain for the treatment of auto-immune disorders, including thyroiditis, and this should be done with the maximum of care.

REFERENCES

1. Bellavia M, Tomasello G, Romeo M, et al. From Gut microbiota imbalance and chaperoning system malfunction are central to ulcerative colitis pathogenesis and can be counteracted with specifically designed probiotics: working hypothesis. Med Microbiol Immunol 2013; 202:393-406.
2. Tralongo P, Tomasello G, Sinagra E, et al. The role of butyric acid as a protective agent against infiammatory bowel disease. Euromediterranean Biomed J 2014; 9(4):24-35.
3. Franchi L. Role of inflammasomes in salmonella infection. Front Microbiol 2011; 2:8.
4. Ogawa H, Fukushima K, Sasaki I, Matsuno S. Identification of genes involved in mucosal defense and inflammation associated with normal enteric bacteria. Am J Physiol Gastrointest Liver Physiol 2000; 279(3):G492-9.
5. Abbas A, Lichtman A, Pilla S. Cellular and Molecular Immunology, Eighth Edition, ELSEVIER 2012.
6. Wen Z, Fiocchi C. Inflammatory bowel disease: autoimmune or immune-mediated pathogenesis? Clin Dev Immunol 2004; 11(3-4):195-204.
7. Björkstén B, Sepp E, Julge K, Voor T, Mikelsaar M. Allergy development and the intestinal microflora during the first year of life. J Allergy Clin Immunol 2001; 108(4):516-20.
8. Hugot JP, Chamaillard M, Zouali H, et al. Association of NOD2 leucine-rich repeat variants with susceptibility to Crohn's disease. Nature 2001; 411(6837):599-603.

9. Ogura Y, Bonen DK, Inohara N, et al. A frame shift mutation in NOD2 associated with susceptibility to Crohn's disease. Nature 2001; 411(6837):603-6.
10. Mori K, Nakagawa Y, Ozaki H. Does the gut microbiota trigger Hashimoto's thyroiditis? Discov Med 2012; 14(78):321-6.
11. Geraci A, Tomasello G, Termine S, Damiani P, Alongi G, Sanfilippo A, D'Arienzo M. Arthritis associated with ulcerative colitis: our experience in Palermo. Libyan J Med 2009; 4(3):94.
12. Shivashankar R, Loftus EV Jr, Tremaine WJ, Harmsen WS, Zinsmeister AR, Matteson EL. Incidence of Spondyloarthropathy in patients with ulcerative colitis: a population-based study. J Rheumatol 2013; 40(7):1153-7.
13. Calvo P, Pablo L. Managing IBD outside the gut: ocular manifestations. Dig Dis 2013; 31(2):229-32.
14. Weizman AV, Huang B, Targan S, et al. Pyoderma gangrenosum among patients with inflammatory bowel disease: a descriptive cohort study. J Cutan Med Surg 2014; 18(5):361.
15. Alkhateeb H, Said S, Cooper CJ, et al. Myopericarditis as a complication of nonspecific colitis. Am J Case Rep 2014; 15:82-4.
16. Lankarani KB, Sivandzadeh GR, Hassanpour S. Oral manifestation in inflammatory bowel disease: a review. World J Gastroenterol 2013; 19(46):8571-9.
17. Nabokina SM, Inoue K, Subramanian VS, Valle JE, Yuasa H, Said HM. Molecular identification and functional characterization of the human colonic thiamine pyrophosphate transporter. J Biol Chem 2014.
18. Costantini A, Pala MI. Thiamine and fatigue in inflammatory bowel diseases: an open-label pilot study. J Altern Complement Med 2013; 19(8):704-8.
19. Costantini A, Pala MI. Thiamine and Hashimoto's thyroiditis: a report of three cases. J Altern Complement Med 2014; 20(3):208-11.
20. Modebe O. Autoimmune thyroid disease with ulcerative colitis. Postgrad Med J 1986; 62(728):475-6.
21. Marino Gammazza A, Rizzo M, Citarrella R, et al. Elevated blood Hsp60, its structural similarities and cross-reactivity with thyroid molecules, and its presence on the plasma membrane of oncocytes point to the chaperonin as an immunopathogenic factor in Hashimoto's thyroiditis. Cell Stress Chaperones 2014; 19(3):343-53.
22. Rodolico V, Tomasello G, Zerilli M, et al. Hsp60 and Hsp10 increase in colon mucosa of Crohn's disease and ulcerative colitis. Cell Stress Chaperones 2010; 15(6):877-84.
23. Füst G, Uray K, Bene L, Hudecz F, Karádi I, Prohászka Z. Comparison of epitope specificity of anti-heat shock protein 60/65 IgG type antibodies in the sera of healthy subjects, patients with coronary heart disease and inflammatory bowel disease. Cell Stress Chaperones 2012; 17(2):215-27.
24. Dr. Thomas Gilmore, Biology Department, Boston University. NF-kB Transcription Factors: http://www.bu.edu/nf-kb/
25. Lührs H, Gerke T, Müller JG, Melcher R, Schauber J, Boxberge F, Scheppach W, Menzel T. Butyrate inhibits NF-kappaB activation in lamina propria macrophages of patients with ulcerative colitis. Scand J Gastroenterol 2002; 37(4):458-66.
26. Round JL, O'Connell RM, Mazmanian SK. Coordination of tolerogenic immune responses by the commensal microbiota. J Autoimmunol 2010; 34(3):J220-25.
27. Foligne B, Zoumpopoulou G, Dewulf J, Younes AB, Chareyre F, Sirad J-C, Pot B, Grangette C. A key role of dendritic cells in probiotic functionality PLoS One 2007; 2(3):e313.
28. Sokol H, Pigneur B, Watterlot L, et al. Faecalibacterium prausnitzii is an anti-inflammatory commensal bacterium identified by gut microbiota analysis of Crohn disease patients. Proc Natl Acad Sci 2008; 105(43):16731-36.
29. Gill HS, Rutherfurd KJ, Prasad J, Gopal PK. Enhancement of natural and acquired immunity by Lactobacillus rhamnosus (HN001), Lactobacillus acidophilus (HN017) and Bifidobacterium lactis(HN019). Br J Nutr 2000; 83(2):167-76.
30. Schmidt EGW, Cleasson MH, Jensen SS, Ravn P, Kristensen NN. Antigen-presenting cells exposed to Lactobacillus acidophilus NCFM, Bifidobacterium bifidum BI-98, and BI-504 reduce regulatory T cell activity. Inflamm Bowel Dis 2010; 16(3):390-400.
31. Mileti E, Matteoli G, Iliev ID, Rescingno M. Comparison of the immunomodulatory properties of three probiotic strains of Lactobacilli using complex culture systems: prediction for *in vivo* efficacy. PLoS

One 2009; 4(9):e7056.
32. Zhou JS, Gill HS. Immunostimulatory probiotic Lactobacillus rhamnosus HN001 and Bifidobacterium lactis HN019 do not induce pathological inflammation in mouse model of experimental autoimmune thyroiditis. Int J Food Microbiol 2005; 103(1):97-104.

EDITORIAL

PERIODONTAL DISEASE AND BONE PATHOGENESIS: THE CROSSTALK BETWEEN CYTOKINES AND *PORPHYROMONAS GINGIVALIS*

A. BALLINI[1], S. CANTORE[2], D. FARRONATO[3], N. CIRULLI[2], F. INCHINGOLO[4], F. PAPA[2], G. MALCANGI[1], A.D. INCHINGOLO[2], G. DIPALMA[2], N. SARDARO[1], R. LIPPOLIS[5], L. SANTACROCE[6], M.F. COSCIA[1], F. PETTINI[4], D. DE VITO[1] and S. SCACCO[1]

[1]Department of Base Medical Sciences, Neurosciences and Sense Organs, University of Bari "Aldo Moro", Italy; [2]School of Medicine, University of Bari "Aldo Moro", Italy; [3]Department of Morphologic and Surgical Sciences, Insubria University, Varese, Italy; [4]Department of Interdisciplinary Medicine, University of Bari "Aldo Moro", Italy; [5]Institute of Bioenergetics and Biomembranes – National Council Research, Bari, Italy; [6]Jonian Department, University of Bari "Aldo Moro", Italy

Received February 12, 2015 – Accepted April 9, 2015

Periodontal disease is the most frequent cause of tooth loss among adults. It is defined as a plaque-induced inflammation of the periodontal tissues that results in a loss of support of the affected teeth. This process is characterized by destruction of the periodontal attachment apparatus, increased bone resorption with loss of crestal alveolar bone, apical migration of the epithelial attachment, and formation of periodontal pockets. Although the presence of periodontal pathogens such as *Porphyromonas gingivalis* is a prerequisite, the progression of periodontal disease is dependent on the host response to pathogenic bacteria that colonize the tooth surface. Nowadays, a growing body of literature has accumulated to investigate the association between bone diseases, periodontal pathogens and periodontal diseases. The integration of pathogen-associated molecular patterns from microorganisms with their surface receptors in the immune cells, induces the production of several cytokines and chemokines that present either a pro- and/or anti-inflammatory role and the activation of mechanisms of controlling this and the related disease, such as osteoporosis and rheumatoid arthritis. This review focuses on the evidence and significance of bone host cell invasion by *Porphyromonas gingivalis* in the pathogenesis of bone disorders, as well as the different lines of evidence supporting the role of cytokines in bone diseases.

Periodontal disease (PD) is a chronic bacterial infection that affects the gingiva and bone surrounding the teeth; the pathogenesis of human periodontitis was placed on a rational footing for the first time by Page and Schroeder in 1976 (1).

The connective tissue of the periodontium is separated from the oral cavity by a thin permeable junctional epithelium that has remarkable cell and fluid dynamics that allow the flow of bacterial toxins and inflammatory mediators (2), so the accumulation of bacteria in the gingival crevice might trigger an inflammatory process, which, if left untreated,

Key words: periodontal disease, Porphyromonas gingivalis, bone loss, cytokines, citrullination, anti–cyclic citrullinated peptide antibodies

Mailing address: Dr Salvatore Scacco, Department of Basic Medical Sciences, Neurosciences and Sense Organs, University of Bari "Aldo Moro", P.zza Giulio Cesare, 11, 70124, Bari, Italy
e-mail: salvatore.scacco@uniba.it

0393-974X (2015)

DISCLOSURE: ALL AUTHORS REPORT NO CONFLICTS OF INTEREST RELEVANT TO THIS ARTICLE.

destroys the periodontium and, eventually, results in tooth loss (3).

Spread of inflammation to the adjacent connective tissue drives the destruction of connective tissue and alveolar bone, that is, the cardinal sign of PD (4-5). Currently, an increasing body of literature has collected to investigate the cross-link between bone diseases and PD, that emerges either with the chronic or the aggressive form, and affects a significant portion of the population (2-5).

In 1998, Page (6) proposed that periodontitis may affect the host's susceptibility to systemic disease in three ways: by shared risk factors, by subgingival biofilms acting as reservoirs of gram-negative bacteria and through the periodontium acting as a reservoir of inflammatory mediators. The present editorial was conducted to focus on scientific published studies that have added to the basic knowledge and broader understanding of clinical and biological links between bone host cell invasion by a specific periodontal pathogen in the pathogenesis of the bone, with references to major historical studies and topical reviews.

Periodontal etiopathogenesis: the role of Porphyromonas gingivalis

The presence of periodontopathogens in the gingival sulcus such as *Porphyromonas gingivalis (P. gingivalis)* (7), in addition to genetic and environmental aspects seem to increase the susceptibility of some individuals to develop PD (8). This pathogen utilizes a multitude of virulence factors to evade host defenses as it establishes itself as one of the predominant pathogens in periodontal pockets (8). The pathogenic factors of *P. gingivalis* including fimbriae, hemagglutinin, capsule, lipopolysaccharide (LPS), outer membrane vesicles, organic metabolites such as butyric acid, and various enzymes such as Arg- and Lys-gingipains, collagenase, gelatinase and hyaluronidase, could contribute to the induction of chronic periodontitis in diverse ways (9). In fact, *P. gingivalis* could colonize gingival crevices by the fimbriae-mediated adherence to gingival epithelial cells, the proteases may have the ability to destroy periodontal tissues directly or indirectly, and the LPS could elicit a wide variety of inflammatory responses of periodontal tissues and alveolar bone loss (8-9).

In PD, gingipains degrade macrophage CD14, thus inhibiting activation of the leukocytes through the LPS receptor, thereby facilitating sustained colonization of *P. gingivalis* (9). Moreover, LPS can induce *in vitro* the osteoclast formation directly, and also indirectly by the cytokine production from gingival fibroblasts (10).

Although chronic exposure to bacteria and their products is a prerequisite for gingival inflammation and periodontal tissue destruction to occur, the major causative factor of soft- and hard- tissue breakdown associated with periodontitis is currently attributed to the host's immune-inflammatory response to bacterial challenge.

Effects of periodontal infection on systemic bone loss

While PDs have historically been deemed to be the result of an infectious process, other authors have proposed that PD may be an early manifestation of osteoporosis (11). The cross-link between these two diseases may be the bone-resorptive process: in fact, the diseases have a common denominator, loss of bone alveolar in PD and generalized in osteoporosis (12-15). Increased local production of cytokines associated with PD could rush systemic bone resorption by modulating the host response (Fig. 1).

Pleiotropic cytokine IL-6, produced by osteoblasts, may play a key role in this possible mechanism, because in normal bone homeostasis, IL-6 production stimulates osteoclastic activity subsequent in bone resorption, and certain lifestyle factors, such as smoking and low calcium intake, may impact the risk of developing osteoporosis and PD (16).

Role of RANK-L and related molecules

Nowadays, studies of crevicular fluid (GCF) from healthy individuals and patients with chronic periodontal disease demonstrated that increases in receptor activator of nuclear factor-kappa B ligand (RANK-L) mRNA and protein levels in periodontal tissues stimulate the differentiation of monocyte-macrophage precursor cells into osteoclasts and the maturation and survival of the osteoclasts, leading to alveolar bone loss (17-19). The severity of periodontal disease correlates slightly with RANK-L and Osteoprogerin (OPG) overexpression and more strongly with the RANK-L/OPG ratio (17).

Studies on humans have demonstrated that

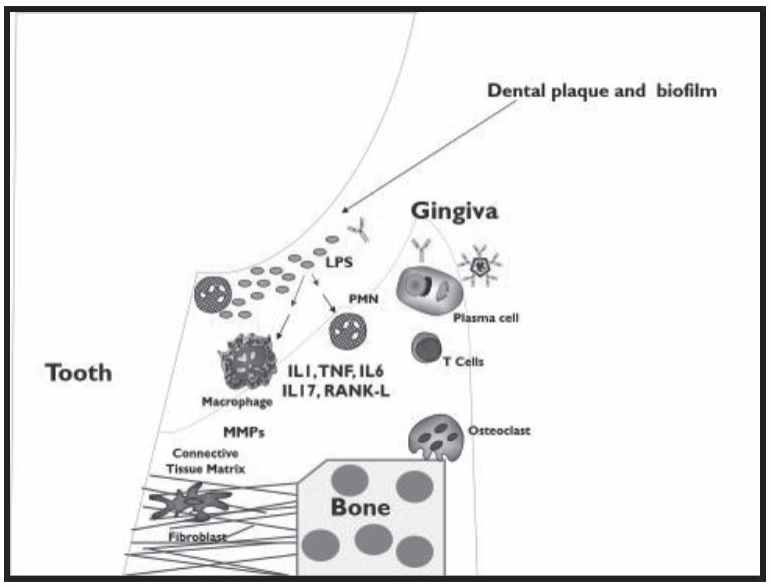

Fig. 1. *The host response. The pathogenetic events in periodontal disease are initiated, conducted and regulated by mediators of the acute and chronic inflammatory process produced by gingival resident cells, activated by infiltrating lymphocytes, junctional epithelium cells, vascular endothelium, mast cells, bone cells, the complement cascade and cytokines system.*

RANK-L levels in GCF were lower in healthy tissues or gingivitis, but increased in periodontitis (18-19) and, on the other hand, OPG levels were higher in healthy tissues than periodontitis, or gingivitis groups (17). Thus, GCF levels of RANK-L and OPG were oppositely regulated in periodontitis, but not in gingivitis, resulting in an enhanced RANK-L/OPG ratio.

Among the components of the oral flora, some organisms such as *P. gingivalis* may be strong inducers of RANK-L expression (18, 19), furthermore, *P. gingivalis* produces a unique class of cysteine proteinases termed gingipains that comprises Arg-gingipain and Lys-gingipain (19).

An amino acid sequence similar to the Arg-gingipain cysteine proteases may be involved in RANK-L production, as *P. gingivalis* strains carrying Lys-gingipain mutations fail to increase RANK-L levels (19). In addition, developments in the field of osteoimmunology, which examine the crosstalk of immune cells and bone, have uncovered a novel role for the RANK-L/RANK/OPG system in other processes such as in controlling autoimmunity or immune responses in the skin (20). The critical balance between osteoblast-mediated bone formation and osteoclast-mediated bone resorption has been described as "coupling" of bone formation to bone resorption (21).

Periodontium as a cytokine reservoir

Cytokines are regulatory low-weight proteins acting as mediators into genesis and control of immune and inflammatory response. During inflammatory response characteristic of periodontitis, proinflammatory cytokines, such as interleukin (IL)-1 α and β, IL-6, IL-17, tumor necrosis factor (TNF)-α, and interferon (INF)-γ can stimulate periodontal osteoblasts to express membrane-bound RANK-L (22-24). In addition to osteoblasts, RANK-L is expressed by a number of other cell types, mainly CD4+ T lymphocytes (25), playing a crucial role in T cell-mediated bone resorption. Through the RANK-L/RANK system, IL-17 may have a role in rheumatoid arthritis (RA), PD, and loosening of joint prostheses (26, 27).

IL-1 is a proinflammatory cytokine that plays an important role in immune regulation and inflammatory processes by inducing expression of many effector proteins, e.g. cytokines/chemokines, nitric oxide synthetase (NOS) and matrix metalloproteinases

(MMPs) (26-28). IL-1 includes two different but functionally similar molecules: IL-1α and IL-1β (28), genes which are all located on the long arm of chromosome 2 (region 2q13–14). IL-1α is mainly produced by keratinocytes of junctional epithelium or pocket epithelium, is a mediator of local inflammation and regulates intracellular event, instead IL-1β is primarily produced by activated macrophages and fibroblasts that release this extracellular protein (29). IL-1 upregulates complement system, Fc-receptor on polymorphonuclear neutrophils and monocytes, the expression of adhesion molecules upon fibroblast and leukocytes and induces the expression of homing receptors into the extracellular matrix for leukocytes and bone resorption by stimulating the proliferation and differentiation of osteoclast progenitors and activating formed osteoclast indirectly (28, 29).

Excessive and/or dysregulated activity of these mediators is associated with tissue destruction and therefore the synthesis, secretion and biological activity of IL-1 cytokines have been identified as therapeutic targets for common inflammatory disorders such as RA, diabetes and PD (30). Single nucleotide polymorphisms (SNPs) in the IL-1 promoter region could modulate this cytokine function that acts a fundamental role in the pathogenesis of PD, by affecting the susceptibility and severity of the affection (31).

The composite IL-1 genotype, known as periodontitis-associated genotype (PAG), obtained by the combination of the two rare alleles at the above-mentioned SNPs, has been extensively investigated in respect to the form of PD (chronic *vs* aggressive), smoke, ethnic group, and oral microbial pathogens present in the plaque biofilm (*P. gingivalis*) and other periodontal clinical parameters related to inflammatory status or to the progression of the disease (31, 32).

In a recent study, osteoblasts obtained from alveolar bone of PD patients underwent apoptosis in the presence of TNF-related apoptosis-inducing ligand (TRAIL), by interacting with its death receptors, (DR4, DR5) (33). However, its activity can be modulated by two decoy receptors, DcR1 and DcR2, as a result that, the sensitiveness of TRAIL-induced apoptosis is determined by the ratio of death and decoy receptor (33). Based on studies such as these, it can be projected that TNF superfamily,

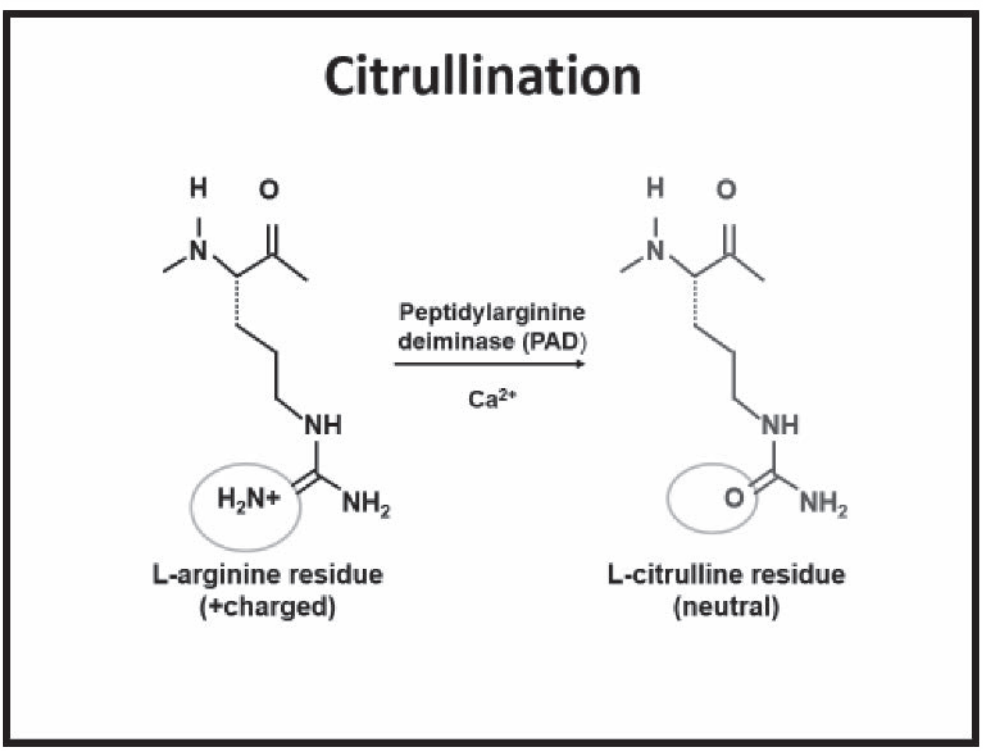

Fig. 2. *Citrullination: changes in secondary and tertiary conformation of proteins, neoepitopes formed.*

and in particular TRAIL, plays a role in controlling the expression of the cytokines that stimulate bone resorption during PD.

Inflammatory cytokines, IL-6 and INF-γ were considered as mediators of periodontal destruction because mononuclear cells and T cells extracted from periodontitis patients expressed more INF-γ and IL-6 compared to their peripheral blood counterparts from healthy controls (31-33).

Rheumatoid arthritis and citrullination : a link with Porphyromonas gingivalis

As reported to date, inflammation is clearly a central component of many chronic diseases.

Post-translational modifications such as phosphorylation, glycosylation and citrullination are very common processes that can increase the morphological and the functional diversity of the proteome, modifying a specific part of an amico acid after its synthesis.

Citrulline formation depends on the conversion of arginine catalyzed by peptidylarginine deiminase (PAD) enzymes (Fig. 2) (32). However, citrulline can be formed even as a side product when nitric oxide (NO) is generated from arginine by NO-synthetase (NOS) (32, 34).

In the oral cavity, nitrate is reduced to nitrite by nitrate-reducing bacteria (71) and nitrite is reduced to NO by nitrite-reducing bacteria (34). Additionally, in the oral cavity, two peroxidases are present; one is salivary peroxidase that is derived from saliva and the other is myeloperoxidase that is derived from leukocytes migrated into the oral cavity, so in this way, the formation of nitrite and NO by oral bacteria results in the production of reactive nitrogen oxide species (RNOS) by various reactions (34). Taking this mechanism into consideration, the decrease in pH in the oral cavity results in the injury of oral tissue cells.

There is a higher salivary arginase activity in periodontitis patients compared to healthy controls; in fact, the increased salivary arginase activity in periodontitis, perhaps causing a decrease in NO synthesis, also leads to a decrease in the antibacterial property of saliva and causes periodontal tissues to become more susceptible to existing pathogens

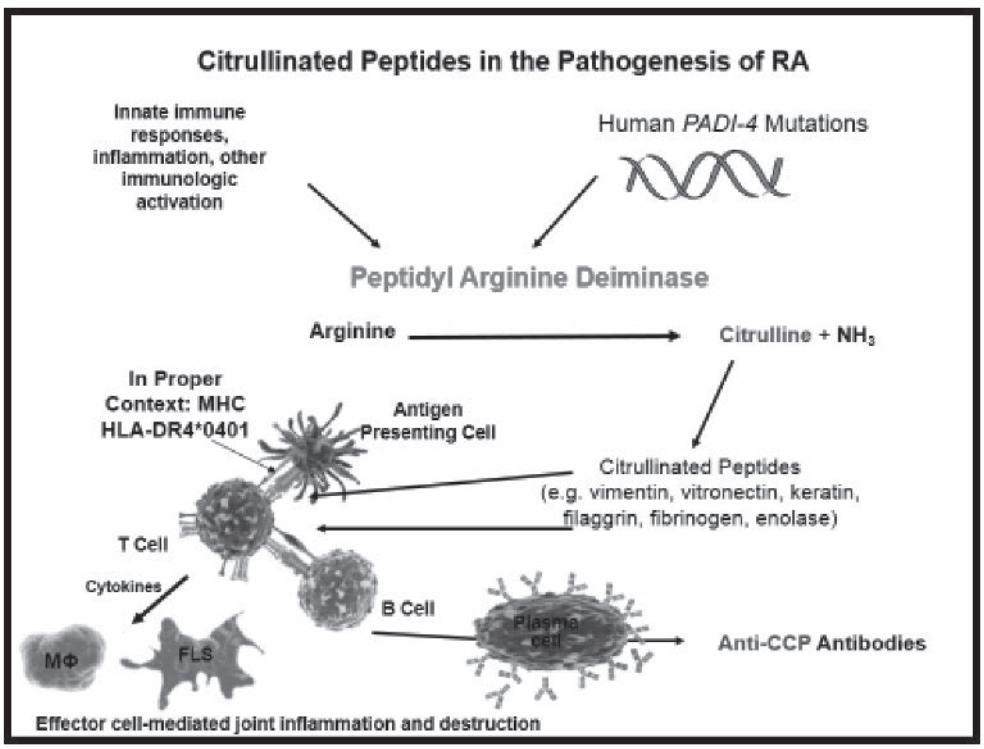

Fig. 3. *Crosslink between PAD and RA. Consistent associations between PAD and antibody responses against citrullinated peptides in the pathogenesis of RA. In RA patients, PD is a strong predictor of anti-CCP antibodies.*

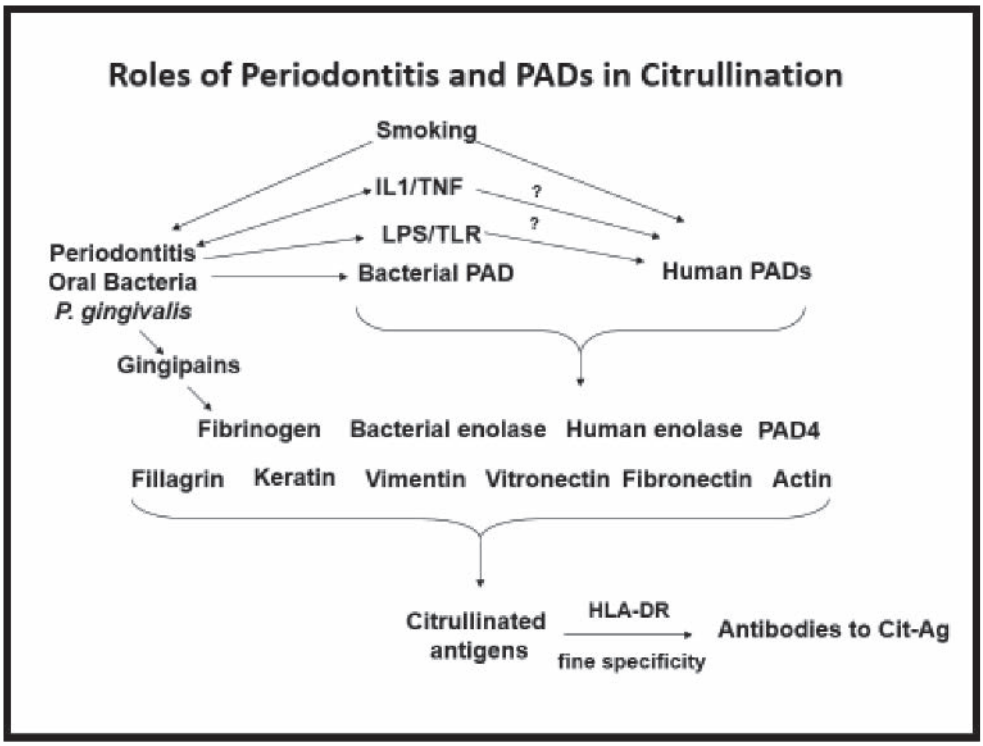

Fig. 4. *P. gingivalis has endogenous PAD. Hypothesized release of NH3+ leads to buffering of crevicular fluid and enhances organism evasion of host defense thus serving as virulence factor.*

(32, 34). Elevated NO production is a reflection of an immune-activated state in which inflammatory cytokines and other mediators have up-regulated inducible nitric oxide synthase (iNOS) (34).

The anti–Cyclic Citrullinated Peptide Antibodies (anti-CCP) are produced locally in the inflamed synovium of Rheumatoid arthritis (RA) patients (Fig. 3), suggesting that citrullinated proteins are located in the inflamed synovium (32). This has led to speculation that individuals predisposed to PD are exposed to citrullinated antigens that, in the proinflammatory context of PD associated to *P. gingivalis* PAD, become systemic immunogens (Fig. 4). In fact*, P. gingivalis* possesses that unique microbial enzyme, PAD, the human equivalent of which has been identified as a susceptibility factor for RA, and its proliferation depends on secretion of PAD (32). PAD catalyzes the deamination of peptidylarginine residues of various peptides to produce peptidylcitrulline and ammonia therefore, from this point of view, is possible to wonder about the presence of anti-CCP antibodies in PD.

DISCUSSION

There is a growing appreciation in international scientific literature of oral bacteria interactions, and their effects alone and in concert emphasizes the complex interplay among different species in amplifying local inflammatory and immunoregulatory pathways. Throughout the microbial world, there are strain differences within a species and these differences sometimes influence virulence.

The results of a recent study of bacterial species showed a potential synergistic partnership between *Aggregatibacter actinomycetemcomitans (A. actinomycetemcomitans)*, *Filifactor alocis (F. alocis)*, and *Streptococcus parasanguinis (S. parasanguinis)* which are key members of localized aggressive periodontitis (LAP), as this consortium

is strongly associated with bone loss (35). However, while it has been proposed that *S. parasanguinis* culd be found in the upper third of the pocket, both *A. actinomycetemcomitans* and *F. alocis* have been shown to be present in the deeper portions of the pocket, resting closer to the pocket epithelium, and these temporal and anatomical associations need additional *in vivo* confirmation.

In recent years, research on the topics of periodontal bacteria in bone diseases, such as *P. gingivalis,* has confirmed long-standing observed cross-talk between these diseases. Although the unique contribution to periodontal disease propagation by *P. gingivalis* as a single species may be considerable, the likelihood for considerable redundancies of function with other bacteria seems likely. In a recent study, conducted on a sample of 22 subjects with PD, the anti-CCP antibody was not found in sera of 21 (U/ml<10), while only in 1 subject with probing depth of 7.1 mm was identified positive for anti-CCP (22.2 U/ml) (32). The results, even if the study was conducted with some limits, i.e. limited sample size, absence of healthy controls not observed levels of *P. gingivalis* antibody response and lower systemic inflammation, do not support a role for anti-CCP in diagnoses of PD (32). We can speculate from these findings alone whether infection with *P. gingivalis* serves as a trigger for RA onset, or alternatively acts to modify immune responses in subjects following disease onset, or both, particularly considering that the levels of bacteria antibody response in this cohort seems to be one of the enrollment criteria including RA positivity. It is possible that these null findings result from its lower specificity and our inability to distinguish smaller differences in anti-CCP expression with a limited sample size. On the other hand, it is also possible that differences in antibody responses to *P. gingivalis* based on disease status may be due to other factors (e.g., gene-environment associations like pollution, tobacco etc.). In fact, gene-environment associations are important in RA susceptibility, with an association existing between smoking, HLA- DRB1 'shared epitope' alleles, PTPN22 and anti-CCP.

Cigarette smoking was much more frequent in subjects with RA and PD compared to healthy controls, which is important given separate associations of smoking with both PD and RA risk. However, these are both multifactorial, chronic diseases, and their complex etiologies and pathogenesis themselves remain incompletely understood.

According to the evidence-based dentistry (36), researchers and clinicians are directed to therapeutic approaches that actually represent the gold standard in PD treatment, such as laser applications (37), bone substitutes (38, 39), and the new emerging field of stem cells from oral tissues (40).

As is evident from the studies in international scientific literature that continue to emerge, a multidisciplinary collaboration is necessary to fully understand the relationships between the host response resulting from periodontal pathogens in the pathogenesis of the bone, as well as the different lines of evidence supporting the role of periodontal bacteria in bone diseases.

CONCLUSIONS

Nowadays, periodontics has evolved from a simplistic model to a more complex interplay between infection and host response, because genetic factors are a new addition to the list of risk factors for periodontal and related systemic diseases. The association between oral and systemic health has highlighted the importance of periodontal health and treatment, with the consequence that dental assessment and attention to oral hygiene assume an increasingly important part for the clinical management of patients with osteoporosis and rheumatoid arthritis.

Together with patient education, these factors improve the probability of patient treatment acceptance, which will improve oral and systemic health. Thus, although many studies have been conducted to understand this process, many questions still need to be clarified in order to utilize this knowledge in the comprehension of the development of PD.

REFERENCES

1. Page RC, Schroeder HE. Pathogenesis of inflammatory periodontal disease. A summary of current work. Lab Invest 1976; 34:235-49.
2. Nunn ME. Understanding the etiology of periodontitis: an overview of periodontal risk factors. Peri-

odontol 2000 2003; 32:11-23.
3. Hugoson A, Norderyd O. Has the prevalence of periodontitis changed during the last 30 years? J Clin Periodontol 2008; 35:338-45.
4. LeResche L, Dworkin SF. The role of stress in inflammatory disease, including periodontal disease: Review of concepts and current findings. Periodontol 2000 2002; 30:91-103.
5. Chandna S, Bathla M. Stress and periodontium: A review of concepts. J Oral Health Comm Dent 2010; 1:17-22.
6. Page RC. The pathobiology of periodontal diseases may affect systemic diseases inversion of a paradigm. Ann Periodontol 1998; 3:108-20.
7. McGraw WT, Potempa J, Farley D, Travis J. Purification, characterization, and sequence analysis of a potential virulence factor from *Porphyromonas gingivalis, Peptidylarginine Deiminase*. Infect Immun 1999; 67:3248-56.
8. Gemmell E, Yamazaki K, Seymour GJ. Destructive periodontitis lesions are determined by the nature of the lymphocytic response. Crit Rev Oral Biol Med 2002; 13:17-34.
9. Kimura S, Tamamura T, Nakagawa I, Koga T, Fujiwara T, Hamada S. CD14- dependent and independent pathways in lipopolysaccharide-induced activation of a murine B-cell line, CH12. LX. Scand J Immunol 2000; 51:392-9.
10. Scheres N, de Vries TJ, Brunner J, Crielaard W. Laine ML, Everts V. Diverse effects of *Porphyromonas gingivalis* on human osteoclast formation. Microb Pathog 2011; 51:149-55.
11. Whalen JP, Krook L. Periodontal disease as the early manifestation of osteoporosis. Nutrition 1996; 12:53-4.
12. Kuo LC, Polson AM, Kang T. Associations between periodontal diseases and systemic diseases: a review of the inter-relationships and interactions with diabetes, respiratory diseases, cardiovascular diseases and osteoporosis. Public Health 2008; 122:417-33.
13. Renvert S. Destructive periodontal disease in relation to diabetes mellitus, cardiovascular diseases, osteoporosis and respiratory diseases. Oral Health Prev Dent 2003; 1:341-59.
14. Azarpazhooh A, Tenenbaum HC. Periodontitis: a syndromic condition. J Can Dent Assoc 2012; 78:c27.
15. Wilder RS, Thomas KM, Jared H. Periodontal-systemic disease education in United States dental hygiene programs. J Dent Educ 2008; 72:669-79.
16. Ershler WB, Keller ET. Age-associated increased interleukin-6 gene expression, late-life diseases, and frailty. Annu Rev Med 2000; 51:245-70.
17. Bostanci N, Ilgenli T, Emingil G, et al. Differential expression of receptor activator of nuclear factor-kappa B ligand and osteoprotegerin mRNA in periodontal diseases. J Periodontal Res 2007; 42:287-93.
18. Wara-aswapati N, Surarit R, Chayasadom A, Boch JA, Pitiphat W. RANKL upregulation associated with periodontitis and *Porphyromonas gingivalis*. J Periodontol 2007; 78:1062-69.
19. Belibasakis GN, Bostanci N, Hashim A, Johansson A, Aduse-Opoku J, Curtis MA, Hughes FJ. Regulation of RANKL and OPG gene expression in human gingival fibroblasts and periodontal ligament cells by *Porphyromonas gingivalis*: a putative role of the Arg-gingipains. Microb Pathog 2007; 43:46-53.
20. Leibbrandt A, Penninger JM. Novel functions of RANK(L) signaling in the immune system. Adv Exp Med Biol 2010; 658:77-94.
21. Parfitt AM. The coupling of bone formation to bone resorption: a critical analysis of the concept and of its relevance to the pathogenesis of osteoporosis. Metab Bone Dis Relat Res 1982; 4:1-6.
22. Moffatt CE, Lamont RJ. *Porphyromonas gingivalis* induction of microRNA-203 expression controls suppressor of cytokine signaling 3 in gingival epithelial cells. Infect Immun 2011; 79:2632-7.
23. Mangan PR, Harrington LE, O'Quinn DB, Helms WS, Bullard DC, Elson CO, Hatton RD, Wahl SM, Schoeb TR, Weaver CT. Transforming growth factor-beta induces development of the T(H)17 lineage. Nature 2006; 441:231-4.
24. Gaffen SL, Hajishengallis G. A new inflammatory cytokine on the block: re-thinking periodontal disease and the Th1/Th2 paradigm in the context of Th17 cells and IL-17. J Dent Res 2008; 87:817-28.
25. Schmidt J, Jentsch H, Stingu CS, Sack U. General immune status and oral microbiology in patients with different forms of periodontitis and healthy control subjects. PLoS One 2014; 9:e109187.
26. Azman R, Lappin DF, MacPherson A, et al. Clini-

cal associations between IL-17 family cytokines and periodontitis and potential differential roles for IL-17A and IL-17E in periodontal immunity. Inflamm Res 2014; 63:1001-12.

27. Yu JJ, Ruddy MJ, Wong GC, Sfintescu C, Baker PJ, Smith JB, Evans RT, Gaffen SL.An essential role for IL-17 in preventing pathogen-initiated bone destruction: recruitment of neutrophils to inflamed bone requires IL-17receptor-dependentsignals. Blood 2007; 109:3794-802.
28. Dinarello CA. The IL-1 family and inflammatory diseases. Clin Exp Rheumatol 2002; 20:S1-13.
29. Chai L, Song YQ. Leung WK. Genetic polymorphism studies in periodontitis and Fcγ receptors. J Periodont Res 2011; 47:273-85.
30. Bartold PM, Marshall RI, Haynes DR. Periodontitis and rheumatoid arthritis: a review. J Periodontol 2005; 76:2066-74.
31. Cantore S, Mirgaldi R, Ballini A, et al. Cytokine gene polymorphisms associate with microbiogical agents in periodontal disease: our experience. Int J Med Sci 2014; 11:674-9.
32. Ballini A, Tetè S, Scattarella A, et al. The role of anticyclic citrullinated peptide antibody in periodontal disease. Int J Immunopathol Pharmacol 2010; 23:677-81.
33. Mori G, Brunetti G, Colucci S, et al. Osteoblast apoptosis in periodontal disease: role of TNF-related apoptosis-inducing ligand. Int J Immunopathol Pharmacol 2009; 22; 95-103.
34. Doel JJ, Hector MP, Amirtham CV, Al-Anzan LA, Benjamin N, Allaker RP. Protective effect of salivary nitrite and microbial nitrate reductase activity against caries. Eur J Oral Sci 2004; 112:424-8.
35. Fine DH, Markowitz K, Fairlie K, Tischio-Bereski D, Ferrendiz J, Furgang D, Paster BJ, Dewhirst FE. A consortium of *Aggregatibacter actinomycetemcomitans, Streptococcus parasanguinis,* and *Filifactor alocis* is present in sites prior to bone loss in a longitudinal study of localized aggressive periodontitis. J Clin Microbiol 2013; 51:2850-61.
36. Ballini A, Capodiferro S, Toia M, Cantore S, Favia G, De Frenza G, Grassi FR. Evidence-based dentistry: what's new? Int J Med Sci 2007; 6:174-8.
37. Grassi FR, Ciccolella F, D'Apolito G, et al. Effect of low-level laser irradiation on osteoblast proliferation and bone formation. J Biol Regul Homeost Agents 2011; 25:603-14.
38. Scattarella A, Ballini A, Grassi FR, et al. Treatment of oroantral fistula with autologous bone graft and application of a non-reabsorbable membrane. Int J Med Sci 2010; 7:267-71.
39. Ballini A, Cantore S, Capodiferro S, Grassi FR. Esterified hyaluronic acid and autologous bone in the surgical correction of the infra-bone defects. Int J Med Sci 2009; 6:65-71.
40. Mori G, Brunetti G, Oranger A, et al. Dental pulp stem cells: osteogenic differentiation and gene expression. Ann N Y Acad Sci 2011; 1237:47-52.

JOURNAL OF BIOLOGICAL REGULATORS & HOMEOSTATIC AGENTS Vol. 29, no. 2, 283-288 (2015)

EDITORIAL

CROSSTALK BETWEEN VITAMIN B AND IMMUNITY

E. SPINAS[1], A. SAGGINI[2], S.K. KRITAS[3], G. CERULLI[4], A. CARAFFA[5], P. ANTINOLFI[5], A. PANTALONE[6], A. FRYDAS[7], M. TEI[4], A. SPEZIALI[4], R. SAGGINI[8], F. PANDOLFI[9] and P. CONTI[10]

[1]Department of Surgery and Odontostomatological Sciences, University of Cagliari, Italy; [2]Department of Dermatology, University of Rome Tor Vergata, Rome, Italy; [3]Department of Microbiology and Infectious Diseases, School of Veterinary Medicine, Aristotle University of Thessaloniki, Macedonia, Greece; [4]Nicola's Foundation, Onlus, Arezzo, Italy; [5]Orthopedic Division, University of Perugia, Perugia, Italy; [6]Orthopedic Division, University of Chieti-Pescara, Chieti, Italy; [7]Aristotelian University, Thessaloniki, Greece; [8]Department of Neurosciences and Imaging, Faculty of Medicine and Surgery, G. d'Annunzio University Chieti-Pescara, Chieti, Italy; [9]Catholic University of Rome, Italy; [10]Immunology Division, Postgraduate Medical School, University of Chieti-Pescara, Chieti, Italy

Vitamin B1 (thiamin) is considered to be the oldest vitamin and in 1936 R.R. Williams and colleagues determined its chemical structure and were able to synthesize this vitamin. Vitamin B1 influences pro-apoptotic proteins, mitochondrial membrane potential, cytochrome C release, protein kinases, p38-MAPK, suppresses oxidative stress-induced NF-kappaB and has anti-inflammatory properties. Deficiency of vitamin B1 may cause beriberi, dysfunction of the nervous system, neuroinflammation, T cell infiltration, chemokine CCL2 activation, over expression of proinflammatory cytokines, such as IL-1, TNF, IL-6, and arachidonic acid products, and induces expression of CD40 by the microglia and CD40L by astrocytes which provoke the death of neurons. Here we report the relationship between vitamin B complex and immunity.

Vitamins originate primarily in plant tissue and are present in animal tissue only as a consequence of consumption of plants. The existence of vitamins was not recognized until about the start of the twentieth century and in 1935-1937 it was reported that cobalt, the central ion in vitamin B12 is a dietary essential for many vital functions.

VITAMIN B

Grains, including breads cereals and rice, are the primary source of the B vitamins and also provide fiber, along with such minerals as iron, potassium, zinc, copper and selenium. Vitamin B is present in legumes, leafy green vegetables, and certain fruits.

Vitamin B1 (thiamin)

Vitamin B1 (thiamin), a component of the vitamin B complex, was discovered in the 1930s. However, long before that time (1880s, K. Takaki) it was noted that the rice-eating people of Asia or people consuming white flour in Europe were deprived of this vitamin, and the incidence of beriberi, which is characterized by numbness, muscle weakness,

Key words: vitamin, immunity, inflammation, cytokine

Mailing address: Prof. Enrico Spinas,
Department of Surgery and Odontostomatological Sciences,
University of Cagliari,
Cso Vittorio Emanuele 340, 09123 Cagliari, Italy
Tel.: +39 330412295
e-mail: enricospinas@tiscali.it

0393-974X (2015)

loss of appetite and disorders of the nervous system, rose to an epidemic level. It was the first water–soluble vitamin to be discovered and therefore is considered the oldest vitamin. Thiamin, like other B-complex vitamins, acts as a biological catalyst, or coenzyme and is a cofactor of key enzymes in glucose metabolism. It is well known and has been extensively studied that thiamin as a coenzyme participates in the production of energy for the body, maintains a constant temperature, is involved in the synthesis of fat and protein metabolism and is important for the functions of the nervous and immune systems.

Chemically, thiamin consists of a molecule of pyrimidine and a molecule of thiazole linked by methylene bridge. Thiamin phosphorylation can take place in most tissue, but particularly in the liver. The most important function of thiamin in the cell is as the coenzyme cocarboxylase or thiamin triphosphate.

Vitamin B1 prevents the expression of the Bcl-2 family of pro-apoptotic proteins, caspase-3 activation, and poly-(ADP-ribose) polymerase (PARP) cleavage. It alters mitochondrial membrane potential, release of cytochrome C, apoptosis-inducing factor and phosphorylation and subsequently the activation of p38-MAPK, stress-activated kinases (SAPK/JNK), protein kinase C, and cytoplasmic phospholipase A2. Acting on macrophages, vitamin B1 has a potential anti-inflammatory effect and suppresses oxidative stress-induced NF-kappaB activation.

Deficiency of thiamin may provoke an abnormal function of heart and circulatory system leading to heart failure, impairment of oxidative metabolism, and immune dysfunctions. Supplementation of thiamin is recommended in stress and fatigue providing instant energy. Its deficiency in the nervous system may impair its ability to synthesize fatty acid and cholesterol, necessary for membrane integrity and function, inducing damage of the central nervous system (CNS) and neuroinflammation. In fact, it has been reported that thiamine deficiency in experimental autoimmune encephalomyelitis promotes the involvement of CCL2 (1), which regulates the migration and activation of monocytes, T cells, NK cells, and basophils and is involved in experimental autoimmune encephalomyelitis (EAE). In addition, the deficiency of vitamin B1 provokes the reduction of activities of the thiamine-dependent mitochondrial enzymes causing a selective neuronal death. Moreover, vitamin B1-deficiency induces expression of CD40 by the microglia and CD40L by astrocyte CD40–CD40L interaction that promotes neuronal death (2).

Furthermore, authors reported that vitamin B1-deficiency in the brain induces an over expression of pro-inflammatory mediators such as IL-1, IL-6, COX-2, and tumour necrosis factor (TNF) which also cause selective neuronal cell death (3).

Vitamin B2 (riboflavin)

Vitamin B2 (riboflavin) was the first growth factor to be characterized from the remaining B-complex vitamins. This vitamin is present in all plants and animals, is necessary for the metabolism of cells and is essential for the utilization of carbohydrates, protein and fat. Animals and humans are unable to synthesize riboflavin and its deficiency is manifested as fissure at the angle of mouth and there is a complete eradication after treatment with riboflavin therapy.

Vitamin B2 is a neuroactive compound with immunomodulatory effects and its deficiency contributes toward a pro-inflammatory gene expression pattern. The amount of inflammatory cytokines/chemokines are increased in inflamed tissues in both human and experimental animals. In addition, riboflavin produces a protective effect against CCL4-induced liver damage, mediated by TNF, in experimental animal model, suggesting that riboflavin may be used as a hepato-protective agent against toxic effects caused by chemical agents in the liver (4).

Results from *in vitro* studies suggest that Hcy, at pathophysiological concentrations, stimulates chemokine expression in vascular cells.

Chemokines are cytokines that stimulate leukocyte movement and regulate their migration in the tissue (5-6). Monocyte chemoattractant protein-1 (MCP-1) is a potent chemokine that stimulates migration of monocytes into the tissues. Some authors (7) indicate that folic acid supplementation can not only reduce MCP-1 released from both plasma and PBMCs of rats with hyperhomocystinemia but can also downgrade MCP-1 expression in the aorta of rats with hyperhomocystinemia. However, other authors reported that in patients with cardiac problems there is no statistically significant association between

treatment with folic acid/vitamin B_{12} and levels of MCP-1 (8).

Riboflavin treatment at high doses (200 and 400 **μ**mol/L) enhances lung cancer cell proliferation, invasion, and migration in cell lines *in vitro*, via activating FAK, p-38 MAPK, NF-**κ**B p50, upregulating fibronectin, ICAM-1, MMP-2, and MMP-9, and increasing inflammatory cytokines (9).

Niacin (nicotinic acid)

Niacin (nicotinic acid), another B-complex vitamin, has an important role in several relevant reactions in the body; for this, it is metabolized to the coenzymes nicotinamide adenine dinucleotide (NAD^+) and nicotinamide adenine dinucleotide phosphate ($NADP^+$). NAD is associated with a number of inflammatory cytokines such as TNF, IL-1β, and IL-6. Niacin has important modulatory effects on the production of inflammatory mediators, and the migration of immune cells. Therefore it has an anti-inflammatory effect even if its effects have not been fully understood. It inhibits CXC chemokine, the induction of CXCL-8/IL-8, lipid mediator leukotriene (LT)B_4-induced neutrophil migration in mice and neutrophil rolling and adherence (10).

Niacin, an amide of vitamin B3, reduces the levels of TNF-α, IL-6 and IL-1β in stimulated alveolar macrophages and inhibits NF-κB activation through the blocking of phosphorylation of NF-κB p65 and IκBα (11).

Niacinamide has antipruritic, antimicrobial, vasoactive, photo-protective, sebostatic and lightening effects, depending on its concentration.

These results support evidence of a role for niacin in the control of inflammation and immunity.

Vitamin B3(panthotenic acid, niacinamide)

Panthotenic acid, formerly called vitamin B3, is a part of Coenzyme A which mediates the release of energy from carbohydrates, fat and proteins, is an essential vitamin in the human diet and influences oxidative stress. Its deficiency is not likely to occur when people eat balanced diets consisting of a variety of foods, however its deficiency may cause the development of pellagra. It occurs in all living cells and its deficiency provokes insomnia, leg cramps or burning feet, reduced growth and food utilization, scaly dermatitis, alopecia, fatty liver degeneration, thymic necrosis and adrenal necrosis. Vitamin B_3 is the common name for precursors of the universal cofactor nicotinamide adenine dinucleotide (NAD^+). High doses of vitamin B3 may play an important role in increasing the number of neutrophils in healthy experimental animal model under steady state, and the mechanism may be dependent on intracellular nicotinamide phosphoribosyltransferase- NAD^+-silencing of sirtuin 1 (SIRT1) signaling pathways.

Vitamin B4

Vitamin B4 is believed to be a mixture of arginine, glycine, riboflavin and pyridoxine and has unconfirmed activity preventing muscular weakness in experimental animal model.

Vitamin B5

Vitamin B5 probably is a niacin and has unconfirmed growth activity in experimental animal model.

Vitamin B6 (pyridoxine)

In 1934, Szent-Gyorgy named a factor that could cure dermatitis in young rats, vitamin B6.

Vitamin B6 is a water-soluble vitamin, refers to a group of three molecules: pyridoxine (pyridoxol), pyridoxal and pyridoxamine. Pyridoxal 5′-phosphate is the metabolically active form of vitamin B6.

Piridoxine is the prominent form in plants, whereas pyridoxal and pyridoxamine are the forms found in animal products.

This vitamin functions in protein metabolism and the requirement is related to the amount of protein eaten and is essential for normal growth, development, and cellular metabolism. In addition, it is involved in the metabolism of fats and carbohydrates and is well tolerated at high doses. Some studies have shown that vitamin B6 deficiency may occur in pregnant women, elderly adults, alcohol abusers, and people with disorders such as kidney disease and Down syndrome. Vitamin B6 deficiency provokes pellagra, described by Goldberger and Lillie in 1926, and is an important nutrient that may protect against several diseases such as atherosclerosis, diabetes and may influence cancer cell development since it has been shown that this vitamin decreases in patients affected by tumor.

Experimental human and animal model indicate

that vitamin B6 deficiency influences both innate and adaptive immunity, and decreased number, function, and proliferation of immune cells, including T lymphocytes, have been reported by several authors. In addition, inhibition of cytokine/chemokine release has been found in vitamin B6-depleted subjects.

Low levels of pyridoxal 5′phosphate (PLP) which is the most commonly used serum marker of vitamin B6 status, have been linked to conditions associated with inflammation, such as rheumatoid arthritis, metabolic syndrome and cardiovascular diseases. These effects suggest that vitamin B6 is an important factor which may exert its effects on activation of IFN-gamma which mediates cellular immune activation (12).

Vitamin B7

Vitamin B7, also called vitamin I, is a mixture which is believed to serve as a factor for promoting digestion.

Vitamin B12 (cobalamin/cyanocobalamin)

Cyanocobalamin is the trivial designation of the vitamin B12-active corrinoid with a cyano-ligand at the beta position of Co atom, that prevents pernicious anemia and promotes body growth.

The deficiency of this vitamin in the body slows down the production of red blood cells, causing anemia. Vitamin B12 is a vitamin B family member, which has been found to have an important antagonist effect on developmental toxicity, teratogenesis and anemia. It also helps the body use folate which is a family of B vitamin compounds. Pernicious anemia which is usually an inherited disease is treated with vitamin B12 to improve the symptoms.

Folate deficiency may occur with decreased intestinal folate absorption and provoke megaloblastic anemia, failure to thrive and infections. Persons with this deficiency can develop severe neurodevelopmental defects due to the decreased folate transport into the central nervous system. The patients may show a combined immunodeficiency with an impaired T-cell proliferation response, pan-hypogammaglobulinemia, and an imbalanced pro-inflammatory cytokine profile. After folate therapy, these effects can be reversed and total immunological recovery achieved (13).

When chronic cobalamin deficiency occurs, there could be a neuropathy, with detriment in myelin by increasing TNF and decreasing epidermal growth factor (EGF) levels, affecting morphologically and functionally the central and peripheral nervous system in experimental animal model. In addition, vitamin B_{12} deficiency increases the levels of some cytokines and growth factors [e.g., TNF-α and nerve growth factor (NGF)] and decreases the levels of others [e.g., epidermal growth factor (EGF) and IL-6] in the rat CNS (14). Excess TNF-α (15) and NGF (16) damages myelin, and decreased levels of EGF reduce its myelinotrophic effect.

Cobalamin-deficiency induces imbalance in the cytokine and growth factor network in CNS. It has been reported that nuclear factor-κB activity is down-regulated by cobalamin with decreases of TNF and NGF and an increase of epidermal growth factor (EGF) and IL-6, and promotes neurite outgrowth and neuronal survival by increasing Erk1/2 and Akt (17).

Moreover, vitamin B12 supplementation may significantly improve sustained viral response rates in hepatitis C virus-infected patients and might be beneficial in the treatment of virus-related chronic diseases (18).

Vitamin B-T (carnitine)

Vitamin B-T (carnitine) plays a role in fat and energy metabolism in the body and is useful for people with heart diseases (19).

It has been found that L-C14-carnitine promoted IL-8 secretion from human epithelial cells lacking Toll-like receptors 2 and 4, and thus, acylcarnitines have the potential to activate inflammation, but the specific molecular and tissue target(s) involved still remain unknown (19).

Biotin

Biotin is another compound of vitamin B complex, and functions metabolically as a coenzyme for carboxylase to which it is bound by C-2 of its thiophene ring via an amid bond. Biotin functions as a mobile carboxyl carrier in four carboxylase enzymes and has important functions in the metabolism of lipids, glucose and energy. Deficiencies of biotin usually manifest as dermatologic lesions such as seborrheic dermatitis, alopecia and achromotrichia. In addition, it is also involved in decrease of growth and appetite, skeletal (perosis) and hepatic steatosis.

Some authors found that biotin administration to biotin-deficient rats increases the synthesis rates of protein rRNA and mRNA *in vitro*, and the abundance of mRNA encoding holocarboxylase synthetase decreases significantly in liver, kidney, and muscle (20).

To date, many laboratory and clinical data indicated that biotin has an essential role in immune function. Biotin administration in experimental animals revealed a decrease of IL-2 and IL-1 beta, two important pro-inflammatory cytokines, and the expression of genes encoding both IL-2 and IL-2 receptor γ depends on biotin. However, these results contrast with those of other authors. Supplementation of biotin also provokes decreased expression of the gene encoding IL-4. In contrast the expression of the genes encoding IL-1β and interferon-γ increased. These effects candidate biotin as an immune regulatory vitamin (21).

Taken together, our observations suggest that vitamins A and B may regulate cytokine/chemokine generation, and mediate the interaction with immune cells involved in pathophysiological pathways and inflammation. Our studies also provide an innovative basis for novel therapeutic strategies in immunocompromised individuals, and in several cases vitamin supplementation could be beneficial in the treatment of inflammatory diseases. However, the mechanism by which these vitamin protective effects occur is still unclear.

REFERENCES

1. Ji Z, Fan Z, Zhang Y, et al. Thiamine deficiency promotes T cell infiltration in experimental autoimmune encephalomyelitis: the involvement of CCL2. J Immunol 2014; 193(5):2157-67.
2. Ke ZJ, Luo J. Response to comment on "Thiamine deficiency promotes T cell infiltration in experimental autoimmune encephalomyelitis: the involvement of CCL2". J Immunol 2014; 193(10):4755-56.
3. Neri M, Cantatore S, Pomara C, et al. Immunohistochemical expression of proinflammatory cytokines IL-1β, IL-6, TNF-α and involvement of COX-2, quantitatively confirmed by Western blot analysis, in Wernicke's encephalopathy. Pathol Res Pract 2011; 207(10):652-58.
4. Al-Harbi NO, Imam F, Nadeem A, et al. Carbon tetrachloride-induced hepatotoxicity in rat is reversed by treatment with riboflavin. Int Immunopharmacol 2014; 21(2):383-88.
5. Xu JM, Weng MZ, Song FB, et al. Blockade of the CXCR6 signaling inhibits growth and invasion of hepatocellular carcinoma cells through inhibition of the VEGF expression. Int J Immunopathol Pharmacol 2014; 27(4):553-61.
6. Kritas SK, Saggini A, Varvara G, et al. Luteolin inhibits mast cell-mediated allergic inflammation. J Biol Regul Homeost Agents 2013; 27(4):955-59.
7. Li M, Chen J, Li YS, et al. Folic acid reduces chemokine MCP-1 release and expression in rats with hyperhomocystinemia. Cardiovasc Pathol 2007; 16(5):305-9.
8. Løland KH, Bleie Ø, Strand E, et al. Effect of folic acid supplementation on levels of circulating Monocyte Chemoattractant Protein-1 and the presence of intravascular ultrasound derived virtual histology thin-cap fibroatheromas in patients with stable angina pectoris. PLoS One 2013; 8(7):e70101.
9. Yang HT, Chao PC, Yin MC. Riboflavin at high doses enhances lung cancer cell proliferation, invasion, and migration. J Food Sci 2013; 78(2):H343-9.
10. Ferreira RG, Matsui TC, Gomides LF, et al. Niacin inhibits carrageenan-induced neutrophil migration in mice. Naunyn Schmiedebergs Arch Pharmacol 2013; 386(6):533-40.
11. Shehadah A, Chen J, Zacharek A, et al. Niaspan treatment induces neuroprotection after stroke. Neurobiol Dis 2010; 40(1):277-83.
12. Christensen MH, Pedersen EK, Nordbø Y, et al. Vitamin B6 status and interferon-γ-mediated immune activation in primary hyperparathyroidism. J Intern Med 2012; 272(6):583-91.
13. Kishimoto K, Kobayashi R, Sano H, et al. Impact of folate therapy on combined immunodeficiency secondary to hereditary folate malabsorption. Clin Immunol 2014; 153(1):17-22.
14. Scalabrino G, Veber D. Cobalamin and normal prions: a new horizon for cobalamin neurotrophism. Biochimie 2013; 95(5):1041-46.
15. Karadag S, Gursu M, Sakin A. The relationship between soluble tumor necrosis factor-like weak inducer of apoptosis levels and cardiac functions in peritoneal dialysis patients. Eur J Inflamm 2014;

12:429-37.
16. Kritas SK, Caraffa A, Antinolfi P. Nerve growth factor interactions with mast cells. Int J Immunopathol Pharmacol 2014; 27(1):15-9.
17. Rocco A, Compare D, Coccoli P, et al. Vitamin B12 supplementation improves rates of sustained viral response in patients chronically infected with hepatitis C virus. Gut 2013; 62(5):766-73.
18. Pescosolido N, Pascarella A, Nebbioso M, Scarsella G. Degenerative events in retina and optic nerve induced by inhibition of carnitine transport. J Biol Regul Homeost Agents 2014; 28(2):263-70.
19. Rutkowsky JM, Knotts TA, Ono-Moore KD, et al. Acylcarnitines activate proinflammatory signaling pathways. Am J Physiol Endocrinol Metab 2014; 306(12):E1378-87.
20. Rodriguez-Melendez R, Zempleni J. Regulation of gene expression by biotin (review). J Nutr Biochem 2003; 14(12):680-90.
21. Malek HA, Shata A. Effect of a high dose of vitamin D on a rabbit model of atherosclerosis. Int J Immunopathol Pharmacol 2014; 27(2):195-201.

THE INFLUENCE OF CARBON MONOXIDE ON THE SECRETION OF MELATONIN BY PINEALOCYTES MEASURED *IN VITRO*

M. ROMEROWICZ-MISIELAK[1], O. KUSAK[1], A. KOZIOROWSKA[2], F. PRZEKOP[3] and M. KOZIOROWSKI[1]

[1]Institute of Applied Biotechnology and Basic Sciences, Center of Applied Biotechnology and Basic Sciences, University of Rzeszow, Poland; [2]Faculty of Mathematics and Natural Sciences, Department of Computer Engineering University of Rzeszow, Poland; [3]The Kielanowski Institute of Animal Physiology and Nutrition, Polish Academy of Sciences, Jabłonna, Poland

Received August 6, 2014 – Accepted February 26, 2015

Photoperiod is considered the most important factor entraining the circannual physiological rhythms through changing circadian patterns of melatonin (MEL) secretion from the pineal gland. The pineal gland of mammals does not respond directly to light but is controlled by light via neuronal phototransduction originating in the retina. In accordance with humoral phototransduction hypothesis, the aim of this study was to determine whether an increased concentration of CO, as a carrier of a light signal in pineal cell culture, affects the synthesis of melatonin. This study demonstrates that a commonly used carbon monoxide donor (CORM-2) markedly stimulated melatonin release from pineal cells incubated *in vitro* in a time-dependent manner, but the mechanism whereby CO modulates MEL release needs to be further explored.

The mammalian pineal gland is a component of the photoneuroendocrine system and is involved in the regulation of circadian rhythms through the nocturnal synthesis of melatonin. The major cellular components of the pineal gland are the pinealocytes but there are also interstitial cells present. The pinealocytes are the neuroendocrine cells responsible for synthesis of melatonin, the darkness hormone secreted into the bloodstream. Melatonin (N-acetyl-5-methoxytryptamine) is produced by pineal gland and released in the circulation in a circadian manner. Its highest concentration occurs during the night due to nocturnal gene transcription and increase of the enzyme arylalkylamine -N-acetyltransferase (AA-NAT) activity, stimulated by induction of beta-adrenoceptors via noradrenaline activation (1-2). Light suppression of MEL production, whether during natural daytime or during interventional nocturnal exposure, is considered to be mediated by changing levels of AA-NAT (3-4). Melatonin exerts its influence on many physiological functions, such as the sleep-wake cycle (5), and the entrainment of circadian (6) and reproductive (7) rhythms. Photoperiod is considered the most important factor entraining the circannual physiological rhythms through changing circadian patterns of melatonin secretion from pineal gland (8). Few studies have conclusively demonstrated the existence of seasonal changes in melatonin rhythmicity in the domestic pig (9-10).

Key words: melatonin, carbon monoxide, pinealocytes in vitro culture

Mailing address:
Prof. Marek Koziorowski,
ul. Rejtana 16C,
Rzeszów 35-959, Poland
Tel.: +48 17 872 32 57
Fax: +48 17 872 32 61
e-mail: mkozioro@ur.edu.pl

0393-974X (2015)

DISCLOSURE: ALL AUTHORS REPORT NO CONFLICTS OF INTEREST RELEVANT TO THIS ARTICLE.

The pineal gland of mammals, in contrast to lower vertebrates, does not respond directly to light but is controlled by light via neuronal phototransduction originating in the retina. This signal passes through the optic nerve and is processed by the hypothalamic circadian pacemakers: the suprachiasmiatic nuclei (SCN) (11). In 1996, D.A. Oren, presented his hypothesis of "humoral phototransduction" of the light signal which proposed that information of light intensity can be transmitted from the retina to the central nervous system, not only by the generally accepted neuronal pathway, but by carbon monoxide and nitric oxide via a humoral pathway (12). Carbon monoxide is formed during heme degradation by the microsomal enzyme heme oxygenase (HO). The expression of the HO system and ability to produce CO have been demonstrated in various animal organs, including eye (13-14). In addition, the induction of HO-1 by intense visible light was demonstrated in the retina in rats (15). CO as a neurotransmitter in the brain operates in a similar way as proposed for nitric oxide (16). CO and NO are known as gaseous transmitters produced exclusively for local regulation, however, there is evidence that they do not participate only in local regulation (17). Prior results indicate that the gaseous messenger CO is released from the eye into ophthalmic venous blood depending on the intensity of sunlight (18). These results are consistent with the "humoral phototransduction" model which predicts that the released CO is directly transferred into the area of cavernous sinus from the eye venous outflow into the arterial blood supplying the brain (12).

This study was designed to determine whether an increased concentration of CO in pineal cell culture affects the synthesis of MEL and therefore, whether CO released from the eye under ambient light can be a carrier of a light signal, a form of humoral phototransduction.

MATERIALS AND METHODS

Isolated pinealocyte culture

Pinealocytes were obtained by trypsin digestion. The glands were removed and immediately placed in ice-cold Dulbecco's Modified Eagle Medium (DMEM). The tissue was incubated at 37°C for 15 min in trypsin (0.25%) solution. After removal of trypsin and its blockage, the cells were mechanically dispersed and resuspended in DMEM supplemented with 7.5% fetal calf serum, 7.5% horse serum, 100U/mL penicillin and 100µg/mL streptomycin to a final concentration of 0.5 x 105 cells/mL. The total number of cells and survival was estimated by Trypan blue exclusion. The survival rate was 90% or higher. Cells were cultivated in 25cm2 culture flasks at 37°C in 5% CO2/95% air for 24 h. After 24 h, the cells in suspension were predominantly pinealocytes, which were separated after the removal of all the culture medium content. The cells were centrifuged and resuspended in DMEM at a concentration of 0.5 x 105 cells/mL, transferred to a 6-well plate (2 mL per well), and kept at 37°C in 5% CO2/95% air for 18 h prior to the CORM-2 treatment. For melatonin determination in the culture medium, the cells were stimulated with CORM-2 (25 and 50 µM) for 24 and 48 h.

Determination of melatonin content

Melatonin content in culture medium was determined by high performance liquid chromatography (HPLC) with electrochemical detection using Chromeleon Chromatography Data System 6.8 software. Melatonin was separated on a Resolve C18 column (5 µm, 250 x 4.6 mm). The chromatographic system was isocratically operated with the following mobile phase: 50 mM sodium acetate, 0.1 M acetic acid and 0.1 mM EDTA, pH 5, at a flow rate of 1mL/min. The elution for melatonin was approximately 10 min. Culture medium was filtered through a syringe filter (0.4 µm). After centrifugation (2 min, 13,000g) 20 µl of the supernatant was injected into the chromatographic system (Dionex UltiMate 3000, equipped with an electrochemical coulometric detector, ESA CoulArray). All the salts and reagents used were obtained from Sigma-Aldrich.

RNA extraction and RT-PCR

Total RNA was extracted from isolated pinealocytes using Total RNA kit (A&A Biotechnology, Gdansk, Poland) according to the manufacturer's instructions. RNA integrity was checked by 2% agarose gel electrophoresis. The quality was expressed as the absorbance ratios at 260:280 nm and the amount of RNA in the sample was measured using a Nano Drop (Thermo, Fisher Scientific Inc., Waltham, MA, USA). cDNA synthesis was performed using High Capacity cDNA Reverse Transcription kit (Applied Biosystems) from 1 µg of total RNA.

Real-time PCR

Messenger RNA (mRNA) levels of Hiomt and Aanat were determined by real-time quantitative PCR using the SybrGreen method (Power SybrGreen Mix, Applied Biosystems). Oligonucleotide primer pairs were constructed based on the GenBank using Primer3 software.

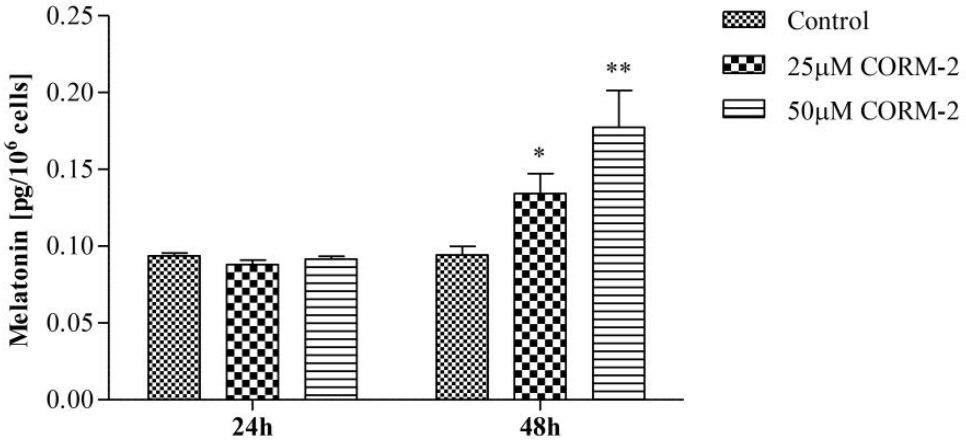

Fig. 1. *Concentration of melatonin in pig pineal cell culture medium after 24 and 48 hours of incubation with CORM-2 in 25 μM and 50 μM concentrations. Data are shown as mean ± SEM, *P≤0.05, **P≤0.01.*

The sequences of the primers are as follows: HIOMT forward primers, 5'-CATGGTGTCCCAGGTTCTCT-3'; HIOMT reverse primer, 5 ' - C A G C T T C A G G G A C A C A C A G A - 3 ' ; AANAT forward primer, 5 ' - T G G A T G T G A C C A G C C A T A G A - 3 ' ; AANAT reverse primer, 5'-TGGAACAGCTTGCTTCATTG-3'. The result for the genes were analyzed on the StepOne Plus System (Applied Biosystems) and normalized against the housekeeping gene - glyceraldehyde-3-phosphate dehydrogenase (19) (GAPDH forward primer, 5'-CGTCCCTGAGACACGATGGT-3'; GAPDH reverse primer 5'- CCCGATGCGGCCAAAT-3').

RESULTS

In pineal cell cultures, carbon monoxide stimulated melatonin release in a time-dependent manner. As shown in Fig. 1, in pinealocyte cultures, 25 μM and 50 μM CORM-2 (P≤0.5), a commonly used CO donor, significantly increased the release of melatonin. 25 μM CORM-2 was responsible for increase of melatonin production after 48 h of incubation from 0.094±0.01 to 0.134±0.02 pg/106 cells (P≤0.05), and 50 μM CORM-2 significantly increased melatonin content from 0.094±0.01 to 0.177±0.06 pg/106 cells (P≤0.01) without any loss in cell viability (data not shown). Twenty-four-hour incubation with CORM-2 had no effect on melatonin synthesis in pineal cells (Fig. 1).

Expression of the enzymes AANAT and HIOMT responsible for the generation of melatonin was detected in pineal cell cultures. Twenty-four-hour incubation with 25 μM CORM-2 was responsible for an almost two-fold increase in melatonin content (P≤0.001), whereas 50 μM CORM-2 increased the release of the MEL almost three-fold (P≤0.001). Twenty-four-hour incubation with CO donor had no effect on Aanat gene expression in relation to control cells (Fig. 2).

Also a difference in Hiomt mRNA was observed; Hiomt mRNA level increased after 24-h incubation with 25 μM CORM-2 (P≤0.001) but significantly decreased (P≤0.001) after incubation with 50 μM used CO donor (Fig. 3). Forty-eight-hour incubation with CORM-2 affected increases of Hiomt mRNA level, in case of 25 μM CORM-2 almost six-fold (P≤0.01) and 50 μM CORM-2 almost two and a half-fold (P≤0.05) in relation to the control culture (Fig. 3).

DISCUSSION

The present study demonstrates that CORM-2, a commonly used carbon monoxide donor, markedly stimulated melatonin release from pineal cells incubated *in vitro* in a time-dependent manner. Melatonin release from pineal cells was independent

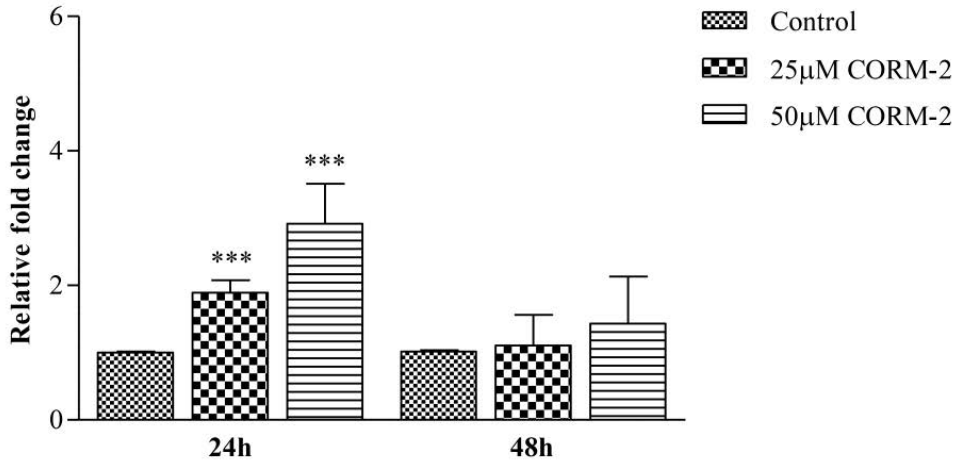

Fig. 2. *Changes in Aanat gene expression in pineal cells in vitro after 24 hours and 48 hours of incubation in the presence of CORM-2 in 25 μM and 50 μM concentrations. Data are shown as the mean ± SEM, ***P≤0.001.*

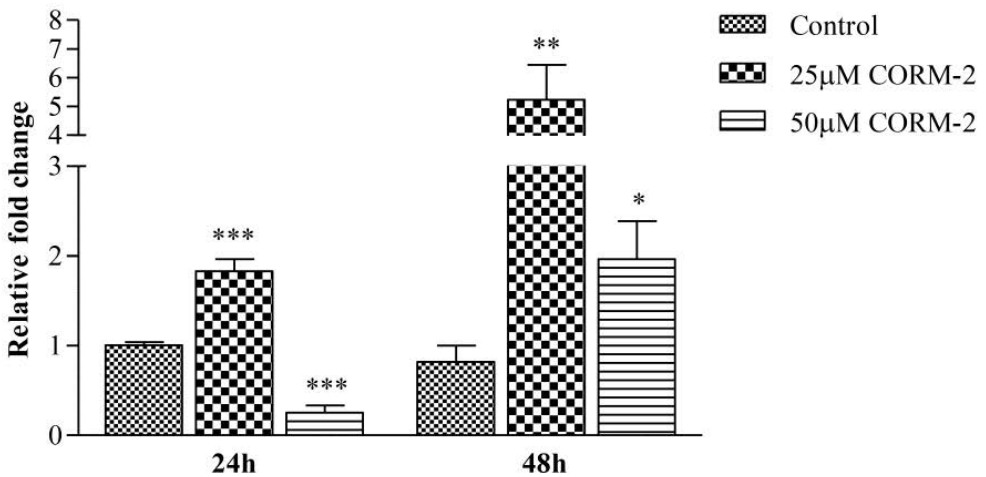

Fig. 3. *Changes in Hiomt gene expression in pineal cells in vitro after 24 hours and 48 hours of incubation in the presence of CORM-2 in 25 μM and 50 μM concentrations. Data are shown as the mean ± SEM, *P≤0.05, **P≤0.01, ***P≤0.001.*

of transcription of arylalkylamine N-acetyltransferase AANAT. Studies in the pineal gland indicate that there is a highly conserved relationship between melatonin synthesis and AANAT activity when hydroxyindole O-methyltransferase (HIOMT) is present (20). The mechanism whereby CO modulates MEL release is unclear. Our recent *in vivo* research on the wild boar and domestic pig crossbreed demonstrated that changes in CO concentration in the ophthalmic venous blood (OphVB) could have an impact on the protein levels of the melatonin synthesis pathway enzyme arylalkylamine N-acetyltransferase (AANAT), with parallel changes in systemic melatonin levels (Romerowicz-Misielak et al., unpublished observation). A study by Gilun et al. performed on an identical animal model has shown that CO can affect the clock gene expression. Elevated concentration of CO in OphVB influenced the expression level of the clock gene in the preoptic area and dorsal hypothalamus. The experimental animals after CO treatment had their master clock machinery deregulated which could

cause chronodisruption (21). In mammals the master circadian clock is located within the suprachiasmatic nuclei (SCN) of the hypothalamus, which receive environmental light-dark information and orchestrate circadian rhythms at the organismal level (22). Recent mammalian clock gene studies have revealed molecular clocks in many other brain regions and peripheral tissues, such as the pineal gland and liver, that are probably synchronized by master clock in the SCN (23-24). Nuclear receptors REV-ERBs that control the rhythmic transcription of BMAL1 are responsive to heme, redox and gases, such as carbon monoxide, suggesting new mechanisms for the systemic coordination of molecular clocks and metabolism (21, 25-26). Oscillation in REV-ERBs ligands (heme, carbon monoxide) may affect not only the phase and amplitude of circadian rhythms, but also physiological outputs of the circadian system (27). The pineal clock genes have been suggested to gate melatonin synthesis through the cAMP signaling cascade in the pineal gland and retina of rodents (28). cAMP signaling can influence both transcription and post-transcriptional regulation of the rate-limiting enzyme for melatonin synthesis (AANAT) and thus melatonin production (3). The gated regulation of melatonin synthesis has also been observed in humans (29). Whereas there is abundant evidence that the cAMP system controls rhythmic gene expression in the pineal gland, it is also possible that other regulatory mechanisms exist, involving release of other transmitters, and additional second messengers (e.g. cGMP). Like nitric oxide, CO may exert its effect via its ability to bind to the heme moiety in hemoproteins such as guanylate cyclase or cyclooxygenase, including a conformation change leading to activation of the enzymes (16) in support of this possibility, CO has been shown to potently regulate cGMP levels in olfactory neurons (30). Several mechanisms can be proposed in which an increase in cGMP regulate AANAT activity: direct regulation of cAMP activity by activation of cAMP-specific cGMP-activated phosphodiesterase (31); adenylate cyclase and presumably cAMP-dependent protein kinase and protein phosphatase could be directly affected by cGMP (32); proteasomal-mediated regulation of AANAT under the control of cGMP (33). However, the role played by cGMP in the pineal gland is still enigmatic.

The cytoprotective and, in particular, anti-apoptotic role of CO is widely described in the airways and cardiovascular system (34). In the central nervous system (CNS), low concentrations of CO suppress neuroinflammation in a model of multiple sclerosis (35). In primary cultures of neurons and astrocytes, CO prevents apoptosis (36). In an adult model of cerebral ischemia, brain lesions were less marked in CO-pre-treated animals (37). However, the association between CO-induced metabolic changes and its cytoprotective role remains unclear. A remarkable body of evidence indicates that melatonin exerts significant neuroprotective effects in numerous brain cell culture and in-vivo systems (38). This is not restricted to scavenging but includes down-regulation of gene expression of pro-oxidant and up-regulation of gene expression of antioxidant enzymes. Chronic melatonin administration in drinking water decreased mRNAs for NOS-1, NOS-2, HO-1 and HO-2 as well as changing their 24-h profile in rats (39).

This work demonstrates that non-physiological changes in CO concentration in pineal cell culture can have an acute impact on MEL synthesis. In order to determine the physiological relevance of this finding, it would be useful to study the effect of normal variation of CO levels. If confirmed, it would support the concept that the effect of light in MEL secretion is mediated, at least in part, via CO.

ACKNOWLEDGEMENTS

The study was carried out with the use of equipment granted by the project “Centre of Applied Biotechnology and Basic Sciences” supported by the Operational Programme “Development of Eastern Poland 2007-2013”. No. POPW.01.03.00-18-018/09.

REFERENCES

1. Reiter RJ. Pineal melatonin: cell biology of its synthesis and its physiological interactions. Endocr Rev 1991; 12:151-80.
2. Ganguly S, Gastel JA, Weller JL, et al. Role of a pineal cAMP-operated arylalkylamine N-acetiltransferase/14-3-3-binding switch in melatonin synthesis. Proc Natl Acad Sci USA 2001;

98:8083-88.
3. Gastel JA, Roseboom PH, Rinaldi PA, Weller JL, Klein DC. Melatonin production: proteasomal proteolysis in serotonin N-acetyltransferase regulation. Science 1998; 279:1358-60.
4. Borjigin J, Zhang LS, Calinescu AA. Circadian regulation of pineal gland rhythmicity. Mol Cell Endocrinol 2012; 349:13-19.
5. Haimov I, Lavie P, Laudon M, Herer P, Vigder C, Zisapel N. Melatonin replacement therapy of elderly insomniacs. Sleep 1995; 18:598-603.
6. Lewy AJ, Ahmed S, Latham-Jackson JM, Sack RL. Melatonin shifts human circadian rhythms according to a phase-response curve. Chronobiol Int 1992; 9:380-92.
7. Goldman BD. The physiology of melatonin in mammals. Pineal Res Rev 1983; 1:145-82.
8. Reiter RJ. Melatonin: the chemical expression of darkness. Mol Endocrinol 1991; 79:C153-58.
9. Mack AC, Unshelm J. Circadian rhythm of the light-dependant hormone melatonin as an indicator for the photic requirement of domestic pig. In: Saloniemi, H. (Ed.), Proceedings of the 9th International Congress in Animal Hygiene. Helsinki, Finland, 1997; p. 216-220.
10. Tast A, Hälli O, Andersson H, Love RJ, Peltoniemi OAT. Seasonal alterations in circadian melatonin rhythms of the European wild boar and domestic gilt. J Pineal Res 2001; 30:43-49.
11. Doyle S, Menaker M. Circadian photoreception in vertebrates. Cold Spring Harb Symp Quant Biol 2007; 72:499-508.
12. Oren DA. Humoral phototransduction: blood is a messenger. Neuroscientist 1996; 2:207-10.
13. Cao L, Blute TA, Eldred WD. Localization of heme oxygenase-2 and modulation of cGMP levels by carbon monoxide and/or nitric oxide in the retina. Vis Neurosci 2000; 17:319-29.
14. Maines MD. The heme oxygenase system and its function in the brain. Cell Mol Biol (Noisy-le-grand) 2000; 49:573-85.
15. Kutty RK, Kutty G, Wiggert B, Chader GJ, Darrow RM, Organisciak DT. Induction of heme oxygenase 1 in the retina by intense visible light: suppression by the antioxidant dimetylthiourea. Proc Natl Acad Sci USA 1995; 92:1177-81.
16. Dawson TM, Snyder SH. Gases as biological messages: Nitric oxide and carbon monoxide in the brain. J Neurosci 1994; 14:5147-59.
17. Wu L, Wang R. Carbon monoxide: endogenous production, physiological functions and pharmacological application. Pharmacol Rev 2005; 57:585-630.
18. Koziorowski M, Stefanczyk-Krzymowska S, Tabecka-Lonczynska A, Gilun P, Kaminski M. The gaseous messenger carbon monoxide is released from the eye into the ophthalmic venous blood depending on the intensity of sunlight. J Biol Regul Homeost Agents 2012; 26:111-18.
19. Barber RD, Harmer DW, Coleman RA, Clark BJ. GAPDH as a housekeeping gene: analysis of GAPDH mRNA expression in a panel of 72 human tissues. Physiol Genomics 2005; 11:21(3):389-95.
20. Klein DC, Baler R, Roseboom PH, et al. The molecular basis of the pineal melatonin rhythm: regulation of serotonin Nacetylation. In: Lydic, R., Baghdoyan, H.A. (Eds.), Handbook of Behavioral State Control: Cellular and Molecular Mechanisms. CRC Press, Boca Raton, FL, 1999; p. 45-59.
21. Gilun P, Stefanczyk-Krzymowska S, Romerowicz-Misielak M, Tabecka-Lonczynska A, Przekop F, Koziorowski M. Carbon monoxide-mediated humoral pathway for the transmission of light signal to the hypothalamus. J Physiol Pharmacol 2013; 64(6):761-72.
22. Reppert SM, Weaver DR. Coordination of circadian timing in mammals. Nature 2002; 418:935-41.
23. Abe M, Herzog ED, Yamazaki S, Straume M, Tei H, Sakaki Y, Menaker M, Block GD. Circadian rhythms in isolated brain regions. J Neurosci 2002; 22:350356.
24. Yoo SH, Yamazaki S, Lowrey PL, et al. PERIOD2: LUCIFERASE real-time reporting of circadian dynamics reveals persistent circadian oscillations in mouse peripheral tissues. Proc Natl Acad Sci USA 2004; 101:5339-46.
25. Raghuram S, Stayrook KR, Huang P, et al. Identification of heme as the ligand for the orphan nucleas receptors REV-ERBalpha and REV-ERBbeta. Nat Struct Mol Biol 2007; 14(12):1207-13.
26. Pardee KI, Xu X, Reinking J, et al. The structural basis of gas-responsive transcription by the human

nuclear hormone receptor REV-ERBbeta. PLoS Biol 2009; 7(2):e1000043.
27. Mazzoccoli G, Cai Y, Liu S, et al. REV-ERBα and the clock gene machinery in mouse peripheral tissues: a possible role as a synchronizing hinge. J Biol Regul Homeost Agents. 2012; 26(2):265-76.
28. Fukuhara C, Liu C, Ivanova TN, Chan GC, Storm DR, Iuvone PM, Tosini G. Gating of the cAMP signaling cascade and melatonin synthesis by the circadian clock in mammalian retina. J Neurosci 2004; 24:1803-11.
29. Berlin I, Touitou Y, Guillemant S, Danjou P, Puech AJ. Beta-adrenoceptor agonists do not stimulate daytime melatonin secretion in healthy subjects. A double blind placebo controlled study. Life Sci 1995; 56:325-31.
30. Verma A, Hirsch DJ, Glatt CE, Ronnett GV, Snyder SH. Carbon monoxide: a putative neural messenger. Science 1993; 259:381-84.
31. Soderling SH, Beavo JA. Regulation of cAMP and cGMP signaling: New phosphodiesterases and new functions. Curr Opin Cell Bio 2000; 12(2):174-79.
32. Iuvone PM. Circadian rhythms of melatonin biosynthesis in retinal photoreceptor cells. In: Kato S, Osborne NN Tamai M. Retinal Degeneration and Regeneration. Kugler Publications bv Amsterdam/ New York 1996.
33. Mason GGF, Hendil KB, Rivett AJ. Phosphorylation of proteasomes in mammalian cells. Identification of two phosphorylated subunits and the effect of phosphorylation on activity. Eur J Biochem 1996; 238:453-62.
34. Ryter SW, Alam J, Choi AM. Heme oxygenase-1/ carbon monoxide: from basic science to therapeutic applications. Physiol Rev 2006; 86(2):583-650.
35. Chora AA, Fontoura P, Cunha A, et al. Heme oxygenase-1 and carbon monoxide suppress autoimmune neuroinflammation. J Clin Invest 2007; 117(2):438-47.
36. Queiroga CS, Almeida AS, Martel C, Brenner C, Alves PM, Vieira HL. Glutathionylation of adenine nucleotide translocase induced by carbon monoxide prevents mitochondrial membrane permeabilisation and apoptosis. J Biol Chem 2010; 285(22):17077-88.
37. Wang B, Cao W, Biswal S, Dore S. Carbon monoxide-activated nrf2 pathway leads to protection against permanent focal cerebral ischemia. Stroke 2011; 42(9):2605-10.
38. Tan DX, Manchester LC, Terron MP, Flores LJ, Reiter RJ. One molecule, many derivatives: a never-ending interaction of melatonin with reactive oxygen and nitrogen species? J Pineal Res 2007; 42:28-42.
39. Jiménez-Ortega V, Cano P, Cardinali DP, Esquifino AI. 24-Hour variation in gene expression of redox pathway enzymes in rat hypothalamus: effect of melatonin treatment. Redox Rep 2009; 14(3):132-8.

INHIBITORY EFFECT OF TETRAMETHYLPYRAZINE ON HEPATOCELLULAR CARCINOMA: POSSIBLE ROLE OF APOPTOSIS AND CELL CYCLE ARREST

J. CAO[1], Q. MIAO[2], J. ZHANG[3], S. MIAO[4], L. BI[4], S. ZHANG[5], Q. YANG[4], X. ZHOU[4], M. ZHANG[4], Y. XIE[4] and S. WANG[4]

[1]Department of Dermatology, Xijing Hospital, Fourth Military Medical University, Xi'an, China; [2]Department of Pharmacy, 401 Military Hospital, Qingdao, China; [3]Department of Hand Surgery, 401 Military Hospital, Qingdao, China; [4]Institute of Materia Medica, Fourth Military Medical University, Xi'an, China; [5]Department of Pharmacy, Tangdu Hospital, Fourth Military Medical University, Xi'an, China

Received November 15, 2014 – Accepted March 2, 2015

The first three authors contributed equally to the paper

Hepatocellular carcinoma (HCC) is the fifth most common cancer. An important approach to control HCC is chemoprevention. This study aims at investigating the antitumor effect of Tetramethylpyrazine (TMP). Rats were injected with N-Nitrosodiethylamine (DEN) to establish HCC. Tumor development was observed. Liver function was evaluated. Apoptosis and cell cycle arrest-related makers and signaling cascades were determined by Western blot, RT-PCR and flow cytometric analysis. The administration of TMP could significantly inhibit tumor development in DEN-induced HCC rats, shown by reduced incidence of tumor, decreased number of tumor nodules and reduced maximal size of tumor. DEN-induced increase of aspartate aminotransferase, alanine aminotransferase, lactate dehydrogenase and alkaline phosphatase activities were significantly inhibited by TMP. TMP exhibited inhibitory effect on HCC through induction of apoptosis and cell cycle arrest in rats. TMP induced apoptosis through increasing Bax, decreasing Bcl-2, increasing the release of cytochrome c, and activating caspase, which consisted of the mitochondrial apoptotic pathway. TMP induced G2/M cell cycle arrest through down-regulation of cyclin B1/cdc2. In addition, inhibition of Akt and ERK signaling and the antioxidant activities of TMP may also contribute to its antitumor effect. These data provide new insight into the mechanisms underlying the antitumor effect of TMP.

Hepatocellular carcinoma (HCC), a tumor with poor prognosis and few treatment options (1), is a major malignancy worldwide and increasingly associated with cancer-related death (2). To date, the incidence of HCC is the third cause of cancer death worldwide (3). The treatment of cancer is still a great challenge in medicine. Chemoprevention is one of the most important approaches to control HCC, in which process one or more non-toxic naturally occurring or synthetic agents are administrated, resulting in prevention, improvement, or reverse of the disease. In this regard, naturally occurring agents

Key words: tetramethylpyrazine, hepatocellular carcinoma, apoptosis, cell cycle arrest

Mailing address: Dr. Siwang Wang,
Institute of Materia Medica,
Fourth Military Medical University 169
Changlexi Road, Xi'an, 710032 China
Tel.: +86-29-8477-4748
Fax: +86-29-8322-4790
e-mails: wangsiw@fmmu.edu.cn

0393-974X (2015)

are receiving more and more attention because of their promising efficacy in various cancer models (4, 5).

Tetramethylpyrazine (TMP) is a purified chemical that has been identified as a component of Ligusticum wallichii Franchat (ChuanXiong), a Chinese herb that is widely used in the treatment of neurovascular and cardiovascular diseases. In recent years, several studies have shown that TMP possesses antitumor effect in several cell lines (6, 7). However, the effects of TMP on tumor growth have not been investigated in HCC, and the underlying mechanisms responsible for antitumor effect of TMP are still far from completely known.

DEN (N-Nitrosodiethylamine) is considered to be a strong hepatocarcinogenic dialkylnitrosoamine, which is a constituent of tobacco smoke, cheddar cheese, curd and fried meals and a number of alcoholic beverages (8). An orthotopic model of HCC is more appropriate for the study of an antitumor agent. To date, DEN treatment of mice is one of the most frequently used models of HCC (9). It is well-known that DEN could damage the nuclear enzymes involved in DNA repair/replication, resulting in DNA damage and mutations as well as hepatocyte death, and thus reproducible HCC animal model (10, 11). Several weeks of DEN administration causes rapid development of tumors (12) and results in 100% HCC in male mice and 10-30% HCC in female mice (13), which may be attributed to the protective role of oestrogens. The molecular characteristic of DEN-induced tumors is similar to the situation of human HCC, with poor prognosis (14). DEN induces irreversible HCC through overexpression of G1/S-phase regulatory proteins (15). In DEN-induced HCC model, Akt and extracellular signal-regulated kinase (ERK) activation was observed (16), and activation of Akt and ERK pathways were involved in the occurrence of HCC induced by DEN (17, 18). Using DEN-induced HCC animal model, the purpose of this study was to (a) determine the effect of TMP on tumor growth in DEN-injected rats; (b) study the effect of TMP on apoptosis and cell cycle progression in tumors; (c) elucidate the possible molecular mechanisms of TMP-induced apoptosis and cell cycle arrest.

MATERIALS AND METHODS

Chemicals and reagents

Cytochrome c (sc-13156), cdc2 (sc-54), cyclinB1 (sc-245), Bax (sc-493), Bcl-2 (sc-492), and β-actin (sc-47778) antibodies were purchased from Santa Cruz Biotechnology. Cleaved caspase 3 (#9661) and 9, Akt (#9272) and P-Akt (#4060) antibodies were purchased from cell signaling. Cleaved caspase 9 antibody (IMG-5705) was purchased from IMGENEX Corporation. ERK (BS1112), P-ERK (BS5016) and Tubulin α (BS1699) antibodies were purchased from Bioworld Technology. DEN, TMP and most of the chemicals and reagents used in this study were procured from Sigma.

Animals

Wistar rats (the Experimental Animal Center of Fourth Military Medical University) were used in this study. Animals were fed in a humidity- and temperature-controlled room and were given free access to food and water. All animal experiments were performed according to the procedures approved by the Fourth Military Medical University Animal Care and Use Committee.

Experimental design

Forty Wistar rats were divided into four groups, and the experimental period was 16 weeks. Control group rats (untreated) were fed with standard diet and water ad libitum. TMP group rats were administered intraperitonially with TMP alone (100 mg/kg b.w.daily). DEN group rats were injected intraperitonially with DEN (100 mg/kg b.w.) once a week for 6 weeks. DEN + TMP group, TMP (100 mg/kg b.w.daily) was administered intraperitonially to DEN-injected rats from 6th week up to16th week.

At the end of the experiments, the rats were euthanized by cervical dislocation. The tumors were counted based on published criteria (19). The blood was collected, processed and stored for further analysis. Tumors tissues were fixed in 75% ethanol and filtered by 500 mesh to get the single cell suspension for flow cytometry analysis. Part of liver was also frozen in liquid nitrogen for Testern blot and RT-PCR analysis. Part of liver was rinsed in ice cold saline and was homogenized in 0.1 M Tris buffer (pH.7.4) for further biochemical analysis.

Flow cytometric analysis

Apoptosis in DEN-induced tumor was assessed by cell cycle analysis using flow cytometry, as previous described (5). At the end of the animal experiment, tumor tissues were fixed in 75% ethanol and filtered by 500 mesh to get the single cell suspension for flow cytometry analysis of apoptosis. Cells were harvested, re-suspended in a hypotonic fluorescent solution (50 mg/ml PI and 0.1% Triton X-100 in 0.1% Na Citrate buffer) for 1 h, at 4°C in the dark. The cell cycle was analyzed by flow cytometry (FL-2) to determine the sub-G0/G1 DNA content and

cell cycle distribution. Sub-diploid populations were considered to be apoptotic. Cellquest software was used to carry out data acquisition and analysis. The results were expressed as percentage of the fragmented DNA.

Biochemical analysis of serum

After the experiment, blood was collected and serum was separated for estimation of LDH, ALT, AST, and ALP by commercial kits (Nanjing Jiancheng Company, China). Assays were conducted according to the manufacturer's instructions.

Determination of caspase activity

The activities of caspase 9 and 3 were assessed using commercial assay kits (Beyotime Institute of Biotechnology) according to the manufacturer's instructions.

qRT-PCR

Total RNA was isolated using TRIzol reagents (Invitrogen) and reversely transcribed using a commercial kit (TIANGEN, China). cDNA was quantified by real-time PCR using SYBR Green (TIANGEN, China)and an BIORAD instrument. Each gene was normalized to GAPDH. Primers used for real-time qPCR were listed: Bcl-2, 5'-GTA CCT GAA CCG GCA TCT G-3' (Forward) and 5'-GGG GCC ATA TAG TTC CAC AA-3' (Reverse); Bax, 5'-CGA GCT GAT CAG AAC CAT CA-3'(Forward) and 5'-GGG GTC CCG AAG TAG GAA-3' (Reverse); GAPDH, 5'-CCA GGT GGT TCC TCT GAC TTC-3'(Forward) and 5'-GTG GTC GTT GAG GGC AAT G-3' (Reverse).

Western blot

In brief, protein extractions were separated by using SDS-PAGE on polyacrylamide gels, and transferred to nitrocellulose membranes (20). After blocking for 1 h with 8% skimmed milk in TBS buffer, the membrane was incubated with indicated primary antibodies overnight at 4°C. After the membrane was washed four times for 15 min each with TBST buffer, it was incubated in the appropriate HRP-conjugated secondary antibody at 37°C for 30 min. The protein bands were visualized using chemiluminescent reagents according to the manufacturer's instructions and quantified using an image analyzer Quantity One System (Bio-Rad, USA). The protein quantifications were adjusted for the corresponding β-actin or Tubulin α level (21).

Determination of redox balance

The activities of antioxidant enzymes, including SOD, CAT, GPx and GR, were determined as previously reported (22). Activities of antioxidant enzymes were expressed as U/mg protein.

Statistical analysis

All experiments were performed at least three times, and results were expressed as the means ± SD. The results were analyzed by one-way ANOVA followed by a SNK-q test for multiple comparisons. All analyses were performed using the Statistical Package for the Social Sciences (SPSS) software. Data were considered statistically significant for $p<0.05$. More specific indices of statistical significance were indicated in individual figure legends.

RESULTS

TMP inhibits tumor growth in DEN-treated rats

In the present study, to evaluate the effect of TMP on tumor growth, we established HCC model using DEN injection. Rats were injected intraperitonially with DEN (100 mg/kg b.w.) once a week for 6 weeks, then the animals were administered intraperitonially with TMP (100 mg/kg b.w.daily) or not from 6th week up to16th week. As shown in Table I, the effect of TMP on tumor development was examined. DEN injection resulted in 90% incidence of HCC in rats, and TMP administration reduced this incidence to 70% (Table I). Moreover, the number of liver tumors in DEN-treated rats was 12.1±3.6, and TMP treatment significantly reduced this value to 7.8±2.3. Furthermore, in livers of DEN-treated rats, the maximal size of tumor was 8.8±2.5 mm. When rats were administrated with TMP, the maximal size of tumor was reduced to 5.5±1.4 mm. These results demonstrate that TMP significantly inhibited tumor development in DEN-induced HCC rats.

TMP protects liver function in DEN-treated rats

Liver function was evaluated by the determination of serum lactate dehydrogenase (LDH), aspartate transaminase (AST), alanine transaminase (ALT) alkaline phosphatase (ALP). Table II shows that, in DEN-treated rats, serum LDH, AST, ALT, and ALP were significantly increased to 246±8.2 U/L, 160±9.7 U/L, 192±10.6 U/L, and 265±10.1 U/L. TMP administration notably reduced serum LDH, AST, ALT, and ALP to 204±4.3 U/L, 105±8.4 U/L, 128±9.3 U/L, 221±5.9 U/L, which were significantly different from that of DEN-treated rats (Table II). In rats treated with TMP alone, serum LDH, AST, ALT, and ALP were not significantly altered (Table III). The results indicate that TMP protected liver

Table I. *Effect of TMP on tumor multiplicity, size, and incidence in DEN-untreated and treated rats.*

Group	No.	Max. size (mm)	Incidence (%)
Control	0	0	0
TMP	0	0	0
DEN	12.1 ± 3.6*	8.8 ± 2.5*	90
DEN + TMP	7.8 ± 2.3#	5.5 ± 1.4#	70

*Forty Wistar rats were divided into four groups, and the experimental period was 16 weeks. Control group: rats (untreated) were fed with standard diet and water ab libitum. TMP group: rats were administered intraperitonially with TMP alone (100 mg/kg b.w.daily). DEN group: rats were injected intraperitonially with DEN (100 mg/kg b.w.) once a week for 6 weeks. DEN + TMP group: TMP (100 mg/kg b.w. daily) was administered intraperitonially to DEN-injected rats from 6th week up to16th week. No. indicates number of tumors. Max. size indicates maximum size of tumor. Results were expressed as means ± SD. *p<0.05, compared with control; # p<0.05, compared with DEN.*

Table II. *Effect of TMP on liver enzyme profiles in DEN-untreated and treated rats.*

Group	LDH (U/L)	ALT (U/L)	AST (U/L)	ALP (U/L)
Control	186 ± 7.9	38 ± 5.1	78 ± 7.9	134 ± 5.3
TMP	185 ± 9.5	37 ± 3.2	80 ± 7.5	137 ± 7.8
DEN	246 ± 8.2*	160 ± 9.7*	192 ± 10.6*	265 ± 10.1*
DEN + TMP	204 ± 4.3#	105 ± 8.4#	128 ± 9.3#	221 ± 5.9#

*Forty Wistar rats were divided into four groups, and the experimental period was 16 weeks. Control group: rats (untreated) were fed with standard diet and water ab libitum. TMP group: rats were administered intraperitonially with TMP alone (100 mg/kg b.w.daily). DEN group: rats were injected intraperitonially with DEN (100 mg/kg b.w.) once a week for 6 weeks. DEN + TMP group: TMP (100 mg/kg b.w.daily) was administered intraperitonially to DEN-injected rats from 6th week up to16th week. Results were expressed as means ± SD. *p<0.05, compared with control; # p<0.05, compared with DEN.*

function against DEN toxicity in rats.

TMP induces mitochondrial-dependent apoptosis in DEN-treated rats

Programmed cell death (apoptosis) is considered to be a pivotal mechanism by which antitumor drugs kill tumor cells. In the next step, we detected the effect of TMP on apoptosis in tumors in DEN-treated rats. As shown in Fig. 1A, apoptosis in DEN-induced tumor was assessed by cell cycle analysis of sub-G0/G1 DNA content. Compared with control rats, the percentage of sub-G0/G1 cells was decreased slightly in DEN-induced tumor (Fig. 1A). The administration of TMP significantly increased the percentage of sub-G0/G1 cells (Fig. 1A), compared with that of DEN-treated rats.

It has been established that mitochondria play a crucial role in the complex process of apoptosis through release of a series of important pro-apoptotic molecules into the cytoplasm (23). In the next step, we examined the effect of TMP on mitochondrial apoptotic pathway. The mRNA expression of Bcl-2 family, including Bax and Bcl-2, were examined by real-time qPCR. In DEN-induced tumors, Bax and Bcl-2 mRNA expression were decreased and increased respectively, compared with that of control (Fig. 1B and C). In tumors, Bax mRNA expression was up-regulated by TMP (Fig. 1B) and increase of Bcl-2 mRNA expression was inhibited by TMP (Fig. 1C). Changes of protein expression of Bax and Bcl-2 were consistent with their mRNA expression (Fig. 1D). In Fig. 1E, the results show that in DEN-

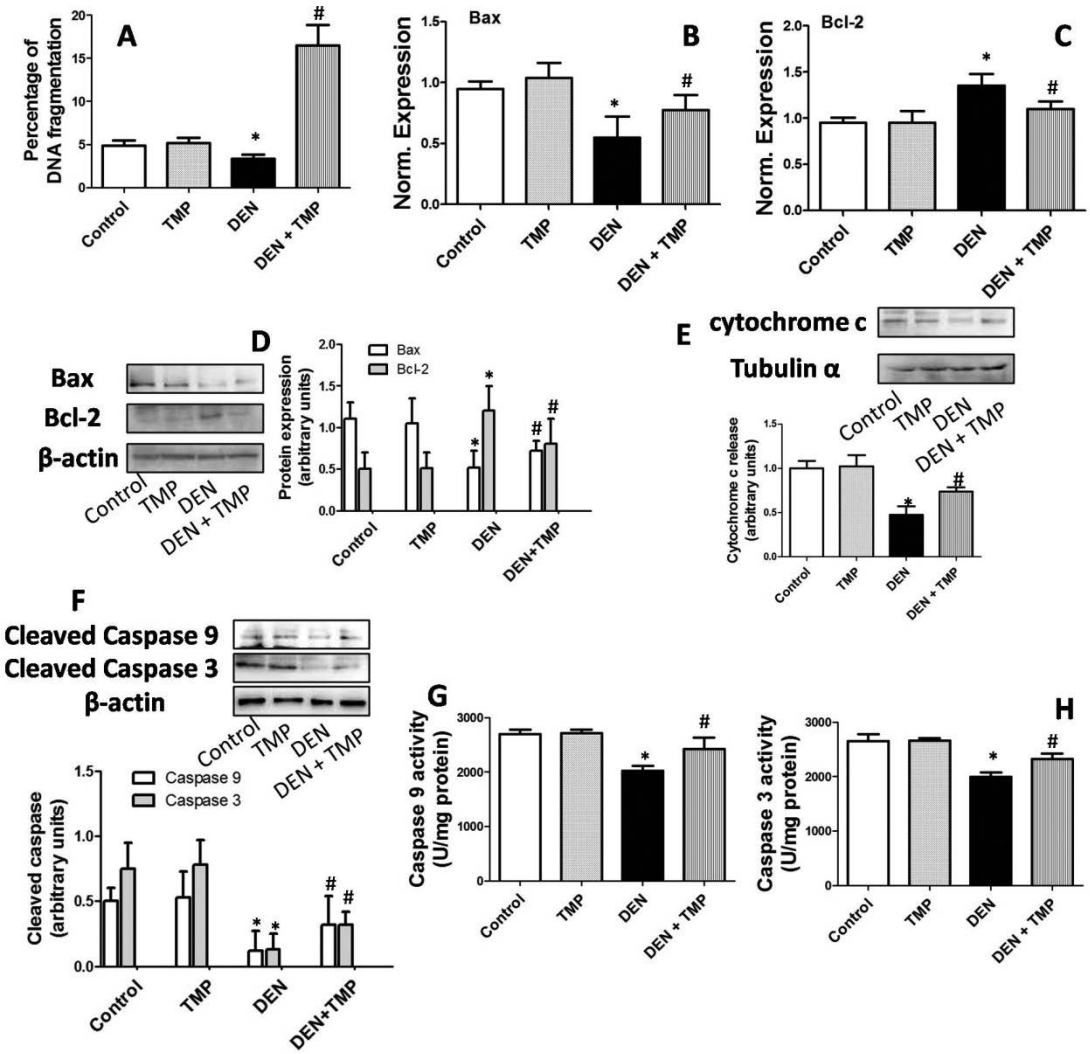

Fig. 1. *The effect of TMP on apoptosis in DEN-induced tumor in rats.* ***A)*** *Tumors were collected and apoptosis was evaluated by flow cytometry analysis. Percentage of sub-G0/G1 DNA content was shown.* ***B***, ***C)*** *mRNA expression of Bax and Bcl-2 were detected by qRT-PCR (5 replicates).* ***D)*** *Protein expression of Bax and Bcl-2. Representative blots were shown. Densitometric analysis was conducted (5 replicates).* ***E)*** *Effect of TMP on Cyto c release in tumors was measured by Western blot analysis of cytosolic protein. Representative blots were shown. Densitometric analysis was conducted (5 replicates).* ***F)*** *Effect of TMP on cleaved expression of caspase 9 and caspase 3 were determined by Western blot. Representative blots were shown. Densitometric analysis was carried out (5 replicates).* ***G***, ***H)*** *Effect of TMP on caspase 9 and caspase 3 activities in tumors were determined by commercial kits (8 replicates). Results were expressed as means ± SD. *p<0.05, compared with control; # p<0.05, compared with DEN.*

induced tumors, cytosolic expression of cytochrome (Cyto) c was decreased, compared with that of control. The administration of TMP significantly promoted cytosolic release of Cyto c compared with that of DEN-treated rats (Fig. 1E). In Fig. 1 F, G and H, the results show that cleaved expression of caspase 9 and 3 and their activities were decreased in DEN-induced tumors compared with that of control. In tumors, TMP administration significantly increased caspase 9 and 3 activities and their cleavage compared with those of DEN-treated rats (Fig. 1E and F). These results demonstrated that TMP induced mitochondrial

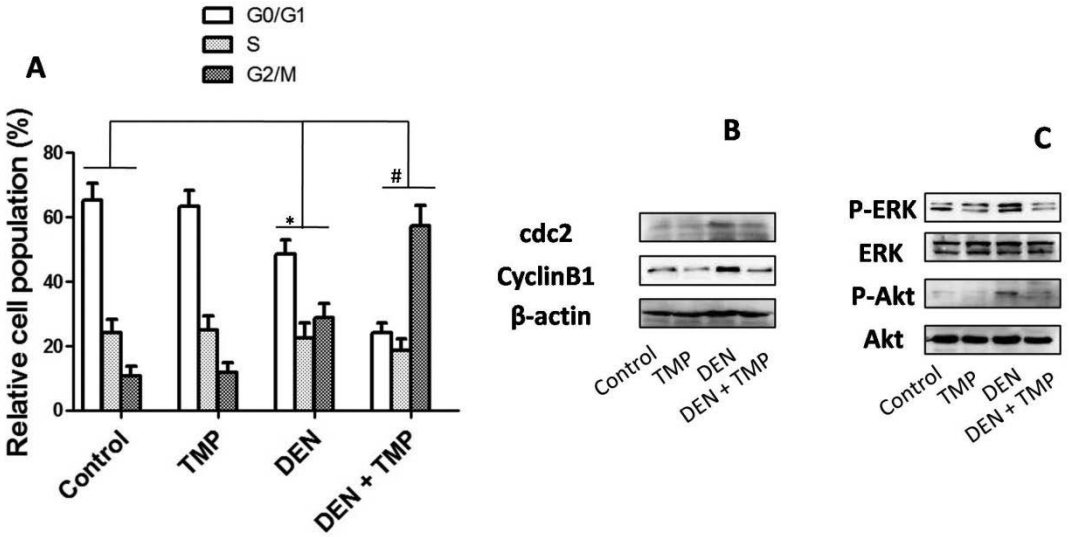

Fig. 2. *The effect of TMP on cell cycle progression and signaling transduction in DEN-induced tumor in rats. **A**) Effect of TMP on cell cycle distribution in tumors were determined by flow cytometric analysis. Results were expressed as percentage of cell population. **B**) Effect of TMP on protein expression of cdc2 and cyclin B1 was measured by Western blot. **C**) Effect of TMP on phosphorylation of ERK and Akt was measured by Western blot. Representative blots were shown.*p<0.05, compared with control; # p<0.05, compared with DEN.*

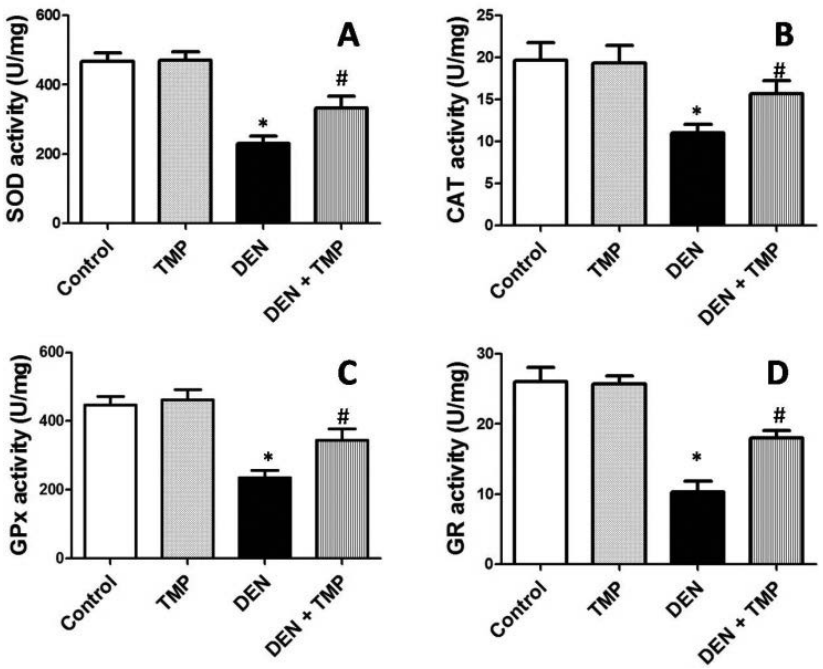

Fig. 3. *The effect of TMP on antioxidant enzyme activities in DEN-induced tumor in rats. At the end of the experiments, activities of SOD, CAT, GPx and GR in livers were determined (8 replicates). Results were expressed as means ± SD. *p<0.05, compared with control; # p<0.05, compared with DEN.*

apoptosis in DEN-induced HCC, with no effect on normal livers.

TMP induces G2/M cell cycle arrest in tumors of DEN-treated rats

It is proved that cell cycle arrest plays a key role in the inhibition of proliferation. Next, we investigated the effects of TMP on cell cycle distribution. The proportions of cells in different phases of cell cycle in tumors treated by TMP were analyzed by the incorporation of PI. In Fig. 2A, we show that TMP induced a significant increase in the number of cells within the G2/M phase, compared with that of DEN-induced tumors (Fig. 2A). Protein expression of cdc2 and cyclin B1, two important G2/M phase transition checkpoints, was notably decreased by TMP in DEN-treated rats (Fig. 2B). Moreover, we detected the phosphorylation of Akt and extracellular signal-regulated kinase (ERK). In livers of DEN-treated rats, phosphorylation of Akt and ERK were significantly activated, compared with that of control (Fig. 2C). TMP administration could inhibit DEN-induced phosphorylation of Akt and ERK (Fig. 2C). The results demonstrated that TMP could induce G2/M cell cycle arrest, which may contribute to the antitumor effect in HCC.

TMP enhances antioxidant activities in DEN-induced HCC

It is reported that during the metabolic process of DEN, reactive oxygen species (ROS) was generated, leading to oxidative stress (24). Oxidative stress has been reported to cause carcinogenesis by several mechanisms including the damage of DNA, lipid and protein, and disorder of intracellular signaling pathways. In the present study, we also detected the effect of TMP on DEN-induced oxidative stress. As shown in Fig. 3, in DEN-induced tumors, the activities of superoxide dismutase (SOD) (A), catalase (CAT) (B), glutathione peroxidase (GPx) (C) and glutathione reductase (GR) (D) were decreased. The administration of TMP significantly inhibited the decrease of SOD, CAT, GPx and GR activities (Fig. 3). The results indicate that DEN induced oxidative stress in livers of rats, and TMP could attenuate the oxidative stress induced by DEN, which may play a role in its antitumor effect.

DISCUSSION

In recent years, several studies have reported that TMP exhibit inhibitory effect on tumor growth *in vivo* and induce apoptosis in several tumor cells. TMP was clinically used to treat lung carcinoma and exhibited potent anti-metastasis activity in the body (25, 26). However, the effect of TMP on HCC is not known. In the present study, we investigated the inhibitory effect of TMP on DEN-induced tumor in rats and elucidated the possible mechanisms.

Mice model of HCC was established by the injection of DEN. The administration of TMP could significantly inhibit tumor development in DEN-induced HCC rats, reflected by reduced incidence of tumor, decreased number of tumor nodules and reduced maximal size of tumor (Table I). DEN-induced liver damage reflects instability of liver cell metabolism which results in distinctive changes of several serum enzyme activities. Generally, liver function could be reflected by AST, ALT, LDH and ALP and increased levels of these indicators may indicate liver damage. Hepatocellular damage is associated with the up-regulation of ALT activity, which is always accompanied by an elevation of AST. In addition, increase of ALP levels reflects the pathological damage in biliary flow. In the current study, DEN-induced increase of these enzyme activities were significantly blocked by TMP (Table II), indicating that TMP played a role in protecting liver cell and decreasing enzyme leakage.

It has been characterized that programmed cell death (apoptosis) is a fundamental process, which may occur under a wide variety of physiological and pathological conditions. The onset of cancer, including liver cancer, is believed to be attributed to the loss of control of normal apoptosis and the disturbance of equilibrium between cellular apoptosis and proliferation (27, 28). Moreover, survival of hepatocytes containing genotoxic lesions attributed to apoptosis inhibition is considered to be crucial for tumor promotion (29, 30). There is literature reporting that suppression of apoptosis by tumor promoting agents (such as Pb) is an important mechanism in tumor promotion (31). For the treatment of cancer, it has been proposed to develop drugs aiming to induce apoptosis in tumor-target

tissues or tumors. For the measurement of apoptosis, DNA fragmentation has been widely accepted as an indicator. In the present study, we found that TMP could significantly induce DNA fragmentation in DEN-induced tumors (Fig. 1A).

Bcl-2 family is a major protein in apoptotic pathway signal transduction cascades. To elucidate the molecular mechanism of TMP-induced apoptosis, we evaluated the mRNA expression of Bax and Bcl-2. Imbalance of the pro- and anti-apoptotic members of the Bcl-2 family is usually a common result in HCC (32). To a degree, Bcl-2 has been considered to be a promising target for anticancer therapy (33). Ectopic expression of Bax has been found to activate caspase signaling and subsequent substrate proteolysis, leading to apoptosis (34). Thus, overexpression of Bax contributes to cell death; conversely, Bcl-2 functions as a suppressor of apoptosis (35). In the present study, TMP induced apoptosis involving increase of Bax, decrease of Bcl-2, release of mitochondrial Cyto c into the cytosol and subsequent activation of caspase-9 and caspase-3 (Fig. 1).

Disruption of cell cycle progression is an important strategy to suppress the growth of cancer cells (36). Evading cell cycle arrest is the most frequent phenomenon observed in tumor development. A series of checkpoints act as surveillance molecules in cell cycle progression. Checkpoints at G1/S and G2/M transitions are essential regulatory gates during cell cycle progression (37, 38). G2/M progression of cell cycle is driven by the maturation promoting factor (MPF), a complex of cyclin B1/cdc2. In this study, we found that TMP induced G2/M cell cycle arrest in DEN-induced tumors, through inhibition of cyclin B1/cdc2 complex (Fig. 2). Moreover, TMP also inhibited Akt and ERK phosphorylation, which may contribute to the pro-apoptotic and cell cycle-arrested effect of TMP.

Redox balance in a cell is closely related with apoptosis and cell cycle progression. SOD acts as the first line of defense against superoxide free radicals, through catalyzing superoxide radicals to H_2O_2 and O_2. Then, CAT and GPx convert H_2O_2 to H_2O, protecting against ROS damage. GR is another important antioxidant enzyme, catalyzing the reduction of glutathione disulfide (GSSG) to the sulfhydryl form (GSH). In the present study, we found that TMP could attenuate the oxidative stress induced by DEN, which may play a role in its antitumor effect (Fig. 3).

In conclusion, this study found that TMP exhibits inhibitory effect on HCC through inducing apoptosis and cell cycle arrest in DEN-induced tumors. TMP induces mitochondrial-dependent apoptosis through Bax/Bcl-2-Cyto c-caspase pathway. TMP induces cell cycle arrest through down-regulation of cyclin B1/cdc2. In addition, the antioxidant activities of TMP may also contribute to its antitumor effect. Taken together, these data provide novel insight into the molecular mechanisms underlying the antitumor effect of TMP, and TMP is a promising pharmacological agent for treating cancer.

ACKNOWLEDGEMENTS

This work was supported by grants from the Science and Technology Projects of Shaanxi Province (2014K11-01-01-01, 2012K14-05-06 and 2011KTZB03-01); and grants from Shaanxi Province, the People's Republic of China (S2010ZDGC105). The work was supported by the Cultivation Project of Collaborative Innovation Center for Chinese Medicine in QinBa Mountains

REFERENCES

1. Aleksic K, Lackner C, Geigl JB, et al. Evolution of genomic instability in diethylnitrosamine-induced hepatocarcinogenesis in mice. Hepatology 2011; 53:895-904.
2. Llovet JM, Burroughs A, Bruix J. Hepatocellular carcinoma. Lancet 2003; 362:1907-17.
3. Parkin DM. Global cancer statistics in the year 2000. Lancet Oncol 2001; 2:533-43.
4. Ramakrishnan G, Raghavendran HR, Vinodhkumar R, Devaki T. Suppression of N-nitrosodiethylamine induced hepatocarcinogenesis by silymarin in rats. Chem Biol Interact 2006; 161:104-14.
5. Wang X, Bai H, Zhang X, et al. Inhibitory effect of oleanolic acid on hepatocellular carcinoma via ERK-p53-mediated cell cycle arrest and mitochondrial-dependent apoptosis. Carcinogenesis 2013; 34:1323-30.
6. Wang Y, Fu Q, Zhao W. Tetramethylpyrazine inhibits osteosarcoma cell proliferation via downregulation

of NF-kappaB *in vitro* and *in vivo*. Mol Med Rep 2013; 8:984-88.
7. Yi B, Liu D, He M, Li Q, Liu T, Shao J. Role of the ROS/AMPK signaling pathway in tetramethylpyrazine-induced apoptosis in gastric cancer cells. Oncology Letters 2013; 6:583-89.
8. Bartsch H, Montesano R. Relevance of nitrosoamines to human cancer. Carcinogenesis 1984; 5:1381-95.
9. Fausto N, Campbell JS. Mouse models of hepatocellular carcinoma. Semin Liver Dis 2010; 30:87-98.
10. Park EJ, Lee JH, Yu GY, et al. Dietary and genetic obesity promote liver inflammation and tumorigenesis by enhancing IL-6 and TNF expression. Cell 2010; 140:197-208.
11. Verna L, Whysner J, Williams GM. N-Nitrosodiethylamine mechanistic data and risk assessment: Bioactivation, DNA-adduct formation, mutagenicity, and tumor initiation. Pharmacol Ther 1996; 71:57-81.
12. Bralet M, Pichard V, Ferry N. Demonstration of direct lineage between hepatocytes and hepatocellular carcinoma in diethylnitrosamine-treated rats. Hepatology 2002; 36:623-30.
13. Naugler WE, Sakurai T, Kim S, Maeda S, Kim K, Elsharkawy AM, Karin M. Gender disparity in liver cancer due to sex differences in MyD88-dependent IL-6 production. Science 2007; 317:121-24.
14. Lee JS, Chu IS, Mikaelyan A, Calvisi DF, Heo J, Reddy JK, Thorgeirsson SS. Application of comparative functional genomics to identify best-fit mouse models to study human cancer. Nat Genet 2004; 36:1306-11.
15. Park DH, Shin JW, Park SK, Seo JN, Li L, Jang JJ, Lee MJ. Diethylnitrosamine (DEN) induces irreversible hepatocellular carcinogenesis through overexpression of G1/S-phase regulatory proteins in rat. Toxicol Lett 2009; 191:321-26.
16. Shimizu M, Sakai H, Shirakami Y, et al. Preventive effects of (-)-epigallocatechin gallate on diethylnitrosamine-induced liver tumorigenesis in obese and diabetic C57BL/KsJ-db/db Mice. Cancer Prev Res (Phila) 2011; 4:396-403.
17. Zhang XF, Tan X, Zeng G, Misse A, Singh S, Kim Y, Klaunig JE, Monga SP. Conditional beta-catenin loss in mice promotes chemical hepatocarcinogenesis: role of oxidative stress and platelet-derived growth factor receptor alpha/phosphoinositide 3-kinase signaling. Hepatology 2010; 52:954-65.
18. Wang Y, Ausman LM, Greenberg AS, Russell RM, Wang XD. Nonalcoholic steatohepatitis induced by a high-fat diet promotes diethylnitrosamine-initiated early hepatocarcinogenesis in rats. Int J Cancer 2009; 124:540-46.
19. Hacker HJ, Mtiro H, Bannasch P, Vesselinovitch SD. Histochemical profile of mouse hepatocellular adenomas and carcinomas induced by a single dose of diethylnitrosamine. Cancer Res 1991; 51:1952-58.
20. Zhang J, Cao R, Cai T, et al. The role of autophagy dysregulation in manganese-induced dopaminergic neurodegeneration. Neurotox Res 2013; 24:478-90.
21. Zhang J, Cai T, Zhao F, Yao T, Chen Y, Liu X, Luo W, Chen J. The role of alpha-synuclein and tau hyperphosphorylation-mediated autophagy and apoptosis in lead-induced learning and memory injury. Int J Biol Sci 2012; 8:935-44.
22. Wang X, Hai CX, Liang X, Yu SX, Zhang W, Li YL. The protective effects of Acanthopanax senticosus harms aqueous extracts against oxidative stress: role of Nrf2 and antioxidant enzymes. J Ethnopharmacol 2010; 127:424-32.
23. Wang X. The expanding role of mitochondria in apoptosis. Genes Dev 2001; 15:2922-33.
24. Balamurugan K, Karthikeyan J. Evaluation of luteolin in the prevention of N-nitrosodiethylamine-induced hepatocellular carcinoma using animal model system. Ind J Clin Biochem 2012; 27:157-63.
25. Chen SX, Wang LX, Xing LL. Effects of tetramethylpyrazine on platelet functions of advanced cases of lung carcinoma. Zhongguo Zhong Xi Yi Jie He Za Zhi 1997; 17:523-31.
26. Zhang P, Pei Y, Qi Y. Influence of blood-activating drugs on adhesion and invasion of cells in lung cancer patients. Zhongguo Zhong Xi Yi Jie He Za Zhi 1999; 19:103-5.
27. Kanzler S, Galle PR. Apoptosis and the liver. Semin. Cancer Biol 2000; 10:173-84.
28. Park YN, Chae KJ, Kim YB, Park C, Theise N. Apoptosis and proliferation in hepatocarcinogenesis related to cirrhosis. Cancer 2001; 92:2733-38.
29. Worner W, Schrenk D. Influence of liver tumor promoters on apoptosis in rat hepatocytes induced

by 2-acetylaminofluorene, ultraviolet light, or transforming growth factor beta 1. Cancer Res 1996; 56:1272-78.
30. Pitot HC. Hepatocyte death in hepatocarcinogenesis. Hepatology 1998; 28:1-5.
31. Shibata MA, Ito Y, Morimoto J, Otsuki Y. Lovastatin inhibits tumor growth and lung metastasis in mouse mammary carcinoma model: a p53-independent mitochondrial-mediated apoptotic mechanism. Carcinogenesis 2004; 25:1887-98.
32. Fabregat I, Roncero C, Fernandez M. Survival and apoptosis: a dysregulated balance in liver cancer. Liver Int 2007; 27:155-62.
33. Baell JB, Huang DC. Prospects for targeting the Bcl-2 family of proteins to develop novel cytotoxic drugs. Biochem Pharmacol 2002; 64:851-63.
34. Finucane DM, Bossy-Wetzel E, Waterhouse NJ, Cotter TG, Green DR. Bax-induced caspase activation and apoptosis via cytochrome c release from mitochondria is inhibitable by Bcl-xL. J Biol Chem 1999; 274:2225-33.
35. Brunelle JK, Letai A. Control of mitochondrial apoptosis by the Bcl-2 family. J Cell Sci 2009; 122:437-41.
36. Chen C, Kong AN. Dietary cancer-chemopreventive compounds: from signaling and gene expression to pharmacological effects. Trends Pharmacol Sci 2005; 26:318-26.
37. Kastan MB, Bartek J. Cell-cycle checkpoints and cancer. Nature 2004; 432:316-23.
38. Hartwell LH, Kastan MB. Cell cycle control and cancer. Science 1994; 266:821-28.

KNOCKDOWN OF CASEIN KINASE 1e INHIBITS CELL PROLIFERATION AND INVASION OF COLORECTAL CANCER CELLS VIA INHIBITION OF THE Wnt/β-CATENIN SIGNALING

L-C. YE[1], C. JIANG[2], J. BAI[2], J. JIANG[2], H-F. HONG[2] and L-S. QIU[2]

[1]Institute of Pediatric Translational Medicine, Shanghai Children's Medical Center, Shanghai Jiaotong University School of Medicine, Shanghai, China; [2]Department of Thoracic and Cardiovascular Surgery, Shanghai Children's Medical Center, Shanghai Jiaotong University School of Medicine, Shanghai, China

Received November 30, 2014 – Accepted February 5, 2015

H-F Hong and L-S. Qiu contributed equally to this paper

Deregulation of casein kinase 1 epsilon (CK1ε) is involved in the development of multiple pathological disorders such as cancer, however the function and molecular mechanism of CK1ε in cancer are still unclear. In the present study, we aimed to investigate the role of CK1ε in human colorectal cancer (CRC). The expression of CK1ε was examined by immunohistochemical assay using a tissue microarray procedure. A loss-of-function experiment was performed to observe the effects of lentivirus-mediated CK1ε shRNA (Lv-shCK1ε) on cell proliferation and invasive potential by MTT and Transwell assays in CRC cell line (SW480). As a result, we found that the expression of CK1ε protein was significantly increased in CRC tissues compared with that in adjacent non-cancerous tissues (ANCT) (68.9% *vs* 42.2%, *P*=0.017), and was correlated with the Duke's staging and depth of invasion in CRC patients (*P*=0.012; *P*=0.015). Knockdown of CK1ε reduced cell proliferation and invasion of CRC cells followed by the downregulation of wnt3α, β-catenin, PCNA and MMP-9. In conclusion, our findings show that high expression of CK1ε is positively associated with the Duke's staging and depth of invasion in CRC patients, and knockdown of CK1ε suppresses the growth and invasion of CRC cells through inhibition of the wnt/β-catenin signaling, suggesting that CK1ε may serve as a promising therapeutic target for the treatment of CRC.

Colorectal cancer (CRC) is the third most common cancer worldwide and the fourth most common cause of death (1). Every year approximately one million new cases of CRC are diagnosed around the world, and more than 0.6 million people die from this disease (2). The standard surgical treatment for CRC is effective, but the outcome is poor with 50% of CRC patients suffering recurrence or death within 5 years of surgery. A multitude of risk factors have been correlated with CRC including hereditary factors, environmental factors and inflammatory syndromes, of which genetic alterations play an important role in the development of CRC (3). The biomarkers for CRC therefore represent opportunities to improve

Key words: casein kinase 1ε, colorectal cancer, proliferation, invasion, β-catenin

Mailing address: Dr. Li-Sheng Qiu,
Department of Thoracic Cardiovascular Surgery,
Shanghai Children's Medical Center,
Shanghai Jiaotong University School of Medicine,
No. 1678 Dongfang Road, Shanghai 200127, China
Tel.: +86-21-38626840 Fax: +86-21-38626873
e-mail: qiulisheng66@163.com

0393-974X (2015)

patient outcome.

Casein kinase 1 (CK1) is a group of ubiquitous Serine/Threonine kinases that are implicated in normal cellular functions and several pathological conditions including digestive cancers (4). Casein kinase 1 alpha (CK1α) has been found differentially expressed between melanoma cells and normal melanocytes, indicating CK1α overexpression as a potential biomarker for distinguishing malignant melanoma from other melanocytic lesions (5). Overexpression of CK1-epsilon (CK1ε) is significantly associated with poor survival in patients with ovarian cancer, and inhibition of CK1ε suppresses the proliferation and invasion of ovarian cancer cells (6). CK1ε, highly expressed in breast tumors, causes cell overgrowth via regulation of mRNA translation and cell proliferation, providing an initial rationale to explore CK1ε blockade as a therapeutic strategy to treat cancers (7, 8).

However, few studies show that loss of CK1ε expression is associated with a poor four-year survival rate in oral cancer patients (9) and suppression of CK1α in primary melanoma cells induces invasive tumor growth (10), suggesting that CK1 may function as a tumor suppressor in some cancers. To further clarify the function and molecular mechanisms of CK1ε in CRC cells, we investigated the expression of CK1ε in CRC tissues and found that CK1ε is positively associated with the Duke's staging and depth of invasion in CRC patients, and knockdown of CK1ε suppresses the growth and invasion of CRC cells, suggesting that CK1ε may serve as a promising therapeutic target for the treatment of CRC.

MATERIALS AND METHODS

Materials

The CRC cell line (SW480) used for these experiments was from the Institute of Biochemistry and Cell Biology (Shanghai, China). Lv-shCK1ε, negative control vector and virion-packaging elements were from Genechem (Shanghai, China). The primers of CK1ε, PCNA and MMP-9 were synthesized by Applied Biosystems (ABI, USA). All antibodies were from Santa Cruz Biotechnology (USA).

Drugs and reagents

Dulbecco's Modified Eagle medium (DMEM) and fetal bovine serum (FBS) were from Thermo Fisher Scientific Inc (Waltham, MA, USA); TRIzol Reagent and Lipofectamine 2000 were from Invitrogen (Carlsbad, CA, USA); M-MLV Reverse Transcriptase was from Promega (Madison, WI, USA); SYBR Green Master Mixture was from Takara (Otsu, Japan). ECL-PLUS/Kit was from GE Healthcare (Piscataway, NJ, USA).

Clinical samples and data

Tissue microarray was prepared for IHC test. Human CRC tissues and the corresponding ANCT were obtained from biopsy prior to chemotherapy in a total of 45 consecutive cases of CRC admitted to our hospital from January 2009 to December 2012. The study was approved by the Medical Ethics Committee of Shanghai Jiaotong University, and written informed consent was obtained from the patients or their parents before sample collection. Two pathologists respectively reviewed all of the cases.

IHC staining

Anti-CK1ε antibody (Santa Cruz Biotechnology, USA) was used for IHC detection of the expression of CK1ε protein in tissue microarrays. Tissue microarray sections were processed for IHC analysis of CK1ε protein as follows. IHC examinations were carried out on 3-mm thick sections. For anti-CK1ε IHC, unmasking was performed with 10 mM sodium citrate buffer, pH 6.0, at 90°C for 30 min. For anti-CK1ε IHC, antigen unmasking was not necessary. Sections were incubated in 0.03% hydrogen peroxide for 10 min at room temperature, to remove endogenous peroxidase activity, and then in blocking serum for 30 min at room temperature. Anti-CK1ε antibody was used at a dilution of 1:200. The antibody was incubated overnight at 4°C. Sections were then washed three times for 5 min in PBS. Non-specific staining was blocked with 0.5% casein and 5% normal serum for 30 min at room temperature. Finally, staining was developed with diaminobenzidine substrate and sections were counterstained with hematoxylin. PBS replaced CK1ε antibody in negative controls.

Quantification of protein expression

The expression of CK1ε was semiquantitatively estimated as the total immunostaining scores, which were calculated as the product of a proportion score and an intensity score. The proportion and intensity of the staining was evaluated independently by two observers. The proportion score reflected the fraction of positive staining cells (score 0, <5%; score 1, 5-10%; score 2, 10-50%; score 3, 50-75%; score 4, >75%), and the intensity score represented the staining intensity (score 0, no staining; score 1, weak positive; score 2, moderate positive; score 3, strong positive). Finally, a total expression score was given ranging from 0 to 12. Based on the analysis in advance, CK1ε was regarded as negative expression in

CRC tissues if the score <2, and positive expression if the score ≥2.

Cell culture and infection

CRC cells were cultured in DMEM medium supplemented with 10% heat-inactivated FBS, 100U/ml of penicillin and 100μg/ml of streptomycin. They were all placed in a humidified atmosphere containing 5% CO2 at 37°C. On the day of transduction, CRC cells were replated at 5×10^4 cells/well in 24-well plates containing serum-free growth medium with polybrene (5 mg/ml). When 50% confluence was reached, cells were transfected with recombinant Lv-shCK1ε or control virus at the optimal MOI (multiplicity of infection) of 50, and cultured at 37°C and 5% CO2 for 4 h. Then supernatant was discarded and serum containing growth medium was added. At 4 days of post-transduction, transduction efficiency was measured by the frequency of green fluorescent protein (GFP)-positive cells. Positive stable transfectants were selected and expanded for further study. The clone in which the Lv-shCK1ε transfected was named as Lv-shCK1ε group, the negative control vectors transfected was named as NC group, and CRC cells untreated were named as control (CON) group.

Quantitative Real-time PCR

To quantitatively determine the mRNA expression level of CK1ε in CRC cells, Real-time PCR was used. Total RNA of each clone was extracted with TRIzol according to the manufacturer's protocol. Reverse-transcription was carried out using M-MLV and cDNA amplification was carried out using SYBR Green Master Mix kit according to the manufacturer's protocol. Target genes were amplified using specific oligonucleotide primer and β-actin gene was used as an endogenous control. Data were analyzed using the comparative Ct method ($2^{-\Delta\Delta Ct}$). Three separate experiments were performed for each clone.

Western blot assay

CRC cells were harvested and extracted using lysis buffer (Tris-HCl, SDS, Mercaptoethanol, Glycerol). Cell extracts were boiled for 5 min in loading buffer and then equal amount of cell extracts were separated on 15% SDS-PAGE gels. Separated protein bands were transferred into polyvinylidene fluoride (PVDF) membranes and the membranes were blocked in 5% skim milk powder. The primary antibodies against CK1ε, PCNA and MMP-9 were diluted according to the instructions of antibodies and incubated overnight at 4°C. Then, horseradish peroxidase-linked secondary antibodies were added at a dilution ratio of 1:1000, and incubated at room temperature for 2 h. The membranes were washed with PBS for three times and the immunoreactive bands were visualized using ECL-PLUS/Kit according to the manufacturer's instructions. The relative protein level in different groups was normalized to β-actin concentration. Three separate experiments were performed for each clone.

Cell proliferation assay

Cell proliferation was analyzed with the MTT assay. Briefly, cells infected with Lv-shCK1ε were incubated in 96-well-plates at a density of 1×10^5 cells per well with DEME medium supplemented with 10% FBS. Cells were treated with 20 μl MTT dye, and then incubated with 150 μl of DMSO for 5 min. The color reaction was measured at 570 nm with enzyme immunoassay analyzer (Bio-Rad, American). The proliferation activity was calculated for each clone.

Transwell invasion assay

Transwell filters were coated with matrigel (3.9mg/ml, 60-80ml) on the upper surface of a polycarbonic membrane (diameter 6.5 mm, pore size 8 mm). After incubating at 37°C for 30 min, the matrigel solidified and served as the extracellular matrix for analysis of tumor cell invasion. Harvested cells (1×10^5) in 100 ml of serum free DMEM were added into the upper compartment of the chamber. A total of 200 ml conditioned medium derived from NIH3T3 cells was used as a source of chemoattractant, and was placed in the bottom compartment of the chamber. After 24 h incubation at 37°C with 5% CO_2, the medium was removed from the upper chamber. The non-invaded cells on the upper side of the chamber were scraped off with a cotton swab. The cells that had migrated from the matrigel into the pores of the inserted filter were fixed with 100% methanol, stained with Hematoxylin, and mounted and dried at 80°C for 30 min. The number of cells invading through the matrigel was counted in three randomly selected visual fields from the central and peripheral portion of the filter using an inverted microscope (200×magnification). Each assay was repeated three times.

Statistical analysis

SPSS 20.0 was used for the statistical analysis. Kruskal-Wallis H test and *Chi*-squared test were used to analyze the expression rate in all groups. One-way analysis of variance (ANOVA) was used to analyze the differences between groups. Statistical significance was set at $P < 0.05$.

RESULTS

The expression of CK1ε protein in human CRC

The expression of CK1ε protein was evaluated

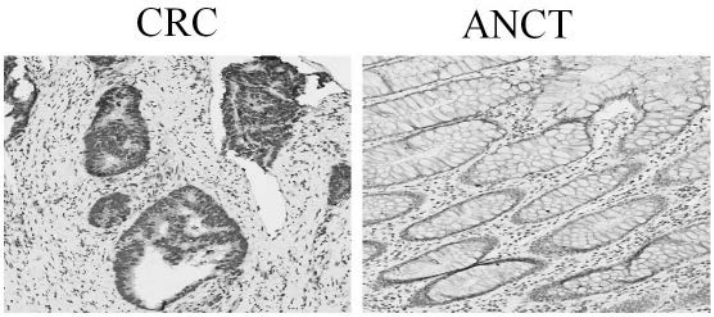

Fig. 1. *The expression of CK1ε protein in human CRC (× 200). The expression of CK1ε protein was examined by IHC staining.* ***A)*** *The high expression of CK1ε in CRC tissues.* ***B)*** *The low expression of CK1ε in ANCT tissues.*

Table I. *The expression of CK1ε protein in CRC.*

Variables	Group	Cases (N)	Expression levels (n)				Positive rate (%)	χ^2	*P*
			-	+	++	+++			
CK1	CRC	45	14	17	9	5	68.9		
	ANCT	45	26	11	5	3	42.2	5.734	0.017

by IHC staining. The positive expression of CK1ε protein was detected in the cytoplasm of CRC tissues and ANCT cells (Fig. 1). The positive rates of CK1ε expression were examined in 68.9% (31/45) of the CRC tissues, and 42.2% (19/45) in the ANCT (P=0.017, Table I).

The correlation of CK1ε expression with clinicopathologic characteristics

The correlation of CK1ε expression with various clinicopathologic characteristics was analyzed. As shown in Table II, CK1ε expression did not associate with the age, gender and CEA level of the CRC patients (each P>0.05). Up-regulation of CK1ε expression did not link to tumor size and degree of differentiation (P=0.988; P=0.904). However, positive expression of CK1ε was correlated with Duke's staging and depth of invasion (P=0.012; P=0.015).

Effect of CK1ε silencing on wnt3α and β-catenin expression

After CRC cells were transfected with Lv-shCK1ε for 24 h, the effect of CK1ε knockdown on wnt3α and β-catenin expression was detected by Real-time PCR and Western blot assays, indicating that the expression level of CK1ε mRNA was significantly silenced in Lv-shCK1ε group compared with the NC and CON groups (each $^{**}P$<0.01) (Fig. 2A), and those of CK1ε, wnt3α and β-catenin proteins were markedly decreased in Lv-shCK1E group in comparison with the NC and CON groups (Fig. 2B).

Effect of CK1ε silencing on cell proliferation

To examine the effect of CK1ε on cell growth, we investigated the proliferative activities of CRC cells by MTT assay. Silencing of CK1ε gene significantly decreased cell proliferative activities of CRC cells in a time-dependent manner (Fig. 3A). Real-time PCR and Western blotting were used to determine the effect of CK1ε on PCNA expression, showing that the amount of PCNA was significantly reduced in Lv-shCK1ε group compared with the NC and CON groups (Fig. 3B, C).

Effect of CK1ε silencing on cell invasion

To determine the effect of CK1ε knockdown on

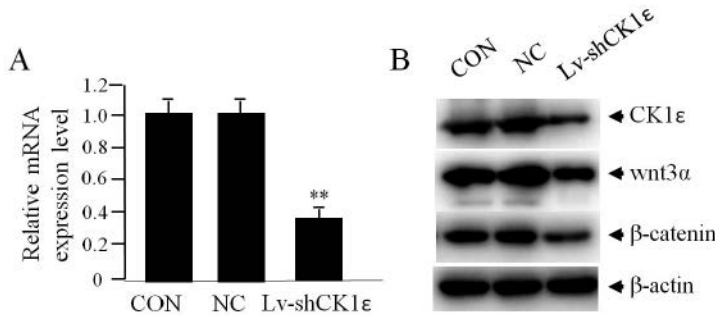

Fig. 2. *Effect of CK1ε silencing on wnt3α and β-catenin expression. The target gene for CK1ε and downstream factors were identified by Real-time PCR (**A**) and Western blot assays (**B**) in CRC cells, indicating that the expression levels of CK1ε, wnt3α and β-catenin were significantly reduced in the Lv-shCK1ε group compared with the CON and NC groups (each **P<0.01).*

Table II. *Association of CK1ε expression with clinicopathologic characteristics.*

Variables	Cases (n)	CK1 expression (n)		*P*
	45	(-)	(+)	
Age				
≤60	28	6	22	
>60	17	8	9	0.075
Gender				
Male	24	7	17	
Female	21	7	14	0.766
Tumor size (cm)				
≤.5	29	9	20	
>5	16	5	11	0.988
Duke's staging				
A+B	14	8	6	
C+D	31	6	25	0.012
Depth of invasion				
Within serosa	17	9	8	
Beyond serosa	28	5	23	0.015
Degree of differentiation				
Well	11	4	7	
Moderately	21	6	15	
Poorly	13	4	9	0.904
CEA(ng/ml)				
≥5	26	9	17	
<5	19	5	14	0.557

cell invasion, Transwell assay was carried out. The invasive potential of CRC cells was attenuated in Lv-shCK1ε group compared to the NC and CON groups (**$P < 0.01$) (Fig. 4 A, B). The endogenous expression of MMP-9 protein, indicated by Western blotting, was down-regulated in the Lv-shCK1ε group compared

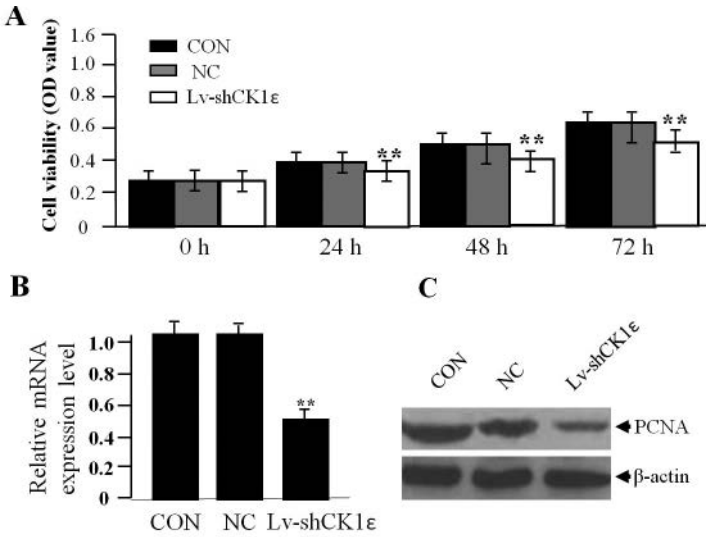

Fig. 3. *Effect of CK1ε silencing on cell proliferation.* ***A)*** *The proliferative activities of CRC cells were assessed by MTT assay, indicating that silencing of CK1ε gene diminished proliferative activities of CRC cells in a time-dependent manner.* ***B, C)*** *The amount of PCNA mRNA and protein was decreased in the Lv-shCK1ε group compared with the CON and NC groups (each **P<0.01).*

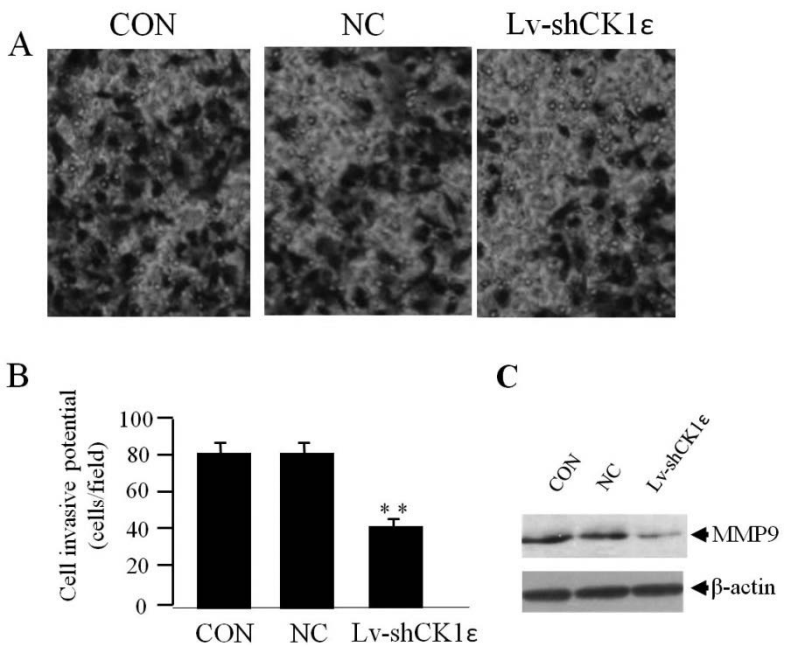

Fig. 4. *Effect of CK1ε silencing on cell invasion.* ***A, B)*** *The effect of CK1ε on cell invasion was observed by Transwell assay. The invasive potential of CRC cells was significantly suppressed in the Lv-shCK1ε group compared with the CON and NC groups (**P<0.01).* ***C)*** *The amount of MMP-9 protein was decreased in the Lv-shCK1ε group compared with the CON and NC groups.*

with the NC and CON groups (Fig. 4C).

DISCUSSION

CK1, a member of the highly conserved and pleiotropic family, plays a critical role in some cellular processes and carcinogenesis including cell proliferation, apoptosis, and cell invasion (11). CK1α is expressed in multiple myeloma (MM) cell lines and patient MM cells, and inhibition of CK1α kinase activity in MM cells with targeted therapy or small hairpin RNAs induces cell G0/G1-phase arrest and apoptosis (12). Importantly, CK delta mutation may promote adenomatous polyp formation via a Wnt/beta-catenin independent mechanism (13), and aberrant localization of CK1α through keratin filament contributes to the progression of CRC (14). However, the clinical significance of CK1ε in colon cancer is not comprehensively understood. In the present study, it was found that CK1ε was highly expressed in the cytoplasm of CRC tissues compared to the ANCT, and was closely correlated with the Duke's staging and depth of invasion in CRC patients, suggesting that CK1ε might be involved in the tumorigenesis of CRC.

CK1 isoforms (alpha, beta, gamma, delta, epsilon) are implicated in diverse cellular processes including cell cycle progression, apoptosis and cellular differentiation (15), of which CK1 delta is highly expressed in pancreatic ductal adenocarcinomas (PDACs) (16), and CK1ε is highly expressed in human sarcoma cells (17). Inhibition of CK1 isoforms (delta, CK1ε or CK1δ) decreases cancer cell growth and induces cell apoptosis (16-18). CK1a inhibition leads to the activation of p53 and results in selective elimination of leukemia cells, revealing CK1a as a potential therapeutic target for the treatment of cancer (19, 20). However, few studies show that CK1α suppresses invasive tumor growth in primary melanoma cells (10). Thus, it is necessary to further explore the function of CK1 in cancer cells. It was found that knockdown of CK1ε inhibited the proliferation and invasion of CRC cells, suggesting a tumor-promoting role of CK1ε in CRC.

Wnt/β-catenin signaling is critical for vertebrate development and tissue maintenance, and dysregulation of this signaling contributes to a host of disease phenotypes, including cancer (21). CK1ε and CK1δI have been reported to be the positive regulators of this pathway linked to cancer development (13, 22). CK1ε as a critical contributor activates the β-catenin signaling in breast cancer (21, 23). Deregulation of Wnt/β-catenin signaling by inactivating mutations of the APC tumor suppressor, or oncogenic mutations of β-catenin has been implicated in colorectal tumorigenesis (24). In the present study, it was found that knockdown of CK1ε downregulated the expression of wnt3α and β-catenin in CRC cells, indicating that CK1ε might be involved in the development of CRC through regulation of the Wnt/β-catenin signaling.

PCNA, as a nuclear protein, is required for maintaining cell proliferation and can be used as independent predictor of recurrence and poor survival in patients with CRC (25). MMPs are important molecules involved in tumor metastasis. They are expressed on the tumor cell surface, activate pro-MMP to exacerbate the malignancy, and serve as a powerful indicator of distant metastasis of colon cancer (26). Specific targeting of Wnt/β-catenin signaling decreases the expression of Wnt target genes (PCNA, MMP-9) in human melanoma cells (27). Our present findings show that knockdown of CK1ε suppressed cell growth and invasion accompanied by the decreased expression of PCNA and MMP-9, suggesting that Wnt/β-catenin signaling might mediate the regulation of CK1ε on the expression of PCNA and MMP-9 in CRC cells.

In conclusion, our findings show that high expression of CK1ε is positively associated with the Duke's staging and depth of invasion in CRC patients, and knockdown of CK1ε suppresses the growth and invasion of CRC cells through inhibition of the wnt/β-catenin signaling, suggesting that CK1ε may serve as a promising therapeutic target for the treatment of CRC.

REFERENCES

1. Siegel R, Naishadham D, Jemal A. Cancer statistics, 2012. CA Cancer J Clin 2012; 62:10-29.
2. Antonic V, Stojadinovic A, Kester KE, Weina PJ, Brücher BL, Protic M, Avital I, Izadjoo M. Significance of infectious agents in colorectal cancer development. J Cancer 2013; 4:227-40.

3. Rawson JB, Bapat B. Epigenetic biomarkers in colorectal cancer diagnostics. Expert Rev Mol Diagn 2012; 12:499-509.
4. Modak C, Chai J. Potential of casein kinase I in digestive cancer screening. World J Gastrointest Oncol 2009; 1:26-33.
5. Sun D, Zhou M, Kowolik CM, Trisal V, Huang Q, Kernstine KH, Lian F, Shen B. Differential expression patterns of capping protein, protein phosphatase 1, andcasein kinase 1 may serve as diagnostic markers for malignant melanoma. Melanoma Res 2011; 21:335-43.
6. Rodriguez N, Yang J, Hasselblatt K, et al. Casein kinase I epsilon interacts with mitochondrial proteins for the growth and survival of human ovarian cancer cells. EMBO Mol Med 2012; 4:952-63.
7. Dolezal T, Kucerova K, Neuhold J, Bryant PJ. Casein kinase I epsilon somatic mutations found in breast cancer cause overgrowth in Drosophila. Int J Dev Biol 2010; 54:1419-24.
8. Shin S, Wolgamott L, Roux PP, Yoon SO. Casein kinase 1ε promotes cell proliferation by regulating mRNA translation. Cancer Res 2014; 74:201-11.
9. Lin SH, Lin YM, Yeh CM, Chen CJ, Chen MW, Hung HF, Yeh KT, Yang SF. Casein kinase 1 epsilon expression predicts poorer prognosis in low T-stage oralcancer patients. Int J Mol Sci 2014**;** 15:2876-91.
10. Sinnberg T, Menzel M, Kaesler S, Biedermann T, Sauer B, Nahnsen S, Schwarz M, Garbe C, Schittek B. Suppression of casein kinase 1alpha in melanoma cells induces a switch in beta-catenin signaling to promote metastasis. Cancer Res 2010; 70:6999-7009.
11. Knippschild U, Krüger M, Richter J, et al. The CK1 Family: Contribution to Cellular Stress Response and Its Role in Carcinogenesis. Front Oncol 2014; 4:96.
12. Hu Y, Song W, Cirstea D, Lu D, Munshi NC, Anderson KC. CSNK1α1 mediates malignant plasma cell survival. Leukemia 2014. doi: 10.1038/leu.2014.202. [Epub ahead of print]
13. Tsai IC, Woolf M, Neklason DW, Branford WW, Yost HJ, Burt RW, Virshup DM. Disease-associated casein kinase I delta mutation may promote adenomatous polyps formation via a Wnt/beta-catenin independent mechanism. Int J Cancer 2007; 120:1005-12.
14. Kuga T, Kume H, Kawasaki N, et al. A novel mechanism of keratin cytoskeleton organization through casein kinase Iα and FAM83H in colorectal cancer. J Cell Sci 2013**;** 126:4721-31.
15. Knippschild U, Wolff S, Giamas G, Brockschmidt C, Wittau M, Würl PU, Eismann T, Stöter M. The role of the casein kinase 1 (CK1) family in different signaling pathways linked tocancer development. Onkologie 2005; 28:508-14.
16. Brockschmidt C, Hirner H, Huber N, et al. Anti-apoptotic and growth-stimulatory functions of CK1 delta and epsilon in ductal adenocarcinoma of the pancreas are inhibited by IC261 in vitro and in vivo. Gut 2008; 57:799-806.
17. Yang WS, Stockwell BR. Inhibition of casein kinase 1-epsilon induces cancer-cell-selective, PERIOD2-dependent growth arrest. Genome Biol 2008; 9:R92.
18. Richter J, Bischof J, Zaja M, Difluoro-dioxolo-benzoimidazol-benzamides As potent inhibitors of CK1δ and ε with nanomolar inhibitory activity on cancer cell proliferation. J Med Chem 2014; 57:7933-46.
19. Järås M, Miller PG, Chu LP, Csnk1a1 inhibition has p53-dependent therapeutic efficacy in acute myeloid leukemia. J Exp Med 2014; 211:605-12.
20. Huart AS, Saxty B, Merritt A. A Casein kinase 1/ Checkpoint kinase 1 pyrazolo-pyridine protein kinase inhibitor as novel activator of the p53 pathway. Bioorg Med Chem Lett 2013; 23:5578-85.
21. Borgal L, Rinschen MM, Dafinger C, et al. Casein Kinase 1 **α** Phosphorylates the Wnt Regulator Jade-1 and Modulates Its Activity. J Biol Chem 2014; 289:26344-56.
22. Schittek B, Sinnberg T. Biological functions of casein kinase 1 isoforms and putative roles in tumorigenesis. Mol Cancer 2014; 13:231.
23. Kim SY, Dunn IF, Firestein R, et al. CK1epsilon is required for breast cancers dependent on beta-catenin activity. PLoS One 2010; 5:e8979.
24. Luu HH, Zhang R, Haydon RC, et al. Wnt/beta-catenin signaling pathway as a novel cancer drug target. Curr Cancer Drug Targets 2004; 4:653-71.
25. al-Sheneber IF, Shibata HR, Sampalis J, Jothy S. Prognostic significance of proliferating cell nuclear antigen expression in colorectal cancer. Cancer

1993; 71:1954-9.

26. Damodharan U, Ganesan R, Radhakrishnan UC. Expression of MMP2 and MMP9 (gelatinases A and B) in human colon cancer cells. Appl Biochem Biotechnol 2011; 165:1245-52.

27. Tarapore RS, Siddiqui IA, Saleem M, Adhami VM, Spiegelman VS, Mukhtar H. Specific targeting of Wnt/β-catenin signaling in human melanoma cells by a dietary triterpene lupeol. Carcinogenesis 2010; 31:1844-53.

FLOW CYTOMETRIC DETECTION OF SUBHAPLOID NUCLEI IN HUMAN SPERM AS A MEASURE OF DNA FRAGMENTATION AND APOPTOSIS

S. GRÖBNER[1], M. FRANZ[1], U. HOBERG[1], B. WETZKA[2] and T. SCHWEIZER[1]

[1]Synlab Medical Services, MVZ Synlab Leinfelden, Leinfelden, Germany; [2]Centre for Gynecological Endocrinology and Reproductive Medicine Freiburg (CERF), Freiburg, Germany

Received July 27, 2014 – Accepted April 14, 2015

The use of assisted reproductive technologies (ARTs) is increasing worldwide. In order to predict the rate of pregnancy after ART the DNA fragmentation index (DFI) of ejaculated spermatocytes may be a better marker than conventional semen quality parameters. Spermatocytes with fragmented DNA are associated with apoptotic stages and are characterized by a low DNA content. The subhaploid nuclei of DNA-damaged spermatocytes can be easily detected by flow cytometry. We here analyzed the percentage of subhaploid nuclei of semen samples from 163 patients aged 26 to 74 years who consulted one of the ten centres for reproductive medicine which routinely send sperm samples to our laboratory in order to determine special sperm parameters. The percentage of subhaploid nuclei indicating the DFI of spermatocytes did not correlate with age and sperm volume, but inversely correlated with sperm concentration and the percentage of motile spermatocytes. This is in concordance with previous studies which demonstrated that DNA damage of spermatozoa correlates with conventional semen quality parameters. Since DNA-damaged spermatocytes are associated with an impaired outcome of assisted conception technologies, this method could help to monitor sperm quality of subfertile men after measures to increase sperm quality and to improve selection criteria of cryopreserved sperm samples in assisted reproduction medicine.

In human sperm samples spermatozoa with damaged DNA exhibiting features of apoptotic cell death have been observed (1). The percentage of DNA-damaged spermatozoa is increased by conditions associated with the creation of oxidative stress such as smoking (2), exposure to radiofrequency electromagnetic radiation (2) and hydrogen peroxide (3), cryopreservation (2), and mild oxidative stress as a result of age (2), dietary deficiencies (4) or bacterial infections (5).

According to the hypothesis of Aitken et al., oxidative stress causes a disruption of spermatogenesis resulting in the production of senescent mature spermatozoa with poorly compacted chromatin (2). Activation of mitochondrial ROS in these defective spermatozoa via lipid peroxidation induces oxidative DNA damage finally resulting in DNA strand breaks and cell death (6). As a consequence, several features of apoptosis such as depolarisation of the inner mitochondrial trans-membrane potential (7), cytochrome c release (8), activation of caspases (8), externalization of phosphatidylserine and annexin V binding (7, 8) have been observed in DNA-damaged human spermatozoa.

Key words: spermatozoa, DNA fragmentation index, male infertility, male subfertility

Mailing address: Dr Sabine Gröbner,
Synlab MVZ Leinfelden,
Max-Lang-Str. 58,
70771 Leinfelden, Germany
Tel.: +49 711 9033 150
Fax: +49 711 9033 160
e-mail: sabine.groebner@synlab.com

0393-974X (2015)

DISCLOSURE: ALL AUTHORS REPORT NO CONFLICTS OF INTEREST RELEVANT TO THIS ARTICLE.

DNA damage in human sperm can be investigated by several assays such as the sperm chromatin structure assay (SCSA) (8), the neutral microgel electrophoresis (COMET) assay evaluating DNA double-strand breaks (2), the DNA diffusion assay (2), and the terminal transferase dUTP nick-end labeling (TUNEL) assay (8-10). Several parameters for determining the DNA status, cell viability and the mitochondrial function, respectively, can be assessed by flow cytometry (11).

Increased DNA damage in human spermatozoa is associated with spontaneous male subfertility and miscarriage (12, 13). It has been suggested to be the result of an abortive apoptotic process of germ cells initiated in early spermatogenesis but not completed during spermiogenesis (10). Human subfertility can be treated by assisted reproduction technologies (ART) such as *in vitro* fertilisation (IVF) or intra-cytoplasmatic sperm injection (ICSI). Using these technologies, DNA-fragmentation index is a better predictor of pregnancy after IVF and ICSI than conventional sperm quality parameters reported by the World Health Organisation (WHO) (12). Moreover, in human sperm samples with a low percentage of DNA strand breaks a "late paternal effect" after ICSI was observed, resulting in higher pregnancy rates and lower miscarriage rates (13).

In the present study, DNA fragmentation of human ejaculates was analyzed by flow cytometric detection of subhaploid nuclei resulting from DNA fragmentation and DNA loss during apoptotic cell death. This rapid and easy to handle method was compared with conventional semen analysis.

MATERIALS AND METHODS

Sperm samples

Sperm samples were from 163 patients who attended one of the ten centres for reproductive medicine associated with our laboratory between May 2012 and February 2014. The main reasons for infertility were idiopathic or tubal factors, endometriosis and male factors. Patients were requested to abstain from ejaculation for two to five days before sample collection. Samples were collected in the centres after masturbation, allowed to liquefy at room temperature, and tubes were transported on ice water to our laboratory within 24 hours.

Determination of sperm concentration

The sperm samples were washed twice with PBS (Euroimmun, Lübeck, Germany), counted in duplicates using a hematocytometer and the sperm concentrations were given as mean values according to the WHO quality parameters (14). Samples were adjusted to a concentration of 10 million spermatozoa per ml PBS and were either immediately analyzed or frozen at –20°C before they were analyzed for the percentage of subhaploid nuclei.

Analysis of subhaploid nuclei by flow cytometry

After the frozen samples had been thoroughly thawed, one ml of each sample containing 10 million spermatozoa was transferred into 7.5 ml cell sorter tubes (Becton Dickinson biosciences, Heidelberg, Germany) and centrifuged at 400 x g for 5 min. According to the protocol of Nicoletti et al. (15), the cell pellet was resuspended in 400 µl lysis/staining buffer (50 µg propidium iodide/ml, 0.1% (w/v) trisodium citrate-2-hydrate, and 0.1% Triton X-100 dissolved in aqua bidest), incubated on ice for 10 min ensuring cell lysis. Thereafter, the remaining nuclei with stained chromatin were analyzed on a FACSCalibur flow cytometer (Becton Dickinson biosciences). The nuclei were gated using the forward-angle light scatter (FSC) and the side-angle light scatter (SSC) in order to exclude artefacts resulting from small particles in the staining buffer alone. To assess their size and DNA content, sperm nuclei with propidium iodide-labelled DNA were detected in the FSC/FL3-PI channel. For each test 10,000 nuclei were examined. All analyses were carried out in duplicate. The mean value of the percentages of subhaploid nuclei (DFI=DNA fragmentation index) was determined by analysis of the nuclei by the FL3-PI histogram using an individual marker (Fig. 1) and calculation by the cell quest pro software version 6.0 (Becton Dickinson).

As a positive control, spontaneous apoptotic cell death of spermatozoa was induced in three sperm samples with low rates of subhaploid nuclei by incubation for 24 h at 37°C in 2 ml MEM (Biochrom, Berlin, Germany) supplemented with 10% fetal serum albumin and 100U/ml penicillin, 100µg/ml streptomycin (all from biochrom) in a 6 well-plate (Greiner Bio-One, Frickenhausen, Germany). Additionally, for each run sperm samples with low DFI (<7%) and high DFI (>15%) were used as negative and positive controls, respectively. Therefore, aliqots of control samples adjusted to a concentration of 10mio/ml were frozen and stored at -20°C. After thawing they were incubated in Nicoletti buffer as described above. Stained control samples were stored up to three days at 4°C in the dark. Using this procedure, the DFI of a representative negative control sample with an initial DFI of 5.3% did not substantially increase after it was used 31 times (mean DFI 6.2%±1.5%).

Analysis of additional sperm parameters

Additional WHO sperm parameters such as volume,

pH, progressive and total motility (14), were evaluated by the IVF centres themselves from freshly taken samples. In order to assure comparability of the data, these additional sperm parameters were evaluated using only the data of the IVF centre [Centre for Gynecological Endocrinology and Reproductive Medicine, Freiburg (CERF), Germany] which was responsible for most (n=91; 55.8%) of the patients included in this study (n=163). pH and spermatocyte morphology was analyzed in sperm samples from 50 and 48 patients, respectively, of these 91 patients.

Statistical analysis

In order to describe the correlation between the percentage of subhaploid nuclei and other sperm parameters, negative linear or logarithmic functions were approximated and the Pearson's correlation coefficient (r) was determined. Differences were considered to be significant if the probability of their occurrence by chance was <0.05 (paired two-tailed Student's *t*-test).

RESULTS

Previous studies have shown that the DNA fragmentation index (DFI) is a better predictor of pregnancy after IVF and ICSI than conventional sperm parameters (12). In the present study sperm samples from patients sent to our laboratory by several infertility centres were analyzed for DNA damage. Therefore, spermatocytes were lysed by a hypotonic lysis buffer containing propidium iodide and nuclei were analyzed for their size and content of DNA by flow cytometric analysis.

As shown in Fig. 1A (upper left panels), artefacts resulting from the buffer alone (data not shown) were excluded from the analysis by appropriate gating using the FSC/SSC analysis.

As a positive control for the induction of DNA damage, a sperm sample of a patient with a low rate of subhaploid nuclei (low DFI) (control) was incubated for 24 h in supplemented MEM medium without fructose to induce spontaneous apoptosis (Fig. 1A, upper panel). To assess their size and DNA content, sperm nuclei were analyzed in the FSC/FL3-PI channel (Fig. 1A, upper mid panels). Non-apoptotic nuclei were characterized by a high FSC and FL3-PI signal (control). Incubation of spermatocytes for 24 h in cell culture medium caused loss of DNA and fragmentation of nuclei indicated by an increase of small nuclei with lowered DNA content (subhaploid nuclei). In order to quantify the percentage of subhaploid nuclei, nuclei were analyzed by the FL3-PI histogram using an individual marker indicating the DNA fragmentation index (DFI) (Fig. 1A, upper right panels).

It has been described that after incubation of spermatocytes for more than 12 hours in cell culture medium containing balanced salts, energy substrates and human serum albumin the rate of DNA damage increases (16). To induce spontaneous apoptosis, sperm samples of three healthy patients with a mean percentage of subhaploid nuclei of 7.6% were chosen (Fig. 1A, lower panel). Incubation of these samples in supplemented MEM medium for 24 h caused an increase of subhaploid nuclei indicated by a DFI of 18.4% (Fig. 1A, lower panel).

Fig. 1B shows some representative analyses of subhaploid nuclei (DFI) of sperm samples from four different patients with low DFI (<15%, upper panel), borderline DFI (15-25%, mid panels) and high DFI (>25%, lower panel).

The distribution of the percentages of subhaploid nuclei among all 163 patients analysed in this study is shown in Fig. 2A (upper left panel). The mean DFI ± standard deviation of the samples was 20.8±19.7%. In 52.8% (86/163) of the samples a rate of less than 15% subhaploid nuclei was detected, whereas 28.8% (47/163) of the patients had a DFI of higher than 25%. The mean age ± standard deviation of the patients analyzed in this study was 38.9±7 years. As shown in Fig. 2A, the distribution of the percentages of subhaploid nuclei was similar in different age groups. In the two groups of patients <35 years and 35-39 years, 53.8% (21/39) and 51.0% (26/51) of the patients, respectively, had a DFI of lower than 15%, 12.8% (5/39) and 15.7% (8/51), respectively, an intermediate DFI of 15-25%, and 33.3% (13/39) and 33.3% (17/51), respectively, a DFI higher than 25%. By contrast, only 23.3% (17/73) of the patients forty years and over showed a DFI higher than 25%. Instead, there were more patients [23.3% (17/73)] with intermediate DFI (15-25%) in this age group, whereas the percentage of patients aged forty years and over with DFI lower than 15% was 53.4% (39/73), similar to that of the younger patients.

The mean sperm concentrations ± standard deviation among all samples was 37.9±30.6 mio/ml. A sufficient sperm concentration of at least 14 mio/ml as defined by the WHO (14) was determined in

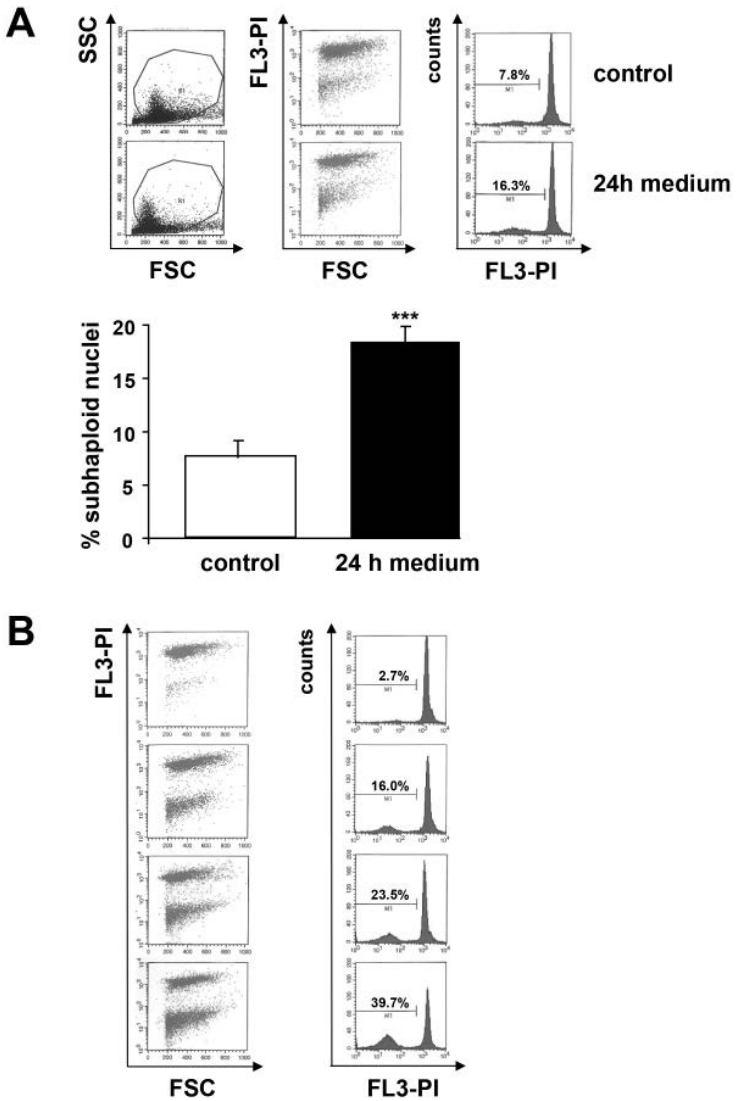

Fig. 1. *Analysis of subhaploid nuclei in sperm. Spermatozoa were incubated in Nicoletti buffer and analyzed by flow cytometry.* ***A)*** *The percentage of subhaploid nuclei (DNA fragmentation index; DFI) is indicated by the marker. Upper panel: Representative result of an untreated sperm sample with a low percentage of subhaploid nuclei (control) and after incubation for 24 h in cell culture medium. Lower panel: Percentage of subhaploid nuclei of sperm samples, which were untreated (control) and incubated for 24 h in cell culture medium, respectively. Data are means + standard deviations resulting from the analysis of three different samples. Significant differences from untreated spermatozoa are indicated by *** ($p<0.001$).* ***B)*** *Representative results of four different patients with low DFI (<15%), intermediate DFI (15-25%) and high DFI (>25%).*

75.5% (123/163) of the patients. As shown in Fig. 2B, in the group of patients with sperm concentration lower than 14 mio/ml the percentage of samples with ≥25% of subhaploid nuclei (DFI) was 70% (28/40). By contrast, in only 13.5% (19/123) of the patients with sperm concentrations of ≥14 mio/ml samples with high DFI (>25%) were observed, indicating an inverse correlation between these two sperm quality parameters.

In Fig. 2C the inverse correlation between sperm concentration and the percentage of subhaploid nuclei is shown. The distribution of the sperm

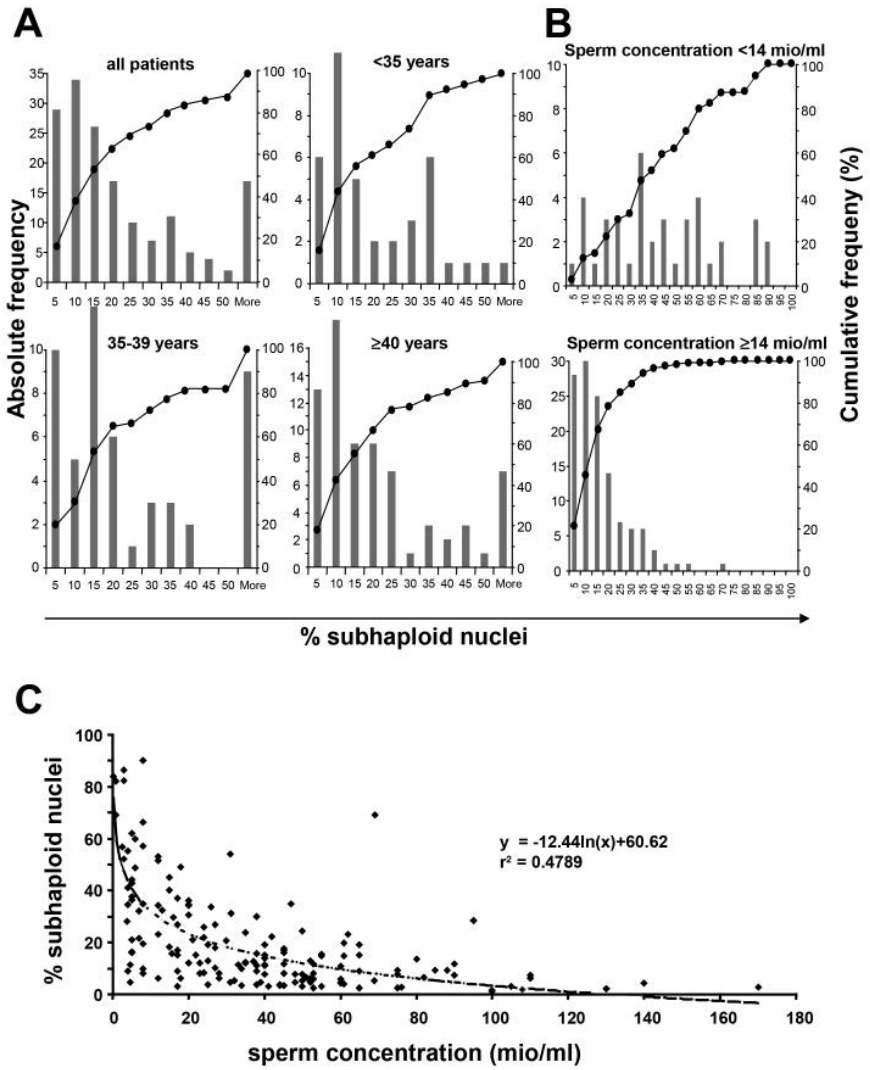

Fig. 2. *Distribution of the percentage of subhaploid nuclei and sperm concentration among the sperm samples (n=163).* ***A****) Absolute and cumulative frequencies of the percentage of subhaploid nuclei among all patients and in different groups of age, respectively.* ***B****) Absolute and cumulative frequencies of the percentages of subhaploid nuclei in two groups of patients with low (<14 mio/ml) and high (≥14 mio/ml) sperm concentration according to the world health organization (WHO).* ***C****) Inverse correlation between the percentage of subhaploid nuclei and sperm concentration.*

concentrations and percentages of subhaploid nuclei of all patients analyzed approximately followed a negative logarithmic function, as depicted in Fig. 2C.

In the present study an inverse correlation between the rate of subhaploid nuclei indicated by the DFI and the concentration of spermatocytes was shown in sperm samples of 163 patients consulting one of the infertility centres included in this study. The percentage of patients with intermediate and high DFI did not increase in patients aged forty years and over when compared to younger patients, indicating that DFI did not increase with age.

In addition to sperm concentration (Fig. 2C), several further WHO sperm parameters were evaluated by the IVF centres themselves from freshly-taken sperm samples (Fig. 3).

As shown in Fig. 3A, no significant correlation was found between the percentage of subhaploid

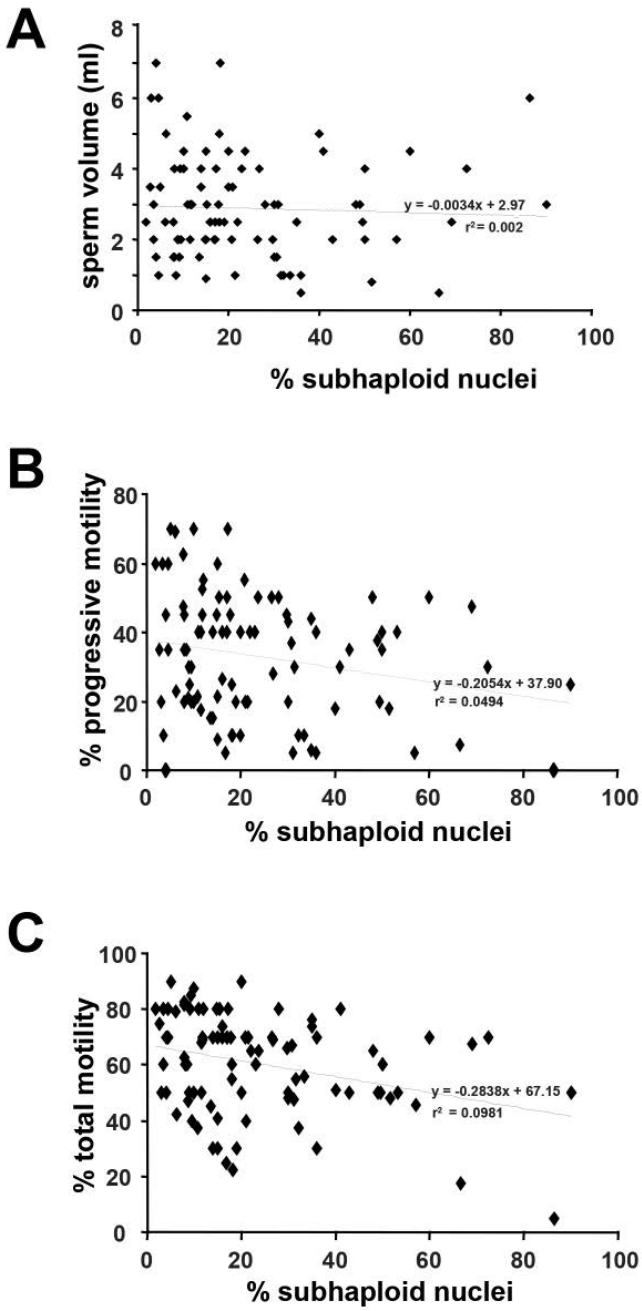

Fig. 3. *Relationship between the percentage of subhaploid nuclei and additional sperm parameters (n=91). **A)** No significant correlation between subhaploid nuclei and sperm volume. Inverse correlation between subhaploid nuclei and progressive motility (**B**) and total motility (**C**).*

nuclei and sperm volume ($p>0.1$). By contrast, both progressive and total sperm motility were negatively correlated with the percentage of subhaploid nuclei, as depicted in Fig. 3B ($p<0.05$) and Fig. 3C ($p<0.005$), respectively.

DISCUSSION

Conventional evaluation of the sperm quality includes the microscopic analysis of the sperm concentration, motility and morphology (14).

However, the predictive value of this conventional analysis is limited as 50% of the couples with failed IVF showed a normal pre-IVF WHO-sperm-analysis (17).

The rate of DNA-damaged, apoptotic spermatozoa not only correlates negatively with conventional WHO semen quality parameters (1), but also with fertility and pregnancy rates after IVF (2, 9, 12, 18). In assisted reproduction medicine intra-cytoplasmatic sperm injection (ICSI) is used in most of the cases (2, 9), thereby circumventing the natural selection process of spermatozoa with damaged DNA. Consequently, a positive correlation between the rate of DNA-damaged spermatozoa and miscarriage and increased risk of defects in the offspring has been observed (2). Correspondingly, the outcome after ICSI was better in the group with ≤20% TUNEL positive spermatozoa indicated by higher pregnancy and lower miscarriage rates when compared to the group with >20% TUNEL positive spermatozoa (9). Moreover, after intrauterine insemination (IUI) no pregnancy was achieved when more than 12% of the spermatozoa were TUNEL positive (19). In general, the rate of apoptosis in human sperm is increased in infertile men (20), whereas only 0.1-10% of spermatozoa of healthy donors are apoptotic (21).

Besides the TUNEL method, several other flow cytometric methods have been described in humans and animals for the assessment of sperm DNA fragmentation or cell death indicated by disintegrity of the plasma membrane (11, 22, 23). Whereas the sperm membrane integrity is related to many sperm functions, especially motility, sperm DNA integrity is important for normal early embryo development (11). With all the methods described above, whole sperm cells are analyzed, either fixed (TUNEL assay) or not (plasma membrane integrity assays). Since propidium iodide, a plasma membrane impermeable dye, can leak in after destabilization of the cell membrane, staining of DNA by PI in whole sperm cells indicates damage of the cell membrane integrity of the sperm head, where most of the sperm DNA is found. Simultaneous assessment of the plasma membrane and acrosomal integrity can be achieved by combination of PI with the acrosome membrane specific dye FITC-PNA (peanut agglutinin) (11). The so called "live/dead staining" uses a combination of the cell membrane impermeable dye PI and the cell membrane permeable dye SYBR-14 to assess not only dead cells (SYBR-14/PI double positive) but also viable cells (SYBR-14 positive/PI negative) (11, 22, 23).

In contrast to all these previously described methods, in the present study we used the DNA-specific dye PI not for staining of whole dead sperm cells, but for staining all sperm nuclei resulting from plasma membrane lysis of sperm cells by hypotonic buffer. With this flow cytometric method, haploid nuclei can easily be distinguished from subhaploid nuclei (Fig. 1B), which result from DNA fragmentation and consecutive DNA loss or fragmentation of nuclei. The advantage of this method compared to other flow cytometric sperm DNA fragmentation assays, like the TUNEL assay, is that samples do not need to be fixed prior to staining of cells. However, a limitation of both of these methods is the lack of quantification of the degree of DNA damage within a single cell, which can be determined with the sperm chromatin structure assay (SCSA). However, SCSA causes DNA strand breaks by the procedure itself (11). Using the method described here, the population of spermatozoa in fact having damaged DNA is measured, and artificial DNA fragmentation induced by short time incubation of sperm cells in hypotonic lysis buffer containing PI can be excluded. Moreover, the flow cytometric events which were included in the analysis were to determine easily as PI-positive and therefore, with high probability as DNA-containing nuclei or nucleus fragments, respectively. Hence, although not completely excluded, both underestimation and overestimation of spermatocyte damage which has been described with several other methods (11) can be widely excluded when analysing the percentage of subhaploid nuclei.

In the present study, sperm samples with lower than 15% subhaploid apoptotic nuclei indicating the DNA fragmentation index (DFI) were interpreted as unsuspicious result which cannot explain male subfertility. Patients with DFI 15% or higher were advised to change their lifestyle (for example, stop smoking), exclude other factors of enhanced DNA fragmentations, such as infections or chemotherapeutic agents, and to supplement their nutrition with anti-oxidants. Whereas patients with DFI between 15% and 25% were advised to

intrauterine insemination (IUI), patients with DFI more than 25% were advised to intra-cytoplasmatic sperm injection (ICSI) since a previous study has shown that after ICSI even patients with >20% TUNEL positive spermatozoa are able to achieve pregnancy, probably due to reparative mechanisms of the oocyte (9).

Usually, density gradient centrifugation and subsequent swim-up technique are used for the preparation of sperm samples for ICSI and IUI, respectively, causing an out-selection of immature, abnormal, DNA-damaged, subhaploid spermatocytes with poorly condensed chromatin and leaky cell membranes (1). On the contrary, DNA fragmentation by the preparation itself probably is enhanced and can be circumvented by renouncing centrifugation and use of special cell culture media supplemented with antioxidants, such as glutathion, N-acetylcystein, hypotaurin, and catalase (9). Additionally, there are attempts to increase the rate of intact spermatocytes in ejaculates by magnetic cell sorting (24). In our study, native, washed cells of human ejaculates were analyzed.

We showed here a negative correlation between the rate of subhaploid nuclei and concentration of spermatocytes (Fig. 2C) and between the percentage of subhaploid nuclei and motility (Fig. 3B and Fig. 3C). This is in correspondence with other groups demonstrating that DNA damage and apoptosis in ejaculated human sperm is correlated with WHO sperm quality markers like sperm concentration and motility (1, 2, 6, 20). A possible explanation is that, as a consequence of accumulated DNA-damage, spermatocytes lose their motility and, induced by production of mitochondrial ROS, undergo apoptotic or necrotic cell death (6). Moreover, evaluation of 48 of the sperm samples included in our study revealed that also the percentage of spermatocytes with normal morphology negatively correlated with the percentage of subhaploid nuclei ($p<0.05$, data not shown), suggesting that DNA-damage might cause development of dysmorphologic spermatocytes. It has been described previously that the inverse correlation between sperm concentration and the apoptotic index can be observed only in normal sperm samples reaching the WHO quality parameters (25). Correspondingly, in our study the variation of the DFI values of sperm samples with sperm concentrations lower than 14 mio/ml was high, whereas sperm samples fulfilling the WHO quality parameter of ≥14 mio/ml strongly correlated with low DFI values (Fig. 2B).

In contrast, neither sperm volume (Fig. 3A) nor pH ($n=50$, data not shown, $p>0.1$) revealed a significant correlation with the percentage of subhaploid nuclei. Since both of these parameters are strongly dependent on the function of the male adnex organ, a correlation was not to be expected.

High rates of sperm DNA fragmentation are associated with recurrent pregnancy loss since DNA repair in spermatocytes is limited (26). Aitken et al. have hypothesized that DNA repair might be performed by the oocyte (2). Thereby, the measurement of subhaploid nuclei described here might be also a useful method for the prediction of the course of a spontaneous pregnancy.

Several anti-oxidative interventions have been described to decrease the DNA fragmentation index of human sperm, such as giving up heavy smoking (2), decrease of the body mass index thereby preventing systemic oxidative stress (27), and oral supplementation with antioxidants such as vitamin C and vitamin E (28). Hence, the success of such measures could be easily monitored by flow cytometric analysis of subhaploid nuclei.

After cryopreservation of sperm, a decrease of the sperm concentration, motility rates and an increase of annexin V positive spermatocytes was observed (29). In accordance, Alvarez et al. reported a case of a successful ICSI procedure using a cryopreserved sperm sample with low DNA fragmentation rate (30). Hence, for assisted reproductive technologies such as ICSI, the very rapid flow cytometric analysis of subhaploid nuclei described here might be useful to easily select cryopreserved sperm samples with low DNA fragmentation rate.

We describe here a very rapid and easy to perform flow cytometric assay to measure the percentage of subhaploid, DNA-damaged nuclei according to the protocol of Riccardi and Nicoletti (15). Advantages of this protocol are the low costs of the reagents required for the combined detergent buffer/staining solution, the long-term storability of the staining buffer, and the missing need of cell fixation and longer incubation periods, respectively. Hence, after a single washing step, spermatocytes can be

analyzed already 10 minutes after resuspension in Nicoletti buffer. Moreover, since the reproducibility of the results after analysis of the same sperm sample even after freezing/thawing was high, also frozen samples could be sent to the laboratory. Therefore, the flow cytometric determination of subhaploid nuclei described here might be a useful method for counselling infertile couples, for monitoring of subfertile men after measures to increase sperm quality, and for screening of cryopreserved sperm samples in assisted reproduction medicine.

REFERENCES

1. Mahfouz RZ, Sharma RK, Said TM, Erenpreiss J, Agarwal A. Association of sperm apoptosis and DNA ploidy with sperm chromatin quality in human spermatozoa. Fertil Steril 2009; 91:1110-18.
2. Aitken RJ, Koppers AJ. Apoptosis and DNA damage in human spermatozoa. Asian J Androl 2011; 13:36-42.
3. Lozano GM, Bejarano I, Espino J, González D, Ortiz A, Garcia JF, Rodriguez AB, Pariente JA. Relationship between caspase activity and apoptotic markers in human sperm in response to hydrogen peroxide and progesterone. J Reprod Dev 2009; 55:615-21.
4. Palmer NO, Bakos HW, Owens JA, Setchell BP, Lane M. Diet and exercise in an obese mouse fed a high-fat diet improve metabolic health and reverse perturbed sperm function. Am J Physiol Endocrinol Metab 2012; 302:E768-80.
5. Fraczek M, Szumala-Kakol A, Jedrzejczak P, Kamieniczna M, Kurpisz M. Bacteria trigger oxygen radical release and sperm lipid peroxidation in *in vitro* model of semen inflammation. Fertil Steril 2007; 88:1076-85.
6. Aitken RJ, Baker MA. Causes and consequences of apoptosis in spermatozoa; contributions to infertility and impacts on development. Int J Dev Biol 2013; 57:265-72.
7. Kim HH, Funaro M, Mazel S, Goldstein M, Schlegel PN, Paduch DA. Flow cytometric characterization of apoptosis and chromatin damage in spermatozoa. Reprod Biomed Online 2013; 24:393-5.
8. Koppers AJ, Mitchell LA, Wang P, Lin M, Aitken RJ. Phosphoinositide 3-kinase signalling pathway involvement in a truncated apoptotic cascade associated with motility loss and oxidative DNA damage in human spermatozoa. Biochem J 2011; 436:687-98.
9. Leberl F, Stadler A, Bulfon S, Boschi A. Sperm TUNEL Test: Is it relevant for IVF Institutes? J Gynäkol Endokrinol 2008; 18:19-22.
10. Sakkas D, Moffatt O, Manicardi GC, Mariethoz E, Tarozzi N, Bizzaro D. Nature of DNA damage in ejaculated human spermatozoa and the possible involvement of apoptosis. Biol Reprod 2002; 66:1061-7.
11. Hossain MS, Johannisson A, Wallgren M, Nagy S, Siqueira AP, Rodriguez-Martinez H. Flow cytometry for the assessment of animal sperm integrity and functionality: state of the art. Asian J Androl 2011; 13:406-19.
12. Larson-Cook KL, Brannian JD, Hansen KA, Kasperson KM, Aamold ET, Evenson DP. Relationship between the outcomes of assisted reproductive techniques and sperm DNA fragmentation as measured by the sperm chromatin structure assay. Fertil Steril 2003; 80:895-902.
13. Benchaib M, Lornage J, Mazoyer C, Lejeune H, Salle B, François Guerin J. Sperm deoxyribonucleic acid fragmentation as a prognostic indicator of assisted reproductive technology outcome. Fertil Steril 2007; 87:93-100.
14. World health organization. WHO laboratory manual for the examination of human semen and sperm-cervical mucus interaction. 5th edition. Cambridge university press, 2010.
15. Riccardi C, Nicoletti I. Analysis of apoptosis by propidium iodide staining and flow cytometry. Nat Protoc 2006; 1:1458-61.
16. Muratori M, Maggi M Spinelli S, Filimberti E, Forti G, Baldi E. Spontaneous DNA fragmentation in swim-up selected human spermatozoa during long term incubation. J Androl 2003; 24:253-62.
17. Liu DY, Baker HW. Defective sperm-zona pellucida interaction: a major cause of failure of fertilization in clinical *in-vitro*-fertilization. Hum Reprod 2000; 15:702-8.
18. Henkel R, Hajimohammad M, Stalf T, et al. Influence of deoyribonucleic acid damage on fertilization and

pregnancy. Fertil Steril 2004; 81:965-72.
19. Duran EH, Morshedi M, Taylor S, Oehninger S. Sperm DNA quality predicts intrauterine insemination outcome: a prospective cohort study. Hum Reprod 2002; 17:3122-8.
20. Weng SL, Taylor SL, Morshedi M, Schuffner A, Duran EH, Beebe S, Oehninger S. Caspase activity and apoptotic markers in ejaculated human sperm. Mol Hum Reprod 2002; 8:984-91.
21. Bacetti B, Collodel G, Piomboni P. Apoptosis in human ejaculated sperm cells (notulae seminologicae 9). J Submicrosc Cytol Pathol 1996; 28:587-96.
22. Yeste M, Estrada E, Rivera Del Alamo MM, Bonet S, Rigau T, Rodriguez-Gil JE. The increase in phosphorylation levels of serine residues of protein HSP70 during holding time at 17°C is concomitant with a higher cryotolerance of boar spermatozoa. PloS One 2014; 9:e90887.
23. Niu ZH, Huang XF, Jia XF, et al. A sperm viability test using SYBR-14/propidium iodide flow cytometry as a tool for rapid screening of primary ciliary dyskinesia patients and for choosing sperm sources for intracytoplasmic sperm injection. Fertil and Steril 2011; 95: 389-92.
24. Said TM, Agarwal A, Zborowski M, Grunewald S, Glander HJ, Paasch U. Utility of magnetic cell separation as a molecular sperm preparation technique. J Androl 2008; 29:134-42.
25. Ricci G, Perticarari S, Fragonas E, et al. Apoposis in human sperm: its correlation with semen quality and the presence of leukocytes. Hum Reprod 2002; 17:2665-72.
26. Carrell DT, Liu L, Peterson CM, Jones KP, Hatasaka HH, Erickson L, Campbell B. Sperm DNA fragmentation is increased in couples with unexplained recurrent pregnancy loss. Arch Androl 2003; 49:49-55.
27. Chavarro JE, Toth TL, Wright DL, Meeker JD, Hauser R. Body mass index in relation to semen quality, sperm DNA integrity, and serum reproductive hormone levels among men attending an infertility clinic. Fertil Steril 2010; 93:2222-31.
28. Greco E, Iacobelli M, Rienzi L, Ubaldi F, Ferrero S, Tesarik J. Reduction of the incidence of sperm fragmentation by oral antioxidant treatment. J Androl 2005; 25:349-53.
29. Sion B, Janny L, Boucher D, Grizard G. Annexin V binding to plasma membrane predicts the quality of human cryopreserved spermatozoa. Int J Androl 2004; 27:108-14.
30. Alvarez JG, Ollero M, Larson-Cook KL, Evenson DP. Selecting cryopreserved semen for assisted reproductive technique based on the level of sperm nuclear DNA fragmentation resulted in pregnancy. Fertil Steril 2004; 81:712-3.

MELATONIN ALLEVIATES BLEOMYCIN-INDUCED PULMONARY FIBROSIS IN MICE

M.H. KARIMFAR[1,2], S. ROSTAMI[3], K. HAGHANI[4], S. BAKHTIYARI[3,4] and A. NOORI-ZADEH[3,4]

[1]Department of Anatomical Sciences, School of Medicine, Ilam University of Medical Sciences, Ilam, Iran; [2]Department of Anatomical Sciences, School of Medicine, Zahedan University of Medical Sciences, Zahedan, Iran; [3]Student Research Committee, Ilam University of Medical Sciences, Ilam, Iran; [4]Department of Clinical Biochemistry, School of Medicine, Ilam University of Medical Sciences, Ilam, Iran

Received February 2, 2015 – Accepted March 25, 2015

Pulmonary fibrosis occurs as a common end-stage sequela of a number of acute and chronic lung diseases. Eicosanoids exert crucial roles in inflammatory processes pertinent to fibrogenesis induction, however, the role of cyclooxygenase 2 (COX-2) is not fully elucidated in most pulmonary fibrosis related-disorders. Recently, melatonin (MLN) has been introduced as an effective immuno-modulator and anti-oxidant agent. The present study aimed to investigate the effect of MLN on COX-2 expression in idiopathic pulmonary fibrosis (IPF). Animals were divided into five groups, including: 1) saline control, 2) 1% ethanol control, 3) MLN control, 4) bleomycin (BLM), in which mice were injected with BLM (15 mg/kg, i.p.) two times per week for four weeks, and 5) BLM+MLN, in which MLN was given to mice (10 mg/kg, i.p.) 30 minutes prior to BLM injections for four weeks. MLN administration significantly reduced body weight loss ($P<0.05$), the rate of mortality, edema formation, lung injury, COX-2 expression ($P>0.05$), interstitial tissue percentage volume ($P<0.05$), and also increased the alveolar space percentage volume. MLN attenuated the BLM-induced lung injury responses such as collagen accumulation and airway dysfunction in mice. Finally, histological evidence supported the ability of MLN to inhibit COX-2 expression. Thus, it may serve as a novel potential therapeutic agent for IPF.

Pulmonary fibrosis is a condition which is characterized by the aggregation of collagen in the extracellular matrix, proliferation and migration of fibroblasts, and alveolar number declining capable of gas exchanging in the lung. The most common and fatal condition subtype of pulmonary fibrosis is called IPF with a median survival of 3-5 years following diagnosis (1). It is a chronic, progressive, irreversible, and usually lethal lung disease with unknown cause. The worldwide incidence of IPF is estimated to be 10.7 cases per 100,000 and 7.4 cases per 100,000 of persons per year for males and females, respectively (2). Unfortunately, the pharmacologic therapy for IPF is limited and there are no effective treatments currently available (3). A large body of evidence suggested that injury to the alveolar epithelium is generated following a burst of pro-inflammatory and fibroproliferative

Key words: melatonin, pulmonary fibrosis, cyclooxygenase 2, bleomycin

Mailing address: Dr. Salar Bakhtiyari, PhD
Department of Clinical Biochemistry,
Faculty of Medicine,
Ilam University of Medical Sciences,
Ilam, I.R. Iran
Tel/Fax: +98 84 32235745;
e-mail: bakhtiyaribio@gmail.com

0393-974X (2015)

mediators associated with normal tissue repair (4, 5). The prostanoid generating enzyme, COX-1 has a constitutive expression in most cells and tissues, whereas COX-2 is expressed only when induced by inflammatory or mitogenic stimuli. One of these prostanoids, i.e. prostaglandin E2 (PGE2), is a major inflammatory mediator, which is derived from endogenous arachidonic acid by COX-1 and COX-2 enzymes (6, 7). It plays important roles in the pulmonary reparative processes via modulating inflammation. Moreover, in IPF, the levels of PGE2 and COX-2 in cultured fibroblasts have been shown to be reduced (8). The limited capacity of fibroblasts to up-regulate PGE2 synthesis has been shown to be due to decreased expression of COX-2 in fibroblasts derived from IPF patients (8-10).

Bleomycin (BLM) is a chemotherapeutic drug used clinically for a variety of human malignancies. Unfortunately, BLM induces pulmonary inflammation through the production of reactive oxygen species (ROS), which eventually progresses to fibrosis. BLM-induced lung fibrosis is a widely used animal model resembling human IPF (11). In response to ROS, resident lung cells release inflammatory mediators and cytokines into the surroundings, induce recruitment of neutrophils, and eventually increase the expression of inducible enzymes such as COX-2 which stimulates the production of large amounts of pro-inflammatory mediators (12, 13). It has been reported that in BLM-induced animal model of pulmonary fibrosis, the inhibitor of cyclooxygenase, such as indomethacin, reduced pulmonary fibrosis (14).

Melatonin (MLN) has a variety of anti-inflammatory, antioxidant, and immunoregulatory effects when it is applied exogenously under both *in vivo* and *in vitro* conditions (15). It has been demonstrated that MLN inhibits the expression of the COX genes and restricts the excessive production of prostanoids, and as well as other mediators of the inflammatory responses (16-21). Considering the strong antioxidant and anti-inflammatory properties of MLN, we conducted this study to better understand its preventive roles and its effect on COX-2 expression in pulmonary fibrosis mouse model. To this end, the MLN deterrent effect on fibrosis development and progression by employing histochemical and morphometric methods was examined. Then, we performed immunohistochemical staining for special COX-2 to evaluate the effect of MLN on its expression.

MATERIALS AND METHODS

Animals

Male C57BL/6 mice (25-30 g), obtained from the Pasteur Institute of Iran, was housed in standard laboratory cages and a 12-h light/dark cycle was maintained while mice had access to water and rodent laboratory chow *ad libitum*. Experiments were carried out according to the ethical guidelines for the care and use of laboratory animals.

Animal model of bleomycin induced lung fibrosis

After recording their weight, the animals were divided into five groups: 1) saline control group; 2) 1% ethanol control group; 3) MLN control group; 4) BLM group, in which mice were injected with BLM (15 mg/kg, i.p.) twice per week for 4 weeks; (5) BLM+MLN group, in which MLN was given to mice (10 mg/kg, i.p.) 30 min prior to BLM injections for 4 weeks.

Preparation of lung tissue

Thirty days after the end of treatment, mice were anesthetized and sacrificed. Through median incision, the thorax of the mice was opened and a small portion of both lungs was cut out and used for histopathological analysis.

Histopathological observation

For preparation of paraffin-embedded samples, pulmonary tissue was fixed using 10% neutral formalin solution and sectioned at approximately 4-6 μm of thickness. The prepared sections were stained with hematoxylin-eosin to analysise routine histology parameters and Masson's trichrome for evaluation of collagen deposition. The slides were examined by light microscopy and photographed.

Immunohistochemical analysis for COX-2

COX-2 immunohistochemistry was performed using a COX detection kit (Abcam, USA) according to the manufacturer's instructions. Tissue samples were embedded in paraffin, sectioned (4-6 μm), deparaffinized in xylene, and then were rehydrated in graded ethanol solutions. The slides were then blocked with 5% BSA (bovine serum albumin) in TBS (Tris-buffered saline) for 2 hours. The sections were then immunostained with primary antibody (rabbit polyclonal IgG against mice COX-2) and incubated overnight at 4°C. After washing the slides with TBS, the sections were incubated with goat anti-rabbit secondary antibody. Sections were

then washed with TBS and incubated for 5-10 min in a solution of 0.02% diaminobenzidine containing 0.01% hydrogen peroxide. Counter staining was performed using hematoxylin, and the slides were visualized under a light microscope.

Counting the number of COX-2 positive cells in the surface unit

To assess cyclooxygenase protein expression, COX-2 positive cells were counted. These cells were characterized by brown cytoplasm. Here, in order to gain a better analysis, 10 serial sections were picked up from each group and the number of positive cells was counted in surface unit. Six µm slides were provided for each group, blocked, and stained based on the detailed immunohistochemical method (which was mentioned earlier). Then, sections were examined using optical microscope with magnification of 40x and graticule. After that, the number of COX-2 positive cells in the surface unit was counted and recorded for each section.

Estimating the percentage volume of alveolar space and interstitial tissue

Ten serial slides were selected from each group and using an optical microscope with magnification of 40x, the number of crossing points of graticule with alveolar space and interstitial tissue sections were counted. Scaled graticule contained 14 longitudinal lines and 14 cross-bar lines which had 196 crossing points in total. For example, in one of the sections, 156 and 40 crossing points for alveolar space and interstitial tissue were recorded, respectively. Finally, considering the graticule section surface and thickness of each section, the volume percentage of alveolar space and interstitial tissue was calculated. So, the total volume percentage was estimated based on summation of volume percentages (10 sections).

Statistical analysis

Data are presented as the means±standard deviation (SD). Multiple comparisons were carried out using one-way analysis of variance (ANOVA) followed by Tukey's post hoc test. Statistical significance was acceptable to a level of $p<0.05$.

RESULTS

Mortality

One-month after BLM and MLN injection, experimental groups were evaluated carefully and the mortality rate was recorded. Our results showed that 5 mice from a total 10 mice belonging to the BLM group had survived (50% of mortality), while for the BLM+MLN group, only 3 mice were dead. Our results suggest that adding MLN reduces the mortality rate from 50% to 30%.

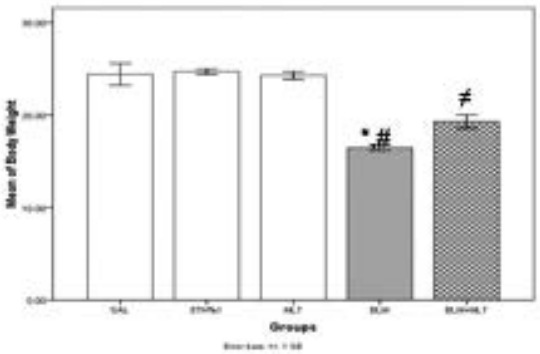

Fig. 1. *Body weight in different groups. Data are presented as the mean ± SD. *, P<0.01 vs control. #, P<0.05 vs BLM+MLN. ≠, P<0.02 vs control.*

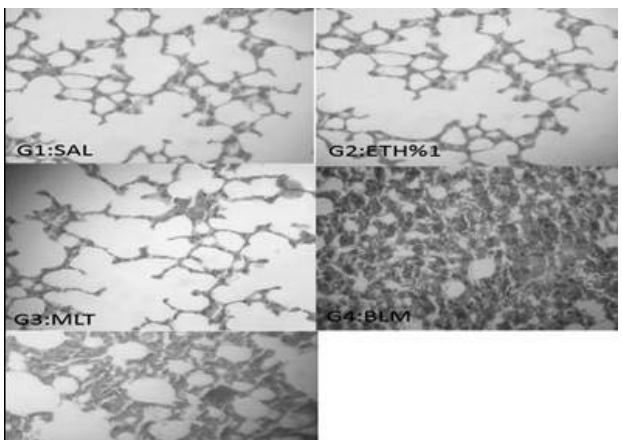

Fig. 2. *Histological analysis of lung tissue after H&E staining: Normal control mice showing alveolar spaces and alveolar septum. (G4) BLM-treated mice showing collapsed and narrower alveolar spaces. The pulmonary interstitium is markedly infiltrated with inflammatory cells, leading to thickening of the interalveolar septa (arrow). (G5) MLN plus BLM-treated mice lung showing more patent alveolar spaces and reduced interstitial infiltrations and these features were less severe.*

Weight changes

As shown in Fig. 1, results indicated that the average weight of the BLM-treated group is significantly ($P<0.05$) lower than the control groups (saline, ethanol %1, MLN). By comparing BLM

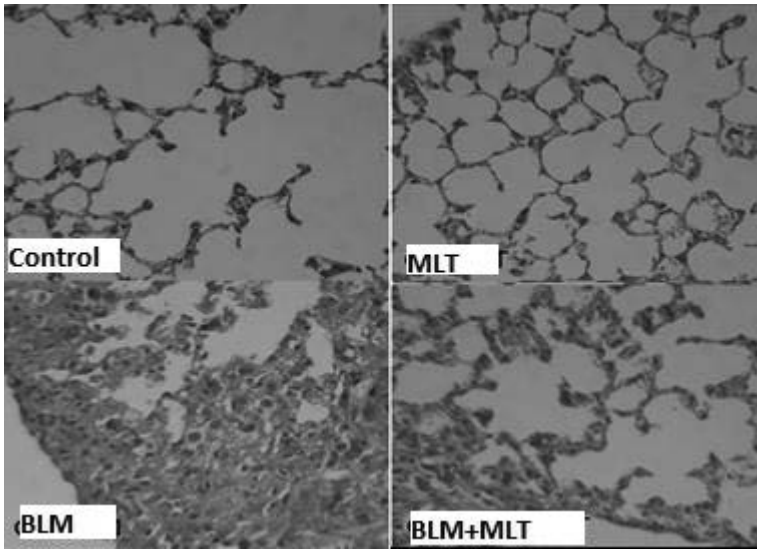

Fig. 3. *Histological analysis of lung tissue (Masson trichrome). Control and MLT-treated mice showing the distribution of pulmonary interstitial reticulin indicated by thin layer. BLM-treated mice showing the excessive collagen deposition in the interstitial lung tissue (thick dark region). MLN plus BLM-treated mice lung showing marked reduction of interstitial deposition of collagen.*

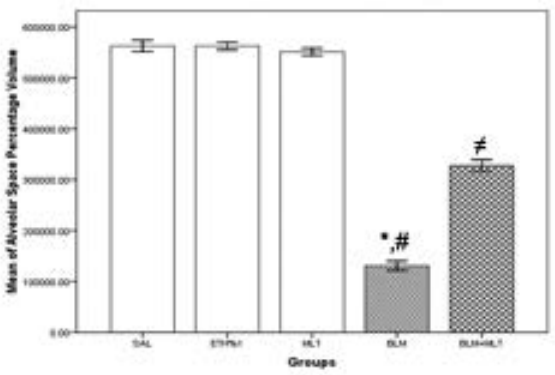

Fig. 4. *Mean of alveolar space percentage volume in different groups. Data are presented as the mean ± SD. *, P<0.001 vs control. #, P<0.01 vs BLM+MLN. ≠, P<0.01 vs control.*

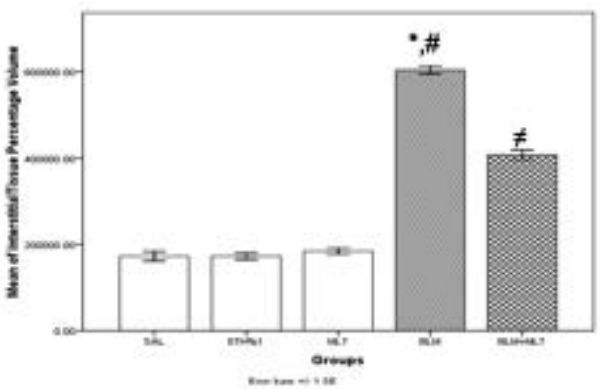

Fig. 5. *Mean of interstitial tissue percentage volume in different groups. Data are presented as the mean ± SD. *, P<0.001 vs control. #, P<0.01 vs BLM+MLN. ≠, P<0.01 vs control.*

and BLM+MLN groups, we observed that the group treated with MLN experienced less weight reduction.

Morphological assessments of pulmonary tissue

Morphological assessments of control mice lung showed the normal characterization of pulmonary alveolar spaces and also septal alveolar thicknesses. The collagen amount and its distribution in the sections stained by Masson trichrome method revealed that around the alveoli, the reticulin distribution was normal. In contrast, the lungs belonging to the BLM-treated mice demonstrated evident collapsed alveoli, obvious interalveolar septal thickening, and densely interstitial infiltration of inflammatory and non-inflammatory cells including lymphocytes, neutrophils, and fibroblasts (Fig. 2).

Moreover, excessive amounts of collagen deposition were detectable around the alveoli. On the other hand, BLM+MLN-treated mice demonstrated outstanding suppression of the BLM-induced inflammatory-related cellular infiltration as evidenced by a reduction in the interalveolar septal thickening and more inflation of the alveoli. Furthermore, the amount of deposited collagen in the alveolar septa was notably reduced in comparison with the BLM-treated lungs (Fig. 3). These protective effects were shown by the significant reduction in the collagen fiber content in the pulmonary of the tissue sections. MLN treatment markedly alleviated the degree of lung fibrosis indicated by decreased collagen deposition and lowered inflammation.

Percentage of alveolar space in volume unit

The results showed a significant difference between the BLM group and all the other groups in terms of alveolar space percentages in volume unit ($P<0.05$). A comparison of alveolar space percentages indicated that MLN had a strong chemo-preventive effect on the further collapsing of the alveolar spaces (Fig. 4).

Percentage of interstitial tissue in volume unit

The average of interstitial tissue in volume unit for BLM group, compared with other experimental groups, indicated a significant increase ($P<0.05$) (Fig. 5).

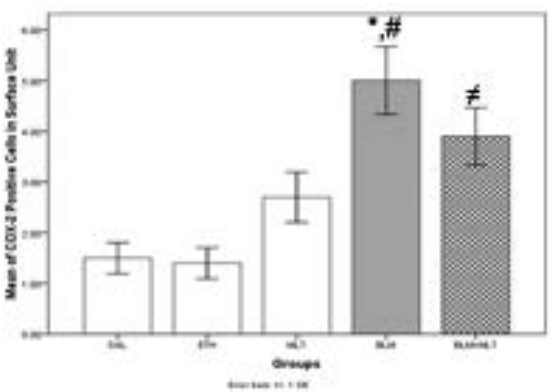

Fig. 6. *Mean of COX-2 positive cells in surface unit in different groups. Data are presented as the mean ± SD. *, P<0.001 vs control. #, P<0.01 vs BLM+MLN. ≠, P<0.01 vs control.*

Table I. *Effects of MLT on COX-2 expression in BLM-induced fibrosis.*

Groups	Number of COX-2 positive cells
BLM	50
SAL	15
BLM+MLT	39
MLT	27
ETH	14
P value between groups	<0.05

Effects of melatonin on COX-2 expression

As shown in Table I, compared with the normal group, the expression of COX-2 in the BLM group (positive cells and the degree of staining) was enhanced significantly ($P<0.05$). The expression of COX-2 was significantly decreased in the BLM+MLT group ($P<0.05$) (Fig. 6). Our results showed that there was a significant difference in COX-2 expression between the BLM and BLM+MLN groups and control groups ($p<0.05$). Furthermore, we found that treatment with melatonin significantly ($P>0.05$) reduced the COX-2 expression in the BLM+MLN group, as compared with that of the BLM group.

DISCUSSION

Pulmonary fibrosis is a respiratory disease that may result from the administration of bleomycin sulfate, an anti-neoplastic agent that can cause this disease as a side effect during the treatment period of patients. This toxic effect has been used in experimental models of animals, but the underlying mechanism involved in the induction of the disease is not clearly understood (22). The results of the present study show the anti-inflammatory, anti-oxidant and immunomudolatory effects of MLN in a 30-day treatment period and improvement in the survival of mice with acute lung injury after BLM administration. A murine model of BLM-induced pulmonary fibrosis was applied to determine the ability of MLN to: 1) inhibit lung inflammation; 2) reduce pulmonary fibrosis; 3) reduce lung architecture destruction and its effects on COX-2 expression. First, the capability of MLN to inhibit pulmonary fibrosis was scrutinized using

histological examination and measurement of alveolar and interstitial percentages in volume unit. It was found that administration of MLN (10 mg/kg, i.p) 30 minutes prior to BLM injections (for 4 weeks until the end of the treatment) could mitigate the progression of pulmonary fibrosis. As shown in previous studies, our results proved the inhibitory and preventive role of MLN on fibrosis. In terms of mortality, the number of surviving mice in the BLM- and also BLM+MLT-treated groups indicated that MLN reducesd it to 30%. Also, the average weight difference between the illness group and other groups (control and treatment groups) was significant, therefore MLN had impeded weight loss in the MLN-treated groups. A comparison between percentage volume of alveolar space and interstitial volume percentage showed that alveolar space had been remarkably decreased and consequently, interstitial percentage was increased in the illness group, while MLN prevented such severe changes in the BLM+MLT-treated group; therefore, the difference between volume percentage of alveolar space and interstitial in control and illness groups and even illness and treatment groups is significant. After evaluation of stained pulmonary tissue sections using H&E and Masson's trichrome method in different experimental groups, the results revealed the increasing number of collapsed alveoli, notable thickening of the inter-alveolar septa, and densely interstitial infiltration of inflammation promoting cells, particularly T-cells, neutrophils, and fibroblasts, in the lungs of the BLM-treated mice. In addition, there was an intense collagen deposition around the alveoli, as manifested by Masson's trichrome staining. On the other hand, BLM+MLT-treated mice showed a marked reduction in the trafficking of the BLM-induced inflammatory cellular infiltrations as evidenced by reducing thicknesses of the inter-alveolar septa and dampening of the alveolar inflation. Furthermore, the amount of collagen deposited in the alveolar septa was markedly reduced in comparison with lungs belonging to the BLM-treated mice. Furthermore, the effect of MLN on COX-2 expression was investigated. Previous studies have shown that MLN acts through multiple mechanisms including radical scavenging, inhibition of prostaglandin production, inhibition of lipoxygenease, and protection against cell membrane damage (21, 23). In the present study, it was found that BLM caused destruction of the lung architecture characterized by focal area of fibrosis with collapse of air alveoli and emphysematous and associated with a significant increase in parenchymal collagen content compared to the control groups. Co-treatment of animals with MLN significantly reduced the collapse of air alveoli in lung tissue and ameliorated the lung fibrosis induced by BLM. These results support the potential anti-fibrotic effect of MLT similar to other antioxidants. The expression of COX-2 was further assessed by immunohistochemical detection. In agreement with previous studies, BLM induced COX-2 expression in lungs (13). Co-treatment of animals with BLM and MLN significantly reduced COX-2 expression. The effect of MLN seems to be mediated mainly by the inhibition of COX-2 and 5-lipogenase enzyme (20). However, it is acceptable that COX-2 enzyme produces anti-fibrogenic agent PGE2 but it also generates fibrogenic factors such as Prostaglandin F2α (24). On the other hand, COX-2 generates the precursor molecules to produce leukotriene fibrogenic factors. Actually, it seems that the beneficial effects of MLN may also be mediated through inhibition of leukotriene synthesis as pulmonary fibrosis protection occurs in leukotriene-deficient mice (25). Anatomical, physiological and pharmacological evidence supports the existence of bilateral interactions between the neuroendocrine and immune systems. In this context, MLN plays an important role as a modulator of producing a great number of immunological molecules involved in pulmonary fibrosis. In conclusion, MLN attenuates the BLM-induced injury response in mice, such as collagen accumulation, airway dysfunction and injury. Finally, histological evidence supported the ability of MLN to inhibit COX-2 expression. The findings of the present study provide evidence that MLN may serve as a target for potential therapeutic approaches of pulmonary fibrosis.

ACKNOWLEDGEMENTS

This paper was extracted from the M.Sc**.** thesis. Deputy for research and technology of Ilam University of Medical Sciences, Iran (grant 901014/65) supported this project financially.

REFERENCES

1. Datta A, Scotton CJ, Chambers RC. Novel therapeutic

approaches for pulmonary fibrosis. Br J Pharmacol 2011; 163:141-72.
2. Harari S, Caminati A. IPF: new insight on pathogenesis and treatment. Allergy 2010; 65:537-53.
3. Baumgartner KB, Samet JM, Coultas DB, Stidley CA, Hunt WC, Colby TV, Waldron JA, Centers C. Occupational and environmental risk factors for idiopathic pulmonary fibrosis: a multicenter case-control study. Am J Epidemiol 2000; 152:307-15.
4. Meltzer EB, Noble PW. Idiopathic pulmonary fibrosis. Orphanet J Rare Dis 2008; 3:8.
5. Kinnula VL, Fattman CL, Tan RJ, Oury TD. Oxidative stress in pulmonary fibrosis: a possible role for redox modulatory therapy. Am J Respir Crit Care Med 2005; 172:417-22.
6. FitzGerald GA. COX-2 and beyond: approaches to prostaglandin inhibition in human disease. Nat Rev Drug Disco 2003; 2:879-90.
7. Chenevard R, Hürlimann D, Béchir M, Enseleit F, Spieker L, Hermann M, Riesen W, Gay S, Gay RE, Neidhart M. Selective COX-2 inhibition improves endothelial function in coronary artery disease. Circulation 2003; 107:405-9.
8. Wilborn J, Crofford L, Burdick M, Kunkel S, Strieter R, Peters-Golden M. Cultured lung fibroblasts isolated from patients with idiopathic pulmonary fibrosis have a diminished capacity to synthesize prostaglandin E2 and to express cyclooxygenase-2. J Clin Invest 1995; 95:1861.
9. Huang SK, Peters-Golden M. Eicosanoid lipid mediators in fibrotic lung diseasesready for prime time? CHEST J 2008; 133:1442-50.
10. Mason RJ, Schwarz MI, Hunninghake GW, Musson RA. Pharmacological therapy for idiopathic pulmonary fibrosis: past, present, and future. Am J Respir Crit Care Med 1999; 160:1771-77.
11. Mouratis MA, Aidinis V. Modeling pulmonary fibrosis with bleomycin. Curr Opin Pulm Med 2011; 17:355-61.
12. El-Demerdash E. Anti-inflammatory and antifibrotic effects of methyl palmitate. Toxicol appl pharmacol 2011; 254:238-44.
13. Kalayarasan S, Sriram N, Sudhandiran G. Diallyl sulfide attenuates bleomycin-induced pulmonary fibrosis: Critical role of iNOS, NF-κB, TNF-α and IL-1β. Life Sci 2008; 82:1142-53.
14. Thrall R, McCormick J, Jack R, McReynolds R, Ward P. Bleomycin-induced pulmonary fibrosis in the rat: inhibition by indomethacin. Am J Pathol 1979; 95:117.
15. Ambriz-Tututi M, Rocha-González HI, Cruz SL, Granados-Soto V. Melatonin: a hormone that modulates pain. Life Sci 2009, 84(15):489-98.
16. Cutando A, Gómez-Moreno G, Arana C, Acuña-Castroviejo D, Reiter RJ. Melatonin: potential functions in the oral cavity. J Periodontol 2007; 78:1094-102.
17. Mauriz JL, Collado PS, Veneroso C, Reiter RJ, González-Gallego J. A review of the molecular aspects of melatonin's anti-inflammatory actions: recent insights and new perspectives. J Pineal Res 2013, 54:1-14.
18. Kannen V, Marini T, Zanette DL, Frajacomo FT, Silva GE, Silva Jr WA, Garcia SB. The melatonin action on stromal stem cells within pericryptal area in colon cancer model under constant light. Biochem Biophys Res Commun 2011; 405:593-98.
19. Dong W-G, Mei Q, Yu J-P, Xu J-M, Xiang L, Xu Y. Effects of melatonin on the expression of iNOS and COX-2 in rat models of colitis. World J Gastroenterol 2003; 9:1307-11.
20. Wang J, Xiao X, Zhang Y, Shi D, Chen W, Fu L, Liu L, Xie F, Kang T, Huang W. Simultaneous modulation of COX-2, p300, Akt, and Apaf-1 signaling by melatonin to inhibit proliferation and induce apoptosis in breast cancer cells. J Pineal Res 2012; 53:77-90.
21. Korkmaz A, Reiter RJ, Topal T, Manchester LC, Oter S, Tan DX. Melatonin: an established antioxidant worthy of use in clinical trials. Mol Med 2009; 15:43-50.
22. Yacoubi L, Rabaoui L, Hamdaoui MH, Fattouch S, Serairi R, Kourda N, Khamsa SB. Anti-oxidative and anti-inflammatory effects of Trigonella foenum-graecum Linnaeus, 1753 (Fenugreek) seed extract in experimental pulmonary fibrosis. J Med Plants Res 2011; 5:4315-25.
23. Genovese T, Paola RD, Mazzon E, Muià C, Caputi AP, Cuzzocrea S. Melatonin limits lung injury in bleomycin treated mice. J Pineal Res 2005; 39:105-12.

24. Oga T, Matsuoka T, Yao C, Nonomura K, Kitaoka S, Sakata D, Kita Y, Tanizawa K, Taguchi Y, Chin K. Prostaglandin F2α receptor signaling facilitates bleomycin-induced pulmonary fibrosis independently of transforming growth factor-β. Nat Med 2009; 15:1426-30.
25. Peters-Golden M, Bailie M, Marshall T, Wilke C, Phan SH, Toews GB, Moore BB. Protection from pulmonary fibrosis in leukotriene-deficient mice. Am J Respir Crit Care Med 2002; 165:229-35.

THE EFFECT OF DIHYDROARTEMISININ ON THE PROLIFERATION, METASTASIS AND APOPTOSIS OF HUMAN OSTEOSARCOMA CELLS AND ITS MECHANISM

W. LIU, D.W. WANG, S.Y. YU, Y. CAO, L. YANG, X.Q. E, G.J. YAO and Z.G. BI

Department of Orthopaedics, the First Affiliated Hospital of Harbin Medical University, Harbin, China

Received January 16, 2015 – Accepted April 24, 2015

This study aims to research the effect of dihydroartemisinin on the proliferation, metastasis and apoptosis in human osteosarcoma cells 143B and the underlying mechanism. This study designed five groups for experiment and control, using dimethylsulfoxide (DMSO), and docosahexaenoic acid (DHA) at concentrations of 15, 25, 35 μmol.L^{-1} respectively. Experiments including methyl thiazolyl tetrazolium (MTT) assay, clone formation assay, Hoechst 33258 staining assay, luciferase reporter plasmid assay, Western blot and scratch test were carried out. In addition, SPSS 18.0 software from IBM was used for statistical analysis and all the data obtained from the experiments were expressed as mean ± SD, and variance was used to compare the difference between the groups. DHA is proved to be able to inhibit the proliferation and metastasis of osteosarcoma cells, as well as leaving a positive effect on apoptosis in the cytomorphosis. It achieves regulation over the human osteosarcoma cells by keeping the expression of related protein under control.

Osteosarcoma originating from the mesenchyme with osteogenic potential results from neoplastic osteoid tissue or immature bone produced by osteosarcoma cells, which is characterized by a high level of malignancy and a high probability of pulmonary metastasis occurring at an early stage (1). The development of neoadjuvant chemotherapy and limb salvage has improved the five-year survival rate to 65%~75%, while there is still 40% death rate resulting from pulmonary metastasis (2). Artemisinin and its derivatives, a malarial drug featuring a rapid and sound curative effect and low toxicity is effective for malaria, especially pernicious malaria and cerebral malaria that are resistant to chloroquine or other drugs; therefore, it is widely used (3). Dihydroartemisinin (DHA) with high anti-malarial activity and strong water solubility is one of the important derivatives of artemisinin, which has a molecular formula of $C_{15}H_{24}O_5$ and a molecular weight of 284.35. It is found that besides anti-malarial activity, DHA also has anti-inflammation, immune regulation, scar proliferation inhibition and anti-tumor effect. Especially in its anti-tumor aspect, it is active in resisting tumor but leaves little toxicity on normal tissue cells.

In the study by Zhan Xiaolong et al. (4), it was found that DHA could effectively inhibit transplanted tumor in nude mice with colorectal cancer. Compared with other derivatives, DHA possesses merits such as quick absorption, short response time, wide distribution within the body and quick excretion and metabolism. Currently there are a great number of studies on

Key words: dihydroartemisinin, osteosarcoma, cell proliferation, metastasis, apoptosis

Mailing address: Dr Zhenggang Bi,
Department of Orthopaedics, the First Affiliated Hospital of Harbin Medical University,
23, Post Street, Nangang District, Harbin, Heilongjiang, 150001, China
Tel./Fax: +86 451 85555485/+86 451 85555125
e-mail: bzg@ibhsedu.com

0393-974X (2015)

protein related to the proliferation and metastasis of osteosarcoma cells. Song Guohui, et al. (5) explored the effect of SCUBE3 on osteosarcoma cell growth and its association with prognosis. An increased expression of SCUBE3 protein in osteosarcoma cells and tissue was found, which promote the growth of osteosarcoma cells by transforming the cell cycle. Based on the study on the effect of expression of RanBP9 on the proliferation, apoptosis and metastasis of osteosarcoma cells, Zhang Xi, et al. (6) found that RanBP9 expressed high in osteosarcoma cell; the expression of RanBP9 had influence on the biological functions of osteosarcoma cells, down regulation of which was able to strengthen proliferation and metastasis of osteosarcoma cells and reduce apoptosis rate.

Starting from the effect of DHA on human osteosarcoma cells, this paper discusses the effect of DHA on the proliferation, metastasis and apoptosis of osteosarcoma cells, and further analyzed the function mechanism of DHA.

MATERIALS AND METHODS

Experimental materials

Human osteosarcoma cells were bought from American Type Culture Collection (ATCC). Cells were cultured in the sterile thermostat incubator at 5% CO_2 and 37°C containing 10% fetal bovine serum (FBS) and 1% penicillin or streptomycin (P/S). Also, in this experiment, methyl thiazolyl tetrazolium (MTT), dimethylsulfoxide (DMSO) and Trypsin/Ethylene Diamine Tetraacetic Acid (EDTA) solution were from Sigma in USA. DHA was bought from Sichuan Sanqi Pharmaceutical Co., Ltd, China, which was dissolved by DMSO to prepare 70mmol/L liquid medicine. DMEM medium, FBS and P/S were all bought from Thermo Scientific in USA, and Hoechst 33258(C1011) was from Beyotime, China; Trypsin/EDTA solution (R-001-100) from Cascade Biologics, USA. The mouse monoclonal antibody VEGF (C-1) (Art. No. sc-7269), goat polyclonal antibody MMP-9 (C-20) (Art. No. Sc-6840) and mouse monoclonal antibody β Actin (Art. No. sc -47758) were all from Santa Cruz Biotechnology Co., Ltd., China.

Experimental methods

Five groups were established, including Control (blank control), DMSO (solvent control), and DHA at concentrations of 15, 25, 35μmol.L^{-1} respectively.

MTT assay

Monolayer adherent cells in the logarithmic phase were digested by 0.25% trypsin and then dried to single cells for preparing the cellular suspension at a concentration of 5×10^6 / L. A quantity of 100 μL cellular suspension was added into each well of a 96-well plate; when cells were adhered, they were processed according to the scheduled grouping (every group was octuplicated). Four hours before processing, 0.02 ml MTT (5 g·L) was added into each well. Absorbance was detected at the wavelength of 492 nm four hours later, and the figure of cell survival was plotted. This experiment was repeated three times.

Clone formation assay

Monolayer adherent cells in the logarithmic phase were digested by 0.25% trypsin and then dried to single cells for preparing the cellular suspension at a concentration of 150/mL. A quantity of 1 ml cellular suspension was added into each well of a 6-well plate. When cells were adhered, they were processed according to the scheduled grouping. Cells were placed into an environment at 37°C with 5% CO_2 and saturation humidity for cultivation for 10 days. Cells were washed with PBS twice after the supernate was removed. Then the cells were fixed in stationary liquid (acetic acid/methyl alcohol 1:3). Fifteen minutes later, cells were stained by crystal violet for 30 min. After the staining fluid was removed by running water, cells were dried. Next, cell clone formation was observed. Under the microscope (low power lens), clone of more than 10 cells were counted and then the clone formation rate was calculated. Rate of clone formation/%= the number of clones/ the number of inoculated cells ×100%.

Hoechst 33258 staining

Monolayer adherent cells in the logarithmic phase were digested by 0.25% trypsin and then dried to single cells for preparing the cellular suspension at a concentration of 5×10^7/L. A quantity of 1 ml cellular suspension was added to each well of a 24-well plate. When cells were adhered, they were processed according to the scheduled grouping. After processing, Hoechst 33258 solution (1g/L) was added and then the cells were dissolved for 7 min at 37°C and cooled over ice. Then the staining liquid was removed. Next, the cells were resuspended in PBS. The blue fluorescence was observed under 450 um ultraviolet. Normal cells and necrotic cells presented weak blue while apoptotic cells presented highlight blue, with karyopyknosis. This experiment was repeated three times.

Luciferase reporter plasmid assay

Cells in the logarithmic phase were spread onto a 24-well plate. When cells had adhered, Lipofectamine2000 was used to transfect 0.3 μg reporter plasmid; five hours later, the transfection was stopped and the plasmid was

placed on normal medium; then cells were processed based on grouping. Cells were lysed 24 h later and then luciferase activity determination was performed according to the instructions on the kit; next, the total protein concentration in lysate was detected and the activity of luciferase was corrected by BCA method. This experiment was repeated three times. The average value was taken as the final result.

Western blot

After human 143B cells were processed with DHA for 24 h, Western blot cell lysate was used according to the instructions and then the protein samples were collected. The correct amount of condensed protein buffer solution was added. The liquid was placed in boiling water for 10 min to achieve a full protein denaturation. Finally, SDS-PAGE was performed. This experiment was repeated three times.

Scratch test

143B cells in a good growth state were spread onto a 6-well plate, with a density of 5×10^5/L (1000 μL in each well) for cultivation for 6~8 h; when the cells had adhered, "#" was marked on them by gel pen and then they were rinsed with PBS. They were photographed at 0 h, 6 h, 12 h, and 24 h after adding DHA in different concentrations. This experiment was repeated three times.

Statistical analysis

SPSS 18.0 of IBM was used for statistical analysis and all data obtained from the experiments were expressed as Mean ± SD; differences among the groups were analyzed by variance.

RESULTS

DHA can inhibit the proliferation of osteosarcoma cell 143 B

In vitro cultured human osteosarcoma cell lines (MG63, U20S, 143B and Saos2) with different grades of malignancy were all found to be sensitive to DHA after being processed by DHA for 24 h and 48 h, as shown in Fig. 1. 143B was taken for the subsequent experiment as it showed the highest sensitivity to DHA.

MTT method was used to detect the survival rate of cells after DHA acted on 143B cells for 24 h. The results are shown in Fig. 2. Compared to the control group, the proliferation rate of the cells in the experimental group remarkably decreased. The inhibition effect became more obvious as the concentration increased. As shown in Fig. 1, the inhibition effect on survival was most obvious when DHA concentration reached 35 μM. There was no statistically significant difference in toxic injury ($P>0.01$).

When DHA obviously inhibited the activity of 143B cell proliferation, it inhibited the ability of clone formation as well, as shown in Fig. 3. The rate of clone formation in these five groups was 0.607, 0.580, 0.453, 0.313 and 0.253 respectively.

In this study, the proliferating cell nuclear antigen (PCNA) was investigated. Western blot assay was performed after DHA acted on 143B human osteosarcoma cell for 24 h, as shown in Figs. 4 and 5. The expression of PCNA protein was found to be decreased; therefore it could not act as the accessory protein of DNA polymerase δ, restrain DNA synthesis nor inhibit the proliferation of 143B cell. Through detecting the expression of c-Myc and Cyclin D1, the main components of Wnt/β-catenin signaling pathway and the target gene that can promote proliferative activity, it was observed that, the expression of both remarkably decreased under the effect of DHA, especially when the concentration of DHA reached 40 μM; besides, the toxic effect was of no statistical significant difference ($P>0.1$).

DHA Induced the apoptosis of 143B human osteosarcoma cells

Hoechst33258 staining results of cell apoptosis are shown in Fig. 6. After DHA acting on 143B cells for 24 h, cells in the control group were observed to have complete form and consistent size of cell nucleus, and weak blue fluorescence showed even distribution and dispersion; compared to the control group, the experimental group was found to have cells with distinctly reduced nucleus, concentrated chromatin and uneven fluorescence, showing a state of apoptosis. The results above proved that, DHA was effective for inducing the apoptosis of 143B cells.

By detecting the members of Bcl-2 families closely associated to apoptosis, including Bcl-2, Bad, and the protein factor Caspase-3 performing apoptosis, the possible mechanism of DHA inducing cell apoptosis was further studied regarding the protein level (7). Results obtained from the Western blot assay are shown in Fig. 6. A down-

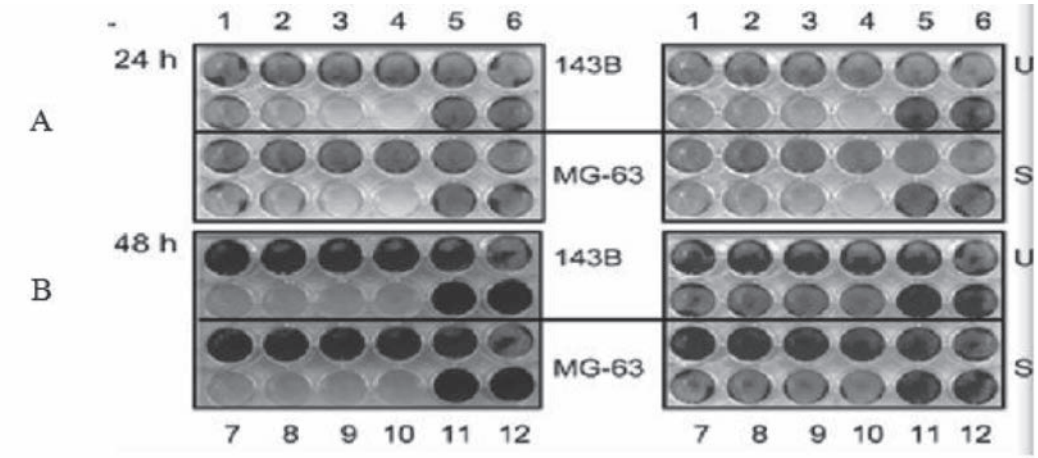

Fig. 1. *Living cells stained with crystal violet.* ***A****) staining results of human osteosarcoma cells (MG63, U20S, 143B and Saos2) processed for 24 h;* ***B****) staining results of human osteosarcoma cells (MG63, U20S, 143B and Saos2) processed for 48 h.*

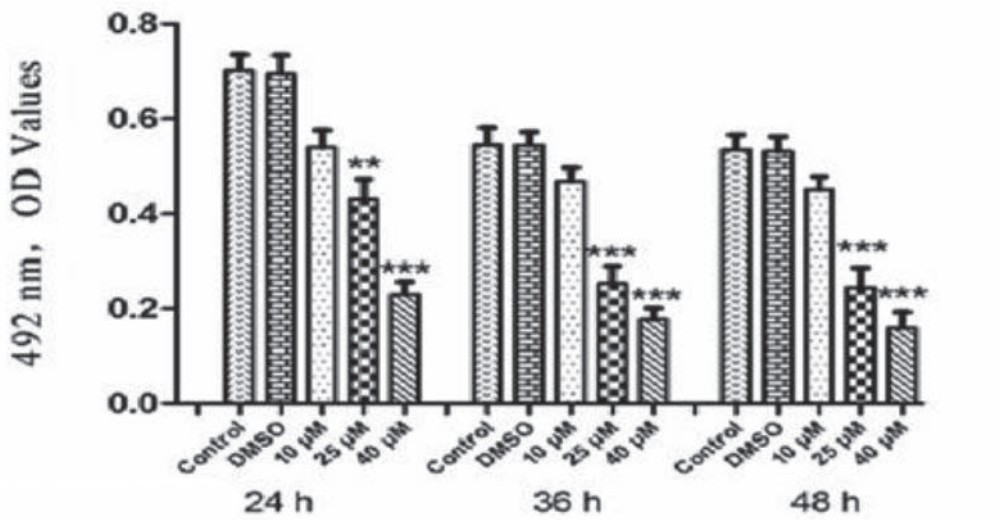

Fig. 2. *OD values of control, DMSO, 10 μM, 25 μM and 40 μM DHA group after the cells were processed for 24, 36 and 48 h.*

regulated expression of Bcl-2 and an up-regulated expression of Bad were found, which promoted the combination of Bad with Bcl-2 (8) and further inhibited the activity of the anti-apoptosis of Bcl-2. Meanwhile, the expression of Caspase-3 increased, which showed an enhanced function on promoting apoptosis. Therefore, the result of the Western blot suggested that DHA could effectively promote the apoptosis of 143B cells, which might be caused by a higher expression of Bad and Capase-3 protein and a lower activity of anti-apoptosis for Bcl-2 protein.

DHA inhibited the ability of metastasis of 143B human osteosarcoma cell (scratch test)

After DHA acted on 143B cells for 6 h, the ability of metastasis of 143B cells in the experimental group was observed to be restricted, as shown in Fig. 8. 12 or 24 h later, the effect was much more obvious, and the speed of cellular metastasis was quite slow in the experiment group, while the cells crossed the scratch test and recovered in the control group. From the above results, it was found that DHA could effectively inhibit the metastasis of 143B cells and

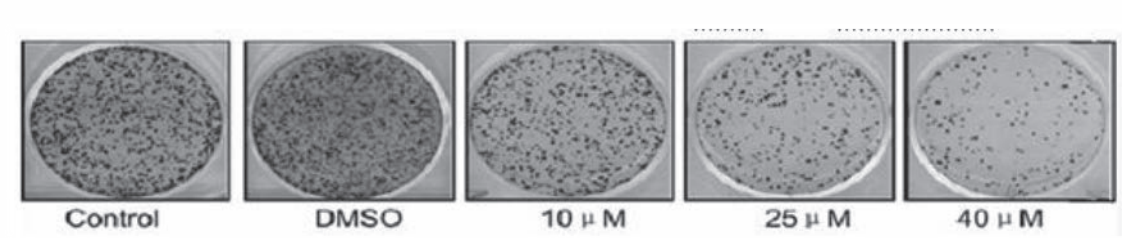

Fig. 3. *Colony formation of control, DMSO, 10 μM, 25 μM and 40 μM DHA group.*

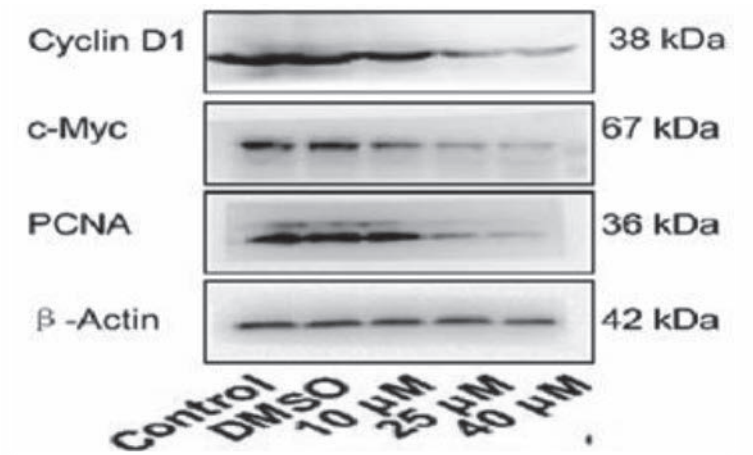

Fig. 4. *Western blotting detection of proliferation associated protein markers (expression of Cyclin D1, c-Myc, PCNA and β-Actin in control, DMSO, 10 μM, 25 μM and 40 μM DHA group, a qualitative analysis).*

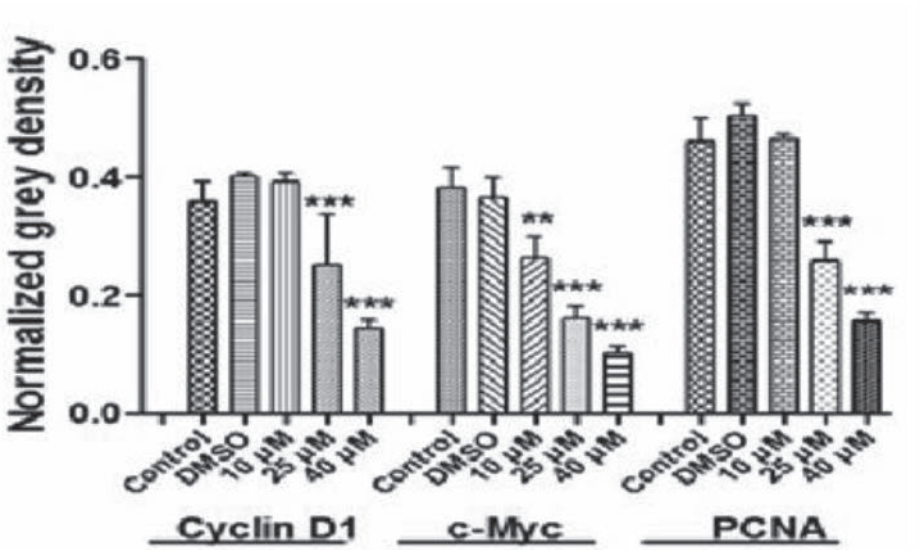

Fig. 5. *Western blotting detection of proliferation-associated protein markers (normalized grey density of expression of Cyclin D1, c-Myc and PCNA in control, DMSO, 10 μM, 25 μM and 40 μM DHA group, a quantitative analysis, by Image J software)*

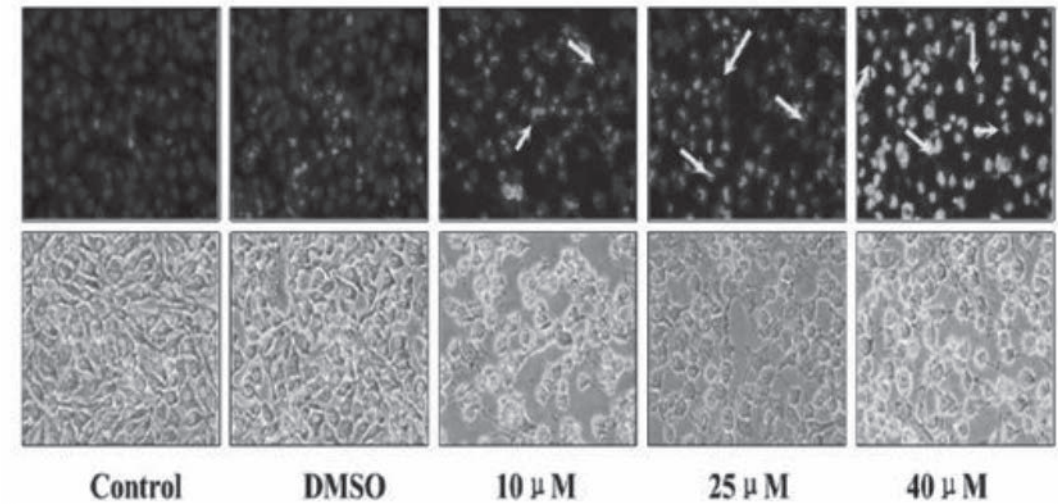

Fig. 6. *Hoechst 33258 staining of cell apoptosis in control, DMSO, 10 μM, 25 μM and 40 μM DHA group (top: fluorescent picture, bottom: non-fluorescent of same).*

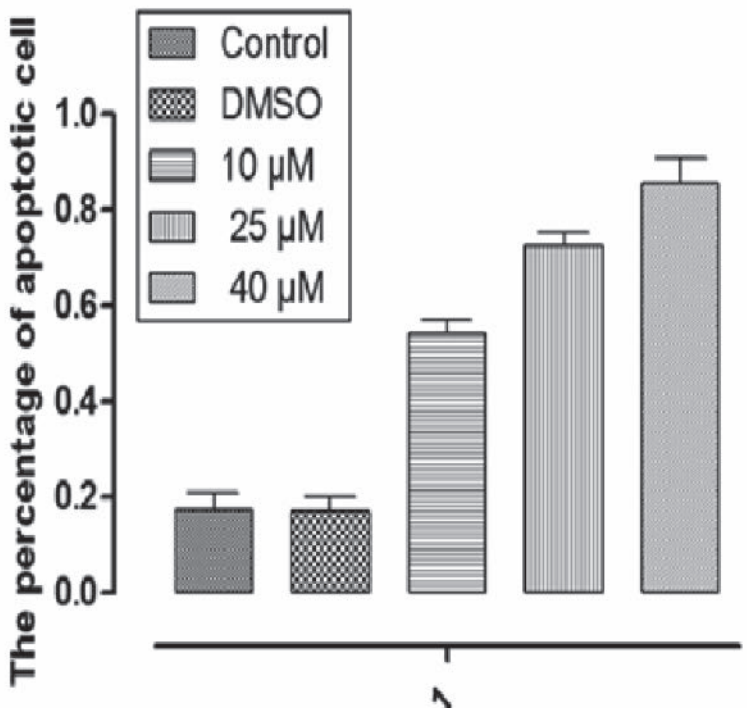

Fig. 7. *The percentage of apoptotic cell (cell count of control, DMSO, 10 μM, 25 μM and 40 μM DHA group, by Image J software).*

the effect became more obvious over time and with an increased concentration.

DISCUSSION

Artemisinin, an effective drug used for resisting malaria, is internationally considered as the front line antimalarials. Previous researches on artemisinin are mainly focused on chemcial structural modifications for efficient anti-malaria activity. To reduce the toxic and side effects, multiple chemical structural modifications have been performed to synthesize

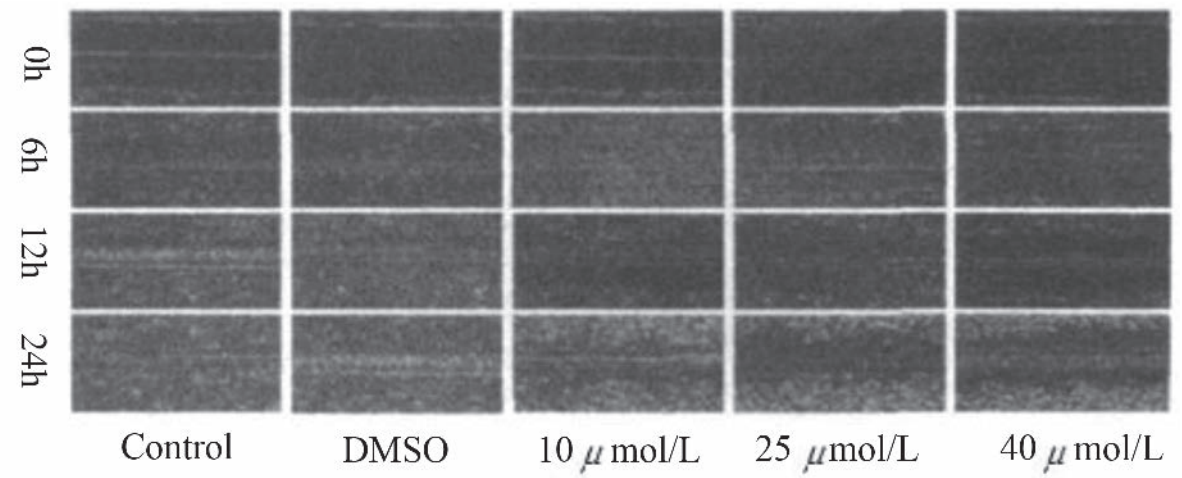

Fig. 8. *Detection of metastasis ability of 143B cells in scratch test (scratch test of control, DMSO, 10 μM, 25 μM and 40 μM DHA groups after cells were processed for 0 h, 6 h, 12 h and 24 h)*

various artemisinin derivatives, of which, DHA which has good water solubility and the least toxicity and side effects. Researches focusing on other biological activities of artemisinin and its derivatives were carried out in the last ten years and found that, artemisinin and its derivatives demonstrate high biological activity in the aspect of treating tumor and bilharziasis as well as improving immunity.

DHA is chemically synthesized by restoring artemisinin and modifying its carbon-12 atom (9); thus, it performs better than other derivatives of the same kind in the aspects of water solubility, cure rate, toxicity, side effects and anti-drug resistance. It possesses especially good effects in the treatment of drug-resistant cerebral malaria and pernicious malaria. Therefore it is widely applied for treating pernicious malaria and cerebral malaria that are resistant to chloroquine or multiple drugs and it is also considered as the first choice for malaria therapy by WHO. DHA has advantages over artemisinin in water solubility, absorption, toxicity and side effects. DHA also has an effect on anti-inflammation regulation, immunoregulation and scar hyperplasia besides specifically and efficiently treating malaria. It is widely appreciated for its strong effect in resisting tumors and its low toxicity on normal tissue cells.

Malignancy and the rate of metastasis of human osteosarcoma are both high. Early pulmonary metastasis is the major cause of death in patients with osteosarcoma, as well being difficult to treat. The incidence and development of osteosarcoma is a complex process with several steps, including changes in gene expression of various types and functions (10, 11). DHA has a high anti-tumor activity, inhibitng the proliferation of tumor cells, inducing the apoptosis of tumor cells, inhibiting the generation of new-born vessels, reversing the drug-resistant tumor cells, improving its ability to kill tumor cells by combining with transferrin and providing sensitization in traditional chemotherapy medicine. Compared with artemisinin, DHA has a high water-solubility and other merits, such as easier assimilation, quick and highly effective excretion and metabolism and less toxicity. It is found that except for its specific anti-malarial effect, DHA also has an anti-inflammatory, immune regulation, and anti-tumor effect, and it can also inhibit the proliferation of scars. Especially in the aspect of anti-tumor effect, it enjoys a high anti-tumor activity but produces little toxicity in normal tissue cells.

In this paper, DHA in different concentration was used to act on the 143B human osteosarcoma cells *in vitro*. Based on the MTT assay, it was found that DHA in different concentrations can inhibit the proliferation of 143B osteosarcoma cells and the rate of inhibition is associated with the concentration and action time

of DHA. When the concentration of DHA reached 35 $\mu mol \cdot L^{-1}$, there was an obvious effect in inhibiting proliferation 48 h later compared with the control group, and the difference was statistically significant ($p<0.01$). Besides, based on Hoechst 33258 staining, luciferase reporter plasmid assay, Western blot and scratch test, DHA can reduce the metastasis of 143B human osteosarcoma cell, compared with the control group; DHA can also effectively inhibit the expression of the relative protein, thereby further inhibiting the proliferation of osteosarcoma cells.

REFERENCES

1. Wu WM, Yang Y, Gao ZL, He WW, Zhao TC, Lin HP. Surgical treatment on osteosarcoma with pulmonary metastases and survival analysis. Chin Oncol 2012; 22(10):774 -78.
2. Rasalkar DD, Chu WCW, Lee V, Lee V, Paunipagar BK, Cheng FWT, Li CK. Pulmonary metastases in children with osteosarcoma: characteristics and impact on patient survival. Pedia Radiol 2011; 41(2):227-36.
3. Kong JQ, Wang W, Cheng KD, Zhu P. Research progresses in synthetic biology of artemisinin. Acta Pharmac Sinica 2013; 48(2):193-205.
4. Zhan XN, Huang Y, Wang L, Liang Z, Li Z. Antitumor effect and mechanism of dihydroartemisinin on colorectal cancer in nude mice with transplanted tumor of human colorectai cancer. Tradi Chin Drug Res Clin Pharmacol 201; 22(5):491- 94.
5. Song GH, Wang J, Lu JC, et al. Role of SCUBE3 in promoting osteosarcoma cell growth and its association with prognosis. J South Med Uni 2014; 34(5):617- 21.
6. Zhang X, Lv YF, Dai HZ, Meng G, Guo QN. Effect of RanBP9 expression on proliferation, apoptosis and metastasis in human osteosarcoma cells. Acta Academ Med Milit Tert 2014; 36(8):745-749.
7. Mou YQ, Zhou LY, Yang QJ, Zhou QX, He BC. Effect of ATRA on the growth of 143B osteosarcoma cells. Chin Pharmacol Bull 2011; 27(8):1091-5.
8. Mou YQ, Zhou LY, Yang QJ, et al. Effect of ATRA on the growth of 143B osteasarcoma cells. Chin Pharmacol Bull 2011; 27(8):1091-5.
9. Shen DD, Shen MM, Jian YX, Yang XC, Ha CY. Research review of dihydroartemisinin derivatives. Chemistry 2008; 71(9):659-63.
10. Strauss SJ, Ng T, Mendoza-Naranjo A, Whelan J, Sorensen PH. Understanding micrometastatic disease and Anoikis resistance in ewing family of tumors and osteosarcoma. Oncologist 2010; 15(6):627-35.
11. Sampo M, Koivikko M, Taskinen M, Kallio P, Kivioja A, Tarkkanen M, Böhling T. Incidence, epidemiology and treatment results of osteosarcoma in Finland - a nationwide population-based study. Acta Oncol 2011; 50(8):1206-14.

4(α-L-RHAMNOSYLOXY)-BENZYL ISOTHIOCYANATE, A BIOACTIVE PHYTOCHEMICAL THAT DEFENDS CEREBRAL TISSUE AND PREVENTS SEVERE DAMAGE INDUCED BY FOCAL ISCHEMIA/REPERFUSION

M. GALUPPO[1§], S. GIACOPPO[1§], R. IORI[2], G.R. DE NICOLA[2], D. MILARDI[1], P. BRAMANTI[1] and E. MAZZON[1]

[1]Experimental Neurology Laboratory, IRCCS Centro Neurolesi "Bonino-Pulejo", Messina, Italy; [2]Council for Agricultural Research and Analysis of Agricultural Economy, Research Centre for Industrial Cultivation (CRA-CIN), Bologna, Italy

Received December 22, 2014 – Accepted March 12, 2015

[§]These authors contributed equally to this work and share the first authorship

Natural compounds are a promising source to treat several pathologies. The present study shows the *in vivo* pharmacological beneficial effect of 4(α-L-rhamnosyloxy)-benzyl isothiocyanate (glucomoringin isothiocyanate; GMG-ITC) obtained from glucomoringin (GMG; 4(α-L-rhamnosyloxy)-benzyl glucosinolate), purified from *Moringa oleifera* seeds and hydrolyzed by myrosinase enzyme (β-thioglucoside glucohydrolase; E.C. 3.2.1.147). Cerebral ischemia/reperfusion (CIR) was induced in rats according to a classic model of carotid artery occlusion for a time period of 1 h and the reperfusion time was prolonged for seven days. GMG-ITC (3.5 mg GMG/ml plus 30 µl enzyme/rat; one ml i.p./rat) was administered 15 min after the beginning of ischemia and daily. The results clearly show that GMG-ITC possesses the capability to counteract the CIR-induced damage reducing TNF-alpha release, IκB-alpha cytosolic degradation/NFκBp65 nuclear translocation, as well as several other direct or indirect markers of inflammation (phospho-ERK p42/44, p-selectin) and oxidative stress (inducible Nitric Oxide Synthase (iNOS), MMP-9). GMG-ITC was shown to exert neuroprotective properties in preventing CIR-induced damage and the related cascade of inflammatory and oxidative mediators that exacerbate the progression of this disease in an experimental rat model. Our results clearly show that the tested phytochemical GMG-ITC possesses the capability to counteract CIR-induced damage.

Among non-communicable diseases, stroke represents the third major cause of mortality (1, 2) and the first cause of adult long-term disability (2) in the world. According to the World Health Organization, 15 million people suffer stroke worldwide each year and of these, 5 million die and another 5 million are permanently disabled (3).

Cerebral ischemia derives from drastic brain blood flow depletion at the level of the so-called ischemic core. In about 85% cases (2) the disease is identified as "ischemic stroke" and is the consequence of a cardiac arrest or of an obstruction.

Key words: cerebral ischemia/reperfusion, glucosinolate, isothiocyanate, Moringa oleifera, stroke

Mailing address: Dr Emanuela Mazzon,
IRCCS Centro Neurolesi "Bonino-Pulejo",
Via Provinciale Palermo,
contrada Casazza, 98124
Messina, Italy
Tel.: +39 090 60128708 Fax: +39 090 60128850
e-mail address: emazzon.irccs@gmail.com

0393-974X (2015)

In other cases, it is due to the breaking of arteries that bring oxygen ("hemorrhagic stroke"). Frequently, the major cause of human stroke seems to reside in cerebral artery thromboembolism (4). Confirmed by epidemiological studies, possible conventional risk factors leading to cerebral ischemia include: hypertension, diabetes mellitus, smoking, excessive drinking, and heart diseases (5-7). Nevertheless, genetic factors (8) were established to having a role in stroke triggering too (9).

On the other hand, reperfusion phase following an ischemic event is considered a paradox, since, even when occurring shortly after ischemia, it can reduce the extent of the ischemic penumbra (referred to a region of reversibly altered tissue surrounding the ischemic core) restoring oxygen and nutrients, but it can also worsen the damage for the afflux of oxidative mediators (10).

Signs of stroke depend on the side and the region of brain affected, and by how severely this is injured. Therefore, each person may have different stroke warning signs. Stroke may be associated with a headache, or may be completely painless. Thus, the symptoms of cerebral ischemia range from mild to severe. Among them, hemiparesis, aphasia, inability to walk without assistance, dependence on others during normal daily activities are all disability hallmarks in survivors (2). Currently, during acute stroke, recombinant tissue plasminogen activator is prescribed in a therapeutic window of intervention from four and a half - six hours (11).

In particular, glucosinolates (GLs), a group of secondary metabolites found almost exclusively in plants belonging to the *Brassicales*, and their derived isothiocyanates (ITCs) have gained great interest as biologically and pharmacologically active compounds most frequently examined for their beneficial therapeutic properties (12). In particular, the phytochemical 4(α-L-rhamnosyloxy)-benzyl ITC (GMG-ITC) obtained from the precursor GL glucomoringin (GMG; 4(α-L-rhamnosyloxy)-benzyl GL) by myrosinase (β-thioglucoside glucohydrolase; E.C. 3.2.1.147) enzyme hydrolysis (12) has been reported to exert anticancer and anti-inflammatory properties (13, 14).

Experimentally, in preclinical studies ischemic stroke is broadly induced in rat through a model of occlusion/reperfusion of the intraluminal middle cerebral artery (15). Therefore, the aim of the present study was to evaluate the efficacy of bioactive GMG-ITC treatment in an experimental rat model of cerebral ischemia/reperfusion (CIR).

MATERIALS AND METHODS

Animals

Male Sprague Dawley rats (Harlan, Italy) weighing 350±50 g were used. Rats were housed in a prefab building animal facility (purchased and certified by Charles River Laboratories International, Inc.) with a controlled environment (temperature, % humidity, air exchange with filtering system) and standard rodent chow and water *ad libitum*. Each cage included no more than 2 rats, and environmental enrichments supplying stimuli that promote the expression of species-specific behaviour and appropriate mental activities, were provided.

The protocol of the present study was approved by a committee belonging to the Italian Higher Health Institute, "General Direction of animal health and veterinary drug". Animal care was in compliance with Italian regulations on protection of animals used for experimental and other scientific purpose (D.M. 116/92) as well as with the European regulations (O.J. of E.C.L 358/1 12/18/1986).

GMG and myrosinase purification

GMG was isolated from *M. oleifera* L. (fam. *Moringaceae)* seeds (cake powder PKM2 provided by Indena India Pvt. Ltd; Bangalore, India) at CRA-CIN of Bologna, Italy according to a standardized protocol (16).

Myrosinase-catalyzed hydrolysis of GMG

GMG was dissolved in PBS solution pH 7.2 at room temperature and before rat intraperitoneally (i.p.) treatment, the action of myrosinase (3.5 mg GMG/ml plus 30 µl enzyme/ml) for 15 min at 37°C allowed having bioactive GMG-ITC quickly (see Fig. 1 A for *in vitro* reaction of GMG-ITC production).

The total conversion of pure GMG into GMG-ITC was confirmed by HPLC analysis using an Agilent Model 1100 HPLC system with an Inertsil ODS3 column (250 mm x 3 mm, 5 µm). Chromatography was performed with 1 ml/min flow rate at 30°C by eluting with a linear gradient of water (A) and acetonitrile (B) from 30% B to 80% in 20 min, monitoring the absorbance at 229 nm.

Induction of CIR and animal treatment

After anaesthesia (a solution of 100 mg/Kg tiletamine plus 15 mg/Kg xylazine administrated at the dosage of 1 ml/Kg, i.p), CIR was induced in rats. Briefly, in the supine position, a cervical parasagittal incision was made and the

left carotid artery was exposed, separated from the vagus nerve and occluded for 1 h by clamping with a small vascular clip, inducing hypotension to generate a cerebral ischemia animal model. GMG-ITC (3.5 mg GMG/ml plus 30 µl enzyme/rat; one ml i.p./rat) was administered 15 min after the beginning of ischemia and daily for a total period of blood flow reperfusion of 7 days. Finally, rats were euthanized and brain samples were taken in order to perform subsequent morphological evaluation and Western blot analysis.

Experimental groups

Rats were randomly allocated into the following groups (n = 30 total animals):

- Group 1 - Untreated CIR group: rats were subjected to 1h of carotid artery occlusion followed by 1 week of reperfusion (n = 10). PBS solution (vehicle of GMG) was administered i.p. 15 min after the beginning of ischemia and daily until the sacrifice;
- Group 2 - GMG-ITC-treated CIR group: rats were subjected to surgical procedures described above and GMG-ITC was administered 15 min after the beginning of ischemia and daily (n = 10).
- Group 3 - Naïve group: control rat group not subjected to CIR-damage (n = 10). Rats were daily administered with PBS solution until sacrifice (7th day).

At the end of the experiment, the animals were euthanized. Brain tissue samples were taken and processed in order to evaluate disease parameters.

Oedema

For all sacrificed animals (n = 10 for each experimental group), a measure of brain hemisphere oedema was established providing left/right ratio (using arbitrary units given by bar size in Fig. 2), and graphing the achieved data. Since mean of naïve left/right ratio was one, we considered this value as a baseline assigning an arbitrary value zero (no oedema). Data from the other two groups were elaborated using the following math formulae: Δ = (mean "group 1 or 2" left/right ratio - mean naïve left/right ratio).

Magnetic Resonance Imaging (MRI)

The study was performed with a 3T Achieva Philips scanner; using a 4-channels NO-SENSE animal coil. 3D high-resolution T1 weighted Fast Field Echo sequence was acquired using the following parameters: repetition time 11 ms; echo time 5.3 ms; flip angle 8 degrees; FOV 120 mm^2; reconstruction matrix 172 × 40; voxel size 1 x 1 x 1 mm; slice thickness 1 mm. The acquisition time was 15.40 min. Representative sagittal sections were extracted from T1-weighted volume acquisition MR imaging data set (29/60).

Gait test

Rat feet were impregnated with a commercial, non-toxic, liquid blue ink and the animals were gently placed a sheet of blotting paper and left to walk freely so that the acquired foot posture after CIR-induction was printed. The relative comparisons among the experimental groups were made and changes in gait were evaluated.

Light microscopy

Brain tissues samples were taken 7 days after CIR-induction. Tissues were fixed in 10% buffered formalin, pH 7.4. After dehydration in graded ethanol and xylene,

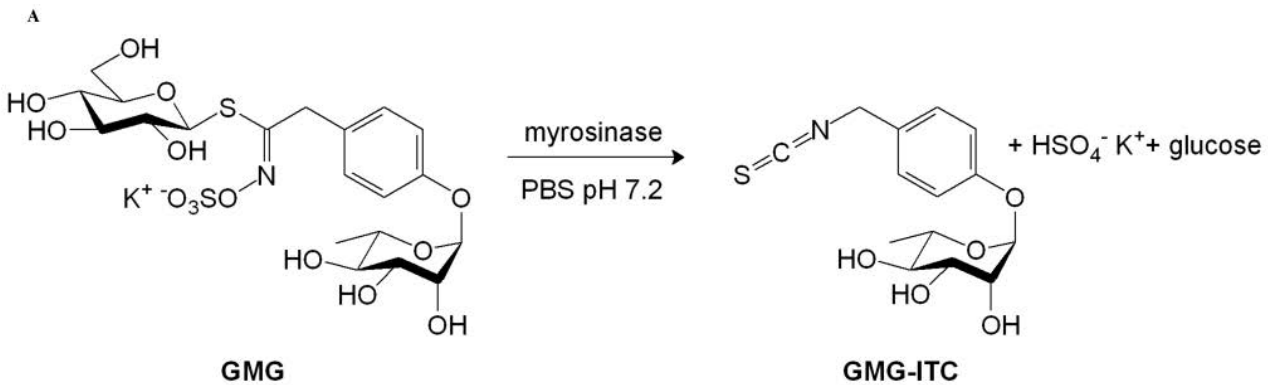

Fig. 1. *Chemical structure and production of 4-(α-L-rhamnosyloxy)benzyl isothiocyanate (GMG-ITC). Myrosinase-catalyzed hydrolysis of GMG to produce GMG-ITC (**A**).*

the tissues were paraffin embedded and cut into 7-µm thick coronal sections. Tissue sections were stained with haematoxylin/eosin (H&E) and studied using light microscopy (Leica ICC50 HD).

Golgi stain

FD Neurotech kit (FD NeuroTechnologies, Ellicott City, MD, USA) was used for Golgi impregnation of tissue, according to the manufacturer's instructions (17). Briefly, brain samples were placed directly into solution (A + B) containing mercuric chloride, potassium dichromate and potassium chromate, without rinsing, and remained there for 2 weeks in the dark at room temperature. Forty-eight hours after placing in solution C (4°C), brains were frozen on dry ice and stored at -70°C until sectioning. Cryostat sections (100 µm) were cut at -25°C and mounted onto gelatinized slides. The slides were allowed to dry in the dark, and the rest of the staining process was carried out as previously described (17). Cresyl violet was used as background colour to counterstain.

Terminal deoxynucleotidyltransferase-mediated UTP end labeling (TUNEL) assay

To test whether spinal cord damage was associated with cell death by apoptosis, we measured TUNEL-like staining in the perilesional spinal cord tissue. TUNEL assay was conducted by using a TUNEL detection kit according to the manufacturer's instructions (Apotag, HRP kit DBA, Milan, Italy). Sections were incubated with 15 mg/ml proteinase K for 15 min at room temperature and then washed with PBS. Endogenous peroxidase was inactivated by 3% H_2O_2 for 5 min at room temperature and then washed with PBS. Sections were immersed in terminal deoxynucleotidyltransferase (TdT) buffer containing deoxynucleotidyl transferase and biotinylated dUTP, incubated in a humid atmosphere at 37°C for 1 h, and then washed with PBS. Sections were incubated at room temperature for 30 min with anti-horseradish peroxidase-conjugated antibody, and the signals were visualized with diaminobenzidine and controstained with methyl green.

Immunohistochemical (IHC) localization

Brain tissues were fixed in 10% (w/v) PBS-buffered formaldehyde, and 6-µm sections were prepared from paraffin-embedded tissues. After deparaffinization, endogenous peroxidase was quenched with 0.3% (v/v) hydrogen peroxide in 60% (v/v) methanol for 30 min. Nonspecific adsorption was minimized by incubating sections in 2% (v/v) normal goat serum in PBS for 20 min. Endogenous biotin or avidin binding sites were blocked by sequential incubation for 15 min with biotin and avidin, respectively.

Sections were incubated overnight with the following primary antibodies:

- anti-IkB-alpha polyclonal antibody (1:100 in PBS v/v; Santa Cruz Biotechnology, Inc),
- anti-MMP9 monoclonal antibody (1:100 in PBS v/v; Cell Signaling Technologies),
- anti-iNOS polyclonal antibody (1:100 in PBS v/v; Santa Cruz Biotechnology, Inc)
- anti-p-selectin monoclonal antibody (1:100 in PBS v/v; Santa Cruz Biotechnology, Inc).

Sections were then washed with PBS and incubated with secondary antibody. Specific labeling was detected with a biotin-conjugated goat anti-rabbit IgG and avidin-biotin peroxidase complex. The counterstain was developed with diaminobenzidine (brown) and ematossilin (blue background).

To verify the binding specificity, some sections were also incubated with only the primary antibody or with only the secondary antibody. In these situations, absence of positive staining was found in the sections, indicating that the immunoreaction was positive in all the experiments carried out. All sections were observed using light microscopy (Leica ICC50 HD). Leica Application Suite V4.2.0 software was used as the image computer program to acquire pictures and to perform densitometric analysis.

Western blot analysis

All Western blot procedures aimed to assess the expression of mediators of CIR development were performed according to protocol published elsewhere used by Galuppo et al. for this procedure (14) and modified here for brain tissue.

Proteins were separated on sodium dodecyl sulfate-polyacrylamide minigels and transferred onto nitrocellulose membranes (Protran nitrocellulose transfer membrane; Whatman Schleicher and Schuell, Dassel, Germany), blocked with PBS containing 5% non-fat dried milk (PM) for 45 min at room temperature, and subsequently probed at 4°C overnight with the follow primary antibodies: TNF-alpha (1:100 in PM 0.1% Tween 20 (PMT) v/v; Cell Signaling Technologies), NFkBp65 (1:1000 in PMT v/v; Cell Signaling Technologies), phospho-ERK p42/44 (1:1000 in PMT v/v; Cell Signaling Technologies), ERK 2 (1:2000 in PMT v/v; Cell Signaling Technologies).

Horseradish peroxidase-conjugated goat anti-mouse IgG or horseradish peroxidase-conjugated goat anti-rabbit IgG were incubated as secondary antibodies (1:2000 in PMT v/v; Santa Cruz Biotechnology, Inc) for 1 h at room temperature. To ascertain that blots were loaded with equal amounts of protein lysates, they were also incubated with GAPDH-horseradish peroxidase conjugated primary

antibody (1:1000 in PMT v/v; Cell Signaling Technology).

Relative proteic band expression was visualized using an enhanced chemiluminescence system (Luminata™ Forte, Western HRP substrate, Millipore) and proteic bands were acquired and quantified with ChemiDoc™ MP System (Bio-Rad, Segrate, Italy) and a computer program (ImageJ software), respectively. Blots are representative of three separately performed and reproducible experiments. Statistical analysis was performed on three repeated blots performed in separate experiments.

Statistical evaluation

Data were elaborated using GraphPad Prism version 6.0 (GraphPad Software, La Jolla, CA, USA). For multiple comparison, one-way analysis of variance (ANOVA) followed by Bonferroni test were conducted to analyze any statistical difference. A p value < 0.05 was considered to be statistically significant. Results are expressed as mean ± S. E. M. of n experiments.

RESULTS

Effect of GMG-ITC treatment on CIR injury in rats: macroscopic and MRI report associated to histological evaluation of brain tissue

Following craniotomy and brain sampling naïve rats did not show any macroscopic alteration or oedema (Fig. 2 A). Conversely, looking at the macroscopic anatomy of the brain, it is clear that 7 days following CIR the craniotomy of untreated rats shows the presence of hyperemia, fibrosis (see arrows) and cerebral oedema (Fig. 2 B). On the contrary, as shown in Fig. 1C, treatment of CIR with GMG-ITC results in the resolution of inflammatory and vascular processes (left panel Fig. 2 C) and in the recovery of a normal volume in the cerebral hemisphere size (right panel Fig. 2 C).

To display this parameter, an arbitrary measure to quantify the dimensional differences between left and right hemispheres in a same brain sample was chosen. Therefore it is possible to appreciate, as in untreated CIR-injured rats, that cerebral capillary dysfunction leads to oedema (right panel Fig. 2 B). However, GMG-ITC treated CIR rats did not show this difference (right panel Fig. 2 C). A measure of brain oedema was arbitrarily obtained providing the mean ratio between left and right hemisphere for each experimental group (Fig. 2 D). Data were correlated with absence of oedema in naïve animals and delta of this difference was shown.

Moreover, brain samples from untreated CIR rats characterized by oedema show also detachment of the cerebellum. This was confirmed by MRI. A sagittal view of rat brain, interpreted by two blinded experienced radiologists, reveals hyperintense areas in the cerebellum, mesencephalon tectum, diencephalon (thalamic portion) and telencephalon (Fig. 3 A).

Also, an exam of gait given by footprint shows some differences in rat foot posture. The ischemic event induced some modifications in gait of untreated CIR-injured rats (left panel Fig. 3 B), while administration of GMG-ITC reducing infarct volume and protecting from CIR-associated damage results in absence of visible changes in footstep (right panel Fig. 3 B).

In addition, rats subjected to CIR but not pharmacologically treated with GMG-ITC showed severe damage of brain tissue with loss of normal structural architecture mainly due to severe CIR. More in detail, at the level of the hippocampus there is an evident zone characterized by oedema and presence of inflammatory cells in the perivascular area (data not shown).

Moreover, also the cerebellum and the cortex of the diencephalon show swelling with diffuse infiltration of lymphocytes and neutrophil cells (Fig. 4 A, B). GMG-ITC reduces the degree of histological alteration as demonstrated by H&E staining. Rats pharmacologically treated with GMG-ITC display absence of cellular mediators of inflammation and oedema both in the cerebellum and cortex of the diencephalon (Fig. 4 C and D).

GMG-ITC preserves brain synaptic functionality and plasticity protecting neuronal cells by apoptosis

Hypoxia resulting from an ischemic event and the following oxidative stress mediator production lead to an abnormal number of dendrite spines that are often permanent associated with brain disorders and correlated to abnormal neuronal cell function in terms of biochemical signals, in particular Ca^{2+}-mediated synaptic plasticity (18). Sections of brains sampled by both GMG-ITC-treated and untreated CIR-injured rats were cut at the level of the dental nucleus of hippocampus and dendrite spine density was analyzed via Golgi impregnation. In the dentate gyrus of CIR-injured rats the number of tree branches

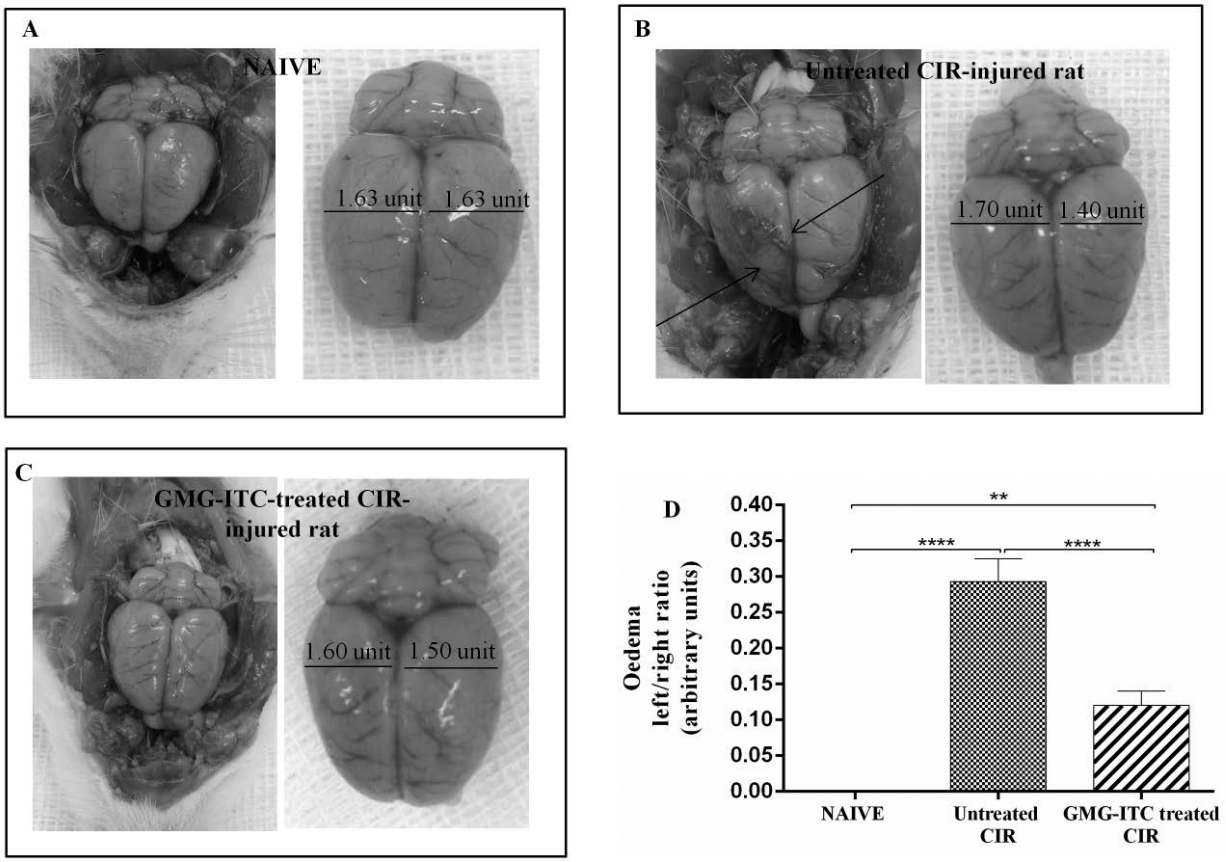

Fig. 2. *Macroscopic anatomy of the brain and oedema following CIR. Representative figures are shown for all experimental groups each consisting of n=10 animals. At the macroscopic analysis, brain sampled by naïve rats shows physiological (**A**) condition and absence of oedema (A, right panel). On the contrary, 7 days after CIR, the craniotomy of untreated rats shows the presence of hyperemia, fibrosis (see arrows) and cerebral oedema (**B**). Treatment of CIR with GMG-ITC results in the resolution of inflammatory and vascular processes as well as in regression of cerebral hemisphere oedema (C, right panel). Units must be considered as an arbitrary measure of the bar put to quantify the dimensional differences between left and right hemispheres in a same image. So it is possible to appreciate as in untreated CIR-injured rats, cerebral capillary dysfunction leads to an alteration of hemisphere proportion (B, right panel). Conversely, GMG-ITC-treated CIR rats do not show this difference (**C**, right panel). Presence of brain oedema in untreated CIR and GMG-ITC-treated rats were compared to naïve (absence of oedema, value 0) and the differences were statistically evaluated and graphed (**D**). A $p < 0.05$ was considered significative. ** $p = 0.0018$; **** $p = 0.0001$*

resulted significantly reduced (Fig. 5 A). Conversely, GMG-ITC-treatment protects the neuronal functional disruption (Fig. 5 B).

To corroborate the above results, TUNEL staining was performed showing the presence of apoptotic bodies both in cortex (Fig. 5 C, see particle C1) and in cerebellum (Fig. 5 E) of untreated-CIR rats. GMG-ITC treated CIR rats showed absence of apoptotic cells both in cortex (Fig. 5 D) and in cerebellum (Fig. 5 F).

Effect of GMG-ITC on TNF-alpha release following CIR

To test whether treatment with GMG-ITC modulates the inflammatory processes triggered by CIR-induction via the regulation of pro-inflammatory cytokine secretion, we analyzed brain expression levels of TNF-alpha by Western blot analysis. This showed a significant increase in TNF-alpha release in brain samples collected 7 days after CIR-induction from untreated rats (Fig. 6 A). Brain levels of TNF-

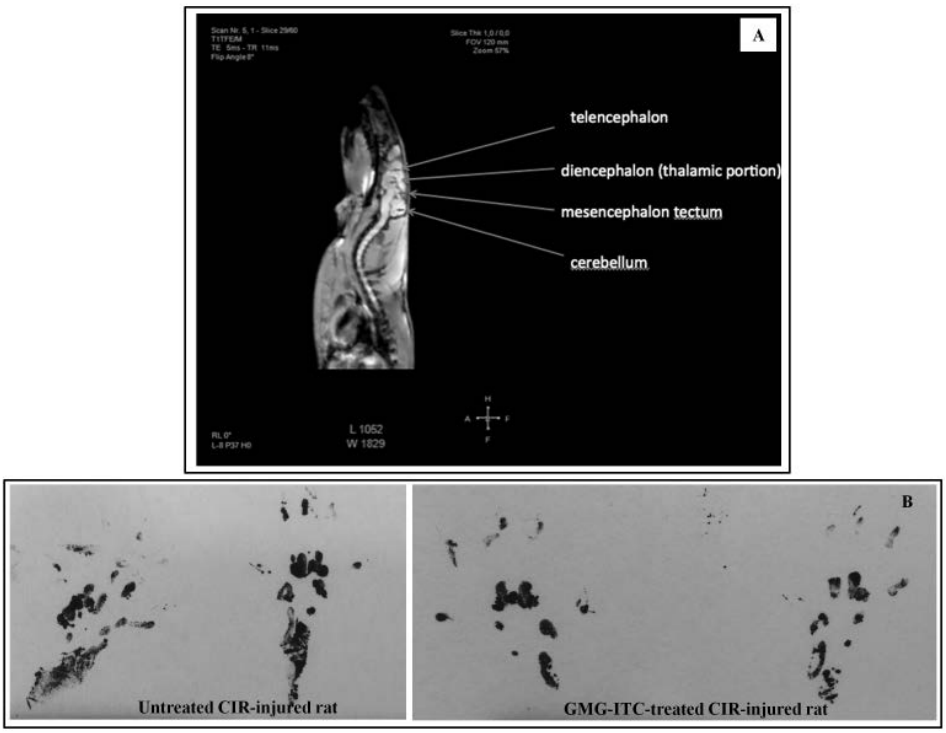

Fig. 3. *CIR caused alterations in brain and in gait. A sagittal view of rat brain by MRI reveals hyperintense areas in the cerebellum, mesencephalon tectum, diencephalon (thalamic portion) and telencephalon (**A**). Also, an exam of gait given by footprint shows some alteration in foot posture of untreated CIR-rat (left panel, **B**). Administration of GMG-ITC reduced infarct volume and provided a significant protection from CIR-associated damage, as reflected in foot gait (right panel, B).*

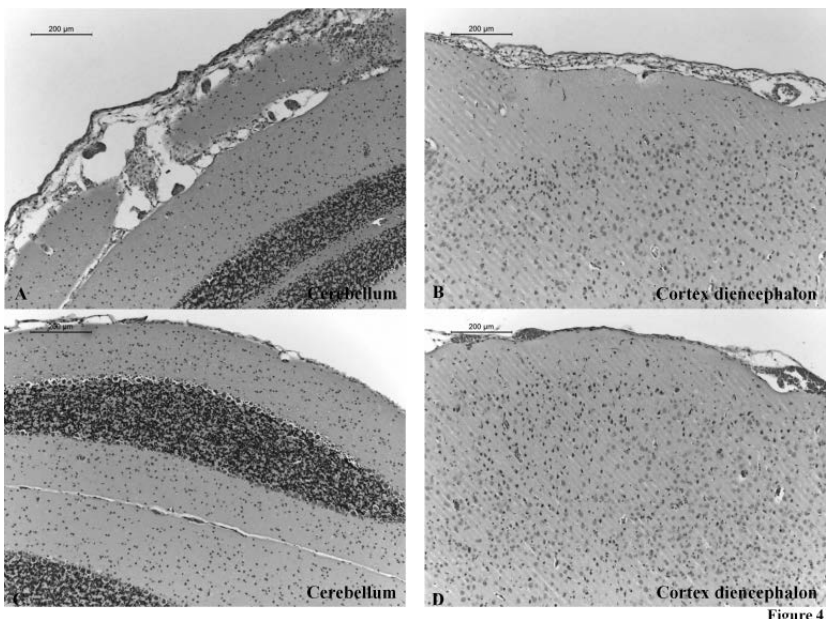

Fig. 4. *GMG-ITC preserves brain following CIR injury. The cerebellum (**A**) and the cortex of the diencephalon (**B**) show swelling with diffuse infiltration of lymphocytes and neutrophil cells. GMG-ITC-treatment in CIR-injured rats reduces the degree of histological alteration displaying absence of cellular mediators of inflammation and oedema both in cerebellum (C) and in the cortex of the diencephalon (**D**).*

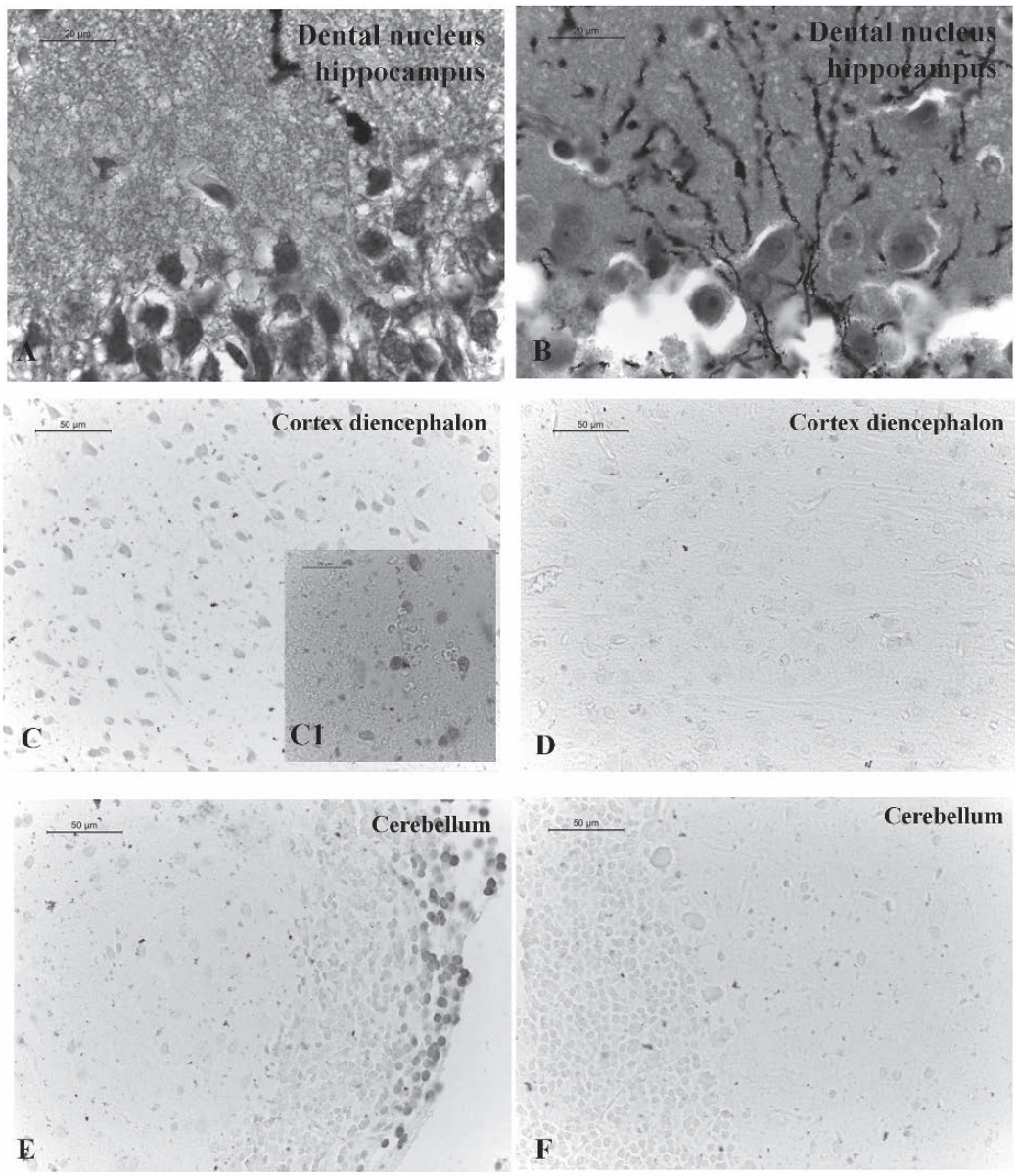

Fig. 5. *GMG-ITC prevents dendritic loss and apoptosis in CIR-injured rats. Golgi impregnation performed on sections cut at level of dental nucleus of hippocampus shows on the dentate gyrus of CIR-injured rats a number of tree branches significantly reduced (**A**). Conversely, GMG-ITC-treatment protects by neuronal functional disruption (**B**). TUNEL staining was used for a measure of apoptosis. Both in cortex (**C**, see particle C1) and in cerebellum (**E**) sections sampled from untreated-CIR rats show the presence of apoptotic bodies. Conversely, GMG-ITC treated CIR rats display absence of apoptotic cells both in cortex (**D**) and in cerebellum (**F**).*

alpha were attenuated by administration of GMG-ITC (Fig. 6 A).

Effect of GMG-ITC on phospho-ERK p42/44 expression following CIR

Western blot analysis of brain tissue homogenates revealed some differences in phospho-ERK p42/44 levels, increased in brain samples taken from rats subjected to CIR (Fig. 6 B) and reduced by treatment with GMG-ITC (Fig. 6 B).

Effect of GMG-ITC on IkB-alpha and NFkBp65 following CIR

To investigate the cellular mechanism by which

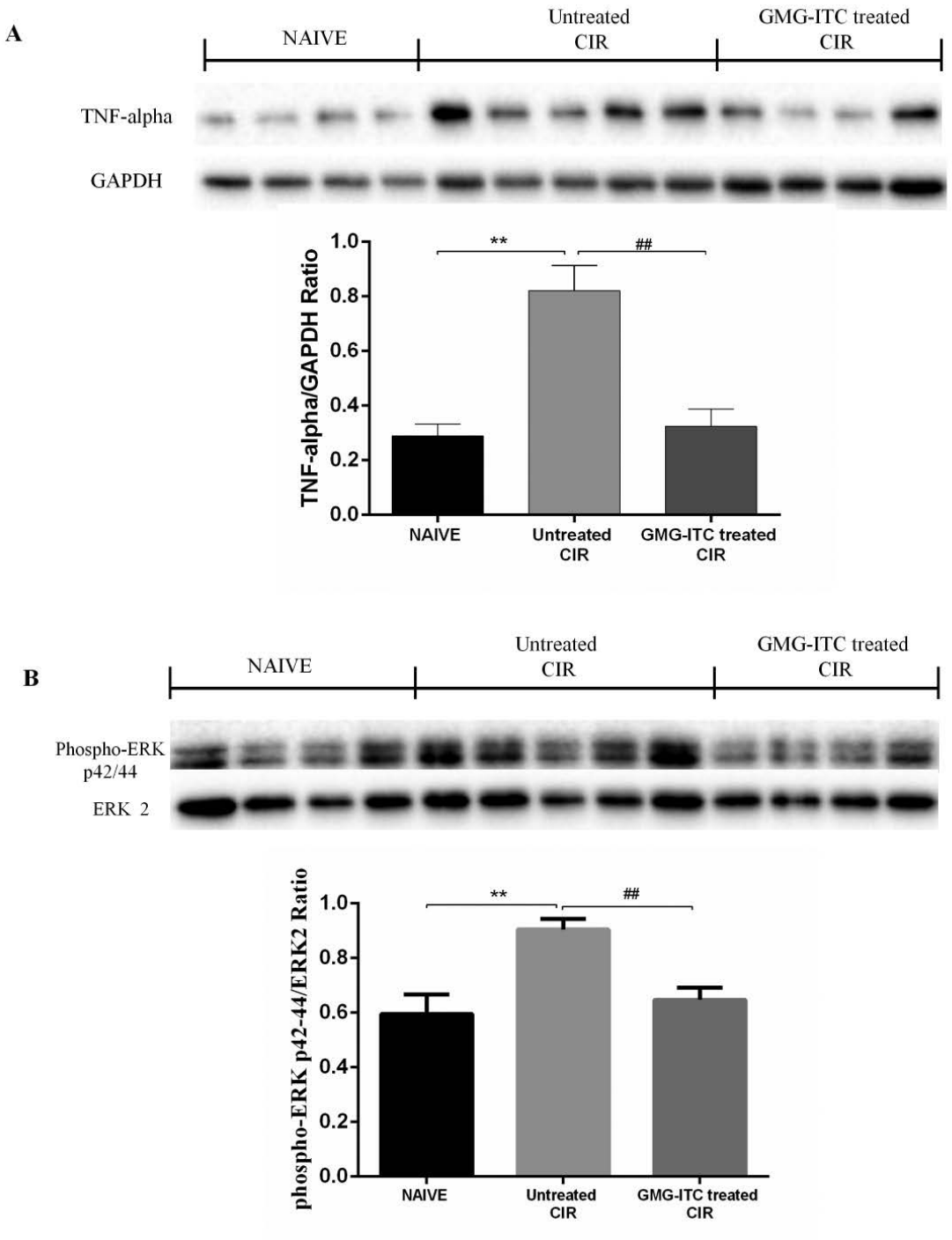

Fig. 6. *GMG-ITC prevents TNF-alpha release following CIR. Brain levels of TNF-alpha were assessed by Western blot analysis. A significant increase in TNF-alpha release is assessed in brain samples collected 7 days after CIR-induction from untreated rats, when compared to naïve rats. Conversely, brain levels of TNF-alpha are attenuated by administration of GMG-ITC (**A**). A p value < 0.05 was considered significative. ** p = 0.0039; ## p = 0.0035. GMG-ITC modulates Mitogen-activated protein kinase (MAPK) signaling pathway. Phospho-ERK p42/44 expression levels normalized on ERK2 display an increase in rats subjected to CIR (**D**), when compared to naïve rats. Treatment with GMG-ITC reduces levels of ERK1/2 (D). A p value < 0.05 was considered significative. ** p = 0.0049; ## p = 0.0064.*

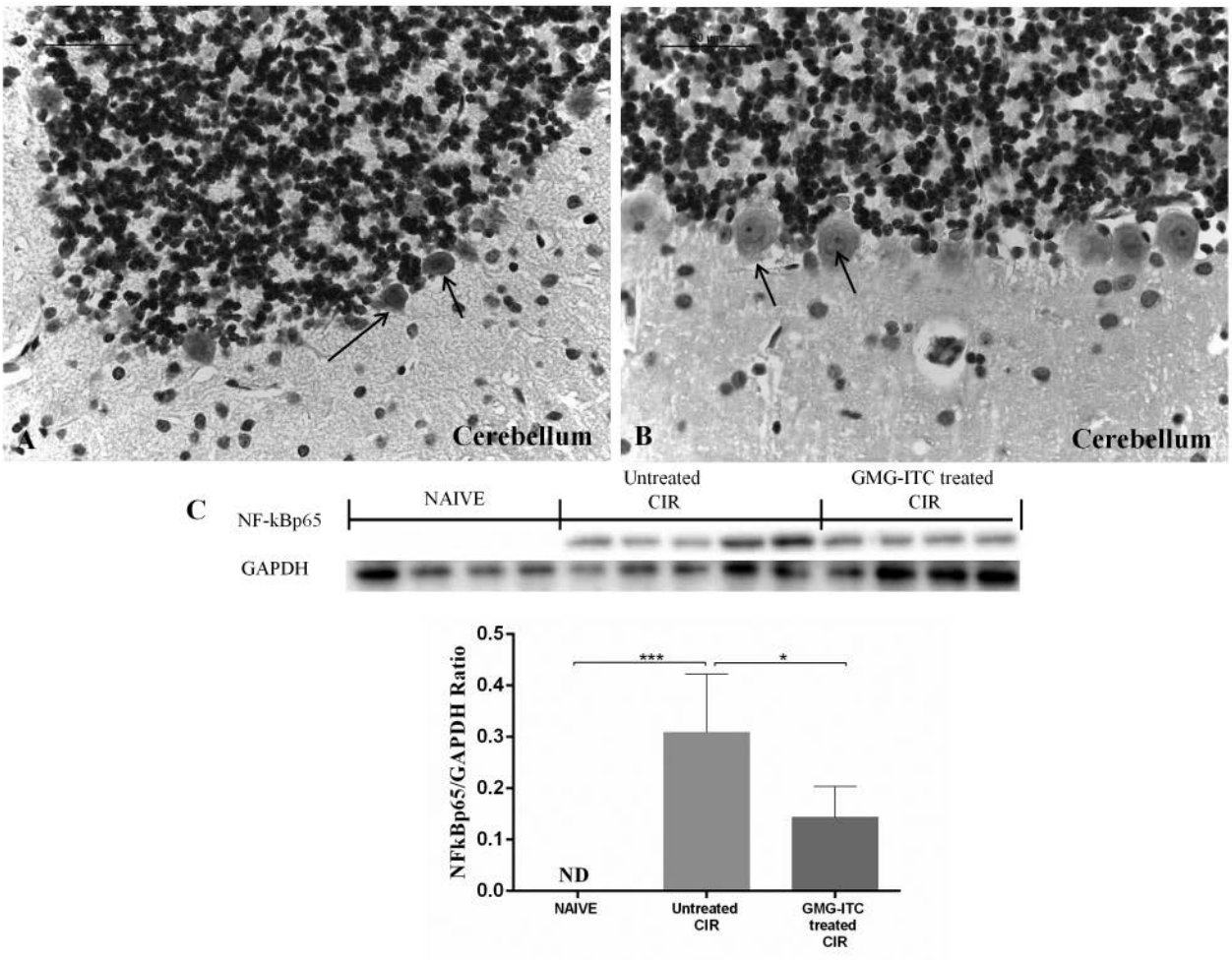

Fig. 7. *GMG-ITC avoids IkB-alpha degradation and nuclear traslocation of NFkBp65. Brain sections of cerebellum samples from rats subjected to CIR show a marked positivity for IkB-alpha into nucleus (**A**), whereas brain sections obtained from rats treated with GMG-ITC exhibited positive staining for IkB-α only in the cytoplasmatic compartment (**B**). In the figures, arrows show tissue localization of the immunopositivity for IkB-alpha. Western blot analysis of NF-kBp65 (**C**) shows in rats subjected to CIR a nuclear traslocation of NF-kBp65 due to its activation (C). On the contrary, treatment with GMG-ITC reduced the expression levels for NF-kBp65 in nuclear protein extract (C). Naïve rat brain shows a totally negative expression for NF-κBp65 in nuclear extract (C). Densitometric analysis was performed to show all differences (**D**). A p value < 0.05 was considered significative. ND not detectable, *** p = 0.0005; * p = 0.0322.*

GMG-ITC treatment may attenuate the development of CIR and the associated damage, we evaluated IkB-alpha degradation in brain sections collected after 7 days of reperfusion by immunohistochemical localization. Brain sections of cerebellum sampled from rats subjected to CIR showed a marked IkB-alpha translocation to nuclear compartment (Fig. 7 A, see arrows), whereas brain sections obtained from rats treated with GMG-ITC exhibited only cytoplasmatic positivity for IkB-alpha staining (Fig. 7 B, see arrows).

This was confirmed by Western blot analysis of NF-kBp65 (Fig. 7 C). Rats subjected to CIR exhibited a nuclear traslocation of NF-kBp65 due to its activation (Fig. 7 C). On the contrary, treatment with GMG-ITC reduced the expression levels for

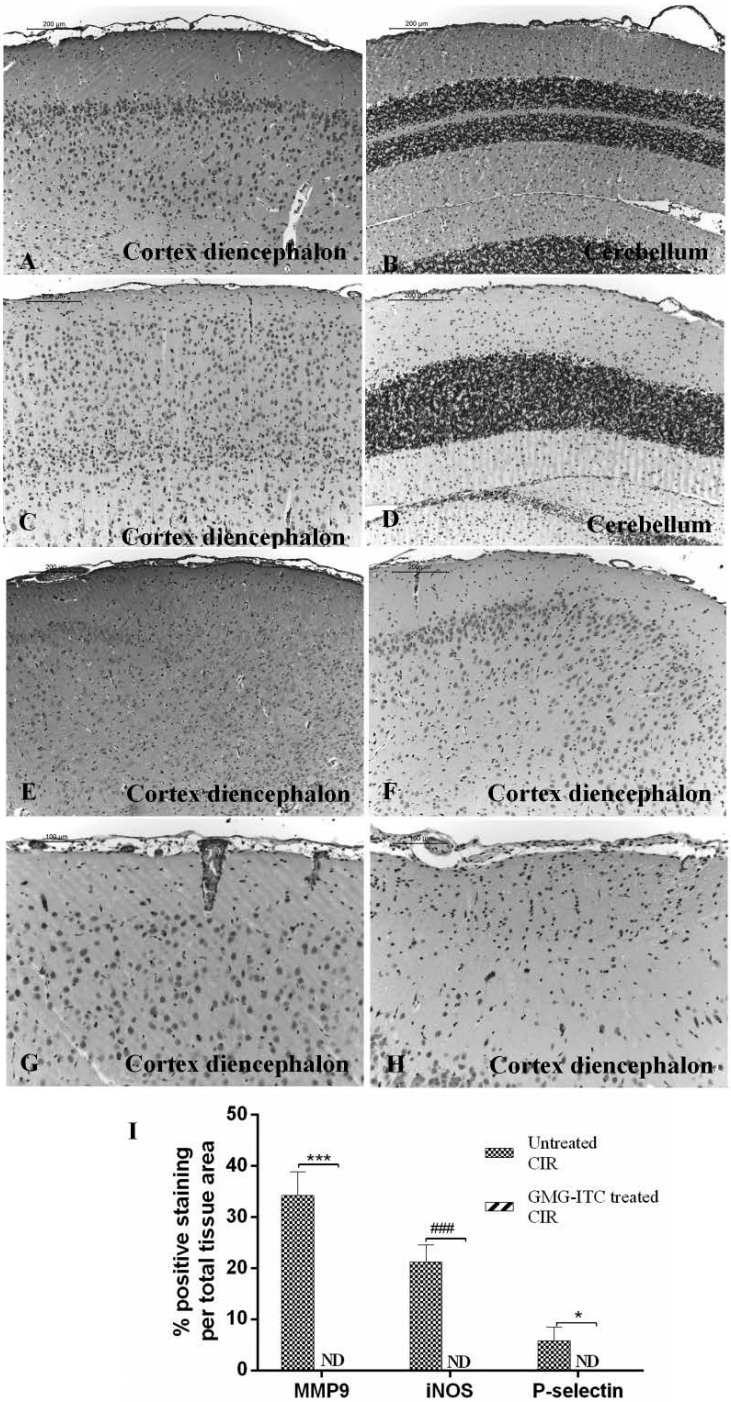

Fig. 8. *Protective role of GMG-ITC against MMP-9, iNOS and p-selectin expression. In diencephalon (**A**) and cerebellum (**B**) sections cut from untreated rats subjected to CIR show a positive immunostaining for MMP-9. Brain section samples from rats treated with GMG-ITC did not stain for MMP-9, either in diencephalon (**C**) or cerebellum (**D**). An increased tissue immunolocalization of iNOS is displayed in untreated rats following CIR (**E**) while, GMG-ITC significantly reduces the degree of positive staining for iNOS (**F**). P-selectin expression is increased in rat brains following CIR in absence of pharmacological treatment (**G**) while, GMG-ITC significantly reduces the degree of positive staining for p-selectin (**H**). Densitometric analysis (**I**): immunohistochemical images of MMP-9, iNOS and p-selectin were quantified and the intensity was represented as % of positive staining on total tissue area. A p value < 0.05 was considered significative. ND = not detectable; *** p = 0.0002; ### p = 0.0004; * p = 0.0274.*

NF-kBp65 in nuclear protein extract (Fig. 7 C).

Effect of GMG-ITC on MMP-9, iNOS and p-selectin expression following CIR

By immunohistochemical stain, brain sections of diencephalon (Fig. 8 A, see densitometric analysis Fig. 8 I) and cerebellum (Fig. 8 B, see densitometric analysis Fig. 8 I) cut from untreated rats subjected to CIR exhibited positive staining for MMP-9, whereas brain sections obtained from rats treated with GMG-ITC did not stain for MMP-9, either in diencephalon (Fig. 8 C, see densitometric analysis Fig. 8 I) or cerebellum (Fig. 8 D, see densitometric analysis Fig. 8 I).

Immunohistochemical localization of iNOS in brain tissues of untreated-CIR rats sampled after seven days of reperfusion, displayed an increased expression of this marker following CIR (Fig. 8 E, see densitometric analysis Fig. 8 I), while treatment with GMG-ITC significantly reduced the degree of positive staining for iNOS (Fig. 8 F, see densitometric analysis Fig. 8 I). Moreover, evaluating p-selectin expression in ischemic cerebral tissue, our results clearly showed an increased expression of adhesion molecules following CIR in the vascular endothelium (Fig. 8 G, see densitometric analysis Fig. 8 I) while, treatment with GMG-ITC significantly reduced the degree of positive staining for p-selectin (Fig. 8 H, see densitometric analysis Fig. 8 I).

DISCUSSION

Ischemic stroke, charged to the cerebrovascular system, leads to serious complications associated with high disability and death (19). With the present experimental model we have clearly shown what happens during CIR in the absence of pharmacological treatment. Signs of disease, recorded following CIR induction, reflect human condition characterized by gait impairment, palpebral ptosis as well as cerebral oedema and fibrosis. Microscopic and immunohistochemical investigations have further clarified the mechanisms involved in the neurodegeneration associated with CIR (loss of synaptic connections and neuronal cell death) and have at the same time demonstrated a protective effect of GMG-ITC. In further detail, inflammatory intermediaries, first released during CIR, such as TNF-alpha, that have been shown to be involved in ischemic stroke development by previous authors (20), are strongly inhibited by GMG-ITC administration. In addition, the contribution of p-selectin as an adhesion molecule that stimulates rolling of leukocytes and other inflammatory cell infiltration in post-ischemic cerebral stroke in the first 15 minutes of ischemia (21) was also modulated by GMG-ITC administration. Data regarding untreated CIR-injured rats have confirmed that when the upregulation of p-selectin resulted more prolonged it appeared to reflect both increased expression on the cerebral endothelial cells and the binding of p-selectin positive platelets to the vessel wall (22), causing, in turn, an exacerbation of the processes leading to neurodegeneration at the origin of CIR. Also, the MAPK pathway, investigated through detection of phospho-ERK p42-44 expression, resulted upregulated in CIR-related mechanisms of pathology (23) but attenuated by GMG-ITC administration.

Upstream of this cascade, NF-κBp65 positively regulates the expression of various genes, including TNF-α, IL-1β, adhesion molecules. Many of them also re-activate NF-κBp65 itself, amplifying and perpetuating the inflammatory response (20). Our results confirmed that CIR injury promoted inflammation by acting on the IkB-alpha/NF-κBp65 pathway and stimulating the downstream-associated response but together they have demonstrated that GMG-ITC administration can inhibit the activation of NF-κBp65 and prevent inflammation in rats with CIR.

A class of enzymes, which resulted up-regulated in CIR, is represented by metalloproteinases (MMP), in particular MMP-9. These, associated to an over-expression of inducible nitric oxide synthase, seem to contribute to brain oedema and to degradation of the blood–brain barrier (24, 25).

In conclusion, 4(α-L-rhamnosyloxy)-benzyl isothiocyanate, a bioactive phytochemical derived from GMG hydrolysis reaction, has proven to block the production of oxidative stress mediators and the related processes, decreasing MMP-9, as well as iNOS over-expression, defending cerebral tissue and preventing severe damages induced by focal ischemia/reperfusion.

In summary, the relevance of the present study consists in the possible use of the bioactive phytochemical GMG-ITC, produced by myrosinase-

hydrolysis of GMG, as a therapeutic agent in counteracting the inflammatory response and oxidative injury induced by CIR. In light of the results achieved, the neuroprotection derived by the treatment of bioactive GMG-ITC could lead to an application of this drug for preventing severe damages induced by focal ischemia/reperfusion. As a natural product the advantage of such preparation will provide huge benefits.

ACKNOWLEDGEMENTS

This work was supported by current research sources 2014 of IRCCS — Centro Neurolesi "Bonino-Pulejo", Messina (Italy).

REFERENCES

1. Bonita R, Mendis S, Truelsen T, Bogousslavsky J, Toole J, Yatsu F. The global stroke initiative. Lancet Neurol 2004; 3:391-93.
2. Baldwin KA, McCoy SL. Making a case for acute ischemic stroke. J Pharm Pract 2010; 23:387-97.
3. http://www.strokecenter.org/patients/about-stroke/stroke-statistics/. Stroke Stat.
4. Jiang Q, Zhang RL, Zhang ZG, Ewing JR, Divine GW, Chopp M. Diffusion-, T2-, and perfusion-weighted nuclear magnetic resonance imaging of middle cerebral artery embolic stroke and recombinant tissue plasminogen activator intervention in the rat. J Cereb Blood Flow Metab 1998; 18:758-67.
5. Yang QD, Niu Q, Zhou YH, et al. Incidence of cerebral hemorrhage in the Changsha community. A prospective study from 1986 to 2000. Cerebrovasc Dis 2004; 17:303-13.
6. He J, Klag MJ, Wu Z, Whelton PK. Stroke in the People's Republic of China. II. Meta-analysis of hypertension and risk of stroke. Stroke 1995; 26:2228-32.
7. O'Donnell MJ, Xavier D, Liu L, et al. Risk factors for ischaemic and intracerebral haemorrhagic stroke in 22 countries (the INTERSTROKE study): a case-control study. Lancet 2010; 376:112-123.
8. Dichgans M. Genetics of ischaemic stroke. Lancet Neurol 2007; 6:149-61.
9. Ou W, Liu X, Shen Y, et al. Association of CVD candidate gene polymorphisms with ischemic stroke and cerebral hemorrhage in Chinese individuals. PLoS One 2014; 9:e105516.
10. Breschi GL, Librizzi L, Pastori C, Zucca I, Mastropietro A, Cattalini A, de Curtis M. Functional and structural correlates of magnetic resonance patterns in a new *in vitro* model of cerebral ischemia by transient occlusion of the medial cerebral artery. Neurobiol Dis 2010; 39:181-91.
11. Wardlaw JM, Murray V, Berge E, del Zoppo GJ. Thrombolysis for acute ischaemic stroke. Cochrane Database Syst Rev 2014; **7**:CD000213.
12. Fahey JW, Zalcmann AT, Talalay P. The chemical diversity and distribution of glucosinolates and isothiocyanates among plants. Phytochemistry 2001; 56:5-51.
13. Brunelli D, Tavecchio M, Falcioni C, et al. The isothiocyanate produced from glucomoringin inhibits NF-kB and reduces myeloma growth in nude mice *in vivo*. Biochem Pharmacol 2010; 79:1141-48.
14. Galuppo M, Giacoppo S, De Nicola GR, et al. Antiinflammatory activity of glucomoringin isothiocyanate in a mouse model of experimental autoimmune encephalomyelitis. Fitoterapia 2014; 95:160-74.
15. McAuley MA. Rodent models of focal ischemia. Cerebrovasc Brain Metab Rev 1995; 7:153-80.
16. Giacoppo S, Galuppo M, De Nicola G, et al. 4(alpha-l-rhamnosyloxy)-benzyl isothiocyanate, a bioactive phytochemical that attenuates secondary damage in an experimental model of spinal cord injury. Bioorg Med Chem 2015; 23:80-88.
17. Feng J, Yan Z, Ferreira A, et al. Spinophilin regulates the formation and function of dendritic spines. Proc Natl Acad Sci U S A 2000; 97:9287-9292.
18. Nimchinsky EA, Sabatini BL, Svoboda K. Structure and function of dendritic spines. Annu Rev Physiol 2002; 64:313-53.
19. Tu Q, Cao H, Zhong W, Ding B, Tang X. Atorvastatin protects against cerebral ischemia/reperfusion injury through anti-inflammatory and antioxidant effects. Neural Regen Res 2014; 9:268-75.
20. Liu X, Mei Z, Qian J, Zeng Y, Wang M. Puerarin partly counteracts the inflammatory response after cerebral ischemia/reperfusion via activating the cholinergic anti-inflammatory pathway. Neural Regen Res 2013; 8:3203-15.

21. Yilmaz G, Granger DN. Leukocyte recruitment and ischemic brain injury. Neuromolecular Med 2010; 12:193-204.
22. Blann AD, Nadar SK, Lip GY. The adhesion molecule P-selectin and cardiovascular disease. Eur Heart J 2003; 24:2166-79.
23. Wang J, Jin H, Hua Y, Keep RF, Xi G. Role of protease-activated receptor-1 in brain injury after experimental global cerebral ischemia. Stroke 2012; 43:2476-82.
24. Simard JM, Kent TA, Chen M, Tarasov KV, Gerzanich V. Brain oedema in focal ischaemia: molecular pathophysiology and theoretical implications. Lancet Neurol 2007; 6:258-68.
25. Iadecola C, Zhang F, Casey R, Clark HB, Ross ME. Inducible nitric oxide synthase gene expression in vascular cells after transient focal cerebral ischemia. Stroke 1996; 27:1373-80.

ANTIPSYCHOTICS REVERSE P-GLYCOPROTEIN-MEDIATED DOXORUBICIN RESISTANCE IN HUMAN UTERINE SARCOMA MES-SA/Dx5 CELLS: A NOVEL APPROACH TO CANCER CHEMOTHERAPY

A. ANGELINI[1,2], G. CIOFANI[1,2] and P. CONTI[3]

[1]Department of Medicine and Aging Sciences, School of Medicine "G. D'Annunzio" University Chieti-Pescara; [2]Aging Research Center, Ce.S.I. " G. D'Annunzio" University Foundation, Chieti-Pescara; [3]Postgraduate Medical School "G. D'Annunzio" University Chieti-Pescara, Chieti, Italy

Received January 14, 2015 – Accepted March 19, 2015

Multidrug resistance (MDR) mediated by P-glycoprotein (Pgp) remains one of the major obstacles to effective cancer chemotherapy. Several chemosensitizers have been used *in vivo* and *in vitro* to reverse MDR but have exhibited several unwanted side effects. Antipsychotics are often administered to treat psychiatric disorders such as delirium, anxiety and sleep disorders in cancer patients during chemotherapy. The present *in vitro* study, examined the effects of two common antipsychotic compounds, haloperidol and risperidone, and a natural compound such as theobromine on reversing MDR Pgp-mediated, to evaluate their potential use as chemosensitizing agents. The human doxorubicin (doxo) resistant uterine sarcoma cells (MES-SA/Dx5) that overexpress Pgp (100-fold), were treated with the antipsychotic alone (1, 10 and 20 μM) or in combination with different concentrations of doxo (2, 4 and 8 μM). The accumulation and cytotoxicity of doxo (MTT assay) and cellular GSH content (GSH assay) in comparison with verapamil, a well-known Pgp inhibitor, used as reference molecule were examined. It was found that the three compounds significantly enhanced the intracellular accumulation of doxo in resistant cancer cells, when compared with cells receiving doxo alone ($p<0.05$). Furthermore, compounds showed strong potency to increase doxo cytotoxicity toward resistant MES-SA/Dx5 cells, when compared with untreated control cells. The antipsychotic compounds also significantly increased GSH content at all concentrations (> 30%) in resistant cells, when compared to untreated control cells ($p<0.05$). These findings suggest that the antipsychotics or their derivatives might represent a novel class of reversal agents for overcoming MDR in cancer therapy, in particular theobromine showed to be an effective Pgp inhibitor with the lowest toxicity.

Multidrug resistance (MDR) of tumour cells to chemotherapeutic agents is a critical problem in the treatment of human cancers (1- 5). One of the main mechanisms for the development of MDR is the overexpression of a 170-kDa integral membrane protein, P-glycoprotein (Pgp), that acts as an energy-dependent efflux pump, exporting a wide variety of structurally and functionally unrelated chemotherapeutic agents from cancer cells. As a result, their intracellular accumulation is reduced,

Key words: P-glycoprotein, antipsychotics, haloperidol, risperidone, theobromine, MDR, GSH, MES-SA/Dx5, doxorubicin

Mailing address: Dr. Antonio Angelini,
Università "Gabriele D'Annunzio",
Centro di Scienze dell'Invecchiamento (Ce.S.I.),
Campus Universitario, Via Colle dell'Ara,
66013 Chieti Scalo, Italy
Tel/Fax: +39 0871 541420
e-mail: aangelini@unich.it

0393-974X (2015)

DISCLOSURE: ALL AUTHORS REPORT NO CONFLICTS OF INTEREST RELEVANT TO THIS ARTICLE.

and consequently their cytotoxicity, in many forms of human malignant tumours (6-12). Generally, MDR is associated with poor survival of cancer patients because by increasing resistant cancer cell population constituting the tumour, the anticancer chemotherapy becomes inefficient. In recent years, several groups of drugs called chemosensitizers have been used *in vivo* and *in vitro* to depress efflux activity of Pgp in multidrug resistant cells and have shown to increase the intracellular accumulation of cytostatics to the cytotoxic concentration for these cells (13-16). However, their clinical application is limited because of their toxicities. Therefore, the search for alternative treatments with safer compounds are needed. Effects of several natural compounds including sedatives, flavonoids, and honokiol and natural hepatoprotective compounds such as cynarin on the resistance cells were tested in our previous reports (17-19). Psychiatric disorders such as delirium, anxiety and sleep disorders affect cancer patients during chemotherapy and are often correlated with worsened disability and poorer quality of life. Therefore, psychopharmacological treatment in clinical oncology is an important tool in order to obtain a more integrated care of cancer (20). The aim of this study, which is a continuation of our previous research conducted on drugs already in clinical use for supportive care in cancer patients, is to assess the effect of two synthetic drugs, haloperidol and risperidone (21-22) , used as first line antipsychotics to manage and treat psychiatric disorders of cancer patient during chemotherapy. In addition, the effect of a natural compound, theobromine (3,7-dimethylxanthine), a methylxanthine present in high concentration in cocoa (23), on Pgp activity in a human resistant sarcoma cell line (MES-SA/Dx5) that expresses high levels of Pgp (100-fold) and is resistant to doxorubicin (doxo), will also be analysed (24). This anticancer drug is a well-known Pgp substrate and is frequently used in combination with other drugs to treat several human tumours. The antipsychotic compounds could interact with Pgp and act as chemosensitizers, modifying drug transport activity and influencing tumour cell sensitivity to chemotherapy. In this study, MES-SA/dx5 cells were treated with three different doxo concentrations (2, 4 and 8 μM), alone and in combination with three different concentrations of antipsychotic compounds achievable in human serum. Intracellular doxo accumulation and cytotoxicity were determined. Furthermore, the levels of total intracellular glutathione (GSH) were measured to evaluate oxidative state after treatment of the resistant sarcoma cells with various concentrations of antipsychotics. Concentrations of doxo which can be achieved in the blood of patients undergoing chemotherapy treatments were used. The results were compared to those obtained with Verapamil (Ver), a calcium blocker, used as positive control (25).

MATERIALS AND METHODS

Chemicals

Doxorubicin (doxorubicin hydrochloride), verapamil and 3-(4,5 dimethylthiazol-2-yl)-2,5-diphenyltetrazolium bromide (MTT), haloperidol, risperidone, theobromine, dichlorofluorescein diacetate (DCF-DA), dithionitrobenzoic acid (DTNB) and dimethyl sulfoxide (DMSO) were purchased from Sigma-Aldrich Co. (St Louis, MO, USA). All chemicals and drugs were freshly dissolved before use, except for doxorubicin, which was stored in a stock solution of 1 mM in PBS at -20° C in the dark.

Cell lines and cell cultures

The doxo-resistant human uterus sarcoma cell line MES-SA/Dx5 was obtained from the European Collection of Cell Cultures (Salisbury, UK) and grown in 25 cm^2 plastic culture flasks (Iwaki Company, Japan) containing 15 ml McCoy's 5a medium (Euroclone, Wetherby West Yorkshire, UK) supplemented with 10% heat-inactivated fetal bovine serum (Euroclone), 2 mM L-glutamine, penicillin (1000 U/ml) and streptomycin (100 μg/ml) in a humidified atmosphere of 95% air and 5% CO_2 at 37°C. Cells were sub-cultured every 3-4 days after treatment with 0.05% trypsin and 0.02 % EDTA in Ca^{++} and Mg^{++} free 1X Phosphate Buffered Saline (PBS). Cells were periodically checked for Mycoplasma contamination.

Intracellular accumulation of doxorubicin

MES-SA-Dx5 cells were seeded on 24-well culture dishes at a density of $1x10^5$ cells/well (Corning-Costar Corp., Corning New York, USA) and incubated for 72 h in growth medium alone at 37°C in an atmosphere containing 5% CO_2 and 95% air to allow cell attachment. At confluence, cells were washed three times with PBS at 37°C and treated with different concentrations of haloperidol (1, 10 and 20 μM), risperidone (1, 10 and 20 μM) or theobromine (1, 10 and 20 μM) at 37°C. After incubation for 24 h at 37°C, all pre-treated cells were

exposed to three different doxo concentrations (2, 4 and 8 μM) and the monolayer cultures were then incubated for 3 h at 37°C. In these experiments, Ver at 10 μM was used as a positive control drug. All values were averaged from at least three wells for each experiment. In the next step, wells were washed three times with ice-cold PBS (pH 7.4) to stop doxo accumulation and cells were solubilized with 250 μl of 4 M NaOH for 2 h and neutralized with 500 μl of 2 M HCl. The concentration of doxo was determined fluorimetrically (excitation, 475 nm; emission, 580 nm) with a fluorescence spectrophotometer (Perkin Elmer LS 45). The amount of doxo accumulated inside cancer cells pre-treated with the antipsychotic compounds or Ver was expressed as a percentage of doxo retention in control cells (doxo alone) at the selected concentrations (2, 4 and 8 μM) and was measured using the following formula: doxo accumulation (%): 100 x (F treated – F control) / F treated, where F treated = mean fluorescence of wells treated with haloperidol, risperidone, theobromine or Ver prior treatment with doxo; F control = mean fluorescence of wells treated with doxo alone.

Cytotoxicity assay

The growth inhibition of MES-SA/Dx-5 cells after treatment with antipsychotics alone or in combination with doxo, was analyzed with MTT cell proliferation assay (26). Briefly, cells were seeded into 96-well microplates (Iwaki Company, Japan) at a density of $1x10^4$ cells/well in growth medium (200 μl) and incubated in atmosphere of 5% CO_2 at 37°C for 24 h. MDR reversal effect of antipsychotics was determined by cultivation of MES-SA/Dx5 cells at different concentrations of doxo (2, 4, and 8 μM) in absence or presence of haloperidol (concentrations used: 1, 10 and 20 μM), risperidone (1, 10 and 20 μM) or theobromine (1, 10 and 20 μM) and incubated at 37°C for 72 h. MES-SA/Dx5 cells containing medium alone were used as negative control for optical density (OD). Doxo with 10 μM Ver was used as positive control. The cytotoxicity of each drug itself was also measured. After incubation, wells were rinsed with PBS before adding 100 μl of MTT (0.5 mg/ml) in drug-free medium to each well. The reaction was run for additional 4 h and the soluble formazan dye produced by metabolically active cells was solubilized in 100 μl of 0.04 N HCl-isopropyl alcohol and quantified at 37°C on a Spectra max 190 Microplate Spectrophotometer reader (Molecular Devices) at the wavelength of 550 nm. Each experiment was performed in triplicate. The percent of cell growth inhibition was evaluated as: (1-OD treated well/OD control well) x 100, where OD treated wells corresponded to the mean absorbance values of cells pre-treated with antipsychotic compounds or Ver, whereas OD control well corresponded to the mean absorbance values of untreated malignant cells.

Measurement of intracellular glutathione

The total intracellular GSH levels of MES-SA/Dx5 cells were measured according to Ellman's method (27). Briefly, MES-SA-Dx5 cells were seeded on 24-well culture dishes at a density of $1x\ 10^6$ cells/well (Corning-Costar Corp., Corning New York) and incubated for 72 h in growth medium alone at 37°C in an atmosphere containing 5% CO_2 - 95% air. The monolayers were then exposed for 3 h to different concentrations of haloperidol (1, 10 and 20 μM), risperidone (1, 10 and 20 μM) or theobromine (1, 5 and 10 μM) and Ver (10 μM) at 37°C. For total GSH determinations, the cells were washed with PBS and solubilized with 250 μl of 4 M NaOH for 2 h and then neutralized with 500 μl of 2 M HCl. After centrifugation 0.1 ml aliquot of supernatants was added to 0.9 ml of phosphate/EDTA buffer (0.2 M potassium phosphate, 0.01 M EDTA, pH 7.4) containing dithionitrobenzoic acid (DNTB, 0.2 mg/ml). The increase in absorbance at 412 nm (TNB formation) was monitored with a Cary 3C UV-visible Spectrophotometer for 15 min against an appropriate blank and quantified using molar adsorption coefficient ε=13600 M^{-1} cm^{-1}. Control MES-SA/Dx5 wells containing medium only were used as control. The assay was carried out in triplicate. Cellular GSH concentrations (nmoles for 1 x 10^6 cells) were expressed as percent of control (100%).

Statistical analysis

The results are expressed as mean ±SD and analyzed for statistical significance with Student's *t*-test between the control and compounds. p-values of <0.05 were considered significant.

RESULTS

Effects of antipsychotics on doxo accumulation in MES-SA/Dx5 cells

As shown in Fig. 1, pre-incubation of cancer cells for 24 h at 37°C with various concentrations of haloperidol, risperidone and theobromine significantly increased the doxo concentration capacity at all doxo concentrations when compared to those cultures treated with doxo alone ($p<0.05$). In particular, as shown in Fig. 2, the mean percentage of doxo accumulation capacity after exposure at 2 μM concentration of doxo in presence of haloperidol, risperidone and theobromine at 1, 10 and 20 μM were 31.9±4.8; 42.5±4.4; 44.5±3 and 43.1±7.2;44.5±4.5; 50.1±3.7 and 38.6±6.5; 43.1±3; 49.2±2.2, respectively. In combination with 4 μM doxo concentration were 30.4±3.1; 33.2±5.6;

Table I. *Cytotoxic effects of doxorubicin (doxo) alone and in combination with the antipsychotic compounds or Verapamil in MES-SA/Dx5 cells.*

	Control	% G.I.*	doxo2μM	% G. I.	doxo4μM	% G. I.	doxo8μM	% G. I.
Medium	1.22±0.03							
doxo2μM	1.03±0.05	15.4±4.6						
doxo4μM	0.94±0.03	23±3						
doxo8μM	0.83±0,02	32.3±1.5						
Ver10μM	1.1±0.04	11.3±4.6	0.57±0.02	53±1.7	0.51±0.02	58±2.2	0.44±0.01	65±1.3
H 1 μM	1.15±0.02	6±1.0	0.88±0.02	28.3±1.1	0.72±0,03	41±2	0.57±0.02	53.3±2
H 10 μM	1.12±0.01	9±1.1	0.72±0,02	41±2	0.58±0.02	53±2	0.52±0,02	58±2
H 20 μM	1.03±0.05	16±5.2	0.6±0.02	51.6±2	0.44±0.05	64.3±4	0.35±0.04	71.6±3.2
R 1 μM	1.16±0.01	5±1.2	0.98±0.05	26.2±7.2	0.77±0.02	37.3±2	0.66±0.02	45.6±1.5
R 10 μM	1.12±0.02	9±2	0.7±0.05	43±4	0.61±0.03	50.3±3	0.57±0.03	53.3±2.5
R 20 μM	1.05±0.08	14.6±7.5	0.55±0.05	55.3±4.5	0.53±0.01	57±1.7	0.48±0.02	61.3±1.5
T 1 μM	1.2±0.01	2±0.9	0.99±0.04	20±4.9	0.88±0.02	28.3±2.3	0.76±0.02	38±1.4
T 10 μM	1.18±0.03	3.3±2.1	0.88+0.01	28±1	0.79±0.04	35.3±3.5	0.7±0.02	43±2
T 20 μM	1.14±0.01	7±1.7	0.8±0.03	34±2.6	0.62±0.02	49.6±2.3	0.57+0.02	53±2

**Percentage of Cell Growth Inhibition. Data are reported as mean ± SD from three independent measurements. H: haloperidol; R: risperidone; T: theobromine; Ver: Verapamil*

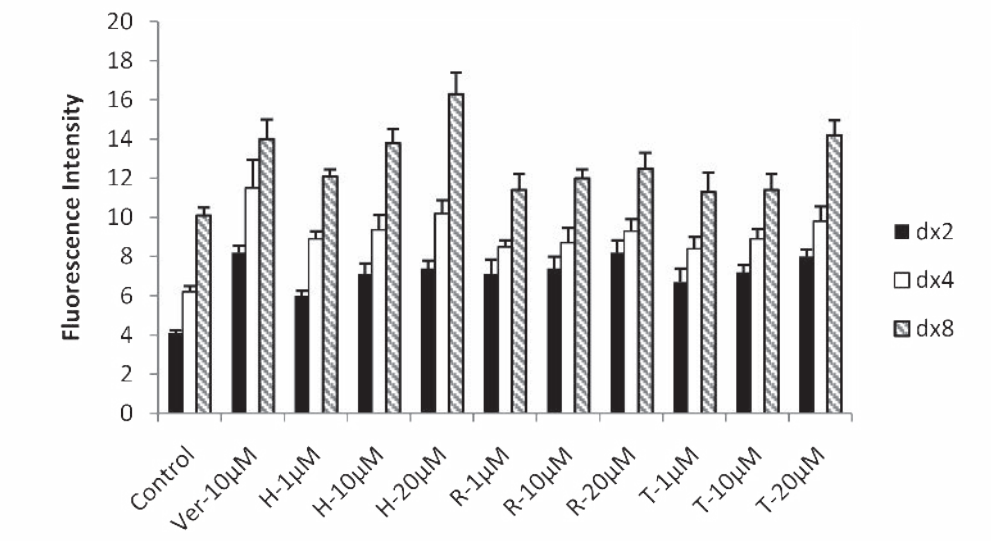

Fig. 1. *Effect of antipsychotic compounds on doxo accumulation on MES-SA/Dx5 cells. The graph shows the doxo fluorescences on resistant cells pre-treated for 24 h at 37°C with Verapamil (10 μM); haloperidol (1, 10, 20 μM), risperidone (1, 10, 20 μM) and theobromine (1, 10, 20 μM) after incubation for 3 h at 37°C with three different concentrations of doxo (2, 4 and 8 μM). Results are expressed as the mean ± S.D. of three different experiments compared with the mean fluorescence of un-pre-treated control cells. All the values were significant ($p<0.05$) when compared with control.*

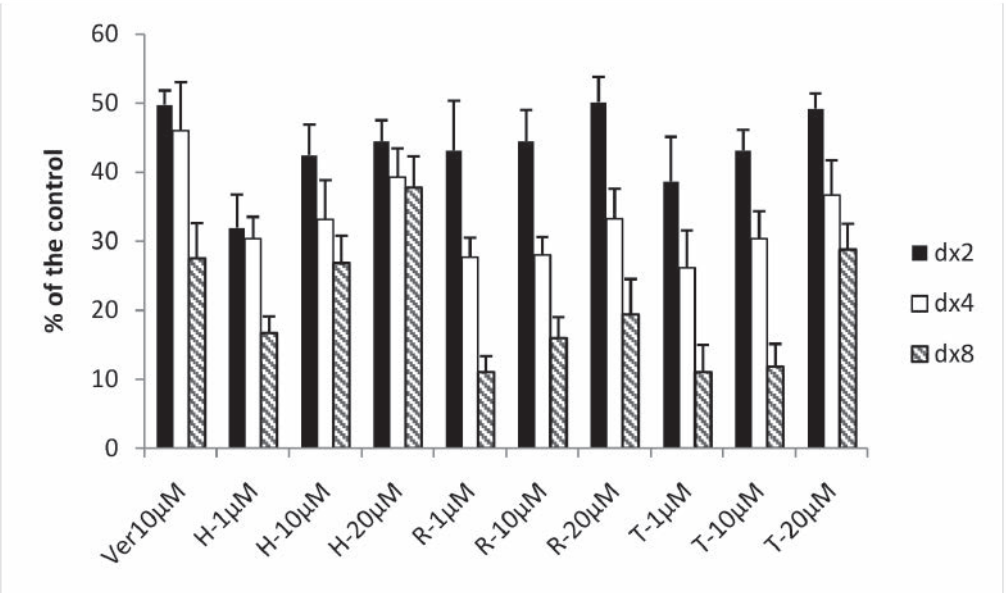

Fig. 2. *Mean percentage of increase in intracellular doxo accumulation in MES-SA/dx5 resistant cells pre-treated for 24 h at 37°C with Ver: Verapamil (10 μM); H: Haloperidol (1, 10, 20 μM),; R: Risperidone (1, 10 20 μM) and T: Theobromine (1, 10, 20 μM) in combination with three different doxo molar concentrations (2, 4 and 8 μM), compared to corresponding untreated cells (doxo alone). All the values were significant compared to control ($p<0.05$). Date are the mean ± S.D. of three experiments.*

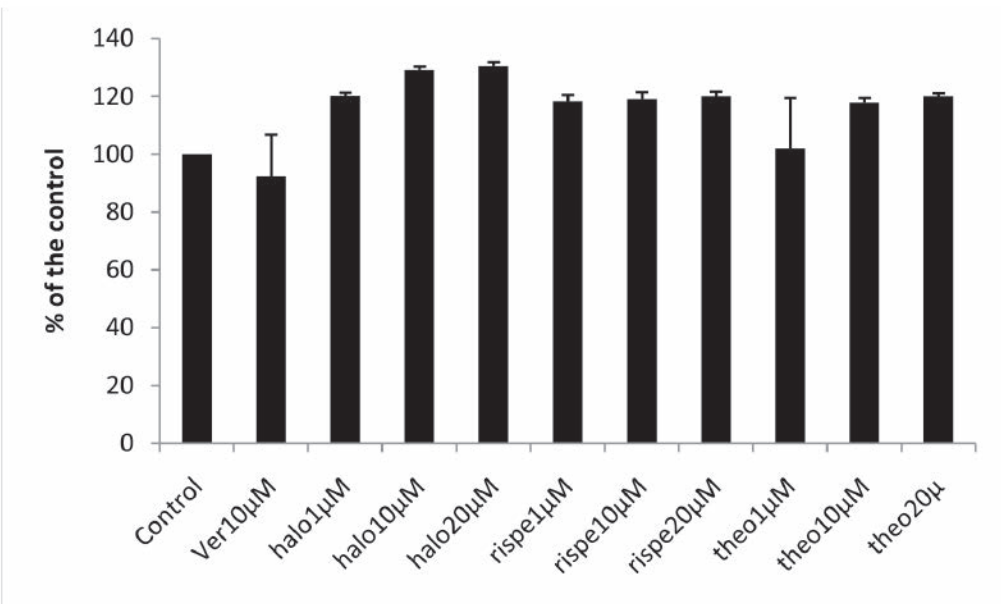

Fig. 3. *Total intracellular GSH concentrations in resistant MES-SA/Dx5 cells after treatment for 3 h with Ver: Verapamil (10 μM), halo: haloperidol (1, 10, 20 μM); rispe: risperidone (1, 10 20 μM) and theo: theobromine (1, 10, 20 μM). Cells treated with medium alone were used as control (100%). Results are expressed as a percentage of control. All the values were significant ($p<0.05$) except the theobromine 1 μM when compared to control untreated cells. Data are the mean ± S.D. of three determinations.*

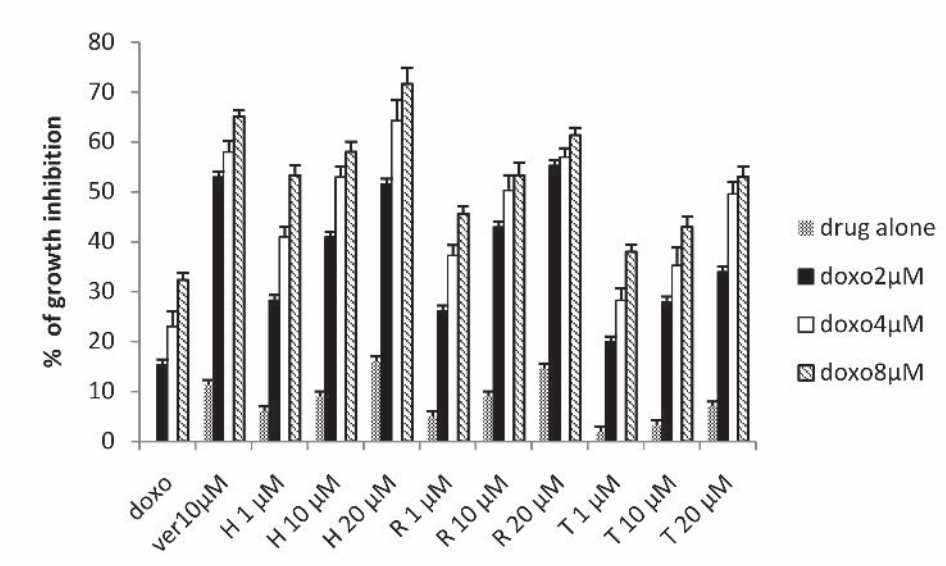

Fig. 4. *Mean percentage of cell growth inhibition (G.I.) in doxo resistant sarcoma cells after treatment for 72 h at 37°C with doxo alone (2,4,8 μM) and in combination with antipsychotic drugs at the indicated concentrations, when compared to untreated control cells. The percentages of G.I. of each compound alone are also reported. Results are the mean ± S.D. of three experiments.*

39.3±4.1 and 27.7±2.8; 28±2.6; 33.3±4.3; and 26.2±5.3; 30.4±3.9; 36.7±5, respectively, and with 8 μM doxo were 16.7±2.4; 26.8±4; 37.8±4.5 and 11±2.3; 15.9±3.1; 19.4±5.1 and 11±4; 11.8±3.3; 28.8±3.7, respectively. The values of Ver (10 μM) used in combination with 2, 4 and 8 μM were 49,7±2.1; 46±7; and 27.5±5.1, respectively (Fig. 2). All values were significant compared to control cells ($p<0.05$).

Effects of antipsychotics on doxo cytotoxicity in MES-SA/Dx5 cells

The data reported in Table I show that antipsychotic compounds combined with doxo significantly increase the sensitivity of MES-SA/Dx5 cells to doxo after 72 h of incubation at 37°C at all doxo concentrations when compared with control cells treated with doxo alone ($p<0.05$). In fact, growth inhibition using 2, 4 and 8 μM doxo concentrations in the presence of haloperidol (1, 10 and 20 μM) showed increases of 1.83; 3.0; 3.3 (haloperidol plus dx 2 μM), 1.78; 2.3; 2.7 (haloperidol plus dx 4 μM) and 1.65; 1.36; 2.2-fold (haloperidol plus dx 8 μM) respectively, whereas in combination with risperidone (1; 10 and 20 μM) increased by 1.7; 2.7; 3.5 (risperidone plus dx 2 μM) and 1.62; 2.1; 2.4 (risperidone plus dx 4 μM) and 1.4; 1.65; 1.89-fold (risperidone plus dx 8 μM), respectively. In presence of theobromine (1, 10 and 20 μM) increased by 1; 1.8; 2.2; (theobromine plus dx 2 μM) and 1.2; 1.5; 2.1; (theobromine plus dx 4 μM) and 1.1; 1.3; 1.6-fold (theobromine plus dx 8 μM) respectively, when compared to the corresponding cells treated with doxo alone. However, results normalized for toxicity of antipsychotic compounds reported in Table I show a recovery of theobromine, in particular at 20 μM concentration in combination with 4 and 8 μM doxo, when compared with cancer cells treated with doxo alone ($p<0.05$).

Effects of antipsychotics on cellular GSH concentrations in MES-SA/Dx5 cells

The effects of antipsychotics and Ver on cellular GSH content in MES-SA/Dx5 cells are shown in Fig.3. All three compounds significantly increased intracellular GSH levels at all concentrations (1, 10 and 20 μM) when compared to control cells ($p<0.05$). However, in cancer cells treated with haloperidol and risperidone we observed that mean cellular GSH levels at 1 μM molar concentration were already

significantly higher (up to 20 and 18%, respectively) when compared to control cells. In contrast, in theobromine series at 1 μM concentration slightly higher values compared to control (100%) were observed, and a significant increase of cellular GSH levels (18 and 20%) at 10 and 20 μM concentration, respectively ($p<0.05$).

DISCUSSION

The Pgp-mediated MDR is the major obstacle to successful clinical cancer chemotherapy, and search of novel, nontoxic and effective compounds against resistance are necessary. In this *in vitro* study, we reported that a group of antipsychotic compounds, haloperidol, risperidone and theobromine, used in combination with doxo, increased doxo accumulation in MES-SA-dx5 cell line (Fig. 1), when compared to corresponding untreated control cultured cells (doxo alone) at all doxo concentrations (2, 4 and 8 μM). In particular, as shown in Fig. 2, exposure of cancer cells to lower doxo concentration (2 μM) in combination with haloperidol, risperidone and theobromine produced a significant increase ($p<0.05$) in cellular doxo accumulation at all concentrations (1, 10 and 20 μM). These gave maximum effect at higher molar concentration (20 μM), about 45%, 50%, and 49%, respectively, similar to that obtained with Ver 10 μM, compared to control cells. In contrast, at higher doxo concentrations (4 and 8 μM) we found a marked reduction capacity to retain doxo which dropped significantly ($p<0.05$) for all three antipsychotics at all concentrations (1, 10 and 20 μM) with minimum effect at lower molar concentration (1 μM). Data indicated this was by up to 16, 11, and 10%, respectively, on MES-SA/Dx5 cells, when compared with the control. The mechanism of the doxo increase in resistant cancer cells is unknown. We suggest that antipsychotics might act as substrates that at low intracellular doxo concentration compete with doxo for binding sites on Pgp such as verapamil, and might saturate these locations, thereby leading to increase in the intracellular doxo accumulation. On the other hand, they might directly inhibit the transporter activity. In contrast, higher intracellular doxo molar concentrations might cause an increase of doxo extrusion by ABC trasporter Pgp in human uterus sarcoma cell line. Consistent with these findings, antipsychotics also increased sensitivity of doxo in resistant sarcoma cells as measured by MTT proliferation cell assay. In fact, as shown in Table I, all three psychotic compounds at all concentrations (1, 10 and 20 μM) enhanced the cytotoxic effects of doxo at all three doxo concentrations (2, 4 and 8 μM) when compared to control cells. The increase was more elevated in presence of the lowest concentrations (2 μM or 1.1 μg/ml) of doxo, (1.83; 3.0; 3.3 and 1.68; 2.7; 3.5; and 1.29; 1.8; 2.23-fold, respectively) which is a concentration lower than the higher serum concentrations achieved when the standard doses of doxo are used in clinical protocols (8-10 μg/ml). However, it is interesting to note that cytotoxic effects of haloperidol and risperidone themselves on tumour cells alone were higher than theobromine, as shown in Table I. Consequently, whether the percentage of growth inhibition was calculated subtracting the cytotoxic activity of both haloperidol and risperidone alone from the respective values obtained in combination with different doxo concentrations, it is possible to note a marked recovery of theobromine at all concentrations (1, 10 and 20 μM) in combination with all doxo concentrations (2, 4 and 8 μM) when compared to control cells. In particular, 20 μM theobromine in combination with doxo 4 and 8 μM was able to significantly ($p<0.05$) reduce cell proliferation of cancer cells (about 43, 46%, respectively), compared to control (Fig. 4). In addition, theobromine is safe and well tolerated *in vivo* with plasma concentrations up to 45 μM attainable after ingestion of 240 mg of theobromine (28) while the maximal plasma concentration attainable *in vivo* of haloperidol and risperidone was about 0.03 μM and 0.1 μM, respectively after a therapeutic oral or i.v. administration (29-30). Therefore, these findings have a clinical importance, because a combined chemotherapy with low dosages of doxo and high dosages of theobromine (side effect free) or its derivatives could increase the efficacy of doxo-based regimens in the treatment of Pgp-mediated MDR tumours as well as reducing its toxic side effects (cardiotoxicity, myelosuppression). Moreover, as shown in Fig. 3, antipsychotic exposure induced a marked increase in GSH production. In particular, haloperidol and risperidone induced a significant increase ($p<0.05$) in GSH production at all concentrations tested (20, 29, 30 and 18, 19, 20%,

respectively) in MES-SA/Dx5 cells when compared to un-pretreated control cells (100%). On the other hand, in the theobromine series the GSH production only slightly increased at low concentration (1 μM) and significantly increased ($p<0.05$) at 10 and 20 μM (18 and 20%, respectively). These results suggest that theobromine at low concentration does not act by affecting the oxidative state of cancer cells inhibiting Pgp activity without severe side effects, while at higher concentrations (10 and 20 μM), the GSH increase could have a protective effect on normal cells against oxidative damage caused by generation of free oxygen radicals during cancer chemotherapy without severe side effects. In summary, the study found that all three antipsychotics tested induce an increase of the cytotoxic effects of doxo in cultured sarcoma cells such as Ver but with less *in vitro* toxic effects. In addition, the results provide a rationale for future clinical studies in order to investigate the use of antipsychotics as potential chemosensitizers. In particular, theobromine is an effective and safe natural compound that, administered at high dosages (side effect free) in combination with conventional chemotherapy, might reverse Pgp-mediated drug resistance and protect normal cells against drug-induced damage in cancer patients.

ACKNOWLEDGEMENTS

The authors thank Federico Angelini for English review of the manuscript.

REFERENCES

1. Ling V. Multidrug resistance: molecular mechanism and clinical relevance. Cancer Chemother Pharmacol 1997; 40:3-8.
2. Gottesman MM. Mechanisms of cancer drug resistance. Annu Rev Med 2002; 53:615-627.
3. Gottesman MM, Pastan I. Biochemistry of multidrug resistance mediated by the multidrug transporter. Annu Rev Biochem 1993; 62:385-427.
4. Gottesmann MM, Fojo T, Bates SE. Multidrug resistance in cancer: role of ATP-dependent transporters. Nat Rev Cancer 2002; 2:48-58.
5. Gillet JP, Gottesman MM. Mechanisms of multidrug rsistance in cancer. Methods Mol. Biol. 2010; 596:47-76.
6. Juliano RL, Ling V. A surface glycoprotein modulating drug permeability in Chinese hamster ovary cell mutants. Biochim Biophys Acta 1976; 455:152-62.
7. Higgins CF. Multiple molecular mechanism for multidrug resistance transporters. Nature 2007; 446:749-57.
8. Ozben T. Mechanisms and strategies to overcome multiple drug resistance in cancer. FEBS lett 2006; 580:2903-9.
9. Sauna ZE, Smith MM, Muller M, Kerr KM, Ambudkar SV. The mechanism of action of multidrug-resistance-linked P-glycoprotein. J Bioenerg Biomembr 2001; 33:481-49.
10. Leonard GD, Fojo T, Bates SE. The role of ABC transporters in clinical practice. Oncologist 2003; 8:411-24.
11. Ward AB, Szewczyk P, Grimard V, et al. Structures of P-glycoprotein reveal its conformational flexibility and an epitope on the nucleotide-binding domain. Proc Natl Acad Sci USA 2013; 110:13386-91.
12. Ambudkar SV, Kimchi-Sarfaty C, Sauna ZE, Gottesmann MM. P-glycoprotein: from genomic to mechanism. Oncogene 2003; 22:7468-85.
13. Trambas CM, Muller HK, Woods GM. P-glycoprotein mediated multidrug resistance and its implications for pathology. Pathology 1997; 29:122-30.
14. Krishna R, Mayer LD. Multidrug resistance (MDR) in cancer. Mechanisms, reversal using modulators of MDR and role of MDR modulators in influencing the pharmacokinetics of anticancer drugs. Eur J Pharm Sci 2000; 11:265-83.
15. Borowski E, Bontemps-Gracz MM, Piwkowska A. Strategies for overcoming ABC-transporters-mediated multidrug resistance (MDR) of tumor cells. Acta Biochim Pol 2005; 52:609-27.
16. Nobili S, Landini I, Giglioni B, Mini E. Pharmacological strategies for overcoming multidrug resistance. Curr Drug Targets 2006; 7:861-79.
17. Angelini A, Di Ilio, Castellani ML, Conti P, Cuccurullo F. Modulation of multidrug resistance P-glycoprotein activity by flavonoids and honokiol in human doxorubicin-resistant sarcoma cells (MES-SA/Dx5): implications for natural sedative as chemosensitizing agents in cancer therapy. J Biol Regul Homeost Agents 2010; 24:197-205.

18. Angelini A, Di Pietro R, Centurione L, Castellani ML, Conti P, Porreca E, Cuccurullo F, Di Ilio C. Inhibition of P-glycoprotein-mediated transport by S-adenosylmethionine and Cynarin in multidrug-resistant human uterine sarcoma MES-SA/Dx5 cells. J Biol Regul Homeost Agents 2012; 26:495-504.
19. Angelini A, Conti P, Ciofani G, Cuccurullo F, Di Ilio C. Modulation of multidrug resistance P-glycoprotein activity by antiemetic compounds in human doxorubicin-resistant sarcoma cells (MES-SA/Dx-5): implications on cancer therapy. J Biol Regul Homeost Agents 2013; 27:1029-37.
20. Caruso R, Grassi L, Nanni MG, Riba M. Psychopharmacology in psycho–oncology. Curr Psychiatry Rep 2013; 15:393.
21. Yoon HJ, Park KM, Choi WJ, Choi SH, Park JY, Kim JJ, Seok JH. Efficacy and safety of haloperidol versus atypical antipsychotics medications in the treatment of delirium. BMC Psychiatry 2013; 13:240.
22. Boettger S, Jenewein J, Breitbart W. Haloperidol, risperidone, olanzapine and aripiprazole in the management of delirium: A comparison of efficacy, safety, and side effects. Palliant Support Care 2014; 5:1-7.
23. Baggott MJ, Childs E, Hart AB, de Bruin E, Palmer AA, Wilkinson JE, de Wit H. Psychopharmacology of theobromine in healthy volunteers. Psychopharmacology 2013; 228:109-18.
24. Wesolowska O, Paprocka M, Koziak J, Motohashi N, Dus D, Michalak K. Human sarcoma cell lines MES-SA and MES-SA/Dx5 as a model for multidrug resistance modulators screening. Anticancer Res 2005; 25:383-89.
25. Tsuruo T, Iida H, Tsukagoshi S, Sakurai Y. Overcoming of vincristine resistance in P388 leukemia in vivo and in vitro through enhanced cytotoxicity of vincristine and vinblastine by verapamil. Cancer Res 2005; 41(5):1967-72.
26. Mosmann TJ Rapid colorimetric assay for cellular growth and survival: application to proliferation and cytotoxicity assay. I. Immunol Methods 1983; 65:55-63.
27. Ellman GC. Tissue sulfhydrylic groups. Arch Biochem Biophys 1959; 82:70-77.
28. Resman BH, Blumenthal P, Jusko W. Breast milk distribution of theobromine from chocolate. J Pediatr 1977; 91:477-80.
29. Zingales IA. A gas chromatography method for the determination of haloperidol in human plasma. J Chromatogr 1971; 54:15-24.
30. Averoso A, Facciolà G, Salemi M, Spina E. Determination of risperidone and its major metabolite 9-hydroxyrisperidone in human plasma by reversed-phase liquid chromatography with ultraviolet detection. J Chromatogr B Biomed Sci Appl 2000; 746:173-81.

LETTER TO THE EDITOR

INFLUENCE OF miR-373 ON THE INVASION AND MIGRATION OF BREAST CANCER AND THE EXPRESSION LEVEL OF TARGET GENES TXNIP

J-G. WANG, L-K. ZHANG, Y-B. CHEN, T. ZHANG, P-F. YUAN and D-C. LIU

Department of Breast Surgery, the First Affiliated Hospital of the Henan University of Science and Technology, Luoyang, China

Received November 21, 2014 – Accepted February 6, 2015

An increasing number of people die from breast cancer every year. Consequently, more research has been concentrated on the study of this type of tumour, and miR-373 resulted as an important gene for treating breast cancer. To explore the influence of miR-373 on the invasion and migration of breast cancer and the expression level of target gene TXNIP, a set of therapeutic methods were designed based on miR-373. The transfection was performed using miR-373 inhibitor; the concentration of miR-373 was controlled by inhibitor, and it was transfected into MCF-7 cell by lipofectin. Fluorescent quantitative polymerase chain reaction was used to detect the expression level of miR-373 in cells after transfection as well as that of Caspase-3 and Caspase-8. MTT assay was used to detect the influence of miR-373 inhibitor on MCF-7 cells. The expression quantity of miR-373 in cell and tissue of breast cancer with high-low invasion and migration ability was detected by qRT-PCR (quantitative real-time polymerase chain reaction), thus the influence of the expression quantity of miR-373 on the invasion and migration of cell was determined. The expression of miR-373, EMT and TXNIP was determined by Western blot. Through the identification of proteomics and bioinformatics, it was finally found that TXNIP was regulated by miR-373. The protein expression level of TXNIP was negatively correlated with the level of miR-373. Thus it was concluded that miR-373 could promote the invasion and migration of breast cancer. In addition, in the tissue and cell of breast cancer with different invasion and migration abilities, the expression level of TXNIP was negatively correlated with the level of miR-373

Both thioredoxin binding protein2 (TBP2) (1) and RAB GTP enzyme binding effect protein1 (RABEP1) have the function of inhibiting cancer induction. It was confirmed that both TBP2 and RABEP1 protein expression levels dropped through luciferase experiment and mutation experiment and they were the direct target gene of miR-373 (2). In recent years, with the increase (3) of miR-373 expression in breast cancer, the recovery rate of breast cancer has improved. However, the pathogenesis and radical solution of breast cancer still need to be researched. MiR-373 is part of miR-371-373 cloud (4). As an extremely conservative endogenous non-coding single stranded small RNA molecule in evolution, miR-373 widely exists in eucaryon with a length of about 21-23 nt. The present research shows that miRNA plays an important role in the process of organism growth, development and disease

Key words: miR-373, TXNIP, breast cancer, MCF-7 cell, fluorescent quantitation polymerase

Mailing address:
Dr Dechun Liu,
Department of Breast Surgery,
the First Affiliated Hospital of Henan,
University of Science and Technology,
Luoyang, 471003, China
e-mail: ldcwjg@163.com

0393-974X (2015)

DISCLOSURE: ALL AUTHORS REPORT NO CONFLICTS OF INTEREST RELEVANT TO THIS ARTICLE.

(5). The report pointed out that the combination between synthetic dsRNAs and promoter could induce gene expression and influence the expression of downstream gene through inducing target gene. It is generally thought that miRNAs plays the role through silencing the expression of target genes. It also plays an important role in the occurrence and development of many diseases, especially which closely related to tumorigenesis.

Thioredoxin-interacting protein (TXNIP), also called Vitamin D3 up-regulating protein1 (VDUP1), is a kind of a-rhodopsin profilin and the only one which can combine with thioredoxin (Trx) in a-rhodopsin profilin family. TXNIP can combine with Trx active cysteine residues thus restraining its antioxidant function, meanwhile it participates in the process of regulating the active oxygen system of the body and mitochondria passage and induces cell apoptosis. Thus mediation function of TXNIP during the cell development process is verified. The gene coding TXNIP locates at chromosome lq21-22 which has 8 exons and is 4174 bp long. TXNIP gene was first found during the process of disposing leukemia cell line HL-60 using 1, 25-dyhydroxy vitamin D-3. Studies suggest that cell generation cycle getting out of control and NK cell developing abnormally of cells related with TXNIP gene are closely related with the formation and transfer of cancer. For now, the expression condition of TXNIP in breast cancer is barely reported and its correlation with clinical symptom of breast cancer is not universally acknowledged. On this account, this paper detected the expression level of miR-373 in breast cancer cells applying qRT-PCR and measured and recorded the influence of miR-373 inhibitor on indicators using MTT assay, qRT-PCR and Western blot and discussed the correlation between protein expression level of TXBIP and miR-373 gene.

MATERIALS AND METHODS

Materials

Enzyme-linked immune detector; flat CR amplification primer of Caspase-3 and Caspase-8; human breast cancer cells; DMEM medium and fetal bovine serum; bovine insulin; thiazole blue; dimethyl sulfoxide; MiR-373 inhibitor and negative control reagent; internal 5s, designed for miR-373 PCR amplification primer; miRNA extraction kit; RNA extraction reagent TRIzol and transfection reagents Lipofectamine2000; fluorescence quantitative PCR kit; real-time fluorescent quantitative PCR; rabbit anti-TXNIP monoclonal antibody; HM315 type paraffin slicing machine; table centrifuge; high-speed refrigerated centrifuge; NANO DROP spectrophotometer; optical microscope; Inverted microscope and thermostat metal bath.

Methods

SNI model: adult SD rats were anesthetized, a cut was made in the lateral skin of the hind leg, the femoral biceps were separated, and the sciatic nerve and its branches were exposed. The distal ligation was implemented. The shin nerve and sural nerve were cut to avoid nerve regeneration and to preserve the sural nerve. Penicillin was injected into the muscle to prevent infection. Sham group: control SNI group. After separating and exposing the sciatic nerve for 3 min the muscle and skin were sutured and penicillin was injected into muscle to prevent infection.

Cell culture

Human breast cancer cell line MCF-7 medium contained DMEM, 10% fetal calf serum and 1% double resistance. It was put into incubator at 37°C, humidity was saturated at 5% CO_2 and its liquid changed once every other day. When the growth area was about 90% these cells resulted as having a ratio of 1:2 or 1:3.

The transfection of miR-373 inhibitor

One day before the transfection, MCF-7 cells in good growth status were chosen and inoculated into 6 orifices with the density of 3x105/hole. After the cell density reached 50%-70%, the experiment was divided into the transfection group, blank group and negative group. Then, according to the conduct manual, transfection with Lipofectamine2000 was carried out, and after 4 h fresh culture solution was added and cultivated for a further 48 h.

Statistical analysis

After comparison with the negative control group, the expression of miR-373 level in the transfection group decreased, the difference was statistically significant ($P < 0.05$).

The mRNA level of Caspase-3 in both the transfection and the negative control group increased by 4.17 times ($P<0.05$), and the mRNA level of Caspase-8 increased 3.32-fold ($P<0.05$). The difference was statistically significant.

The inhibition rate after miR-373 on MCF-7 cell proliferation increased with the increase of concentration ($P < 0.05$) and the difference was statistically significant.

The TXNIP mRNA expression quantity in breast

cancer tissues was 39.07±12.34, in para-carcinoma tissue was 40.12±13.13, there was no statistically significant difference (P <0.05).

The TXNIP protein levels in breast cancer tissues was 0.43±0.11, which was lower than that in breast cancer tissues of 0.85±0.01 The difference was statistically significant (P<0.05).

RESULTS

Difference between miR-373 inhibitor before and after transfection on MCF-7 cells

After miR-373 inhibitor transfected into MCF-7 cells for 48 h, Real-Time PCR was used to detect the expression situation of miR-373 in cells. Compared with negative control group, the expression level of miR-373 decreased (P<0.05), as shown in Fig. 1. The result indicated that miR-373 inhibitor can effectively suppress the miR-373 expression in MCF-7 cells.

The mRNA level of caspase-3 and caspase-8 before and after miR-373 inhibitor transfection on MCF-7 cells

Compared with negative control group, the mRNA level of Caspase-3 increased 4.17 times (P<0.05), and the mRNA level of Caspase-8 increased 3.32-fold (P<0.05), as shown in Table I.

Table I. *The mRNA expression situation of Caspase-3 and Caspase-8 before and after miR-373 inhibitor transfection.*

Group	Ct0	Ct1	Ct2	ΔCt1	ΔCt2	ΔΔCt1	ΔΔCt2	2-ΔΔCt1	2-ΔΔCt2
Trans-fection group	22.14±0.32	20.94±0.71	21.03±1.12	-1.2±0.92	-1.11±0.85	-2.06	-1.73	4.17	3.32
The negative control group	23.51±0.42	24.37±0.57	24.13±1.32	0.86±1.32	0.62±0.84				

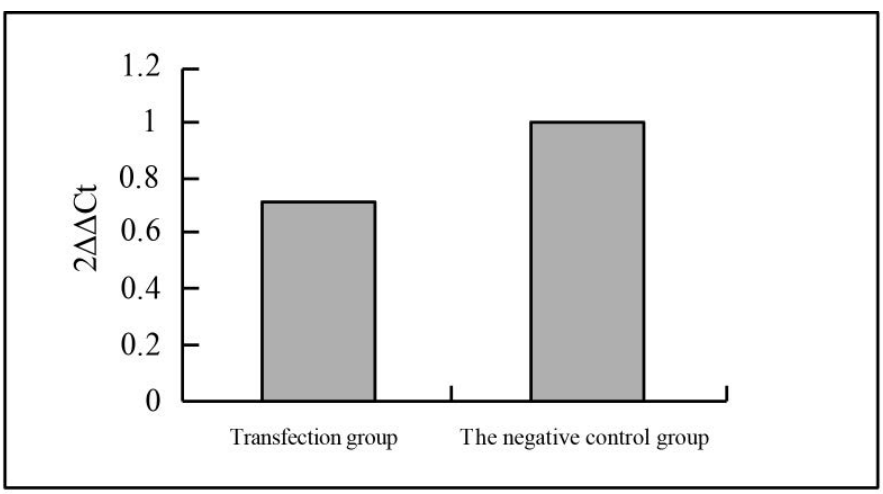

Fig. 1. *The miR-373 change situation after miR-373 inhibitor transfection.*

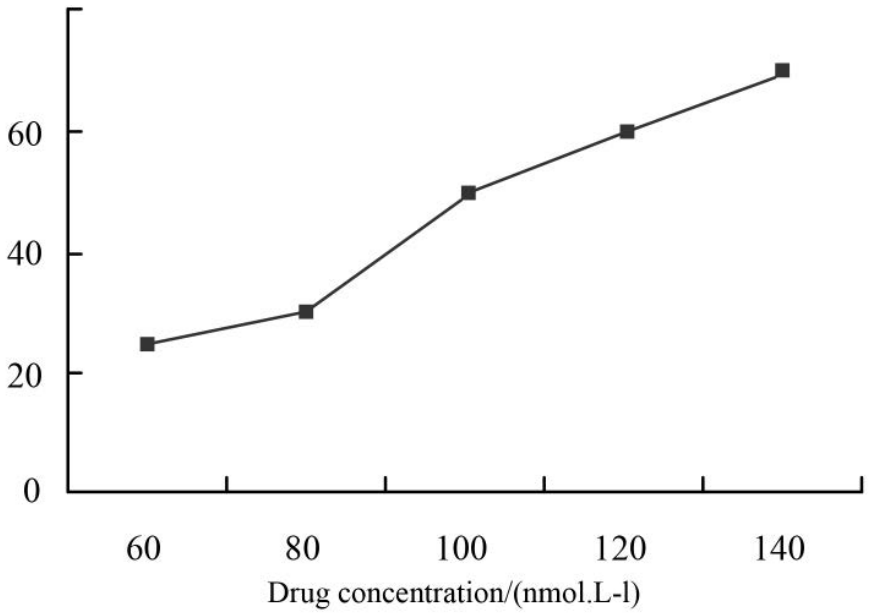

Fig. 2. *The influence of miR-373 Inhibitor on MCF-7 cell proliferation.*

The influence of miR-373 Inhibitor on MCF-7 cell proliferation

By using MTT inhibitor to MTT colorimetric assay, miR-373 inhibitor in 60-140nmol/L concentration section was detected to have an inhibiting effect on MCF-7 cell growth, and the inhibition ratio increased with the increase of concentration ($P<0.05$) as shown in Fig. 2. From the combination of the above three studies, we can conclude that miR-373 can promote the invasion and migration of breast cancer by inhibiting the expression of TXNIP gene.

qRT-PCR detected TXNIP mRNA level

The expression quantity of TXNIP mRNA in breast cancer tissues was 39.07±12.34, and in para-carcinoma tissue was 40.12±3.13. It was concluded that miR-373 presented up regulation in breast cells and high invasion and migration ability of tissue.

Western blotting detected TXNIP protein level

The protein level in breast cancer tissue was 0.43±0.11 which was lower than that in breast cancer tissues of 0.85±0.01, thus we concluded that the expression level of TXNIP protein was negatively correlated with that of miR-373.

DISCUSSION

Since the discovery of the first miRNA, with the continuous research of miRNA function, more studies have shown that the ability of micromRNA to regulate and control the body's normal physiological activities is closely related to the occurrence of tumor. Domestic research shows that the low expression quantity of miRNA cells could increase by adopting the vector construction method. In addition, after the constructed plasmid transfected into human cells, it could be integrated into cellular genome thus obtaining stable expression. After the expression of promoter in carrier fused with fluorescin, the fluorescin could indirectly report the microRNA expression situation and could also measure the transfection efficiency and expression situation during process of plasmid imported into cells. Many researchers concentrated on the study of miR-373. Voorhoeve et al. identificated miR-372 and miR-373 in the germ cell of testicles very early, along with the characteristic high expression level

and oncogene. The expression of miR-373 was also found in the sample of squamous-cell carcinoma tissues of human esophagus cancer. MiR-373 inhibited the p53 access inhibiting the expression of tumor repressor and eliminated its inhibiting function on cell cycle dependency kinase, thus promoting the development of cancer (6); Takamizawa, et al. used pH1-RNApuro plasmid to effectively up-regulate the expression of miRNA gene; Schultz, et al. (7), transfected miR-373 in human immortalized epidermis cells and found that TGF-βreceptor1 (TGFBR1) and receptor2 (TGFBR2) combined with miR-373, and the mRNA level of TGFBR2 decreased. Because TGF-β played an important role in cell proliferation, apoptosis and tumor metastasis and the down-regulation of its expression, it could promote deterioration and metastasis of tumor. The function of miRNA in tumor was mainly in these aspects, such as angiogenesis (8), cell apoptosis (9), invasion and metastasis, cell proliferation (10) and tumorigenesis (11). Due to the close relationship between miRNA and tumor, researchers termed it the living inhibiting gene of cancer. Mature miRNA were led into RNA induced complexus, and coupled on target gene mRNA through the function of complementary alkali genes, regulating gene expression (12). We could reduce the sensitivity of cell to p53 allele of normal expression by blocking the aging induced by RAS and disturbing cell transformation mediated by RAS, blocking the path of CDK inhibition mediated by p53 or directly inhibiting the expression of cancer suppressor gene LATS2 and promote the formation of embryonic cell in the testicle. MiR-373 could also promote the proliferation of human esophagus cancer through expression inhibition of cancer suppressor gene LATS2. These studies indicated that miR-373 was closely related to the invasion and migration ability of tumor (13).

In this study the variation of miR-373 caused by miR-373 inhibitor transfecting MCF-7 cell suggested miR-373 inhibitor can effectively restrain the expression of miR-373 in MCF-7 cells. After the transfection, mRNA level of Caspase-3 and Caspase-8 increased by 4.17 times and 3.32 times respectively comparing with negative control group($P<0.05$). MTT colorimetric experiment suggested that the inhibition function of miR-37 to the development of MCF-7 is active when the concentration is 60~140nmol/L and the inhibition ratio increased as the concentration increased ($P<0.05$). So miR-373 can promote breast cancer invasion and migration by restraining the expression of TXNIP gene. The experiment of qRT-PCR found the expression quantity of TXNIP mRNA in breast cancer was 39.07±12.34, while the expression in fatigue tissues was 40.12±13.13, which suggested that miR-373 expresses as up-regulation in breast cancer cells and tissue with high ability of invasion and migration. The detecting applied to Western blotting method showed the protein level of TXNIP in breast cancer tissue was 0.43±0.11 which was lower than 0.85±0.01 to the tissue near the cancer, suggesting the protein expression level of TXNIP was negatively correlated with miR-373 level. In short, the reduction of TXNIP protein expression leads to dysdifferentiation of breast cancer cells, bad histopathological classfication and maliganancy increaseof the cells, resulting in easily occurred recurrence and metastasis (12).

REFERENCES

1. Masutani H, Yoshihara E, Masaki S, Chen Z, Yodoi J. Thioredoxin binding protein (TBP)-2/Txnip and á-arrestin proteins in cancer and diabetes mellitus. J Clin Biochem Nutr 2012; 50(1):23-34.
2. Yan GR, Xu SH, Tan ZL, Liu LX, He QY. Global identification ofmiR-373-regulated genes in breast cancer by quantitative proteomics. Proteomics 2011; 11(5):912-135.
3. Chen W, Cai F, Zhang B, Barekati Z, Zhong XY. Chen W, Cai F, Zhang B. The level of circulatingmiRNA-10b and miRNA-373 in detecting lymph nodemetastasis of breast cancer: potential biomarkers. Tumour Biol 2013; 34(1):455-62.
4. Nikaki A, Piperi C, Papavassiliou AG. Role of microRNAsin gliomagenesis: targeting miRNAs in glioblastoma multiforme therapy. Expert Opin Investig Drugs 2012; 21(10):1475-7.
5. Y. R. Wei, Q. X. Lu, Q. J. Lu. Research progress of microrna and cell signal transduction pathway. Biological Technology Bulletin 2010; 28-32.
6. Lee KH, Goan YG, Hsiao M, Lee CH, Jian SH, Lin JT, Chen YL, Lu PJ. MicroRNA-373post-transcriptionally regulates large tumor suppressor,

homolog 2 and stimulates proliferation in human esophageal cancer. Exp Cell Res 2009; 315(15):2529-38.
7. Schultz N, Marenstein RD, De Angelis DA, et al. Off-tar-get effects dominate a large-scale RNAi screen for modulators of the TGF-β pathway and reveal microRNA regulation of TGFBR2. Silence 2011; 2:1-20.
8. Bonauer A, Carmona G, Iwasaki M, et al. miRNA-92acontrols angiogenesis and functional recovery of ischemic tissues in mice. Science 2009; 324(5935):1710-3.
9. Wang Y, Lee CG. miRNA and cancer focus on apoptosis. J Cell Mol Med 2009; 13(1):12-23.
10. Lee KH1, Goan YG, Hsiao M, Lee CH, Jian SH, Lin JT, Chen YL, Lu PJ. MicroRNA-373 (miR-373) post-transcriptionally regulates large tumor suppressor, homolog 2 (LATS2) and stimulates proliferation in human esophageal cancer. Exp Cell Res 2009; 315(15):2529-31.
11. Pineau P, Volinia S, Mcjunkin K, et al. miR-221 overexpression contributes to liver tumorigenesis. Proc Natl Acad Sci USA 2010; 107(1):264-9.
12. O'Day E, Lal A. MicroRNAs and their target gene networks in breast cancer. Breast Cancer Res 2010; 12(2):201-2.
13. Vasudevan S. Functional validation of microRNA-targetRNA interactions. Methods 2012; 58(2):126-34.

LETTER TO THE EDITOR

HOW EXPRESSIONS OF CLAUDIN-1 AND MMP-2 IN RETINOBLASTOMA CORRELATE WITH HISTOLOGICAL DIFFERENTIATION AND OPTIC NERVE INVASION

WC. WAN, XM. JIN, GY. ZHENG, FY. ZHANG, Y. LV and Y. ZHU

Ophthalmology, the First Affiliated Hospital of Zhengzhou University, Zhengzhou, China

Received January 9, 2015 – Accepted March 9, 2015

Retinoblastoma is a commonly seen and dangerous intraocular malignant tumor in infants. Studies have found that Claudin-1 and MMP-2, whose expressions may be connected, play roles in tissues of retinoblastoma. In this study we analyze and discuss changes of Claudin-1 and MMP-2 expressions, and the correlation between the expressions and retinoblastoma histological differentiation and optic nerve invasion. MaxVisionTM was applied to detect expressions of Claudin-1 and MMP-2 in 45 samples of retinoblastoma and 15 paraffin-embedded samples of normal retina. The correlation between Claudin-1 expression and MMP-2 expression was analyzed based on *chi*-squared test and Spearman's correlation test. Positive expressions of Claudin-1 in retinoblastoma were fewer than those in retina; higher positive expressions were found in differentiated tissues than in undifferentiated tissues; while compared to expressions in invasive optic nerves, Claudin-1 expressed more positively in optic nerves without invasion. As for MMP-2, its expressions were higher in retinoblastoma than in normal retina; undifferentiated tissues had higher positive expressions than differentiated tissues, which were not statistically significant; higher positive expressions were detected in invasive optic nerves. Thus, it could be concluded that the correlation between Claudin-1 expression and MMP-2 expression in retinoblastoma was negative. Expressions of Claudin-1 were positively related to histological differentiation and optic nerve invasion of retinoblastoma; while MMp-2 expression had negative correlation with histological differentiation and optic nerve invasion of retinoblastoma. Clandin-1 and MMP-2 played a negative role in the optic nerve invasion and tumor development of retinoblastoma.

Retinoblastoma (RB), a commonly seen and dangerous intraocular malignant tumor in infants, originates from embryonic nuclear layer cell in the retina. It is thought that the prognosis of RB is closely related to optic nerve invasion and tumor distant metastases. Recent studies have found that abnormal expressions of Claudin-1 and MMP-2 are linked with the invasion and metastases of tumor. Claudin is one of the major structures for inter-cell tight junction proteins, while Claudin-1 belongs to Claudin family with more than 20 members which express differently (up-regulation or down-regulation) in various tumors. Furthermore, the expression with differences has been proved to be involved in tumor advancement (1). MMP-2, a core member of matrix metalloproteinase (MMP),

Key words: protein Claudin-1, protein MMP-2, retinoblastoma, histological differentiation, optic nerve invasion

Mailing address: Dr Yu Zhu,
Ophthalmology,
First Affiliated Hospital
of Zhengzhou University,
No.1, Jianshe East Road,
Zhengzhou, Henan, 450052, China
e-mail: zy@ibhsedu.com

0393-974X (2015)

degrades extracellular matrix, basement membrane included, to cause damage. MMP-2 increases tumor invasion when it destroys organic prevention of tumor invasion and metastasis.

With MaxVisionTM, Yan Sun et al. tested immunohistochemistry (IHC) of Livin, PTEN and MMP-9 in tissues of RB and normal retina, and discussed their correlations. The results showed that positive expressions in RB had clinical significance (2). Lijuan Meng adopted the grouping method to test changes of MMP-9 and VEGF expressions, ending up with high clinical values that MMP-9 and VEGF expressions in RB were increased (3). Based on MaxVisionTM, Jia Yu et al. detected expressions of MMP-9 and NF-kB by their monoclonal antibodies to see how the expressions connected with RB differentiation and optic nerve invasion. The results could be used as biological indicators to reflect RB invasion and metastasis, helping select high-risk patients (4).

Having adopted MaxVisionTM, this research detected Claudin-1 and MMP-2 expressions in tissue slices of RB, to observe their relationship with tumor cell differentiation, optic nerve invasion and metastasis, as well as clinical stages.

MATERIALS AND METHODS

Study subjects

Eyeball tissues were taken of RB infants who had undergone ophthalmectomy from 2001 to 2012 in all hospitals in Zhengzhou, China. In total there were 45 paraffin-embedded samples, 17 with differentiation and 28 with undifferentiation. Furthermore, a total of 19 were intraocular (stage I), 17 glaucoma (stage II), and 9 extraocular (stage III). RB was diagnosed by the completion of eyeball tissue reproduction and Hematoxylin and eosin (HE) dyeing. Of the 45 samples, 23 were from males and 22 from females; 24 samples were of right eye RB, and 21 of the left eye, and binocular incidence was not detected; the average age of the subjects was two years and eight months. No patient had received radiotherapy or chemotherapy prior to surgery. Ten out of fifteen samples of normal retina were pathologically proved to be adjacent after ophthalmectomy, and five samples were from pathologically normal retina from subjects who had undergone ophthalmectomy because of external damage.

Major reagents

Rabbit anti-human polyclonal Claudin-1 antibody from ABGENT company with 1:50 working concentration; rabbit anti-human polyclonal MMP-2 antibody from BOSTER company (Wuhan, China) with 1:200 working concentration; ready-to-use kit of MaxVisionTM (KIT-5030), goat anti-mouse or anti-rabbit IgG polymer with enzyme labels, and DAB dyeing liquor from MXB company (Fujian, China).

Methods

Samples were fixed with 10% neutral formalin and embedded with paraffin. Every paraffin block was cut into 3 to 5 pieces, 3-μm thick. Then blocks were rinsed under 40°C water. Pellets were taken out and kept at 4°C after drying at room temperature. Before MaxVisionTM, the following steps were taken in order: blocks were kept overnight in an oven at 60°C, de-waxed with dimethylbenzene and hydrated with alcohol, and rinsed with PBS. Completed steps of MaxVisionTM were taken according to the manufacturer's insstructions for KIT-5030, when blocks finished antigen retrieval with citric acid repair liquid (PH=6) at 95°C. Finally the blocks were colored with 3,3'-Diaminobenzidine (DAB). Positive Claudin-1 referred to tissue blocks of colon cancer with known positive expressions of Claudin-1, as did MMP-2. Reference for negative expressions was PBS solution rather than primary antibody.

Evaluating standards for research results

Positive expressions were performed as brown particles in cell membranes of tumor cells and normal retina cells. Each block was observed under 5 random high power fields (X200). Two hundred cells under each field were counted and the rate was calculated of positive cells with 1000 cells from five fields. For Claudin-1 protein grading, <1% referred to negative expression, 1%-25% (+) positive expression, 25%-50% (++) neutral positive, and >50% (+++) strong positive. For MMP-2, <1% signified negative expression, 1%-10% (+) positive expression, 10%-25% (++) neutral positive and >25% (+++) strong positive, which was on the basis of positive rate (5 high power fields).

Statistic analysis

Research data were analyzed with SPSS 17.0 software for statistics). *Chi*-squared test was adopted to compare expressions of Claudin-1 and MMP-2 in adjacent tissues and RB tissues, and the correlation between those expressions were analyzed by Spearman 's correlation test. The result was statistically significant with $P<0.05$.

RESULTS

Claudin-1 expression

Positive expressions of Claudin-1 resulted

Table I. *Relationship between Claudin-1 expression and RB clinical and pathological characteristics.*

Clinical and pathological characteristics	Gender		Clinical stage			Pathological type		Optic nerve invasions	
	Male	Female	Stage I	Stage II	Stage III	Undifferenitation	Differentiation	Without invasion	With invasion
Samples (n)	23	22	19	17	9	28	17	26	19
Positive expression (n)	13	11	16	7	1	11	13	20	4
Negative expression (n)	10	11	3	10	8	17	4	6	15
Positive rate (%)	56.52	50.00	84.21	41.18	11.11	39.29	76.47	76.92	21.05
P		0.661	P1, 2#=0.001	P2, 3*<0.001	P1, 3**<0.001		0.015		<0.001

*# refers to P between stage I and stage II, * refers to P between stage II and stage III, and ** refers to P between stage I and stage III.*

Table II. *Relationship between MMP-2 expression and RB clinical and pathological characteristics.*

Clinical and pathological characteristics	Gender		Clinical stage			Pathological type		Optic nerve invasion	
	Male	Female	Stage I	Stage II	Stage III	Undifferentiation	differentiation	Without invasion	With invasion
Samples (n)	23	22	19	17	9	28	17	26	19
Positive expression (n)	15	16	9	13	9	20	11	14	17
Negative expression (n)	8	6	10	4	0	8	6	12	2
Positive rate (%)	65.22	72.73	47.37	76.47	100.00	71.43	64.71	53.84	89.47
P		0.586	P1, 2#=0.006	P2, 3*<0.001	P1, 3**<0.001		0.636		<0.011

*# refers to P between stage I and stage II, * refers to P between stage II and stage III, and ** refers to P between stage I and stage III.*

Table III. *Relation between Claudin-1 and MMP-2 in RB.*

Claudin-1	MMP-2		Total
	Positive	Negative	
Positive	13	11	24
Negative	18	3	21
Total	31	14	45

56.52% in male and 50.00% in female. Brown particles were present in the dyed parts of cell membranes and or endochylema in RB cells and normal retina cells. In clinical stages, the highest positive rate reached 84.21% in intraocular, reduced to 41.18% in glaucoma, and finally remained at the lowest in extra-ocular with 11.11%. As shown in Table I, the positive expressions were reduced with tumor occurrence and development.

MMP-2 Expression

Dyed parts of MMP-2 were similar to Claudin-1, but MMP-2 positive expression occupied 6.22% in male and 72.73% in female. Positive rate in the differentiation group (64.71%) was lower than in the undifferentiation group (71.43%), which was

not statistically significant. Brown particles in cell membranes and/or endochylema of RB cells and normal retina cells indicated that MMP-2 had no impact on the differentiation of tumor cells. Thdrefore it was possible that MMP-2 expression did not connect to the differentiation degree of tumor cell (Table II).

Relationship between Claudin-1 and MMP-2

Based on Spearman's rank correlation, Claudin-1 expression in RB was found to be in negative relation with MMP-2. To be specific, positive Claudin-1 was accompanied by 13 cases of positive MMP-2 expression and 11 cases of negative MMP-2 expression; while if Claudin-1 was negative, 18 MMP-2 cases were discovered to be positive and 3 cases were negative [Table III ($r=-0.537$ and $P=0.023$)].

DISCUSSION

RB is an intraocular malignant tumor, usually occurring in children. The key biological features of RB, and main cause of patients' death, were the invasion and metastasis of malignant tumor. Inter-cell adhesion in common organism contains adhesion junction and tight junction, which acts significantly in maintaining health structure and function of epithelial cells and endothelial cells. Tight junction consists of adhesion molecules of trans-membrane cell whose main trans-membrane proteins refer to Claudin and Occludin, regulating cell proliferation and differentiation, maintaining cell polarity and permeability (5). Generally speaking, Claudin expresses and distributes on membranes of adjacent surfaces in epithelial cells, which leads to inter-cell tight junction; furthermore, Claudin forms lateral distribution along base membranes and epithelial cells. It has been reported that Claudin expresses with specificity in a variety of tissues and organs (6). The correlation between Claudin-1 expression and RB (including malignant tumor occurrence, development and metastasis) was a slow process involving various elements. But how this worked isstill unknown. It is generally maintained that damage of cell junction caused by the loss of inter-cell adhesion is linked to malignant tumor development and metastasis (7). Recent finding presented that abnormal expressions of Claudin (the main end-blocking protein for tight junction), could influence the tight junction. Moreover, abnormal expressions also related to malignant tumor occurrence, development and prognosis (8).

This study, based on MaxVisionTM (9), detected 53.33% positive expression of Claudin-1 in RB cells, but the positive rate reached 93.33% in normal retina cells, which signified a remarkable difference with $P<0.001$. Positive rate with 76.47% in the differentiation group was higher than 39.29% in undifferentiation, $P=0.015$; while 76.92% in optic nerves without invasion was greater than 26.32% in optic nerves with invasion. As for expressions in clinical stages, positive rates were 84.21% in stage I, 41.18% in stage II and 11.11% in stage III. Expressions between stages I and II (10), stages II and III, and stages I and III had statistic difference with $P<0.01$, and reduced as tumor occurring and developing. All the above indicated that Claudin-1 expression did have a relationship to clinical stage of RB, differentiation degree of tumor cell and optic nerve invasion. In addition, it was also shown in the results that if Claudin-1 expression reduced, the inter-cell tight junction was likely to be destroyed, causing optic nerve RB invasions (11) and tumor occurrence and development. However, gender did not play a role in Claudin-1 expressions in RB, which was in accordance with studies based on the close relationship between abnormal expressions of Claudin-1 and malignant tumor occurrence, development and prognosis (12).

MMP, with dependence on Zn^{2+}, belongs to endogenous proteolytic enzyme that has gelatinase with gelatinase A (MMP-2) and gelatinase B (MMP-9) degrading gelatin and basement membrane collagen (type-VI, V, VII and X), which means greater adhesion between cell and ground substance (13, 14). With regard to the correlation between MMP-2 and RB, it is generally thought that the core step of malignant tumor local invasion and metastasis is the degradation of extracellular matrix (ECM). Enzymes could degrade big molecule proteins of ECM. MMP-2 from the Matrix metalloproteinase (MMP) family was named type IV collagenase, and it could damage ECM around tumor surfaces by degrading IV collagen to cause tumor invasion and metastasis. The increase of MMP-2 expression could

enhance tumor ability for invasion and metastasis (15).

In the present study, MMP-2 expression in RB was tested and 68.89% positive expressions were found in RB and 6.67% in normal retina cells. The increase of MMP-2 expression in RB with P<0.01 showed that the increase caused RB occurrence. With P=0.636, the difference between 64.71% positive expressions in differentiation group and higher percentage of 71.43% in undifferentiation did not have statistical significance. But the difference showed that MMP-2 expression did not make a difference to tumor cell differentiation and did not have relativity with differentiation degree. MMP-2 expression promoted optic nerve invasion, which was noted by the statistic difference (P=0.011) between 89.47% positive expressions in optic nerves with invasion and 53.84% in optic nerves without invasion. In clinical stages, positive rates differ from 47.37% in stage I, 76.47% in stage II and 100% in stage III. Expressions between stage I and stage II had statistical difference with P<0.05, as did expressions between stage II and stage III, and expressions between stage I and stage III. Thus, MMP-2 could make tumor expand. Moreover, gender made no difference to MMP-2 expression (16).

The experiment calculcated the close bond between MMP-2 expression and RB clinical stages and optic nerve invasion. Therefore, MMP-2 over-expression was likely to lead to optic nerve invasion and tumor clinical process. The result was consistent with reports in literature that tumor potential for invasion and metastasis was positively affected by tumor cell production of MMP-2.

In summary, by statistic analysis, the simultaneously testing of Claudin-1 expression and MMP-2 expression in RB is proof of the correlation between the expressions and tumor differentiation and invasion as well as clinical stages. With different working mechanisms, Claudin-1 and MMP-2 function differently in RB invasion and metastasis, but their expressions are connected. It is possible that normal expressions of Claudin-1 can sustain cell stability. While in RB tissues, low level expression of Claudin-1 destroys inter-cell tight junction, and high level expression of MMP-2 degrades ECM; the combination of the mentioned low level and high level expressions makes RB more invasive and pushes tumor cell processing forward. To the best of our knowledge, this is the first study to demonstrate low level expression of Claudin-1 and high level expression of MMP-2 as indexes for optic nerve invasion and high risk development of RB. However, more time is necessary to put the research results into application for guiding clinical practices. Further research should be carried out before the results of this study can be applied in clinical practice with accuracy and practicability of test methods.

REFERENCES

1. Zhuang XM, Cao YH, Fan XS. Study on correlation between tight junction protein claudin-1 and breast neoplasms. Chinese Journal of Bases and Clinics in General Surgery 2012; 19(2):192-96.
2. Sun Y, Zhang X, Wang DT, Zhu J, Zheng JQ. Expression of Livin, pten and mmp-9 in retinoblastoma and their correlation. Recent Advances In Ophthalm 2014; 34(2):135-39.
3. Meng LJ. Changes of expressions of MMP-9 and VEGF in retinoblastoma. Shandong Medical J 2011; 51(38):96-97.
4. Yu J, Wang JF, Qin M, Yue XL, Zhou Q, Li J. Expressions of MMP-9 and NF-KB in retinoblastoma. Internat Eye Sci 2012; 12(8):1470-73.
5. Zuo L, Li W, You SJ. Progesterone reverses the mesenchymal phenotypes of basal phenotype breast cancer cells via a membrane progesterone receptor mediated pathway. Breast Cancer Res 2010; 12(3):109-121.
6. Bronstein JM, Chen K, Kornblum HI. Developmental expression of OPS/Claudin11. Neurosci Res 2000; 60(3):284-90.
7. Yang Y, Wu LQ. Research status of inter-cell tight junction proteins- claudins in malignant tumors. Experimen and Laborator Med 2013; 31(2):146-148.
8. Liu YY, Li LL, Xia X, Xue XD, Fu JH. Research progress on the correlation between tight junction proteins and lung diseases. J Clinic Pediatric 2012; 30(5):492-95.
9. Zhang WQ. The application of immunohistochemistry in pathological diagnosis. Anhui Medical and Pharmaceutical J 2012; 16(11):1700-702.
10. Long H, Zhou P. Expression and significance of

MMP-2 and MMP-14 in retinoblastoma. Internat J of Ophthalm 2011; 11(10):1719-21.
11. Tang S, Lu XH, Zhang GM, Zhao JY, Zhao DS,Liu GQ. Clinical analysis of combined therapy of retinoblastoma. J of Practic Oncolog 2013; 28(2):167-70.
12. Xu JH, Cui M. Research advances in relationship between tight junction protein-claudins and tumors. Medical Recapitulate 2008; 14(7):1014-16.
13. Ogata Y, Miura K, Ohkita A, et al. Imbalance between matrix metalloproteinase 9 and tissue inhibitor of metalloproteinase 1 expression by tumor cells Implicated in liver metastasis from colorectal carcinoma. Kurumc Med J 2001; 48(3):211.
14. Zhang S, Li L, Lin JY, Lin H. Imbalance between expression of matrix metalloprotcinase-9 and tissue inhibitor of metalloprotcinase-1 in invasiveness and metastasis of human gastric carcinoma. World J Gastrocntcrol 2003; 9(5):899.
15. Wang SZ, Ma XM. Advancing research on relationship between extracellular matrix and tumor metastasis. Acta Academiae Medicinae Neimongol 2009; 31(1):76-80.
16. Lippoldt A, Liebner S, Andbjer B, et al. Organization of choroid plexus epithelial and endothelial cell tight junctions and regulation of Claudin-1, -2 and-5 expression by protein kinase C. Neurore Port 2000; 11(7):1427-31.

LETTER TO THE EDITOR

SIDE EFFECTS OF TUBERCULOSIS TREATMENT WITH FIXED-DOSE COMBINATIONS

HQ. ZHANG, XE. XI, YL. WANG, W. HAN, CX. ZHANG and JH. JIAO

Tuberculosis Medicine, the First Affiliated Hospital of Xinxiang Medical University, Weihui, China

Received January 9, 2015 – Accepted March 10, 2015

This paper aimed to explore the therapeutic effect and safety of Fixed-dose Combinations (FDCs) on tuberculosis. A computer search was carried out to review the literature related to clinical randomized controlled trials (RCTs) and clinical controlled trails (CCTs) on the curative effect and safety of treating pulmonary tuberculosis with FDCs. The results demonstrated that, in the 22 studies examined, comparison of sputum negative conservation rate of treating smear-positive pulmonary tuberculosis with FDCs and single drug, the relative risk (RR) value and 95% confidence interval (CI) were 1.02 (1.01, 1.03) and 1.01 (1.00, 1.02), respectively, at the end of the 2nd month and 6th month (P<0.05), while comparison of the relapse rate within six months showed that RR value and 95% CI was 1.72 (0.98, 3.02) (P>0.05). No statistically significant differences were found between the two groups in total occurrence of the rates of side effects pertaining to skin reaction, gastrointestinal tract side reaction, occurrence rate of liver and gall side reaction or occurrence rate of drug withdrawal because of side effects (P>0.05). After sensitivity analysis, it was found that occurrence rate of gastrointestinal tract side effects and occurrence rate of liver and gall side effects were unstable. All the findings suggest that the curative effect of treating tuberculosis with FDCs is better than that of a single drug. More reliable evidence is required since the safety evaluation results are not stable.

Tuberculosis, is a chronic infectious disease is highly prevalent in China. Tuberculosis, featured by its highly infectious, high drug resistance, and low declining rates, occurs mostly among young and middle-aged people and evidently differs in various areas (1, 2). Treatment of tuberculosis mainly includes traditional Chinese medicine and Western medicine, combinations of these two, surgical operation, endobronchial therapy for caseous lesion drainage, and physical therapy, immunotherapy and gene therapy (2).

Fixed dose combination (FDC) is a compound mixture preparation combined with different antituberculosis drugs in varying doses in chemotherapy regimens. Through observation of domestic FDCs in the initial treatment of smear-positive pulmonary tuberculosis, Cai and Feng (3) proved that domestic quadruple FD preparations were highly efficient antituberculosis drugs worth promoting. Du J et al. (4) studied the effectiveness and safety of antituberculosis FDCs and found that the effect corresponded to the Chinese national standard therapeutic regimen, with easy adjustment of dose and fewer untoward side effects, therefore, it is promising for promotion. In addition, based on the comparison of effects of FDCs and plate

Key words: FDCs, tuberculosis, side reaction, safety analysis

Mailing address: Dr Huiqiang Zhang,
Tuberculosis Medicine,
First Affiliated Hospital
of Xinxiang Medical University,
Weihui, Henan, 453100, China
Tel.: +86 0373 4402322
e-mail: zhq@ibhsedu.com

0393-974X (2015)

combination in the initial treatment of smear-positive pulmonary tuberculosis, Yin et al. (5) proved that the curative effect of FDCs was better than plate combination in the treatment of smear-positive pulmonary tuberculosis, but further discussions and examinations are needed based on more high-quality comparative studies.

Based on the above research, this study collected data on clinical randomized controlled trails (RCTs) and clinical controlled trails (CCTs) from the literature to compare the curative effects and safety of FDCs in the initial treatment of smear-positive pulmonary tuberculosis in order to provide positive reference for clinical application.

MATERIALS AND METHODS

Materials

The search was carried out on cases of patients over 14 years of age who needed initial treatment for smear-positive pulmonary tuberculosis. Pregnancy, breast feeding, severe liver disease and kidney disease were criteria for exclusion. The baseline conditions of the experimental group and the control group were comparable. Repeated publications for the same research objects were excluded. Research data on the same subjects were divided or reported from different points of view and only one high quality reference was maintained. Literature with research subjects not conform to the inclusion standard were excluded. Studies with undefined main outcome indicators and nonrelevant data were also excluded. All materials concerned studies on the EDC anti-tuberculosis curative effect, safe randomized controlled trial (RCT) and clinical control trial (CCT) in China and elsewhere.

Method of administration

FDC, including duplex, triplex and quadplex FDCs, was administered in an experimental group; while non-FDC was used in a control group, including single drug, plate-type combined drugs.

Outcome indicators

i) Outcome indicators of the curative effect were: sputum negative conservation rate at the end of the 2nd month; sputum negative conservation rate at the end of the 6th month after treatment; relapse rate. ii) Outcome indicators of the safety were: total occurrence rate of medication side effects; occurrence rate of side effects on skin, gastrointestinal tract, liver and gall; rate of drug withdrawal because of side effects (drug withdrawal or therapeutic method alteration caused by serious side effects whilst using FDCs and non-FDCs for treating tuberculosis).

Literature search

Eight databases were searched by computer, including PubMed, EMBAS, ISI Web of Science, CNKI, CBM, Wanfang, and CqVip, and the studies were all relevant to the therapeutic effects and safety of antituberculosis therapy with FDCs published in journals in China and elsewhere before March, 2012. The English index words included "tuberculosis, pulmonary", "lung tuberculosis", "Fixed-dose Combination", "Rifater", and Rifamate", while the Chinese index words included "Feijiehe", Feilao", "Guding Jiliang Fuheji", and "Feining". November 11, 2013 was time for retrieval. Chinese and English literature were both available. Quality evaluation was performed on the incorporated studies according to the 'Risk of bias' Assessment Tool in the System Assessor Handbook 5.1.0 of Cochrane Collaboration updated in March, 2011, including random member generation, allocation and conceal, group blinding, outcome evaluation blinding, data missing report and selective ending report. Evaluation of each aspect was divided into L (Low risk), H (High risk) and U (Unclear risk).

Statistic analysis

Stata 12.0 software was used for the meta-analysis. Outcome indicators of this study were all enumerated data. Relative risk (RR) was served as the pooled statistical magnitude, and 95% confidence interval (CI) of RR was calculated. Heterogeneity of the included literature was detected using Q-test. If $P>0.05$, then the literature was of no obvious heterogeneity, thus it was analyzed using the fixed effect model; otherwise, it was analyzed using the random effect model, followed by sensitivity analysis. Evaluation of publication bias was detected using Begg's correlation test .

RESULTS

Comparison of basic literature feature and curative effect by different drug deliveries

The studies included in the paper were mostly from China, followed by areas with high occurrence of tuberculosis, such as Southeast Asia and Africa. As for the research strategy, 6-month short-course chemotherapy recommended by World Health Organization (WHO) was adopted, referring to 2 months of intensive treatment and 4 months of after treatment, which is shown in Table I.

A total of 22 studies included in the paper

Table I. *Basic literature features.*

Included literature	Case source	Design pattern	Experimental group		Control group		
			Drug delivery	Treatment strategy	Drug delivery	Treatment strategy	
Chen YH 2009 (6)	China	CCT	4FDC/2FDC	2RHZE/4RH	Plate-type combined drug	2H3R3E3Z3/4H3R3	HHUULL
Zhang SY 2010 (7)	China	RCT	3FDC+E/2FCD	2RHZE/4RH	Plate-type combined drug	2H3R3E3Z3/4H3R3	LHLULL
Tan WG 2007 (8)	China	RCT	3FDC+E/2FCD	2RHZE/4RH	Plate-type combined drug	2H3R3E3Z3/4H3R3	LHLLLL
Cai XF 2010 (9)	China	CCT	4FDC/2FDC	2RHZE/4RH	Plate-type combined drug	2H3R3E3Z3/4H3R3	HHUULL
Du JJ 2011 (10)	China	RCT	3FDC+E/2FCD	2RHZE/4RH	Plate-type combined drug	2H3R3E3Z3/4H3R3	UHUULL
Du YC 2007 (11)	China	CCT	3FDC+S/2FDC 3FDC /2FDC	2RHZE+2S3/4RH 2HRZ/4RH	Plate-type combined drug	2H3R3E3Z3/4H3R3	UHUULL
Liang Y 2007 (12)	China	RCT	3FDC+E/2FDC	2RHZE/4RH	Plate-type combined drug	2RHZE/4RH	LHUULL
Ma LP 2010 (13)	China	RCT	4FDC/2FDC	2RHZE/4RH	Plate-type combined drug	2RHZE/4RH	LHUULL
Qiu ZH 2010 (14)	China	RCT	4FDC/2FDC	2RHZE/4RH	Plate-type combined drug	2H3R3E3Z3/4H3R3	LHUUU;
Wang J 2007 (15)	China	RCT	3FDC+E/2FDC	2RHZE/4RH	Plate-type combined drug	2H3R3E3Z3/4H3R3	LHLLLL
Xu WG 2004 (16)	China	CCT	3FDC/2FDC	2RHZ/4RH	Plate-type combined drug	2RHZE/4H3R3	HHUULL
Zhao QR 2006 (17)	China	RCT	4FDC/2FDC	2RHZE/4RH	Single drug	2RHZE/4RH	LHUUUL
Zhao Chunxiao 2006 (18)	China	RCT	3FDC /2FDC	2RHZ/4RH	Single drug	2H3R3E3Z3/4H3R3	UHUULL
Zhong Q 2006 (19)	China	CCT	3FDC+S/2FDC	2RHZE+2S3/4RH	Plate-type combined drug	2H3R3E3Z3/4H3R3	HHUULL
Zhu LZ1998 (20, 21)	China	RCT	3FDC /2FDC	2RHZ/4RH	Single drug	2RHZE/4RH	UHUULL
Huang C 2005 (22)	China	RCT	3FDC+E/2FDC	2RHZE/4RH	Plate-type combined drug	2RHZE/4H3R3	UHUULL
Su. WJ 2002 (23)	Taiwan in China	RCT	3FDC+E/2FDC	2RHZE/4RH	Single drug	2RHZE/4RH	UHUULL
Bartacek.A 2009 (24)	Egypt, India, Pakistan, Philippines, Thailand	RCT	4FDC/2FDC	2RHZE/4RH	Single drug	2RHZE/4RH	LLLLLL
Gravendeel. JM 2003 (25)	Indonesia	RCT	4FDC/2FDC	2RHZE/4RH	Single drug	2RHZE/4RH	UHUULL
Lienhardt. C 2001 (26) (27)	Nine countries from Africa, Asia and Latin America	RCT	4FDC/2FDC	2RHZE/4R3H3	Single drug/2FDC	2RHZE/4H3R3	LLLLLL
Zaka-Ur-Rehman. Z 2008 (28)	Pakistan	RCT	4FDC/2FDC	2RHZE/4RH	Single drug	2RHZE/4RH	UHUULL

H: isonicotinyl hydrazide; R: rifampicin; Z: pyrazinamide; E: ethambutol; S: Streptomycin; FDC contains H, R and Z and 4FDC includes H, R, Z and E.

possessed different FDC deliveries in 2-month intensive treatment, including 3FDC, 3FDC+E/S and 4FDC. At the end of the second month, sputum negative conservation rate indicated that 4FDC did better than single drug combination. Furthermore, the remaining two patterns of drug delivery and their single drug combinations did not demonstrate statistically significant curative effects, as shown in

Table II. *Comparison of results between different FDC delivery and single drug delivery.*

Drug delivery	Literature number	χ^2	P value in heterogeneity test	I^2	RR (95% CI of RR)
3FDC	5	6.38	0.17	37%	1.01 (0.980, 1.03)
3FDC+E/S	8	7.03	0.43	0%	1.01 (0.98, 1.04)
4FDC	9	13.84	0.09	42%	1.03 (1.01, 1.05)

Table III. *Comparative result of each side reaction rate between FDCs group and single drug group.*

Outcome indicator	Number of studies	χ^2	Detection of the heterogeneity of P value	I^2	RR (95%CI of RR)	P value detected by Begg's
Total occurrence rate of side reaction	20	47.27	<0.05	60%	0.89 (0.77, 1.03)	0.33
Skin side reaction	20	15.27	0.71	0	1.06(0.89, 1.25)	0.02
Gastrointestinal reaction	20	36.75	<0.05	48%	0.86(0.72, 1.03)	0.48
Liver and gall side reaction	17	41.62	<0.05	62%	1.09(0.83, 1.44)	0.54

Note: skin side effects include rash, itching; gastrointestinal side effects include nausea, vomiting, stomach ache, loss of appetite; liver and gall side effects include abnormal liver function, jaundice.

Table IV. *Sensitivity analysis result of each side reaction occurrence rate of FDCs and single drug.*

pharmaceutical way	number of studies	χ^2	P value of heterogeneity detection	I^2	RR (95%CI of RR)
Total recurrence rate of side reaction [a]	18	19.89	0.28	15%	0.93(0.85, 1.01)
Gastrointestinal tract side reaction [a]	18	25.56	0.08	33%	0.84(0.74, 0.94)
Liver and gall side reaction [b]	16	11.04	0.75	0%	1.35(1.19, 1.53)

a: apart from literature written by Zhao Xiaochun in 2006 and by Zhong Qiu written in 2006; b: apart from literature written by Zhao Xiaochun in 2006.

Table II.

Comparison of sputum negative conservation rate

Analyzing and comparing sputum negative conservation rates of FDCs in the treatment of tuberculosis at the end of January, it was found that 22 studies all involved that indicator, and they were of good homogeneity (heterogeneity test showed that χ^2 =33.45, P=0.07, I^2=33%). Comparing sputum negative conservation rates between the FDC group and the single drug combination group in treating new tuberculosis at the end of January, no statistically significant difference was found (P=0.006), and RR value and its 95% CI were 1.02 (1.01, 1.03). The sputum negative conservation rates at the end of January of treating new pulmonary tuberculosis in the FDC group was superior to that in the single drug combination group. Publication bias detected

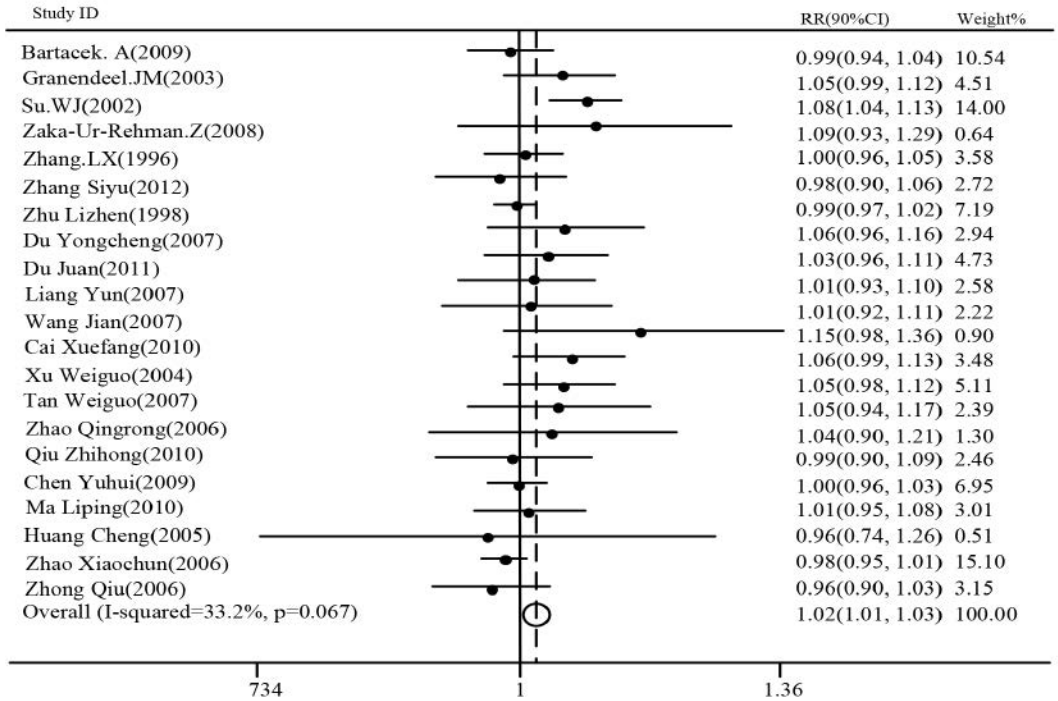

Fig. 1. *Forest graph of comparison of sputum negative conservation rates at the end of the 2nd month between FDCs group and single drug combination group.*

by Begg's showed that P=0.12, which indicated that there was no obvious publication bias, as shown in Fig. 1.

Sputum negative conservation rates of FDCs in the treatment of tuberculosis at the end of the 2nd month were compared. Altogether 16 studies involved sputum negative conservation rate, and no obvious heterogeneity was found (χ^2=22.21, P=0.30, I^2=14%). Comparing sputum negative conservation rates between the FDC group and the single drug combination group in treating smear-positive pulmonary tuberculosis at the end of the 2nd month, no statistically significant difference was found (P=0.02), and RR value and its 95% CI was 1.01 (1.00, 1.02). The curative effect in the FDC group was superior to that in single drug combination. The publication bias detected by Begg's showed that P=0.02, which indicated that there was obvious publication bias (Fig. 2).

Comparison of relapse rate

At the end of treatment course, the cured patients showing negative sputum smear examination twice resulted as positive in sputum smear examination or sputum culture during the follow-up period. There were a total of 8 studies with follow-up data, 7 with 2-year follow-up and 1 with 5 to 8 months. Comparing the relapse rate between the FDC group and the single drug combination group, it was found that all the eight studies had good homogeneity (χ^2=1.84, P=0.97, I^2=0%), and RR value and its 95%CI was 1.72 (0.98, 3.02). The publication bias detected by Begg's showed that P=0.81, which indicated that the publication bias was not obvious (Fig. 3).

Safety evaluation

No statistically significant differences were found while comparing the total occurrence rate of medication side effects, skin side effect, gastrointestinal tract side effect and liver and gall side effects between the FDC group and the single drug group, as shown in Table III.

Data was merged after eliminating two studies by carrying out sensitivity analysis on indicators with

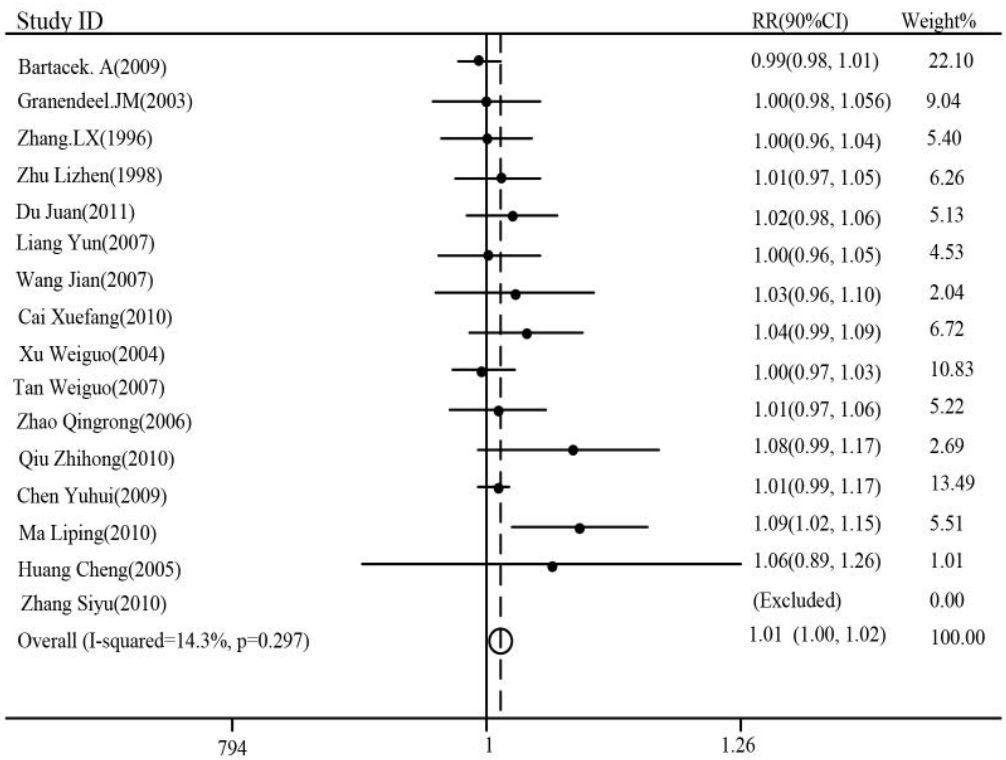

Fig. 2. *Forest graph of comparison of sputum negative conservation rates at the end of the 6th month between FDCs group and single drug combination group.*

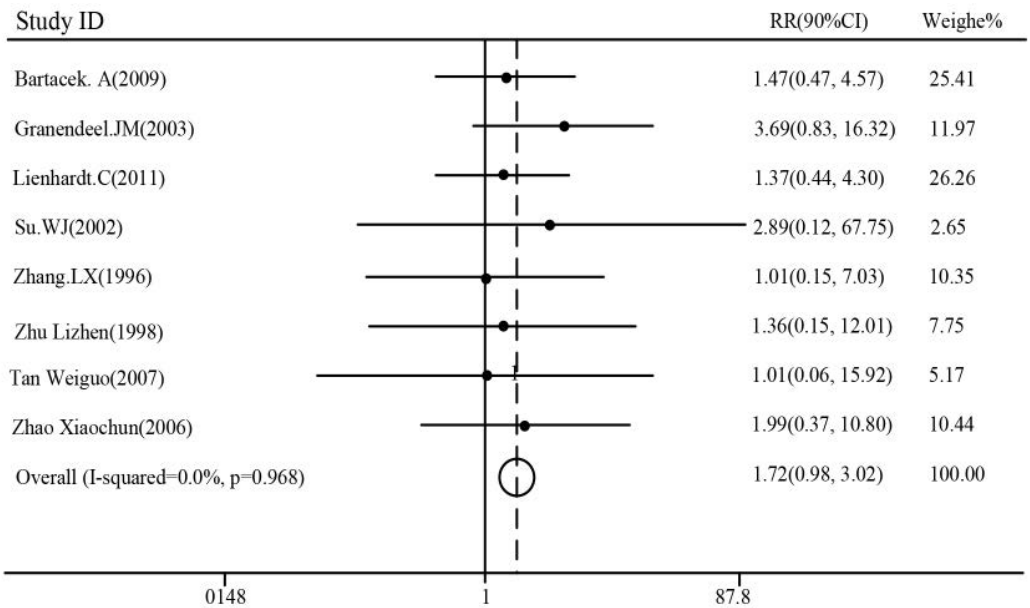

Fig. 3. *Forest graph of comparison of relapse rate between FDCs group and single drug combination.*

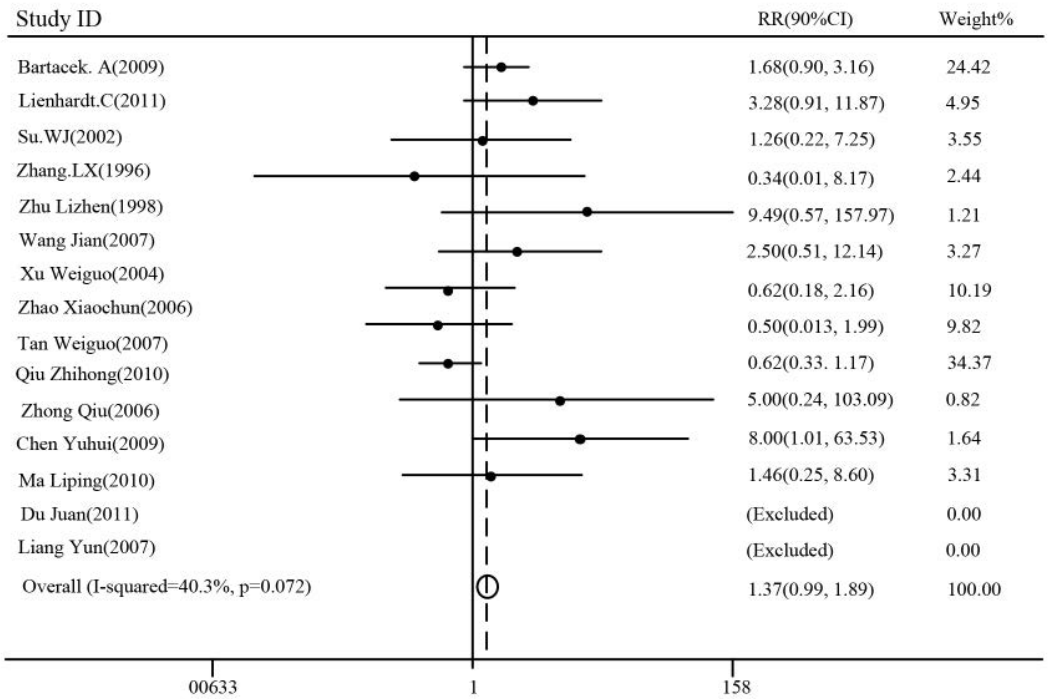

Fig. 4. *Forest graph of comparison of the drug withdrawal between FDCs group and single drug combination.*

significant heterogeneity, i.e., indicators with P<0.05 in heterogeneity test. Combined RR value and its 95%CI of occurrence rate of gastrointestinal side effect and liver and gall side effect was statistically significant, indicating the results were not stable (Table IV).

Comparison of drug withdrawal rate of side reaction

Rate of drug withdrawal because of side effects was compared between the FDC group and the single drug group. A total of fourteen studies involved merging, with good homogeneity (χ^2=18.44, P=0.07, I^2=40%). Comparison of the side reaction drug withdrawal rates between the two groups showed no statistically significant differences (P=0.06), and RR value and its 95%CI was 1.37(0.99, 1.86). The publication bias detected by Begg's showed that P=0.58, which indicated that the publication bias was not obvious, as shown in Fig. 4.

DISCUSSION

FDCs, a compound preparation composed of multiple first line antituberculosis drugs, was widely used clinically. FDCs, as the new progress in treating tuberculosis, has attracted much attention (29, 30). General use has created the condition for the popularization and application of FDCs in China. Cai XF, Qiu ZH, et al. (3, 31) proved that the Chinese FDCs were similar to the imported FDCs. As is well known, treatment of tuberculosis needs long-term medicine administration. The current conventional drugs for treating tuberculosis involve multiple categories and large dosage. Patients may show poor drug therapy compliance because of unpleasant drugs, leading to poor effect. However, FDCs featured by good absorption effect simplifies the prescription drug, improves the drug supply system and reduces the occurrence rate of drug resistance in the treatment of tuberculosis, which might be the main primary reason that the recovery rate of treating smear-positive pulmonary tuberculosis with FDCs is significantly higher than that with plate-type combined drug (2, 30, 32).

The present study shows that the efficacy of treating smear-positive pulmonary tuberculosis with

FDCs and single drug combination was statistically significant. Compared with single drug combination, the efficacy of FDCs was more effective in controlling tuberculosis. Through comparing the different pharmaceutical combinations of FDCs, we found that the quadplex FDCs was the most effective. In addition, of the 22 clinical studies investigated, 8 reported the follow-up situations, and only the design for the relapse rate of quadplex FDCs in 2 non-Chinese studies were elaborated (1, 27). There might have been bias since only indicators from sputum smear examination and sputum culture were confirmed as data of recurrence. In addition, this study also evaluated the safety of treating tuberculosis with FDCs regarding skin side effects, gastrointestinal tract side effect and liver and gall side effects. Skin side effect includes rash and itchiness, and the results show that the occurrence rate between the two groups was of no statistical difference and the result was stable. Gastrointestinal tract side effects include nausea, vomiting and loss of appetite. The whole-process blind method was not used in most of the studies included, thus the investigator might have considered the side reactions occurring in the gastrointestinal tract as being caused by other reasons than the drugs. Liver and gall side effects include abnormal liver function, jaundice and hepatalgia. Comparison of the rates of the liver and gall side effects between the two groups showed no statistically significant difference. Bias might have occurred due to the different detection methods for liver and gall abnormity and different determination standards for abnormal liver function used in the studies (1, 33).

To sum up, the paper shows that it is necessary and valuable to promote the application of FDCs on a larger scale, to undertake a control study of higher quality and thoroughly discuss its short-term and long-term curative effects. On the one hand, the existing research results can be further discussed and verified. On the other hand, it can provide sufficient scientific basis for China to formulate and develop the control strategy of tuberculosis (30).

REFERENCES

1. Ma JJ, Zhou ZW, Yan T, Wu X, Wang RH, Yi J. Meta-analysis on efficacy and safety of fixed-dose combination (FDC) in treatment of pulmonary tuberculosis. Chinese J of Clinical Pharmacology and Therapeutics 2012; 17(10):1143-50.
2. You XH, Li GQ. Present status of treatment of tuberculosis and its prospect. Chinese Community Doctors 2012; (20):10.
3. Cai XF, Feng YJ. A clinical observation in new smear positive pulmonary tuberculosis patients under domestic fixed-dose combination treatment. Zhejiang J of Preventive Medicine 2010; 22(7):21-23.
4. Du J, Tian D, Zhang ZB. Analysis on the effect of fixed-dose combination therapy for the initial treatment of smear-positive pulmonary tuberculosis in Wuhan. J of Public Health and Prevent Med 2011; 22(4):35-8.
5. Yin JJ, Zhong Q, Zhou L, Li HC, Chen YX, Liu JH, Zhao MG. Effect of treating new pulmonary tuberculosis with FDCs and plate-type combined drug-meta analysis. J of Practic Med 2013; (24):178-84.
6. Chen YH. A study on clinic efficacy of fixed-dose combinations with four drugs in treating tuberculosis patients. Jinan University, 2009. http://cdmd.cnki.com.cn/Article/CDMD-10559-2009108232.htm
7. Zhang SY. Randomized controlled clinical trial of fixed-dose combination and assembled drugs to pulmonary tuberculosis. Central South University 2010. http://cdmd.cnki.com.cn/Article/CDMD-10533-2010189503.htm
8. Tan WG. Fixed-dose Combinations in tuberculosis control. Beijing Tuberculosis and thoracic Tumor Research Institute 2007. http://cdmd.cnki.com.cn/Article/CDMD-87112-2007147197.htm
9. Cai XF, Feng YJ. A clinical observation in new smear positive pulmonary tuberculosis patients under domestic fixed-dose combination treatment. Zhejiang Journal of Preventive Medicine 2010; 22(7):21-23.
10. Du J, Tian D, Zhang ZB. Analysis on the effect of fixed-dose combination therapy for the initial treatment of smear-positive pulmonary tuberculosis in Wuhan. Journal of Public Health and Preventive Medicine 2011; 22(4):35-38.
11. Du YC, Chen QY, Lin SF, et al. Application of fixed-dose streptomycin-free combinations in primary treatment of patients with smear positive pulmonary

tuberculosis. Strait Journal of Preventive Medicine 2007; 13(6):89-90.
12. Liang Y, Yan XX, Wang JY, et al. Curative effect of fixed-dose anti-tuberculosis combinations in primary treatment of tuberculosis. Chinese Journal of Anti-tuberculosis Association 2007; 29(2):180-81.
13. Ma LP, Wu XG, Chu NH, et al. Feasibility study of domestic four-drug fixed-dose combination under DOTS as initial treatment in patients with smear positive pulmonary tuberculosis. Chinese Journal of Anti-tuberculosis Association 2010; 61(5):21-25.
14. Qiu ZH, Zhang SC. Comparison of fixed-dose combination and co-packaged combination drug therapies in patients with tuberculosis. China Preventive Medicine 2010; 11(6):605-607.
15. Wang J, Zhao J, Zhong T. Feasible evaluation of fixed-dose combination (FDC) in anti-tuberculosis therapy: a community-controlled study. Modern Preventive Medicine 2007; 33(13):2590-2591.
16. Xu WG, Lu W, He HJ, et al. randomized control study on domestic fixed-dose combinations in the initial treatment of smears positive tuberculosis. Chinese Journal of Tuberculosis and Respiratory Diseases 2004; 52(10):45-48.
17. Zhao QR, Tian M, Pan R, et al. Randomized control study on domestic 4FDC/2FDC combinations in initial treatment of smear positive tuberculosis patients. Parastoses and Infectious Diseases 2007; 15(3):122-27.
18. Zhao XC. Observation on curative effect of fixed-dose combination in treating tuberculosis. The Journal of The Chinese Antituberculosis Association 2006; 57(5):114-15.
19. Zhong Q, Huang GQ & Zhang M et al.. Study on using fixed-dose combinations in provincial tuberculosis programe. Chinese Journal of Anti-tuberculosis Association 2006; 57(5):274-77.
20. Zhu LZ, Yan BY. Controlled clinical study on efficacy of fixed-dose compounds rifinah in anti-tuberculosis chemotherapy. Chinese Journal of Tuberculosis and Respiratory Diseases 1998; 21(11):645-647.
21. Zhu LZ,Yan BY. Controlled clinical study on efficacy of fixed-dose compounds rifinah in anti-tuberculosis chemotherapy: results of two-year follow Up. Tuberculosis and Thoracic Tumor 2000; 48(5):320.
22. Huang C. Controlled study on efficacy of fixed-dose compounds in anti-tuberculosis. Jiangsu Journal of Preventive Medicine 2005; 16(3):31-33.
23. Su WJ, Perng RP. Fixed-dose combination chemotherapy (Rifatcr/Rifinah) for active pulmonary tuberculosis in Taiwan: a two-year follow-up. Int J Tuberc Lung Dis 2002; 6(11):1029-32.
24. Bartacck A, Schutt D, Panosch B, et al. Comparison of a four-drug fixed-dose combination regimen with a single tablet regimen in smear-positive pulmonary tuberculosis. Int J Tuberc Lung Dis 2009; 13(6):760-66.
25. Gravendeel JM, Asapa AS, Bccx-Blcumink M, et al. Preliminary results of an operational field study to compare side-effects, complaints and treatment results of a single drug short course regimen with a four-drug fixed-dose combination(4FDC) regimen in South Sulawesi, Republic of Indonesia. Tuberculosis (Edinb) 2003; 83(1-3):183-86.
26. Licnhardt C, Cook SV, Burgos M, et al. Efficacy and safety of a 4-drug fixed-dose combination regimen compared with separate drugs for treatment of pulmonary tuberculosis: the study c randomized controlled trial. JAMA 2011; 305(l4):1415-14,,23.
27. Zaka-Ur-Rchman Z, Jamshaid M, Chaudhry A. Clinical evaluation and monitoring of adverse effects for fixed multidose combination against single drug therapy in pulmonary tuberculosis patients. Pak J Pharm Sci 2008; 21(2):185-94.
28. Zhang F, Liu SJ, Zhang GL, Zhang MX, Nie G, Wang J. Evaluation of the adverse drug reactions of fixed-dose combination on primary TB treatment and its coping strategies. Shenzhen J of Integrated Traditional Chinese and Western Medicine 2012; 22(4):204-7.
29. Du ZX, Luo SZ, Fan RL, Li WM. Effect of treating new pulmonary tuberculosis with fdcs and plate-type combined drug—meta analysis. The J of Practic Med 2013; 29(24):4106-10.
30. Qiu ZH, Zhang SC. Comparison of FDC and co-packaged combination drug therapies in patients with tuberculosis. China Preventive Medicine 2010; 11(6):605-7.
31. Chen QT, Tan SY, Guo WR, Liu JX, Xue ZQ. Factors affecting treatment failure of new smear positive pulmonary tuberculosis patients. Chinese J of Antituberculosis 2011; 33(4):219-26.

32. Licnhardt C, Cook SV, Burgos M, Yorke-Edeards V, Rigouts L, Anyo G. Efficacy and safety of a 4-drug fixed-dose combination regimen compared with separate drugs for treatment of pulmonary tuberculosis: The study C randomized controlled trial. JAMA 2011; 305(14):1415-23.
33. Yu J, Yang RZ, Zhang TJ. Research progress of the bioavailability of FDC of antitubercular agent. J of Shenyang Pharmaceutical University 2012; 9(5):406-10.

LETTER TO THE EDITOR

THE INFLUENCE OF POSTERIOR APPROACH CERVICAL INTRASPINAL TUMOR RESECTION ON THE STABILITY OF CERVICAL VERTEBRA

XP. GENG[1], X. WANG[2], T. MENG[1], JJ. LI[1], XC. LI[1] and GY. FU[1]

[1]Department of Spinal Surgery, Binzhou Medical University Hospital, Binzhou, China; [2]Department of Orthopedics, Binzhou People's Hospital, Binzhou, China

Received January 9, 2015 – Accepted March 13, 2015

The first two authors contributed equally to this manuscript

This paper discusses the influence of posterior approach cervical intraspinal tumor resection on the stability of cervical vertebra. A total of 32 patients with cervical intraspinal tumor were included and divided into a group undergoing posterior approach bilateral vertebral lamina resection (group A) (n=16) and a group undergoing posterior approach semi-laminectomy (group B) (n=16). It was found, through follow-up visits, that the incidence rate of cervical instability of the patients was 25% and the incidence rate of cervical curvature deterioration of the patients was 37.5% in group A, whereas the two incidence rates of group B were 6.25% and 12.5% respectively; the incidence rates of cervical curvature deterioration and instability were significantly increased compared to group B (P< 0.05). It is concluded that, both regular posterior approach vertebral lamina resection and semi-laminectomy influence the biomechanical change of cervical vertebra, but the influence of the latter is less. Also, it is found that, applying titanium connectors and titanium nails for rigid internal fixation maintains the completeness and stability of the structure of the cervical vertebra.

Clinically, cervical intraspinal has a high incidence rate, and is very likely to be misdiagnosed (1) since the tumor shows no typical clinical symptoms in the early stage. The clinical symptoms do not show until the tumor becomes large (2). Surgery by that time is dangerous and complex, and may threaten the patient's life (3), making it difficult to treat the tumor.

The medical field has advanced in regard to the recognition of the properties and local dissection of tumors. Jiang Lin et al. (2), studied the treatment of cervical cancer by lamina resection. After carrying out tumor resection, it was found that, the physiological curvature of cervical vertebra was well maintained and the range of motion of the cervical vertebra also achieved an ideal effect. Fang Zhen et al. (4), reported tumor resection based on posterior cervical vertebra and internal fixation. A drill was used to cut lamina and the lateral mass was preserved. Cervical posterior surgery was carried out and the centrum of focal zone established according to the situation. None of the patients showed symptoms of unstable cervical vertebra or swan-neck deformity, proving that primary cervical intraspinal tumor can be cut by a posterior approach. Deng Guibin et al. (5) applied posterior cervical laminectomy to cut intraspinal tumor together with lateral mass fixation and fusion

Key words: cervical vertebra, posterior cervical intraspinal tumor resection, stability of cervical vertebra

Mailing address:
Dr Xiaopeng Geng,
Department of Spinal Surgery,
Binzhou Medical University Hospital,
No.661, Huanghe'er Road,
Binzhou, China
e-mail: gxp@ibhsedu.com

0393-974X (2015)

to treat the cervical intraspinal tumor. It was found that the cervical vertebra of the patients remained stable, without deformity.

As the surgical reconstruction and technology become more advanced, treatment for this disease focuses on excision, so as to relieve cervical cord compression in the early state and promote function recovery of the cervical cord. This study discusses the influence of posterior cervical intraspinal tumor resection on the stability of cervical vertebra by treating patients with cervical intraspinal tumor in Taizhou People's Hospital. We performed posterior cervical intraspinal tumor resection and semi-laminectomy on thirty-two cases of cervical intraspinal primary tumor to cut tumor focus and reconstruct the stability of the cervical spine and then compared the clinical curative effect, hence, providing reference for this kind of research.

MATERIALS AND METHODS

Materials

Data in the research regarded 32 patients confirmed as having cervical intraspinal tumor who were treated in Taizhou People's Hospital between January, 2009 and December, 2013. These patients were divided into group A and group B, 16 cases in each group. Group A included 11 males and 5 females, with age ranging from 23~76 years (mean 42.8±13.2 years) and treatment course of 15d ~7 years (mean 2.1±0.5 years); group B included 9 males and 7 females, with age ranging from 22~77 years (mean 43.1±12.7 years) and treatment course of 14 days to 7 years (mean 2.3±0.6). There was no statistical significance between age, gender ratio and treatment course ($P>0.05$). All patients conformed to the standard clinical diagnosis (6).

Research methods

The research subjects above were divided into groups A and B. Patients in group A were treated by posterior approach bilateral vertebral lamina resection approach while group B by the semi-laminectomy approach. Then the clinical effects of these two groups were compared based on the observation indexes of instability incidences of the cervical spine, 3 months after treatment, incidences of cervical spine curvature deterioration, cervical spine movement degree variations and long-term curative effects.

Surgical method

Group A: posterior approach bilateral vertebral lamina resection. The patients treated by general anesthesia were in a prone position or lateral position. The neck was placed in neural and flexion position after the head was fixed. The muscle in the neck was separated along the center line until reaching the supraspinous ligament. The supraspinous ligament was protected, the periosteum expanded and the paravertebral muscle was separated to expose spinous process in the lesion segment and bilateral lamina. After protecting the bilateral joint capsule, the tumor resection was performed.

Group B: semi-laminectomy. The patients were previously treated as group A. Then the muscle was separated along the center line until reaching the supraspinous ligament. The supraspinous and interspinous ligaments were protected, the periosteum was expanded and the paravertebral muscle was separated to expose the spinous process in the lesion segment and bilateral lamina. After cutting the tumor, the excised semi-lamina was reset and fixed, thereby maintaining the stability and completeness of the cervical spine structure (Figs. 1 and 2).

Statistical analysis

In this study, the relative data were processed by SPSSS18.0 software. Data for age and course of disease of the patients were expressed as mean ± standard deviation Mean ± SD. Student's *t*-test was applied to compare the measurement data and for the count data the c^2 test was adopted. $P< 0.05$ was considered to have statistical significance.

RESULTS

Incidence of instability and curvature deterioration of cervical spine after surgery

It was found through statistics that group A had a high incidence of instability and curvature deterioration of the cervical spine (Fig. 3) while group B had low incidence (Fig. 4). After surgery, the incidences of instability and curvature deterioration of group A were significantly increased compared to group B ($P<0.05$). The data is shown in Table I.

Change of movement degree of cervical spine

It was found that, statistically, the movement range of the cervical spines of group A after surgery decreased by (17.3±2.1%) while group B had no obvious change. It was apparent that the movement degree of the cervical spines of patients in group B was superior to group A after surgery ($P< 0.05$).

Long-term clinical effect

It was found that the cure rate, effective rate

Table I. *Comparison of incidence of instability and curvature deterioration of cervical spine of group A and B after surgery.*

Group	Case number	Instability of cervical spine (n, %)	Curvature deterioration of cervical spine
Group A	16	4(25.00)	6(37.50)
Group B	16	1(6.25)	2(12.50)
χ^2	-	5.109	5.221
p	-	0.0152	0.0121

(n, %)

Table II. *Comparison of long-term curative effect in the two groups.*

Group	Case number	Cure	Effective	Invalid	Total effective rate
Group A	16	6(37.50)	6(37.50)	4(25)	12(75.00)
Group B	16	8(50.00)	5(31.25)	3(18.75)	13(81.25)
χ^2	-	2.109	3.111	2.791	2.503
p	-	0.7161	0.6829	0.6573	0.6719

(n, %)

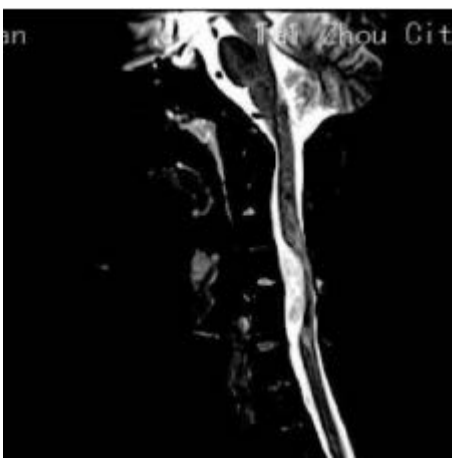

Fig. 1. *Optic nerve neurinoma locates in veutro before surgery.*

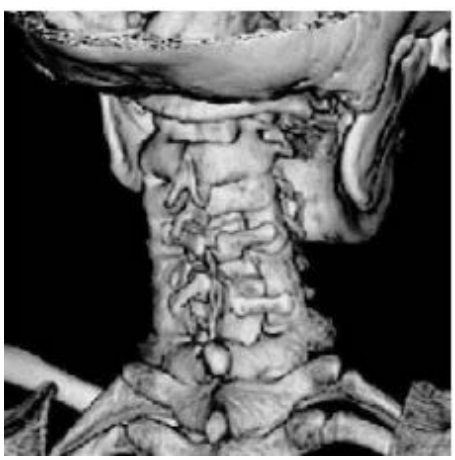

Fig. 2. *Reset of vertebral plate is fixed by titanium connector after surgery.*

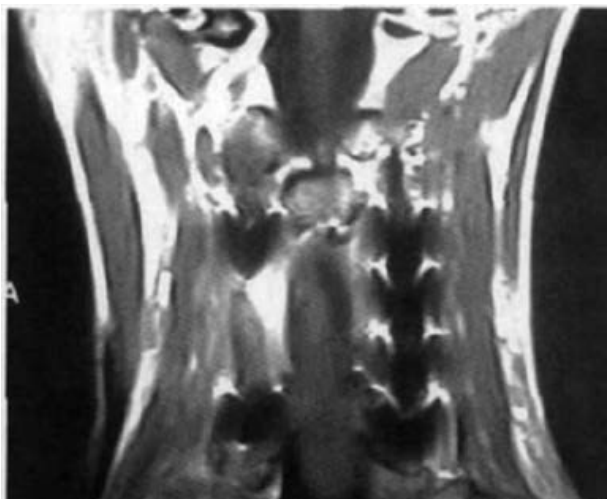

Fig. 3. *Structure of cervical vertebra processed after posterior bilateral vertebral lamina resection.*

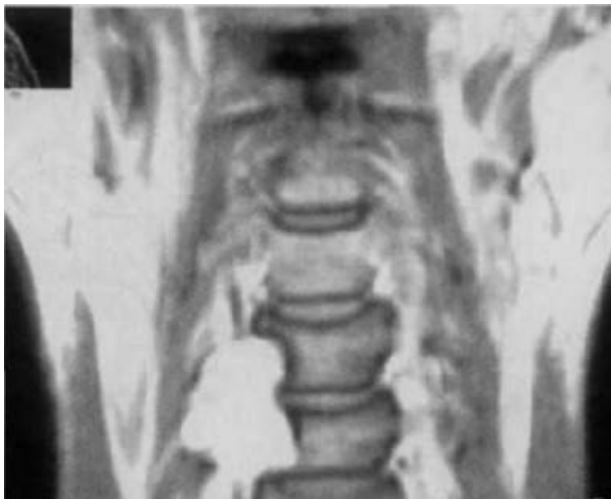

Fig. 4. *Structure of cervical vertebra processed after posterior semi-laminectomy.*

and total effective rate of group A was very close to group B, and had no remarkable difference (P>0.05), indicating that the long-term curative effect was similar in both groups, as shown in Table II.

DISCUSSION

Cervical intraspinal tumor can be primary or metastatic. Primary cervical intraspinal tumors originate from the cervical spine skeleton or its affiliated vessels, nerves, spinal dura mater, blood vessels or adipose tissue. According to the relationship of the tumor with the spinal dura mater and spinal cord, primary cervical intraspinal tumors can be divided into eqidual tumors, extramedullary, spinal subdural tumors and intramedullary tumors. Schwannoma and neurofibroma start from the tunica vaginalis or fibres in the dorsal nerve root; spinal meningioma grows upon arachnoid and spinal pia mater, and a few upon the nerve root; a dumbbell-shaped cervical intraspinal tumor is mostly benign and has a slow growth. It has been proved by clinical research that, intraspinal tumors have no typical clinical performance in the early stage, therefore, they are prone to be diagnosed as occipital neuralgia or cervical spondylosis. Tumors, to some extent, compress the cervical cord, nerve root and adjacent tissues as they grow, thereby inducing symptoms of pain, restrained movement and numbness of limb. In the later stage, the large tumor can severely compress and damage adjacent structures. The cervical cord under compression can induce spastic paralysis of limbs, nervus phrenicus can cause emesis upon stimulation, and the damaged nervus phrenicus can lead to dyspnea and paralysis of respiratory muscles, even threatening life (4).

Recently, a wealth of research on the stability of the spine after intraspinal tumor resection has been carried out. To discuss the influence of posterior intraspinal tumor resection on the stability of cervical vertebra, this research studied, by treating the patients with intraspinal tumor from Taizhou People's Hospital, different methods and compared the clinical effects. Finally, this study drew a conclusion, consistent with related literature, that posterior bilateral vertebral lamina resection had higher incidence of instability of cervical vertebra and deterioration of curvature than posterior semi-laminectomy and the long-term effects of these two resections had no distinct difference. This proved that, treating intraspinal tumor by posterior bilateral vertebral lamina resection approach could decrease the stability of cervical vertebra. He cervical spine is a particular site for dissection; moreover, tumor

diagnosis and treatment in that position is more complex compared to intraspinal tumor in other parts. Surgical resection is still the preferred method as recognized by the public. Primary cervical intraspinal tumors are mostly benign, and may not recur in a lifetime after completed resection. Therefore, patients should undergo surgery as early as possible, so as to relive the compression and promote recovery of the functions of the cervical cord. Primary cervical intraspinal tumors closely correlating with the cervical cord, vertebral artery and nerve root are able to compress the cervical cord, and enwrap the vertebral artery and nerve root, hence, surgery may do harm to these positions or cause instability of the cervical cord after surgery, which increases the risks of surgical resection and causes difficulties for the total resection of tumors (8).

Meanwhile, if the tumor is close to a vital center such as the medulla, this increases the surgical risks. It is difficult to perform surgical resection and stability reconstruction since tumors have a wide range of infiltration, involving multiple cervical cord stages, as well as dumbbell neurogenic tumors inside and outside the spinal canal (9). Based on the above analysis and conclusions, this research holds that, the application of posterior cervical spinal surgery has the following advantages: firstly, the operation is relatively simple; there is little trauma, thus minimizing the stimulation on the cervical cord, and patients can recover faster. Secondly, the surgery has less risks. Surgery through the posterior approach can fully expose and protect the vertebral artery and nerve root, avoiding unnecessary damage. Patients in this research have not had the vertebral artery ligatured and suffered from no post-operative complications. Thirdly, it can completely cut out the tumor and lower recurrence rate. No recurrence cases were found in the follow-up visits of the patients who underwent the above surgery. The resection range of the vertebral plate can be increased if necessary. To fully expose the tumor and completely remove it, hemilaminectomy or total laminectomy resection can both be selected. Fourthly, it can achieve ideal stability (10). Complete tumor resection is crucial for thoroughly reducing pressure and tumor recurrence, but a wide span of resection may bring damage and instability to the overall structure of the spine. Therefore, it is necessary to maintain the stability of the spine during surgery. Ways to cut the tumor and yet maintain the biomechanical stability of the spine (11) are continually being investigated. Means of internal fixation of the spine offer multiple choices for the reconstruction after resection of a spinal tumor. It is also important to select a reasonable fusion scope and reconstruction method for surgery by the posterior approach. Some patients in this research underwent posterior spinal fusion, and all achieved bone union. Patients with tumors involving the first and second cervical vertebra can have the the stability of cervical vertebra reconstructed by adopting short-segment occipitocervical fusion from the occipital bone to C2 pedicle after performing posterior decompression resection. Usually, tumors involving other parts need to have the facet joint cut. Fixation by posterior nail-stick system or lateral mass iron plate can not only cut out a large-scale tumor within the spine canal, but also maintain the posterior structure of the cervical vertebra and effectively maintain the stability of the cervical vertebra, with little trauma and few complications (12).

This study proved that the posterior bilateral vertebral lamina resection approach in intraspinal tumor resection can induce instability, exacerbate curvature, and affect the flexibility of the cervical vertebra while the semi-laminectomy approach has fewer effects; both methods are able to change the degree of physical movement. With the development of microneurosurgery and minimally invasive technology, the semi-laminectomy approach has been able to improve vision during surgery, enabling the complete removal of tumors. The semi-laminectomy approach has less influence on the stability of the cervical vertebra and is more in keeping with biomechanical principles. The excised vertebral plate can be reset and a rigid internal fixation performed with a titanium connector and titanium nail after the tumor is removed, thereby maintaining the completeness and stability of the cervical vertebra structure and achieving anatomical reduction. Notably, the middle and posterior column of the cervical vertebra in group B is strengthened. The quality of life of those patients greatly improved as their physical curvature after surgery was well maintained and an ideal degree of movement of their cervical vertebra was achieved. Therefore, more

importance should be given to cervical intraspinal tumor resection through the semi-laminectomy approach.

REFERENCES

1. Wang XD, Zhao HW, Liu HP, Duan F. Laminoplasty remaining spinous process in the treatment of intraspinal tumor based on clinical observation on 58 cases. Chin J Practic Neruous Diseas 2010; 13(15):22-23.
2. Jiang L, Gao GZ. To investigate the effects of cervical posterior resection of cervical cancer and related factors of stability. Guide Chin Med 2014; 12(23):42-43.
3. Cheng J, Yang Y. Nursing Strategies of safe nosocomial transfer for patients with cervical spinal cord tumors Resection. Nursing J Chin People's Liberation Army 2013; 30(16):48-49.
4. Fang Z, Wang KM, Liao L, Yang DS, Qin J, Dai YL, Li JY, Fang GM. Clinical analysis of cervical posterior approach surgery in the treatment for primary intraspinal tumor. J Oncol 2011; 17(8):586-91.
5. Deng JB, Zhang CH, Huang CM, Luo SJ, Zhong CF, Li XM. Posterior cervical laminectomy at the same time lateral mass fixation and fusion in treatment of cervical cancer. Chin J Trauma Disabil Med 2011; 19(7):13-14.
6. Lin GZ, Wang ZY. Application of finite element method in research of postoperative stability of cervical laminectomy. Chin J Neurosurg Dis Res 2010; 15(4):192-94.
7. Zhang MG, Xu QW, Che XM. Minimally invasive surgery for the intra- and extra-spinal tumors. Chin J Minimally Invasive Neurosurg 2010; 21(11):188-89.
8. Liu XB, Lin AG, Tang HT, He C. Application of spinous process and lamina replantation laminoplasty in intraspinal tumor surgery. Chin J Clin Neurosurg 2010; 17(4):76-78.
9. Gao FY, Wang Q, Liu CX, Han GQ, Xiong YB, Yin H, Wang C, Yang CY, Ma J. One-stage Microsurgical Excision for Intra- and Extra-spinal Dumbbell-shaped Tumors in Cervical Spine: A Report of 11 Cases. Chin J Contemp Neurol and Neurosurg 2013; 13(7):636-40.
10. Wang C, Xiao YF, Zhao XJ. Cervical Intraspinal tumor resection and stability reconstruction. Guide of China Med 2011; 9(25):293-95.
11. Liu JG, Chen HF, Hu Y, Huang SQ. Analysis of classification and surgical treatment of cervical dumbbell-shaped tumors. Chin J Contemp Neurol and Neurosurg 2013; 13(11):941-45.
12. Ye ZP, Qin F, Cai MT, He HY, Shi DJ, Guo Y. Hemilaminectomy procedures for the microsurgicai management of intradural- extramedullary tumors of the cervical spinal. The J Practic Med 2012; 28(6):955-57.

LETTER TO THE EDITOR

BERBERIS VULGARIS FRUIT CRUDE EXTRACT AS A NOVEL ANTI-LEUKAEMIC AGENT

TA. SAEDI[1,2], S. GHAFOURIAN[3], M. JAFARLOU[2], M.N. SABARIAH[4], P. ISMAIL[5], R.M.T. EUSNI[4] and F. OTHMAN[2]

[1]Institute of Bioscience, Universiti Putra Malaysia, Serdang, Selangor, Malaysia; [2]Department of Anatomy, Faculty of Medicine and Health Sciences, Universiti Putra Malaysia, Serdang, Selangor, Malaysia; [3]Clinical Microbiology Research Center, Ilam University of Medical Sciences, Ilam, Iran; [4]Department of Pathology, Faculty of Medicine and Health Sciences, Universiti Putra Malaysia, Serdang, Selangor, Malaysia; [5]Department of Biomedical Sciences, Faculty of Medicine and Health Sciences, Universiti Putra Malaysia, Serdang, Selangor, Malaysia

Received December 31, 2014 – Accepted March *11, 2015*

Tumor protein p53 encoded by the *TP53* gene in humans is known as a cancer biomarker in patients diagnosed with cancer, and it plays an essential role in apoptosis, genomic stability, and inhibition of angiogenesis. Cancer therapies with common chemotherapy methods are effective, as known, but have some side effects. *Berberis vulgaris* is traditionally administrated as a cancer drug. The current research aims to evaluate p53 as a biomarker in WEHI-3 cell line and to demonstrate the *Berberis vulgaris* fruit crude extract (BVFCE) as a new anticancer drug. For this purpose, we evaluated the effect of BVFCE in different concentrations against WEHI-3cell line *in vitro* and determined the quantitative level of p53 gene in the treated WEHI-3 cells. The results demonstrated that even at only 1 mg/ml concentration of *Berberis vulgaris* crude extract, there was a low level of p53 biomarker expression on WEHI-3 cells in comparison with doxorubicin. Therefore, the current study suggests BVFCE as a reliable anti-leukaemic drug and candidate for anticancer therapy. However, further investigation need be carried out to confirm its efficiency *in vivo*.

Apoptosis, or programmed cell death, is a biological process essential for the regular development and maintenance of tissue homeostasis (1). Failure of apoptotic mechanism leads to abnormal cell proliferation or differentiation arrest, giving rise to tumor cell formation and cancer development. Mechanisms of apoptotic pathways are widely investigated, and the causes of incorrect apoptotic process are clarified. Various anticancer drugs are tested for their ability to re-establish proper apoptotic machinery in cancer cells with minimal effect on surrounding tissue or normal cells. Leukaemia belongs to a large group of diseases in which variability of factors contributing to tumor development requires individual therapeutic approach. A growing number of prognostic factors helps to better define optimal therapy regimen, but extensive adverse effects together with acquired resistance to chemotherapy are calling for novel therapy strategies in leukaemia.

Key words: BVFCE, anti-leukaemia, WEHI-3, qRT-PCR, p53

Mailing address: Prof. Dr. O. Fauziah,
Department of Human Anatomy,
Faculty of Medicine and Health Sciences,
Universiti Putra Malaysia,
43400 Serdang, Selagor, Malaysia
Tel.: +603 89472315 Fax: +603 89422341
e-mail: fauziah@upm.edu.my

0393-974X (2015)

The barberry also known as *Berberis vulgaris* is a plant that grows in Iran. It is estimated that more than 5×10^6 kg of barberries are produced each year. It is also extensively applied as a medicinal plant in traditional medicine (7).

The human neoplasia could be detected via high-level expression of p53 (2-4). High level p53 protein is related to poor prognosis in many tumors (5-6).

The current study aimed to evaluate the effect of crude extract of barberry on WEHI-3 cell *in vitro* line and compare its efficiency with doxorubicin as an anticancer drug.

MATERIALS AND METHODS

Preparation of crude extracts

Berberis vulgaris fruit crude extract (BVFCE) was prepared with some modification as described by Campbell et al. (2002). The barberry fruit was purchased from markets in Iran. Ethanolic extract of barberry was prepared by adding 10 gr of dry, ground herb to 100 ml ethanol and then stirred at 250 rpm in an orbital shaker for 1 h at room temperature. This thick syrup was evaporated completely using the freeze drying system (8).

Cell culture

Murine myleomonocytic leukaemia cell line, WEHI-3 and mouse embryonic fibroblast cell line 3T3 were purchased fromATCC. Cells were maintained in RPMI 1640 (NacalaiTesque, USA) supplemented with 10% heat-inactivated fetal bovine serum (FBS), 1% antibiotics (100 IU/ml penicillin, 100 µg/ml streptomycin) at 37°C in a humidified incubator containing 5% CO_2, after which the medium was replaced with new culture medium containing different concentrations ranging from 1 to 30mg/ml of the herbal extract. The cells were cultured in 5mg/ml of doxorubicin (Sigma-Aldrich, USA) and used as a control (9).

Cell viability assay

Twenty-four hours later, the amount of cell death was assayed using an MTT kit (Vybrant MTT Cell Proliferation Assay Kit, Life Technologies, USA) following the manufacturer's protocol. The absorbance was read at 570 nm using the microplate ELISA reader. Percent of cell viability was calculated using the following formula:

$$(\%) = (\text{Abs}_{\text{Treatment}} / \text{Abs}_{\text{Control}}) \times 100\%$$

DNA extraction of Staphylococcus aureus

DNA was extracted from the *S. aureus* using the DNA extraction KIT (Gene ALL, South Korea).

Real-time quantitative PCR (RT-qPCR)

Real-time quantitative PCR was conducted using the Syber Green Hot-Start Real-Time PCR-Mix kit (GENECRAFT; Germany) with *nuc*gene as a reference gene for standards. Use of 2x QuantiFast SYBER Green RT-PCR master mix together with a QuantiFast RT mix allowing both reactions were added at the beginning. QuantiFast RT Mix, 2x QuantiFastSyber Green RT-PCR Master Mix, diluted primers, and RNase-free water were stored at -20°C.

Standard curve for RT-qPCR

The procedures for RT-qPCR and standard preparation were as follows: first, the concentration of extracted DNA was evaluated. Then the genome size of *S. aureus* was obtained from http://www.cbs.dtu.dk/databases/DOGS/index.html. Subsequently the mass of DNA per genome was obtained by using the following formula (Applied Biosystems):M = [n]. [1.096e-21 g/bp], whereas n = genome size (bp), M = Mass, and e-21= $\times 10^{-21}$

Thus, for *S. aureus* RN4220, as obtained from the database, the genome size was 2821361, soM = [2.8 e6 bp]. [1.096e-21g/bp]→M = 3e-15→M = 0.003 pg

As the bacteria are haploid, a single copy of the gene exists in the genome. Therefore, 0.003 pg of *S. aureus* genome contain one copy of *nuc* gene. Thus, 300000× 0.003 pg=900 pg of DNA needed. In each reaction, 3 µl was used. So, 900pg ÷3=300 pg/ul of DNA. The concentration of DNA was 6.5 ng/µl (6500 pg/ µl).
Each dilution was prepared at 100 µl, using the formula below:

C1V1=C2V2

[6500 pg/µl] . V1 = [300pg/µl]. [100µl]→V1 = 4.6 µl

We can therefore have the volume of diluents to be= 100 µl – 4.6 µl = 95.4 µl. Thus, 4.6 µl of DNA should be adjusted to 95.4 µl of distilled water. Other concentrations were prepared by serial dilution as listed in Table I.

RESULTS

Cytotoxicity of Berberisvulgaris fruit crude extraction WEHI-3 and 3T3 cell lines

To study the cytotoxicity effect of BVFCE *in vitro*, WEHI-3and 3T3 cell lines were incubated with various concentrations of BVFCE. The anti-proliferative effect was determined using MTT assay, which is considered more reliable. The MTT results demonstrated that BVFCE inhibited the proliferation of WEHI-3 cell line in a dose-dependent manner.

Moreover, the IC_{50} values of BVFCE for normal cells (13mg/ml) were decreased in WEHI-3 cells (8 mg/ml). One of the most important signals in cancer

Table I. *Preparation of standard by serial dilution.*

Dilution	Volume of DNA (µl)	Volume of diluents (µl)	Final Volume	Copy number
Standard 1	4.6	95.4	100	300000
Standard 2	10	90	100	30000
Standard 3	10	90	100	3000
Standard 4	10	90	100	300
Standard 5	10	90	100	30

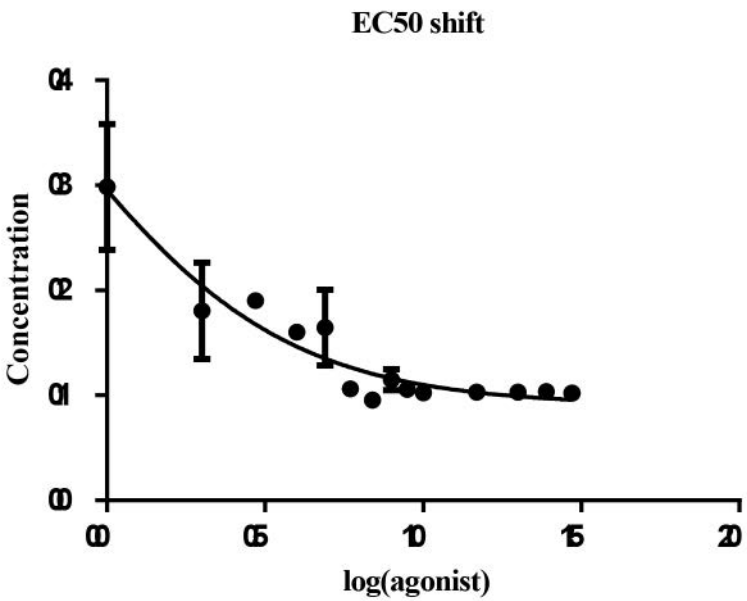

Fig. 1. *The effect of Berberis vulgaris crude extract on 3T3 cell line after being treated with IC50 value at 0 and 48 h by MTT assay (3T3 cell line, IC50= 13 mg/ml).*

is p53 that could be followed (Figs. 1, 2).

Berberis vulgaris fruit crude extract decreased the expression level of p53 gene

The analysis by qPCR indicated the level of p53 was in normal condition for both the cells, but after treatment with BVFCE, it demonstrated an excellent quantitative expression of p53 in WEHI-3 cells which is more than the one found in 3T3 cell lines (Fig. 3). On the other hand, when the cells were treated

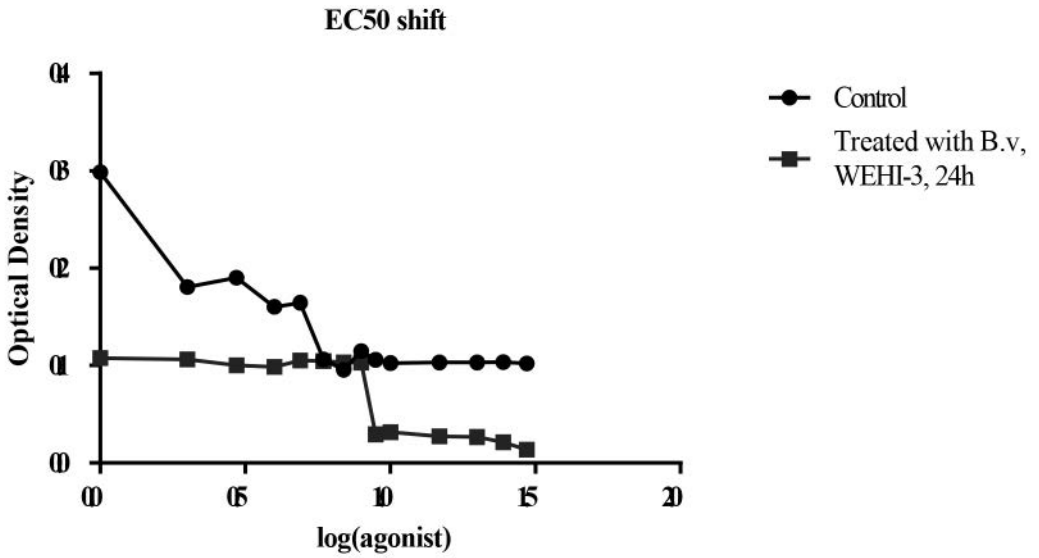

Fig. 2. *The effect of Berberis vulgaris crude extract on WEHI-3 cell line after being treated with IC_{50} value at 24 h by MTT assay (WEHI- 24 h cell line, IC_{50}= 8mg/ml, EC50 Ratio =0. 17).*

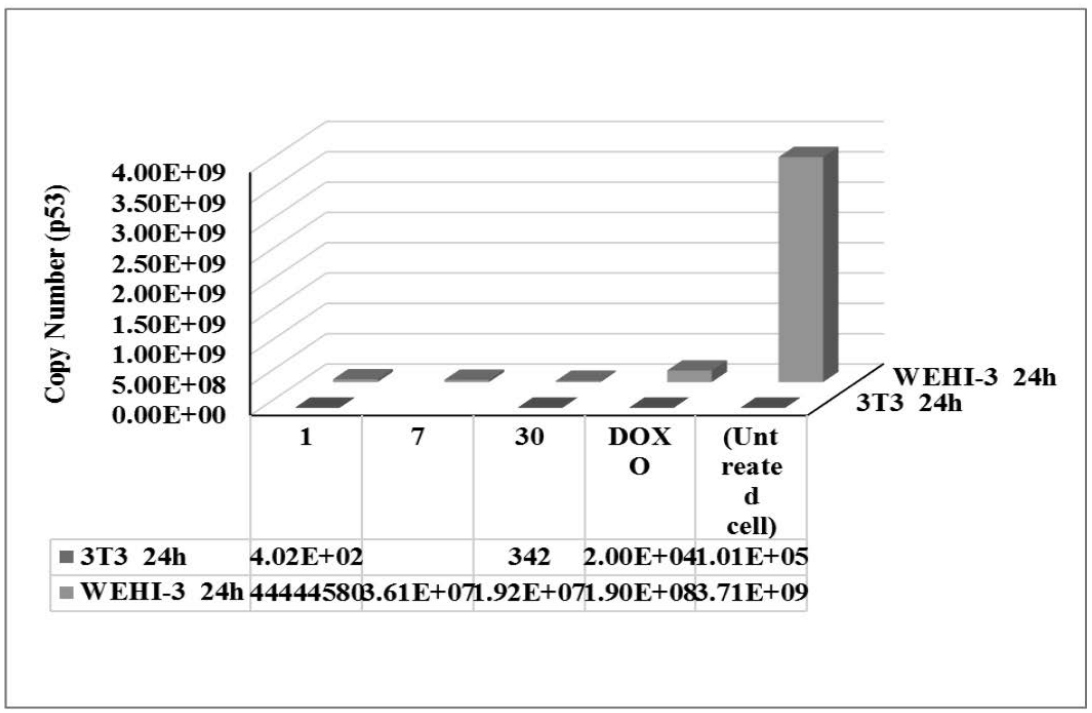

Fig. 3. *Expression level of p53 in WEHI-3 and 3T3 cell lines. The 3T3 used as a control and doxorubicin as a chemotherapeutic drug for treatment of cancer. As shown in presence of Berberis vulgaris crude extract the expression level of p53 was decreased more than doxorubicin.*

with doxorubicin, the level of p53 showed a decrease that demonstrated the efficiency of doxorubicin but BVFCE showed more decreasing effects on the p53 than the compared doxorubicin drug. The level of p53 expression decreased more when the BVFCE concentrations were increased (Fig. 3).

DISCUSSION

Leukaemia remains a cancer disease which can not be treated in many patients. The rate of mortality and morbidity is high. It is important to diagnosis early and treat the infected patients. The current treatment is monitoring via examination for fifteen days and then 21 to 28 days aspiration of bone marrow. Therefore, it is important to identify the reliable marker and also a new method for treatment of infected patients. The marker that predicts the stage of disease and also demonstrates the success prior to therapy is important.

In this survey, we found p53 as a potential biomarker for poor prognosis and also effectiveness of *Berberis vulgaris* fruit crude extract on decreased expression of this p53 gene. The analysis revealed high expression level of p53 in WEHI-3cell lines in comparison with normal 3T3 cell line. Also the findings demonstrate that the doxorubicin cause a decrease of p53 in both normal and leukaemic cell lines. On using the lower and highest concentrations of IC_{50} to evaluate the efficiency of extract, the results demonstrated a decreased expression of p53 to its minimal level. These results therefore indicate the role of p53 as a reliable marker for poor diagnosis of leukaemia. Moreover, BVFCE had a specific effect on p53 gene and consequently might improve cancer therapy in the near feature.

In conclusion, the current study recommended *Berberis vulgaris* fruit crude extract as a candidate for anti-cancer therapy in leukaemia with efficiency on p53. However, further studies should be carried out with emphasis on different cancer markers.

ACKNOWLEDGEMENTS

The authors are very grateful to the Faculty of Medicine and Health Science, University Putra Malaysia for providing facilities for this research work and, our special thanks also go to Mr Umar Ahmad for his instructive editing.

REFERENCES

1. Gautrey H L, Tyson-Capper AJ. Regulation of Mcl-1 by SRSF1 and SRSF5 in cancer cells. PloS one 2012; 7(12), e51497.
2. Cattoretti G, Rilke F, Andreola S, D'Amato L, Delia D. p53 expression in breast cancer. Int J Cancer 1988; 41:178-83.
3. Crawford LV, Pim DC, Lamb P. The cellular protein p53in human tumors. MolBiol Med 1984; 2:261-72.
4. Iggo R, Gatter K, Bartek J, Lane D, Harris AL. Increased expression of mutant forms of p53 oncogene in primary lung cancer. Lancet 1990; 335:675-79.
5. Martin HM, Filipe MI, Morris RW, Lane DP, Silvestre F. p53 expression and prognosis in gastric carcinoma. Int J Cancer 1992; 50:859-62.
6. Thor AD, Moore DH, Edgerton SM, et al. Accumulation of p53 tumor suppressor gene protein: an independent marker of prognosis in breast cancers. J Nat Cancer Inst 2004; 84:845-55.
7. Food and Agriculture Organization (FAO), 2005. Report, Rome.
8. Campbell MJ, Hamilton B, Shoemaker M, Tagliaferri M, Cohen I, Tripathy D. Antiproliferative activity of Chinese medicinal herbs on breast cancer cells *in vitro*. Anticancer Res 2002; 22:3843-52.
9. Li Z, Meng Z, Sayeed A, Shalaby R, Ljung B-M, Dairkee SH. Genome wide alleotyping of a new *in vitro* model system reveals early events in breast cancer progression. Cancer Res 2002; 62:5980-87.

LETTER TO THE EDITOR

EFFECT OF PREGNANE XENOBIOTIC RECEPTOR ACTIVATION ON INFLAMMATORY BOWEL DISEASE TREATED WITH RIFAXIMIN

Y-C. WAN[1], T. LI[2], Y-D. HAN[2], H-Y. ZHANG[3], H. LIN[4] and B. ZHANG[5]

[1]Department of Endocrinology, China-Japan Union Hospital, Jilin University, Jilin University, Changchun, China; [2]Department of Anesthesiology, China-Japan Union Hospital, Jilin University, Jilin University, Changchun, China; [3]Department of Gastrointestinal Surgery, China-Japan Union Hospital, Jilin University, Jilin University, Changchun, China; [4]Department of Internal Medicine, Outpatient Department of Air Force Aviation University, Jilin University, Changchun, China; [5]Microscopic Examination Department, China-Japan Union Hospital, Jilin University, Changchun, China

Received February 10, 2015– Accepted March 31, 2015

The causes and pathogenesis of Inflammatory Bowel Disease (IBD) are still not clearly understood. This study aims to prove the important role of rifaximin played in inflammatory reaction caused by abnormity of the intestinal mucosal immune system. Intestinal microflora can greatly promote and maintain the inflammatory reaction of IBD, therefore, antibiotics can be used to treat IBD. Rifaximin is a medicine usually used for local intestinal infection. Many clinical and basic studies have shown that both a single application of rifaximin and the joint application with other medicines could achieve a good efficacy. This paper studied the activation of Pregnane Xenobiotic Receptor (PXR) in treating IBD with rifaximin and analyzed its efficacy in IBD when PXR was involved in the transport of medicine and metabolism. The results prove that rifaximin can not only serve as an anti-microbial drug, but can activate PXR and actually weaken the reaction of IBD. Thus it is safe to say that rifaximin has great potential in treating IBD.

Pregnane Xenobiotic Receptor (PXR), also called the steroid and xenobiotic receptor (SXR), is an important member of nuclear receptor families. It is encoded by the NRI12 gene and activated by several natural or synthetic progestogens (1). PXR is a newly discovered key factor of CYP3A4 transcription regulation. Many medicines and environmental chemicals can achieve CYP3A4 transcription by the regulation of PXR, and can therefore have an effect on the metabolism of several medicines with substrate of CYP3A4 or environmental chemicals, which may induce mutual reactions among medicines and even create some adverse effects.

Apart from its important role in metabolism and mutual reactions of medicines, there are increasingly more studies showing that PXR and its regulation target genes play a great part in sustaining the stability of the internal condition of the body and giving full play to the important physiological functions. Therefore, it is necessary to study the enzyme regulation and related pharmacological effects of traditional Chinese medicine and natural products on cytochrome P450, which will provide information for discovering new pharmacological

Key words: rifaximin, PXR, IBD, activation

Mailing address:
Dr B. Zhang,
Microscopic Examination Department,
China-Japan Union Hospital,
Jilin University,
Changchun 130033, China
e-mail: Zhang_bin_z@163.com

0393-974X (2015)

effects.

Rifaximin is an antibiotic which fails to be assimilated orally and which has a local effect on the bowel. It is the semi-synthesis derivative of rifamycin, which is characterized by a wide antibacterial spectrum and strong antibacterial activity. Rifaximin has a high antibacterial activity towards several Gram-positive bacteria, gram-negative aerobes and anaerobes, while the activity of gram-positive bacteria is much stronger than that of gram-negative (2, 3). By irreversibly combining it with the RNA polymerase β subunit dependent on DNA, rifaximin can inhibit the synthesis of bacterial RNA, prevent the connection between this enzyme and DNA, and the block of transcription of DNA and finally inhibit the synthesis of bacterial protein and shows the effect of disinfection (4, 5). Mencarelli et al. (6) found that rifaximin could effectively improve the expression of PXR and its related genes and inhibit the effect of TNFα in intestinal epithelial cells (IEC), thus inhibiting the reaction of IBD. These antibacterial effects can maintain the complete defense in bowel against any damage from foreign matter and bacterial products within the enteric cavity.

IBD is a chronic non-specific gastrointestinal disease which mainly includes Ulcerative colitis (UC) and Crohn's disease (CD) (7). With the improvement in lifestyle leading to changes in dietary habits, there is an increasing incidence of IBD year by year. Some studies claim that there is an incidence of one in five people with IBD in the USA, and the ratio continues to increase. The pathogenesis of IBD is related to the local abnormal immunity in intestinal mucosa. The imbalance between pro-inflammatory cytokines and anti-inflammatory cytokines is considered as an important finding of IBD. Rifaximin can be mediated by PXR (8, 9) and then activate the CYP3A4. However, the classical ligand of rifampicin (RIF) can be applied to treat UC by activating PXR. This experiment took rifaximin as the object of study and built an IBD model by employing Dextran sodium sulfate (DSS) (MW 36-50 KDa). Furthermore, it led to an initial discussion over the molecular mechanism of rifaximin in treating IBD, which provided the experimental evidence and basis for further study of functions of rifaximin and an exploration of the effect of PXR compound on IBD.

MATERIALS AND METHODS

Materials

Rifaximin with a purity over 98% (National Institute for the Control of Pharmaceutical and Biological Products, China); Dulbecco's modified Eagle's medium (DMEM), hematogenous fetal bovine serum (FBS) and pamcreatin (Hyclone Inc., US); rifampicin (Merck Inc., Germany); Dextran sodium sulfate(DSS) (MW36-50 KDa, MP Biomedical LLC, Solon, OH, Russia); Dimethyl Sulphoxide (DMSO) and pregnenolone16a-carbonitrile (PCN) (Sigma Inc., Japan); RNApure kit for a rapid extract of the total RNA (Biomed Inc., Beijing, China); TransScriptTM One-Step RT-PCR SuperMix (TransGen Biotech Inc., Beijing, China); Fast SYBR@ Green Master Mix (Applied Biosystems Inc., USA); NE-PERTM nucleoprotein and plasmosin extract kit and LightShift® Chemiluminescent EMSA kit (Pierce, Rockford, IL, USA); camellia oil to be injected (Academy of Military Medical Sciences, China); the other reagents are all commercially available.

Cellular incubator (NAPCO 5410, Japan); reversed microscope (Nikon 120, Japan); clean bench (Great wall Air Purifier Equipment Engineering Inc, Beijing, China); PCR: GeneAmp PCR System 2400 (PE Applied Biosystem Inc., USA); ice maker (Manitowoc QM20, US); Ultra-low temperature freezer (MDF-U53V, Sanyo Inc, Japan); digital precise scale (Sartorius BS110S, Germany); water purifier (Millpore Simplicity, USA); Enzyme-labeled meter (PerknElmer VictorX, USA); Vortex oscillator (XH-89, Zhejiang Yuecheng Electric Factory, China); StepOne PlusTM Real Time PCR (Applied Biosystems, USA).

Method

Rifaximin and RIF were dissolved in DMSO. 4% (wt/vol) DSS was dissolved in distilled water; PCN (42 mg·kg-1): 151.2 mg PCN were dissolved it 36 mL camellia oil.

Rifaximin: for a low dosage (20 mg·kg-1) 72 mg rifaximin were dissolved in 36mL camellia oil; for a medium dosage (40 mg·kg-1) 144 mg rifaximin were dissolved in 36 mL camellia oil; for a high dosage (80 mg·kg-1) 288 mg rifaximin were dissolved in 36 mL camellia oil.

Cell culture

LS174T cell strain was obtained from the cell bank in Peking Union Medical College and was placed into a culture flask with DMEM+10 % FBS to serve as the medium. This cell strain was cultured at 37°C with 5% CO_2 against an appropriate saturated humidity. When cells grew to cover 80% of the medium, it was digested

by pamcreatin including 0.25% trypsin and 0.02% EDTA, and then subcultured at the ratio of 1:3.

Detection of mRNA expression of CYP3A4 and PXR in LS174T by Realtime PCR

The LS174T cells were in a six-well plate by medium including 0.1, 1, 5, 10, 20, 50, and 100μmol·L^{-1} rifaximin; 24 and 48 h later, based on the instructions on the RNApure kit, the total RNA was rapidly extracted; the result of electrophoretic analysis clearly showed the 18S and 28S stripe and showed that the ratio between A260 and A280 was between 1.7 and 2.0, and the fragment of total RNA was complete without degradation. Using 2 μg reverse transcription was carried out at 42°C for 30 min and at 85°C for 5 min, respectively, according to the manufacturer's instructions on TransScriptTM One-Step RT-PCR SuperMix; PCR was carried out by ABI StepOne PlusTM Realtime PCR and 2.0 μL reverse transcription reaction product was taken as the PCR reaction model; 0.5 μL 20 μmol· L^{-1} upstream and downstream primer and 10 μL Fast SYBR@ Green Master Mix were added respectively, Rnase-free water was made up to 20 μL. The reaction parameters were shown as follows: initial denaturation at 95°C for 20 s, denaturation at 95°C for 3 s, and annealing at 60°C for 30 s with 40 cycles in all; β-actin was set up as the inner reference at each proliferation and Realtime quantitative analysis of the proliferation product of PCR was carried out by means of $2^{-(\Delta\Delta Ct)}$. Finally, 10μmol·L^{-1} RIF was used as the positive control group and 0.1% DMSO as the solvent control group. The specific primer sequence is shown in Table I.

Effect of rifaximin on the CYP3A4 and PXR protein expression in LS174T cell detected by Western-blot

The cell samples were precooled twice with different processing in the plate wells with PBS; 1 mL PBS was added and then cells and collagen were scraped from the plate wells with a cell scraper; cells were then put into a 1.5 mL EP tube which was placed on ice and then suspended until the collagen within was dissolved and cells were released; the cells were centrifuged at 4°C and 1500×g for 4 min and then the supernatant was removed; the cellular sediment was rinsed twice in PBS and then centrifuged and enriched by adding 200 μL RIPA lysate, kept at 4°C for 10 min and then centrifuged at 12000×g for 10 min, then the sediment and supernatant were removed, namely the lysate of whole-cells. Protein was quantified by the Basic Competency Assessment (BCA) method and bovine serum protein was taken as the protein quantification standard. 20 μg protein was simmered in water at 95°C for 4 min. All samples were electrophoresed through 12% SDS-polyacrylamide 8×10 cm until the bromophenol blue moved towards the bottom of gel at the constant pressure of 100V. After electrophoresis, the protein was transferred from the gel to the membrane of Polyvinylidene Fluoride (PVDF) at 30V for 3 h; the PDVF membrane was submerged in 1×TTBS (10 mM Tris-HCl pH8.0, 150 mM NaCI pH7.7, 0.05%Tween) including 5% skimmed milk powder (SMP), and was kept at 4°C overnight and the sites were combined with sealing non-specificity; the appropriate amount of primary antibodies diluted with 1×TTBS including 5% SMP at the ratio of 1:1000 was added and then cultured at room temperature for 1 h; the membrane was washed three times in 1×TTBS for 15 min each time; next secondary antibodies [IgG marked by Horseradish Peroxidase (HRP)] diluted with 1×TTBS including 5% SMP at the ratio of 1:1000 were added and cultured at room temperature for 1 h; the membrane was washed three times in 1×TTBS for 15 min each time; then washed in TBS again for 10 min; and was finally developed according to the manufacturer's instructions on the electrochemiluminescence (ECL) kit.

Effect of rifaximin on activation of PXR in the detection by EMSA

One day after spreading LS174 cells on the plate, they were treated with rifaximin (10-100 μmol·L^{-1}) and RIF (10 μmol·L^{-1}) to culture for a further 24 h; the nucleoprotein was extracted for detection according to the manufacturer's instructions on the NE-PERTM nucleus

Table I. *Specific primer sequence under real-time PCR.*

Gene	Primer sequence
CYP3A4	5'-CAAGACCCCTTTGTGGAAAA-3'
	5'-CGAGGCGACTTTCTTTCATC-3'
PXR	5'-AGCTGGAACCATGCTGACTT-3'
	5'-AGGGGCGTAGCAAAGGGGTG-3'
β-actin	5'-CTACAATGAGCTGCGTGTGG-3'
	5'-TAGCTCTTCTCCAGGGAGGA-3'

and cytoplasm protein extract kit (Pierce, Rockford, IL, USA). The protein quantification was carried out by the BCA method and the bovine serum protein was taken as the standard. Probe was synthesized by Invitrogen and marked with biotin(5'-GAATGAACTTGCTGACCCT CTATATGAACTCAAAGGAGGTCAGTG-3, and its complementary), but its competitive probe failed to be marked. 5 μg nucleus protein were prepared according to the instructions on LightShift® Chemiluminescent EMSA kit (Pierce, Rockford, IL, USA) and left at room temperature for 30 min; native polyacrylamide gel with a 6% concentration by 0.5×TBE was prepared and added with 0.5×TBE into the electrophoresis equipment so as to cover the upper sample well; then it was prerun at 100V for 30 min and samples were loaded in the 20 μl system and electrophorese at 100V until the bromophenol blue moved towards $^{2}/3$ or $^{3}/4$ part of the whole gel; gel and nylon membrane were fixed on the electroporation equipment according to the manufacturer's instructions; then precooled 0.5×TBE buffer was added and electrophoresed at 38 0mA for 45-50 min; cross-linking was carried out by applying the UV lamp in the length of 254 nm and the side of nylon membrane was turned with DNA up and the cross-linking lamp placed at a 0.5 cm from membrane under the UV lamp to carry out cross-linking for 10 min. The detection of chemoluminescence was carried out based on the manufacturer's instructions, and finally, photo exposure detection was carried out.

Animal grouping and administration

Sixty male C57BL/6J mice between 20 and 25 g in weight were used in this study, all provided from the experimental animal center in the Academy of Military Medical Sciences, China. All the mice were placed in an environment of (23±2)°C and (55±10)% humidity and fed *ad libitum*. The mice were randomly divided into six groups, ten in each group, including a control group, model group, low dosage group, middle dosage group, high dosage group and positive medicine group (PCN). All groups were treated with intraperitoneal injection. All mice were pre-administrated for three days and the control group was treated with the camellia oil in an equal dosage. From the 4th day, the model group, low dosage group, middle dosage group, high dosage group and positive medicine group freely drank the camellia oil including 4% DSS until the 10th day, and meanwhile they were treated with rifaximin or PCN correspondingly. The changes in weight as well as their diarrhea and hemafecia conditions were monitored of these mice. Disease activity index (DAI) was evaluated for all mice according to the Murano standard (10). All mice were kept from food but still provided with water 12 h before sacrificing. the lung, heart, liver, kidney, stomach, spleen, duodenum, intestinum jejunum, ileum, cecum, and colon were removed from the mice in all six groups and were conserved at -80°C until use. Some parts of the colon were fixed in 10% neutral buffer formalin for the preparation of pathological slicing and HE dyeing; and the length of other parts was measured.

Extract of DNA and Real-time PCR analysis

After administering for 10 days, the lung, heart, liver, kidney, stomach, spleen, duodenum, intestinum jejunum, ileum, cecum, and colon were taken from the mice in all six groups and preserved at -80°C until use. Based on instructions on the RNApure kit, tissues were taken to extractthe total RNA; the result of electrophoretic analysis clearly showed the 18S and 28S stripe and showed that the ratio between A260 and A280 was between 1.7 and 2.0, and the fragment of total RNA was complete without degradation. TransScriptTM One-Step RT-PCR SuperMix 2μg RNA was used for reverse transcription at 42°C for 30 min and at 85°C for 5 min, respectively, according to the manufacturer's instructions; PCR reaction was carried out by ABI StepOne P1usTM Realtime PCR and 2.0 μL reverse transcription reaction product was taken as the PCR reaction model; 0.20 μmol· L^{-1} upstream and downstream primer and 10 μL Fast SYBR@ Green Master Mix were added respectively, the Rnase-free water was made up to 20 μL. The reaction parameters were shown as follows: initial denaturation of 20S at 95°C, denaturation of 3S at 95°C, and annealing of 30S at 60°C with 40 cycles in all; β-actin was set up as the inner reference at each proliferation and the Realtime quantitative analysis of the proliferation product of PCR was conducted by means of $2\text{-}(^{\Delta\Delta Ct})$. Gene sequence was carried out according to the study of Cheng J et al. (11).

Statistical analysis

To ensure the accuracy of results, all the experiments were repeated three times and statistical analysis was carried out by SAS software, using the data collected from these experiments. The experimental data was expressed by mean ± standard deviation. The comparison between every two groups was carried out by *t*-test, $p<0.05$.

RESULTS

Effect of rifaximin on the CYP3A4 and PXR mRNA expression in LS174T cell in the detection by real-time PCR

In this study, 0.1% DMSO was used as the solvent control and 10 μmol·L^{-1} RIF as the positive control. By studying the transcription regulation effect of rifaximin on CYP3A4, it was found that RIF could

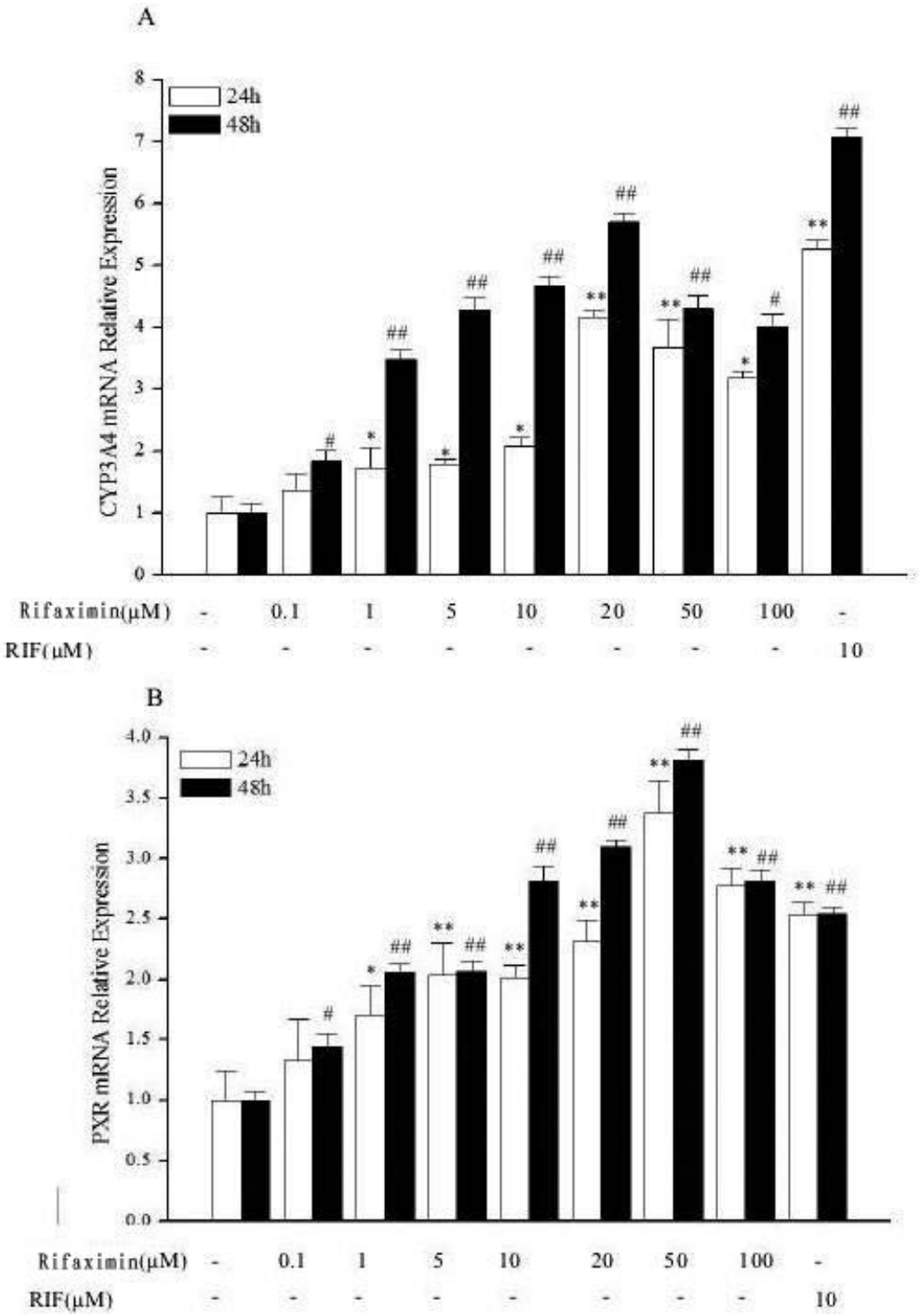

Fig. 1. *Effect of rifaximin on mRNA in LS174T cell.* ***A)*** *Influence of rifaximin on concentration-dependent effect of CYP3A4 mRNA relative expression in LS174T cell.* ***B)*** *Influence of rifaximin on concentration-dependent effect of PXR mRNA relative expression in LS174T cell (n=3). When compared with the control group, * = p<0.05, ** = p<0.01 (24h) in graph A; when compared with the control group, # = p<0.05, ## = p<0.01 (48h) in graph B.*

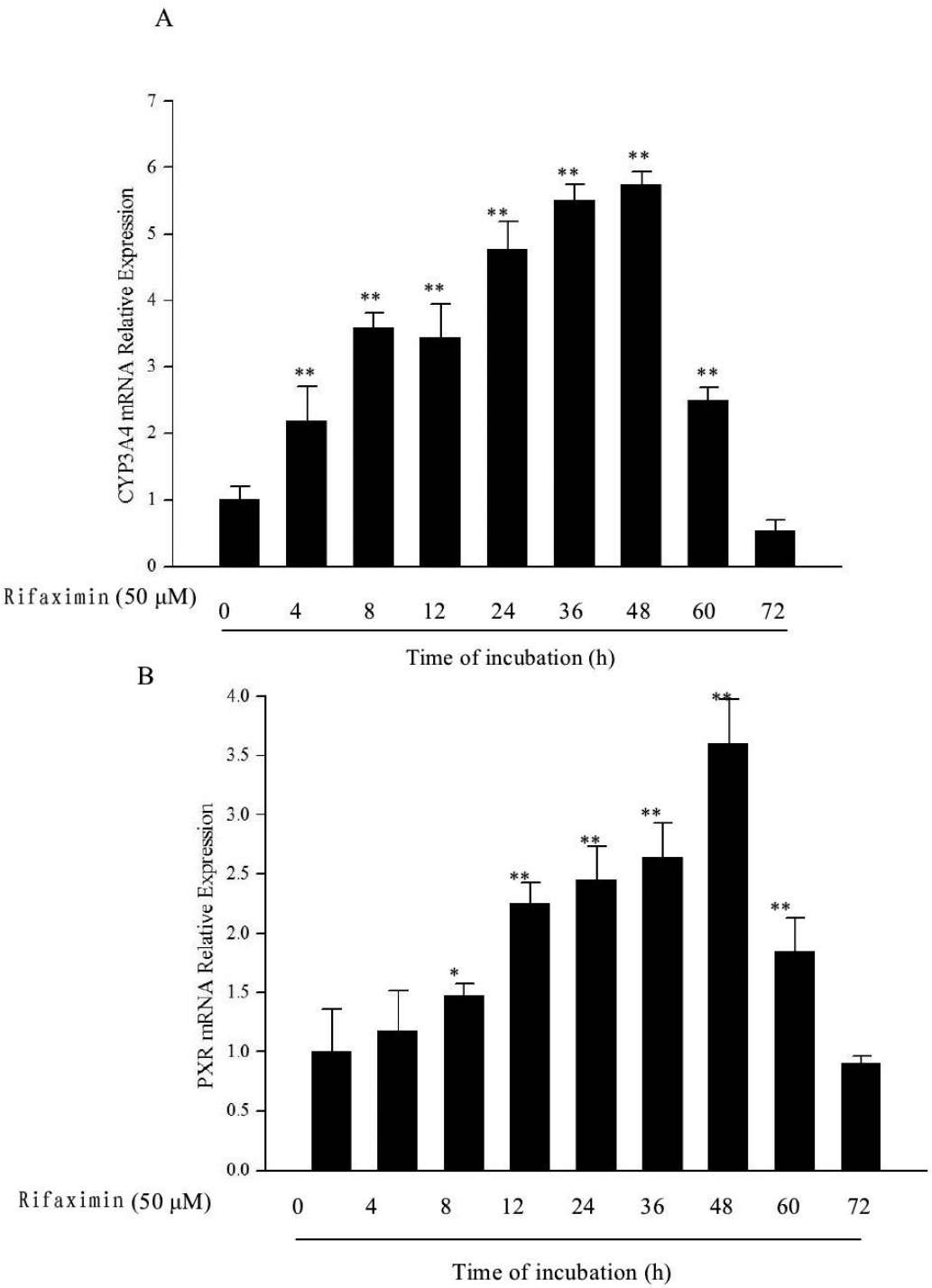

Fig. 2. *Effect of rifaximin on mRNA in LS174T cell.* ***A****) Influence of rifaximin on time-dependent effect of CYP3A4 mRNA expression in LS174T cell.* ***B****) Influence of rifaximin on time-dependent effect of PXR mRNA expression in LS174T cell (n=3). When compared with the control group, *= p<0.05, and ** = p<0.01.*

both activate PXR and induce the transcription expression of CYP3A4. Rifaximin could induce the transcription expression of CYP3A4 within the concentration of 0.1-100 μmol·L^{-1} 24 and 48 h later and showed a tendency of increase at first but later decreased and reached the maximum at 20 μmol·L^{-1}, as was the tendency for the transcription of PXR activation which reached the maximum at 50 μmol·L^{-1}, Fig. 1.

Effect of rifaximin on CYP3A4 and PXR mRNA in different time-points

After the action of rifaximin, the CYP3A4 and PXR mRNA expression were detected at 0, 4th, 8th, 12th, 24th, 36th, 48th, 60th, and 72nd h, respectively. Results showed that the 20μmol·L^{-1} rifaximin could improve its expression at the 4th h, while the mRNA expression was improved at the 8th, 12th, 24th, 36th, 48th, 60th, and 72nd h. At the 72nd h, the expression was reduced and it was of statistical significance when compared with that at 0 h, which showed a clear time-dependent effect, Fig. 2.

Protective mechanism of rifaximin for mice with IBD caused by DSS

Clinical grading for mice with IBD caused by DSS

All 60 mice in this experiment were randomly divided into six groups of 10 mice each, including control group, model group, low dosage group, middle dosage group, high dosage group and positive medicine group (PCN), which were all treated with intraperitoneal injection. All mice were pre-administered for 3 days and the control groups were treated with camellia oil in equal dosage. From the 4th day, the model group, low dosage group, middle dosage group, high dosage group and positive medicine group drank camellia oil freely including 4% DSS until the 10th day, and meanwhile they were treated with rifaximin or PCN correspondingly. By noting changes of weight, diarrhea and hemafecia condition in these mice, the DAI was evaluated based on the Murano standard. The results showed that the change of weight, diarrhea and hemafecia condition in mice from the model group was much worse than other groups. However, the changes in weight, diarrhea and hemafecia were successively alleviated for mice in the low dosage group, middle dosage group and high dosage group. The colon of mice in the model group was shorter in length than other groups. From the perspective of the appearance of colon, the colon from mice in the model group was congested and had turned red, while the colon from mice in the low dosage group, middle dosage group and high dosage group had an alleviated congestion successively. However, there was almost no congestion on the surface of colon from mice in the positive group.

Preparation of pathological slicing for mice with IBD caused by DSS

To achieve a direct understanding of the severity of colonitis in mice caused by DSS and the protective effect of rifaximin, we made a histological examination. The results showed that when compared with the control group, in the model group treated with DSS for seven days freely, edema and inflammatory cellular infiltration was clearly shown on the intestinal wall of colon tissues. However, the damage of colon tissues was much alleviated after being treated with 20-80mg·kg^{-1}, PCN (42 mg·kg^{-1}) rifaximin. Moreover, with the increased dosage of rifaximin, the damage to the colon tissues was much less, without obvious surface of ulcer but only with edema and inflammatory cellular infiltration. Meanwhile, the damage to colon tissues was also obviously improved. However, as to the grading for pathological slicing, there was a much higher pathological grading for the model group than the control group. After treatment with 20-80 mg·kg^{-1}, PCN (42 mg·kg^{-1}) rifaximin, the pathological grading for the two groups was reduced. However, when compared with the model group, there was a much lower pathological grading in the PCN group.

PXR relative expression in mice with IBD caused by DSS in the detection by Realtime PCR

In order to achieve a better understanding of the protective mechanism of mice with IBD caused by DSS, we detected the CYP3α11, CYP3α13 , GSTα1 and MDR1α in colon tissues and the PXR mRNA expression of lung, heart, liver, kidney, stomach, spleen, duodenum, intestinum jejunum, ileum, cecum, and colon from mice in each group. This result clearly showed a lower expression of CYP3α11, CYP3α13, GSTα1 and MDR1α in the model group but a successively higher expression

in the low dosage group, middle dosage group and high dosage group. Moreover, they all showed a dependence on concentration to some extent. But the PCN group ranked the first in the increase of PXR mRNA expression. It was stated as above that PXR mRNA all had an expression in the above mentioned organs of mice, among which the liver and duodenum ranked the first in its expression, and then the cecum and colon. In addition, the PXR mRNA expression of all tissues in the model group was much lower than other groups, and the low dosage group, middle dosage group and positive medicine group tended to be higher subsequently.

NF-κB relative expression in mice with IBD caused by DSS detected by Realtime PCR

Nuclear factor -kappa B(NF-κB) is an important signal regulation pathway. Past studies have shown that the activation of PCR could inhibit the NF-κB signal pathway. To further study the protective effect of the rifaximin on mice with IBD caused by DSS, we conducted gene expression of related factors to NF-κB (Chemokine (C-C)motif receptor2 (CCR2), ICAM-1, IL-1β, IL-6, IL-10, inducible nitric oxide synthase(iNOS), monocyte chemoattractantprotein 1 (MCP-1)) by realtime PCR. Results showed that the model group could obviously induce the mRNA expression of CCR2, ICAM, IL-1β, IL-6, IL-10, iNOS, MCP-l and TNFa, while the inductive effect of the low dosage group, middle dosage group and high dosage group decreased successively, while the positive medicine group could obviously inhibit the expression of CCR2, ICAM, IL-1p, IL-6, IL-10, iNOS, MCP-l and TNFa mRNA. These results were in line with other literature.

DISCUSSION

Cytochrome P450 is the critical enzyme of medical metabolism, which takes part in the metabolism of several medicines and natural products. However, CYP450 itself can also be induced or inhibited by several medicines, which will change the metabolism and clearance velocity of the other medicine that is taken at the same time. This is the common mutual reaction of medicine. The protein regulated and mediated by PXR is involved in several segments of medicinal process, including: the phase I metabolic enzyme CYP3A, CYP2B6, CYP2C,CYP1A; the phase II metabolic enzyme UGT, SULT, GST; medicine transporter MDR1, MRP2, MRP3,MRP4, MRPS, BCRP, OATP, OCTP. PXR is the critical transcription factor of CYP3A4 for expression control. The transcription expression of CYP3A4 mediated by PXR is considered as the important molecular basis of medical mutual reaction. PXR report gene experiments are based on the molecular mechanism of PXR in regulating the expression of CYP3A4. Basing on this experimental model, the induction of medicine to CYP3A4 and its effect produced by means of PXR can be ascertained.

IBD has a high rate of recurrence and major clinical symptoms, such as diarrhea, celialgia and Mucopurulent hemafecia (12). There is a higher incidence of IBD in western countries than Asian countries. However, with the improvement of lifestyle in Asian countries, the incidence of IBD is higher year by year. However, the cause of IBD is still far from clear, and the study of IBD pathological mechanism and development of new treatment remains an issue of great contention. Rifaximin can activate CYP3A4 by mediating PXR, while the classical ligand RIF of PXR can be applied to treat UC by activating PXR. Therefore, this experiment applied the internationally accepted IBD model caused by DSS, and then discussed the molecular mechanism of rifaximin in treating IBD, which provides the reference for further study on the functions of rifaximin and further discussion on the effect of PXR in inducing the compound to treat IBD (13).

In this study, we first carried out the cellular experiment, then selected the human colon cancer cell strain LS174T and studied the effect of rifaximin on the CYP3A4 and PXR mRNA expression. Results showed that rifaximin could induce the CYP3A4 and PXR mRNA expression in cellular level with time and concentration dependence, which was consistent with transcription level as to its effect on the CYP3A4 protein. In order to have further insight into the inductive mechanism of rifaximin for CYP3A4, the potential mechanism was inferred as the shift of PXR from cytoplasm to nucleus which combined with the consistent sequence in the transcription region of CYP3A4 after activated by allogene and then the formation of ligand-receptor compound to induce the transcription of CYP3A4 and the expression of

protein. Thereafter, the EMSA was carried out and this result showed that the combination of PXR with the transcription region of CYP3A4 was quite specific, demonstrating that the inductive effect of rifaximin on CYP3A4 began in the combination phase of PXR with the transcription region of CYP3A4. Recently, a great number of studies have shown that PXR as a critical transcription regulation factor played an important role in the CYP3A4 expression. Thus it was estimated that the activation of rifaximin for PXR might simply represent its mechanism to induce the CYP3A4 expression. In order to prove this estimation, reporter gene technology was applied to examine the activation of rifaximin for PXR. The result of this experiment shows that rifaximin can promote its transcription activation and then induce a higher expression of CYP3A4, while this process is mediated by CYP3A4 regulation sequence including PXR response.

Rifaximin can activate CYP3A4 by mediating PXR, while the classical ligand RIF of PXR can be applied as the therapy for IBD by activating PXR. Thus the UC model caused by DSS applied in this paper, was pre-treated with rifaximin or PCN (Pregnenolone 16a-carbonitrile, as the inductor of classical CYP3A4 expression for rodent animals) for three days and then treated with 4%DSS at the 4th day. The result showed that the low, middle and high dosage of rifaximin could all relieve the symptoms of IBD. The result of pathological slicing revealed that rifaximin could effectively improve the condition of ulcer, which hinted that rifaximin could serve as a therapy for IBD caused by DSS.

In this study CYP3α11, CYP3α13, GSTα1 and MDR 1α were detected in colon tissues from mice in each group, as well as the PXR mRNA expression of lung, heart, liver, kidney, stomach, spleen, duodenum, intestinum jejunum, ileum, cecum, and colon from mice in each group. Results showed that the mRNA expression of CYP3α11, CYP3α13, GSTα1 and MDR 1α in the model group was all reduced to some extent. However, the mRNA expression of CYP3α11, CYP3α13, GSTα1 and MDR 1α in the low dosage group, middle dosage group and high dosage group was successively higher, and was also dependent on concentration. As stated above, PXR mRNA was expressed in the above mentioned organs of mice, among which the liver and duodenum ranked the first in its expression, and then the cecum and colon. In addition, the PXR mRNA expression of all tissues in the model group was much lower than other groups, and the low dosage group, middle dosage group and positive medicine group tended to be higher successively. Previous studies have shown that the activated PXR could inhibit the NF-KB signal pathway. In order to further examine the protective effect of rifaximin on IBD in mice caused by DSS, the mRNA expression of CCR2, ICAM, IL-1β, IL-6, IL-10, iNOS, MCP-1 and TNFa was detected by Realtime PCR. Results led to conclude that the model group could obviously induce the mRNA expression of CCR2, ICAM, IL-1β, IL-6, IL-10, iNOS, MCP-1 and TNFa, while the inductive effect of low, middle and high dosage was weakened successively and PCN could obviously inhibit the mRNA expression of CCR2, ICAM, IL-1β, IL-6, IL-10, iNOS, MCP-1 and TNFa. Therefore, rifaximin as the xenobiotic ligand was inferred to be one which could be applied to alleviate IBD by activating PXR and then inducing CYP3α11, CYP3α13, GSTal and MDRIα. Besides, it could also be applied to inhibit the mRNA expression of CCR2, ICAM, IL-1β, IL-6, IL-10, iNOS, MCP-1 and TNFa and could be safely applied for treatment.

In conclusion, the results obtained in this study show that rifaximin can activate PXR and the expression of CYPA4 mRNA at cellular level; the EMSA experiment and report gene experiment demonstrate that rifaximin can induce the expression of CYP3A4 by activating PXR. In the IBD model induced by DSS, PXR is the critical factor in treating IBD. When a compound can induce the PXR expression, it means that it has a potential ability in treating IBD, while rifaximin may be safely applied to treat IBD by activating PXR. The pathogenesis of IBD is yet far from clear, while the intestinal microorganisms play a leading role in the development of IBD. Therefore, antibiotics have great potential for treating IBD. At present, rifaximin is an antibiotic with local effect on bowel which fails to be assimilated orally but it has a low systematic effect, there are several studies proving its efficacy and safety. However, quite a number of problems in treating IBD with rifaximin are waiting for answers from further studies and more clinical experiments, such as whether it can be administered at intervals,

whether it is effective to administer in low dosage and whether it has drug resistance.

REFERENCES

1. Liu Y, Yin Y, Chen Y, Zhou HZ. Effects of genetics variants of pregnanexenobiotic receptor and on pharmacogenetics and drug metabolism. Chinese J of Clinical Pharmacology and Therapeutics 2007; 12(8):84-849.
2. Prantera C, Lochs H, Grimaldi M, Danese S, Scribano ML, Gionchetti P. Rifaximin-extended intestinal release induces remission in patients with moderately active Crohn's disease. Gastroenterology 2012; 142(3):473-81.
3. Shafran I, Burgunder P. Adjunctive antibiotic therapy with rifaximin may help reduce Crohn's disease activity. Dig Dis Sci 2010; 55(4):1079-84.
4. Ojetti V, Lauritano EC, Barbaro F, Miqneco A, Ainora ME, Fontana L, Gabrielli M, Gasbarrini A. Rifaximin pharmacology and clinical implications. Expert Opin Drug Metab Toxicol 2009; 5(6):675-82.
5. Maccaferri S, Vitali B, Klinder A, et al. Rifaximin modulates the colonic microbiota of patients with Crohn's disease: An *in vitro* approach using a continuous culture colonic model system. J Antimicrob Chemother 2010; 65(12):2556-65.
6. Mencarelli A, Migliorati M, Barbanti M, Cipriani S, Palladino G, Distrutti E, Renga B, Fiorucci S. Pregnane-X-receptor mediates the anti-inflammatory activities of rifaximin on detoxification pathways in intestinal epithelial cells. Biochem Pharmacol 2010; 80(11):1700-707.
7. Yarur AJ, Strobel SG, Deshpande AR, Abreu MT. Predictors of aggressive inflammatory bowel disease. Gastroerol Hepatol 2011; 7(10):652-59.
8. Mencarelli A, Renga B, Palladino G, et al. Inhibition of NF-κB by a PXR-dependent pathway mediates counter-regulatory activities of rifaximin on innate immunity in intestinal epithelial cells. Eur J Pharmacol 2011; 668(1-2):317-24.
9. Cheng J, Shah YM, Gonzalez FJ. Pregnane X Receptor as a target for treatment of inflammatory bowel disorders. Trends Pharmacol Sci 2012; 33(6):323-30.
10. Wang YG, Zhou JM, Ma ZC, et al. Pregnane X Receptor mediated-transcription regulation of CYP3A by glycyrrhizin: a possible mechanism for its hepatoprotective property against lithocholic acid-induced injury. Chem Biol Interact 2012; 200(1):11-20.
11. Cheng J, Ma X, Krausz KW, et al. Rifampicin-activated human pregnane X receptor and CYP3A4 induction enhance acetaminophen-induced toxicity. Drug Metab Dispos 2009; 37(8):1611-21.
12. Xu JR. Summary of Chinese traditional medicine and Western medicine in treatment of inflammatory bowel disease. Chinese Medicine Modern Distance Education of China 2010; 8(4):176-78.
13. Wang ZL, Li SX. The influence factors of establishment of the inflammatory bowel disease model in BALB/c mice induced by TNBS. J of Tropical Med 2012; 12(5):573-76.

LETTER TO THE EDITOR

CLINICAL DIAGNOSIS OF CAROTID ATHEROSCLEROSTIC PLAQUE IN HYPERTENSIVE PATIENTS WITH HIGH RESOLUTION MAGNETIC RESONANCE ANGIOGRAPHY

L. ZHANG[1], C-M. TIAN[2], Q-Y. LIU[1], S-S. WANG[1], X. WANG[1], L. CHEN[1], Y. FENG[1] and L-T. GUO[1]

[1]Department of Radiology, Affiliated Hospital of Binzhou Medical University, Binzhou, China;
[2]Department of Pediatrics, Affiliated Hospital of Binzhou Medical University, Binzhou, China

Received March 6, 2015 – Accepted April 9, 2015

As the incidence of ischemic cerebrovascular disease increases continuously over the years, carotid atherosclerosis as an important dangerous factor has drawn a lot of attention from many experts and scholars. To explore the clinical significance of high resolution magnetic resonance angiography (MRA) in carotid atherosclerosis and ischemic cerebrovascular disease, a group contrasting method was adopted. One hundred patients with ischemic cerebrovascular disease and 100 patients without ischemic cerebrovascular disease were taken as observation group and control group, respectively. High resolution MRA was used for examining and observing the development of carotid atherosclerostic plaque in patients in the two groups. We found that the proportion of carotid atherosclerostic plaque in the experimental group and control group had statistical difference (P<0.05); and the proportion of carotid atherosclerostic plaque in patients over 60 years of age was higher than in patients under 60 years, and the difference was statistically significant (P<0.05). The proportion of carotid atherosclerostic plaque in patients with high blood pressure was also higher than in patients without high blood pressure, and the difference was statistically significant (P<0.05). Moreover, the proportion of carotid atherosclerostic plaque in patients with hyperlipidemia was higher than in patients without hyperlipidemia, and the differences were statistically significant (P<0.05). We can therefrore draw a conclusion that the development of carotid atherosclerostic plaque affects the occurrence of ischemic cerebrovascular disease, which is related to patient's age, level of blood pressure and blood lipids. In addition, high resolution MRA is helpful to early discovery of the formation of carotid atherosclerostic plaque.

Stroke, one of the main leading causes of death in the world, ranked second in the global cause of death, and its death toll reached 6.2 million in 2011, based on the data released by the World Health Organization (WHO) in 2013; its high incidence rate and mortality rate are obvious (1). Stroke, including hemorrhagic stroke and ischemic stroke (about 80%), is mainly caused by artery thrombosis or blood clots induced by embolism, such as atherosclerosis (the most common and dangerous pathogenic factor), cardiogenic embolism, lacunar infarction. For this reason, many experts and scholars have carried out extensive research in this field. In the article of Li ML (2), the color Doppler ultrasound detection

Key words: ischemic cerebrovascular disease, hypertension, high resolution MRA, atherosclerostic plaque

Mailing address: Dr Lin Zhang,
Department of Radiology, Affiliated Hospital of Binzhou,
Medical University, No.661, Huanghe Second Road,
Bincheng District, Binzhou,
Shandong, 256603, China
E-mail: az@ibhsedu.com

0393-974X (2015)

method was explained, and was proved to have unique advantages on detecting the nature of carotid atherosclerostic plaque and could evaluate the potential risks of atherosclerotic plaque rupture, thus providing diagnostic basis for developing effective treatment protocols. In the study of Qian JL, et al. (3), carotid arteries of 210 patients with cerebral infarction underwent Color Doppler Flow Imaging (CDFI) detection, and the results showed that carotid atherosclerostic plaque was closely connected with cerebral infarction, and also indicated that CDFI was conducive to preventing and treating the cerebral infarction. In the paper by (4) Li and Liang, they proved that probucol+aspirin+statins (PAS) triple therapy had significant effect on treating carotid atherosclerostic plaque in patients with cerebral infarction by grouping contrast experiments. Traditional radiological technologies, such as computed tomography (CT) angiography, transcranial Doppler ultrasound, magnetic resonance angiography (MRA), angiography, etc. can only show the stenosis degree of blood vessels but cannot observe pathological changes of vascular walls. To date, high resolution MRA is applied in studying conditions of the intracranial vascular wall, including atherosclerotic plaque, irregular wall thickening, wall reconstruction, intraplaque hemorrhage, aortic dissection and vasculitis, etc (5, 6).

It is not difficult to see that in atherosclerostic detection methods, Doppler ultrasonic detection is commonly applied with a higher precision rate (7), however it is limited in examining bifurcations of total artery and plaques in internal carotid artery, while magnetic resonance angiography (MRA) has better results in this aspect. In this study, the relationship between ischemic cerebrovascular disease and carotid atherosclerostic plaque was analyzed by observing patients in our hospital with and without ischemic cerebrovascular disease using high resolution MRA, which lays a solid foundation for future treatment of cerebrovascular disease in.

MATERIALS AND METHODS

A total of 100 patients with ischemic cerebrovascular disease (61 male and 39 female) and 100 patients without ischemic cerebrovascular disease (58 male and 42 female) who were admitted to our hospital from May 2010 to May 2014 were taken as an observation group and a control group, respectively. Symptoms of patients in the two groups were confirmed by Magnetic Resonance Imaging (MRI) or Computed Tomography (CT) (Table II).

Methods

Patients in the two groups were examined using 1.5 T MRA scanners, and the imaging sequences included: axial 3-dimensional time-of-flight magnetic resonance angiography (3D - TOFMRA); axial fast spin echo (FSE) and double inversion recovery (DIR); axial FSE PDWI and T2 WI with EcG gating (8). In horizontal FSE sequence, upward and downward side of carotid artery lesion applying radio frequency saturated zone inhibited blood flow signal of carotid artery and jugular vein. Using the above methods, in both groups we analyzed the results of MRA, recorded the number of patients with and without ischemic cerebrovascular disease who were found with carotid plaque, and analyzed the number of patients who were over 60 and under 60 years of age with carotid plaques, as well as the formation of carotid plaque in patients with hypertensive history.

Statistical analysis

Statistical software SPSS17.0 was used for statistical analysis. Measurement data were expressed as mean±SD and processed by *t*-test, enumeration data was processed by χ^2 test, and the difference was considered to have statistical significance if $P<0.05$.

RESULTS

Comparison of development of carotid atherosclerostic plaques of patients in the two groups

By comparing the observation group with the control group, it was found that general characteristics in the two groups were obviously different (Table II). The results indicated that 68 patients in the observation group (68%) and 35 patients in the control group (35%) were found with carotid atherosclerostic plaques, and the difference of the proportion of patients with carotid plaques in the two groups was statistically significant ($P<0.05$).

Influence of patients' age on formation of carotid atherosclerostic plaques

Of 104 patients over 60 years of age, 78 developed carotid plaques; and of 96 patients under 60 years, 25 developed carotid plaques; the proportion of carotid plaques among patients over 60 years was higher than that among patients below 60 years, and the difference was statistically significant ($P<0.05$).

Table I. *Characteristics of patients in the two groups studied.*

Group	Gender (male/ female)	Age	Hyperlipemia patients (number)	Hypertensive Patients (number)
Observation group	61/39	42±2.12	61	42
Control group	58/42	38±2.12	59	41

Table II. *Comparison of general clinical characteristics in the observation group and control group.*

Variables	Observation group (n=100)	Control group (n=100)	P value
Age (n, mean±SD)	63.9±13.6	63.1±12.4	0.86
Male (n, %)	61(61.00)	58(58.00)	1
Hypertension (n, %)	42(42.00)	41(41.00)	1
Hyperlipemia (n, %)	61(61.00)	59(59.00)	0.28

mean±SD, χ^2

Table III. *Effect of different influence factors of patients in two groups on formation of carotid atherosclerostic plaques.*

Influence factors		Observation group (n=100)	Control group (n=100)	Total	With carotid plaques	Proportion of forming plaque (%)
Age (O)	O≥60	50	54 54	104	78	75.0
	O<60	50	46	96	25	26.0
Hypertension	Yes	44	39	83	48	57.8
	No	56	61	117	55	47.0
Hyperlipidemia emia	Yes	59	61	120	72	60.0
	No	33	47	80	31	38.8

Influence of patients' blood pressure on formation of carotid atherosclerostic plaques

Of 83 patients with high blood pressure in the two groups, 48 developed carotid atherosclerostic plaques; and of 117 patients without high blood pressure, 55 developed carotid atherosclerostic plaques; the proportion of carotid atherosclerostic plaques among patients with high blood pressure was higher than that among patients without high blood pressure, and the difference had statistical significance (P<0.05).

Influence of patients' blood lipids on formation of carotid atherosclerostic plaques

Of 120 patients with hyperlipemia in the two groups, 72 developed carotid atherosclerostic plaques; and of 80 patients without hyperlipemia, 31 developed carotid atherosclerostic plaques.

The proportion of carotid atherosclerostic plaques among patients with hyperlipemia was higher than that among patients without hyperlipemia, and the difference had statistical significance ($P<0.05$). The effect of different influence factors of patients on formation of carotid atherosclerostic plaques is shown in Table III.

DISCUSSION

Cerebrovascular diseases threaten human life and health worldwide, in which, ischemic stroke, as a commonly and frequently encountered disease occurring in the central nervous system, has high incidence, fatality rate and invalidism rate. In addition, the incidence of cerebrovascular disease shows an increasing trend with aging of populations and an increase in the smoking population (9, 10). In clinical events of ischemic cardia-cerebrovascular disease, carotid atherosclerosis is closely related to ischemic stroke, and its main pathogeneses lie in rupture of vulnerable plaques and thrombosis. To date, color Doppler ultrasound and Digital Subtraction Angiography (DSA), as the main method applied in evaluating atherosclerotic plaques, cannot make a detailed analysis on the vulnerability of plaques. In clinical practice, it is found that ultrasonic Doppler is limited greatly in evaluating common carotid artery bifurcation (CCAB) and internal carotid atherosclerosis plaque, especially plaque calcification, although it is able to show stenosis degree of CCA. High resolution MRA applied in this study is a good way to compensate the defects of ultrasonic Doppler. This study examined the degree of carotid atherosclerosis in patients with ischemic cerebrovascular disease and without ischemic cerebrovascular disease, and analyzed the correlation of carotid atherosclerosis and ischemic cerebrovascular disease.

Carotid atherosclerosis is a dangerous factor for the formation of cerebrovascular disease, the rupture or failure of which are able to lead to complete occlusion or incomplete obstruction of distal arteries of carotid arteries, thus causing ischemia and hypoxia of brain tissue in the blood supply (11). In this study, 68% of the patients with ischemic cerebrovascular disease in the observation group were diagnosed with carotid atherosclerostic plaques by MRAand 35% in the control group, which explained that the formation of ischemic cerebrovascular disease was connected with carotid atherosclerostic plaques to some extent. Therefore, early discovery of carotid atherosclerostic plaques contributes to the prevention of ischemic cerebrovascular disease. Besides its non-invasive characteristic, MRA is also featured by high sensibility and specificity compared with carotid ultrasound, and its results are very close to the results obtained from carotid angiography. The results obtained in this study showed that, the proportions of carotid atherosclerostic plaques developed in the elderly, hypertensive and hyperlipemia patients over 60 years of age were relatively high, which indicated that patients conforming to the above conditions were more likely to develop carotid atherosclerostic plaques, and they should attach importance to preventing ischemic cerebrovascular disease.

In conclusion, MRA has many advantages over carotid ultrasound. The application of high resolution MRA is able to intuitively reflect significant biological characteristics, such as structure of carotid arterial blood wall, size and ingredient of carotid atherosclerostic plaque, etc., and it has exceptional advantages in evaluating different types of atherosclerotic plaques, stability of vulnerable plaques in particular, compared to other examination methods. However, the high costs of MRA limit a large-scale investigation for carotid atherosclerotic plaques, therefore must be chosen based on a patient's specific clinical symptoms.

REFERENCES

1. Zhang XN, Wu SZ, Zhang SK. Advances in the research of high-resolution magnetic resonance imaging used for treating carotid atherosclerotic plaques in ischemic stroke patients. Chinese J of Contemporary Neurology and Neurosurgery 2014; 14(1):56-59.
2. Li ML. Color Doppler Flow Imaging (CDFI) in the application of the carotid atherosclerotic plaques of cerebral infarction. J of Minimally Invasive Medicine 2014; 9(5):628-30.
3. Qian JL, Xuan LM, Zhou WH. Color Doppler Flow Imaging (CDFI) in the observation of characteristics of carotid atherosclerotic plaque in patients with

cerebral infarction. Chinese J of Ultrasound Diagnosis 2006; 7(1):41-43.
4. Li SF, Liang K. Observation of curative effects of trigeminy therapy with probucol, antiplatelet agents and statins on atherosclerotic plaque of the carotid in cerebral infarction patients. J of Clinical Neurology 2011; 24(2):134-36.
5. Caplan LR. Intracranial branch atheromatous disease: a neglected, understudied, and underused concept. Neurology 1989; 39(9):1246-1250.
6. Kwan MWM, Mak W, Cheung RTF, et al. Ischemic stroke related to intracranial branch atheromatous disease and comparison with large and small artery diseases. Journal of the Neurological Sciences 2011; 303(1):80-84.
7. Miao F, Shen YL. Imaging studies of ischemic stroke. Chinese Journal of Contemporary Neurology and Neurosurgery 2011; (11):138-42.
8. Liu D, Wang Q, Cai J, Cai Y, Wang Y, Han X. Quantitative measurement of carotid atherosclerotic plaque by high-resolution three-dimensional black-blood magnetic resonance imaging. Journal of Southern Medical University 2013; (3):365-69.
9. Millon A, Mathevet JL, Boussel L, Faries PL, Fayad ZA, DouekPC, Feugier P. High□resolution magnetic resonance imaging of carotid atherosclerosis identifies vulnerable carotid plaques. J Vasc Surg 2013; (57):1046-1051.
10. Ji T. Ultrasound and magnetic resonance imaging analysis of carotid atherosclerostic plaque. Contemporary Medicine 2011; 17(28):42-43.
11. Swartz RH, Bhuta SS, Farb RI, et al. Intracranial arterial wall imaging using high resolution 3-Tesla contrast-enhanced MRI. Neurology 2009; 72(7):627-634.

LETTER TO THE EDITOR

A CASE OF MULTIPLE BILATERAL TESTICULAR CAPSULE MAST CELL TUMOURS IN A DOG

I.L. OIKONOMIDIS[1], T.K. TSOULOUFI[1], G.D. BRELLOU[2], N. SOUBASIS[3], C. VERVERIDIS[3], I. VLEMMAS[2] and M. KRITSEPI-KONSTANTINOU[1]

[1]Diagnostic Laboratory, School of Veterinary Medicine, Faculty of Health Sciences, Aristotle University of Thessaloniki, Greece; [2]Laboratory of Pathology, School of Veterinary Medicine, Faculty of Health Sciences, Aristotle University of Thessaloniki, Greece; [3]Companion Animal Clinic, School of Veterinary Medicine, Faculty of Health Sciences, Aristotle University of Thessaloniki, Greece

Received October 11, 2014 – Accepted March 20, 2015

A 5-year-old intact male German Shepherd dog was referred with a diagnosis of leishmaniasis. Several testicular masses were palpated during the physical examination, while the diagnostic screening yielded no remarkable findings. Fine needle aspiration cytology of the masses revealed the presence of intermediately differentiated mast cell tumours. Scrotal ablation and orchiectomy were performed as a definitive treatment option. The pathological examination of the surgical specimens confirmed the diagnosis of grade II mast cell tumours and showed that they were all confined to the testicular capsule. At 7 months post-admission, the dog exhibited neither postsurgical complications nor metastatic foci and was, therefore, given a favourable prognosis. Despite their exceptionally rare occurrence, mast cell tumours should be considered for the differential diagnosis of testicular tumours.

Mast cell tumours or mastocytomas are the most commonly encountered cutaneous tumours in dogs (1). The latter are usually affected at a mean age of 8-9 years, while certain breeds, such as boxers, seem to be predisposed to mast cell tumour development. Mast cell tumours are characterised by a variable appearance, ranging from solitary (most often) to multifocal (1). In about one half of the cases, mast cell tumours arise on the trunk (2, 3). Apart from skin, mast cell tumours may also be encountered in gastrointestinal system, liver, spleen or elsewhere (4).

Primary sites for mast cell tumour development involve the dermis and/or subcutis and occasionally, internal viscera (1). Mast cell tumours constitute the most commonly reported scrotal tumours in dogs (5). However, according to the literature under study, cases of intra-scrotal mast cell tumours, with or without associated cutaneous involvement, have not been previously described in this species. The present case concerns a 5-year-old dog, which had been diagnosed with multiple bilateral mast cell tumours located at the testicular capsule.

Case description

A 5-year-old intact male German Shepherd dog was presented for a routine follow-up appointment after a past diagnosis of leishmaniasis. The dog resided

Key words: epididymis, mastocytoma, neoplasm, scrotum, testicle

Mailing address: Dr Ioannis L. Oikonomidis,
Diagnostic Laboratory, Department of Clinical Studies,
School of Veterinary Medicine,
Faculty of Health Sciences,
Aristotle University of Thessaloniki,
Stavrou Voutyra 11, 54627, Thessaloniki, Greece
e-mail address: economidis.john@gmail.com

0393-974X (2015)

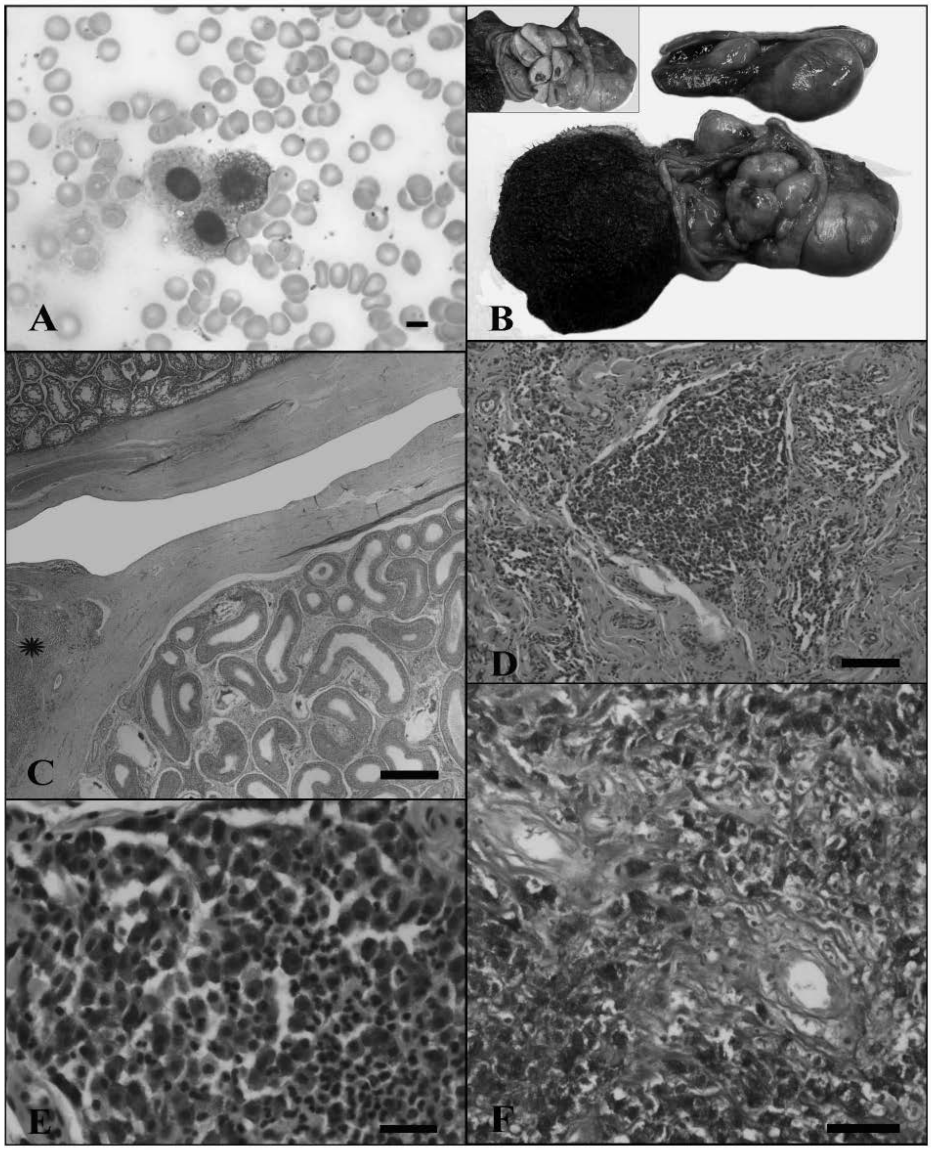

Fig. 1. ***A)*** *Mast cells with moderate amount of cytoplasmic granules in a haemorrhagic background, (Giemsa, x100, bar = 6 μm).* ***B)*** *Grey-whitish nodules are prominent in the capsule of both testicles. Note the firm and homogenous cut surface of the masses (inset).* ***C)*** *Panoramic overview of the tissue reveals that the neoplasm (asterisk) is strictly localised in the capsular layers of the testicle. Seminiferous tubules (upper left) and epididymis (lower right) appear intact, (Hematoxylin and Eosin, x4, bar = 500 μm).* ***D)*** *Numerous neoplastic mast cells admixed with eosinophils are aggregated in the centre. Smaller foci of mast cell accumulations are shown in the dense fibrous surrounding stroma, (Hematoxylin and Eosin, x20, bar =50 μm).* ***E)*** *Higher magnification from the previous figure. Moderately pleomorphic neoplastic mast cells showing granular cytoplasm, intermingled with eosinophils with lobulated nucleus (Hematoxylin and Eosin, x40, bar =25μm).* ***F)*** *Multiple neoplastic mast cells containing varying amounts of the characteristic granules (Toluidine blue staining, x20, bar =50 μm).*

in northern Greece, had an outdoor lifestyle and was currently on vaccinations and antiparasitic treatment. On physical examination, lymphadenomegaly of right prescapular and popliteal lymph nodes, as well as splenomegaly were reported. Moreover, the presence of multiple, firm, cold, non-painful, intra-scrotal masses of variable size (approximately 1x1 to 3x3 cm) was disclosed during the testicular palpation.

The results of complete blood count (ADVIA 120, Siemens Healthcare Diagnostics, USA) and fasting serum biochemical profile (Flexor E, Vital Scientific N.V., The Netherlands) were within the laboratory reference intervals. Indirect fluorescent antibody titre for anti-leishmanial antibodies was 1/200 (cut-off titre: 1/100). Thoracic radiographs were unremarkable, while ultrasonography of the abdomen and scrotal area revealed hepatomegaly, splenomegaly and multiple masses on the testicle and epididymis bilaterally, without abnormalities in the regional lymph nodes. Ultrasound-guided fine needle aspiration (FNA) of the spleen and liver were performed, while the enlarged lymph nodes and the intra-scrotal masses were also aspirated. The samples were submitted for cytological evaluation.

All specimens were stained with Giemsa. Cytological examination of spleen and liver samples was unremarkable, whereas in terms of lymph node status, a diagnosis of reactive lymphadenopathy was made. Samples obtained from the intra-scrotal masses, were of small to moderate cellularity and contained well-preserved nucleated cells and many red blood cells. The main cell population was comprised of mast cells with a moderate amount of cytoplasm, usually containing a moderate number of metachromatic granules of variable size. The nucleus of the aforementioned cells was round to oval, usually centrically located and was rarely masked by cytoplasmic granules (Fig. 1A). Numerous eosinophils were observed, either as single or in small groups. A scant population of normal epithelial cells arranged in clusters, with a moderate amount of lightly basophilic cytoplasm and a mainly round nucleus, which was devoid of prominent nucleoli, was also reported. The cytological appearance of the masses was consistent with a mast cell tumour diagnosis.

The removal of both testicles and scrotum was subsequently suggested. A bilateral radical orchiectomy with scrotal ablation was performed, which was followed by post-surgical administration of analgesics. No adjuvant therapy was suggested, due to the pending histopathological report.

The operative specimens were submitted for histopathological evaluation. Macroscopically, multiple, ovoid to round, solid, well circumscribed nodules of variable size (0.5 to 3 cm in diametre) were detected. All nodules appeared to be attached to both testicles, occupying the vaginal cavity (Fig. 1B). The cut surface of each nodule displayed a grey-white homogenous appearance (Fig. 1B inset). Histopathological examination of sections stained with hematoxylin and eosin revealed that the nodules were located in the outer part of the *tunica albuginea* of the testicle and in the connective tissue surrounding the ductus epididymis and the ductuli efferents, without penetrating the testicular parenchyma though (Fig. 1C). The masses consisted of numerous, sizable, round to polygonal cells, with usually abundant basophilic cytoplasmic granules and round to ovoid nucleus. The cells showed mild to moderate anisokaryosis and varying quantities of granules, while mitoses were less than 1 per high power field. Among the neoplastic cells and at the periphery of the nodules, multiple eosinophils were detected (Fig. 1, D, E). Collagenolysis and haemorrhages were also reported. Histochemical staining toluidine blue was carried out on serial sections to identify the purple cytoplasmic granules of mast cells (Fig. 1F). Histopathology verified the diagnosis of multiple mast cell tumours, and the neoplasms were classified as grade II (4).

The full clinical, haematological and biochemical profile of the patient was re-evaluated 7 months post-admission, yielding only a mild eosinophilia (1,400/μl, reference intervals: 0-600/μl). The latter was confirmed by a differential white blood cell count performed manually on a Giemsa-stained blood smear. Giemsa-stained buffy coat smears revealed no abnormalities. An aspiration of prescapular and popliteal lymph nodes was attempted without any satisfactory results, as lymph nodes were not palpable during physical examination due to their normal size and patient's obesity. Thoracic radiographs and ultrasonography of the abdomen were unremarkable. No post-surgical complications were referred.

DISCUSSION

Mast cell tumours located at the inguinal area have been previously described on the cutis of the scrotum and prepuce in dogs (6). To the authors' knowledge, this case constitutes the only documented report of intra-scrotal mast cell tumours without scrotal involvement, whether bi- or uni-lateral, single or

multiple in dog. No other species, except for a horse, have been reported to have developed a mast cell tumour with a similar anatomical location (7).

The dog was initially presented for a scheduled leishmaniasis follow-up visit, during which the presence of intra-scrotal masses was an incidental finding. On physical examination, the scrotum bilaterally had no remarkable findings, while multiple intra-scrotal masses were palpated, delineating a diagnosis of a primary testicular tumour. The initial differential diagnosis included the interstitial cell tumour, Sertoli cell tumour and seminoma.

Scrotal ultrasonography was thereafter performed, as it is acclaimed as a highly sensitive method for testicular neoplasia detection, which revealed the presence of multiple masses (8). FNA cytology of the masses disclosed the presence of mast cell tumours of intermediate differentiation. In terms of mast cell tumour diagnosis, FNA cytology attains high sensitivity and specificity rates and is, therefore, considered conclusive in the majority of the cases (1). In the present case, histopathological examination was additionally performed, which confirmed the cytological diagnosis and suggested the grade of tumour malignancy. However, most essentially, histopathology disclosed the unique anatomical location of the tumours at the testicular capsule and indicated no associated cutaneous involvement.

On admission, peripheral lymphadenomegaly and hepatosplenomegaly were also observed. A diagnosis of reactive lymphadenopathy was established based on FNA cytology, while, regarding the enlarged spleen and liver, ultrasound-guided FNA cytology revealed no abnormalities. Both lymphadenopathy and hepatosplenomegaly were attributed to leishmaniasis, as they constitute well-described entities of the disease (9).

At 7 months post-admission, the main investigation was targeted towards the evaluation of the regional lymph nodes, liver and spleen, as they are regarded as common sites for mast cell tumour metastasis (10). FNA yielded no remarkable findings. In fact, aspiration cytology of regional lymph nodes has been considered as a method of high sensitivity and specificity (100% and 96% respectively) for the detection of solid tumour metastasis in dogs and cats (11). Additionally, the physical and clinicopathological examination, as well as the thoracic radiographs were unremarkable. Based on the absence of local recurrence, systemic signs and metastatic disease and considering the previously reported favourable outcome of dogs with grade II cutaneous or subcutaneous mast cell tumours treated exclusively with surgical excision, the prognosis for the patient remained good (10, 12, 13).

This is the first fully described report of a dog affected with mast cell tumours, which were all attached to the testicle and epididymis bilaterally, without any cutaneous penetration or penetration of testicular lobules and epididymis. Although extremely rare, mast cell tumours should be considered also for the differential diagnosis of testicular neoplasms.

REFERENCES

1. Thamm DH, Vail DM. Mast cell tumors. In Withrow and Macewen's Small Animal Clinical Oncology. Withrow SJ, Vail DM, ed. 4th ed. Saunders Elsevier, St. Louis, 2007; p. 402-424.
2. Bostock DE. Neoplasms of the skin and subcutaneous tissues in dogs and cats. Brit Vet J 1986; 142:1-19.
3. Rothwell TLW, Howlett CR, Middleton DJ, Griffiths DA, Duff BC. Skin neoplasms of dogs in Sydney. Aust Vet J 1987; 64:161-64.
4. Goldschmidt MH, Hendrick MJ. Tumors of the skin and soft tissues. In: Tumors in Domestic Animals. Meuten D, ed. 4th ed. Iowa State Press, Ames, 2002; p. 45-117.
5. Cerundolo R, Maiolino P. Cutaneous lesions of the canine scrotum. Vet Dermatol 2002; 13:63-76.
6. Raskin RE. Skin and subcutaneous tissues. In Canine and Feline Cytology: A color atlas and interpretation guide. Raskin RE, Meyer DJ, ed. 2nd ed. Saunders Elsevier, St. Louis, 2010; p. 26-76.
7. Brown JA, O'Brien MA, Hodder DJ, Peterson T, Claes A, Liu IKM, Ball BA. Unilateral testicular mastocytoma in a Peruvian Paso stallion. Equine Vet Educ 2008; 20(4):172-75.
8. Pugh CR, Konde LJ. Sonographic evaluation of testicular and scrotal abnormalities: A review of 26 case histories. Vet Radiol Ultrasoun 1991; 32(5):243-50.

9. Koutinas AF, Polizopoulou ZS, Saridomichelakis MN, Argyriadis D, Fytiannou A, Plevraki KG. Clinical considerations on canine visceral leishmaniasis in Greece: a retrospective study of 158 cases (1989-1996). J Am Anim Hosp Assoc 1999; 35:376-83.
10. Welle MM, Rohrer Bley C, Howard J, Rufenacht S. Canine mast cell tumours: a review of the pathogenesis, clinical features, pathology and treatment. Vet Dermatol 2008; 19(6):321-39.
11. Langenbach A, McManus PM, Hendrick MJ, Shofer FS, Sorenmo KU. Sensitivity and specificity of methods of assessing the regional lymph nodes for evidence of metastasis in dogs and cats with solid tumors. J Am Vet Med Assoc 2001; 218(19):1424-28.
12. Seguin B, Leibman NF, Bregazzi VS. Clinical outcome of dogs with grade-II mast cell tumors treated with surgery alone: 55 cases (1996-1999). J Am Vet Med Assoc 2001; 218(7):1120-23.
13. Thompson JJ, Pearl DL, Yager JA, Best SJ, Coomber BL, Foster RA. Canine subcutaneous mast cell tumor: characterization and prognostic indices. Vet Pathol 2011; 48(1):156-68.

LETTER TO THE EDITOR

EXPRESSION MECHANISM AND CLINICAL SIGNIFICANCE OF NOB1 IN GASTRIC CANCER TISSUE AND ADJACENT NORMAL TISSUE

W-P. ZHOU[1], X. LIU[2], Y. YANG[3] and Y-F. LIU[4]

[1]Oncology Department, the First Affiliated Hospital of Zhengzhou University, Zhengzhou, Henan, China; [2]Blood Bank Center, the First Affiliated Hospital of Zhengzhou University, Zhengzhou, Henan, China; [3]Geriatrics Department, the First Affiliated Hospital of Zhengzhou University, Zhengzhou, Henan, China; [4]Biological Treatment Center, the First Affiliated Hospital of Zhengzhou University, Zhengzhou, Henan, China

Received December 22, 2014 – Accepted April 9, 2015

This paper studies the effect and relationship of NOB1 in the development of gastric cancer, based on an analysis of NOB1expression in gastric cancer tissue and adjacent tissue. Thirty gastric cancer tissue samples taken during surgery with complete pathological data and their related adjacent normal tissue were examined in this study. NOB1 protein expression in gastric cancer tissue and adjacent normal tissue was detected by immunohistochemistry (IHC). Real-time PCR was used to detect NOB1 mRNA expression, which provided a basis on which to explore the clinical pathological characteristics for patients with gastric cancer. Results show that NOB1 protein in gastric cancer tissue and adjacent normal tissue were diffusely expressed both in the cytoplasm and nucleus. The positive expression rate in gastric cancer tissue was 73%, higher than that in adjacent normal tissue (47%). Both the reference NAPDH and NOB1 amplification are reflected in the amplification curve in standard S-shape and the unimodal solubility curve which was not altered by non-specific amplification and primer dimer. NOB1 mRNA relative expression in cancer tissue was 4.899±1.412. NOB1 expression had no direct relationship with the patients' age, gender, tumor differentiation or infiltration degree, lymphatic metastasis, distant metastasis nor pTNM periodization, but was directly related to the size of the tumor. All the findings in this paper suggest that NOB1 can be one of the focuses for diagnosing and treating gastric cancer and that its protein expression is likely to increase with the growth of tumor, thus playing a great role in the incidence and development of gastric cancer.

Gastric cancer is a common malignant tumor in the digestive tract. There are some epidemiological studies which show that it ranks fourth in the most common tumors after lung cancer, ovarian cancer, and colorectal cancer. It has a higher incidence in developing countries, especially in the southeast countries such as China (1-2). The incidence of gastric cancer is a complicated pathological process with many factors and steps. In addition to the environment, most attention is presently paid to its pathogenesis, including gene expression and polymorphism (3). The conclusion of the relationship between NOB1

Keywords: NOB1, gastric cancer tissue, adjacent normal tissue, PCR

Mailing address: Dr Xin Liu
Blood Bank Center, the First Affiliated Hospital of Zhengzhou University,
Zhengzhou, Henan, 450052, China
e-mail: lx@ibhsedu.com

0393-974X (2015)

and tumor reached by Dong B., et al. (4) suggests the close relationship between NOB1 and gastric cancer and other tumors. He XW et al. (5) studied the effect of NOB1 on the proliferation and apoptosis of RKO cells in colorectal cancer. Then they observed an obvious reduction of NOB1 mRNA and its protein expression. There were also decreases in the number of clone formation and in the dimension of tumors, but an increase in the number of cells. Their study showed that NOB1 plays an important role in the incidence and proliferation of malignant tumors. Zhong Junxin, et al. (1) also observed the increasing expression of NOB1 in gastric cancer with an inspection of that expression, and they considered NOB1 very important in the incidence of gastric cancer. Based on the above results, this paper examins NOB1 mRNA expression in gastric cancer tissue and adjacent normal tissue by IHC and Real-time PCR, so as to explore the function mechanism and relations of NOB1 in the development of gastric cancer.

MATERIALS AND METHODS

Thirty gastric cancer patients with complete pathological data who were treated with surgical resection from April 2013 to July 2013 are included in this paper. The gastric cancer tissue samples and relative adjacent normal tissue samples (distance over 5.0cm) were taken and then kept the lab of Gastroenterology department at -80°C. The latter was set as control group. There were 22 males and 8 females with a mean age of 56.03. The AJCC method was taken for the pathological grading from I to III of all cases. All patients were treated with radiotherapy, chemotherapy or immunization therapy before surgery.

Main reagents

cDNA reverse transcription kit, Real-time PCR reagent and Trizol reagent (from TAKARA company);DEPC (from Sigma company, USA), RNasin (from Promega company, USA); NOB1 antibody with working concentration of 1:25 (from PROTEINTECH company); second antibody DAB chromogenic substrate system (from Genentech).

Real-time PCR

The upstream primer for NOB1 is 5'-TCTTCCTCATCCCTCTCAAC-3', and the downstream primer is 5'-ATCCCATCCACTCTCCTCAT-3'. GAPDH is the reference, the upstream primer is 5'-CCCTCTCACCCACCCAACAT-3' and the downstream primer, 5'-CCTATTCCCCTAACCCCTCC-3'. The total DNA was extracted according to the Trizol method. A reverse transcription reaction system was made up in accordance with the instructions on TAKARA and the first strand in cDNA was synthesized. The concentration of Mg2+ and primers were optimized. The reaction system for amplifying by Real-time PCR was 25 μL and 40 cycles were run according to the following conditions: 2 min at 95°C, 30s at 95°C, 30s at 60°C and 30s at 72°C. The changes in NOB1 mRNA expression by Real-time PCR were examined. When the reaction was over, the original value of Ct was read, and then the relative expression of NOB1 by $2^{-\Delta\Delta Ct}$ was analyzed.

Immunohistochemistry

Tissues were embedded in paraffin, and paraffin tissue slicing and HE dyeing were performed according to instructions on the SP immunohistochemistry staining kit. The given positive section was taken as a positive control, and PBS was taken in place of the primary antibody as negative control. Data analysis: the semi-quantitative immunity grading method was adopted and the product between the two grades from the straining intensity and ratio of positive cells was considered as standard. Staining intensity of positive cells: the staining results with double-blind method were evaluated. The staining result of immunohistochemistry showed no color, or light yellow, tan or brown granules in the endochylema or nuclei. The four types of staining intensity were marked with grades 0, 1, 2, 3 respectively. Staining ratio of positive cells: every section of the specimens was selected with 5 typical visions under the high-power microscope (400x). Two hundred cells within each vision were randomly counted and the total amount was no fewer than 1,000. The positive cells in 26%~50% were marked as grade 2, 51%~75% as grade 3, 76%~100% as grade 4, and below or equal to 25% as grade 1. The product was divided into four grades: grade 0~2 were -, grades 3~5 were --, grades 6~8 were---, and grades >8 were+. Cells whose grades were between 3 and 5 had positive expression.

Statistical analysis

The experiment result was statistically analyzed by SPSS 17.0 software. The comparison in positive rates between gastric cancer tissue and adjacent normal tissue was tested by χ^2. $P<0.05$ showing that the difference was of statistical significance.

RESULTS

Expression of NOB1 protein in the gastric cancer tissue and adjacent normal tissue

When staining NOB1 protein in the gastric cancer tissues and adjacent normal tissues with HE, it was

Table I. *Positive rates in the gastric cancer tissue and adjacent normal tissue.*

Performance	-	+	++	+++	Positive rate
Gastric cancer tissue	8	7	8	7	73%
Adjacent normal tissue	16	8	3	3	47%

Table II. *Relative expression of NOB1 mRNA in 30 specimens.*

Relative expression			Relative expression			Relative expression		
Serial NO.	Gastric cancer tissue	Adjacent normal tissue	Serial NO.	Gastric cancer tissue	Adjacent normal tissue	Serial NO.	Gastric cancer tissue	Adjacent normal tissue
1	4.01866	1	11	4.18816	1	21	5.18354	1
2	3.42076	1	12	4.19296	1	22	5.19335	1
3	5.79738	1	13	3.60481	1	23	7.55833	1
4	6.80478	1	14	4.10296	1	24	4.42435	1
5	4.37841	1	15	3.33994	1	25	4.46009	1
6	3.55095	1	16	4.25408	1	26	7.35111	1
7	4.92873	1	17	6.55864	1	27	6.38600	1
8	7.27997	1	18	3.44855	1	28	3.57170	1
9	7.82932	1	19	3.77022	1	29	4.31691	1
10	3.01391	1	20	5.32609	1	30	4.70928	1

found that there were fewer adenoid structures and a higher ratio between nucleus and cytoplasm. Some staining results are shown in Fig. 1.

NOB1 protein was diffused both in gastric cancer tissue and in adjacent normal tissue. There was no significant difference in the staining intensity between the cytoplasm and nucleus (Fig. 2).

In the immunochemistry experiment, the positive expression rate was 73%, obviously higher than that in adjacent normal tissue samples (χ^2= 4.444, P<0.05) (Table I).

Expression of NOB1 MrNA in gastric cancer tissue and adjacent normal tissue.

During the process of applying the Real-time PCR, it continued to produce the amplification curve. The solubility curve continued to be produced after the PCR was over. The amplification of reference NAPDH and NOB1 were seen in the standard amplification and solubility curve. The amplification curve showed a typical S-shape. The solubility curve showed a typical unimodal with a uniform solution temperature. This unimodal solubility curve illustrated that the amplification product was quite specific. The experiment results were apart from the interruption of non-specific amplification and primer dimer, and were used for data analysis (Fig. 3 a, b, c, d).

The results from the formula $2^{-\Delta\Delta Ct}$ are the multiple of target genes from samples in the experiment group regulated by the reference gene expression when compared with that in the control group. The relative NOB1 mRNA expression in gastric cancer tissue and adjacent normal tissue is shown in Table II.

The results showed that the expression of NOB1 mRNA in gastric cancer tissue was 4.899±1.412 (Mean±SD) based on $2^{-\Delta\Delta Ct}$, higher than the relative expression in the adjacent normal tissue (Fig. 4).

Table III. *Relationship between the expression of NOB1 and the clinical pathological characteristics of gastric cancer (Mean±SD).*

Clinical pathological characteristics	Cases	Expression of NOB1		Value of P
		Positive	Negative	
Age				
≥60	16	14	2	0.101
□60	14	8	6	
Gender				
Male	22	15	7	0.391
Female	8	7	1	
Diameter of tumor(cm)				
≥5	15	14	1	0.035
□5	15	8	7	
Differentiation Degree				
High and moderate	7	5	2	1.000
Low and no	23	17	6	
Infiltration degree				
T1+T2	3	1	2	0.166
T3+T4	27	21	6	
Lymphatic metastasis				
N0+N1	16	11	5	0.689
N2+N3	14	11	3	
Distant metastasis				
With	4	4	0	0.550
Without	26	18	8	
pTNM periodization				
Period I and II	14	11	3	0.689
Period III and IV	16	11	5	

Expression of NOB1 and analysis of clinical pathological characteristics for patients with gastric cancer

The expression of NOB1 had no significant relationship to the patients' age, gender, cancer differentiation, infiltration degree, lymphatic metastasis, distant metastasis or pTNM periodization (P□0.05 in all cases, difference was of no statistical significance), but it was directly related to the size of the tumor (P□0.05, difference was of statistical significance) (Table III).

DISCUSSION

Gastric cancer is a common malignant tumor in the digestive tract. The genetic factor is one of the main causes of gastric cancer. Diet, benign lesions of the stomach and bacterial infection are also likely to induce gastric cancer. Without a clear clinical record in the early stage of gastric cancer, it is hard to make an accurate diagnosis. At present, the diagnosis for gastric cancer, apart from the observation of symptoms and signs, is dependent on auxiliary

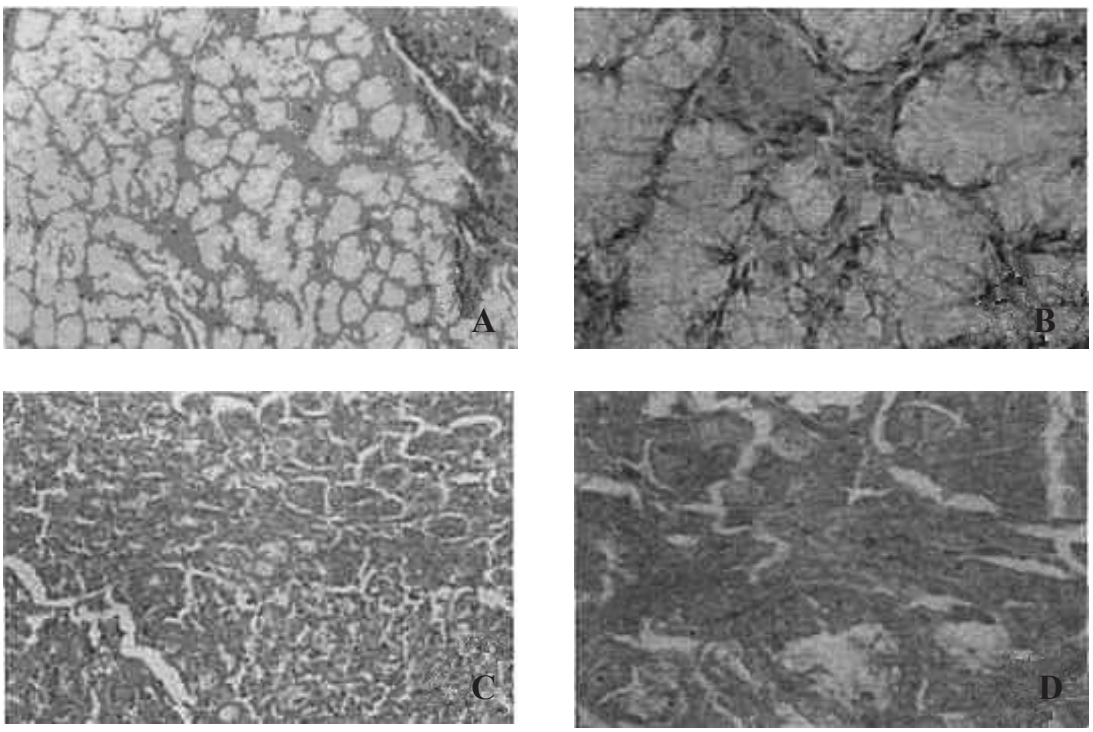

Fig. 1. *Staining results with HE of NOB1 protein.* ***a/c*** *gastric cancer tissue (100x);* ***b/d*** *adjacent normal tissue (400x).*

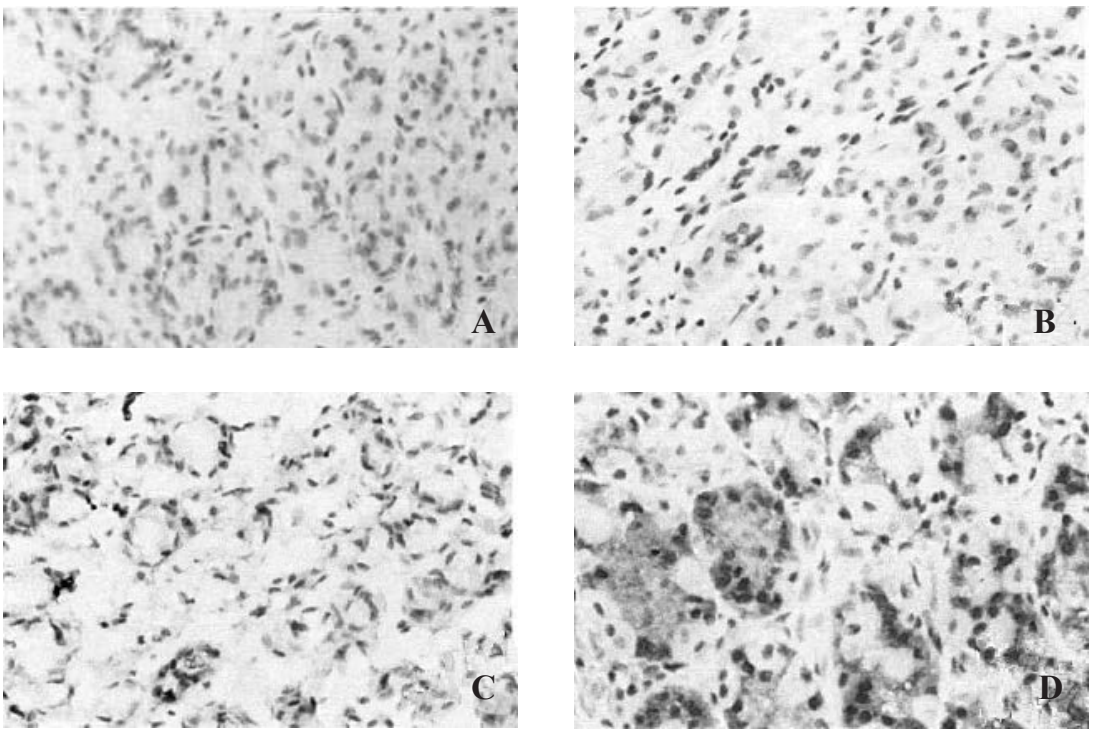

Fig. 2. *Immunochemistry staining results of NOB1 protein (400x).* ***a****) (-), adjacent normal tissue;* ***b****) (+), gastric cancer tissue;* ***c****) (++), gastric cancer tissue;* ***d****) (+++), gastric cancer tissue.*

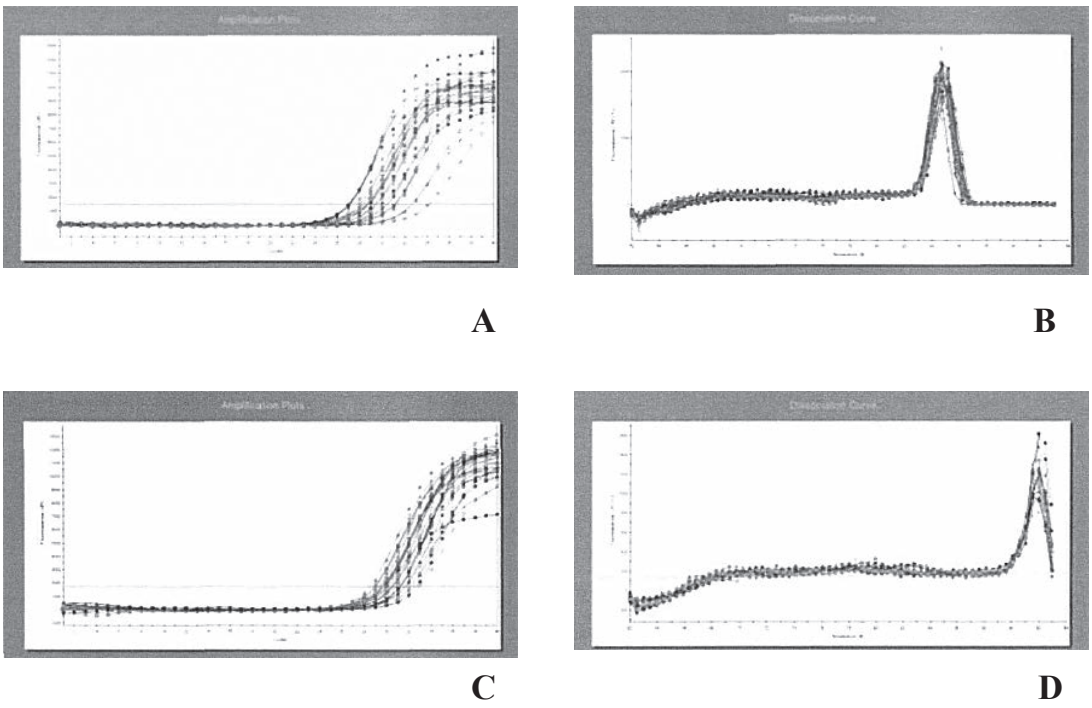

Fig. 3. ***a)*** *Amplification curve of reference GAPDH.* ***b)*** *Solubility curve of reference GAPDH.* ***c)*** *Amplification curve of NOB1.* ***d)*** *Solubility curve of NOB1.*

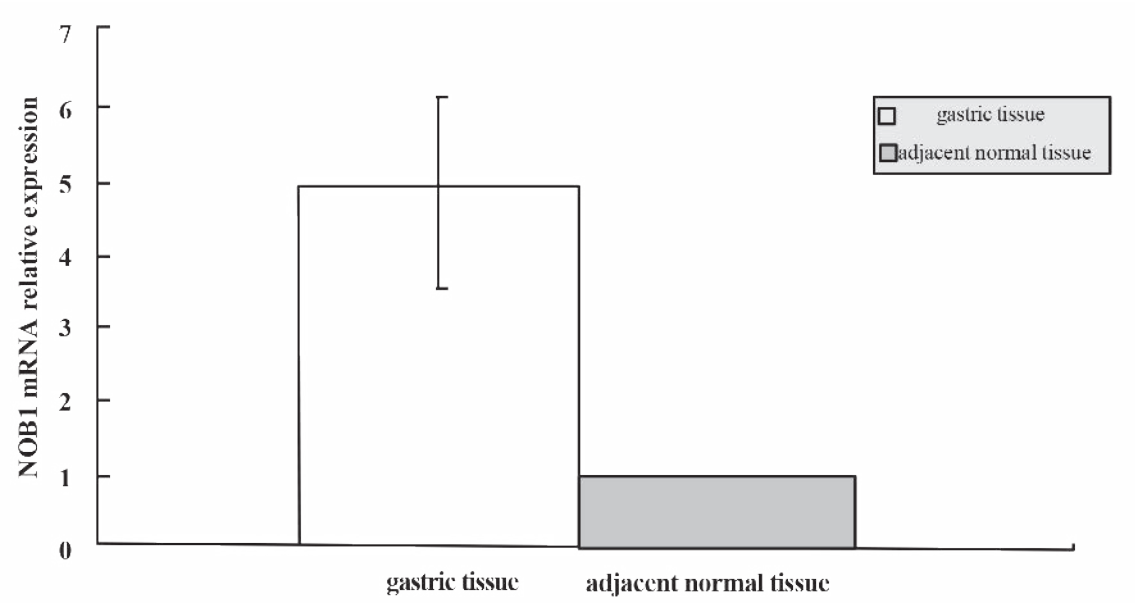

Fig. 4. *Comparison of expression of NOB1 mRNA between gastric tissue and adjacent normal tissue.*

examination or laboratory examination (6). There are some tumor markers in the clinical examination of gastric cancer, including CEA, CA19-9 and CA72-4. In Li Yan's study on the tumor markers and clinical significance of gastric cancer, he proved that a combined examination could improve the detection rate. He also revealed that a combined examination was likely to reduce the specificity while improving the sensibility, so that a marker with strong specificity was a necessary choice (7). Nowadays, as to gastric cancer treatment, surgery still predominates with a quite good response. However, because of the difficulty of detecting the tumor in the early stage, most patients arrive at a progressive stage and the gastrectomy fails to achieve a good response. Therefore, it is safe to say that the cancer survival rate can effectively be improved by improving the diagnosis rate of early gastric cancer. The gene diagnosis and treatment is the present focus of medical research. Moreover, the present research on gastric cancer aims at making an earlier diagnosis by identifying the gene which plays a decisive role in gastric cancer.

NOB1 is a multi-functional protein, whose change in expression will directly affect the biosynthesis of ribosome and proteasome. NOB1 is believed to play an important role in treating tumors since change in ribosome and proteasome is related to the incidence, development, metastasis and suppression of tumor (8). Its effects on the incidence and development of tumor have attracted the attention of a great number of scholars. Studiesby Lin, et al. (9) showed that the application of RNA interruption technique could effectively silence NOB1 in HEY and SKOV3 ovarian cells, reduce the proliferation of ovarian cancer cells, and arrest cell cycle in G1 phase. Some research groups have also studied the performance of NOB1 in colorectal cancer, finding NOB1 expression in colorectal cancer significantly higher than in normal colorectal tissue. In this case, NOB1 may be the proto-oncogene which leads to a malignant hyperplasia, therefore, it has become the new tumor marker and new target gene (1, 8). Moreover, it may be closely related to the high selectivity within eukaryotes and the ubiquitin-proteasome pathway (UPP) with high efficacy. Gastric cancer is induced by interrupting the process of protein degradation by UPP (6). The 26S proteasome in UPP recognizes and degrades the substrate protein after ubiquitination. The 26S proteasome is made up of one 20S core protease and two 19S regulatory particles. NOB1 protein serves as the molecular companion in the formation process of 19S regulatory particles. In this formation process, the precursor compound of 20S core protease is first produced by the combination of semi-proteasome (α7β7) with the molecular companion Umplp subunit, and then this precursor compound goes from cytoplasm to nucleus. Meanwhile, another precursor compound of 19S proteasome is produced by the mutual reaction between NOB1 protein, as the molecular companion, and the subunit Nin1p/Rpn12 of RP together with 19S regulatory particles. Next, these two compounds are combined, and the molecular companion Umplp and NOB1 protein are separated from these two precursors and degraded. When cells grow into the exponential phase, NOB1 takes part in the transcription process of new proteasome. UPP is able to degrade cancer genes, inhibit production of cancer genes, metaprotein and allosteric protein, and preserve the normal functions of cells. If there is a lack of NOB1, it is likely to induce the tumor with abnormal functions of UPP.

In this study, the difference between NOB1 mRNA relative expression in gastric cancer tissue and that in adjacent normal tissue is of statistical significance. The positive NOB1 expression rate in gastric cancer tissue (73%) is statistically higher than that in adjacent normal tissue (43%). It suggests that NOB1 is possibly one of the focuses for gene diagnosis and treatment for gastric cancer. Moreover, the rising NOB1 expression in gastric cancer shows that NOB1 may play an important role in the incidence and development of gastric cancer.

In conclusion, the results obtained by these two methods revealed that NOB1 mRNA and protein expression in gastric cancer tissue was higher than that in adjacent normal tissue. Therefore, NOB1 enjoys a great potential as one of the focuses of gene diagnosis and treatment for gastric cancer. Besides, NOB1 protein expression is not related to the age, gender, tumor's differentiation and infiltration degree, lymphatic metastasis, distant metastasis and pTNM periodization, but related to the size of tumor. This signifies that NOB1 protein expression is likely to increase with the growth of the tumor. All

findings as stated above suggest that NOB1 plays an important role in the incidence and development of gastric cancer with its increasing expression.

REFERENCES

1. Zhong JX, Duan XF, Li JJ, Wu CT. Expression of NOB1 and its significance in gastric cancer. Guangdong Med J 2014; 35(6):870-72.
2. Jacques F, Hai-Rim S, Freddie B, Dacid F, Colin M, Donald MP. Estimates of worldwide burden of cancer in 2008. GLOBOCAN 2008 2010; 127(12):2893-917.
3. Wang JM, Lin SR. Progress in the clinical research of gastric cancer. Chin J Gastroenterol Hepatol 2012; 21(1):3-5.
4. Dong B, Zou SW, Ai KX. NOB1 gene and tumors. Acad J Sec Milit Med Uni 2011; 32(4):432-34.
5. He XW, Tao F, Luo SS, Yu XK. Effect of Lentivirus-mediated NOB1 gene silencing by RNA interference on proliferation and apoptosis of human colon cancer cells. Chin J Gastroint Surg 2012; 15(11):1182-86.
6. Zhong JX. Expression and its significance of NOB1 in the gastric cancer and its adjacent normal tissues. J South Med Uni 2014; http://cdmd.cnki.com.cn/Article/CDMD-90023-1014340028.htm
7. Li Y. Tumor marker for gastric cancer and its clinical significance. Pract J Clin Med 2011; 8(1):11-15.
8. He XW. Development in Studying NOB1. Chin J Clin (e-ed). 2011; 5(8):2360-63.
9. Lin Y, Peng S, Yu H, Teng H, Cui M. RNAi-mediated down regulation of NOB1 suppresses the growth and colony-formation ability of human ovarian cancer cells. Med Oncol 2012; 29(1):311-17.

JOURNAL OF BIOLOGICAL REGULATORS & HOMEOSTATIC AGENTS Vol. 29, no. 2, 431-436 (2015)

LETTER TO THE EDITOR

EXPRESSION AND CLINICAL SIGNIFICANCE OF APOPTOSIS-ASSOCIATED PROTEINS SURVIVIN AND LIVIN IN CONDYLOMA ACUMINATUM

G-W. YIN, J. LI and H-B. ZHANG

Department of Dermatology, The First Affiliated Hospital, Zhengzhou University, Zhengzhou City, Henan Province, China

Received January 20, 2015 – Accepted April 13, 2015

The objective of the present study was to explore the expression and significance of survivin and Livin in lesions of Condyloma acuminatum (CA). Streptavidin-perosidase (SP) immunohistochemistry method was used to measure the expression of survivin, Livin and Ki-67 in 48 cases of CA and 25 cases of normal foreskin tissues. The positive expression rates of survivin, Livin and Ki-67 were 72.91% (35/48), 77.08% (37/48) and 85.42% (41/48) in CA tissues, and 4% (1/25), 4% (5/25) and 60% (15/25) in the control group, respectively. The expression intensity of survivin, Livin and Ki-67 in CA tissues (++ ~ +++) was significantly higher than that in the normal control group (- ~ ++). There were significant differences (P <0.05) both in the positive rates and the expression intensity of survivin, Livin and Ki-67 between the two groups. There was positive correlation between the expression of survivin and Livin in CA group (P < 0.01); the expressions of survivin and Ki-67 were positively correlated with each other (P < 0.01); Livin and Ki-67 expressions were positively correlated with each other (P < 0.01). There were over-expressions and excessive proliferations of survivin and Livin in CA tissues, and apoptosis suppressors survivin and Livin were correlated with CA.

Condyloma acuminatum (CA), one of the sexually transmitted diseases, severely threatens people's life all over the world, especially in the depressed areas. CA can also be induced by indirect contact infection such as underwear, briefs, bath towel, tub, and closestool circle. Mother-to-child transmission is another reason for occurrence of CA.

Research has found that in recent years, tumor has a close relationship with cell apoptosis. CA was infected by human papilloma virus (HPV), and common sexually transmitted diseases (STD). The clinical manifestations of CA are similar to those of papilloma or cauliflower thickening. CA is a benign proliferative disease, and excessive proliferation of body warts can induce giant condyloma acuminatum (GCA), also named Buschke-loewenstein tumour (1). Proteins survivin and Livin were discovered in recent years and became new members of the family of apoptosis protein inhibitors (IAP), and they may inhibit apoptosis through various ways, and participate in the development of tumor (2, 3). Ki-67 antigen is one of the most widely used cell proliferation markers, and it can accurately reflect the activity of cell proliferation. CA hyperplasia is fast, and its relapse is easy.

The present study detected expressions of survivin, Livin and Ki-67 proteins in acute CA tissues to explore the possible role of survivin and Livin in

Key words: survivin, Livin, Ki-67, Condyloma acuminatum

Mailing address:
Dr Guang-wen Yin,
The First Affiliated Hospital of Zhengzhou University,
No.1, East Jianshe Road,
Zhengzhou City, 450052,
Henan Province, China
e-mail: bhushan2015@163.com

0393-974X (2015)

the pathogenesis of CA by using the Streptavidin-perosidase (SP) immunohistochemical method.

MATERIALS AND METHODS

Cases

Forty-eight patients with CA (29 male and 19 female; aged 18 to 62 years median 27.94±9.69 years) consecutively treated in the skin venereal outpatient department of our hospital were enrolled in this study. The patients had not received any drug, laser, freezing, or other treatment previously. Disease duration was 4 weeks (w) ~ 25 w with an average of 9.93±4.12 w. They all exhibited typical clinical manifestations, and were diagnosed with CA by clinical and laboratory criteria. A total of 25 cases of normal prepuce tissues served as the control group.

Reagents

Poly-clonal antibody against survivin was bought from Wuhan Boster Biological Engineering Co.Ltd. The rabbit-anti-Livin, and SP polyclonal antibody (concentrated) general detection kits were provided by Beijing Bioss Biological Co. Ltd. Ki-67 ready-to-use SP detection kits and DAB enzyme substrates were purchased from Fujian MXB Biological Engineering Co. Ltd.

Antibodies against survivin, Livin and Ki-67 were employed in the SP method. According to the directions of the kits, all tissue samples were stained under the same conditions.

Survivin and Livin expressed tan particles of positive cells in the cytoplasm, while Ki-67 positive color tan particles were in nuclei.

According to Birner et al. (4), the comprehensive staining intensities of survivin, Livin and Ki-67 and positive cell percentage in all the cells were analyzed by semi-quantitative processing method according to the semi-quantitative classification scoring system of positive cell percentage and tinting strength grade in tissue sections. Positive cell percentage of 10% or less was designated as 0 point. Positive cell percentage of 10~25% was designated as 1 point. Positive cell percentage of 26~50% was designated as 2 points. Positive cell percentage of 51~75% was designated as 3 points. Positive cell percentage of 76% and more was designated as 4 points.

In the tinting strength analysis, no color was designated as 0 point; light yellow was designated as 1 point; yellow was designated as 2 points; tan color was designated as 3 points.

The combined results of the above two scores were defined as follows: 0 point was designated as negative result (-), and 1~4 points were designated as weak and positive result (+), and 6~8 points were designated as positive result (+ +), and 9~12 points were designated as strong positive result.

Statistical analysis

The SPSS11.0 statistical software was employed for χ^2 test, *t*-test, and Spearman's correlation analysis was used for variance between survivin, livin and Ki-67. A *P* valueless than 0.05 indicated that the difference was statistically significant.

RESULTS

Expression of survivin in CA tissue and normal epithelial tissue

Thirty-five of 48 cases had CA tissues, and the survivin positive expression rate was 72.92% (35/48), and the positive expressing intensity was ++ ~ +++ (Fig. 1A). The positive cells mostly showed focal or flake distributed in the upper and particle

Table I. *Positive rate comparison between survivin, Livin and Ki-67 in CA tissue and normal tissue in control group.*

Classification		Case Quantity	Positive	Negative	Positive Rate	*P*
survivin	CA Group	48	35	13	72.92%	<0.01
	Control Group	25	1	24	4.0%	
Livin	CA Group	48	37	11	77.08%	<0.01
	Control Group	25	5	20	20.00%	
Ki-67	CA Group	48	41	7	85.42%	<0.01
	Control Group	25	15	10	60.00%	

Note: Positive rate comparison between survivin, Livin and Ki-67 in CA tissue and normal tissue in control group, P < 0.05

Table II. *Expression intensity comparison of survivin, Livin and Ki-67 in CA tissue and normal tissue in control group.*

Classification		Case Quantity	Expression Intensity (case quantity)				*P*
			-	+	++	+++	
survivin	CA Group	48	13	8	13	14	<0.01
	Control Group	25	24	1	0	0	
Livin	CA Group	48	11	5	13	22	<0.01
	Control Group	25	20	3	2	0	
Ki-67	CA Group	48	7	18	21	2	<0.01
	Control Group	25	10	11	3	1	

Note: expression intensity comparison of CA tissue and normal control group survivin, Livin, and Ki-67 in normal control group, P < 0.05.

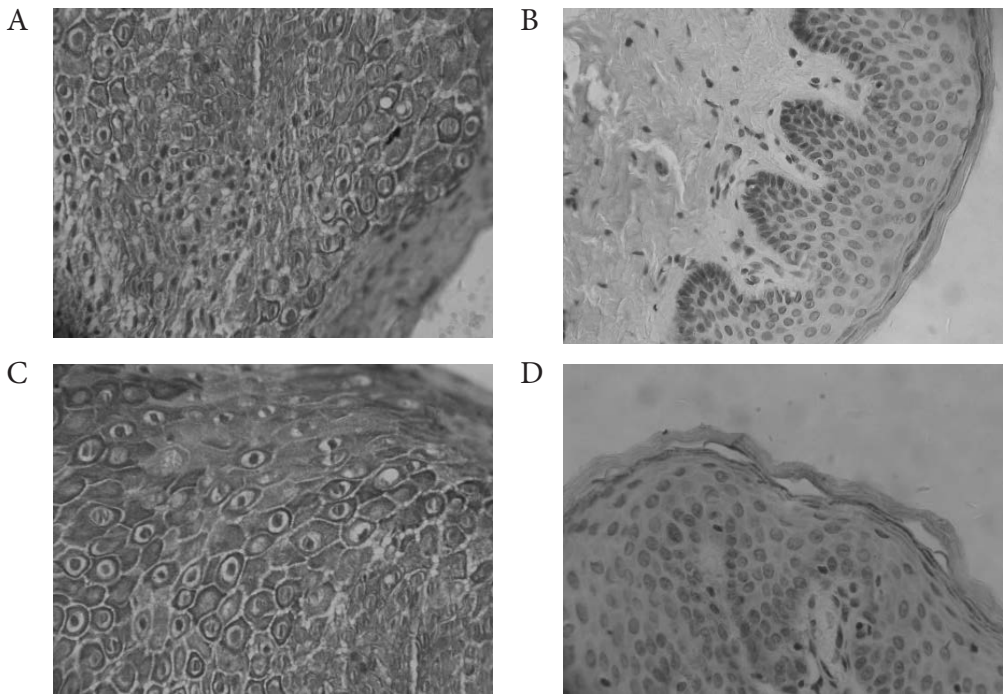

Fig. 1. ***A)*** *Expression of Survivin in CA tissue. CA tissues were collected and subjected to immunohistochemical analysis with antibody targeting Survivia as staining.* ***B)*** *Expression of survivin in normal tissue. Normal tissues were collected and subjected to immunohistochemical analysis with antibody targeting Survivia as staining.* ***C)*** *Expression of Livin in Condyloma acuminatum tissue. Condyloma acuminatum tissues were collected and subjected to immunohistochemical analysis with antibody targeting Livin as staining.* ***D)*** *Livin expression in normal foreskin tissue. Normal tissues were collected and subjected to immunohistochemical analysis with antibody targeting Livin as staining. (DAB staining SP X 400).*

layer of stratum spinosum (Fig. 1A), and lower layer of stratum spinosum and bottom base layer also showed expression of the protein of survivin. Positive cells mostly had large nuclei, which were easy to be seen, and abundant cytoplasms were illustrated (Fig. 1A) (Table I). There was 1 case with survivin expression of 25 cases of normal tissues, and the positive expression rate was 4% (1/25), and the expression intensity was - ~ + (Fig. 1B) (Table II). The difference of the positive rate was statistically

significant (χ^2 = 23.826, P < 0.05), and the positive intensity expression of similarity between the two groups was statistically significant (χ^2 = 24.314, P < 0.05) (Table I, Table II)

Expression of Livin in CA tissue

Thirty-seven of 48 cases had Livin-positive expression in CA tissues, and the positive expression rate was 77.08% (37/48), and the expressing intensity was ++ ~ +++ (Fig. 1C). Positive cells showed focal or diffuse distribution of stratum spinosum, and the expression was more significant in stratum spinosum layers (Fig. 1C) . In the control group, there were 5 cases with Livin positive expression, the positive expression rate was 20% (5/25), and the expression intensity was mostly - ~ ++ (Fig. 1D) (Table I, II). The positive expression rate between the two groups was statistically different (P < 0.05), and the positive expression intensity of similarity between the two groups was statistically significant (P < 0.05) (Table I and Table II).

Ki-67 expression in CA tissues and normal epithelium

Forty-one of 48 cases had ki-67 positive expression, and the positive expression rate was 85.42% (41/48), and the expressing intensity was mostly ++ ~ +++. The main positive cells were stained in the nuclei with tan grains, and the positive cells were throughout base layer and the lower part of stratum spinosum, and upper stratum spinosum and particle layer had Ki-67 expression. The positive expression rate of the normal control group was 60% (15/25), and the intensity of expression intensity was mostly - ~ +, mainly observed in the underlying cells; The differences of positive rates were statistically significant (P < 0.05), and the positive intensity expression between the two groups was statistically significant (P < 0.01) (Table I and Table II).

Correlation analysis of expression of survivin and Livin in CA tissues

Spearman correlation analysis illustrated that the expressions of survivin and Livin in CA tissues of 48 cases were positively correlated with CA (*P* < 0.01). The expressions of survivin and Ki-67 were positively correlated with CA (P < 0.01), and Livin and Ki-67 expressions were positively correlated with CA (P < 0.01).

DISCUSSION

Survivin was discovered to be a new member of the IAP family screened in human genome library by Effector Cell Protease Recepor-1 (EPR-1) cDNA, and studies have shown that survivin was specifically expressed in tumor tissues. In comparison, normal tissues had no expression or lower expression of surviving, and its expression in cancer tissue was corrected with progression of cancer (5, 6). Survivin can inhibit apoptosis, and affect cell proliferation and angiogenesis (7). Its inhibiting effect on cell apoptosis is mainly by the following two pathways: firstly, it can directly interact with caspase-3 and caspase-7, and inhibit caspase activity, and block apoptosis process; secondly, it can indirectly inhibit the activity of caspase-3 and inhibit apoptosis through P21 (8).

The present experiment adopted the immunohistochemical method to research survivin protein expression in CA tissues, and the results showed that survivin protein positive expression rate and expression intensity in CA tissues were significantly higher than those of the normal control group (Fig. 1A, B) (P < 0.05). The expression of survivin protein in CA tissues was increased (Fig. 1A), and its mechanism might be the survivin gene in different signaling pathways of apoptosis. Survivin directly inhibited the terminal effects on caspase-3 and caspase-7, or certain cycle protein kinases such as CDK4 for blocking the signal transduction of apoptosis, inhibiting apoptosis of epithelial cells and promoting excessive proliferation, and promoting the CA excessive proliferation, and participating in the development of CA.

In recent years, Livin was found to be a new member of IAP family (2). The protein was cloned from the human genome cDNA library. Because it was found in human fetal renal cDNA libraries, it was also named as kidney inhibitor of apoptosis protein (KIAP) (9). It was reported that livin was highly expressed in a variety of tumor tissues, and it could inhibit the apoptosis of tumor cells, and promote the role of the abnormal proliferation of tumor cells, and it was involved in the development of tumors. We used the SP immunohistochemical method to detect expression of apoptosis-related proteins in CA tissues. The results demonstrated that the livin

positive expression rates and positive expression intensity in CA tissues were higher than those of the control group (Fig. 1C, D). Livin expression in CA tissues was increased (Fig. 1C), and it might directly inhibit apoptosis by caspase, and then lead to increase of cell quantity and CA excessive hyperplasia.

Ki-67 antigen is a DNA binding protein, with molecular weight of 359 kD. Its gene location is on chromosome 10, composing of 15 exons in proliferating cells (10). Its expression is closely related to cell cycle through its auto-phosphorylation and anti-phosphorylation effect on the cell cycle, and it can accurately control the cell cycle. Ki-67 can comprehensively reflect cell proliferation, and it is considered as the most ideal index of cell proliferation. This study found that the Ki-67 positive expression rates and expression intensity in CA tissues were higher than those in the normal tissues, thus prompting high proliferation stage of cells in CA tissues.

The present study also found that the expressions of survivin and Livin were positively correlated with CA tissue. Moreover, survivin was positively correlated with the expression of Ki-67, and Livin was positively correlated with the expression of Ki-67, indicating that survivin and Livin might be responsible for abnormal proliferation of CA tissues, and participate in the occurrence and development of CA .

Previous studies on survivin and Livin expression in CA or other related diseases have been reported (11-13). Expressions of survivin and Livin were abnormal in lesions of patients, which might be involved in the pathogenesis of the diseases, and CA and apoptosis could be responsible for the occurrence of the diseases. These results were consistent with the findings in the present study, however, because only limited numbers of patients were involved in all the studies, it remains to be investigated whether and how survivin and Livin is involved in the related diseases.

There are some limitations to the study. First of all, the sample size was small, and is therefore of limited power, which may weaken the conclusion of this study. Further studies should collect more samples to further confirm the conclusion. Secondly, only the immunofluorescence staining method was employed in the study, and other methods including RT-PCR and Western blot should be used in further investigation to explore role of survivin and Livin in lesions of CA from mRNA and protein levels.

In conclusion, over-expression and excessive proliferation of survivin and Livin were found in CA tissues, and apoptosis suppressors survivin and Livin were correlated with CA and pathogenesis of the disease.

REFERENCES

1. Bertram P, Treutner KH, Rübben A, Hauptmann S, Schumpelick V. Invasive squamous-cell carcinoma in giant anorectal condyloma (Buschke-Lowensteintumor). Langenbecks Arch Chir 1995; 380:115-18.
2. Xi RC, Biao WS, Gang ZZ. Significant elevation of survivin and livin expression in human colorectal cancer: inverse correlation between expression and overall survival. Onkologie 2011; 34(8-9):428-32.
3. Kasof GM, Gomes BC. Livin, a novel inhibitor of apoptosis protein family member. J Biol Chem 2001; 276(5):3238-46.
4. Birner P, Schindl M, Obermair A. Overexpression of hypoxia-inducible factor 1alpha is a marker for an unfavorable prognosis in early-stage invasive cervical cancer. Cancer Res 2000; 60:4693-96.
5. Fuzhong T, Nan L, Jiajia G, Miao L, Deqi Y. Clinical significance of the relationship between expression of survivin and effects of neoadjuvant chemotherapy in locally advanced breast cancer. Gan To Kagaku Ryoho 2008; 35(8):1319-23.
6. Rohayem J, Diestelkoetter P, Weigle B, Oehmichen A, Schmitz M, Mehlhorn J, Conrad K, Rieber EP. Antibody response to the tumor associated inhibitor of apoptosis protein Survivin in cancer patients. Cancer Res 2000; 60(7):1815-17
7. Yang YL, Li XM. The IAP family: endogenous caspase inhibitors with multiple biological activities. Cell Res 2000; 10(3):169-177.
8. Suzuki A, Kawano H. Survivin initiates procaspase 3 / P21 complex formation as a result of interaction with CDK4 to resist Fas-mediated cell death. J Oncogene 2000; 19(10):1346-1353.
9. Bhushan M, McLaughlin B, Weiss JB, Griffiths CE. Levels of endothelial cell stimulating angiogenesis

factor and vascular endothelial growth factor are elevated in psoriasis. Br J Dermatol 1999; 141:1054-60.
10. Nassar A, Lawson D, Cotsonis G, Cohen C. Survivin and caspase-3 expression in breast cancer: correlation with prognostic parameters, proliferation, angiogenesis, and outcome. Appl Immunohistochem Mol Morpho 2008; 16(2):113-20.
11. Lin JH, Deng G, Huang Q, Morser J. KIAP, a novel member of the inhibitor of apoptosis protein family. Biochem Biophys Res Commun 2000; 279(3):820-31
12. EndlE, Gerdes J. The Ki-67 protein: fascinating forms and an unknown function. Exp Cell Res 2000; 257(2):231-37.
13. Zhang Y, Huang H, Zhou H, et al. Activation of nuclear factor kB pathway and downstream targets survivin and livin by SHARPIN contributes to the progression and metastasis of prostate cancer. Cancer 2014; 120(20):3208-18.
14. Xi RC, Sheng YR, Chen WH, Sheng L, Gang JJ, Tong Z, Shan Z, Ying GH, Dong LC. Expression of survivin and livin predicts early recurrence in non-muscle invasive bladder cancer. J Surg Oncol 2013; 107(5):550-4.
15. Zhao X, Yuan Y, Zhang Z, Feng X, Zhang J, Yuan X, Li J. Effects of shRNA-silenced livin and survivin on lung cancer cell proliferation and apoptosis. J BUON 2014; 19(3):757-62.

LETTER TO THE EDITOR

EFFECT OF RELATIVE GENE EXPRESSION ON PLAQUE VULNERABILITY IN PATIENTS WITH STABLE ANGINA AND PATIENTS WITH ACUTE CORONARY SYNDROME

N. CHEN[1], J.Y. ZHANG[1], S.Z. YANG[2] and Y.D. LI[2]

[1]Department of Cardiology, the First Affiliated Hospital of Zhengzhou University, Zhengzhou, China; [2]Department of Cardiology, Nanyang Central Hospital, Nanyang, China

Received February 13, 2015 – Accepted April 29, 2015

This study was conducted to investigate the effect of relative gene expression on plaque vulnerability in patients with either stable angina or acute coronary syndrome (ACS). A total of 30 patients with ACS, 28 patients with stable angina and 17 healthy volunteers were selected. High resolution ultrasound was used to detect carotid arterial intima-media thickness (IMT) and plaque score, Sandwich enzyme linked immunoassay to determine the change of matrix metalloproteinase (MMP)-9 and tissue inhibitor of matrix metalloproteinase (TIMP)-1. The three groups had no statistically significant difference in age, gender, total cholesterol, triglyceride, high-density lipoprotein cholesterol and low-density lipoprotein cholesterol. MMP-9, TIMP-1, MMP-9/TIMP-1 and IMT, total plaque score, soft plaque score and hard plaque score of patients' acute coronary syndrome were obviously higher than those with stable angina and normal people. It was also found that MMP-9 was in a positive correlation with IMT, total and soft plaques score, TIMP-1 was positively correlated with IMT as was MMP-9/TIMP-1. Regardless of age, IMT was in a positive correlation with MMP-9, TIMP-1 and MMP-9/TIMP-1 in partial correlation analysis. All these findings suggest that ACS patients have remarkably higher MMP-9, 1TIMP-1, MMP-9/TIMP-1, IMT, total plaque score, soft plaque score and hard plaque score compared to patients with stable angina pectoris and healthy subjects (P<0.05) and there are positive correlations between MMP-9, TIMP-1, 1MMP-8/TIMP-1, total plaque and soft plaque score.

The incidence and development of acute coronary syndrome (ACS) is closely related to the stability of atherosclerotic plaques and rupture of vulnerable plaques is considered as the major pathogenesis for ACS (1). Recently, research tends to diagnose ACS by identifying vulnerable plaques.

Zhao Wei, et al. found that the inflammation markers interleukin-6 (IL-6), matrix metalloproteinase (MMP)-9 and matrix metalloproteinase (TIMP)-1 could directly reflect the instability of plaques in patients with ACS and play an important role in its incidence and development. Detecting their levels might help to diagnose patients at high risk of developing ACS and predict the incidence of cardiovascular diseases (2). Zhao Kai, et al. found that autophagy of monocyte from the peripheral blood of a patient with coronary heart disease tended to decrease as the instability of coronary atherosclerotic plaques increased. They believed that strengthening autophagy of peripheral

Key words: High resolution ultrasound, acute coronary syndrome, MMP-2, IMT

Mailing address:
Dr Jinying Zhang,
Department of Cardiology,
the First Affiliated Hospital of Zhengzhou University,
No.1, Jianshe East Road,
Zhengzhou, 450052, China
e-mail: zjy@ibhsedu.com

0393-974X (2015)

DISCLOSURE: ALL AUTHORS REPORT NO CONFLICTS OF INTEREST RELEVANT TO THIS ARTICLE.

blood monocytes could be a new way of stabilizing coronary atherosclerotic plaques, reducing the frequency of acute coronary arterial diseases and reducing the mortality (3). Zhu Zhebei, et al. proposed that INF-γ was able to thin the fiber caps of atherosclerotic plaques and restrain the formation of vulnerable plaques by reducing the immersion and regeneration of smooth muscle cells, reducing the synthesis of collagen and increasing the expression of extracellular matrix protein degradation, thereby promoting the formation of vulnerable plaques (4).

Through analyzing the correlation between MMP-9, TIMP-1 and carotid arterial intima-media thickness (IMT) in patients with ACS, this study explored its significance in identifying the vulnerable plaques for those patients.

MATERIALS AND METHODS

Study group

A total of 30 patients (21 males, 9 females; mean age of 62.3±9.4 years) with ACS were enrolled in one group of the study. Of these 30 patients, 5 suffered from unstable angina and the remaining 25 from acute myocardial infarction. In the other study group, 29 patients (14 males, 15 females; mean age 58.6±6.8) were confirmed with stable angina. Seventeen volunteers (10 males, 7 females; mean age 57.5±8.1) were enrolled as control group. All volunteers in the control group were confirmed non-smokers with normal blood pressure and without any record of coronary heart disease, diabetes or hypertension. They all signed a written informed consent before enrolment. The diagnosis for acute myocardial infarction was performed according to the criteria from World Health Association (WHO), while the diagnosis for unstable angina and stable angina were carried out according to criteria from The American Heart Association. Subjects with acute infection, severe kidney disease, severe heart failure, malignant tumor, cerebral apoplexy, gestation, rheumatism, trauma or who had undergone surgery within the last month, were not included in the study.

Carotid arterial IMT and plaque detection

Agilent Sonos 5500 color Doppler ultrasound imaging and linear-array probe with 11-3L frequency conversion (7.0MHz) were used for detection. Probing depth was set at 4 cm. Patients in supine position were examined by horizontal scanning from the internal extremity of the clavicle to the common carotid artery. The probe moved towards the head along the scanning direction to examine the carotid bifurcation, internal carotid and external carotid. The probe then turned 90° to detect the IMT of the common carotid artery. Plaques are usually defined as vessel lumen prominence exceeding 1.3 mm, which is used as the standard to determine its formation. Plaques can be divided into soft plaques and hard plaques. The former is defined as plaque with a different degree of mixed echo and the latter is defined as plaque with a local strengthened echo and sound shadow or obvious sound attenuation. This study adopted the Crouse method for the plaque score. Length of plaques were excluded and then the maximum thickness value of atherosclerotic plaques in common carotid artery, carotid bifurcation, internal carotid and external carotid on the same side were taken; the sum of these values was the plaque score of carotid artery on that side and the total plaque score was the sum of plaque scores of carotid artery on both sides.

Determination of plasm MMP-9 and TIMP-1

Blood samples were taken from all patients within 24 h after the occurrence of acute myocardial infarction, while patients with unstable or stable angina had blood samples taken in the early morning after being admitted to hospital. The normal control group had blood samples taken in the early morning. A quantity of 4 ml blood was drawn from every patient and they were treated with heparin as an anticoagulant. All blood samples were centrifuged at 3000r/min for 15min. Plasma was obtained and preserved at -20°C. MMP-9 and TIMP-1 were then detected by Sandwich Enzyme Linked Immunoassay. Devices for these tests included MMP-9 enzyme linked immunoassay kit (DMP900, Quantikine US), TIMP-1 enzyme linked immunoassay kit (DMP100, Quantikine, US) and Bio-tech Microplate Reader (A450nm Finland) which was used to detect spectroscopic luminosity. MMP-9 or TMP-1 monoclonal antibody was coated in advance in microplates and then injected with standard substance and sample. MMP-9 or TIMP-1 was combined with immobilized antibody to form specific MMP-9 or TIMP-1 enzyme-linked polyclonal antibody compound. When reaction terminated, it was found that MMP was in proportion to TIMP-1 or the compound. Foreign matter was rinsed away and substrate, i.e., the chromatic product catalyzed from enzyme within reaction wells, was added. Next, the standard curve was formulated according to the standard tube density value and the content of MMP-9 or TIMP-1 in samples was calculated based on standard curve.

Determination of blood lipids

Fasting blood samples were taken in the early morning to detect the blood lipids. Total serum cholesterol was detected by triple enzyme end-point colorimetric method; triglyceride was detected by 4-chlorophenol colorimetric method; high-density lipoprotein cholesterol and low-density lipoprotein cholesterol were detected by direct

method based on the full-automatic biochemical analyzer.

Statistical analysis

All measurement data were expressed by mean ± standard deviation and they were tested based on homogeneity of variance. Data that did not distribute normally were treated with logarithmic transformation before analysis. The comparison among these three groups was analyzed by single-factor variance and the comparisons between two groups were tested by LSD-t. All numerical data were tested by c^2. The analysis of correlation between unit linear, partial indexes and relative coefficients was applied by *t*-test. When $p<0.05$, the difference was of statistical significance. Statistical analysis was performed by applying SPSS 11.0 software.

RESULTS

General clinical data

The difference in age, gender, total cholesterol, total cholesterol, triglyceride, high-density lipoprotein cholesterol, and low-density lipoprotein cholesterol between these three groups was of no statistical significance (P>0.05) (Table I).

Comparison of ratio of MMP-9 and TIMP-1 and carotid artery ultrasound index

From experimental results It can be concluded that MMP9, TIMP-1, MMP-9/TIMP-1, IMT, total plaque score and in ACS group was much higher than stable angina group and control group (P<0.01), as shown in Table II.

Relative analysis of multiple factors

Among the three groups of data treated by elemental linear analysis, MMP-9 was in positive correlation with IMT, total plaque score and soft plaque score (r=0.468, P<0.01; r=0.592, P<0.01; r=0.677, P<0.0l); TIMP-1 was positively correlated with IMT, total plaque score, soft plaque score and hard plaque score (r=0.449, P<0.0l; r=0.493, P<0.01; r=0.435, P<0.01; r=0.227, P<0.05); MMP-9/TIMP-1 was positively correlated with IMT, total plaque score, and soft plaque score (r=0.253, P<0.05; r=0.431, P<0.0l; r=0. 547, P<0.0l). Regardless of age, the analysis of partial correlation showed that IMT was positively correlated with MMP-9 (r=0.461, P<0.001), TIMP-1 (r=0.441, P<0.001), and MMP-9/TIMP-1 (r=0.241, P<0.01).

DISCUSSION

Coronary atherosclerotic heart disease (CAHD) is one of the main causes of death worldwide (5). To date, the incidence of cardiovascular and

Table I. *Comparison of general clinical data from the three groups (mean±standard deviation).*

Indexes	ACS group (n=30)	Stable angina group (n=29)	Normal control group (n=17)
Age(year)	62.3±9.4	58.6±6.8	57.7±8.1
Male/female	21/9	14/15	10/7
Total cholesterol(mmol/L)	4.36±0.77	4.42±0.80	4.04±0.62
Triglyceride (mmol/L)	1.35±0.64	1.34±0.61	1.21±0.54
HDLC(mmol/L)	1.13±0.39	1.13±0.37	1.00±0.22
LDLC(mmol/L)	2.34±0.47	2.36±0.51	2.23±0.41

Table II. *Ratio between plasm MMP-9 and TIMP-1 and comparison among ultrasound indexes of carotid artery in these three groups (mean ± standard deviation).*

Index	ACS group(n=30)	Stable angina group (n=29)	Normal control group (n=17)
MMP-9(μg/L)	13.15±9.80ac	2.21±2.00	1.66±1.27
TIMP-1(μg/L)	1.36±0.61ac	0.69±0.39	0.58±0.42
MMP-9/TIMP-1	10.01±7.20ac	3.25±1.99	5.17±7.42
IMT(mm)	1.01±0.21bd	0.83±0.12a	0.66±0.08
Total plaque score	4.47±1.90bd	2.24±1.70a	0.31±0.89
Soft plaque score	2.30±2.21bd	0.40±0.69a	0.00±0.00
Hard plaque score	2.17±1.56b	1.84±1.60a	0.31±0.89

cerebrovascular diseases dominated by CAHD is in rapid growth. ACS is an acute situation of CAHD and once it occurs the condition of patients becomes serious. Various studies reveal that ACS is a group of clinical syndromes mainly caused by the rupture of atherosclerotic vulnerable plaques and the formation of secondary complete or incomplete obliterative thrombus (6).

The so-called vulnerable plaques refer to easily ruptured plaques with thin fiber caps, a big lipid core and abundant macrophages and new blood vessels which can cause thrombus and acute closure in coronary artery (7). However, the stable atherosclerotic plaques act the opposite way as they are featured by thick fiber caps and small lipid core and they will not cause occlusion in coronary artery. Therefore, a deep understanding of the mechanism of unstable plaques acts as a key in mastering the stability of vulnerable plaques. It can stabilize the vulnerable plaques, greatly reduce the incidence of ACS and further reduce the mortality of CAHD.

ACS is mainly caused by unstable atherosclerotic plaques, and the thrombus formation induced by its rupture leads to vascular cavity obliteration and promotes myocardial ischemia or necrosis in the distal vascular supply area (8). Extracellular matrix which is the important composition of the vascular wall, is also a key part in the complete plaques. Extracellular matrix with great elasticity and tenacity is rich in collagen, therefore its content, thickness and strength play a vital role in preventing the rupture of plaques. On the normal artery wall, the synthesis and resolution of extracellular matrix is in a relative balance and its composition is relatively stable. Extreme degradation of extracellular matrix is likely to induce the break of plaques and the incidence of ACS. MMP is a family of zinc iron-dependent proteinase which plays a major role in the degradation of extracellular matrix. Secreted by macrophages, smooth muscle cells and epithelial cells, it can quicken the break of plaques by digesting the composition of fiber caps and destroying their structure, which is one of major causes of unstable plaques (9). Therefore, the relation between MMP and plaque stability has drawn great attention recently.

This study found that in the ACS group there was not only the rupture of plaques in coronary artery, but a much higher carotid arterial IMT, total plaque score, soft plaque score and hard plaque score than those in the stable angina group and control group. Coronary plaques found in patients suffering from stable angina pectoris are dominated by stable fibrous plaques, while vulnerable and soft lipid plaques account for the main part in ACS patients.

Patients with acute myocardial infarction are usually found with obviously lower MMP-9 after being treated with pravastatin for three days (10). Therefore, this study recruited patients who had suffered acute myocardial infarction within 24 h, so as to exclude interference from other treatment factors. The results found that plasm MMP-9, TIMP-9/TIMP-1 and carotid arterial IMT, total plaque score, soft plaque score and hard plaque score in the ACS group were obviously higher than those in the stable angina group and normal control group.

Further analysis demonstrated that MMP-9 was positively correlated with IMT, total plaque score and soft plaque score; TIMP-1 was positively correlated with IMT, total plaque score, soft plaque score and hard plaque score; MMP-9/TIMP-1 was in positive relation with IMT, total plaque score and soft plaque score. Regardless of age, the partial correlation analysis showed that IMT was in a positive correlation with MMP-9, TIMP-1, and MMP-9/TIMP-1. MMP-9, MMP-9/TIMP-1was strongly linked to soft plaque score. The imbalance between MMP-9 and TIMP-1 is thought to be the direct cause of the rupture of vulnerable plaques in compromised patients. However, the imbalance process between MMP-9 and TIMP-1 is as follows: excessive higher MMP-9 weakens the inhibition ability of TIMP-1 with compensatory increasing to excessive high activity of MMP-9, thereby resulting in the degradation of extracellular matrix and rupture of plaques. Soft plaques with higher MMP-9, MMP-9/TIMP-1 detected by carotid arterial ultrasound can further reflect the instability of plaques.

In conclusion, plasm MMP-9, TIMP-1, MMP-9/TIMP-1, carotid arterial IMT, total plaque score, soft plaque score and hard plaque score of ACS patients are obviously higher than those with stable angina and healthy subjects. In addition, Plasma MMP-9, TIMP-1, MMP-9/TIMP-1 are found in a positive correlation with carotid arterial IMT, total plaque score and soft plaque score. As a result, the detection

of serum MMP-9 and MMP-9/TIMP-1 by carotid artery ultrasound was considered to have a great clinical significance in the detection of vulnerable plaques.

REFERENCES

1. Niu JF, Li J. Changes of interleukin-18 in patients with acute coronary syndrome and its clinical significance. Adv Cardiov Dis 2013; 34(1):118-20.
2. Zhao W, Li TT, Li Y. Relative analysis of inflammation markers in patients with coronary disease and acute coronary syndrome. Chinese J Ger Heart Brain Ves Dis 2014; 16(2):207-8.
3. Zhao K, Chen WQ, Xu XS, Meng X, Zhang Y, Li JF. The study of relationship between autophagy related proteins expression in mono-cytes and vulnerability of coronary atherosclerotic plaque. Chinese J Art 2014; 22(1):37-42.
4. Zhu ZB, Jiang JJ, Li RZ, Wang L. The relationship between atherosclerotic plaque characteristics and Th-cell drift in the patients with coronary artery disease. Chinese J Art 2012; 20(7):643-6.
5. Liu EQ, Fan JL. Recent advances in translational research of atherosclerosis. J of Xi'an Jiaotong University (Medical Sciences) 2014; 35(5):565-74.
6. Wang LJ. High-sensitive c-reaction soluble protein OX40l in patients with acute coronary syndromes and changes of matrix metalloproteinase-9. Shanxi Med J 2014; 3(1):75-6.
7. Wang TT, Huang YN. Recognition and processing of carotid arterial plaque. Chinese J Front Med Sci (e-version) 2014; 6(7):6-16.
8. He C, Yuan JQ. Relationship between inflammation markers and acute coronary syndromes. Adv Cardio Dis 2014: 32(5):680-4.
9. Wang J, Tan XJ. Research progress of effect of MMP-9 on coronary heart disease. J Mod Med & H 2013; 29(5):731-3.
10. Chen Y, Duan XY, Zhang SF, Guan HZ, Wu XW. Effect of large dose of pravastatin on serum CRP and MMP-9 level in patients of acute myocardial infarction. Chinese J New Clin Med 2012; 5(3):198-200.

JOURNAL OF BIOLOGICAL REGULATORS & HOMEOSTATIC AGENTS Vol. 29, no. 2, 443-450 (2015)

LETTER TO THE EDITOR

EVALUATION OF ANTIVIRAL THERAPY TREATMENT FOR LIVER CIRRHOSIS CAUSED BY CHRONIC HEPATITIS C AND HEPATITIS C BY ^{31}P-MRS, BASED ON METABOLITE DETECTION

JS. GU, RR. SUN, S. SHEN and ZJ. YU

Department of Infectious Diseases, the First Affiliated Hospital, Zhengzhou University, Zhengzhou, Henan, China

Received February 11, 2015– Accepted May 6, 2015

This study discusses the application of magnetic resonance spectrum (MRS) to evaluate the efficacy of antiviral therapy in the treatment of liver cirrhosis caused by chronic hepatitis C and hepatitis C, based on metabolite detection. A total of 54 patients with liver cirrhosis caused by chronic hepatitis C and hepatitis C were selected and divided into treatment group and control group. ^{31}P-MRS imaging was carried out on patients in the two groups both before receiving antiviral treatment and 6 months after treatment to compare the change of metabolite ratio (PE+PC)/(GPE+GPC). It was revealed that no statistically significant difference was found in the comparison of (PC+PE)/(GPC+GPE) ratio in the two groups before treatment, but the difference was found 6 months after treatment; ratio of (PC+PE)/ (GPC+GPE) in the treatment group distinctly decreased 6 months after treatment compared to before treatment, with a statistically significant difference, while the control group had no remarkable change or statistical significance. Moreover, 32 patients were found with sustained virus response to antiviral therapy. Of these, 25 patients possessed a decreased ratio of (PC+PE)/ (GPC+GPE), 4 remained without change and 3 had a slightly increased ratio after antiviral treatment. Of 12 patients with no response, 1 had a decreased ratio of (PC+PE)/ (GPC+GPE), 2 remained without change and 9 had a slightly increased ratio. The differences were all statistically significant in comparison of the two groups. ^{31}P-MRS is thought to be effective for evaluating the efficacy of antiviral therapy through non-invasive detection of liver energy metabolism.

Chronic hepatitis C is a worldwide liver disease, with 1,700 million infectors (1). Many cases develop into liver cirrhosis and even liver cancer in the advanced stage. To date, liver puncture is used to determine the degree of hepatitis and staging of chronic hepatitis (2); however, this invasive examination is painful for patients. Therefore, magnetic resonance spectrum (MRS) is now being applied to acquire liver tissue information.

MRS is a molecular imaging method which makes use of atomic nuclei such as 1H, 31P, 13C, 19F, 23Na. Usually, ^{31}P-MRS is applied in liver diffuse lesion. For instance, Sevas-tianova et al. (3), with the help of 3.0-T ^{31}P-MRS spectroscopy with proton decoupling, distinguished different stages of nonalcoholic fatty liver disease by analyzing the composition of phosphomonoester and phosphodiesterase and detecting phosphorous

Key words: chronic hepatitis C, liver cirrhosis, magnetic resonance, spectrum, antiviral

Mailing address: Dr Zujiang Yu,
Department of Infectious Diseases,
the First Affiliated Hospital,
Zhengzhou University,
Jianshe East Road No.1,
Zhengzhou, Henan 450052, China
e-mail: yzj@ibhsedu.com

0393-974X (2015)

DISCLOSURE: ALL AUTHORS REPORT NO CONFLICTS OF INTEREST RELEVANT TO THIS ARTICLE.

compound such as nicotinamide adenine dinucleotide phosphate. Wang Lijuan (4) proposed a ^{31}P-MRS liver cancer diagnosis method based on genetic algorithm and neural network to improve the identification rate of liver cancer.

Based on the current technologies, MRS images and metabolite peaks of 54 cases of liver cirrhosis caused by chronic hepatitis C and hepatitis C before treatment and 6 months after treatment were analyzed. ^{31}P-MRS in the efficacy evaluation of interferon and ribavirin treating vital hepatitis C was also discussed.

MATERIALS AND METHODS

A total of 54 patients (32 male and 22 female; age 32-69 years - mean 49.3 years) with liver cirrhosis caused by chronic hepatitis C and hepatitis C who were admitted to the infections department of the First Affiliated Hospital of Zhengzhou University, Henan, between October 2012 and September 2013 were enrolled in this study based on inclusion and exclusion criteria. None of the patients had contraindication for magnetic resonance spectroscopy.

Inclusion criteria was as follows: (1) Hepatitis C virus (HCV) RNA> 500 copies/mL; (2) no complications, such as gastrointestinal bleeding, hepatic encephalopathy and primary liver cancer; (3) with Child-Pugh staging of level A or B (evaluated based on serum bilirubin, serum albumin, ascites, hepatic encephalopathy and thrombin time); (4) patients who had twice undergone successful MRS with an interval of 6 months; (5) patients who had not undergone any antiviral therapy.

Exclusion criteria was as follows: (1) infection with hepatitis A, B, D or F, EB virus, cytomegalovirus or human immunodeficiency virus and chronic hepatitis C; (2) liver disease induced by alcohol or drugs, pulmonary heart disease, serious heart attack, and liver function damage induced by brain or kidney.

According to this criteria, 54 eligible patients were selected. Patients who accepted antiviral therapy were classified into treatment group (n=42) and control group (n=12). This study was approved by the Ethics Committee of Zhengzhou University, and signed informed consent was obtained from each participant.

Clinical evaluation

With regard to treatment efficacy, the primary endpoints were: (1) sustained virological response (SVR) (5) (defined as: viral RNA of hepatitis C could not be detected or detected as < 500 copy/ml, and the drugs stopped after at least 24 weeks); (2) recurrence (defined as: viral RNA of hepatitis C could not be detected or detected as < 500 copies/mL in the antiviral therapy, but it could be detected within 24 weeks after stopping taking drugs). The secondary endpoint is evaluation of disease progress (defined as Child-Pugh score increases of 2 or more); for instance, liver disease induces primary liver cancer, renal insufficiency, spontaneous bacterial peritonitis, variceal bleeding or death (6).

Treatment

Prior to the study, patients in the treatment group were examined for serum HCV antibody, liver function, viral RNA of hepatitis C, coagulation function, thyroid function, alpha fetoprotein, liver CT scanning, blood routine and urine routine. Blood routine and liver function were controlled every week for the first month, every four weeks during the study and every eight weeks within twenty-four weeks after having stopped taking medication. Viral RNA of hepatitis C was detected before treatment, twenty-four weeks and forty-eight weeks after treatment and six months after having stopped taking drugs. RNA level of hepatitis C was detected using real-time polymerase chain reaction (PCR) (Roche Group).

Liver function and HCV-RNA were checked in patients in the control group. Blood routine and liver color Doppler ultrasound performed every twelve weeks.

All the patients were given symptomatic and supportive treatment, including lowering transaminase and bilirubin and supplementing albumin level. Patients in the treatment group with neutrophil granulocyte $\geq 1.0\times10^9$/L, blood platelet $\geq 50\times10^9$/L, hemoglobin >10g/L were also treated with PEG-IFNα-2a and ribavirin. Initial dosage of PEG-IFNα-2a was 180 μg/kg (subcutaneous injection). Dosage of PEG-IFNα-2a was reduced to 90 μg/kg once a week if neutrophil

granulocyte and blood platelet became $\leq 0.75\times10^9$/L or $<50\times10^9$/L, respectively, but if they increased to $>0.75\times10^9$/L and $\geq50\times10^9$/L, respectively, then the dosage was returned to 180 μg/kg. Once neutrophile granulocyte reached $\leq0.5\times10^9$/L or blood platelet $<30\times10^9$/L, the treatment stopped. The treatment lasted for forty-eight weeks if the patients could tolerate the dosage of PEG-IFNα-2a for 180 μg/kg every week; otherwise, the treatment lasted for 72 weeks with reduced dosage of 90 μg/kg every week.

Patients were treated with standard dosage of ribavirin at first if hemoglobin >100g/ L (genotype 1: weight > 75 kg, dosage of 1200 μg /d and weight ≤75kg, dosage of 1000 μg /d; non-genotype 1: weight > 75 kg, dosage of 1000 μg /d and weight ≤75kg, dosage of 800 μg /d). The dosage was reduced if the increased dosage of ribavirin induced hemoglobin level to be less than 100g/ L. When hemoglobin level reached ≤80g/L, then ribavirin treatment stopped. Treatment lasted for forty-eight weeks if the patients could tolerate ribavirin.

Patients were treated with cell growth simulator or erythrogenin if hemocyte reduced during treatment. All the patients were followed-up for three years.

^{31}P-MRS

Philips Achieva 3.OT MR scanner and P-140 coil (emitting-receiving loop coil, diameter of 14 cm) (Fig. 1) were applied. All the patients fasted 6 h before scanning and exercised breathing. A position was marked 2-2 ins below the right rib (Fig. 2).

Firstly, regular T1WI and T2WI fat-suppression sequence and in-phase and out-phase T1WI were scanned. The parameters were as follows: i) breath freely T1-TFE-IP: TR13ms, TE2.3ms, ACQ M×P matrix 268×149, NSA 1, FOV400mm×300mm ×156mm, 24 layers, layer thickness of 6 mm, interval of 1 mm, pixel of 1.5×2mm, direction of layer: transverse direction, reverse direction: forward and backward, direction of fat reposition: left, scanning time of 20 s; ii) T1WI in-phase and out-phase scanning dual-FFE-fast-BH: TR 101ms, TE out-phase 1.15ms, in-phase 2.3ms, FOV 400×300×167, pixel of 1.8×1.89, ACQ M×P matrix 224×158, 24 layers, layer thickness of 6 mm, interval of 1 mm, scanning time of 15 s; iii) hold breath T2W-spair-sense sequence: TR 1250ms, TE 70ms, NSA 1, FOV 400×300×167, pixel of 1.4×1.58, ACQ M×P matrix 288×188, 24 layers, layer thickness of 6 mm, interval 1 mm, scanning time of 15 s.

Q-Body coil was used to locate the image in axial, coronal, and sagittal planes. Region of interest at the size of $6\times5\times6cm^3$ on right liver robe was selected. The volume of the region of interest was put on the same level of the coil mark, thus the optimal signal noise ratio could be acquired and meanwhile the influence of fat, blood vessel, air and bone around the liver could be excluded (7).

Before scanning V should be at the highest clarity and the top of V should be sharp (Fig. 3). Scanning parameters are as follows: TR 5000ms, the shortest TE 0.10, NSA 128, spectral resolution 1.46Hz, phase period, SAR/local torso<68%, local torso/level<6. 8W/kg/normal, Blrms 1.55uT, PNS/level 48%/ normal, read time 682. 67ms, acquisition time 11 min, total acquisition time 40 min. All the patients underwent ^{31}P-MRS scanning prior to and 6 months after antiviral therapy.

Data processing

Spectroview software was used for correcting baseline and frequency of the data acquired. The image acquired lacked phosphocreatine peak since the image avoided the pollution from muscle. Generally, chemical shift of phosphocreatine in skeletal muscle is considered as 0 while the positions of other chemical shifts were confirmed based on phosphocreatine. Another metabolic product was needed for reference since there was no phosphocreatine in liver. With reference of γ-ATP (-2.5ppm), frequency shift was manually corrected. Spectral lines of ^{31}P-MRS acquired were PE, PC,Pi, GPE, GPC,γ-ATP, α-ATP, β-ATP, from left to right. As 3.0T MR classifies metabolic products more detailed, PME was presented as two peaks, PE and PC, and PDE as GPE and GPC. Peak value and areas below peak were calculated by software.

Statistical analysis

Age and HCV RNA level were in normal distribution, expressed by mean and standard deviation. Differences of age and HCV RNA between the two groups were compared by carrying out the *t*-test on two independent samples. Child-Pugh grading score was in non-normal distribution, expressed by median and inter-quartile range

(IQR). Difference of Child-Pugh grading scores in the two groups were performed by non-parameter Mann-Whitney test. Other classified variables were expressed by mean and percentage. Correlation between the variables in the treatment group was tested by Fisher's exact test.

All the statistical tests were double blind. $P< 0.05$ was considered to be statistically significant. SPSS19.0 software was used for all the statistical analyses.

RESULTS

Population statistics and basic characteristics of patients

As shown in Table I, 54 eligible patients were enrolled in the study. Forty-two patients with sufficient blood cell count were able to undergo antiviral therapy and the remaining 12 patients were classified into the control group as they were not suitable to receive antiviral therapy due to either rejection or health status. No statistical significant difference was found in gender and HCV RNA level between the two groups, nor for end-stage liver disease (MELD) score. Child-Pugh score, total bilirubin and hepatic encephalopathy situation were different between the two groups and gender, serum albumin, prothrombin time and ascites were found with significant difference between the two groups ($P<0.01$; $P<0.002$; $P<0.018$; $P<0.001$).

Comparison of ratio of (PC+PE)/(GPC+GPE) of the two groups before and after antiviral treatment

In the control group, the ratio of (PC+PE)/(GPC+GPE) before and after treatment was (0.86±0.17) and (0.78±0.19), respectively, and the difference between them was of no statistical significance. In the treatment group, the ratio before and after treatment was (1.14±0.24) and (0.59±0.21), respectively, and no statistically significant difference

Table I. *Population statistics and basic characteristics of patients.*

		Treatment group (n=42)	Control group (n=12)	P value
Age (y)		52.7±10.1	58.3±12.5	<0.001
Gender	Female	17 (40.4%)	5(41.7%)	0.451
	Male	25(40.0%)	7(58.3%)	
HCV RNA level (log copy/mL)		5.30±1.18	5.23±1.15	0.641
MELD score		12.6(9.8,15.2)	12.5(9.4,15.8)	0.637
Child-Pugh score		5.0(4.0,7.0)	5.0 (3.0,7.0)	0.791
Total bilirubin (mg/dL)	<2	5(11.9%)	2(16.7%)	0.660
	2-3	19(45.2%)	6(50.5%)	
	>3	18(42.9%)	4(33.3%)	
	>3.5	4(9.5%)	1(8.3%)	0.002*
Serum albumin (g/dL)	2.8-3.5	18(42.9%)	7(58.4%)	
	<2.8	20(47.6%)	4(33.3%)	
	<1.7	12(28.5%)	3(25.0%)	0.018*
Prothrombin time	1.7-2.3	23(54.8%)	5(41.7%)	
	>2.3	7(16.7%)	4(33.3%)	
Hepatic encephalopathy	None	42(100.0%)	12(100.0%)	NA
Ascites	None	40(95.2%)	10(83.3%)	<0.001*
	Easy to control	2(4.8%)	2(16.7%)	

** statistical difference between two groups. Normal distribution of age and HCV RNA level is expressed by mean and standard deviation; abnormal distribution of Child-Pugh score is expressed by median and inter-quartile range; other types of variables are expressed by quantity and percentage.*

Table II. *Ratio of (PC+PE)/(GPC+GPE) of the two groups.*

	Control group	Treatment group	P value
Before treatment	0.86±0.17	1.14±0.24	0.108
6 months after treatment	0.78±0.19	0.59±0.21	0.034
P	0.895	0.002	

Table III. *Ratio of (PC+PE)/(GPC+GPE) of response group and non-response group before and after antiviral treatment.*

Group	(PE+PC)/ (GPC+GPE) Decrease	(PE+PC)/ (GPC+GPE) No change	(PE+PC)/ (GPC+GPE) increase
Response group (n=32)	25 (78%)	4(13%)	3(9%)
Non-response group (n=12)	1 (8%)	2(17%)	9(75%)
p	<0.05	<0.05	<0.05

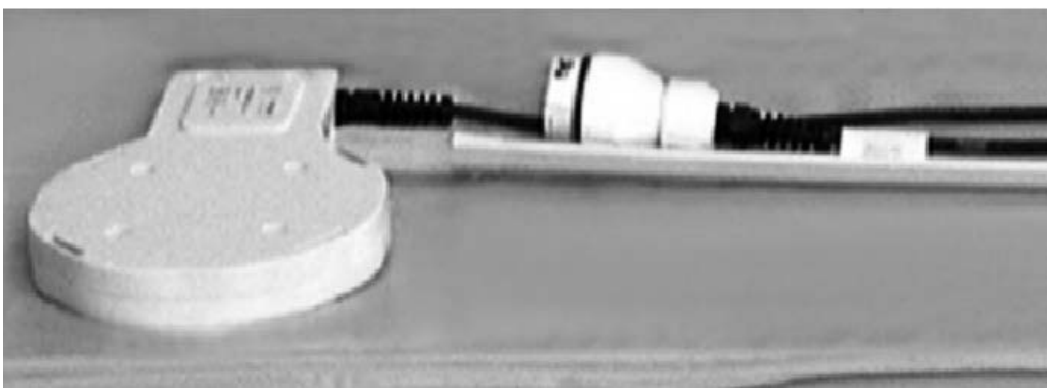

Fig. 1. *Phosphorus spectrum coil.*

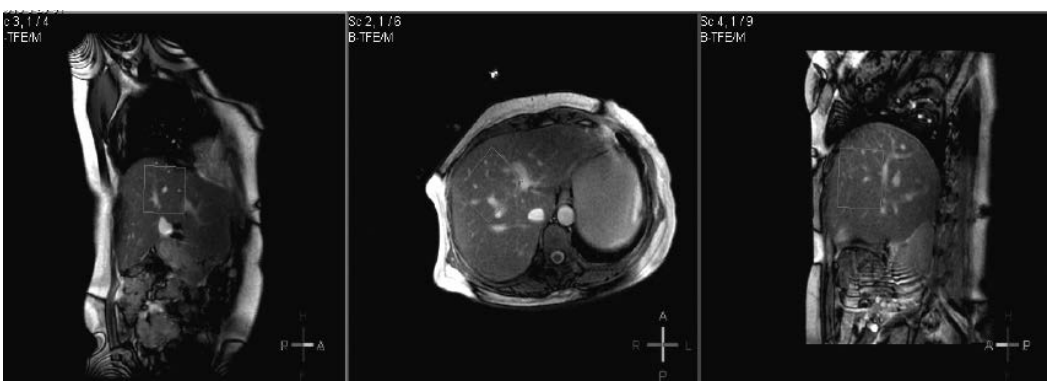

Fig. 2. *Location map for phosphorus spectrum of liver.*

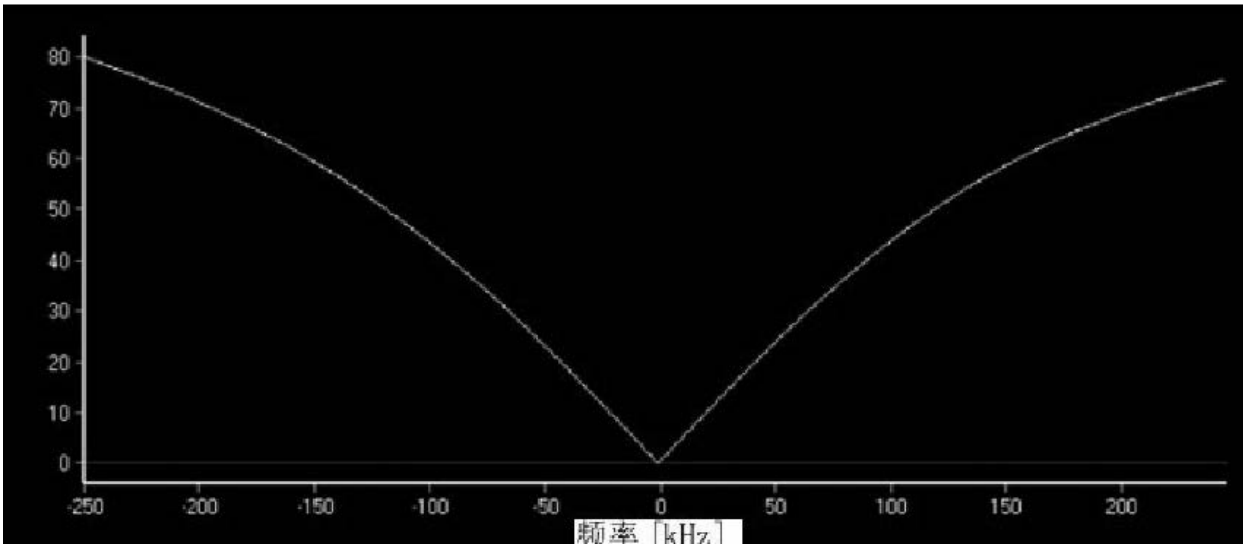

Fig. 3. *Manual tuning window.*

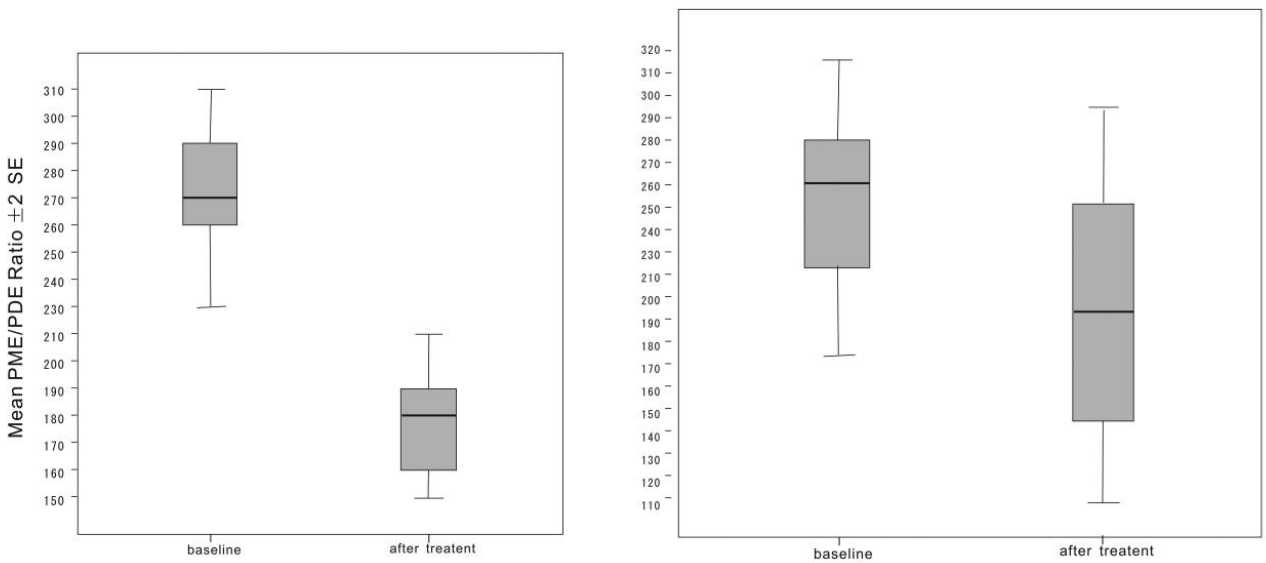

Fig. 4. *Analysis of changes of (PC+PE)/(GPC+GPE) ratio of response group and non-response group before and after antiviral treatment.*

was found, however, the difference had statistical significance after 6 months of treatment (Table II).

Changes of ratio of (PC+PE)/(GPC+GPE) of response group and non-response group before and after antiviral treatment

A total of 32 patients exhibited sustained virological response to antiviral treatment, of whom 25 had decreased ratio of (PC+PE)/(GPC+GPE) (78%) after antiviral treatment, 4 patients showed no change and 3 patients had a slightly increased ratio. Of 12 patients with no response, 1 had a decreased ratio (8%), 2 showed no change and 9 had a slightly higher ratio ($P<0.05$). Less than 0.03 higher or lower was defined as no change of (PC+PE)/(GPC+GPE) ratio, more than 0.03 higher was defined as increase,

and more than 0.03 lower was defined as decrease (Table III).

Through further analyzing the changes of (PC+PE)/(GPC+GPE) ratio in the two groups before and after treatment, it was found that the ratio of the response group distinctly decreased after treatment and the difference had statistical significance; however, the ratio of the non-response group remained unchanged (Fig. 4).

DISCUSSION

MRS is a non-invasive method for effectively evaluating the metabolic process of viable tissues. Chemical changes occur in compound or metabolic products from tissues under certain environments since they possess protons. These slight changes are transformed into numerical value spectrum standing for the concentration of relevant metabolic product in tissue or humor after being collected by an MR scanner (8). ^{31}P-MRS is widely applied in studies on liver because compounds containing ^{31}P in liver involved in energy metabolism of cells and phospholipid metabolism correlate with biological membrane (9). ^{31}P-MRS is featured by high sensitivity. Notably, it can effectively detect the change of metabolite in liver tissue of patients with chronic hepatitis C who are clinically treated by antiviral therapy.

Several different resonance peaks can be detected while patients are examined by ^{31}P-MRS, including phosphocreatine, triphosadenine, phosphomonoester, phosphate diester, inorganic phosphate. Phosphomonoester contains message of phosphorylated sugar produced through glycolysis, as well as message of membrane precursor such as phosphorylethanolamine and phosphorylcholine, correlating with anabolism of membrane. Phosphate diester contains endoplasmic reticulum and degradation product of membrane such as message of phosphatidyl ethanolamine, phosphatidyl cholines and phosphodiester, correlating to catabolism of membrane (10). Many studies indicate that increased phosphomonoester and decreased phosphate diester are in a definite correlation with liver cirrhosis (11). Repairing of injured liver cells in hepatitis C and liver cirrhosis presents as increased anabolism, decreased catabolism and rising (PC+PE)/(GPC+GPE), which can be used for quantitatively evaluating the damage of liver cells. ^{31}P-MRS is a potential and non-invasive method for monitoring hepatitis as it can directly reflect metabolism of liver cells. Some studies have demonstrated that chronic liver disease becomes more severe as ratio of phosphomonoester and phosphate diester increases, and increase of this ratio is more sensitive in liver cirrhosis (12). As MRS develops, we can use the ratio of phosphomonoester and phosphate diester to evaluate the severity of liver disease related to HCV.

In this study, before treatment, difference of the ratio of (PC+PE)/(GPC+GPE) between the control group and the treatment group was not statistically significant, but 6 months after treatment, there was a statistically significant difference in the treatment group. Ratio of (PC+PE)/(GPC+GPE) distinctly decreased in the sustained virological response group but remained unchanged or increased in the non-response group. Phosphomonoester is correlated to anabolism of membrane and phosphate diester is correlated to catabolism. Repairing of injured cells in liver cirrhosis presents as increased anabolism, decreased catabolism and rising (PC+PE)/(GPC+GPE) ratio. But this study demonstrated that the ratio decreased after effective antiviral therapy; patients in the response group also had increased ratio. Moreover, it was also found that, the ratio of (PC+PE)/(GPC+GPE) was in a good correlation with liver fibrosis degree and liver cirrhosis grading.

In general, ^{31}P-MRS can be taken as a non-invasive method for evaluating the reaction of liver to antiviral therapy and efficacy of antiviral. The ratio of phosphomonoester and phosphate diester does not have 100% sensitivity or specificity. In this research, as to patients with no sustained response, some patients had decreased ratio of (PC+PE)/(GPC+GPE). Similarly, some patients among those with sustained virological response also had increased ratio of (PC+PE)/(GPC+GPE). This ratio was obtained before treatment and 6 months after treatment. But most patients should continue to be treated for more than one year. Therefore, repeated detection of the ratio of (PC+PE)/(GPC+GPE) may bring higher sensitivity and specificity. On the other hand, it can provide biochemical information of the liver metabolism process which can show the progression of liver fibrosis (13).

This study demonstrates that ^{31}P-MRS can quantitatively detect the ratio of phosphomonoester and phosphate diester before and after antiviral therapy of patients with liver cirrhosis, therefore can be used for evaluating efficacy of treatment of this disease caused by chronic hepatitis C and hepatitis C. ^{31}P-MRS is a new invasive technology for evaluating liver metabolism process and an effective method for evaluating efficacy of antiviral therapy.

REFERENCES

1. Bini EJ, Perumalswami PV. Hepatitis B virus infection among American patients with chronic hepatitis C virus infection: prevalence, racial/ethnic differences, and viral interactions. Hepatol 2010; 51(3):759-66.
2. Shen MR, Li ZP, Ding XH, Chu F, Hu GC. Clinical significance of liver biopsy in diagnosis and treatment of liver disease. Chinese J Clin Hepatol 2012; 28(7):545-46.
3. Sevastianova K, Hakkarainen A, Kotronen A, et al. Nonalcoholic fatty liver disease: detection of elevated nicotinamide adenine dinucleotide phosphate with in vivo 3.0-T ^{31}P MR spectroscopy with proton decoupling. Radiol 2010; 256(2):466-473.
4. Wang LJ. 31P-MRS for liver cancer diagnosis based on genetic algorithm and neural network. Shandong; Shandong Light Industry University 2010:3-4.
5. Brook G, Soriano V, Bergin C. European guideline for the management of hepatitis B and C virus infections. Int J STD AIDS 2010; 21(10): 669-78.
6. Lundbom J, Hakkarainen A, Soderlund S, Westerbacka J, Lundbom N, Taskinen MR. Long-TE 1H-MRS suggests that liver fat is more saturated than subcutaneous and visceral fat. NMR Biomed 2011; 24(3):238-45.
7. Zhang LJ, Yao XZ. Magnetic resonance imaging of the abdomen (liver): technological state of the Art. Chinese J Clin Med 2014; 21(4):497-99.
8. Jiang MJ, Zhang LN. Progress in magnetic resonance spectroscopy for liver. Bulletin of Chinese Cancer 2011; 20(8):597-600.
9. Zhao S, Li CY, Gao FX, Li YC, Wang W, Li JM, Li QX, Liu XW. The diagnostic value of combined with proton magnetic resonance spectroscopy and DWI in cirrhosis by 3.0 T MRI. J of Clinical Radiology 2013; 32(3):344-47.
10. Mariana VF, de Fatima GG, Maria Pde G. The effect of mechanical lymph drainage accompanied with heat on lymphedema. J Res Med Sci 2011; 16(11):1448-51.
11. Lim AK, Patel N, Hamilton G, Mylvahan K, Kuo YT, Goldin RD, Taylor-Robinson SD. 31P MR spectroscopy in assessment of response to antiviral therapy for hepatitis C virus-related liver disease. AJR Am J Roentgenol 2007; 189(4):819-23.
12. Dreze M, Charloteaux B, Milstein S, et al. 'Edgetic' perturbation of a *C. Elegans* BCL2 ortholog. Nat Methods 2009; 6(11): 843-9.
13. Chen XL. Experiment on quantitative evaluation of magnetic resonance imaging on liver fibrosis. Sichuan, North Sichuan Med Coll 2013:10-11.

LETTER TO THE EDITOR

META-ANALYSIS OF HIGH RISK FACTORS OF RESIDUE OR RELAPSE OF CERVICAL INTRAEPITHELIAL NEOPLASIA AFTER CONIZATION

J. JIN[1], L. LI[2] and F. ZHANG[3]

[1]Obstetrics and Gynecology Department, the First Affiliated Hospital of Henan University of Science and Technology, Luoyang, China; [2]Neonatology, Luoyang Women and Children's Medical Center, Luoyang, China; [3]Dermatological Department, Luoyang Central Hospital Affiliated to Zhengzhou University, Luoyang, China

Received January 23, 2015 – Accepted may 6, 2015

This study assesses the high risk factors of residue or relapse after conization of cervical intraepithelial neoplasia. Literature on high risk factors of residue or relapse after conization of cervical intraepithelial neoplasia from January 2006 to June 2011 were selected from the Pubmed Database, Elsevier Database, Chinese Biomedicine Database and Chinese Journal Full-text Database of China National Knowledge Internet (CNKI). Software RevMan 4. 2 provided by Cochrane collaboration network was used in the statistical analysis of the data. According to the inclusion criteria, 10 essays were retrieved, including 348 cases in case groups and 1,608 cases in control groups. Information about residue or relapse after conization, incisal edge, HIV infection after six months of surgery, age, menopause status was obtained through the above method. Meta-analysis showed that positive surgical margin groups had a higher residual or recurrence rate than negative surgical margin groups after conization; groups where glands were involved had a higher residual or recurrence rate than non-involved glands groups after conization; positive HR-HPV infection after six months of conization groups had higher residual or recurrence rates than negative HR-HPV infection groups; 50 years or older groups had higher residual or recurrence rate than under 50 year-old groups after conization; postmenopausal groups had higher residual or recurrence rate than premenopausal groups. Menopause, 50 years old or older, gland involvement, positive surgical margin and HR-HPV infection after six months are high risk factors of residue or relapse after α - β conization of CIN.

A series of pathological changes of tissues in the early stage of invasive carcinoma of the cervix is called CIN, which can reflect the disease progression of cervical cancer (1). Recently, the number of new cases of cervical intraepithelial neoplasia (CIN) has been increasing and the patients tend to be younger and younger, which is seriously threatening the health of women (2).

The commonly used surgical approaches are loop electrosurgical excision procedure (LEEP) and cold knife conization (CKC). Scholars have analyzed a series of relevant risk factors of lesion residual or relapse cases found in postoperative follow-up, which is important for clinical evaluation and management (3). However, a number of studies show that CIN has a higher recurrence rate after

Key words: conization, cervical intraepithelial neoplasias, relapse, high risk factors

Mailing address: Dr Jian Jin,
Obstetrics and Gynecology, Xinqu Hospital of the First Affiliated Hospital of Henan University of Science and Technology, northern side of the road 300 meters western to the crossroad of Guanlin Road and Xuefu Street, Luoyang, Henan, 471000, China
e-mail: jj@ibhsedu.com

0393-974X (2015)

surgery, which influences the prognosis of patients (4). To further improve the prognosis quality of CIN patients and the treatment effect, Zhou Ping, et al. pointed out that in order to diagnose lesion residue or recurrence of CIN in the early stage, postoperative follow-up is highly significant (5). Deng Yuanzheng, held the view that the positive pathological detection of surgical margin excision, persistent infection of high-risk HPV and menopause were high risk factors of relapse after CIN surgery, which could be taken as a foundation strengthen postoperative follow-up to patients, so as to achieve an early detection and treatment of recurrent patients and further optimize the prognosis of patients (6).

This study explores the quantitative relation between incisal edge, involved glands, HPV infection six months after surgery, age, menopause, HIV infection and postoperative lesion residue or relapse.

MATERIALS AND METHODS

Source of data

Inclusion criteria:

(1) primary literature published home and abroad with studies of independent cases on high risk factors of residue or relapse after CIN conization;

(2) patients in control groups and case groups from the same area and comparable in age;

(3) the data integral with comprehensive statistical index odds ratio (OR) or 95% confidential intervals or calculable with sufficient information;

(4) clear, identical or similar definitions given to incisal edge, involved glands, HPV infection six months after surgery, age, menopause and HIV infection;

(5) at least a two-year follow-up after conization.

Exclusion criteria: (1) review literature; (2) literature without control group; (3) repeated reporting with same author and similar content; (4) incomplete original data.

Document retrieval and data collection

A database was formed from Pubmed (1/2006 to 6/2011), Elsevier (1/2006 to 6/2011), Chinese Biomedicine (1/2006 to 6/2011), Chinese Journal Full-text of China National Knowledge Internet (CNKI) (1/2006 to 6/2011) and some other references. Key search words were CIN, cervical conization, persistence, recurrence, risk factors. Information, such as persistence or recurrence after cervical conization, incisal edge, involved glands, HPV infection six months after surgery, age, menopause, HIV infection, was extracted from the literature in accordance with the criteria.

Statistical analysis

Software RevMan 4.2 provided by Cochrane collaboration network was adopted for statistics. Continuous variable was represented by weighted mean difference (WMD) and 95% confidence interval (CI) while binary variable was represented by OR value and 95% CI. Firstly, statistical heterogeneity included in the study was analyzed, then fixed model and random model were adopted respectively. If there was significant heterogeneity in the result, revised Dersimonian-Laird was adopted to detect it, and if there was no remarkable heterogeneity in the result, Peto Mantell Iaenszel, the fixed effect model, was applied to combine data and calculate the gross OR value. As for researches that were low in quality, high in weight or had apparently different outcomes, sensitivity analysis was required before deciding whether or not to include them.

RESULTS

Fifty-five relevant articles were retrieved, among which 10 (7-17) conformed to the inclusion criteria (Table I). There were 348 cases in case groups and 1,608 cases in control groups. Other literature was excluded because the research purposes did not coincide with this study or they did not meet the inclusion criteria. The main findings of the research are shown in Table II.

Incisal margin status

Nine studies (7-9, 11-16) reported relevant results regarding incisal margin status and the residue or relapse rate after conization. Heterogeneity test was p=0.29, which indicated that there was no heterogeneity among studies, so a fixed effect model was adopted to combine and analyze the data (Fig. 1). The OR value of combinative effect was 4.30 [95%CI(3. 28~5. 63)], p<0.00001, the difference of which was statistically significant and showed that the positive incisal edge groups had a higher rate of residue or relapse after conization than the negative incisal edge groups.

Gland involvement

Six studies (7, 9, 11, 12, 15, 16) reported relevant results regarding cervical glandular and the rate of residue or relapse after conization. Heterogeneity test was p=0.03, which suggested that there was

Table I. *Research projects and relevant content of the selected literature.*

No.	Publication time	Case Group (case)	Control group (case)	Follow-up	Research project	Investigation project
1	2006	64	385	449	Taiwan, China	Incisal edge,involved glands, age
2	2006	36	167	203	Barcelona, Spain	Incisal edge, age, HPV infection after six months of surgery
3	2007	41	36	77	Seoul, Korea	Incisal edge, involved glands, age, menopause
4	2007	44	41	85	Chiang Mai, Thailand	Age, menopause
5	2008	10	226	236	Seoul, Korea	Incisal edge, involved glands, age, menopause
6	2009	40	161	201	Brazil	Incisal edge,involved glands, HIV infection
7	2009	16	227	243	Seoul, Korea	Incisal edge,HPV infection after six months of surgery
8	2010	43	309	352	France	Incisal edge,HPV infection after six months of surgery
9	2010	21	152	173	Hunan,China	Incisal edge,involved glands, menopause
10	2011	33	105	138	Brazil	Incisal edge, involved glands, HIV infection

Table II. *Analysis of high risk factors of persistence or recurrence after conization of CIN[OR(95% CI)].*

No.	Incisal edge	Involved glands	HPV infection six months after surgery	Age	Menopause	HIV infection
1	9.33 (5.10~17.06)	4.37 (2.03~9.43)		5.79 (3.31~10.14)		
2	3.49 (1.66~7.34)		153.5 (20.25~1164.09)	1.91 (0.83~4.40)		
3	3.89 (1.37~11.06)	1.73 (0.69~4.33)		2.74 (1.01~7.44)	2.65 (0.94~7.48)	
4				1.76 (0.73~4.23)	1.47 (0.61~3.53)	
5	3.45 (0.84~14.18)	1.92 (0.48~7.61)		3.30 (0.80~13.54)	0.81 (1.24~37.39)	
6	3.53 (1.65~7.54)	11.58 (4.37~32.13)				5.36(2.39~12.01)
7	2.03 (0.62~6.69)		18.28(5.55~60.20)			
8	3.48 (1.77~6.82)		43.67(21.19~90.02)			
9	4.41 (1.7~11.45)	6.09 (2.33~15.97)			3.61(1.42~9.20)	
10	2.94 (1.25~6.93)	11.43 (3.64~35.89)				4.17(1.72~10.10)

heterogeneity among studies, so the random effect model, Dersi-monian-Laird, was used for data combination, and statistical results are shown in Fig. 2. The OR value of combinative effect was 4.51 (95%CI 3. 01~6.74), P<0.00001, which showed that the rate of residue or relapse after conization of the involved glands groups was 4.51-fold higher than non-involved gland groups.

HPV infection six months after surgery

Three studies (8, 13, 14) reported relevant results regarding HPV infection six months after surgery and the rate of residue or relapse after conization. Heterogeneity test was p=0.17, which indicated that there was no heterogeneity among studies, so fixed effect model was adopted to combine and analyze the data (Fig. 3). The OR value of combinative effect was 43. 67 (95% CI 21. 19~90. 02), P < 0. 00001, whose difference was statistically significant and showed that the positive HPV infection six months after surgery groups had an obviously higher rate of residue or relapse after conization than the negative

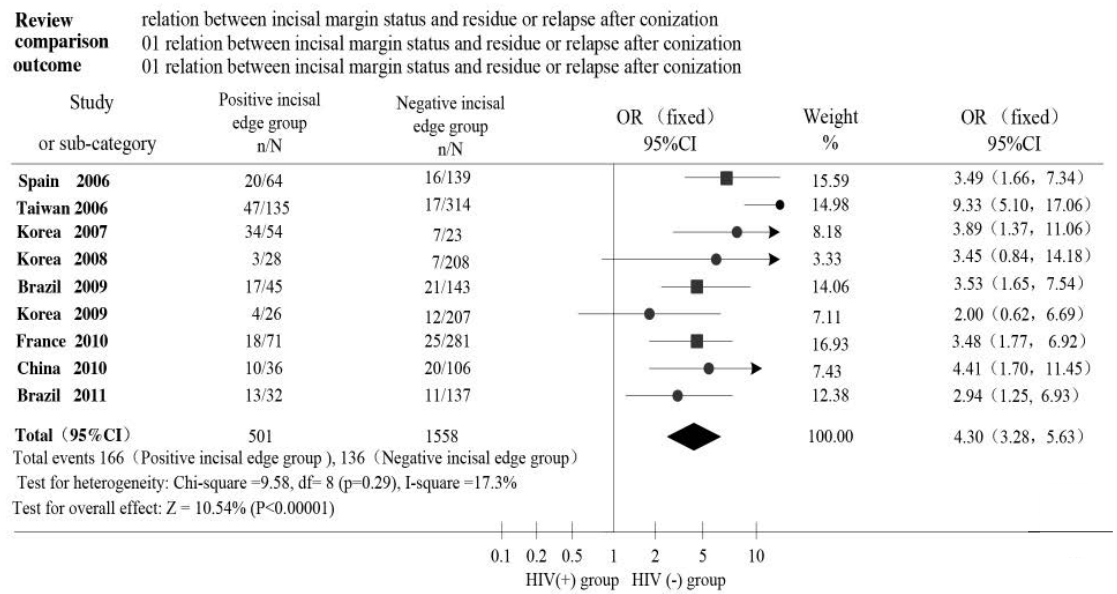

Fig. 1. *Relationship between incisal margin status and the residue or relapse rate after conization.*

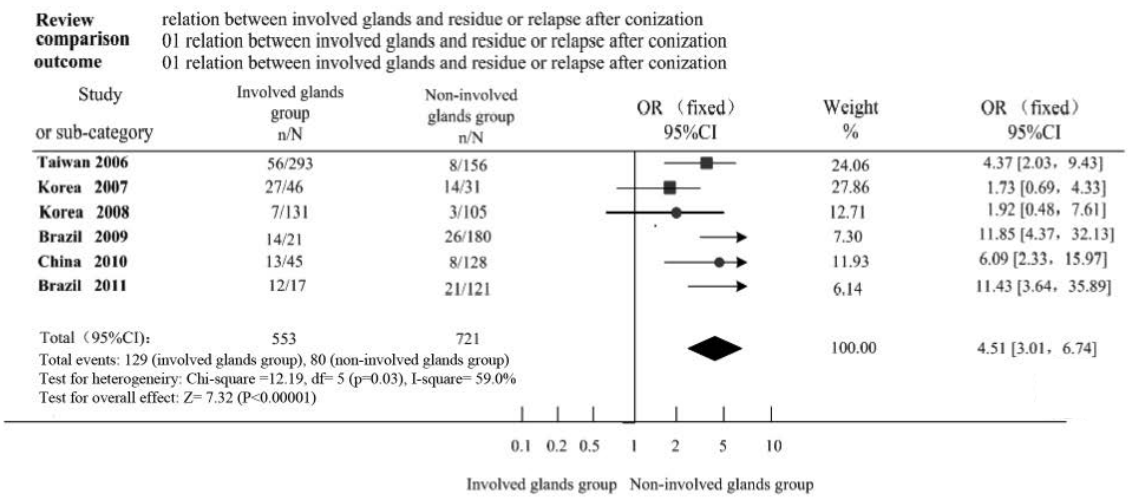

Fig. 2. *Relationship between involved glands and the rate of residue or relapse after conization.*

HPV groups.

HIV infection

Two studies (12, 16) reported relevant results regarding HIV infection and the rate of residue or relapse after conization. Heterogeneity test was p=0.68. which indicated that there was no heterogeneity among studies, so a fixed effect model was used to combine and analyze the data (Fig. 4). The OR value of combinative effect was 4.79 (95% CI 2. 64~8. 68), P < 0.00001, whose difference was statistically significant and showed that the positive

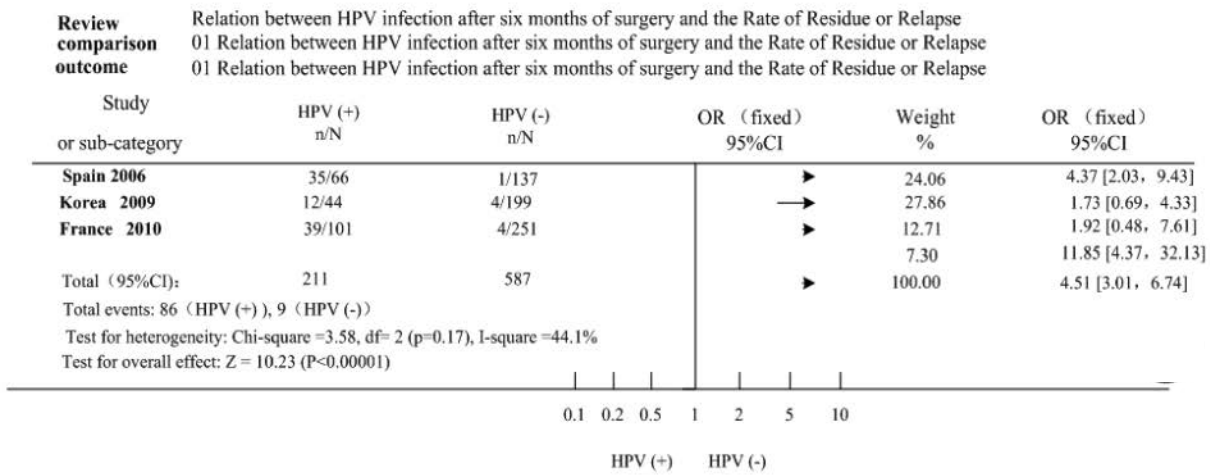

Fig. 3. *Relationship between HPV infection after six months of surgery and the rate of residue or relapse after conization*

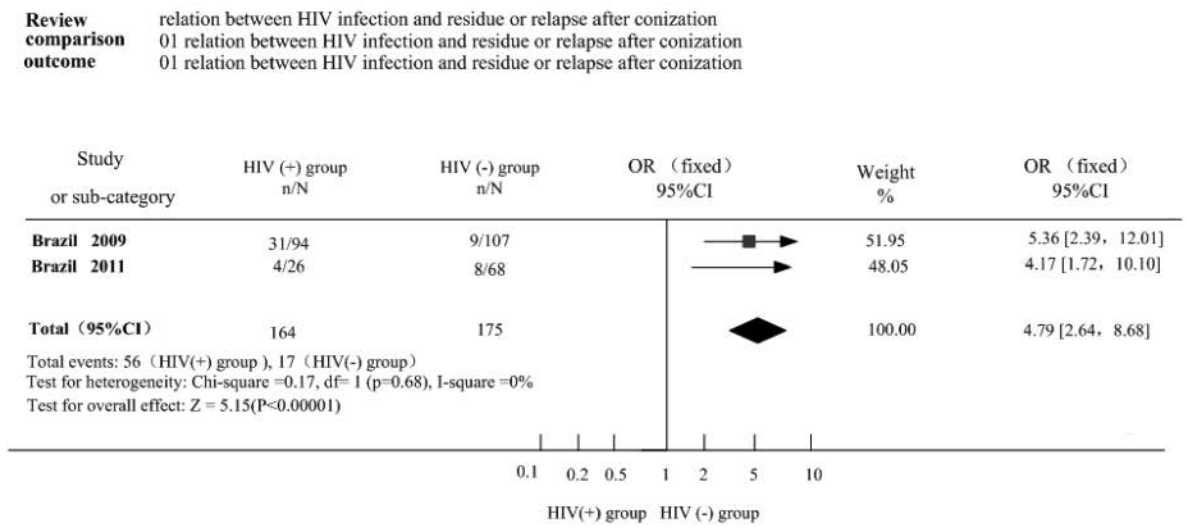

Fig. 4. *Relationship between HIV infection and the rate of residue or relapse after conization.*

HIV infection group had a higher rate of residue or relapse after conization than the negative HIV infection group.

Menopausal status

Four studies (9-11, 15) reported relevant results regarding the menopausal status and the rate of residue or relapse after conization. Heterogeneity test was p=0.34, which indicated that there was no heterogeneity among studies, so a fixed effect model was used to combine and analyze the data (Fig. 5). The OR value of combinative effect was 2.46 (95%CI 1. 45~4. 15), P = 0.0008, whose difference was statistically significant, indicating that the menopause groups had a higher rate of residue or relapse after conization than the premenopause group.

Age

Five studies (7-11) reported relevant results

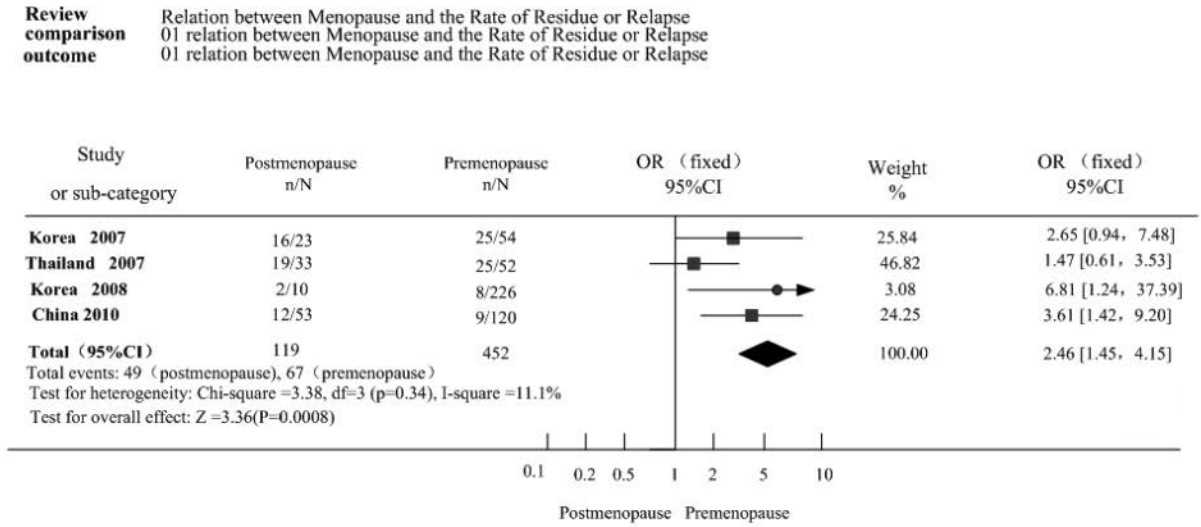

Fig. 5. R*elationship between menopause and the rate of residue or relapse after conization.*

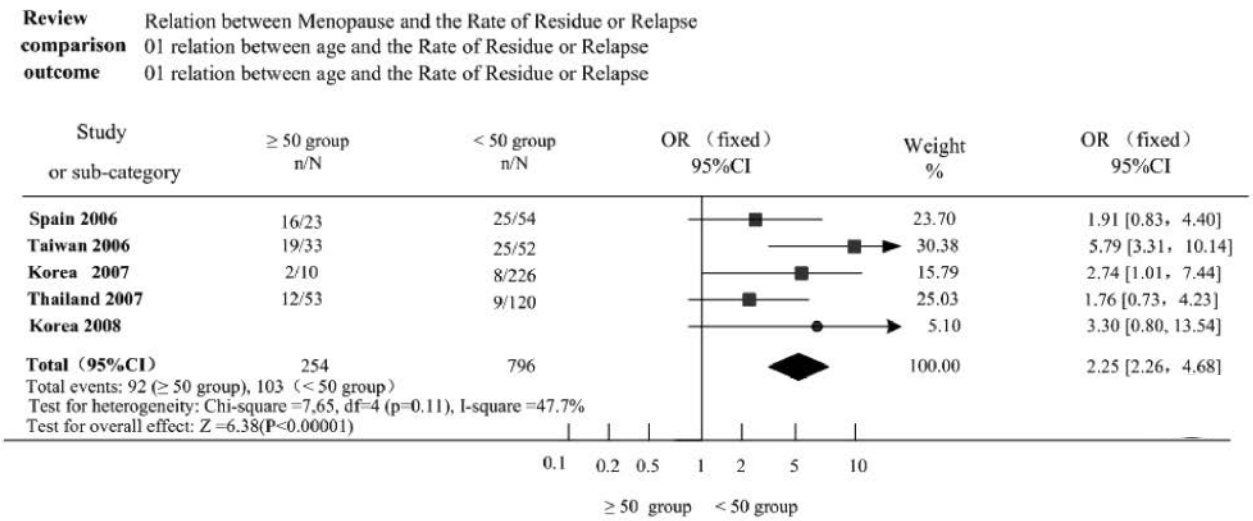

Fig. 6. *Relationship between age and the rate of residue or relapse after surgery.*

regarding age and the rate of residue or relapse after conization. Heterogeneity test was p=0.11, which indicated that there was no heterogeneity among studies, so a fixed effect model was used to combine and analyze the data (Fig. 6). The OR value of combinative effect was 3.25 (95% CI 2. 26~4.68), P <0.00001, whose difference was statistically significant, indicating that 50 year or older groups had a higher rate of residue or relapse after conization than under 50 years old groups.

DISCUSSION

CIN is a precancerous lesion that is closely related to invasive carcinoma of the cervix. CIN II/III patients after vaginoscopy tend to receive cervical conization treatment. The CIN II/III lesion residue or recurrence after surgery is the combined result of multiple factors as well as correlation among internal factors. Therefore, in the postoperative follow-up, the risk of individual disease progression can be predicted by synthesizing multiple high risk factors.

The ten studies included in this thesis had all conformed to the rigorous scientific requirements in design, object selection, sample size, time for follow-up, and reliable results. There was a meta-analysis on the high risk factors of residue or relapse after conization, and the results showed that positive incisal edge, involved glands, HPV infection six months after surgery, HIV infection, menopause and being over 50 years old are high risk factors of the residue or relapse after surgery.

The relationship between factors of positive incisal edge, involved glands, HPV infection six months after surgery, HIV infection, menopause, being over 50 years old and the CIN II /III lesion residue and recurrence after surgery was studied, and it was found that the OR value greatly differed between studies. General research methods do not easily achieve better results while a meta-analysis can evaluate the potential bias and sources of heterogeneity in studies and make a quantitative comprehensive assessment of results. Moreover, evaluation of the effect size (OR value) was improved and a comprehensive conclusion was reached.

Bias may occur while consulting the literature, such as sampling bias including searching bias, publication bias, etc. Owing to different inclusion criteria, there may be a selection bias in meta-analyses on the same subject, which may result in different conclusions.

Although there were confounding factors as bias, the conclusion reached by this meta-analysis still offers an overview of high risks of residue or relapse after conization in the past five years. It distinguishes groups with a high risk rate of residue or relapse in the postoperative follow-up suggests pertinent precaution and therapeutic measures. Sarian, et al. (17) found that in CIN II/III patients with lesion residue after treatment of LEEP, their specificity of cervical cell cytology six months after surgery can reach 81%, while the positive predictive value was only 32%. When detected by joint HR-HPV and cytology, the specificity reaches 96%, while its positive predictive value can reach 70% and negative predictive value 100%, which is significantly higher than single detecting. Hence, the cervical cytology test together with the HR-HPV test has a higher specificity and sensitivity, which would be an effective supervision method of the residue and relapse after conization of CIN II /III patients. The therapeutic HPV vaccine is still been in phase II of clinical trials, once it is used in clinic, it could prevent the recurrence of CIN II/III and cure the relapse of lesions, and could become the choice of high risk CIN II/III patients.

Owing to limited inclusive cases and bias within the study, the reliability of conclusions needs to be improved by more reasonable randomized controlled trials with strict design, multicenter and large samples.

REFERENCES

1. Zhang H. Analysis on relevant factors of relapse of cervical intraepithelial neoplasias after surgery. Liaoning, Dalian Med Uni 2013; 5-29.
2. Chen YM, Jin L, Chen HQ. Evaluation of clinical efficacy of different cervical conization in treatment of cervical intraepithelial neoplasia grade III. Contem Medi 2012; 18 (19):102-4.
3. Yang X, Qian DY. Relevant risk factors of residue and relapse after high-level conization of cervical intraepithelial neoplasia. Chin J Clin Obstet Gynecol 2011; 12(1):73-75.
4. Qu XF. Analysis on relevant factors of relapse of cervical intraepithelial neoplasias after conization. Inner Mongolia Med J 2012; 11(9):1319-21.
5. Zhou P, Wang QF. Meta-analysis on relevant factors of cervical intraepithelial neoplasia residual or recurrence after cervical conization. Chin J Pract Gynecol Obstet 2014; 30(7):546-52.
6. Deng YZ. Meta-analysis on high risk factors of relapse of cervical intraepithelial neoplasias after cervical conization. Chin Pract Med 2014; 9(36):105-6.
7. Lu CH, Liu FS, Kuo CJ. Prediction of persistence or

recurrence after conization for cervieal intraepithelial neoplasia III. Obstet Gynecol 2006; 107:830-35.
8. Alonso I, Tome A, Puig-Tintore LM. Pre-and post-conization high-risk HPV testing predicts residual/ recurent disease in patients treated for CIN2-3. Gynecol Oncol 2006; 103:631-36.
9. Park JY, Lee SM, Yoo CW. Risk factors predicting residual disease in subsequent hysterectomy following conization for cervical intraepithelial neoplasia (CIN) III and microinvasive cervical cancer. Gynecol Oncol 2007; 107:830-40.
10. Kietpeerakool C, Khunamornpong S, Srisomboon J. Cervical intraepithelial neoplasia II-III with endocervical cone margin involvement after cervical loop conization: is there any predictor for residual diseas? Obstet Gvnaecol Res 2007; 33:660-64.
11. Park JY, Lee KH, Dong SM. The Association of pre-onizationhigh-risk HPV load and the persistence of HPV infection and persistence/recurrence of cervical intraepithelial neoplasia after conization. Gynecol Oncol 2008; 108:549-54.
12. Lima MI, Tafuri A, Araujo AC. Cervical intraepithelial neoplasia recurrence after conization in HIV-positive and HIV-negative women. lnt J Gynecol Obstet 2009; 104:100-104.
13. Park JY, Bae J, Lim MC. Role of high risk-human papilloma virus test in the follow-up of patients who underwent conization of the cervix for cervical intraepithelial neoplasia. J Gynecol Oncol 2009; 20:86-90.
14. Lequevaque P, Motton S, Decharme A. Predictors of recurrence in high-grade cervical legions and a plan of management. Eur Surg Onco1 2010; 36:1073-79.
15. Mao YZ. Analysis of Recurrence after conization of cervical intraepithelial neoplasia. Chin Med Herald 2010; 7:32-33.
16. Lodi CT, Michelin MA, Lima MI. Factors associated with recurrence of cervical intraepithelial neoplasia after conization in HIV-infected and non-infected women. Arch Gvnecol Obstet 2011; 284:191-97.
17. Sarian LO, Derchain SF, Andrade LA. HPV DNA test and pap smear in detection of residual and recurrent disease following loop electro-surgical excision procedure of high grade cervical intraepithelial neoplasia. Gynecol Oncol 2004; 94:181-86.

JOURNAL OF BIOLOGICAL REGULATORS & HOMEOSTATIC AGENTS Vol. 29, no. 2, 459-464 (2015)

LETTER TO THE EDITOR

PROTEIN EXPRESSION OF METADHERIN AND SENSIBILITY OF BREAST CANCER MDA-MB-231 CELLS TO TREATMENT BEFORE AND AFTER TRANSFECTION

H. ZHAO[1,2], QT. WANG[2], SQ. GENG[3], J. XU[3], YZ. YU[2] and ZG. YU[1]

[1]Department of Breast Disease, the Second Hospital of Shandong University, Jinan, China; [2]Department of Breast Disease, the Second Affiliated Hospital of Qingdao University Medical College, Qingdao, Chin; [3]Department of Pathology, the Second Affiliated Hospital of Qingdao University Medical College, Qingdao, Shandong, China

Received February 3, 2015 – Accepted May 7, 2015

Breast cancer tends to have an increasing mortality, severely threatening the health of females. The invasion and metastasis of breast cancer are the leading causes of death. It has been reported that breast cancer is caused by the activation of a series of proto-oncogenes and inactivation of anti-oncogenes. In the present study, Real-time PCR and Western blot were used to detect the protein expression level of metadherin before and after transfecting MDA-MB-231 cells to identify the effect, while the sensitivity of MDA-MB-231 cells to 1 mg/L doxorubicin and 8mg/L taxol was measured by methylthiazolyldiphenyl-tetrazolium bromide (MTT). The results demonstrated that mRNA and protein expression level of metadherin both improved after transfection. The inhibition effect of 1 mg/L doxorubicin and 8 mg/L taxol on breast cancer cells decreased after transfection. Detected by flow cytometry, the apoptosis rate of breast cancer cells was 39.68±0.42%, 20.64±0.55%, respectively, under the effect of 1 mg/L doxorubicin; while under the effect of 8 mg/L taxol, the rate was 24.89±0.41% and 13.8±0.63%, respectively. Thus the inhibition effects of 1 mg/L doxorubicin and 8mg/L taxol to breast cancer cells and their effects on apoptosis were different, and the differences were statistically significant (P<0.05). Based on the statistics on the expression level of metadherin after transfecting breast cancer cells MDA-MB-231 and the exploration of the sensitivity of the cells to treatment, the effect of metadherin on breast cancer MDA-MB-232 cells was proved.

Breast cancer is one of the most frequent malignant carcinoma for females, with an annual increase of 1.3 million females, according to the statistics at the end of the 20th century (1-4). Breast cancer is a systemic malignant disease, and the invasion and metastasis of tumor cells are the leading cause of death. According to related studies, metadherin, a proto-oncogene, has no or low expression in normal tissues but high expression in endocrine tissues such as cardiac muscle, thyroid, skeletal muscle and adrenal glands. A delayed response gene infected by HIV-1 or treated by recombination HIV-1 capsid protein (gp120) was first reported in 2002 (5), following the successful clone of full-length cDNA by the joint effort of four separate study groups (6, 7). In 2004, scientists found the lung homing domain which can regulate lung metastasis of mouse mammary cell 4T1 by means of phage

Key words: breast cancer MDA-MB-231 cells; metadherin gene, MTT assay, FCM, chemosensitivity

Mailing address: Dr Zhigang Yu,
Department of Breast Disease,
the Second Hospital of
Shandong University,
247#, Beiyuan St, Tianqiao District,
Jinan, 250033, China
e-mail: yzg@ibhsedu.com

0393-974X (2015)

DISCLOSURE: ALL AUTHORS REPORT NO CONFLICTS OF INTEREST RELEVANT TO THIS ARTICLE.

display screening and named it Metadherin. Kang, along with other colleagues, was the first to clone the full-length sequence of metadherin and analyze its structure. Metadherin is composed of 86082 bases, including 12 exons and 11 introns, while cDNA is made up of 3611 bases (not including poly-A) which code a single transmembrane protein with molecular weight of 64KD. Metadherin plays a prominent part in regulating progress of tumor including cancerization, apoptosis, invasion and metastasis, drug resistance and angiogenesis, thus it is regarded as a potential tumor therapeutic target. Furthermore, metadherin expresses highly in multiple tumor cells such as liver cancer, non-small cell lung cancer, melanoma, malignant neuroglioma, neuroblastoma, esophageal carcinoma, breast cancer, carcinoma of prostate and carcinoma of gallbladder (8, 9). Liu et al. (10) found that metadherin highly expressed in cells and tissues of glioma could improve its own expression by acting on the matrix metalloprotein-9 (MMP-9) promotor and further enhance the ability of invasion of glioma cells. Wang et al. (11) found that metadherin plays an important role in the development of tumor, including promoting the proliferation, invasion and metastasis, avoiding the apoptosis and producing resistance against chemotherapy treatment. In addition, they also found that metadherin could promote the incidence and progress of tumor by activating the signal pathway of NF-KB, PI3K/AKT, MAPK and wnt/β-catenin. This study made a comparison between the protein expression of metadherin before and after transfecting breast cancer cells MDA-MB-231, then discussed the relationship between them and finally further explored the sensitiveness of breast cancer cells MDA-MB-231 to treatment before and after transfection

MATERIALS AND METHODS

Human Breast cancer MDA-MB-231 cells were all bought from the cell bank of the Institute of Biochemistry and Cell Biology, Chinese Academy of Sciences (CAS), China. All cells were placed in 5 mL RPMI 1640 medium of containing 10% fetal calf serum (FCS) at 37°C with 5% CO_2.

Main reagents: TransStart Top Green qPCR Supermix (Transgen BIotech, China); Reverse transcription kits (ThermoFisher Scientific Company, China); metadherin monoclonal antibody against human metadherin (Invitrogen, USA); methyl thiazolyl tetrazolium (MTT) (Sigma Inc., USA); RPMI1640 and FCS without mycoplasma (Shijiazhuang Bosheng Chemical Reagent Co. Ltd., China); Doxorubicin (Zhejiang Hisun Chemical Co. Ltd., China); isopropanol, Trichloromethane, Pancreatin, Phosphate Buffered Saline (PBS), Dimethyl sulfoxide (DMSO) and 75% Ethanol (the Fourth Hospital of Hebei Medical University, China); OPTI medium and Lipofectamine 2000 transfection reagent (Invitrogen Inc., USA).

Cell culture

Cells were placed in 5 mL RPMI 1640 containing 10% PCS in a sterile culture flask which was placed in an incubator containing 5% CO_2 at 37°C and the culture liquid was changed every one or two days; cells in a good state were selected and subcultured when 90% of the flask bottom was covered; after removing the supernatant, the cells were rinsed with 2 mL PBS and then added with 0.75% pancreatin to immerge all cells; as observed by microscope, the digestion was completed when cells became round and the gap increased; 3 or 4 mL RPMI 1640 culture liquid was placed in the incubator containing 5% CO_2 at 37°C and then subculture was performed every 2-3 days.

Plasmid amplification, extraction and transfection

Kanamycin was added to lysogeny broth (LB) medium (500 mL/flask), and the concentration of the liquid was adjusted to 25 μg/ml. A quantity of 50 μl DH5α *Escherichia coli* was added with 4 μl (0.5 μg/ μl) metadherin plasmid and 500 μl LB medium without antibiotics. The cells were shaken at 200 rpm at 37°C for 1-1.5 h. All the above liquid was added to 500 ml LB fluid nutrient medium containing antibiotics. The liquid was then shaken at 200 rpm at 37°C for 12-16 h, and afterwards centrifuged at 8000 rpm at 4°C to extract plasmid. A quantity of about 0.2-0.6 million cells (cell amount was determined by the size and growth speed of cells) was cultured in a 6-well plate for 24 h. Plasmid transfection was performed once the cells covered 70-80%. The cells were then incubated for 5-6 hour culture. After nutrient solution containing Lipofectamine 2000-DNA was removed, every well was added with 2 ml fresh nutrient for continuous culture. Forty-eight hours later, transfection was detected.

Detection of metadherin expression in breast cancer cells before and after transfection by real-time PCR

Breast cancer cells with a good growth were selected. After the medium was removed, the cells were rinsed twice by PBS. Then 1 ml Trizol reagent was added to the culture flask to extract RNA from cells. OD260/280 of RNA

detected was between 1.8-2.0 and RNA concentration was between 980-1100 ng/μg. Then 5 μg RNA was taken for reverse transcription. Real Time amplification of breast cancer MDA-MB-231 cells was detected by SYBGGreenI kit according to the manufacturer's instructions.

Detection of protein expression of metadherin before and after transfection by Western blot

When the cells covered 70-80%, a nutrient solution without fetal calf serum was used and an equal quantity of plasmid mixing liquid was added. After 4-6 h culture, the nutrient solution was removed. The cells were collected after culture with nutrient solution containing 10% fetal calf serum for 48 h. Non-transfection cells were taken as controls. A quantity of 20 μl protein standard substance (25mg/ml) was taken and diluted with 0.9% NACl. Then the standard substance was added to a 96-well plate in quantities of 0, 1, 2, 4, 8, 12, 16, 20 μl, and standard dilution buffer was added until the quantity reached 20 μl. The plate was added with 200 μl BCA working fluid and left at 37°C for 20-30 min. A562 was detected at a wavelength between 540-595 nm. Protein concentration of the sample was calculated based on standard curve. After SDS-PAGE electrophoresis and transmembrane, immune color developing was carried out. Gel image analysis system was used to scan bands to obtain gray value, and the results were analyzed by semi-quantitative method. Relative expression quantity of target gene was expressed by the ratio of gray value of target gene and gray value of β-actin.

Detection of sensitivity of breast cancer cells to chemotherapy treatment before and after transfection by MTT assay

Cells were taken in logarithmic phase; medium was added according to the condition of cells and then the number of cells was measured by cell counter; the cellular suspension concentration was adjusted to 1000-10000/well; 32 wells of a 96-well plate were filled with sterile PBS so that cells could be evenly distributed in the incubator at constant 37°C with 5% CO_2 till the bottom of the wells were spread with a monolayer of cells; then 1 mg/L Doxorubicin and 8 mg/L Taxol were added respectively until every well reached 100 μl. Another nine wells were set as controls. The control wells were added with medium of the same amount without chemotherapeutic drugs. Culture was continued for another 4 h after adding 10 μl MTT solution (0.5%) into every well. 100 μl DMSO was added and the solution was shaken on a table concentrator at low speed for 10 min. Light absorption value of every well was measured by enzyme-linked immunometric meter at OD 490 nm and the inhibition rate was also calculated. Next, MDA-MB-231 cells in logarithmic phase were selected and digested with 0.25% pancreatic enzymes. After counting, RPMI-1640 nutrient solution containing 10% fetal bovine serum was added for cell suspension with a concentration of 2.5×10/ml. Then the cell suspension was transferred into a six-well plate, 2 ml each well, and cultured at 37°C with 5% CO_2 for 18-24 h. When cells grew 80- 90% and were evenly distributed, they were added with different treatment factors for reaction. Cells were collected finally as the reaction finished and then placed on the device for detecting cell apoptosis rate.

Statistical analysis

Statistical analysis was performed by SPSS 18.0 software and all data was expressed as mean ± standard deviation. For data in the two groups before and after transfection, the average was compared by *t*-test. A p value of less than 0.05 was considered to be statistically significant.

RESULTS

Detection of protein expression of metadherin in breast cancer MDA-MB-231 cells before and after transfection

Through detecting the protein expression of 0.8 μg metadherin gene with real-time PCR and Western blot before and after 48-hour transfection, it was found that the expression of mRNA of metadherin was 1.00±0.00 before the transfection and 3.25±0.02 after 48-hour transfection while the expression of protein in metadherin was 0.46±0.05 before transfection and 1.24±0.07 after transfection. Statistical analysis showed that there was a significant difference between the gene and protein expression of breast cancer before and after transfection, and the difference between the two groups was considered to be statistically significant ($p<0.05$) (Fig. 1).

Detection of chemosensitivity of breast cancer MDA-MB-231 cells to doxorubicin

By MTT, the inhibition ratio of breast cancer cell under the effect of 1mg/L doxorubicin was 60.69±0.02% before transfection and 41.92±0.03% after 24-hour transfection. Detected by flow cytometry, the apoptosis rate of breast cancer cell under the effect of 1mg/L doxorubicin was 39.68±0.42% before transfection and 20.46±0.55% after 24-hour transfection. Statistical analysis showed that there was a statistically significant

Table I. *Inhibition and apoptosis ratio of doxorubicin for breast cancer cells before and after transfection.*

Doxorubicin	Inhibition Ratio	Apoptosis Ratio
Before transfection	60.69±0.02%	39.68±0.42%
After transfection	41.92±0.03%	20.64±0.55%

Table II. *Inhibition and apoptosis ratio of taxol for breast cancer cells before and after transfection.*

Taxol	Inhibition Ratio	Apoptosis Ratio
Before transfection	57.68±0.38%	27.89±0.41%
After transfection	40.89±0.02%	13.88±0.63%

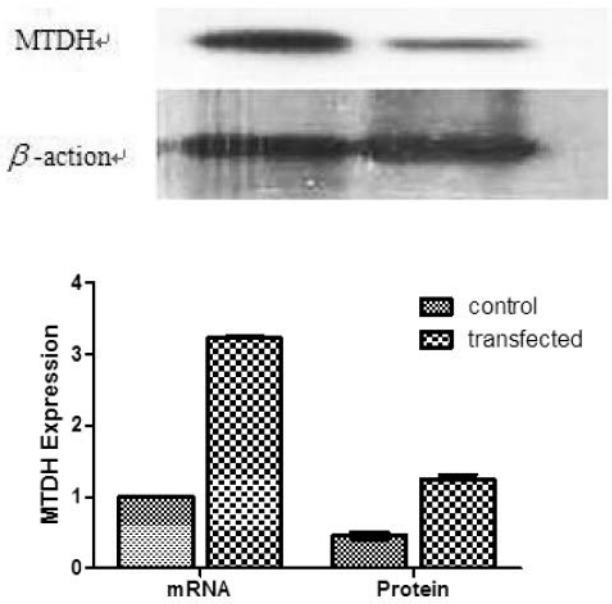

Fig. 1. *mRNA and protein expression of metadherin before and after transfection.*

difference between the inhibition and apoptosis ratio of breast cancer cells under the effect of doxorubicin before and after transfection ($p<0.05$) (Table I).

Detection of chemosensitivity of breast cancer MDA-MB-231 cells to taxol

Through MTT, the inhibition ratio of breast cancer cell under the effect of 8mg/L taxol was 57.68±0.3% before transfection and 40.89±0.02% after 24-hour transfection, while the apoptosis rate of breast cancer cell was 24.89±0.41% before transfection and 13.88±0.63% after 24-hour transfection, which showed that there was a statistically significant difference between the inhibition and apoptosis ratio of breast cancer cells under the effect of taxol before and after transfection ($p<0.05$) (Table II).

DISCUSSION

Breast cancer occurring among females has had an increasing incidence in recent years. It is one of the most frequent diseases threatening the health of

all populations. However, the traditional therapy is mostly surgery excision, but patients are likely to suffer mental problems as well as poor prognosis after surgery. Neoadjuvant chemotherapy carried out before surgery has been the leading therapy for advanced breast cancer (12). This method is able to reduce the pathological staging of cancer tissues, render surgery much easier and improve the success rate of breast-conserving surgery. A wealth of studies have proved that the incidence and development of breast cancer is a complex process, involving the transformation of several genes. Gene therapy has become a new approach and focus of research for breast cancer treatment, including oncogene therapy, anti-oncogene therapy, immunogene therapy, multidrug resistance gene therapy, suicide gene therapy, antiangiogenesis therapy, miRNA therapy and joint gene therapy (13).

Metadherin, i.e., the metastatic adhesive gene/protein, was named astrocyte elevated genel (AEG-1) when it was first discovered in the initial human embryo astrocyte in patients affected by HIV-1 virus. Many studies revealed that metadherin was expressed highly in several malignant tumors, such as breast cancer, liver cancer, and cerebral glioma. It is considered as an oncogene as is closely related to several malignant biological behaviors, such as proliferation, metastasis, angiogenesis and drug resistance. Metadherin expressing in cytoplasm, cell membrane and nucleus produces effect by taking part in the regulation of several signal pathways, including PI3K/AKT and NF-KB (14). Du et al. (15) found that metadherin as an oncogene played an important role in the incidence and development of breast cancer, and artificial intervention of metadherin can effectively control the malignant biological behaviors of breast cancer cells.

This study transfected the eukaryotic expression carrier pCMV6-ENTRY carrying metadherin into the cell strain of breast cancer MDA-MB-231 using cation liposome transfection. Forty-eight hours after transfection, the mRNA and protein expression of metadherin in MDA-MB-231 cells was detected by real-time PCR and Western-blot. Results revealed that the mRNA and protein expression in transfected cells was higher than that non-transfected cells ($p<0.05$) and the expression product of metadherin was acquired finally, providing some experimental technology support for further studies on metadherin. Furthermore, it was confirmed that pCMV6-ENTRY-mediated metadherin could successfully transfect the MDA-MB-231 cells and obtain target proteins.

To date, the specific chemosensitive gene of solid tumor has still not been discovered. However, a number of genes relating to the proliferation and apoptosis of tumor is in correlation with the sensitivity of tumor cells to chemotherapy treatment. At the same time, several chemotherapy treatments are able to induce the apoptosis to some extent. The sensitivity of tumor cell apoptosis appears to be an important factor affecting the chemotherapy result (13). In this study the apoptosis ratio was detected by flow cytometry of the breast cancer MDA-MB-231 cells under the effect of 1mg/L doxorubicin and 8mg/L taxol 24 h before and after transfection, and statistical analysis showed that this ratio had a statistically significant difference ($p<0.05$).

Metadherin is considered as an efficient target gene with high potential as a new treatment for breast cancer. This study improved the expression of mRNA and proteins in breast cancer cell by MDA-MB-231 transient transfected by metadherin. Comparing the sensitivity of MDA-MB-231 to adriamycin and taxol before and after transfection, we found that the high expression of MDTH may be linked with drug resistance of breast cancer cell to adriamycin and taxol. The higher the expression of metadherin, the lower the inhibition rate and apoptosis rate of adriamycin and taxol to MDA-MB-231. However, the specific mechanism of the influence of metadherin on the chemosensitivity of tumor cell remains to be studied further. The research carried out in this study may be of help for future targeted therapy or chemotherapy of breast cancer genes.

REFERENCES

1. Ma XQ, Deng XJ, Chen H, Pan YY. Clinical analysis of treating 34 breast cancer patients with modified radical mastectomy. Contemporary Medi 2011; 17(6):2-3.
2. Li N, Zheng RS, Zhang SW, et al. Analysis and prediction of breast cancer incidence trend in China. Chinese J of Preventive Medicine 2012; 46(8)703-7.
3. Zheng Y, Wu CX, Wu F. Status and trends of breast

cancer mortality in Chinese females. Chinese J of Preventive Medicine 2011; 45(2):150-54.
4. Liang JL, Feng JF, Yang Y, Ma CL, Li X. The clinical efficacy comparison of conserving therapy and modified radical mastectomy in the treatment of early breast cancer. China Medical Herald 2011; 8(5):14-16.
5. Li J, Zhang N, Song L B, et al. Astrocyte elevated gene-1 is a novel prognostic marker for breast cancer progression and overall patient survival. Clinical Cancer Research 2008; 14(11):3319-26.
6. Wang L, Wang J. MicroRNA-mediated breast cancer metastasis: from primary site to distant organs. Oncogene 2012; 31(20): 2499-511.
7. Martinez I, Cazalla D, Almstead LL, et al. miR-29 and miR-30 regulate B-Myb expression during cellular senescence. Proceedings of the National Academy of Sciences 2011; 108(2):522-27.
8. Wang Z, Liang QM. Discussion over the relation between metadherin gene and breast cancer. China & Foreign Medical Treatment 2013; (9):182-83.
9. Liu ZZ, Cao H, Ding ZY, Du C, Wang L, Han YL, Xie XD. Mechanism research on influence of down-regulating metadherin gene expression in breast cancer cell metastasis. Chinese J of Cancer Prevention and Treatment, ISTIC 2014; 21(8).
10. Liu L, Wu J, Ying Z, et al. Astrocyte elevated gene-1 upregulates matrix metalloproteinase-9 and induces human glioma invasion. Cancer Research 2010; 70(9):3750-59.
11. Wang QM, Xie XD. Progress in research of metadherin and its relation with tumors. Chinese J of Cancer Prevention and Treatment 2011; 18(14):1138-40.
12. Xu WY, Yang W. Progress in treatment of breast cancer. J of Naval General Hospital 2012; 24(1):29-33.
13. Liu XH, Shui QL. Study on gene therapy for breast cancer. Modern Diag & Treatment 2011; 1:013.
14. Yoo BK, Emdad L, Lee SG, et al. Astrocyte elevated gene-1 (AEG-1): a multifunctional regulator of normal and abnormal physiology. Pharmacol Ther 2011; 130(1):1-8.
15. Du C, Liu ZZ, Ding ZY, Guo F, Ma DC, Xie XD. Influence of metadherin gene down regulation on proliferation and apoptosis of human breast cancer SK-BR 3 cells. J of Endocrine Surg 2013; 7(5):359-63.

JOURNAL OF BIOLOGICAL REGULATORS & HOMEOSTATIC AGENTS Vol. 29, no. 2, 465-470 (2015)

LETTER TO THE EDITOR

EFFICACY OF DIFFERENT RESECTIONS ON NON-MUSCLE-INVASIVE BLADDER CANCER AND ANALYSIS OF THE OPTIMAL SURGICAL METHOD

GF. CHEN, TP. SHI, BJ. WANG, XY. WANG and Q. ZHANG

Department of Urology, the General Hospital of the Chinese People's Liberation Army, Haidian, Beijing, China

Received January 29, 2015 – Accepted May 6, 2015

This study aimed to analyze the clinical efficacy of different resections in treating non-muscle-invasive bladder cancer (NMIBC), including partial cystectomy, transurethral resection of bladder tumor (TURBT) and holmium laser resection of bladder tumor. Two hundred and sixteen patients were recruited with NMIBC who were available for follow-up visits in hospital, including 62 cases treated with partial cystectomy, 90 cases treated with TURBT and 64 cases with holmium laser resection. Analysis was made on the cases with tumor relapse in the two years, on operation time, blood loss, time for indwelling urinary catheter, hospital stay and complications after operation. Results were compared to the clinical efficacy of these operation patterns. It was found that the two-year relapse rate for TURBT group, partial cystectomy group and Holmium laser resection group was 41%, 31%, and 33% respectively, and the difference had no statistical significance ($p>0.05$). Both the TURBT group and holmium laser resection group had shorter operation time, hospital stay and time for indwelling urinary catheter as well as much less blood loss when compared with the partial cystectomy group; the difference had statistical significance ($p<0.001$). In terms of complications, the TURBT group was likely to induce obturator nerve reflex and bladder perforation while the partial cystectomy group was likely to induce bladder spasm. Therefore, this study presumes that holmium laser resection and TURBT are much safer and quicker for recovery and obviously superior to the partial cystectomy.

With the changes in diet, lifestyle and the public working environment, there is a higher incidence of bladder cancer and patients tend to be much younger. However, bladder cancer is likely to suffer relapse, and leaves serious physical and mental pressure on the patients and their families (1). Based on tumor pathological grading, a proper operation pattern can effectively promote the recovery for patients, and reduce the relapse of tumor.

W. Ping, et al. made a comparison between clinical data from 52 patients with muscle-invasive bladder cancer treated with the combination of partial cystectomy with chemotherapy and the total survival rate of 47 patients treated with radical bladder resection simultaneously. It made a statistical analysis of the related influencing factors and their application value. This study showed that partial cystectomy combined with chemotherapy could serve as an effective operation pattern for treating invasive bladder cancer for patients with high selectivity (2). Bladder cancer ranks the second common malignant tumor in the uro-genital system.

Key words: Non-muscle-invasive bladder cancer, operation pattern, clinical efficacy

Mailing address:
Guangfu Chen, MD. PhD
Department of Urology,
The General Hospital
of the Chinese People's Liberation Army,
No.28, Fu-xing Road, Beijing, 100853 China
e-mail: cgf@ibhsedu.com

0393-974X (2015)

Therefore X. Shuxiong, et al. made a retrospective analysis of patients with non-muscle-invasive bladder cancer (NMIBC) treated with transurethral resection of bladder tumor (TURBT) in recent years and made a comparison between 2 μm laser group and bipolar electrotome group in operation time, complications, hospital stay after operation and rate of relapse. It reached the conclusion that compared with bipolar electrotome, 2 μm laser was safer and more effective in treating NMIBC and had fewer complications (3). Presently the traditional therapy still fails to cure all patients with bladder cancer. Both the chemotherapy medicine perfusion into bladder and treatment with immunosuppressant has failed. W. Hua, et al. raised a large number of preclinical and clinical studies so as to prove the security and efficacy of oncolytic adenovirus perfusion into bladder to treat bladder cancer. Moreover, they made a discussion over the feasibility of intravenous administration in treating muscle-invasion or metastasis bladder cancer (4).

In recent years, there were a total of 327 patients with NMIBC who were operated on in our hospital but only 216 patients were available for follow-up visit.

MATERIALS AND METHODS

We report the clinical efficacy of three different operational patterns carried out on 216 patients with NMIBC who were admitted to our hospital and consequently followed-up.

Inclusion criteria: 1) patients whose tumor location, size and quantity were confirmed by urinary system color Doppler ultrasound, intravenous pyelography, Computed Tomography (CT), cystoscopy and were pathologically diagnosed with non-muscle-invasive bladder cancer; 2) patients with first-time attack; 3) patients who had no severe heart and lung disease and could tolerate surgery.

Exclusion criteria: patients who had blood coagulation disorders, severe liver and kidney function deficiency or chronic and acute infections.

Based on the above criteria, the 216 patients were divided into three groups. In the partial cystectomy group, there were 42 males and 20 females ranging in age from 22 to 75 years (mean 63 years). In the second group, there were 20 patients with tumor within 2 cm around the ureteral orifice, 4 with tumor at the posterior wall, 16 at sidewall, 4 at the top part, and 18 at the anterior wall. In the TURBT group, there were 68 males and 22 females ranging in age from 20 to 82 years (mean 65 years). Thirty-six patients had tumor at the sidewall, 4 at the anterior wall, 44 at the posterior wall and 6 at the triangle. In the holmium laser resection group, there were 48 males and 16 females ranging in age from 18 to 81 years (mean 61years). Thirty patients had tumor at the sidewall, 10 at the anterior wall, 10 at the top part, 2 at the triangle, and 12 at the posterior wall. The study was carried out at the General Hospital of the Chinese People's Liberation Army, and all the patients signed the informed consent. All patients received the cystoscopic biopsy before the operation. Based on the WHO bladder pathological grading 2004 and International Anti-cancer Association 2002, there was no statistical significance among these three groups in TNM staging, number and size of tumor ($p>0.05$), as shown in Table I.

Operation methods

After successful Continuous Epidural Anesthesia (CEA) (5), the patients in the TURBT group were placed in lithotomy position. German R-WOLF resectoscope annular cutting electrode and the matching supervising system with 160W of resection and 60W of coagulation was applied; 1.5% glycine as irrigation fluid was taken and the bladder capacity within 150 mL was controlled to observe size, number and distance from ureteral orifice of the tumor. Small-sized tumors were resected together with partial bladder walls of their bases through to the deep muscle. Tumors of larger size were resected gradually above the surface of the bladder and at the bases. The resected bases should include the deep muscle of the bladder wall. The healthy bladder wall tissues were resected within 2 cm around the tumor.

After successful CEA in the holmium laser, patients in resection group were placed in lithotomy position. This study applied the Holmium laser machine equipped with 365 μm or 550 μm holmium laser of end lasing type and the laser power was set between 15 W and 40 W (the exported energy between 0.5 and 1.5J, frequency between 20 and 30 Hz). Optical fiber was fixed on n. 5 catheter. Tumors less than 1 cm in size were directly vaporized and tumors over 1cm in size were resected with holmium laser, which not only cuts off the blood supply in the tumor body to reduce blood loss, but also clarifies the pathology. Vaporization was then carried out by aiming at the bases of the tumor and the healthy bladder wall tissues within 2 cm around the tumor by optical fiber until the muscle in the bladder wall was in sight. The Fr20-22 catheter was located after the operation bladder irrigated. Open operation was selected for tumors within a 2 cm distance from the ureteral orifice with wide bases and a high grade. On the partial bladder cystectomy group median incision of lower abdomen was applied to open the bladder; the healthy bladder wall within 2 cm around

the tumor was resected; tumor within a 2 cm distance from the ureteral orifice together with ureter was resected; ureter was again built in with indwelled Double-J, and pulled out one month later; surgical field was soaked in distilled water for 5 min and the incisions in bladder sewn up with 0~1 self-absorbent string; Patients in these three groups were all treated with Shenzhen Wangle Pirarubicin (theprubicine, THP) in single dose of 10 mg per bottle and 30 mg plus 5% GS30 mL and received bladder irrigation once. All patients changed their body position once every ten minutes and excreted the perfusion liquid every 40 min. In the first eight weeks, one perfusion was carried out. For the following 2 years perfusion is carried out once a month. All patients were invited to come back to hospital every 3 months in the first two years post-operation, every 6 months in the 3rd year and once a year from the 5th year on.

Clinical efficacy

Based on statistical comparison of cases of relapse, operation time, blood loss, time of indwelling ureter, hospital stay and post-operation complications among these three operation patterns in two years, this paper also analyzed the benefits and weaknesses of these three patterns respectively.

Statistical analysis

Statistical analysis was performed by SPSS 17.0 software and all measurement data in normal distribution was expressed by mean ± variance. Comparison between every two groups was carried out by LSD-t test and comparison in measurement data among these three groups was carried out by variance analysis. Numeration data was inspected by the chi-square test and the standard of test was as follows: if $p<0.05$, the difference was of statistical significance.

RESULTS

The three groups all completed the operation. The difference of operation time, blood loss and time of indwelling ureter and hospital stays between these groups was analyzed by variance, and the difference was quite obvious. The TURBT group and Holmium laser resection group had more benefits than the partial cystectomy group and the difference was of statistical significance (Table II).

Of 327 patients with NMIBC, 216 were available for follow-up visits: 62 patients were treated with partial cystectomy, of whom 19 suffered relapse in two years; 37 patients were treated with TURBT, of whom 37 suffered relapse within two years; 64 patients were treated with holmium laser, of whom 21 suffered relapse within two years. The difference in 2-year relapse rate among these groups was of statistical significance ($p>0.05$). Fifteen patients had obturator nerve reflex and 6 had bladder perforation in the TURBT group, but they could still successfully finish the operation. Ureter was kept in the body of 6 patients with perforation indwelled for 7 to 10 days. The partial bladder cystectomy had a higher rate of spasms than the other two groups (6), and the difference was of statistical significance (Table III).

DISCUSSION

NMIBC makes up 75%-85% of primary bladder tumor (7), among which Ta makes up 70%, T1 makes up 20% and Tis makes up 10% (8). Partial cystectomy, TURBT and Holmium laser resection are common operation patterns for NMIBC. However, bladder tumor is a multi-centric disease in time and space and is susceptible to relapse. Therefore, a proper operation pattern based on the patients' conditions is of great clinical significance to promote the recovery and reduce relapse and development of tumor. The holmium laser is 2.1μm in length, which lies within the absorption range of water, producing a low rate of injuries to the surrounding tissues. It is 0.4 mm deep which means high precision in resection. Resection and homeostasis can be carried out simultaneously. There is a clear surgical field, less pain for patients and a quicker recovery. Energy produced by the holmium laser enables the water between the terminal end of optical fiber and stone to vaporize and promotes the formation of tiny vacuoles.

TURBT is both the important diagnosis method for NMIBC (9), and the major operation pattern. It can not only resect the tumor but also resect the tumor bases and healthy partial bladder walls surrounding the tumor through to the deep muscle which is beneficial for tumor grading and staging and is able to establish a diagnosis. The drawback is the requirements of a very high standard of skilled operators. The simultaneous resection of complicated hyperplasia of the prostate can not only shorten the residence time of cancer-causing matter in urine and reduce the relapse of bladder cancer in a much safer, more effective and feasible

Table I. *Basic indexes of patients in the three groups before operation.*

Item	TURBT group	Holmium laser resection group	Partial cystectomy group	χ^2	p
Number t of tumor					
Solitary	38	26	30	0.877	0.645
Multiple (from 2 to 7)	52	38	32		
Size of tumor					
≤3cm	50	28	26	3.432	0.180
>3cm	40	36	36		
T staging					
Ta	60	42	44	0.471	0.790
T1	30	22	18		
Grading					
Papilloma	29	16	11	13.329	0.055
Low malignant tendency	28	20	13		
Low grade	25	19	22		
High grade	8	9	16		

Table II. *Comparison of items in three groups in and after operation.*

Item	TURBT group	Holmium laser resection group	Partial cystectomy group	F	P	Comparison between two groups		
						P(TURBT *vs* Holmium laser)	P(Holmium laser *vs* Partial)	P(TURBT *vs* Partial)
Operation time/min	39.6±10.1	29.2±14.1	92.5±13.9	474.56	<0.001	<0.001	<0.001	<0.001
Blood loss/ml	43.3±10.2	20.1±9.1	98.2±15.6	741.93	<0.001	<0.001	<0.001	<0.001
Time of indwelling ureter/d	6.1±2.1	4.0±1.5	11.7±1.6	311.13	<0.001	<0.001	<0.001	<0.001
Hospital days/d	8.3±2.8	7.5±2.6	14.3±3.1	11.89	<0.001	0.087	<0.001	<0.001

manner. Partial cystectomy widely applied in China at present is effective for tumor with high grade and invasion tendency, especially for tumor near the ureteral orifice (10).

Observing three resections over a length of time, we found that holmium laser resection was characterized by small trauma, less bleeding and rapid recovery compared to TURBT, but there were also setbacks such as excessive broken tumor tissue and consequent incompleteness of tumor samples therefore pathologists were unable to determine the overall differentiation of the tumor due to severe burn, compression and damage caused by the resection. As to partial resection of bladder tumor, tissue adhesion is major after surgery,thereby lowering the repeatability of it, though complete

Table III. *Comparison of complications in and after operation among these three groups and cases of relapse in two years.*

Item	TURBT group	Holmium laser resection group	Partial cystectomy group	χ^2	p
Relapse condition					
Relapse	37	21	19	2.072	0.355
No relapse	53	43	43		
Perforation					
Yes	6	0	-	-	0.042
No	84	64	-		
Bladder spasm					
Yes	19	12	25	9.494	0.009
No	71	52	37		
Obturator nerve reflex					
Yes	15	-	-	-	-
No	75	-	-		

resection of both tumor and bladder wall is useful to confirm invasion depth of tumor (11). Holmium laser combined with electric resection is thought to have a future in treating bladder tumor, helping to lower the incidence of obturator nerve reflex and reduce bleeding. For tumors less than 1 cm, electric resection removes tumor along with part of the bladder wall on the base and invasion scope can be confirmed after pathological examination. Holmium laser is prone to damage samples during vaporization cutting, which affects pathological staging and classification. For tumors of more than 1 cm, holmium laser combined with electric resection is feasible. The tumor close to the operation microscope is removed and the root of tumor pedicle is clearly displayed (12). Electric resection is used to remove the mass on the base and adjacent to the tumor. The bordering area of the tumor is then removed. Pathological examination of these three parts is beneficial to confirm invasion scope and is of great significance in lowering the recurrence and development of bladder tumor.

The constant studies on tumor molecular mechanism not only enable the combination of nuclear matix proteins with exfoliated urothelial cells to improve the accuracy of diagnosing bladder cancer, but also enable the combination of vascular endothelial growth factor (VEGF) with Ki67 to enhance the prognosis. Together with the improved operation level and chemotherapy perfusion into bladder regularly after operation, we can choose the second TURBT to reduce the tumor residue and reduce the rate of relapse from 2 to 6 weeks after operation. It is also believed that TURBT and Holmium laser resection has a much more promising future in treating NMIBC.

ACKNOWLEDGEMENTS

National Natural Science Funds (No. 81171971).

REFERENCES

1. Zhong H, Wang B. Gender difference and the major risks in bladder cancer. Shandong Medical Journal 2011; 51(39):102-3.
2. Wang P, Shen SY, Bo JJ, Zhang LH, Li Z, Liu DM, Huang YR. Clinical study of partial stectomy combined with chemotherapy for muscle-invasive bladder cancer. China Oncology 2012; 22(10):766-9.
3. Xu SX, Dai SY, Zhu JG, et al. Effect observation on different transurethral resection patterns for treating patients with non-muscle invasive bladder cancer. Chongqing Medicine 2014; 43(25):3284-6.

4. Wang H, Wang ZP. Research progress in oncolytic adenovirus in the treatment for bladder cancer. China Cancer 2014; 23(2):148-52.
5. Hu HM. Ankylosis of knee joint after treatment with manipulation and traditional chinese medicine under continuous epidural anesthesia. Nei Mongol Journal of Traditional Chinese Medicine 2013; 32(14):32-3.
6. Xie D, Zheng J, Su LR. Effects of different irrigation fluid temperature on postoperative bleeding and cystospasm in patients after transurethral resection of the prostate. Chinese Journal of Nursing 2011; 46(4):334-6.
7. Wang X, Cui S, Gu JQ. Current treatment of non-muscle-invasive bladder cancer. Journal of North Sichuan Medical College 2013; 28(2):176-80.
8. Kirkali G, Chan T, Manoliaran M, et al. Bladder cancer: epidemiology, staging and grading, and diagnosis. Urology 2005; 66(S6A):4-34
9. Zhan WZ, Liang YY, Yuan QP. A comparative study of recurrence and progression in non-muscle-invasive bladder tumor after 2 μm continuous-wave thulium laser or transurethral resection using European transurethral resection organization of research and treatment of cancer scoring system. Chinese Journal of Endourology 2013; 7(3):170-4.
10. Hu MJ. Comparison in efficacy between transurethral resection of bladder tumor and partial cystectomy in treating patients with bladder tumor. Chinese and Foreign Medical Research 2014; 12(31):67-9.
11. Luo J, Zhang JS, Wang CZ, Liu N. Association of WHO 2004 pathological classification of bladder urothelial tumors with the outcome. Journal of Capital Medical University 2012; 33(5):656-60.
12. Li CC. Efficacy observation and analysis of transurethral resection of bladder tumor combined with medicine perfusion in treating superficial bladder tumor. Guide of China Medicine 2013; 11(23):564-5.

CORRELATION BETWEEN C-erbB-2 WITH GASTRIC MUCOSAL ATYPICAL HYPERPLASIA AND GASTRIC CARCINOMA

B. SONG[1], J. YU[2], and T.S. WU[3]

[1]Department of Gastroenterology, Yantaishan Hospital, Yantai, Shandong, China; [2]Department of Pediatrics, Yantaishan Hospital, Yantai, Shandong, China; [3]Emergency Center, the First Teaching Hospital of Xinjiang Medical University, Urumqi, Xinjiang, China

Received January 9, 2015 – Accepted April 13, 2015

C-erbB-2 is a cancer gene originating from cells. The high-expression and amplification of C-erbB-2 and its protein products (P185) are found in a wide variety of tumors. The abnormal expression of C-erbB-2 has great influence on the occurrence and development of gastric carcinoma. This paper aimed to analyze the expression of C-erbB-2 in the tissues of gastric carcinoma, gastric mucosal atypical hyperplasia and gastritis, and discuss its role in the occurrence and development of gastric carcinoma. The morphological differences and connections among simple intestinal metaplasia (SIM), atypical intestinal metaplasia (AIM) and dysplasia in intestinal metaplasia through hematoxylin and eosin (HE) staining were studied. Three groups were set to detect the expression condition of C-erbB-2 by immunohistochemical method (IHC). The result showed that C-erbB-2 had no significant difference in AIM and gastric carcinoma, that is, AIM was closely related to gastric carcinoma. The positive expression was demonstrated of C-erbB-2 products (P185) in medium and gastric mucosa dysplasia tissues and was 29.41% and 66.67%, respectively, while it was 25%, 50% and 77.78% in high, medium and low differentiation of gastric carcinoma. It can be seen that there was a significant difference between them ($P<0.05$), and the expression degree was significantly enhanced ($P<0.05$); the expression degree in high differentiation gastric cancer tissue was significantly higher than the middle and low differentiation gastric cancer tissue. It was concluded that C-erbB-2 played an important role in the pathogenic mechanism of gastric carcinoma, and it might act on the later period of the gastric carcinoma, which provides objective reference index for the diagnosis and prognosis of gastric carcinoma and meanwhile provides instructional theoretical reference for the application of targeted drugs in the clinical treatment of gastric carcinoma.

Gastric carcinoma is a common malignant cancer, whose death rate can be reduced by early detection and treatment. Now it is widely believed that the process of atypical hyperplasia is the main cause of gastric carcinoma, therefore atypical hyperplasia is considered to be precancerous lesions (1, 2). Gastritis is a benign disease of gastric mucosa, and can be treated by medical treatment, while the intestinal metaplasia is a common concomitant lesion in gastric mucosa of gastritis, and it is closely associated with gastric carcinoma. This paper aimed to study the change of gastric mucosa and achieve an early discovery and timely treatment of gastric cancer through the gene expression of C-erbB-2. Intestinal metaplasia is

Key words: gastric carcinoma, atypical hyperplasia, C-erbB-2 Gene, p185 protein

Mailing address: Dr Tianshan Wu,
Emergency Center,
the First Teaching Hospital of Xinjiang,
Medical University, No.8, Liyushan Road,
Xinshi District, Urumqi,
Xinjiang, 830054, China
e-mail: wts@ibhsedu.com

0393-974X (2015)

divided into simple intestinal metaplasia (SIM) and atypical intestinal metaplasia (AIM) according to pattern and tissue. It is reported that the main reason of tumor occurrence, development, invasion and metastasis is the activation of oncogene (C-erbB-2) and the functional loss of tumor suppressor genes. With the activity of tyrosine kinase C-erbB-2 receives the information of epidermal growth factor and stimulates cell proliferation. Wei Xueming et al. found in "Expressions and Significance of EGFR, C-erbB-2, VEGF and COX-2 in Human Gastric Cancer Tissues" that over expression of C-erbB-2 which is closely related with the invasion and metastasis of many solid tumors can aggravate the atypical hyperplasia of gastric mucosa (3-5); Ding Chunming, et al. indicated that the positive abnormal expression of C-erbB-2 was a hazard in the deterioration of gastric carcinoma (6), and it was correlated to the expression of p53 (cancer inhibition). This paper analyzed the expression of C-erbB-2 in tissues of gastritis, atypical hyperplasia and gastric carcinoma by HE staining and IHC and discussed the role and clinical significance in the occurrence and development of gastric carcinoma. It aimed to provide theoretical basis for the early discovery, early diagnosis and timely treatment of gastric carcinoma.

MATERIALS AND METHODS

A total of 192 wax specimens of fiberscope biopsy from a hospital were selected and divided into three groups according to pathologic histology types, including Gastric carcinoma group, Gastric mucosa dysplasia group and Chronic gastritis group (Table I). The age of groups was of no statistical significance ($P>0.05$). In the gastric carcinoma group, there were 48 cases of poorly and moderately differentiated gastric carcinoma, 12 moderately differentiated patients and 18 highly differentiated; as for the Gastric mucosa dysplasia group, there were 8 mild samples, 34 medium samples and 6 severe samples.

The rat anti-human monoclonal antibody of C-erbB-2 was purchased from Santa Cruz, and immunohistochemical SP kit and DAB (3,3'-diaminobenzidine) colorimetric solution were both purchased from Beijing Biotechnology Company Co., Ltd.

All specimen were treated with 10% formalin fixation, paraffin embedding and cut into 4 μm section followed by HE staining and immunohistochemical experiments. After HE staining, pathological morphology of gastric mucosa tissues was observed under the light microscope. For SP immunohistochemistry Envision was used according to the manufacturer's instructions; paraffin sections were dewaxed with xylene, and hydrated with gradient alcohol. After emerging in 0.01 mol/L boiling citrate buffer (PH=6.0) for 18 min, sections were cooled at room temperature, and washed twice with distilled water. After PBS washing for 3×5 min, peroxidase blockers were added. Ten min later, sections were washed again with PBS for 3×5 min, and stored at 4°C for one night adding one drip of immune animal serum (room temperature for 10 min) and mouse anti-human monoclonal antibody and rewarming it at 37°C for 45 min. Sections were washed with PBS (3×5 min), and then mixed with streptomyces anti-biotin peroxidase (at room temperature for 10 min). After PBS washing again for 3×5 min, the sections were observed through a microscope for 2-5 min after the addition of 50 μl of freshly prepared DAB color liquid after rinsing and the nucleus counterstained with hematoxylin after which it was rinsed with distilled water. It was then differentiated with hydrochloric acid and rinsed with tap-water and dehydrated again with gradient alcohol. The positive biopsies were taken as positive control and PBS as negative control.

Morphological observation of gastric mucosa lesion

The difference between SIM and AIM was found based on the morphologic observation of gastric mucosa lesion, shown in Table II and Table III.

Test results

C-erbB-2 was considered positive cell when its cell nucleus or cell nucleus together with cytoplasm appeared with brown granules and only cytoplasm that was positive was regarded as non-specific staining. Cytoplasm staining was positive in IM while cell membrane staining was positive in gastric carcinoma. Positive cells were classified in three types according to the proportion of cells: with none or less than 10% positive cells (-); more than 10% of positive cells were regarded as weakly positive (I); more than 25% of positive cells were regarded as positive (II).

Statistical analysis

Data analysis was performed by using SPSS 19.0 software and Spearman's correlation index, statistical significance $p<0.05$.

RESULTS

The positive expression of C-erbB-2 was found in cytoplasm in IM while it was found in cell membrane

Table I. *General characteristics of the studied patients.*

Group	Total specimen	Gender Proportion	Age range (year)	Average age (year)
Gastric carcinoma	78	64/14	29-80	59.6
Gastric mucosa dysplasia	48	34/14	30-75	57.8
Chronic gastritis	66	28/38	30-74	56

Table II. H*istomorphology characteristics of SIM and AIM.*

Histomorphology	SIM	AIM
Tissue structure	Regular gland	The cells were crowded and pseudostratified; the cell nucleus showed adenomatous standing and overlap; polarity was chaos
Goblet cell	Regular morphology; the nucleus was located at the base of cell	Cells were oblate-shaped; large nucleus with obvious nucleolus; usually off normal; the polarity was changed
Columnar cell	The cell was columnar with bright cytoplasm, the nucleus was located at the bottom	Cells were oblate-shaped; large nucleus with obvious nucleolus; chaos
Paneth cell	Regular morphology; the nucleus was located at the bottom	Cells were inverted; the polarity was changed
Gastric pit	Regular morphology; the mucosa among depressions was smooth	Mutability of form, depressions became deeper, hackly

Table III. *Morphological comparison between AIM and hyperplasia.*

Histomorphology	AIM	Hyperplasia
Tissue structure	The cells were crowded and pseudostratified; the cell nucleus showed adenomatous standing and overlap; polarity was chaos	Nuclear arrangement was loose with a larger proportion
Goblet cell	Cells were oblate-shaped; large nucleus with obvious nucleolus; usually off normal; the polarity was changed	No goblet cell
Paneth cell	Cells were inverted; the polarity was changed	No Paneth cell

in gastric carcinoma (7, 8). The expression in the tissue of chronic gastritis, gastric mucosa dysplasia and gastric carcinoma is shown in Fig. 1 and Table IV. Table IV shows that the positive expression rate and level of C-erbB-2 in gastric carcinoma tissue and gastric mucosa dysplasia was significantly higher than in the chronic gastritis tissue, and among them, the rate of positive expression of C-erbB-2 in chronic gastritis was 30.3%, 65.38% in gastric mucosa dysplasia, and 61.54% in gastric carcinoma. The expression in chronic gastritis was significantly different compared with gastric mucosa dysplasia and gastric carcinoma ($P<0.05$); the difference between gastric mucosa dysplasia and gastric carcinoma had no statistical significance ($P>0.05$).

The expression of C-erbB-2 in gastric mucosa tissue with mild, medium and serious degree is shown in Table V. The Table shows that the positive expression degree in mild, medium and serious gastric mucosa dysplasia was respectively 0, 29.41% and 66.67%, showing an upward trend ($P<0.05$). The positive expression degree in serious gastric mucosa dysplasia was significantly increased compared with mild gastric mucosa dysplasia ($P<0.05$), and it showed that the positive expression of C-erbB-2 increased as the lesion deteriorated.

Table IV. *The expression of C-erbB-2 in the tissue of chronic gastritis, gastric mucosa dysplasia and gastric carcinoma.*

Group	Cases (number)	The degree of positive reaction			Positive Rate (%)
		-	I	II	
Chronic gastritis	66	46	12	8	30.30
Gastric mucosa dysplasia	52	18	20	14	65.38
Gastric carcinoma	78	30	20	28	61.54

Table V. *The expression of C-erbB-2 in mild, medium and serious gastric mucosa dysplasia.*

Gastric mucosa dysplasia	Cases (number)	The degree of positive reaction			Positive rate (%)
		-	I	II	
Mild	8	8	0	0	0 (0.00)
Medium	34	26	4	6*	10 (29.41)*
Serious	6	2	0	4*	4 (66.67)*

Table VI. *Expression condition of C-erbB-2 in gastric cancer tissue of different differentiation degrees.*

Gastric carcinoma	Cases (n)	The degree of positive reaction			Positive cases (%)
		-	I	II	
Poorly differentiated	48	36	10	2	12 (25.00)
Moderately differentiated	12	6	4	2	6 (50.00)*
Highly differentiated	18	4	4	10	14 (77.78)*

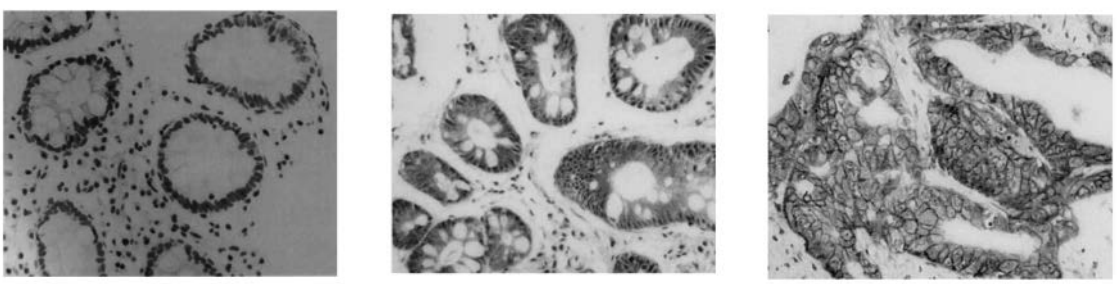

Fig. 1. *The expression of C-erbB-2 in the tissue of chronic gastritis, gastric mucosa dysplasia and gastric carcinoma;* ***A****) The negative expression of C-erbB-2 in gastritis tissue;* ***B****) The positive expression of C-erbB-2 in gastric mucosa dysplasia tissue;* ***C****) The positive expression of C-erbB-2 in gastric carcinoma tissue.*

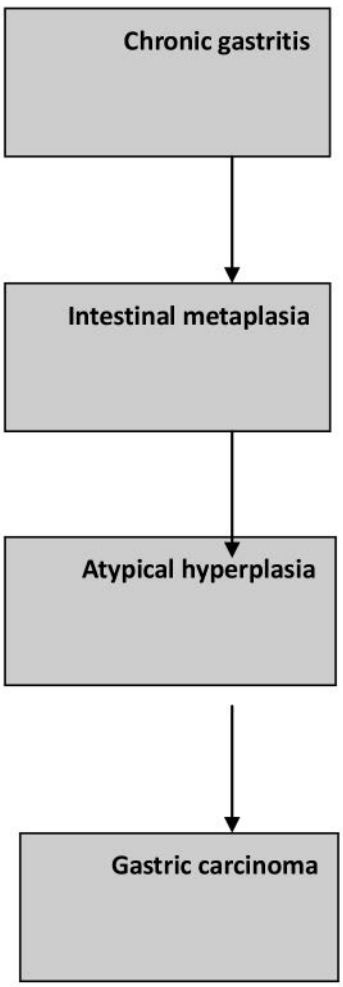

Fig. 2. *The process of gastric mucosal canceration.*

The relationship between C-erbB-2 expression and clinical and pathological factors of gastric carcinoma is shown in Table VI. It is obvious that C-erbB-2 expression was not related to differentiation degree ($P>0.05$), while it was positively correlated with depth of invasion and lymphatic metastasis ($P<0.05$). C-erbB-2 expression of infiltrating into muscle layer below the lymph node metastasis is high.

DISCUSSION

Gastric carcinoma is a cancer originating from gastric mucosal epithelium, which is one of the most common cancers (9). It remains the leading cause of cancer-related death, especially for the elderly (10, 11). Gastric mucosa dysplasia is closely associated with the occurrence of gastric carcinoma. It may be an important link of the precancerous process and is listed as gastric precancerous lesion (12, 13). Gastric mucosal canceration is a complicated process which can be divided into four steps (Fig. 2).

This paper analyzed the expression of C-erbB-2 in tissue of chronic gastritis, atypical hyperplasia and gastric carcinoma by HE staining and IHC, which provides theoretical basis for understanding the occurrence of gastric carcinoma. Besides, this research can be a reference to clinical screening of high-risky patients with gastric carcinoma.

It has been reported that oncogene is a gene segment existing in chromosomes, and it remains inactive and does not express itself in normal situations. However, cell transmission or even malignant tumor occurs if oncogene causes genes amplification, absence, ectopia or mutation (14, 15). Proto-oncogene C-erbB-2 is also called neu gene or HER-2 gene, and it encodes a transmembrane glycoprotein with tyrosine kinase activity. In normal circumstances it is inactive and participates in the regulation of growth and differentiation of the cells, but if it is affected by oncogenic factors C-erbB-2 can be out of control, leading to the activation, amplification and the excessive expression of protein P185. It produces many growth factor receptors and the mitosis is enhanced (16, 17). As a proto-oncogene, C-erbB-2 can act as a biomarker to the diagnosis of gastric carcinoma. C-erbB-2 is an important biomarker in the early diagnosis of gastric carcinoma (18).

Many studies indicate that the expression of C-erbB-2 occurs in the later period of gastric carcinoma. It is closely related to lymphatic metastasis and prognosis. However, this study indicates that C-erbB-2 expression may take place earlier since expression was found in tissues of serious gastric mucosa dysplasia and gastric carcinoma and also in the tissues of mild and medium gastric mucosa dysplasia and intestinal metaplasia. C-erbB-2 was mainly located in cell membrane, performing as a brown and positive particle. Positive dyeing in cytoplasm was found in a few cells. In the process of gastric mucosa canceration, cell proliferation activity increased gradually with increasing positive expression of C-erbB-2. C-erbB-2 also expressed

more positively in serious gastric mucosa dysplasia and gastric carcinoma than in medium dysplasia, ($P<0.05$). It was inferred that C-erbB-2 high-expression leads to increase of EGF in cell membrane sample information capacity which promotes cell proliferation activity. No remarkable difference was noted between proliferation index of serious gastric mucosa dysplasia and gastric carcinoma, nor in the condition of C-erbB-2. This showed that serious dysplastic tissues were more likely to cancerate. The increase of its proliferation ability may be associated with the increased expression of C-erbB-2.

This study showed that C-erbB-2 did not express in mild gastric mucosa dysplasia tissue, and expressed slightly in chronic gastritis tissue. Furthermore, C-erbB-2 expression in atypical hyperplasia was close to the high differentiation of gastric carcinoma. The expression degree in medium and serious gastric mucosa dysplasia was respectively 29.41% and 66.67%, and it had a significant difference ($P<0.05$). The expression in gastric carcinoma with poor, medium and high differentiated degree was respectively 25%, 50% and 77.78% and the expression had a significant difference between each two groups ($P<0.05$); the expression in the high differentiation group was significantly higher than it was in the medium and poor differentiation ($P<0.05$) groups. This demonstrates that the C-erbB-2 participated in the regulation of gastric carcinoma cell differentiation, and the expression increased as the lesion of gastric mucosal deteriorated. High expression may lead to the malignant transformation of cells. It might act on the later period of gastric carcinoma occurrence, and had a close relationship with the occurrence and development of gastric carcinoma and the activation of a variety of cancer genes.

REFERENCES

1. Li Y. Gastric mucosa atypical hyperplastic bowel and atypical hyperplasia: study of morphology and biology. Peking Union Med College 2012. http://cdmd.cnki.com.cn/Article/CDMD-10023-1012447604.htm
2. Hu WH. research of the relationship of *Helicobacter pylori* infection to gastritis lesions, atypical hyperplasia and gastric carcinoma. Jilin Med J 2013; 24:4882-3.
3. Wei XM, Gu GL, Ren L, Xiong M, Wang SL, Li DC. Expressions and significance of EGFR, C-erbB-2, VEGF and COX-2 in human gastric cancer tissues. Chinese Journal of Bases and Clinics in General Surgery 2009; 16 (11):900-5.
4. Wang FL, Xie H. Expression and clinical significance of C-erb-B2 and Topo II α in breast cancer. Jiangsu Med J 2011; 37(5):541-3.
5. Mu JP, Liu L, Fang W, Ao JB, Cheng JM, Zhou LZ. The changes of colon proto-oncogene C-fos expression on experimental colitis in rats. Chin J of Gastroenterol and Hepatol 2010; 19(11):988-90.
6. Ding CM, Yu G, Zhu BH. Study on the expression of p53 and C-erbB-2 and their relationship with tumor progression in gastric cancer. The Practical J of Cancer 2011; 26(1):31-3.
7. Li M, Liu LN, Wang ZH, Feng L, Li YN, Zhang QP. Significance of the sites of EGFR expressions in gastric carcinogenesis. J of Dalian Med Univ 2010; 3(2):170-2.
8. Fan P. The relevant research of EGFR gene mutation in the gastric carcinoma. Xinjiang: Shihezi Univ 2010.
9. Zou XN, Sun XB, Chen WQ, Zheng RS, Zhang SW, Dai Z, Liu WD, Zhao DL. Analysis of incidence and mortality of stomach cancer in China from 2003 to 2007. Tumor 2012; 32(2):109-14.
10. Wang SB, Liu CM. Comparative studies on the expression of Ki-67 and MVD count in gastric carcinoma between, young and aged patients. Chin J of Clinic Gastroenterol 2010; 22(4):221-3.
11. Li KB. The comparation and prognostic analysis of clinical manifestation, pathological feature in gastric carcinoma between, young and aged patients. Anhui Med and Pharmace J 2013; 17(2):285-6.
12. Wei Q, Wang L, Huang RF, Tang Y. The expression and significance of Shh in gastritis, atypical hyperplasia and gastric carcinoma. Military Surgeon in Southwest China 2012; 14(4):608-10.
13. Song R. The application status and clinical value of NCCN Guideline for gastric cancer patients in a comprehensive teaching hospital in Shanghai. Shanghai: Fudan Univ 2012. http://cdmd.cnki.com.cn/article/cdmd-10246-1013102458.htm
14. Wei YY, Hou J, Tang WR, Luo Y. The cooperation between p53 and Ras in tumorigenesis. Hereditas

2012; 34(12):1513-21.
15. Wang HB, Ji CS. Progress of the relationship between p53 and c-erbB-2 in gastric cancer. Chin J of Bases and Clinics in General Surg 2010; 17(8):880-4.
16. Liu JB, Shen K. The relationship between P185 protein within antibody and breast cancer. J of Basic and Clinical Oncol 2010; 23(4):368-9.
17. Tang Y, Wang LJ, Ma LY. The expression and clinical significance of HER2 in the gastric cancer tissue. J of Xinjiang Med Univ 2012; 35(2):202-5.
18. Wang QM, Wang LF, Yu XL, Qin HM, Zhang WB, Song LY. Expressions and significance of EGFR, C-erbB-2, Topo II α and P-gp in human gastric cancer tissues. J of Mod Oncol 2013; 21(4):834-7.

JOURNAL OF BIOLOGICAL REGULATORS & HOMEOSTATIC AGENTS Vol. 29, no. 2, 479-484 (2015)

LETTER TO THE EDITOR

THIN-LAYER CHROMATOGRAPHY IDENTIFICATION FOR RHUBARB AND PHELLODENDRI AMURENSIS CORTEX IN SHUANG-BAI CATAPLASM AND STUDY OF SKIN IRRITATION ASSAY

YG. TIAN, SM. QIN and L. DING

School of Pharmaceutical Engineering, Guangdong Food and Drug Vocational College, Guangzhou, China

Received January 29, 2015 – Accepted April 21, 2015

This paper aimed to raise a thin-layer chromatography (TLC) identification method for rhubarb and Phellodendri Amurensis Cortex and inspected skin irritation induced by them. It applied the TLC identification for Rhubarb and Phellodendri Amurensis Cortex in Shuang-bai cataplasm prescription. In this study six rabbits were divided into two groups to observe the skin irritation from Shuang-bai cataplasm on intact and defected skin. Another 36 were randomly divided into 6 groups to observe the acute toxicity from Shuang-bai cataplasm on intact and defected skin. Also 30 guinea pigs were divided into 3 groups to observe skin allergy to Shuang-bai cataplasm. The results showed that the average weight of the group of intact-skin rabbits was 2.026±0.10 kg and 2.427±0.023 kg after medication; the average weight of the group of defected-skin rabbits was 2.170±0.05 kg and 2.540±0.15 kg after medication; Shuang-bai cataplasm produced no irritation on intact or defected rabbit skin, no acute toxicity in rabbits and no allergy on the skin of guinea pigs. The skin allergy rate on guinea pigs of the medication group was 0 at each time quantum. Therefore, it can be concluded that this preparation produces no extreme skin irritation for rabbits, guinea pigs or human beings, and it can be safely put into practice.

Cataplasm, also called hydrogel plaster, is a new plaster for external use. The medicine is dissolved or blended with water-soluble polymer material matrix, and then spread on the surface of backing materials for skin application (1). In the 1970's Japan first modified and developed the age-old cataplasm formulation into the modern-day cataplasm and in the 1980's it found its way into the European and American market as well as China. Cataplasm was defined by medicinal extracts and plaster spread onto the surface of backing materials after blending the medicine, chemical drugs and proper hydrophilic matrix together as shown in Chinese Pharmacopoeia, 2005.

Compared with traditional plaster, cataplasm has several merits which include large drug capacity, no allergy or irritation on skin, good moisture and ventilation performance. It can also be used repeatedly (2).

Shuang-bai cataplasm is composed of five herbal medicines, namely rhubarb, Cacumen Platycladi, Phellodendri Amurensis Cortex, Lycopus lucidus and mint (3). It boasts several benefits such as lowering fever and detoxifying, relieving pain and eliminating stasis. It is mainly applied in the treatment of traumatic injury, sores and ulcers in

Key words: Shuang-bai cataplasm, TLC, skin irritation

Mailing address:
Dr Yuguang Tian,
Guangdong Food and Drug Vocational College,
No.321, Longdong North Road,
Tianhe District, Guangzhou,
Guangdong, 510520, China
e-mail: tyg@ibhsedu.com

0393-974X (2015)

their early stage, local inflammation and pain, pelvic inflammation and phlebitis (4). Shuang-bai powder was usually applied with Vaseline ointment and hydromel in past clinical practice and was probably likely to induce skin allergies (5) and stain clothes. In order to avoid these problems, this study created a cataplasm from the original combination which was less likely to induce allergy and skin irritation and easier to apply without staining clothes. To control the quality of Shuang-bai cataplasm, thin-layer chromatography was applied to identify Rhubarb and Phellodendri Amurensis Cortex within. Skin irritation was inspected in the hope of providing a reference for future studies.

MATERIALS AND METHODS

Forty-two healthy rabbits with a body mass between 2 and 2.5 kg and the same number of rabbits of different sex were used; thirty healthy white guinea pigs with a body mass 300-400 gr and the same number of guinea pigs of different sex were used. All animals were provided by the Experimental Animal Center of Zhengjiang Chinese Medical University and their certification number was SCXK (Shanghai) 2008-0016. All animals received one-week adaptive feeding before this experiment.

Rhubarb identification

Three plasters of this drug and 3 plasters of negative control sample without Rhubarb were cut up. The backing materials were removed and then placed into a Soxhlet extractor; Petroleum ether (30-60°C) was added; heating reflux was operated until the color of the extracts disappeared and the petroleum ether fluid was removed. The petroleum ether was patched and volatilized and 120 ml 70% ethanol was added, heating reflux was operated for 1 h and was then filtered in boiling water. Filtrate was dried and 25 ml water was added to dissolve the residue; 6 ml hydrochloric acid was added and heating hydrolysis operated for 30 min and immediately cooled down, shaken and extracted using 30 ml ethyl acetate twice. It was then combined with the ethyl acetate liquid and rinsed for three times in 15 ml of water; the solvent was volatilized and 1 mL of methyl alcohol was added to dissolve the residue which would serve as a solution for experiments and for controls. Another 0.5 g of rhubarb was obtained as a control sample, 50 mL petroleum ether was added (30-60°C). Another rhein was obtained as a control sample and methyl alcohol was added to make a solution including 1.0 mg in each 1 mL to serve as the control solution. Inspection was based on the TLC (an appendix VIB of Chinese Pharmacopoeia, 2010 edition), from which 4 µl and 6 µl solution was drawn for control material and control sample. The solution was then spread upon the same silica gel G thin-layer plates taking sodium carboxymethyl cellulose (CMC) as adhesive, petroleum ether (30-60°C), ethyl formate and Performic acid (15:7:1) as developing solvent; it was taken out and dried under the sun then placed under an ultraviolet lamp (254 nm) for inspection. On the chromatogram for test sample, the spots of fluorescence appeared to be the same color in the corresponding location on the chromatogram for control material and control sample. After fumigation in ammonia vapor, the spots turned red. (Fig. 1).

Two plasters of this drug and 3 plasters of negative control sample without Phellodendri Amurensis Cortex were taken and cut up; the backing materials were removed and then 60 mL of absolute ethyl alcohol was added; heating reflux for 1 h was operated, the filtrate was dried out and water was added to dissolve the residue; the pH was regulated to the value 8 or 9 by strong ammonia solution; 20 mL trichloromethane was extracted twice, combined with the trichloromethane liquid and rinsed for three times in 15 mL water; the solvent was volatilized and then 2 mL of methyl alcohol was added to dissolve the residue which would serve as a solution for experiments and for negative control. Another 0.1 g of Phellodendri Amurensis Cortex was taken for control sample, 30 mL absolute ethyl alcohol was added and medical solution for control was fabricated in the same way. Inspection was based on TLC (an appendix VIB of Chinese Pharmacopoeia, 2010); 12 µl solution was taken from the above-mentioned experiments and 0.5 µl both for control material and control sample; the solution was spread upon the same silica gel G thin-layer plates using sodium carboxymethyl cellulose (CMC) as adhesive and ethyl acetate, butanone, performic acid and water (10:7:1:1) as developing solvent; it was dried under the sun then placed under the ultraviolet lamp for inspection (365 nm). On the chromatogram for test sample, the spots of fluorescence appeared to be the same color in the corresponding location on the chromatogram for control material and control sample. (Fig. 2).

Skin irritation assay

Six healthy white rabbits (3 of each sex) were randomly divided into two groups, namely the intact skin group and defected skin group (scratched by sterilized needle without bleeding); the rabbits were shaved on both sides of the spine in an area of about 150 cm^2 24 h before this assay; any shaved area with skin injury was not used for the assay. This assay applied the self-contrast for both sides on the same body. Five $g\cdot(100g)^{-1}$ of Shuang-bai cataplasm was applied to both groups on the left side, treated with drugs once and applied with cataplasm

matrix on the right side, fixed with gauze of the same length. Plasters were removed, treated with drugs for 24 h and then rinsed with tepid water. Observation was carried out by the naked eye to determine whether there was any erythema and edema in local parts 1, 24, 48, and 72 h later, after removing the test sample.

Skin acute toxicity assay

Thirty-six healthy white rabbits were taken and then randomly divided into 6 groups including four experimental groups, namely the intact skin group, low dosage group, defected group and high dosage group. There were also 2 control groups, namely the intact skin control group and defected skin control group. Before the experiment, both sides of the spine were shaved on 10% of the total surface area (about 150 cm^2); 24 h after shaving detection was carried out to establish whether there was any injury caused by shaving and to determine whether the defected skin was improper for toxicity assay. The control groups were treated with 5g·Kg^{-1} drug once and the intact skin group and defected skin group were treated with the cataplasm matrix; high dosage group was treated with 5g·Kg^{-1} drug once; the intact skin group and defected skin group were treated with the 150 cm^2 cataplasm in high concentration and low dosage group was treated with 1.25g·Kg^{-1} drug once; the intact skin group and defected skin group were treated with the cataplasm in the same area in low concentration. The method of fixation was the same as above, and each animal was kept in an individual cage. After 24-h treatment the residue was rinsed with tepid water; the body mass, skin, hair, eyes, and changes of mucosa, breathing, central nervous system, the activity of four limbs and poisoning effects were observed at the 1^{st}, 24^{th}, 48^{th} and 72^{nd} h and at the 14th day after removing the test medicine, respectively .

Skin allergy assay

Thirty healthy white guinea pigs were taken (the same number for each sex) and shaven symmetrically on both sides of their backs (3cm x 3cm) 24 h before receiving the treatment. The guinea pigs were randomly divided into three groups, including treatment group, blank control group (treated with matrix), and positive control group (1% 2, 4-dinitrochlorobenzene (DNCB). Allergy contact: 0.2 g Sanhuang Sanyu cataplasm was obtained to apply on the shaven area on the left side and the fixation method was as stated above, removed 6 h later and residue rinsed away with tepid water and repeated once on the 7^{th} and 14^{th} day, for a total of three times. The blank control group and positive control group carried out the allergy assay in the same way. Irritation contact: Sanhuang Sanyu cataplasm was applied for 14 days and 0.2 g of Sanhuang Sanyu cataplasm was applied on the shaven area in the right side, rinsed away 6 h later and observed; skin allergy was observed at 24, 48 and 72 h. Positive control group (treated with 1% 2, 4-DNCB) and blank control group were observed in the same way.

Statistical method

The database was built by combining diseases, solvents, major clinical performance, therapies and treatment results drawn from literature. Statistical analyses were carried out using EXCEL 2003 software.

RESULTS

Skin irritation assay

When the intact rabbit skin group came into contact with the Shuang-bai cataplasm, there was no erythema and edema in local parts. There were no abnormal reactions on either side of the body.

Skin acute toxicity assay

At the 1^{st}, 24^{th}, 48^{th} and 72^{nd} h and on the 14^{th} day after the intact rabbit skin group and defected skin group came into contact with the test medicine, there was no poisoning in their body mass, skin, hair, eyes, mucosa, breathing or in the central nervous system or activity of the four limbs. Moreover, there was no erythema or edema in the skin. The changes in body mass of the rabbits in different groups are shown in Table I.

Skin allergy assay

There was no allergy in the blank group and treatment group, such as erythema and edema. After the positive control group received the treatment for 6 h, there was erythema in the skin without edema, and the erythema still remained 24, 48 and 72 h later without edema. The morbidity of allergy in these three groups is shown in Table II.

DISCUSSION

Shuang-bai powder is a prescription of the late professor Huang Yaoshen in Guangzhou University of Chinese Medicine (6). In 1964, it was recorded in the textbook *Lectures on Chinese Medicine Traumatology* on trial in Chinese Medicine School and is presently widely applied in China. It has been effective in clinical application for over four decades,

Table I. *Changes in body mass of rabbits in three groups.*

Group	Rabbits	Before treatment	7d after treatment
Intact skin			
Control	6	2.026±0.10	2.427±0.023
High dosage	6	2.217±0.03	2.460±0.052
Low dosage	6	2.095±0.21	2.285±0.077
Defected skin			
Control	6	2.170±0.05	2.540±0.15
High dosage	6	2.349±0.17	2.503±0.03
Low dosage	6	2.083±0.04	2.250±0.12

Table II. *Mean and morbidity of allergy of guinea pigs in thethree groups.*

Group	Guinea pigs	6h(n%)		24h(n%)		48h(n%)		72h(n%)	
——		Mean	Morbidity	Mean	Morbidity	Mean	Morbidity	Mean	Morbidity
Control	10	0	0	0	0	0	0	0	0
Treatment	10	0	0	0	0	0	0	0	0
Positive	10	1.8	100.0	3.2	100.0	2.6	100.0	1.3	52.0

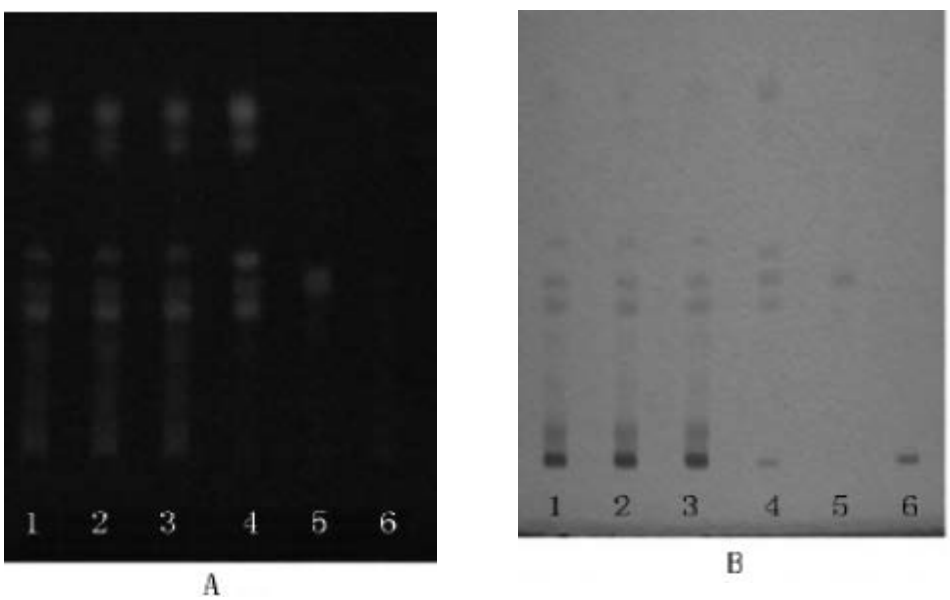

Fig. 1. *TLC chromatogram of rhubarb under ultraviolet lamp (**A**) and after fumigation in ammonia vapor (**B**). 1-3 refer to the Shuang-bai cataplasm test sample; 4 refers to the rhubarb control material, 5 refers to the rhein control sample and 6 refers to the rhubarb negative control.*

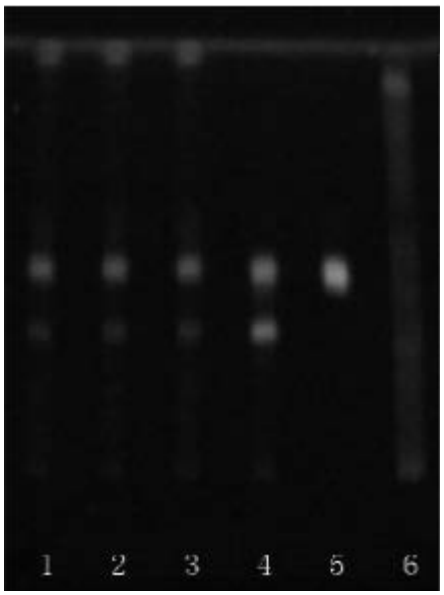

Fig. 2. *TLC chromatogram of Phellodendri Amurensis Cortex. 1-3 refer to the Shuang-bai cataplasm test sample; 4 refers to the Phellodendri Amurensis Cortex control medicine; 5 refers to the berberine hydrochloride control sample and 6 refers to the Phellodendri Amurensis Cortex negative control.*

which is a precious and classical prescription in our medical world.

Shuang-bai powder is much more effective in treating diseases, such as acute soft tissues injury, phlebitis, cancer pain and pressure sore (7). When applied, traditional powder needs a temporary allocation.

Shuang-bai powder is considered efficient in clearing away heat and detoxifying, detumescence and abirritation, dissipating stasis and activating the blood circulation according to the traditional Chinese medicine (TCM) theory. This prescription includes the external application of rhubarb so as to clear heat from blood and dissipate stasis (9). Phellodendri Amurensis Cortex, the major herbal medicine in this prescription, clears away heat and eliminates dampness, detoxifies and heals ulcers and dissipates stasis (10). However, the production of cataplasm is complex and tedious, which makes the application inconvenient. Moreover, it consumes too many medicinal materials (8).

Shuang-bai powder has many advantages, for example, it leaves no residue, does not pollute and it is simple to use. Moreover, it has good breathability and moisture retention, it is not irritant and has no sensitization; in addition, it can be pasted and uncovered repeatedly. It helps the drug to react rapidly and enduringly on skin and it evaporates waste and cools down the skin (11).

This study adopted the TLC identification and clear spots were found in the chromatogram. The results found that there was no interference of foreign spots in the area and this method was quite specific and reproducible. Because Shuang-bai cataplasm contains a large amount of glycerine, in the identification of Phellodendri Amurensis Cortex, the extracted sample methyl alcohol was affected by the glycerine, thus spots after development were inconsistent with the spots in control medicine and control sample. Through trial and error, this paper removed the methyl alcohol within the extract liquid, regulated the pH to 8 or 9 by strong ammonia solution and then extracted by trichloromethane. In this way, it acquired a good result by overcoming the effect of glycerine on development.

With further studies and the constantly newly-emerging technologies and equipment, TCM cataplasm has achieved a gradual improvement in several aspects, including matrix, craft-work and quality standard. Meanwhile, this paper achieved an integration of new traditional Chinese trans-dermal absorption system with traditional Chinese external treatment and developed a new Chinese medicine cataplasm through new preparation technology. By exploring new applications, it applied the medicine on some corresponding acupoints and maximized the therapy of acupoint administration in TCM. This medicine can permeate through the skin into the blood circulation, and then give full play to its function of channel tropism and further to the merits of TCM cataplasm. Because it has several merits, such as a large capacity of medicine, less animal consumption, speed in producing effects, pain- and stimulus-free, TCM cataplasm will increasingly win more approval from doctors and patients, which shows a favorable development trend and foreground of market application. Moreover, the social and economic benefits derived from this medicine will be promising.

This study proved that Shuang-bai cataplasm produced no irritation on the intact skin and defected skin of rabbits, and no acute toxicity on the intact skin and defected skin of guinea pigs, as well as no extreme allergy on the skin of human beings. These findings all suggest that Shuang-bai cataplasm is quite safe and effective with little skin irritation. Thus it is safe to say that it is of great worth for clinical use.

REFERENCES

1. Peng LP, Zhu CC, Xiao LX. Modern progress of orthopedics external application of Chinese medicine formulations. China J of Traditional Chinese Medicine and Pharmacy 2011; 26(6):1363-6.
2. Xue B, Xi XB, Li FY. Progress of clinical application of external application in treating soft tissue injury. Chinese J of Traditional Medical Traumatology and Orthopedics 2014; 6:34.
3. Wu XR, Huang XB, Yuan WB, et al. Optimization of matrix prescription of Shuang-bai Cataplasm by orthogonal test. Traditional Chinese Drug Research and Clinical Pharmacology 2012; 16(6):681-3
4. Wu KY, Wu XR, Wu QD. Summary and comment of Shuang-bai powder. New J of Traditional Chinese Medicine 2013; 45(8):174-5.
5. Ouyang WS, Liu DH, Wei G, Lin HL, Huang WJ, Ye MR. Study of anti-inflammation, abirritation and eliminating stasis effect of Shuang-bai powder and the effective parts of its single herb. Pharmacology and Clinics of Chinese Materia Medica 2011; 27(2):118-21.
6. Xu ZW, Liu XB. Collection and academic features of prescriptions from famous doctors in Guangzhou area. Journal of Guangzhou University of Traditional Chinese Medicine 2009; 26(5):488.
7. Shi QH, Cheng L, Chen GF, Zhang NH, Gao HL. The effect of acupoint catgut-embedding therapy combined with the external application of Chinese traditional medicine Shuang-bai powder on 40 patients with cancer pain. Jiangxi J of Traditional Chinese Medicine 2014; (4):21-4.
8. Chang ZR, Li J, Fu XT. Qualitative and quantitative methods for xuanji huapi plaster. Chinese Traditional Patent Medicine 2012; 34(10):1919-25.
9. Song HZ, Li SJ, Yu J, Dong SZ, Ouyang F, Qiu LH, Huang Y. Clinical examples of external application of rhubarb licorice root decoction in treating *tinea pedis* from Professor Huang. Modern Traditional Chinese Medicine 2012; 32(2):7-8.
10. Zhang JH, Wang WN, Liu YX, Wang YN, Pei YH, Liu XQ. Influence of salt processing on the dissolution of com positions from *phellodendri amurensis* cortex. J of Shenyang Pharmaceutical University 2012; 29(7):551.
11. Guo MH, Song YX, Liu SP, Hu BR, Ma YY, Li XH. Study on skin toxicity of liuwei qiangu cataplasms. China Pharmacist 2014; 17(7).

LETTER TO THE EDITOR

THE INFLUENCE AND REGULATORY MECHANISM OF Y-BOX BINDING PROTEIN 1 IN OSTEOSARCOMA AND ITS SIGNIFICANCE

W-P. ZHOU[1], X. LIU[2], Y. YANG[3] and Y-F. LIU[4]

[1]Oncology Department, the First Affiliated Hospital of Zhengzhou University, Zhengzhou, Henan, China; [2]Blood Bank Center, the First Affiliated Hospital of Zhengzhou University, Zhengzhou, Henan, China; [3]Geriatrics Department, the First Affiliated Hospital of Zhengzhou University, Zhengzhou, Henan, China; [4]Biological Treatment Center, the First Affiliated Hospital of Zhengzhou University, Zhengzhou, Henan, China

Received January 23, 2015 – Accepted April 27, 2015

This study quantified the expression of Y-box binding protein 1 (YB-1) by the immunohistochemical method based on pathological paraffin block specimens of aspiration biopsy from patients with osteosarcoma to explore the influence and regulatory mechanism of YB-1 in osteosarcoma and its significance. Patients were divided into two groups with high and low expressed YB-1, and results showed that 7 cases (13.7%) and 18 cases (26.1%) were in level III, and 44 cases (86.3%) and 51 cases (76.9%) were in level IV respectively, and patients with high YB-1 expression quantity had higher malignant tumor degree (p=0.03). Moreover, the tumor necrosis rate induced by chemotherapy in the two groups were 21 cases (41.2%) and 38 cases (51.8%), respectively. By survival analysis, it was found that a 5-year overall survival rate of patients with high YB-1 expression and low YB-1 expression were 61.2% and 76.6%, respectively (p = 0.054), and 5-year event free survival rates were 52.5% and 72.4%, respectively (p = 0.033). Furthermore, metastasis rate of high YB-1 expression and low YB-1 expression were 41.8% and 22.7%, respectively (p = 0.036), indicating that patients with high YB-1 expression had higher pulmonary metastasis rate. Through further study, we discovered that possibly miR-382 plays a regulatory role in YB-1 gene in osteosarcoma.

Osteosarcoma, the most common primary malignant bone tumor, mostly occurs in children and adolescents, with a high invasiveness and early metastasis. About 20% of patients with osteosarcoma have metastasis (1, 2). The lung is the most common metastasis organ of osteosarcoma, which seriously affects the prognosis of patients with osteosarcoma (3, 4). The traditional treatments of osteosarcoma include amputation surgery, preoperative and postoperative chemoradiotherapy adjuvant treatment, etc (5, 6). Although researchers all over the world have carried out much relevant clinical and basic research on osteosarcoma over the past 30 years, an improvement in the prognosis of patients with osteosarcoma is still not forthcoming. While in the study on blood cancer, many patients achieved a lot of benefits by performing assessment before treatment, using molecular markers, and then

Key words: YB-1, osteosarcoma, expression regulation

Mailing address:
Dr Xin Liu,
Blood Bank Center,
the First Affiliated Hospital of
Zhengzhou University,
Zhengzhou, Henan, 450052, China
e-mail: lx@ibhsedu.com

0393-974X (2015)

developing individualized regimen according to the results of evaluation (7-8). Unfortunately, reliable prognostic markers are still needed in the treatment of osteosarcoma. There is much in depth research of occurrence, metastasis and drug resistant molecular targets of osteosarcoma, using advanced molecular biology techniques, currently being carried out. In addition, the application of gene therapy has a good prospect in the treatment of osteosarcoma. After large-scale sequencing of human genome, stem cell treatment has become the most dynamic, the most influential and promising disciplinary in the research field.

YB binding protein, a type of highly conservative multi-functional protein, participates in the regulation of transcription and metastasis. There are three kinds of YB binding proteins in humans, in which, Y-box binding protein 1 (YB-1), as one of the members of the cold shock protein family with highly conservative nucleic acid combined sequences in YBX1 genetic codes, is the most important one. Recently, with the constant increase of research on YB-1, abnormal expression of YB-1 protein was found in a variety of human tumors, playing an important role in occurrence, evolution, metastasis and multidrug resistance of the tumor (9). This study tried to clarify the role of YB-1 in osteosarcoma and its regulatory mechanism by molecular biology, cell biology and gene chip, in order to provide new methods for molecular diagnosis and prognosis of osteosarcoma.

MATERIALS AND METHODS

General materials

One hundred and twenty patients who had well preserved biopsy tissue paraffin specimens and who had undergone aspiration biopsy in our hospital from 2005 to 2012 were selected. They were diagnosed with highly malignant osteosarcoma, and received formal preoperative chemotherapy, excision and postoperative adjuvant chemotherapy. There were, 67 males and 53 females (mean age: 16.2 years), divided into two groups, with high and low expressed YB-1. The main anatomic sites were: thighbone (62 cases), tibia (22 cases), humerus (27 cases), pelvis (5 cases) and 4 cases with other sites. The tumor types were: mother cell osteosarcoma (72 cases), cartilage mother cell osteosarcoma (17 cases), fibroblast mother cell osteosarcoma (19 cases), angiotelectasis osteosarcoma (6 cases) and 6 cases of other types. Histological grading was: level III (25 cases), level IV (95 cases). Enneking staging were: stage A at level II (33 cases), stage B at level II (87 cases) respectively. Rates of tumor necrosis induced by chemotherapy were: 59 mild cases, 61 severe cases.

Reagents and instruments

YB-1 antibody (Santa Cruz Inc., America), Actin antibody (Sigma Inc., America), paraffin embedding machine (Leica Inc., Germany), optical microscope (BX41TF) (Olumpus Inc., Japan), Constant temperature drying oven (PHO50) (Experimental Instrument co., LTD, Shanghai, China), microsyringe (5 μl) (Zhenhai Glass Factory, Ningbo, China).

Correlation of YB-1 expression and clinical index in osteosarcoma tissue

Immunohistochemical staining was carried out on the paraffin sections, and the results were evaluated. Tan or brown cells presented positive; positive YB-1 was seen in the cytoplasm, in the cell nucleus and also in karyoplasm. Five different grades were defined according to the cell ratio after dyeing: colorless or light colored cells (<5%) zero, colored cells (>5% to 25%) 1 point, colored cells (>25% to 50%) 2 points, colored cells (>50% to 75%) 3 points, colored cells (>75%) 4 points. Dyeing grades showing 0-2 points were low and 3-4 points were high.

Influence and expression regulatory mechanism of YB-1 in osteosarcoma tissue

Cells were placed in Dulbecco Modified Eagle Medium (DMEM) containing 10% Fetal Bovine Serum (FBS), and were cultured in a humid atmosphere at 5% CO^2 at 37°C. The cells were removed from the incubator when they grew from 80% to 90%, the medium was removed and they were rinsed with Phosphate Buffer solution (PBS). 0.25% pancreatin was added and they were digested for 1-2 min. The appropriate complete medium was added when cells became round and remained submerged. The cells were dried and then the cell suspension was equally divided into petri dishes. They were cultured in an incubator in a humid atmosphere with 5% CO^2 at 37°C, for 2-3days.

Cells with 70%-80% convergence taken from the petri dishes were infected with plasmid. Part of the cell samples were removed from the medium 24 h after transfection. The cells were rinsed twice with PBS, digested with 0.25% pancreatin, and suspended in complete medium containing 10% FBS. The number of cells was counted under microscope, and density adjusted to 2.0×10^4/ml. They were planted in a 96-well plate at 2000 cells per well, cultured in an incubator in a humid atmosphere with 5% CO^2 at 37°C, and survival rate was detected. At the same time, colony-forming assay was performed

and the clone that was over 50 cells was counted under microscope after 24-hour transfection. Then the plasmid (containing puromycin resistance gene) that expressed YB-1 and YB-1 shRNA was transferred into SaOS2 and LM-7 osteosarcoma cell line using Lipofectamin 2000, and cells were managed with puromycin (2ng/ml) after plasmid had been transfected for 36 h. Moreover, medium was changed once every three days, and then stable cell line was screened after two weeks. The medium was changed after 72 h and the total RNA extracted from cells was kept at -80°C. Relevant protein expression was detected with quantitative fluorescence and Western blot method. Furthermore, differential expression of microRNA (miRNA) in osteosarcoma tissue was tested applying Hualian small RNA chip, and expression of mRNA of relevant gene was detected with quantitative fluorescence PCR. In addition, patients were followed up after postoperative adjuvant chemotherapy to evaluate the influence of YB-1 on prognosis of tumor.

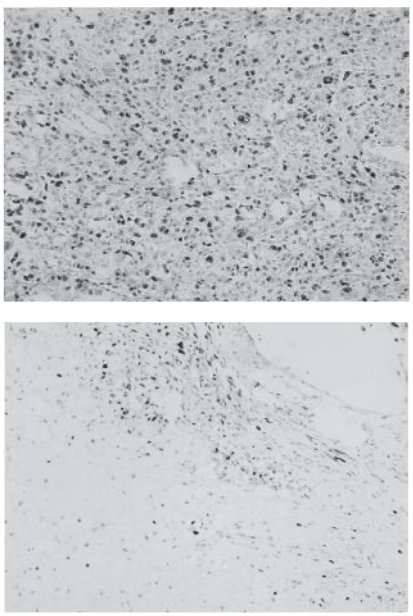

Fig. 1. *High YB-1 expression and low YB-1 expression in immunohistochemical staining.*

Detection index

Cell survival rate, external cell migration ability, expression of relevant protein and the mRNA expression of relevant gene were detected.

Statistical analysis

Data analysis adopted SPSS 18.0 statistical analysis software, and measurement data were expressed with (%, x±s). In addition, mean value between the groups was compared by one-way analysis of variance (One-way ANOVA), and pairwise comparison applied q test. Difference was considered to have statistical significance if $P<0.05$.

RESULTS

YB-1 expression

According to the immunohistochemical staining score, 120 cases of YB-1 expression in osteosarcoma tissue were absolutely positive. Of them, 55 cases (45.83%) had high YB-1 expression quantity (high YB-1 group), 65 cases (54.17%) had low YB-1 expression quantity (low YB-1 group) (Fig. 1).

Highly expressed YB-1 group and lowly expressed YB-1 group had no statistical significance on gender, age and distribution of anatomical site. Histological grading of those two groups were: 7 cases (13.7%) and 18 cases (26.1%) at level III respectively, 44 cases (86.3%) and 51 cases (73.9%) at level IV respectively, and patients with high YB-1

Table I. *Correlation of YB-1 expression quantity and clinical parameter.*

Biopsy tissue of osteosarcoma patients					
	YB-1 High		YB-1 Low		
Clinical variables	No.	%	No.	%	p
Total Patients	51	42.5	69	57.5	
Histologic Grade					0.03
III	7	13.7	18	26.1	
IV	44	86.3	51	73.9	
Enneking Grade					0.77
II a	13	25.5	20	29.0	
II b	38	74.5	49	71.0	
Response to chemotherapy					0.02
GR	21	41.2	38	55.1	
PR	30	58.8	31	44.9	

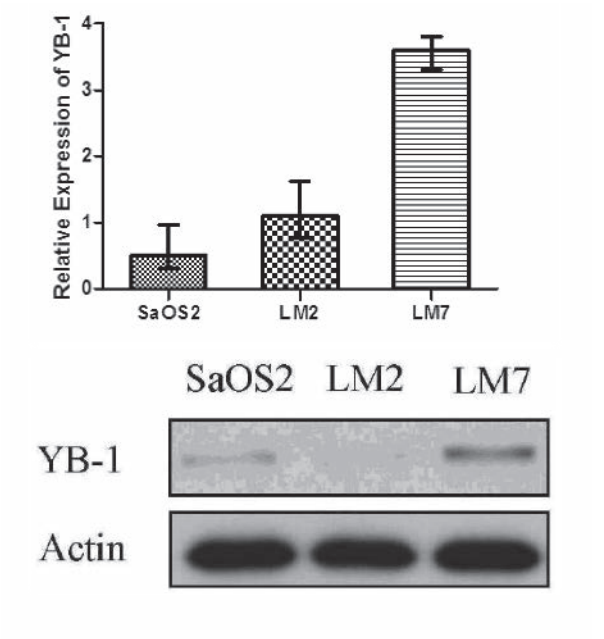

Fig. 2. *Expression of YB-1 protein in high transferred and low transferred osteosarcoma cells.*

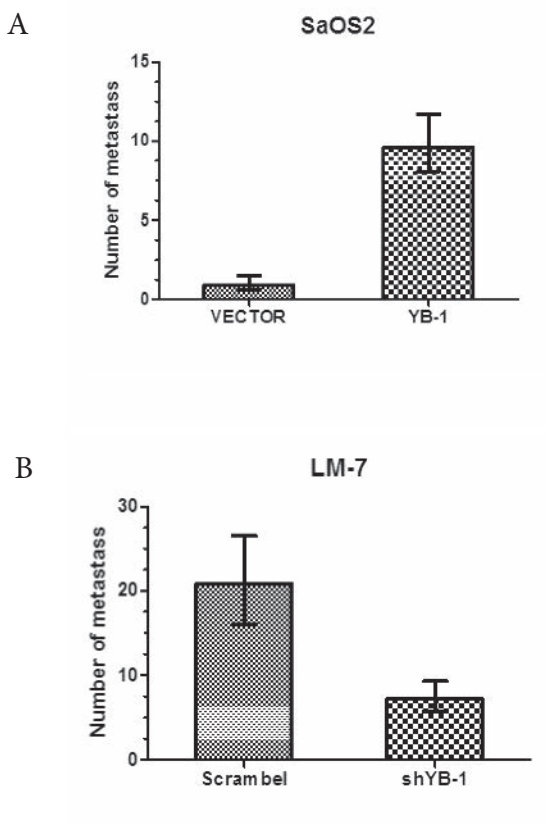

Fig. 3. ***A****) Pulmonary metastasis of SaOS2 cells after over expressing YB-1.* ***B****) Pulmonary metastasis of LM -7 cells after lowering YB-1 expression.*

expression quantity had higher tumor malignant degree (p=0.03). Enneking staging was: 13 cases (25.5%) and 20 cases (29%) in stage A at level II, 38 cases (74.5%) and 49 case (71%) in stage B at level II, and there was no statistical significance (p=0.77). Tumor necrosis rates of the two groups induced by chemotherapy were: 21 (41.2%) and 38 (55.1%) mild cases respectively, 30 (58.8%) and 31 (44.9%) severe cases respectively; the chemotherapy response of patients with low YB-1 expression were better, and the difference was statistically significant (p=0.02) (Table I).

Correlation of YB-1 expression quantity and prognostic parameter

The five-year overall survival rates of all patients were 69.5% (95%CI: 61.8%-79%), and 5-year event free survival rates were 62.4% (95%CI: 54.1%-72.1%). Five-year overall survival rates of patients with high YB-1 expression and low YB-1 expression were 61.2% (95%CI: 49.3%-76%) and 76.6% (95% CI: 67.7%-89.6%) (p=0.054), respectively, and 5-year event free survival rates were 52.5% (95%CI: 39.8%-67.1%) and 72.4% (95% CI: 62.9%-85.5%) (p=0.033), respectively. Metastasis rates of patients with high YB-1 expression and low YB-1 expression were 41.8% (95% CI: 26.7%-57.7%) and 22.7% (95%CI: 3.7%-37.3%) (p=0.036), respectively. Therefore, the patients with highly expressed YB-1 have higher pulmonary metastasis possibility and worse prognosis.

The promotion of YB-1 on invasion and migration of osteosarcoma cells

To detect the correlation of YB-1 expression and metastasis ability of osteosarcoma cells, this study measured YB-1 expression quantity in osteosarcoma cell lines with different metastasis abilities. The

results showed that YB-1 at mRNA level (Fig. 1) and protein level (Fig. 2) in high transferred LM-7 cell lines were significantly higher than other cell lines.

The promotion of high YB-1 expression on pulmonary metastasis of osteosarcoma cells

Previous experiments indicated that YB-1 has the ability of enhancing metastasis of osteosarcoma cells; hence, this research further studied the influence of YB-1 on internal pulmonary metastasis. SaOS2 cells (Fig. 3 A) of high YB-1 expression and LM -7 cells (Fig. 3 B) of lower YB-1 were injected into nude mouse through caudal vein injection. The results show that high YB-1 expression significantly promoted pulmonary metastasis of SaOS2 cells, on the contrary, the pulmonary metastasis ability of LM -7 cells with naturally high metastasis was inhibited after the YB-1 expression was lowered.

Differential expression of miRNA in metastatic and non-metastatic osteosarcoma cell

Through analyzing the miRNA chips of two patients who had metastasis in early stage and drug resistance, and had no metastasis but obtained good therapeutic effect, we discovered that 23 miRNA obviously declined in the samples of metastatic patients. Furthermore, we verified that the expression level of miR-382 and miR-30d in samples of osteosarcoma metastatic patients (n=6) and non-metastatic patients (n=6) using fluorescent quantitation PCR method. Based on the results, miRNA-382 expression presented obvious decline in samples of metastatic patients, but there was no change of miRNA-30d, and it also showed that it was miR-382 that plays a regulatory role in YB-1 gene in osteosarcoma.

DISCUSSION

Osteosarcoma, one of the most common malignant tumors in children and teenagers, accounts for about 20% of malignant bone tumor patients who are under 20 years of age, which is one of the most frequent reasons leading to child and adolescent death (10). Although the concept of neoadjuvant chemotherapy is known, a variety of multi-drug chemotherapy are being used and improved and extensive tumor resection is constantly advancing as well as limb-salvage technology, the overall survival rate of osteosarcoma is still poor. Five-year overall survival rate is about 65% (11). Through studying large samples, we find that clinical and pathological factors related to prognosis are as follows: tissue necrosis rate induced by chemotherapy, content of serum alkaline phosphatase, tumor histological type and grade, tumor size, pathogenic site and metastasis or non-metastasis and more. In addition, a lot of prognosis related molecular markers have been widely studied, but they are not all used in all clinical institutions, and as prognostic factors evaluating sensibility and specificity, there still exists a certain difference when compared with the requirements of clinical application. Therefore, exploring new molecular markers is still the focus of research on osteosarcoma.

This study combines the expression of specific molecules with clinical follow-up data with immunohistochemistry and PCR technology to verify the relationship of targeted molecules and occurrence, development of osteosarcoma, and metastasis and resistance mechanism, and explores in depth its mechanism by research means such as cell biology and molecular biology. It is not only beneficial to reveal the occurrence and development of osteosarcoma and metastasis and resistance mechanism, but also provides a fundamental basis for taking those molecules as diagnostic and prognostic markers. In the meantime, research on the mechanism of those molecules also shows how to effectively interfere osteosarcoma cell proliferation, metastasis and resistance through intervening on the molecules and pathways involved, which offers strong evidence for osteosarcoma molecular targeted therapy.

YB-1 coded by YBX1 gene, belongs to the cold shock protein super family, and this kind of protein includes one highly conserved DNA sequence motif combined with DNA and RNA. This sequence motif is located in a the cold shock domain made up of 65 amidogens, and the pronucleus cold shock protein homology of the domain is more than 40% (12). This high conservation indicates that this kind of protein plays an important role in pronucleus and eukaryotic cells.

In recent years, studies have found that the high YB-1 expression and tumor progression relate to poor prognosis, thus more attention is paid to YB-1.

YB - l, as a tumor protein (13, 14), regulates genetic codes of a variety of inflammatory kinesins so as to promote the development of tumors. Tumor cell proliferation and drug resistance will occur when its expression level rises, which can control tumor cell proliferation and survival from different sources in the body. It prevents the apoptosis of tumor cells through a variety of ways, and regulates the energy metabolism of tumor cells, thereby promoting aerobic glycolysis. Furthermore, YB-1 can promote unlimited replication and genome stability, and also can induce angiogenesis, control and adjust multi proteins and pathways relating to metabolism and invasion. Studies have shown that expression quantity and prognosis of YB-1 have significant correlation in many kinds of tumors including osteosarcoma, non-small cell lung cancer, synovial sarcoma, prostate cancer, melanoma and multiple myeloma.

In this study, patients with high YB-1 expression had higher metastasis rates, and had relatively poorer 5-year event free survival rate and overall survival rate than patients with low YB-1 expression, and the difference was statistically significant. These results suggest that the presence of YB-1 gives a possibility of evaluating prognostic markers, and might play a key role in tumor metastasis.

In the specimens, we found that YB-1 showed a high expression in transferred osteosarcoma. Metastasis ability of the osteosarcoma cell line was directly related to the expression of YB-1, and LM-7 cell line and highly expressed YB-1 had the strongest metastasis ability. LM-7 cells with high metastasis ability obviously lost its metastasis ability after its YB-1 expression lowered under RNA interference; in contrast, metastasis ability of SaOS2 cell line with lowly expressed YB-1 was also at a low level. The metastasis ability of SaOS2 increased significantly after over-expression of YB-1. Thus YB-1 was proved to be an important molecular promoting metastasis of osteosarcoma.

In conclusion, risks in the treatment of osteosarcoma can be classified on the basis of the quantity of YB-1 expression, and YB-1 expression is believed to be closely associated with the metastasis ability of the osteosarcoma cell line, miR-382 expression level is closely related to tumor metastasis, and YB-1 expression level is in close relationship with the prognosis of endostar adjuvant chemotherapy.

REFERENCES

1. Ayerza MA, Farfalli GL, Aponte-Tinao L, Muscolo L. Does increased rate of limb-sparing surgery affect survival in osteosarcoma? Clin Orthopaedics Rel Rese 2010; 468(11): 2854-59.
2. Salah S, Fayoumi S, Alibraheem A, et al. The influence of pulmonary metastasectomy on survival in osteosarcoma and soft-tissue sarcomas: a retrospective analysis of survival outcomes, hospitalizations and requirements of home oxygen therapy. Interact Cardiovasc Thorac Surg 2013; 17(2):296-302.
3. Leary SES, Wozniak AW, Billups CA, Wu JR, McPherson V, Neel MD, Rao BN, Daw. NC. Survival of pediatric patients after relapsed osteosarcoma: the St. Jude Children's Research Hospital experience. Cancer 2013; 119(14):2645-53.
4. Li X, Moretti VM, Ashana AO, Lackman RD. Impact of close surgical margin on local recurrence and survival in osteosarcoma. Int Orthop 2012; 36(1):131-37.
5. Kim HJ, Chalmers PN, Morris CD. Pediatric osteogenic sarcoma. Curr Opin Pediatr 2010; 22(1):61-66.
6. Bi WZ, Wang W. Status quo in treatment of osteosarcoma and its prospect. Chin Med News 2011; 26(14):15.
7. Brooks SA, Lomax-Browne HJ, Carter TM, Kinch CE, Hall DMS. Molecular interactions in cancer cell metastasis. Acta Histochemica 2010; 112(1):3-25.
8. Thomas X, Chelghoum Y, Fanari N, Cannas G. Serum 25-hydroxyvitamin D levels are associated with prognosis in hematological malignancies. Hematol 2011; 16(5):278-83.
9. Lin F, Zheng S, Shen Z, Tang LN, Chen P, Sun YJ, Zhao H, Yao Y. Relationships between levels of CXCR4 and VEGF and blood-borne metastasis and survival in patients with osteosarcoma. Med Oncol 2011; 28(2): 649-53.
10. Whelan JS, Jinks RC, McTiernan A. Survival from high-grade localised extremity osteosarcoma: combined results and prognostic factors from three

European osteosarcoma intergroup randomised controlled trials. Ann Oncol 2012; 23(6):1607-16

11. Chen J, Liu YX. Research progress of osteosarcoma chemotherapy. Zhejiang J Integr Trad Chin West Med 2010; 20(1): 53-55.
12. Eliseeva IA, Kim ER, Guryanov SCE. Y-box-binding protein 1 (YB-1) and its functions. Biochemistry-Moscow 2011; 76(13):1402-33.
13. Zhang Y. Progress of human YB-1 protein in the study of tumor. Nei Mongol J Trad Chin Med 2014; 33(10):115-16.
14. Cui Y, Li J, Shi JG, Yan QG. Effect of Y-box binding protein 1 on tumor and its research. Prog Mod Biomed 2010; (18): 3564-68.

LETTER TO THE EDITOR

GLYOXALASE I A111E, PARAOXONASE 1 Q192R AND L55M POLYMORPHISMS IN ITALIAN PATIENTS WITH SPORADIC CEREBRAL CAVERNOUS MALFORMATIONS: A PILOT STUDY

C. RINALDI[1], P. BRAMANTI[2], A. FAMÀ[1], C. SCIMONE[1], L. DONATO[1], C. ANTOGNELLI[3], C. ALAFACI[4], F. TOMASELLO[4], R. D'ANGELO[1] and A. SIDOTI[1]

[1]Department of Biomedical Sciences and Morphological and Functional Images, Division of Medical Biotechnologies and Preventive Medicine, University of Messina, Messina, Italy; [2]IRCCS Centro Neurolesi "Bonino-Pulejo", Messina, Italy; [3]Department of Experimental Medicine, University of Perugia, Perugia, Italy; [4]Department of Neurosciences, University of Messina, Messina, Italy

Received November 10, 2014 – Accepted April 2, 2015

It is already known that the conditions of increased oxidative stress are associated to a greater susceptibility to vascular malformations including cerebral cavernous malformations (CCMs). These are vascular lesions of the CNS characterized by abnormally enlarged capillary cavities that can occur sporadically or as a familial autosomal dominant condition with incomplete penetrance and variable clinical expression attributable to mutations in three different genes: *CCM1(Krit1)*, *CCM2 (MGC4607)* and *CCM3* (*PDCD10*). Polymorphisms in the genes encoding for enzymes involved in the antioxidant systems such as glyoxalase I (GLO I) and paraoxonase I (PON I) could influence individual susceptibility to the vascular malformations. A single nucleotide polymorphism was identified in the exon 4 of GLO 1 gene that causes an amino acid substitution of Ala for Glu (Ala111Glu). Two common polymorphisms have been described in the coding region of PON1, which lead to glutamine → arginine substitution at 192 (Q192R) and a leucine → methionine substitution at 55 (L55M). The polymorphisms were characterized in 59 patients without mutations in the CCM genes versus 213 healthy controls by PCR/RFLP methods using DNA from lymphocytes. We found that the frequency of patients carrying the GLO1 A/E genotype among the case group (56%) was four-fold higher than among the controls (14.1%). In the cohort of CCM patients, an increase in the frequency of PON192 Q/R genotype was observed (39% in the CCM group versus 3.7% in the healthy controls). Similarly, an increase was observed in the proportion of individuals with the genotype R/R in the disease group (5%) in respect to the normal healthy cohort (0.5%). Finally, the frequency of the PON55 heterozygotes L/M genotype was 29% in patients with CCMs and 4% in the healthy controls. The same trend was observed in PON55 homozygous M/M genotype frequency (CCMs 20% *vs* controls 10%). The present study aimed to investigate the possible association of GLO1 A111E, PON1 Q192R and L55M polymorphisms with the risk of CCMs. We found that individuals with the GLO1 A /E genotype, PON192/QR-RR genotypes and PON55/LM-MM genotypes had a significantly higher risk of CCMs compared with the other genotypes. However, because CCM is a heterogeneous disease, other additional factors might be involved in the initiation and progression of CCM disease.

Key words: cerebral cavernous malformation, glyoxalase I, paraoxonase I

Mailing address: Dr Rosalia D'Angelo,
Department of Biomedical Sciences
and Morphological and Functional Images,
Division of Medical Biotechnologies
and Preventive Medicine, University of Messina,
via C. Valeria 1, 98125 Messina, Italy
Tel.: +39 0902213372 Fax: +39 090692449
e-mail address: rdangelo@unime.it

0393-974X (2015)

Cerebral cavernous malformations (CCMs) are vascular malformations characterized by abnormally enlarged sinusoidal channels, with a simple endothelial lining devoid of elastin and smooth muscle (1). CCMs affect up to 0.5% of the human population (2, 3), although only 20-30% of affected individuals develop symptomatic disease (4, 5). They have been reported in infants, children, and old people, but the majority of patients present with symptoms between the second and fifth decades.

The most common manifestations include seizures, recurrent headaches, hemorrhagic stroke, focal neurological deficits and also cognitive impairment, that may occur especially in the earliest onset presentation of the disease (2, 3). CCMs may arise sporadically or be inherited as an autosomal dominant condition with incomplete penetrance and variable expressivity. Sporadic cases usually present with a single lesion, whereas the familial forms are characterized by multiple and evolutive lesions and are associated with mutations in three distinct loci: *KRIT1/CCM1*, *MGC4607/CCM2* e *PDCD10/CCM3* (6-8).

Loss-of-function mutations in genes enconding CCM proteins causes destabilization of endothelial barrier function leading to increased vascular permeability (9-11). Experimental studies have clearly demonstrated that the homozygous loss of CCM genes is not sufficient to induce CCM lesions, suggesting that additional factors, relative to the neurovascular microenvironment, are necessary to cause CCM disease (12). For example, it is known that krit1 is involved in the maintenance of the intracellular reactive oxygen species (ROS) homeostasis to prevent the oxidative stress (13) like glyoxalase I (GLO1) (14) and paraoxonase I (PON1) genes (15).

With regard to GLO 1 a single nucleotide polymorphism was identified in the exon 4 of GLO 1 gene that causes an amino acid substitution of Ala for Glu (Ala111Glu) (16). The presence of an additional acidic charge from the Glu residue was associated with a decreased enzyme activity which may cause accumulation of AGEs in cells or tissues. This decrease in the activity of GLO 1 causes an accumulation of MG and glycation of High-Density Lipoprotein (HDL). The glycation of HDL also results in a decrease in the activity of PON 1(15). This also inhibits the production of the monocyte chemotactic protein-1 (MCP-1) by the endothelial cells (17). For these reasons, PON 1 has been considered an important mediator with anti-inflammatory and antioxidants capacity.

In the coding region of PON1 gene, two genetic polymorphisms which change the paraoxon hydrolysis activity among individuals have been reported (18): Q192R which lead to glutamine → arginine substitution at amino acid 192 and L55M to leucine → methionine substitution at amino acid 55 (19). Furthermore, the histological analysis of CCM showed the presence of cholesterol crystals around the vessels (18, 20), probably index of a wrong cholesterol efflux and of a hypothetical malfunction of PON1 (21-23).

In our previous study, a CCM gene mutation analysis in a cohort of 40 Italian sporadic patients was performed and only four novel mutations were identified in 3 patients (24). Here, a case-control study on 59 CCM patients lacking CCM mutations and 213 healthy controls was performed to evaluate the possible relationships between PON1 and GLO1 genes allelic variants and CCM risk.

MATERIALS AND METHODS

Patients

A total of 59 CCM patients (39 male and 20 female) were recruited. All were negative for mutations and polymorphisms in the 3 CCM genes to coding exons and intron–exon boundaries sequencing and Multiplex ligation-dependent probe amplification (MLPA). Twenty patients were recruited from previous screening and 39 during recent months. Patients with single or multiple malformations, but without known clinically affected relatives, were classified as apparently sporadic.

Clinical and neuroimaging information on the number and localization of CCM lesions was collected through direct interview and review of medical records. Lesions were single in 56 patients (95%) and multiple in 3 patients (5%). In 32/59 (54%) patients, lesions were located supratentorially; in 16/59 (27%) lesions were subtentorial and in 11/59 (19%), were supra/subtentorial. The data available did not reveal the existence of patients with skin, spinal cord, retinal, hepatic or vertebral lesions. Additional clinical data included: age of symptoms onset and neurological events classified in: headache, epilepsy, cerebral hemorrhages and focal neurological deficits.

Headache was reported in 12 patients, epilepsy in

22, and cerebral hemorrhages in 8; 14 patients had focal neurological deficits, while 3 patients were asymptomatic. The mean age at onset of symptoms was 46.0±12.0 years (median: 47; range: 20-65 years) (Table I).

The control group consisted of 213 unrelated, randomly selected, ethnically matched, healthy individuals, subjects of a previous case-control study on the possible role of GLOI and PON polymorphisms in multiple sclerosis (25). Demographic data on controls are summarized in Table I. Age at onset of symptoms of male *vs* female was matched in the CCM patients, as well as age of male *vs* female in the controls. Overall patient age at onset of symptoms versus overall healthy control age were matched. Table I indicates no significant differences (P<0.05). This study was approved by the Scientific Ethics Committee of the Azienda Ospedaliera Universitaria - Policlinico 'G. Martino' Messina. Informed consent was obtained from all patients and controls.

Molecular analyses

Genomic DNA was extracted from peripheral blood using the standard salting out method. DNA was extracted from lymphocytes by the salting out method (26). Nucleotide sequence of primers is shown in Table II. PCR with a final volume of 50 µl, containing 50 ng of DNA, 20 pmoles of each primer, 100 µM each of dNTP, 1.5 mM of MgCl2, 10 mM Tris-HCl pH 8.3, 50 mM of KCl and 1U of Taq DNA polymerase were performed in a Gene Amp PCR System 2700 (Life Technologies) at the following conditions: initial denaturation step at 94°C for 5 min and then 35 cycles consisting of denaturation at 94°C for 40 s, annealing for 30 s and extension at 72°C for 30 seconds. The final extension step at 72°C was extended to 10 minutes. The annealing temperature was optimized for each primer set.

Genotyping

The three polymorphisms were characterized in CCM patients and in healthy controls. Genotyping of these polymorphisms was performed using polymerase chain reaction/restriction fragment length polymorphism (PCR/RFLP) method. The C to A substitution in GLO 1 exon 4, which changes Ala111Glu in the encoded protein, leads to the loss of a recognition site for SfaNI (New England Biolabs GmbH, Germany) restriction enzyme. Single-base substitutions in PON1 exon 3 and 6, which lead to the change of leucine to methionine and glutamine into arginine, at positions 55 and 192, respectively, create recognition sites for Nla III (PON1/55) and Alw1 (PON1/192) (New England Biolabs GmbH, Germany) restriction enzyme. PCR products were digested using either SfaNI for 16 h at 37°C, Alw1 for 1 h at 37°C or NlaIII for 15 min at 37°C. The digested product was resolved by 2% agarose gel electrophoresis and the fragments were visualized under UV light after staining with ethidium bromide to identify the single base pair change. The expected DNA fragments, upon digestion, are listed in Table II.

Statistical analysis

Analysis of the data was performed using the computer software SPSS for Windows (Version 6.0.1) and Epi Info

Table I. *Demographic and disease-related data on CCM patients and controls.*

CCM patients (n=59)				
			Age of onset	
Gender	n	Mean ±SD	Range	Median
Male	39	45.2±12.22	20-64	46
Female	20	47±11.0	27-65	48
Overall		46±12.0	20- 65	47
Healthy controls (n=213)				
			Age	
Gender	n	Mean ±SD	Range	Median
Male	61	45/±12	25-60	48
Female	152	43±11	22-59	50
Overall		44±11.4	20- 60	49

P </0.05 indicates significant differences. Statistical analysis was tested by the Student's t-test.
CCM: Cerebral cavernous malformations; SD: standard deviation

Table II. *Oligonucleotide primer sequences used for genotyping.*

Gene	Oligonucleotides	Sequence	RFLP		
PON1 192Q/R	PON192F	5'-GAATGCCAGTTAATAATCCTG -3'	QQ	QR	RR
	PON192R	5'-ACCAGTATGCCTTCACAATG -3'	473	473,146,327	146,327
PON1 55L/M	PON55F	5'-TAAGAGGATTCAGTCTTTGA -3'	LL	LM	MM
	PON55R	5'-GTATACAGAAAGCCTAAGTG -3'	423	423,123,300	123,300
GLO1 A111E	GLO1F	5'-TCAGAGTGTGTGATTTCGTG-3'	AA 453,260	AE 713, 453,260	EE 713
	GLO1R	5'-CATGGTGAGATGGTAAGTGT-3'			

PON1 192Q/R, paraoxonase 1 Q192R; PON1 55L/M, paraoxonase 1 L55M; GLO1: glyoxalase 1; F: Forward; R: Reverse; base pair(s)

(Version 6.0.4).

For each group (control and patients), allele frequencies were calculated by direct gene counting. Deviations from the Hardy-Weinberg equilibrium (HWE) were tested by the χ^2-test on a 2x3 contingency table, with two degrees of freedom. Associations between the gene genotypes and the risk of CCM were assessed by odds ratios (Ors) and 95% confidence intervals (CIs).

Ors express the relative risk (OR) of CCM with a specific genotype and are calculated by dividing the odds of a CCM having a specific genotype by the odds of a control subject having the same genotype. Estimates of statistical significance were calculated by standard χ^2, analysis included Student's *t*-test of means and the respective standard deviation (SD) for case and controls. A two-side probability value of <0.05 was considered to indicate statistical significance.

RESULTS

GLO1, PON 1 192, PON1 55 gene polymorphisms and the risk of CCM in healthy controls and CCM patients are given in Table III.

For GLO1, the prevalence of the wild type GLO1 A/A genotype was significantly lower (P<0.001) in the CCM group (13.5%) than in the healthy controls (37%). We also found that the frequency of patients carrying the A/E genotype among the case group (56%) was four-fold higher than among the controls (14.1%). For individuals with the E/E genotypes, the prevalence was found to be 1.6-fold lower among the CCM cohort (30.5%) compared with the healthy controls (49.3%) (P<0.0001).

Patients with the A /E genotype had a significant increase for CCM risk (OR= 10.7, 95% CI= 4.4-25.8, P< 0.0001) compared with the A/A genotype. Therefore, the presence of the E allele significantly increases the risk of CCM. This might be explained by the fact that the A to E substitution, due to the SNP, may determine conformational modification in the enzyme, leading to an isoenzyme with a lower detoxification capacity (16).

With regard to PON192, the prevalence of the wild type PON1 192 Q/Q genotype was significantly lower (P<0.0001) in the CCM group (56%) than in the healthy controls (96%). In the cohort of CCM patients, an increase in the frequency of PON192 Q/R genotype was observed (39% in the CCM

Table III. *Prevalence of GLO1, PON1 192, PON1 55 genetic polymorphisms and risk of CCM.*

	Genotype	Controls (n)	(n=213) %	CCMs (n)	(n=59)%	OR	95%CI	p
GLO1	A/A	78	37.0	8	13.5	1.0	0.3-2.8	1
	A/E	30	14.1	33	56.0	10.7	4.4-25.8	< 0.0001
	E/E	105	49.3	18	30.5	1.67	0.7-4.04	p=0.25
PON1 Q192R	Q/Q	204	96	33	56.0	1.0	0.6-1.7	1
	Q/R	8	3.7	23	39.0	17.7	7.3-43.0	< 0.0001
	R/R	1	0.5	3	5.0	18.5	1.9-183.7	0.001
PON1 L55M	L/L	183	86	30	51.0	1.0	0.6-1.7	1
	L/M	9	4.0	17	29.0	11.5	4.7-28.2	< 0.0001
	M/M	21	10.0	12	20.0	3.48	1.5- 7.8	0.002

Genotypes with Q/R, L/M and A/E alleles, respectively. OR: odds ratios are calculated relative to subjects with the Q/Q, L/L and A/A genotypes, respectively CI: confidence interval Two-sided $\chi 2$ test; $p< 0.05$ indicates statistical significance

Table IV. *Haplotype of PON1 gene frequencies in CCM patients.*

Haplotype	n (%)
LLQQ	9 (15.25)
LLQR	18 (30.5)
LLRR	3 (5.08)
LMQQ	13 (22.0)
MMQQ	11 (18.6)
LMQR	3 (5.08)
MMQR	2 (3.38)

Q=/glutamine and R=arginine at position 192 of the peptide sequence;
L=leucine and M=methionine at position 55 of the peptide sequence

group *vs* 3.7% in the healthy controls) (P<0.0001), with an OR of 17.7 (95% CI=7.3-43.0, P<0.0001). Similarly, an increase was observed in the proportion of individuals with the genotype R/R in the disease group (5.0%) with respect to the normal healthy cohort (0.5%) OR of 18.5 (95% CI=1.9-183.7, P= 0.001).

Regarding the PON1 55 polymorphism, the prevalence of the wild type PON1 55 L/L genotype was significantly lower (P<0.0001) in the CCM group (51%) than in the healthy controls (86%). The frequency of the PON55 heterozygotes L/M genotype was 29% in patients with CCM and 4% in the control group. Individuals belonging to the CCM cohort had a significantly higher risk for CCM (OR= 11.5, 95% CI=4.7-28.2, P<0.0001).

Finally, we observed differences in the frequency also of the PON155 homozygotes M/M among the two groups (CCMs 20% *vs* controls 10%), resulting in an elevation of CCM risk (OR=3.48, 95% CI=1.5-7.8, P=0.002).

In addition, the association between the PON 1/55 and PON1/192 polymorphisms was estimated, and PON1 haplotypes were reconstructed (Table IV). In particular, we described 22% of haplotype LMQQ and 15.25% LLQQ. Thus, 37.25% of all CCM patients expressed, either single or double quantities of leucine instead of methionine at 55 position of PON1, with a significant reduction of serum enzyme activity (27).

DISCUSSION

In an effort to further elucidate pathogenic mechanisms of CCM and to increase our understanding of the role of additional genetic factors in the predisposition to this disease, we determined the frequencies and ORs of GLO 1 and PON I gene polymorphisms in a healthy control and in a population of patients with CCM.

We hypothesized a possible relationship between GLO1 A111E and PON1 Q192R/L55M polymorphisms with the risk of CCM because the increase of oxidative stress induced by the incorrect function of these enzymes would make the endothelial cells more susceptible to the vascular malformations and so contribute to CCM pathogenesis especially in the absence of CCM gene mutations. Because CCM is a heterogeneous disease, further possible non-genetic mechanisms could influence the final phenotype of CCM, besides the oxidative stress (28, 29). This hypothesis is supported by the fact that in our study, on GLOI A/E polymorphism, the frequency of patients carrying the E/E genotype was 1.6-fold lower than among the healthy controls. Exogen factors, environmental conditions, dietary habits, in combination with the potential susceptibility due to A/E polymorphism, possibly lead to the risk of CCM. Recently, endocrinological factors also were proposed as important in the pathophysiology of progression and/or worsening of vascular (and/or lymphatic) malformations (30, 31).

ACKNOWLEDGEMENTS

We are thankful to Prof. Saverio Francesco Retta, coordinator of CCM Italia (Community for Cerebral Cavernous Malformations), who contributed to study stimulation.

REFERENCES

1. Clatterbuck RE, Eberhart CG, Crain BJ, Rigamonti D. Ultrastructural and immunocytochemical evidence that an incompetent blood-brain barrier is related to the pathophysiology of cavernous malformations. J Neurol Neurosurg Psychiatry 2001; 71:188-92.
2. Labauge P, Denier C, Bergametti F, Tournier-Lasserve E. Genetics of cavernous angiomas. Lancet Neurol 2007; 6:237-44.
3. Revencu N, Vikkula M. Cerebral cavernous malformation: new molecular and clinical insights. J Med Genet 2006; 43:716-21.
4. Otten P, Pizzolato GP, Rilliet B, Berney J. 131 cases of cavernous angioma (cavernomas) of the CNS, discovered by retrospective analysis of 24,535 autopsies. Neurochirurgie 1989; 35:82-83,128-31 (in French).
5. Robinson JR, Awad IA, Little JR. Natural history of the cavernous angioma. J Neurosurg 1991; 75:709-14.
6. Heros RC, Morcos JJ. Cerebrovascular surgery: past, present, and future. Neurosurgery 2000;47(5):1007-33.
7. Folkersma H, Mooij JJ. Follow-up of 13 patients

with surgical treatment of cerebral cavernous malformations: effect on epilepsy and patient disability. Clin Neurol 2001; 103(2):67-71.
8. D'Angelo R, Marini V, Rinaldi C, et al. Mutation analysis of CCM1, CCM2 and CCM3 genes in a cohort of Italian patients with cerebral cavernous malformation. Brain Pathol 2011; 21:215-24.
9. Stockton RA, Shenkar R, Awad IA, Ginsberg MH. Cerebral cavernous malformations proteins inhibit Rho kinase to stabilize vascular integrity. J Exp Med 2010; 207(4):881-96.
10. Whitehead KJ, Chan AC, Navankasattusas S, et al. The cerebral cavernous malformation signaling pathway promotes vascular integrity via Rho GTPases. Nat Med 2009; 15:177-84.
11. Zheng X, Xu C, Di Lorenzo A, et al. CCM3 signaling through sterile 20-like kinases plays an essential role during zebrafish cardiovascular development and cerebral cavernous malformations. J Clin Invest 2010; 120:2795-804.
12. Meng Q, Xia Y. c-Jun, at the crossroad of the signaling network. Protein Cell 2011; 2:889-898.
13. Goitre L, Balzac F, Degani S, Degan P, Marchi S, Pinton P, Retta SF. KRIT1 regulates the homeostasis of intracellular reactive oxygen species. PLoS One 2010; 5:e11786.
14. Thornalley PJ. The glyoxalase system in health and disease. Mol Aspects Med 1993; 14(4):287-371.
15. Bacchetti T, Masciangelo S, Armeni T, Bicchiega V, Ferretti G. Glycation of human high density lipoprotein by methylglyoxal: effect on HDL-paraoxonase activity. Metabolism 2014; 63(3):307-11.
16. Junaid MA, Kowal D, Barua M, Pullarkat PS, Sklower Brooks S, Pullarkat RK. Proteomic studies identified a single nucleotide polymorphism in glyoxalase I as autism susceptibility factor. Am J Med Genet 2004; 131:11-17.
17. Mackness B Hine D, Liu Y, Mastorikou M, Mackness M. Paraoxonase-1 inhibits oxidised LDL-induced MCP-1 production by endothelial cells. Biochem Biophys Res Commun 2004; 318(3):680-83.
18. Camps J, Marsillach J, Joven J. The paraoxonases: role in human diseases and methodological difficulties in measurement. Critical Reviews in Clin Lab Sci 2009; 46(2):83-106.
19. Mackness B, Mackness MI, Arrol S, Turkie W, Durrington PN. Effect of the human serum paraoxonase 55 and 192 genetic polymorphisms on the protection by high density lipoprotein against low density lipoprotein oxidative modification. FEBS Lett 1998; 423(1):57-60.
20. Frischer JM, Pipp I, Stavrou I, Trattnig S, Hainfellner JA, Knosp E. Cerebral cavernous malformations: congruency of histopathological features with the current clinical definition. J Neurol Neurosurg Psychiatry 2008; 79(7):783-88.
21. Rozenberg O, Shih DM, Aviram M. Human serum paraoxonase 1 decreases macrophage cholesterol biosynthesis: possible role for its phospholipase-A2-like activity and lysophosphatidylcholine formation. Arterioscler Thromb Vasc Biol 2003; 23:461-67.
22. Rosenblat M, Vaya J, Shih D, Aviram M. Paraoxonase 1 (PON1) enhances HDL-mediated macrophage cholesterol efflux via the ABCA1 transporter in association with increased HDL binding to the cells: a possible role for lysophosphatidylcholine. Atherosclerosis 2005; 179:69-77.
23. Aviram M, Rosenblat M. Paraoxonases 1, 2, and 3, oxidative stress, and macrophage foam cell formation during atherosclerosis development. Free Radic Biol Med 2004; 37(9):1304-16.
24. D'Angelo R, Alafaci C, Scimone C, Ruggeri A, Salpietro FM, Bramanti P, Tomasello F, Sidoti A. Sporadic cerebral cavernous malformations: report of further mutations of ccm genes in 40 italian patients. Biomed Res Int 2013; 459253.
25. Sidoti A, Antognelli C, Rinaldi C, D'Angelo R, Dattola V, Girlanda P, Talesa V, Amato A. Glyoxalase I A111E, paraoxonase 1 Q192R and L55M polymorphisms: susceptibility factors of multiple sclerosis? Mult Scler 2007; 13:446-453.
26. Sambrook J, Fritsch EF, Maniatis T. Molecular Cloning: A Laboratory Manual, 1st and 2 nd edns. Cold Spring Harbour Laboratory1989; New York.
27. Mackness MI, Arrol S, Mackness B, Durrington PN. Alloenzymes of paraoxonase and effectiveness of high-density lipoproteins in protecting low-density lipoprotein against lipid peroxidation. Lancet 1997; 349(9055):851-2.
28. Ferrè N, Camps J, Fernandez-Ballart J, et al. Regulation of serum paraoxonase activity by genetic,

nutritional and life style factors in the general population. Clin Chem 2003; 49:1491- 97.
29. Choquet H, Nelson J, Pawlikowska L, et al. Association of cardiovascular risk factors with disease severity in cerebral cavernous malformation type 1 subjects with the common Hispanic mutation. Cerebrovasc Dis 2014; 37(1):57-63.
30. Kulungowski AM, Hassanein AH, Nosé V, et al. Expression of androgen, estrogen, progesterone, and growth hormone receptors in vascular malformations. Plast Reconstr Surg 2012; 129(6):919e-924e.
31. Salpietro V, Ruggieri M, Alterio T, Mallamace R, Chirico V, Arrigo T, Romano C. Is there a risk of pubertal worsening in primary intestinal lymphangiectasia? J Endocrinol Invest 2013; 36(11):1128.

LETTER TO THE EDITOR

QUALITY OF LIFE FOLLOWING SURGICAL TREATMENT OF LOWER LIMB METASTASES IN LONG BONE

C. PERISANO[1], L. SCARAMUZZO[2], V. DE SANTIS[1], A. PICCIOLI[3], A. ZIRANU[1], C. BARONE[4] and G. MACCAURO[1]

[1]Department of Geriatrics, Neurosciences and Orthopaedics, University Hospital Agostino Gemelli, Catholic University of the Sacred Heart, Rome, Italy; [2]Spine Surgery Division, IRCCS Istituto Ortopedico Galeazzi Spa, Milan, Italy; [3]Orthopedics Oncology, "Palazzo Baleani", Azienda Policlinico Umberto I, Rome, Italy; [4]Department of Internal Medicine, Division of Medical Oncology, University Hospital "Agostino Gemelli", Catholic University of the Sacred Heart School of Medicine, Rome, Italy

Received January 27, 2015 – Accepted April 29, 2015

Pathological fractures have a high incidence in musculo-skeletal oncology, and localization in long bone causes severe pain, disability and poor quality of life. The aim of this retrospective case series is to evaluate the clinical results, in particular regarding the quality of life, in patients affected by lower long bone pathological fractures surgically treated. We analyzed 93 patients with pathological fractures of tibia and femur surgically treated in our Orthopaedic Department and followed up for at least 3 years or until their death. Intramedullary nailing or endoprosthetic reconstruction for pathologic fractures located in the metadiaphyseal and diaphyseal or proximal regions in advanced-stage cancer patients are suitable methods for a stable fixation or reconstruction. These approaches guarantee a good mechanical stability, a faster mobilization, a better control of pain with an overall improvement in quality of life in all patients, confirmed also by the trend of the ECOG performance status and QOL-ACD.

Pathological fractures are the most frequent emergencies in orthopaedic oncology (1). Ten to twenty-nine percent of metastatic patients have fractures (1, 2). Approximately 280,000 US adults are living with metastatic bone disease although the true frequency is probably underestimated. The prevalence of metastatic bone disease changes according to age and sex and becomes higher over the 5th decade (2).

Metastatic disease particularly affects pelvis, spine and long bone (1-4). Femur, humerus and tibia are the most commonly affected long bones and induce a wide bone loss resulting in severe pain, disability and fracture (1-4).

Pathological fractures have a low healing rate, and reduce the prognosis and the quality of life, although improvements in the method of fixation have a better outcome than only radiotherapy and conservative treatment, providing a better pain control relief or return of limb normal function (1). Surgery is now recommended for intractable pain and impending or established pathologic fractures (1, 5, 6). Surgical

Key words: bone metastasis, pathological fractures, impending fracture, quality of life

Mailing address: Dr Perisano Carlo,
Department of Geriatrics, Neurosciensces and Orthopaedics,
University Hospital Agostino Gemelli,
Catholic University of the Sacred Heart,
Largo A.Gemelli 1, 00168, Rome, Italy
Tel.: +39 3295416825
e-mail: carloperisano@hotmail.it

0393-974X (2015)

DISCLOSURE: ALL AUTHORS REPORT NO CONFLICTS OF INTEREST RELEVANT TO THIS ARTICLE.

intervention aims to achieve local tumour control, durable stability, immediate reduction of pain, and acceptable function of the affected extremity and an early restoration of full weight-bearing as quickly as possible, minimizing the morbidity associated with the operative procedure and hospitalization (1, 5, 6).

The aim of this clinical study is a retrospective analysis on patient with lower long bone pathological fractures reviewed in terms of surgical strategy, quality of life, return to function and complications related to these procedures

MATERIALS AND METHODS

We reviewed our previous analysis on patients with bone metastasis in lower long bone. From 1998 to 2010, more than 500 patients were treated at our institution for metastatic lesions involving the appendicular skeleton. Of these, we electively reviewed patients with lesions involving the lower long bones (femur, tibia) managed surgically. Exclusion criteria were open fractures, primary bone tumours, non-unions and lesions with uncertain diagnosis. Patients with fibular metastasis were excluded from the study because of the limited number of cases. Preoperative evaluation included cancer staging with total body CT scan, alternatively bone scan or positron emission tomography (PET)-CT was carried out to ascertain the primary tumor and the presence of visceral or multiple bone metastases. Primary lesions were identified in all patients before surgery. Preoperative blood samples, chest XR and biplanar XR of the affected long bone were carried out before surgery. Surgical procedures were performed according to Capanna and Campanacci criteria (7) adjusted with reference to the Karnofsky general status scale (8). Indications to surgery were considered a complete or impending fracture, presence of intractable pain unresponsive to opioids, complete inability to walk because of pain, and more than 3 months of life expectancy. Biopsy was performed only on patients for whom the diagnosis of primary carcinoma had not been previously established.

In the patients with metastasis of thyroid and kidney carcinoma, neoadjuvant embolisation was performed to reduce intraoperative bleeding and an easy and accurate tumour resection. Tumour debulking or curettage was performed after open reduction when tumour extended widely in the soft tissues around the fracture. Surgical strategy was planned taking into account several factors, including size and site of the lesion, histology, and the presence of visceral metastasis.

All patients with pertrochanteric or diaphyseal femoral fracture were treated with a titanium Proximal Nail (Standard or Antirotation) or Lateral Anterograde Femoral Nail (PFN, PFN-A or LAFN, respectively, Synthes, USA) inserted in a locked static mode after a closed or open reduction of the fracture. The diameter of PFN and PFNA was 10 mm, while LAFN changed from 10 to 12 mm. One screw in PFN and PFN-A or two distal screws in LAFN were always inserted in a static mode. Acrylic cement was used to fill the bone cavity after PFN insertion to improve mechanical stability of the system; this was not necessary with PFN-A or LAFN stabilisation because the proximal diameter of the nail was selected to entirely fill the transverse diameter of the femoral lesion.

All patients with multiple metastasis and a tibial metadiaphyseal localisation were treated by the insertion of an unreamed static intramedullary locked nail. Lesions at the proximal tibia were treated by intralesional piecemeal removal, and filled with bone cement. In one patient the insertion of 2 Rush nails across the bone cement was used to obtain a stiffer construction. In one patient with metastasis of breast cancer, cement loaded with doxorubicine was used. In two locations at the proximal tibia secondary to thyroid and urothelial metastatic disease, a modular prostheses (Mutars System, Implantcast, Germany) was implanted. The latter patient (urothelial) had a contemporary involvement of the metaepiphyseal fibula as well as the proximal tibia: in this patient, before the implanting of a knee prosthesis, a wide proximal fibular and tibial resection including peroneal nerve, was performed. In the involvement of the distal tibia, treatment was differentiated according to the histotypes and the overall prognosis (life expectancy) of the patient. In a case with a bladder primary tumor and metastatic diffusion, treatment was curettage and cement with metal pinning. In another patient, where kidney was the primary tumor, distal tibial metaepiphyseal diffusion of the metastatic lesion was treated by the insertion of a locked anterograde intramedullary nailing, while the gap was filled with cement. Patients with fibular metastasis are not involved in the study because of the few number of cases.

Antibiotic therapy with third generation cephalosporin was administered from 2 h preoperatively to the third day postoperatively. Low-dose heparin was administered from the day of admittance to 30 days postoperatively. Additional treatment regimens, such as postoperative radiation therapy or preoperative embolisation, were recorded. In addition to demographic and primary tumor data, surgical and postoperative complications, hardware failure and survival rate were collected. Clinical outcomes focused on pain relief, postoperative mobility, and functional status using both the Eastern Cooperative Oncology Group (ECOG) and quality of life questionnaire for cancer patients treated with anticancer drugs (QOL-ACD). All patients were evaluated at time of fracture and 1, 3, 6 months after surgery. They were followed up for

at least 3 years or until their death. The median follow-up was 22 months.

The results obtained were analyzed using the student's *t*-test and χ^2 test; and verified with Fisher's exact test. Significance was accepted at $p < 0.05$.

RESULTS

Ninety-three patients met inclusion criteria (50 male) with a mean age of 62.4 years (range 39–81). Details of demographic aspects, histotype, localization and surgeries are described in Table I.

The most common primary malignancy in total patients was carcinoma of the breast (25 patients, 26.88%); in patients with femoral metastases the most common histotype was breast carcinoma with 23 patients (28.75%) while in patients with tibial metastases it was lymphoma in 3 patients (23.01%).

Sixty-nine patients (74.19%) had synchronous visceral and bone localizations at time of surgery.

In both groups of patients there were no pathological fractures after surgery and no implant

Table I. *Details of demographic aspects, histotype, localization and surgeries of patients.*

	Femur	**Tibia**
Mean Age	61.2	70
n.	80	13 (1 bilateral)
Type of Cancer		
Breast	23	2
Prostate	12	/
Lung	8	/
Colon	6	1
Thyroid	4	1
Kidney	2	3
Myeloma	16	1
Lymphoma	4	3
Bladder	3	1
Liver	2	/
Urothelial	/	2
Localisations		
Proximal	52 (65%)	5
Dyaphiseal	28 (35%)	6
Distal	/	3
SURGERY		
Nail	PFN= 16 PFN-A=10 L-AFN= 54	7
PMMA Adjuvant Nail	8	1
Prosthesis		2
Curettage + PMMA		2
Rush/PIN + PMMA		3
ADJUVANT TREATMENT		
Postoperative radiotherapy	80	
Embolisation	6	4

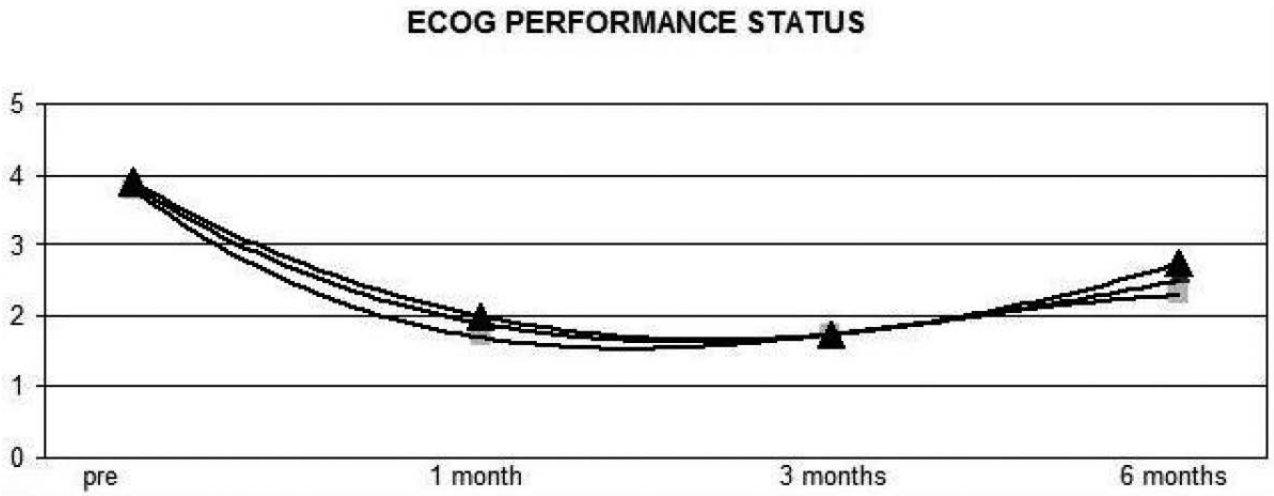

Fig. 1. *ECOG Performance Status in total, femoral and tibial patients.*

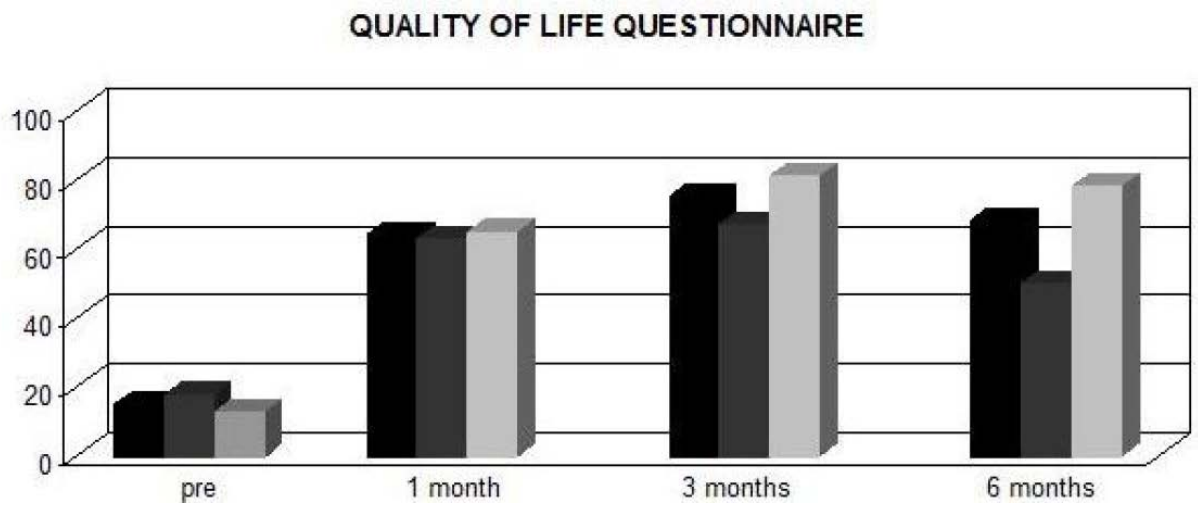

Fig. 2. *Histogram showing QoL questionnaire results.*

failures, while in the femoral group 11 patients (13.75%) suffered from non-fatal DVT post-surgery, with no pulmonary embolism, 6 (7.5%) developed superficial wound infections and 2 (2.5%) developed pneumonia; in the tibial group there was only one case of superficial wound infection and one case of tumor relapse that required radiotherapy.

In the femoral group 76 patients had died at the time of review, with a mean survival of 10 months (maximum, 48 months). Forty-eight patients (60%) died within 12 months after surgery because of progression of the primary disease. The patients' survival rate was 25% at 2 years and 15% at 3 years. In the tibial group the average survival time observed was different according to different histotypes. In 6 patients it was approximately 6 months, in the haematological lesions it was 23 months and in a kidney lesion it was 5 years. Operating time, blood loss, length of hospitalisation and postoperative complications did not correlate with survival.

In femoral patients lung cancer appears to be a predisposing factor in reducing survival time than other histotypes and the presence of visceral or cerebral metastases is a negative prognostic factor.

All patients attained satisfactory pain relief, as gauged by postoperative use of analgesics. 74.2% of patients occasionally used non-narcotic analgesics, with excellent pain relief, while 25.8% used them regularly and narcotic analgesics occasionally with good pain relief.

In the femoral group, the mean interval to weight-bearing was 4 days. In 3 months, 68 patients (85%) were able to walk with or without an aid, while in the tibial group partial weight-bearing with 2 crutches was allowed 4 days postoperatively, except for the patient affected by bladder carcinoma with distal tibia lesion in which emptying and filling with cement and pins was performed, and in patients treated with modular prostheses in which weight bearing was allowed 5 days after surgery.

This study showed an overall improvement in quality of life in all patients, confirmed also by the trend of the ECOG performance status and QOL-ACD (Fig.1, 2). The ECOG index showed an improvement of the patients' general condition up to 12 months after the index procedure, with an average score improving from 3.80 preoperatively, to 1.70 at 1 month, 1.75 at 3, 2.30 at 6, 3.40 at 12, 3.70 at 24 and 3.85 at 36 months (Fig.1) in femoral patients, while tibial patients showed an improvement in the general condition up to 6 months minimum follow-up after the index procedure, with an average score improving from 3.75 preoperatively, to 1.90 at 1 month, 1.80 at 3 months, and 2.50 at 6 months (Fig. 1).

The QOL-ACD index showed an improvement of the patients' general condition. In femoral patients the improvement was up to 6 months after the index procedure, with an average score improving from 13% preoperatively, to 65% at 1 month and 81% at 3 months ($p = 0.0001$) with 85% of patients able to walk without an aid (Fig. 2). At 10 months a worsening score was noted (43%), but was still statistically significant compared with the pre-operative value ($p = 0.005$), because of deterioration in mental and physical aspects, due to the progression of the primary pathology, with 48 patients dead by that time. In tibial patients the improvement was observed until 3 months after the index procedure, with an average score improving from 17% preoperatively, to 62% at 1 month, 66% at 3 months, and averaged 48% because of a worsening in mental and emotional aspects due to the progression of the primary disease.

DISCUSSION

Advances in adjuvant and neoadjuvant therapies have recently improved the prognosis of cancer patients leading consequently to an increased incidence of skeletal metastases and subsequent pathological fractures of long bones (9). Twenty-five percent of lesions involving a long bone eventually evolve into a pathological fracture; conversely, a pathological fracture is the initial manifestation of a long bone metastasis in 10% of patients (10, 11). The femur, in particular the proximal femur, is the long bone most commonly affected by metastases (12-14), instead the pathological fractures of the tibia as a result of a cancer localisation are quite rare, with an incidence ranging from 2.6% to 5% (15, 16) and normally the tibia is involved in a very advanced stage of the primary tumor (15).

Preoperative estimation of postoperative survival time is used to help select the best treatment for a pathological fracture from a choice of a conservative treatment or an intramedullary nailing or other more aggressive surgical options, such as resection and reconstruction with tumor prostheses (1, 7, 14). Studies in the literature indicate that when patients live longer than 3 years postoperatively, there is a risk of nail failure with the possibility of reoperation (17). Surgery has to be considered as a treatment option in patients with a life expectancy of more than 3 months, for pain relief, to accelerate the mobilisation and to improve the quality of life (1, 10, 11).

In the treatment of tibial articular lesions or when a fracture is located in the femoral head or neck, bone resection and prosthetic replacement is indicated, especially in solitary lesions and in histotypes of better prognosis (kidney and haematological cancer (14). Intramedullary nailing is considered for metadiaphyseal and diaphyseal fractures in patients whose tumor responded to radiation therapy and who have a short life expectancy (5, 6). In the proximal metaepiphyseal a good indication is the use of

cement eventually combined with plates or cement alone in the epiphyseal lesions (6). Amputation has to be reserved only in the presence of large soft ulcerated or infected masses, or finally when there is surgery failure (6).

The gold standard is to stabilise the whole segment to avoid unpleasant events such as fractures above and below the instrumentation (1, 10, 11, 14). The secondary lesion, in fact, has to be considered as an illness of the whole segment and not as a part of it (1, 10, 11, 14). According to this principle, the authors prefer to use an intramedullary locked nailing instead of a plate and screw system.

The current study supports the favourable outcomes of surgical management of pathological lower long bone fractures regarding the mechanical stability and quality of life. The mechanical stability gave a marked reduction of painful symptoms and the authors observed a reduction of analgesic drug use in all the treated patients; the surgical strategy and technique are selected based on the patient's medical condition, and considering staging, prognosis and mechanical consequences of bone metastases.

Intramedullary nailing improved the quality of life in patients suffering from pathologic femoral fractures, as shown by ECOG and QOL. The value of ECOG and QOL improved at 3 and 6 months postoperatively, but reduced at 12 months, by which time many patients (60%) had died. In some patients, tumour progression influenced functional activity, as we observed previously in the survival rate and functional activity after acetabuloplasty for acetabular metastasis due to carcinoma (9, 18). In tibial patients the value of ECOG and QOL improved at 3 months, but worsened 6 months after surgery because of a deterioration of the general condition due to progression of primary pathology.

In our series no hardware failure was observed, but in the medical literature some mechanical complications with the use of nails have been reported; for example, break-up of the distal locking screws, or a breakage of the implant (19) or failure of compression in plates and failure of Rush nails. There is an increasing risk for implant failure, ranging from 3.1% to 42% for the few patients with cancer who survive more than one year after fixation for femoral pathologic fracture (15, 17, 19).

No pulmonary embolism was seen in our series; however, we usually implant unreamed intramedullary locked nail inserted in a static mode to reduce this risk (20).

External bracing, radiotherapy, hormone therapy, biphosphonate therapy and radioisotopes can be performed in cases where life expectancy is less than 3 months, in particular in tibia but also in femur (21).

In conclusion, the improvement of cancer patients' estimated survival means that resection and endoprosthetic reconstruction can be considered as a preferable method of treatment for proximal femoral metastases in patients with good general fitness and life expectancy. Although there is a high risk of dislocations and infections, this method ensures major local tumor control, and complication rates or failure rates are not significantly higher compared with osteosynthesis, especially when the latter procedure is associated with curettage and adjuvant cement. On the other hand, the finding of multiple lesions besides the level of fracture, the low incidence of intra- and postoperative complications and the possibility of early mobilisation strongly support the use of intramedullary nailing for pathologic fractures located in the metadiaphyseal and diaphyseal regions in advanced-stage cancer patients. It is a suitable method for a stable fixation of inter/sub-trochanteric and shaft pathologic fractures and enables early and painless postoperative mobilisation and weight-bearing, thus improving the quality of life.

There are some limitations that need to be acknowledged and addressed regarding the present study. The number of cases is small to make broad generalisations. Further empirical evaluations and larger series of patients are necessary to validate the present results, in particular in patients with tibia metastasis. However, we feel that provision of good mechanical stability of the affected segment in these patients is vital in order to achieve pain control, faster mobilisation and overall improvement in their quality of life.

REFERENCES

1. Manglani HH, Marco RA, Picciolo A, Healey JH. Orthopedic emergencies in cancer patients. Semin Oncol 2000; 27(3):299-310.
2. Li S, Peng Y, Weinhandl ED, et al. Estimated number of prevalent cases of metastatic bone disease in the

US adult population. Clin Epidemiol 2012; 4:87-93.
3. Kelly CM, Wilkins RM, Eckardt JJ, Ward WG. Treatment of metastatic disease of the tibia. Clin Orthop Relat Res 2003; 415(S)219-29.
4. Piccioli A, Maccauro G, Rossi B, Scaramuzzo L, Frenos F, Capanna R. Surgical treatment of pathologic fractures of humerus. Injury 2010; 41:1112-16.
5. Piccioli A, Rossi B, Scaramuzzo L, Spinelli MS, Yang Z, Maccauro G. Intramedullary nailing for treatment of pathologic femoral fractures due to metastases. Injury 2014; 45(2):412-7.
6. Piccioli A, Maccauro G, Scaramuzzo L, Graci C, Spinelli MS. Surgical treatment of impending and pathological fractures of tibia. Injury 2013; 44(8):1092-6.
7. Capanna R, Campanacci DA. The treatment of metastases in the appendicular skeleton. J Bone Joint Surg Br 2001; 83(4):471-81.
8. Karnofsky DA, Burchenal JH. The clinical evaluation of chemotherapeutic agents. In: McLeod E, editor. Evaluation of chemotherapeutic agents. New York: Columbia University Press; 1949.
9. Maccauro G, Liuzza F, Scaramuzzo L, et al. Percutaneous acetabuloplasty for metastatic acetabular lesions. BMC Musculoskelet Disord 2008; 5;9:66.
10. Ruggieri P, Mavrogenis AF, Casadei R, et al. Protocol of surgical treatment of long bone pathological fractures. Injury 2010; 41:1161-67.
11. Nilsson J, Gustafson P. Surgery for metastatic lesions of the femur: good outcome after 245 operations in 216 patients. Injury 2008; 39:404-10.
12. Jacofsky DJ, Haidukewych GJ. Management of pathologic fractures of the proximal femur: state of the art. J Orthop Trauma 2004; 18:459-69.
13. Bickels J, Dadia S, Lidar Z. Surgical management of metastatic bone disease. J Bone Joint Surg Am 2009; 91:1503-16.
14. Piccioli A, Capanna R. Il trattamento delle metastasi ossee. Linee Guida S.I.O.T 2008.
15. Kelly CM, Wilkins RM, Eckardt JJ, Ward WG. Treatment of metastatic disease of the tibia. Clin Orthop Relat Res 2003; 415(S):219-29.
16. Maccauro G, Liuzza F, Muratori F, Gosheger G, Salgarello M, Logroscino CA. A very rare localization of metastatic lung carcinoma to the interosseous membrane. Arch Orthop Trauma Surg 2003; 123:563-66.
17. Miller BJ, Soni EE, Gibbs CP, Scarborough MT. Intramedullary nails for long bone metastases: why do they fail? Orthopedics 2011; 11:34.
18. Scaramuzzo L, Maccauro G, Rossi B, Messuti L, Maffulli N, Logroscino CA. Quality of life in patients following percutaneous PMMA acetabuloplasty for acetabular metastasis due to carcinoma. Acta Orthop Belg 2009; 75(4):484-9.
19. van Doorn R, Stapert JW. Treatment of impending and actual pathological femoral fractures with the long Gamma nail in The Netherlands. Eur J Surg 2000; 166:247-54.
20. Cole AS, Hill GA, Theologis TN, Gibbons CL, Willett K. Femoral nailing for metastatic disease of the femur: a comparison of reamed and undreamed femoral nailing. Injury 2000; 31:25-31.
21. Picci P, Ruggeri P. Advances in Bone Metastasis Management. Future Medicine Ltd (1 gennaio 2012).

LETTER TO THE EDITOR

POTENTIAL USE OF MELATONIN IN PROCEDURAL ANXIETY AND PAIN IN CHILDREN UNDERGOING BLOOD WITHDRAWAL

L. MARSEGLIA[1], S. MANTI[2], G. D'ANGELO[1], T. ARRIGO[2], C. CUPPARI[2], C. SALPIETRO[2] and E. GITTO[1]

[1]Neonatal Intensive Care Unit, Department of Paediatrics, University of Messina, Italy; [2]Unit of Paediatric Genetics and Immunology, Department of Paediatrics, University of Messina, Italy

Received October 27, 2014 – Accepted April 30, 2015

The recognition of the value of pain, especially in the pediatric population, has increased over the last decade. It is known that pain-related anxiety can increase perceived pain intensity. There are several different approaches to the treatment of pre-procedural anxiety and procedural pain in children. Melatonin, a neurohormone with the profile of a novel hypnotic-anaesthetic agent, plays an important role in anxiolysis and analgesia. This study investigated the effects of oral melatonin premedication to reduce anxiety and pain in children having blood samples taken. The investigations were carried out on 60 children, aged 1-14 years, divided into 2 equal groups. Using a computer-generated randomization schedule, patients were given either melatonin orally (0.5 mg/kg BW, max 5 mg) or placebo 30 min before blood draw. Pre-procedural anxiety was assessed using the scale from the Children's Anxiety and Pain Scales, while procedural pain used the Face, Legs, Activity, Cry and Consolability assessment tool for children under the age of 3 years, Faces Pain Scale-Revised for children aged 3-8 years and Numeric Rating Scale for children over the age of 8 years. Oral administration of melatonin before the blood withdrawal procedure significantly reduced both anxiety ($p<0.0005$) and pain levels than placebo ($p<0.0002$ for children under 3 years and $p<0.0039$ for children over 3 years). These data support the use of melatonin for taking blood samples due to its anxiolytic and analgesic properties. Further studies are needed to support the routine use of melatonin to alleviate anxiety and pain in pediatric patients having blood samples taken.

Procedures carried out with a needle are the most important sources of pain for children. Pain causes children to be frightened of needles and this leads children to unwillingness to have procedures such as having blood samples taken. Pain management in pediatric patients has great clinical importance and pharmacological and/or non-pharmacological treatments of pre-procedural anxiety and procedural pain are helpful (1). Melatonin has antioxidant, anxiolytic and sedative properties and plays an important role in the regulation of sleep and circadian rhythms (2-5). Among the broad range of effects attributed to melatonin, its role in analgesia emerges as important because of its clinical implications (6). Its potential anti-nociceptive and anti-inflammatory actions have been studied in an animal model of acute pain (7) and has been demonstrated in studies conducted on patients with extensive tissue injury

Key words: melatonin, anxiety, pain, blood withdrawal, children

Mailing address: Lucia Marseglia, MD
Neonatal Intensive Care Unit,
Department of Pediatrics,
University of Messina,
Via Consolare Valeria, 1 98125 Messina, Italy
Tel.: +390902213100 Fax: +39090692308
e-mail: lmarseglia@unime.it

0393-974X (2015)

DISCLOSURE: ALL AUTHORS REPORT NO CONFLICTS OF INTEREST RELEVANT TO THIS ARTICLE.

and chronic pain, e.g., due to fibromyalgia, irritable bowel syndrome, and migraine (8-10). Despite the evidence from animals and adult humans studies, data are lacking on the use of melatonin for analgesic purposes in pediatric patients.

Gitto et al. (11) demonstrated that melatonin has beneficial effects as an analgesic antioxidant in preterm newborns subject to painful procedures, such as endotracheal intubation and mechanical ventilation, especially when an inflammatory component is involved. Melatonin administration has been found to raise pain thresholds (12). However, little is known about the short-term anti-nociceptive effects of melatonin on acute procedural pain. The positive relationship between anxiety and pain is a common experience in the clinical settings and it is known that pain-related anxiety can increase perceived pain intensity (13). Pre-procedural anxiety, assessed as pre-procedure anxiety, also impacts pain perception. In the paediatric population, melatonin has been successfully used in the treatment of anxiety associated to sleep disorders (14).

The objective of this randomized, double-blind clinical study was to investigate the possible effect of oral melatonin in comparison with placebo on children having blood samples taken, evaluating its efficacy for alleviating anxiety and pain.

MATERIALS AND METHODS

Subjects

The present study was a double-blind, placebo-controlled, randomized, clinical trial with the aim of assessing anxiety and pain levels of children subjected to medical procedures, such as having blood samples taken. Children, aged 1-14 years, who required blood tests were enrolled at the Pediatric Department of University Hospital of Messina, Italy, over a 4-month period.. Exclusion criteria were patients with sleep disorders, neuro-developmental delay, on-going treatment with hypnotics or psychotropic drugs (including opioids) within a week before admission, daily analgesic treatment, corticosteroids. The study was conducted in accordance with the principles of the Declaration of Helsinki (15). The Institutional Review Board approved the study. Participation in this study was voluntary. The children and their parents enrolled were informed about the aims of the research. They were fully informed about the study protocol and provided written informed consent. A physician carried out the physical examination on each child. Using a computer-generated randomization schedule, patients were given either 0.5 mg/kg (max 5 mg) oral melatonin (Melamil®) or placebo (5% glucose solution) 30 min before blood drawing. Melatonin and placebo solutions were prepared by a pharmacist who was unaware of the study. The melatonin and placebo solutions were identical in respect to preparation and packaging and were indistinguishable; only a coded label was maintained to ensure the double-blind nature of the study. The patients received drugs via oral route by a blinded nurse. Other sedative or analgesic agents were not used. The data were obtained by interviewing the children, their parents and the observer.

Instruments

Pre-procedural anxiety levels were assessed for children over 3 years by a parent and a blinded resident using the Children's Anxiety and Pain Scales (CAPS) (16), a well-established method for evaluating paediatric pain and anxiety (17). The CAPS is a 0 - 5 scale and consists of two sets. The first set includes five cartoon faces that range from a neutral expression (0 - no anxiety) to a frightened face (5 - severe anxiety), whereas the second set consists of five cartoon faces that range from a neutral expression (0 - no pain) to a suffering face (5 - severe pain). In this study, the first set was used for evaluating pre-procedural anxiety.

Procedural pain was assessed by different scales, according to the children ages. The FLACC (Face, Legs, Activity, Cry and Consolability) assessment tool was used to provide a simple consistent method of pain evaluation in non-verbal or pre-verbal children (18). This tool incorporates 5 categories of behaviour included in the acronym, each of which is scored from 0-2 with total scores ranging 0-10. The scale was used for children under 3 years of age.

The Faces Pain Scale (FPS) was used for children under 8 years and the Numeric Rating Scale (NRS)for the participants over 8 years. FPS requires selecting a picture of a face that represents one's pain intensity (19). They fall into two categories: drawings and photographs. Face scales may not require the ability to seriate or estimate quantities. Generally, children prefer face scales to NRS that estimates pain using numbers representing increasing pain severity (20). Both scores were between 0 and 10. The patients were asked about the average level of their pain during the medical procedures according to the pain score. Pain was evaluated 5 min after blood sampling by an investigator blinded to group assignment who performed all tests scoring in the post-procedure period.

Data analysis

All statistical analyses were performed using standard SPSS package (version 12.0 for Windows). Continuous variables are expressed as arithmetic mean (SEM), and

categorical variables were expressed as frequencies and percentages. Variables that were not normally distributed were transformed, as appropriate, by either logarithmic or square root transformations to satisfy normality assumptions. To compare the differences between the melatonin and placebo groups, the χ^2 test was used for categorical variables and the independent sample *t*-test for continuous variables. The paired *t*-test was used to compare differences in the melatonin group before and after treatment. A two tailed *p* value less than 0.05 was considered statistically significant.

RESULTS

Sixty children 1-14 years old volunteered to participate in the study and were randomly assigned to melatonin (group M) or placebo (group P)(30 per group). The distribution of male subjects was 16/30 (53%) and 13/30 (43%), respectively, in melatonin and placebo solutions groups. All the participating subjects were of Italian origin. There were no significant differences between the two groups with respect to the demographic properties (age, body weight, and duration of performance). Demographic data and other clinical characteristics of the study subjects are reported in Table I. There were significant differences between melatonin and placebo groups in anxiety and pain scores after blood sampling; in fact, patients who received melatonin showed anxiety levels statistically lower than those treated with placebo ($p<0.0005$). In addition, the melatonin-treated children had significantly lower pain score than did the placebo controls ($p<0.0039$); moreover, pain was more significantly reduced in children under 3 years ($p<0.0002$). None of the children treated with melatonin indicated that their pain level during the last experience was greater compared with the previous experience during blood withdrawal.

DISCUSSION

The principle goal of anxiolysis and analgesia is

Table I. *Patient characteristics.*

Characteristic	Melatonin (group M)	Placebo solutions (group P)	*P*
Age (yr)	4.4 ± 3.5	5.1 ± 2.6	0.38
Sex (M/F)	16/14 (53%)	13/17 (43%)	
Weight (kg)	16.5 ± 6.5	16.3 ± 4.2	0.88
CAPS	1.3 ± 1	2.2 ± 0.9	0.0005
FLACC	2.5 ± 1.16	5.2 ± 1.4	0.0002
FPS and NRS	1.2 ± 0.8	2.1 ± 0.8	0.0039

Data are shown as percentage (%), and mean ± standard deviation (SD).
CAPS: children's anxiety and pain scales; FLACC: face-legs-activity-cry-consolability; FPS: faces pain scale; NRS: numeric rating scale.

to prepare the patients to stay calm during painful procedures, avoiding harmful complications.

The results of this study revealed that premedication with oral melatonin decreased anxiety and pain levels in paediatric patients between the age of 1-14 years. Placebo (5% glucose solution) or melatonin (Melamil®) at the recommended dose of 0.5 mg/kg (max 5) was administrated 30 min before blood sampling. The onset of melatonin-induced sedation in children is reported to begin approximately 20-30 min after oral administration, and further elevated blood melatonin concentrations remain constant for approximately 1.5 h (21). Our findings support the anxiolytic effect of melatonin reported in previous studies (22), although some reports (23, 24) claimed that melatonin premedication failed to reduce anxiety in elderly and anxious children undergoing surgery. The difference between these results might be explained by differences in populations (age, gender, types of medical procedures, and different pain scores of our patients) or methodologies. In the present study, children of both groups were comparable for age and clinical conditions, and all underwent the same medical procedure.

The anxiolytic properties of melatonin were demonstrated to involve the non-selective MT1/MT2 receptor (25, 26). Pharmacological studies targeting MT2 receptors suggest the mechanism by which the indolamine modulates anxiety involves this receptor. Animal models showed that the administration of UCM765, a selective MT2 receptor ligand, reduced anxiety at a dose of 10 mg/kg (27). Considering the involvement of the MT2 receptor in modulating anxiety levels, this receptor may become a novel target for the treatment of anxiety disorders. It has also been demonstrated that the anxiolytic effect of melatonin occurs following the activation of the GABAergic system through the mutual interaction between GABA and MT2 receptors (28). In fact, melatonin produces marked dose-dependent increases in GABA concentrations in the central nervous system (29).

The precise mechanism underlying the analgesic effect of melatonin however, has not been clarified. The analgesic action has been shown potentially to involve MT1 and MT2 receptors present in the spinal cord and various brain regions (11, 30). One report also suggested that the opioid system may be involved in this effect (31). In experimental studies, melatonin showed potent dose-dependent analgesic effects (32). The effects may be linked to Gi-coupled melatonin receptors, to Gi-coupled opioid μ receptors or GABA-B receptors. Possibly, melatonin may augment GABA-ergic systems and morphine anti-nociception, enhancing GABA-induced currents and inhibiting glycine effects (30). Melatonin also may enhance the levels of β-endorphins and the anti-nociception induced by delta opioid receptor agonists and could activate MT2 melatonin receptors in the dorsal horn of the spinal cord (22, 33). The analgesic effect of melatonin remains controversial as there were opioid-sparing effects or reduced pain scores in 5 studies, while 3 studies yielded contradictory findings (34).

The present study assessed the anxolytic and analgesic role of melatonin in painful procedures. Oral melatonin administered to children undergoing blood withdrawal significantly reduced anxiety and pain, when compared to placebo. Moreover, pain was more significantly reduced in children under 3 years of age ($p<0.0002$ *vs* $p<0.0039$ in children more than 3 years), probably because the awareness of the painful experience can increase perceived pain intensity.

Currently, is well known that an adequate pain control is a fundamental right of every patient at any age and the American Academy of Pediatrics recommends that pain be recognized and treated more aggressively in paediatric subjects. Melatonin, based on its properties as an anxiolytic and analgesic, may provide beneficial effects in a variety of paediatric painful procedures. Equally important to point out is that no significant short- or long-term side-effects after administration of standard doses of melatonin in children have been reported (35, 36). Therefore, melatonin could serve as an effective and safe drug to control anxiety and pain perception.

This study investigated whether oral melatonin premedication would reduce the anxiety and pain levels of paediatric patients undergoing blood withdrawal. The results revealed that melatonin decreased the anxiety and pain scores in the treated children who received premedication with melatoninin in comparison to placebo, supporting its use in the treatment of anxiety and pain in children. Moreover, several studies showed that melatonin

can be administered in large doses with very low acute toxicity or side effects (35, 36). Although the available data are encouraging, further studies are needed to recommend the routine use of melatonin as an efficacious anxiolytic and analgesic drug for medical painful procedures in children.

REFERENCES

1. Rogers TL, Ostrow CL. The use of EMLA cream to decrease venipuncture pain in children. J Pediatr Nurs 2004; 19:33-39.
2. Shin DJ, Jeong CW, Lee SH, Yoon MH. Receptors involved in the antinociception of intrathecal melatonin in formalin test rats. Neurosci Lett 2011; 494:207-10.
3. Hardeland R, Madrid JA, Tan DX, Reiter RJ. Melatonin, the circadian multioscillator system and health: the need for detailed analyses of peripheral melatonin signaling. J Pineal Res 2012; 52:139-66.
4. Gitto E, Marseglia L, Manti S, et al. Protective role of melatonin in neonatal diseases. Oxid Med Cell Longev 2013; 2013:980374.
5. Galano A, Tan DX, Reiter RJ. On the free radical scavenging activities of melatonin's metabolities, AFMK and AMK. J Pineal Res 2013; 54:245-57.
6. Marseglia L, D'Angelo G, Manti S, Aversa S, Arrigo T, Reiter RJ, Gitto E. Analgesic, anxiolytic and anaesthetic effects of melatonin: new potential uses in pediatrics. Int J Mol Sci 2015; 16:1209-20.
7. Esposito E, Paterniti I, Mazzon E, Bramanti P, Cuzzocrea S. Melatonin reduces hyperalgesia associated with inflammation. J Pineal Res 2010; 49:321-31.
8. Citera G, Arias MA, Maldonado-Cocco JA, Lázaro MA, Rosemffet MG, Brusco LI, Scheines EJ, Cardinalli DP. The effect of melatonin in patients with fibromyalgia: a pilot study. Clin Rheumatol 2000; 19:9-13.
9. Mozaffari S, Rahimi R, Abdollahi M. Implications of melatonin therapy in irritable bowel syndrome; a systematic review. Curr Pharm Des 2010;16:3646-55.
10. Peres MF, Zukerman E, da Cunha Tanuri F, Moreira FR, Cipolla-Neto J. Melatonin 3 mg is effective for migraine prevention. Neurology 2004; 63:757.
11. Gitto E, Aversa S, Salpietro CD, Barberi I, Arrigo T, Trimarchi G, Reiter RJ, Pellegrino S. Pain in neonatal intensive care: role of melatonin as an analgesic antioxidant. J Pineal Res 2012; 52:291-95.
12. Srinivasan V, Pandi-Perumal SR, Spence DW, Moscovitch A, Trakht I, Brown GM, Cardinali DP. Potential use of melatonergic drugs in analgesia: mechanisms of action. Brain Res Bull 2010; 81:362-71.
13. Ploghaus A, Narain C, Beckmann CF, et al. Exacerbation of pain by anxiety is associated with activity in a hippocampal network. J Neurosci 2001; 21:9896-903.
14. Ross C, Davies P, Whitehouse W. Melatonin treatment for sleep disorders in children with neurodevelopmental disorders: an observational study. Dev Med Child Neurol 2002; 44:339-44.
15. World Medical Association (WMA). Declaration of Helsinki. Amended by the 64th WMA General Assembly, Fortaleza, Brazil, October 2013. WMA Archives, Ferney-Voltaire, France.
16. Kuttner L. Management of young children's acute pain and anxiety during invasive medical procedures. Pediatrician 1989; 16:39-44.
17. Meyerhoff AS, Weniger BG, Jacobs RJ. Economic value to parents of reducing the pain and emotional distress of childhood vaccine infections. Pediatr Infect Dis J 2001; 20:57-62.
18. Merkel SI, Voepel-Lewis T, Shayevitz JR, Malviya S. The FLACC: a behavioral scale for scoring postoperative pain in young children. Pediatr Nurs 1997; 23:293-97.
19. Champion GD, Goodenough B, Von Baeyer CL, Thomas W. Measurement of pain by self-report. In: Finley GA, McGrath PJ, eds. Measurement of Pain in Infants and Children. Seattle: IASP Press; 1998:123-60.
20. Gaffney A, Mcgrath P, Dick B. Measuring pain in children: Developmental and instrument issues. In: Schechter N, Berde CB, Yaster M, eds. Pain in Infants, Children and Adolescents. 2. Philadelphia: Lippincott Williams & Wilkins; 2003:128-41.
21. Goldman SE, Adkins KW, Calcutt MW, et al. Melatonin in children with autism spectrum disorders: endogenous and pharmacokinetic profiles in relation to sleep. J Autism Dev Disord 2014; 44:2525-35.

22. Ismail SA, Mowafi HA. Melatonin provides anxiolysis, enhances analgesia, decreases intraocular pressure, and promotes better operating conditions during cataract surgery under topical anesthesia. Anesth Analg 2009; 108:1146-51.
23. Capuzzo M, Zanardi B, Schiffino E, Buccoliero C, Gragnaniello D, Bianchi S, Alvisi R. Melatonin does not reduce anxiety more than placebo in the elderly undergoing surgery. Anesth Analg 2006; 103:121-23.
24. Isik B, Baygin O, Bodur H. Premedication with melatonin vs midazolam in anxious children. Paediatr Anaesth 2008; 18:635-41.
25. Golombek DA, Martini M, Cardinali DP. Melatonin as an anxiolytic in rats: time dependence and interaction with the central GABAergic system. Eur J Pharmacol 1993; 237:231-36.
26. Papp M, Litwa E, Gruca P, Mocaer C. Anxiolytic-like activity of agomelatine and melatonin in three animal models of anxiety. Behav Pharmacol 2006; 17:9-18.
27. Ochoa-Sanchez R, Rainer Q, Comai S, et al. Anxiolytic effects of the melatonin MT(2) receptor partial agonist UCM765: comparison with melatonin and diazepam. Prog Neuropsychopharmacol Biol Psychiatry 2012; 39:318-325.
28. Wan Q, Man HY, Liu F, Braunton J, Niznik HB, Pang SF, Brown GM, Wang YT. Differential modulation of GABAA receptor function by Mel1a and Mel1b receptors. Nat Neurosci 1999; 2:401-3.
29. Naguib M, Gottumukkala V, Goldstein PA. Melatonin and anesthesia: a clinical perspective. J Pineal Res 2007; 42:12-21.
30. Zahn PK, Lansmann T, Berger E, Speckmann EJ, Musshoff U. Gene expression and functional characterization of melatonin receptors in the spinal cord of the rat: implications for pain modulation. J Pineal Res 2003; 35:24-31.
31. Arreola-Espino R, Urquiza-Marín H, Ambriz-Tututi M, Araiza-Saldaña CI, Caram-Salas NL, Rocha-González HI, Mixcoatl-Zecuatl T, Granados-Soto V. Melatonin reduces formalin-induced nociception and tactile allodynia in diabetic rats. Eur J Pharmacol 2007; 577:203-10.
32. Wilhelmsen M, Amirian I, Reiter RJ, Rosenberg J, Gögenur I. Analgesic effects of melatonin: A review of current evidence from experimental and clinical studies. J Pineal Res 2011; 51:270-77.
33. Yu CX, Zhu CB, Xu SF, Cao XD, Wu GC. Selective MT2 melatonin receptor antagonist blocks melatonin-induced antinociception in rats. Neurosci Lett 2000; 282:161-64.
34. Yousaf F, Seet E, Venkatraghavan L, Abrishami A, Chung F. Efficacy and safety of melatonin as an anxiolytic and analgesic in the perioperative period: a qualitative systematic review of randomized trials. Anesthesiology 2010; 113:968-76.
35. Carr R, Wasdell MB, Hamilton D, et al. Long-term effectiveness outcome of melatonin therapy in children with treatment-resistant circadian rhythm sleep disorders. J Pineal Res 2007; 43:351-59.
36. Seabra ML, Bignotto M, Pinto LR Jr, Tufik S. Randomized, double-blind clinical trial, controlled with placebo, of the toxicology of chronic melatonin treatment. J Pineal Res 2000; 29:193-220

JOURNAL OF BIOLOGICAL REGULATORS & HOMEOSTATIC AGENTS Vol. 29, no. 2, 515-520 (2015)

LETTER TO THE EDITOR

MIXED DENTITION SPACE ANALYSIS OF A SOUTHERN ITALIAN POPULATION: NEW REGRESSION EQUATIONS FOR UNERUPTED TEETH

N. CIRULLI[1], A. BALLINI[2], S. CANTORE[1], D. FARRONATO[3], F. INCHINGOLO[4], G. DIPALMA[1], M.R. GATTO[5] and G. ALESSANDRI BONETTI[5]

[1]School of Medicine, University of Bari Aldo Moro, Bari, Italy; [2]Department of Basic Medical Sciences, Neuroscience and Sense Organs, University of Bari Aldo Moro, Bari, Italy; [3]Department of Surgical and Morphological Science, Dental School, University of Varese, Varese Italy; [4]Department of Interdisciplinary Medicine, University of Bari Aldo Moro, Bari, Italy; [5]School of Medicine, University of Bologna, Bologna, Italy

Received February 16, 2015 – Accepted March 10, 2015

Mixed dentition analysis forms a critical aspect of early orthodontic treatment. In fact an accurate space analysis is one of the important criteria in determining whether the treatment plan may involve serial extraction, guidance of eruption, space maintenance, space regaining or just periodic observation of the patients. The aim of the present study was to calculate linear regression equations in mixed dentition space analysis, measuring 230 dental casts mesiodistal tooth widths, obtained from southern Italian patients (118 females, 112 males, mean age 15±3 years). Student's *t*-test or Wilcoxon test for independent and paired samples were used to determine right/left side and male/female differences. On the basis of the sum of the mesiodistal diameters of the 4 mandibular incisors as predictors for the sum of the widths of the canines and premolars in the mandibular mixed dentition, a new linear regression equation was found: y = 0.613x+7.294 (r= 0.701) for both genders in a southern Italian population. To better estimate the size of leeway space, a new regression equation was found to calculate the mesiodistal size of the second premolar using the sum of the four mandibular incisors, canine and first premolar as a predictor. The equation is y = 0.241x+1.224 (r= 0.732). In conclusion, new regression equations were derived for a southern Italian population.

The amount of discrepancy between the total tooth material (mesiodistal width) present and the dental arch perimeter available to contain the teeth is probably the most critical estimate of any in the orthodontic diagnostic procedure (1, 2). Nowadays, three main approaches have been used to estimate the mesiodistal crown widths of permanent canines and premolars in mixed dentition patients: measurement of the unerupted teeth using radiographs (3, 4), the application of regression equations that relate the mesiodistal widths of erupted teeth to those of unerupted teeth (5, 6) and combination of measurements from erupted teeth and radiographs of unerupted teeth (7, 8).

The approach by Moyer proposed a very simple and easy way to use regression scheme to predict

Key words: mixed dentition, regression equations, space analysis, mesiodistal width, dental casts

Mailing address: Dr Stefania Cantore,
School of Medicine,
University of Bari Aldo Moro,
P.zza Giulio Cesare, 11,
70124, Bari, Italy
Tel./fax: +39 0803430475
e-mail: stefaniacantore@pec.omceo.bari.it

0393-974X (2015)

DISCLOSURE: ALL AUTHORS REPORT NO CONFLICTS OF INTEREST RELEVANT TO THIS ARTICLE.

mesiodistal widths of permanent canines and premolars on the basis of mandibular incisors widths using a statistical coefficient (r), called correlation coefficient (5). Coefficients of determination (r^2) are indicators of predictive accuracy of the regression equations for y (the sum of mesiodistal widths of canine and premolars) based on values of x (the corresponding sum of mesiodistal widths of four mandibular incisors), that is, the proportion of the total variance of y, which is determined then value of x for each regression equation (6). Although a regression equation must have an r^2-value of at least 0.5 to be clinically useful (7), the r^2 tends to overestimate the true reliability (8).

This method was developed on a Caucasian population, therefore the applicability of this method to populations of other ethnic groups has been studied and doubted (9-12). In addition, there has been some evidence of secular trends of changing dimensions of teeth, which may require progressive modification of mixed dentition analysis for different populations (13).

The aim of the present study was to calculate a regression equation, suitable for southern Italians which predicts the sum of the canine, first and second premolars using the sum of the four mandibular incisors as the predictor. To better estimate the width of the leeway space, another regression equation was found to predict the second premolar width, using the sum of the four mandibular incisors, the canine and first premolar as a predictor.r.

MATERIALS AND METHODS

By using methodology from a previous similar experience (14), we collected the dental cast models of 230 consecutive subjects (118 females and 112 males, mean age 15±3 years) between 2006 and 2014, from a private practice in the city of Bari (Centri Odontoiatrici Specialistici).

This work was carried out according to the recommendations of the Declaration of Helsinki, and all patients and parents gave informed consent. Patients were included in the study according to the following criteria :

- fully erupted permanent teeth in the mandibular jaw (except the third molar);
- absence of alterations in form, size and number;
- absence of inter-proximal restorations, fracture and caries, or age-related attrition in the measured teeth;
- no fractures or bubbles on the analyzed casts;
- no orthodontically treated patients;
- all Italian subjects, born and still resident in Puglia (southern Italy) for at least one previous generation.

All impressions and study casts were obtained with alginate and plaster models for high quality (orthodontic extra strong white stone 164-450-89 Orthosnow,

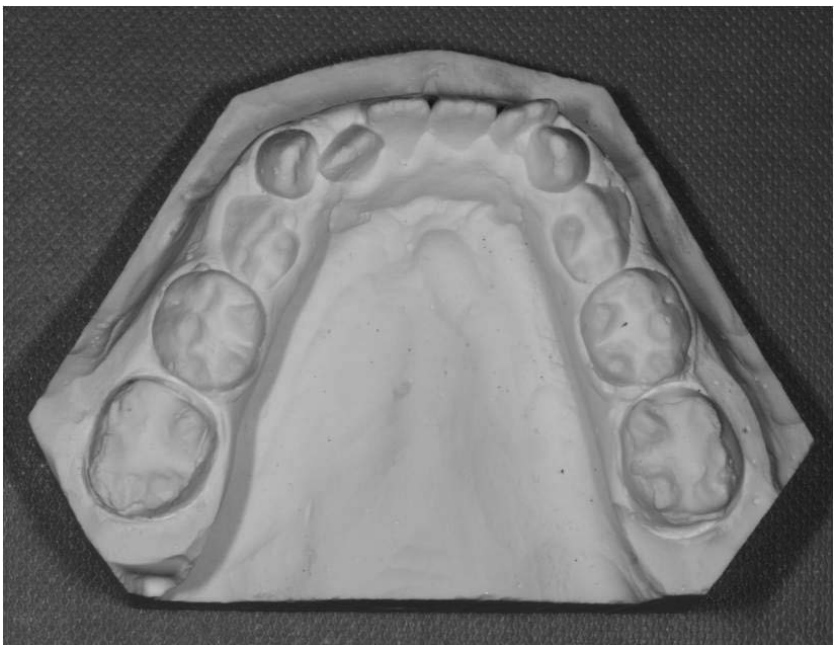

Fig. 1. *Study cast model of mixed dentition.*

Dentaurum, Italy) which had been shaped using the Tweed technique (Fig. 1). A digital caliper (Mauser® A/08 10825 Pforzheim, Germany) with an accuracy of 0.01 mm was used to measure each tooth (15), and to better adapt to the interdental space, the measuring tips were also narrowed. The mesiodistal widths of all the mandibular incisors, canines and premolars were measured, and the caliper was adjusted to the greatest mesiodistal diameter (contact point) of the teeth, parallel to the occlusal surface and perpendicular to the longitudinal axis (15, 16). Duplicate measurements were made 2 weeks later by a single investigator on 15 randomly selected dental casts.

Statistical analysis

On the basis of the study conducted on a northern Italian population (14) and hypothesizing a normal distribution of the predictor (sum of widths of the four mandibular incisors), with a precision of 0.15 mm in the estimate of such sum, a standard deviation of 1.16 mm and a confidence level of 95%, a number of at least 230 casts was defined. All statistical analyses were performed using the SPSS software package (SPSS for Windows 98, release 16.0, SPSS Inc., Chicago, Illinois, USA).

Descriptive statistics (mean, standard deviation, minimum and maximum values) were computed; normality of the distribution of the variables was assessed using the Shapiro-Wilk test. None of the *p*-values was greater than 0.05, for all the parameters except for the sum of the width of the incisors, and for the mean between the sum of the width of canine and first and second premolar of right and left arch. For these parameters, comparisons between genderes and arches were carried out by using *t*-test for independent and paired samples and for the other parameters comparisons between the genderes and arches were carried using Mann-Whitney U-test for independent samples or Wilcoxon test for paired samples.

Correlation coefficients (r) and linear regression equations were constructed to evaluate the relationship between the sum of widths of the four mandibular incisors (independent variable) and the sum of the widths of the canine and first and second premolars (dependent variable).

The constants of the models, the coefficients of linear determination (r^2) and the standard error of the estimated (SEE) were computed and the significance of the difference between the correlation coefficients was computed by using Z- transformation of the coefficients.

Significance value was *a priori* set at 0.05; accuracy of measurements was tested using Dahlberg's formula (17), and the method error for the measurement of individual permanent teeth ranged from 0.01 to 0.03 mm with a mean of 0.004 mm (standard deviation=0.02 mm).

For the intra-examiner calibration, intra-class correlation coefficient (ICC) was used to determine measurement consistency.

The values for each type of tooth were high (ICC=0.995, p=0.001 for incisors; ICC=0.958, p=0.001 for canines; ICC=0.969, p=0.001 for premolars) indicating high measurement reliability and consequently all tooth measurements for the remaining 215 dental casts were performed only once.

RESULTS

Statistically significant differences were observed in the sums of both the mandibular canine and premolar diameters (p=0.001) and in the widths of incisors (p=0.006) by gender, resulting that males seem to have teeth slightly larger (Table I).

No statistically significant difference was observed between the left and right side in either gender, so the results of right and left summations were averaged.

Table II presents the linear regression equation, the standard error of the estimate and correlation coefficients between the mandibular incisors and the mandibular lateral segments. Residual plots showed fairly even distribution of the residuals above and below zero, and the normal plots of the residuals were fairly straight.

The predictive accuracy of the regression equation of the sums of the widths of the canine and premolars based on the values of the sums of the widths of the four mandibular incisors was better in females than in males.

Analysis of variance (ANOVA) (F = 217.28 with 1 and 229 degrees of freedom, with all statistically significant P values equal to 0.001) demonstrate that all variances due to regression were highly significant, so that it is unlikely that the relationship between the sums of widths of the four mandibular incisors and the sums of widths of the canine and first and second premolars in the linear model was due to chance.

The percentage of observations having an absolute error (computed as the difference between observed and predicted values) greater than 1 mm was 13.00% (29/230), greater in males (17/112=15%) than in females (12/118=10%). The regression equation for the total sample is: $y = 0.613x+7.294$ ($r= 0.701$)

No statistically significant difference in the second premolar of the two sides was observed

Table I. *Descriptive values for the sums of the four mandibular incisors and the mandibular canine and premolar segments.*

GROUP	N	Summation	Mean (mm)	SD (mm)	Min (mm)	Max (mm)
Combined	230	Mandibular incisors Mandibular canine and premolars	23.55 21.72	1.59 1.39	18.90 17.85	28.40 27.10
Females	118	Mandibular incisors * Mandibular canine and premolars **	23.27 21.34	1.44 1.06	19.60 17.85	28.40 25.35
Males	112	Mandibular incisors* Mandibular canine and premolars**	23.84 22.13	0.16 1.41	19.60 18.85	28.40 27.10

*SD: standard deviation; *t-test=2.75, p=0.006, males vs females;*
*** Mann-Whitney U-test=4187, p=0.001, males versus females.*

Table II. *Regression parameters for prediction of summation of mesiodistal widths of the canine and second premolars in mandible.*

Group	Arch	r	a (mm)	b	SEE(mm)	r^2
Combined	Mandible	0.701	7.294*	0.613*	0.991	0.491
Females	Mandible	0.713	6.874*	0.621*	0.884	0.508
Males	Mandible	0.670	8.773*	0.560*	1.053	0.449

*SEE: standard error of estimates; *Significant at p=0.001*

by gender or between the sums of the mandibular incisors, canines and first premolar segments of the two sides, therefore the results of the right and left sides were averaged. Statistically significant differences in these mean values were observed by gender (respectively p=0.005 and p=0.001) (Table III), with the result that the males' teeth are slightly larger than those of the females.

Table IV shows the linear regression equation, the standard error of the estimate and the correlation coefficients between the mandibular second premolar and the sum of mandibular incisors, canine and first premolar for each gender. Residual plots showed a fairly even distribution of the residuals above and below zero, and the normal plots of the residuals were fairly straight.

The correlation coefficients were not significantly different between males and females.

The predictive accuracy of the regression equation of the sums of widths of the incisors, canine and first premolar based on the values of the sums of widths of the second mandibular premolar was better in females than in males. Analysis of variance (ANOVA) (F = 260.33 with 1 and 229 degrees of freedom, and all statistically significant p = 0.001) indicated that all variances due to regression were highly significant, so that it is unlikely that the relationship between the sums of widths of the second mandibular premolar and the sums of widths of the incisors, canine and first premolar in the linear model was due to chance.

The percentage of observations having absolute error greater than 0.5 mm was 6.09% (14/230), and was smaller among females (6/112=5.35%) than among males (8/118=6.78%). The regression equation for the total sample is: y=1.224+0.241x (r=

Table III. *Descriptive values for the sums of the four mandibular incisors canine and first premolar and the mandibular second premolar.*

Group	N	Summation	Mean (mm)	SD (mm)	Min (mm)	Max (mm)
Combined	230	Mandibular incisors canine and I premolar	26.00	1.61	21.25	31.75
		Mandibular II premolars	7.50	0.53	6.05	9.55
Females	118	Mandibular incisors canine and I premolar	25.57	1.45	21.25	30.30
		Mandibular II premolars	7.40	0.50	6.05	8.65
Males	112	Mandibular incisors canine and I premolar	26.46	1.64	22.70	31.75
		Mandibular II premolars	7.59	0.54	6.45	9.55

Table IV. *Regression parameters for prediction of summation of mesiodistal widths of the incisors, canines and first premolar in mandible.*

Group	Arch	r	a (mm)	b	SEE	r^2
Combined	Mandible	0.732	1.224	0.241***	0.361	0.535
Females	Mandible	0.704	1.206	0.242***	0.356	0.496
Males	Mandible	0.735	1.712	0.244***	0.370	0.541

*SEE: standard error of estimates; ***Significant at p = 0.001*

0.732).

DISCUSSION

During the mixed dentition period, the mesiodistal dimensions of unerupted canines and premolars were extrapolated from measurements of the erupted permanent mandibular incisors using the Tanaka and Johnston prediction equations (5) or calculated using Moyers probability tables (6). It is essential to remember that tooth size varies in different ethnic groups and among genders, so prediction equations and tables specific to each population for both males and females must be made (14, 18). Consequentially, the different methods proposed for mixed dentition space analysis are relevant only for the population from which it was developed (13, 16).

As previously reported, only Caucasian-born subjects were evaluated who had been residents in Puglia (southern Italy) at least from one generation and referring to the Dr. Cirulli private practice in Bari. Obviously, the data collected in the present study do not represent the southern Italian population in general, but can be considered representative of a certain population of southern Italy. In fact, as reported by Rickards et al. in 1995 (19), southern and central Italian populations, Greek and Aegean populations appeared very homogeneous and quite differentiated from the rest of Europe, both continental (including northern Italy) and south-eastern, stressing the major impact of the heavy Greek colonization on the genetic pools of the circum-Mediterranean people.

Certainly, according to evidence-based dentistry (20), further investigation with a larger sample size is required to collect more representative odontometric

data for southern Italians.

In conclusion, the findings of this study provide southern Italian odontometric data which were previously unavailable. Validating studies need to be carried out to confirm the applicability and precision of the new regression equations proposed.

REFERENCES

1. Musich DR, Ackerman JL. Am J Orthod 1973; 63:366-75.
2. Nance HN. The limitations of orthodontic treatment; mixed dentition diagnosis and treatment. Am J Orthod 1947; 33:177-223.
3. Bull RL. Radiographic method to estimate the mesiodistal dimension of unerupted teeth. Am J Orthod 1959; 45:711-712.
4. de Paula S, Almeida MA, Lee PC. Prediction of mesiodistal diameter of unerupted lower canines and premolars using 45 degrees cephalometric radiography. Am J Orthod Dentofacial Orthop 1995; 107:309-14.
5. Moyers RE. In: Handbook of Orthodontics. 3th ed. Chicago: Mosby Year Book; 1973: p. 370-1.
6. Tanaka MM, Johnston LE. The prediction of the size of unerupted canines and premolars in a contemporary orthodontic population. J Am Dent Assoc 1974; 88:798-801.
7. Hixon EH, Oldfather RE. Estimation of the sizes of unerupted cuspid and bicuspid teeth. Angle Orthod 1958; 28:236-40.
8. Staley RN, O'Gorman TW, Hoag JF, Shelly TH. Prediction of the size of the unerupted canine and premolars in a contemporary orthodontic population. J Am Dent Assoc 1984; 108:185-90.
9. Al-Khadra BH. Prediction of the size of unerupted canines and premolars in a Saudi Arab population. Am J Orthod Dentofacial Orthop 1993; 104:369-72.
10. Ferguson FS, Marco DJ, Sonnenburg EM, Shakun M.L. The use of regression constants in estimating tooth size in the Negro population. Am J Orthod 1978; 73:68-72.
11. Yuen KK, Tang EL, So LL. Mixed dentition analysis for Hong Kong Chinese. Angle Orthod 1998; 68:21-28.
12. Van der Merwe SW, Rossouw P, Van Wyk Kotze T, Trutero H. An adaptation of the mixed dentition space analysis for a Western Cape Caucasian population. J Dent Assoc S Afr 1991; 46:475-9.
13. Marinelli A, Alarashi M, Defraia E, Antonini A, Tollaro I. Tooth wear in the mixed dentition: a comparative study between children born in the 1950s and 1990s. Angle Orthod 2005; 75:340-3.
14. Alessandri Bonetti G, Verganti S, Zanarini M, Bonetti S, Gatto MR. Mixed dentition space analysis for a northern Italian population: new regression equations for unerupted teeth. Prog Orthod 2011; 12:94-9.
15. Hunter WS, Garn SM, Miller RL. Commutator-operated digital caliper with visual display and card-punch capacity. J Dent Res 1970; 49:176.
16. Oakley C, Brunette DM. The use of diagnostic data in clinical dental practice. Dent Clin North Am 2002; 46:87-115.
17. Dahlberg G. Statistical Methods for Medical and Biological Students. Br Med J 1940; 2:358-59.
18. Johnston (Jr) LE. Regression. Is your guess as good as mine? Seminars in Orthod 2002; 8:87-91.
19. Rickards O, Scano G, Martinez-Labarga C, Taraborelli T, Gruppioni G, De Stefano GF. Genetic history of the population of Puglia (southern Italy). Gene Geogr 1995; 9:25-40.
20. Ballini A, Capodiferro S, Toia M, Cantore S, Favia G, De Frenza G, Grassi FR. Evidence-based dentistry: what's new? Int J Med Sci 2007; 6:174-8.

ERRATA CORRIGE

In Vol. 29 No. 1, January - March,

page 221, the authors names and affiliations should read:

Y. SUN[1] DG. LI[1,2], Q. LI[3] L. HUANG[4], Z. HE[5], F. ZHANG[6] and CB. WANG[7]

[1]Department of Clinical Laboratory, the PLA General Hospital, Beijing, China; [2]Department of Nephrology, Chinese PLA General Hospital, Beijing, China; [3]Clinical Laboratory Center, Xiyuan Hospital, China Academy of Chinese Medical Sciences, Beijing, China; [4]Department of Clinical Laboratory, the Fifth People's Hospital of Chengdu, China; [5]Beijing Center for Physical and Chemical Analysis, Beijing, China; [6]Department of Clinical Laboratory, the PLA General Hospital, Beijing, China; [7]Department of Clinical Laboratory,the PLA General Hospital, Beijing, China

page 159, the authors names should read:

L. WANG, GY. SHAN, XA. LIU and XY. SUN